

The Synthesis and Assembly of Linear-Dendritic Rod Diblock Copolymers

by

Catherine Marie Bambenek Santini

Bachelor of Science, Chemistry
South Dakota State University, 1995

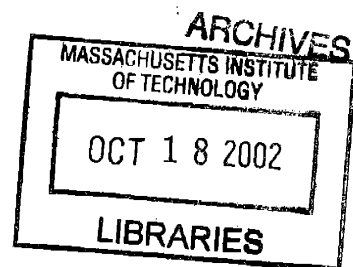
Submitted to the Department of Materials Science and Engineering in Partial Fulfillment of the
Requirements for the Degree of

Doctor of Philosophy in Polymers

at the

Massachusetts Institute of Technology

September 2002



© 2002 Massachusetts Institute of Technology. All right reserved.

Signature of Author..... *Catherine Marie Bambenek Santini*
Catherine Marie Bambenek Santini
Department of Materials Science and Engineering
August 9, 2002

Certified by..... *Paula T. Hammond*
Paula T. Hammond
Joseph P. Mares Associate Professor of Chemical Engineering
Thesis Supervisor

Certified by..... *T. Alan Hatton*
T. Alan Hatton
Ralph Landau Professor of Chemical Engineering Practice
Thesis Supervisor

Certified by..... *Anne M. Mayes*
Anne M. Mayes
Professor of Polymer Physics
Department of Materials Science and Engineering Thesis Supervisor

Accepted by..... *Harry L. Tuller*
Harry L. Tuller
Professor of Ceramics and Electronic Materials
Chair, Departmental Committee on Graduate Students

The Synthesis and Assembly of Linear-Dendritic Rod Diblock Copolymers

by

Catherine Marie Bambenek Santini

Submitted to the Department of Materials Science and Engineering on August 9, 2002
in partial fulfillment of the requirements for the degree of
Doctor of Philosophy in Polymers

Abstract

Dendrimers are three-dimensional, hyperbranched macromolecules that possess a uniform size and shape. Most dendrimers are spherical in shape; however, the shape of the dendrimer can be adjusting using the number and the position of the branching groups in the core. For example, dendritic rods have been prepared by assembling a dendron around each repeat unit of a linear polymer core, and hybrid-linear dendritic diblock copolymers have been prepared by attaching a dendron to the end functional group of a linear polymer. This linear block in the diblock copolymers also adds physical integrity and an assembly mechanism for arrangement of the polymer. Nonetheless, no one has combined the unique shape of the dendritic rod with that of the linear dendritic diblock copolymer. The objective of this research was to prepare a linear-dendritic rod diblock copolymer, and to examine its assembly behavior in solution, at the air/water interface, and in the bulk. These polymers consisted of a linear poly(ethylene oxide)-poly(ethylene imine) diblock copolymer around which poly(amido amine) branches were divergently synthesized. The dendritic branches were terminated with amine and ester groups, as well as alkyl chains of various lengths in order to “tune” the amphiphilic nature of the polymer.

A fundamental change in the assembly behavior of the polymers was observed at generation 4.0 (eight end-groups). In solution, the hydrodynamic and viscometric radii were found to increase to a much greater extent than expected for the generation 4.0 and 4.5 polymers, consistent with a breakdown of the spherical approximation as the dendritic block extended into a rod-like shape. Similarly, at the air/water interface, the dendritic block of generation 4.0-alkyl terminated polymers all adopted a horizontal rod configuration, while the dendritic block of the lower generation polymers took on a random coil configuration, whose shape depended on the length of the terminal alkyl groups as well as the generation number of the dendritic block. Finally, in the bulk, direct observation of the generation 4.0-dodecyl terminated polymer with TEM indicated that the polymer was adopting a rod- or worm-like conformation, while the lower generation polymers only exhibited traditional diblock copolymer or polymer brush behavior.

Thesis Supervisor: Paula T. Hammond

Title: Joseph P. Mares Associate Professor of Chemical Engineering

Thesis Supervisor: T. Alan Hatton

Title: Ralph Landau Professor of Chemical Engineering Practice

Acknowledgements

This thesis would not have been possible without the assistance that I received from many people. I would especially like to thank my advisors, Professors Paula Hammond and T. Alan Hatton for the intellectual, financial, and emotional support that I have received over the years. First, I really appreciate the technical suggestions and advice that they offered. Second, I am very grateful for the emotional support that they showed as my project faced many challenges; their patience and encouragement helped me to make something of a project, which at times seemed hopeless. Third, I really value the latitude that they gave me in my experimental work, as this autonomy has helped me to become a better researcher. Finally, I am very thankful for the flexibility and understanding that they have shown as I balanced finishing a thesis with pregnancy and motherhood.

I would also like to thank my thesis committee members Professors Anne Mayes and Klavs Jensen. Your suggestions and input have helped to make this a better thesis.

Similarly, I would like to thank Professors Ed Merrill, Bob Cohen, Greg Rutledge, Daniel Blankstein, and Paul Laibinis for their attention and helpful ideas during 10.975 and 10.981 seminars.

I am also very grateful for having the opportunity to work with undergraduates James Boedicker and Claudia Couto. James' patience and hard work in collecting the SAXS and OM data, as well as help in preparing samples for TEM came at a critical time and helped me to finish off the bulk characterization of the polymers. I especially appreciated his willingness to come in and finish off the work in the fall and early winter, even after he had started another UROP. I couldn't have asked for a better UROP.

Experimentally, I am also very much indebted to several people. First there is Laurel Ng of the Professor Christine Ortiz's group, who helped me collect the AFM images of my individual polymers. Second, Dr. Peter Dvornic, Peter Carver, and Dr. Tom Chamberlin of the Michigan Molecular Institute/Impact Analytical were very helpful and responsive as I sent them samples for GPC-MALLS. Third, are Steve Wetzal, Tony Modestino, and Peter Maloof of the Chemical Engineering Department. Steve was always very patient and helpful when I had facilities questions; Tony was great help with the NMR; and Peter helped to reconfigure the computer on a crucial piece of old equipment during Y2K. Finally, are Mark Johnson, Dean DeLongchamp, Greg Pollock, and Geoff Moser of the Hammond and Hatton groups. Mark Johnson was responsible for all of the TEM images presented in this thesis as well as helpful discussions of dendrimers in general. Dean was always very willing to help me with computer issues (no matter how stupid), and he wrote an important Excel macro for me so that I could process my Langmuir data much more quickly. Greg very kindly conducted some last minute WAXD experiments for me, and Geoff was always willing to help with the light scattering equipment.

Finally, I must thank those who helped to fund my stay at MIT. The Starr Foundation kindly provided me with a graduate fellowship during my first year. The 3M Innovation Fund and the Environmental Protection Agency funded the research and my stipends. Finally, the MIT graduate student office, kindly covered my tuition during this past spring.

My time at MIT has helped me to grow in many ways, both personally and professionally. I have experienced some of my greatest highs, as well as lowest lows while I have been here. There are several people I have to thank for helping me to make it here, make it through, and make the time more enjoyable.

Before coming to MIT, there were several people who fostered my interest in science and engineering. Back in high school, Mr. Saelens, Mr. Swanson, and Mrs. Leak (Lind) not only encouraged me to pursue a scientific career, but also provided opportunities for several of us to participate in activities, such as the Science Olympiad and the Math Team, that helped us to further develop our scientific and engineering skills. When doing undergraduate work at South Dakota State University (SDSU) Doctors Rita Majerle, Jim Rice, and Rolland Rue were also a big influence. Specifically, Doctors Majerle and Rice helped to get me involved in undergraduate research in their labs, and they gave me the latitude to discover what true research was all about. I did not think that I would enjoy doing research or going to graduate school until they opened my eyes.

Here at MIT, I am very grateful to Yot, Ken, Darrell, Anne-Valerie (A.V.), and Bindu, my fellow PPST class members who helped me to make it through the first year of core classes and qualifiers.

Also the first year, I really appreciated my roommate Rosanna, and suitemates Kate, Mary, and Winnie at Ashdown House who gave me so much encouragement and support during the difficulties of adjusting to life at MIT. I will never forget the good times that we had, and I have not yet bought a rice cooker.

Through the course of my stay at MIT, I am very happy that I had the opportunity to be a part of the Hammond and Hatton groups. The friendship and fun that we shared made going to work so much easier. As my desk was in the Hammond group, I got to know you a little better. To the old crew (Wen-Yue, Jyotsna, Sarah, Aaron, Bindu, Mitch, Dave, Jung Sheng (J.S.), Mark, and Xueping, I will always remember, lunches, coffee, and movies and Sarah's. To the new ones (Don, Dean, Greg, LaRuth, LaShanda, Shoshana, Ilsoon, Haipeng, Heejae, Mike, and Hiro) I really appreciate the support and encouragement that you gave me as I was finishing up and pregnant.

I am also so grateful that I had the opportunity to be part of the Catholic Fellowship (CF) group at MIT. Through the group I met a number of wonderful people, (including my husband John) and I had the opportunity to learn a lot more about and grow in my faith. CF provided me with a group where I felt that I really belonged, and I will always cherish the memories of the CF meeting and activities. Similarly, I really appreciate the fellowship that I received from Maricarmen and Cynthia. Even though you were not a part of CF, our study of the catechism helped me to become a better person. Finally, I really value the opportunity that I had to be a part of the pro-life group at MIT. The people in the group are some of the most caring that I have met at MIT, and I hope that they will be able to keep up the wonderful work.

On the family side, I would like to thank my parents, Jerry and Mary Ann Bambenek, who have been so incredibly supportive of everything that I have done, especially as I have been balancing completion of this thesis with parenthood. I am very grateful to my Dad for passing on to me his boundless curiosity and perfectionism, and to my Mom for passing on to me not only her interest in science and engineering but who also has been a great role model for me. My brother Joe has also been a wonderful influence in my life. He has opened up many opportunities for me, including coming to MIT, and has showed me what it means to be a loving

person. I also want to thank my new parents, John and Pat Santini, and my brother-in-law Andrew, for their support, encouragement, and prayers as I have been finishing up.

In addition, I have to thank my little daughter, Alexandra Mary (Allie) for your patience as your Mom has been finishing her thesis. You've been a very understanding baby and have brought so much joy to my life. I am looking forward to spending more time with you now that this project and thesis (my other "baby") are done.

Finally, I would like to thank my wonderful husband, John. I couldn't have made it through this thesis without all of your love and support, both emotional and physical. In addition to being there through the highs and lows, you also sacrificed your own time, energy, and sleep to help with laundry, dishes, cooking, taking care of Allie, and whatever else came up. You make being married easy.

Last, but certainly not least, I have to thank Our Heavenly Father above and Our Lord Jesus Christ for blessing me with my life and the opportunity to have completed a doctorate at MIT. I couldn't have made it through all of this without You.

Table of Contents

| | |
|---|----|
| List of Figures..... | 14 |
| List of Tables..... | 19 |
| | |
| Chapter 1 – Introduction and Objectives..... | 21 |
| 1.1 Introduction..... | 21 |
| 1.2 Research Objectives and Scope..... | 23 |
| 1.3 References..... | 25 |
| | |
| Chapter 2 – Synthesis and Chemical Characterization of the Linear-Dendritic Rod | |
| Diblock Copolymers..... | 29 |
| 2.1 Introduction..... | 29 |
| 2.2 Background..... | 31 |
| 2.2.1 Spherical Dendritic Homopolymers..... | 31 |
| 2.2.2 Dendritic Rods..... | 32 |
| 2.2.3 Hybrid-Linear Dendritic Diblock Copolymers | 34 |
| 2.3 Experimental..... | 35 |
| 2.3.1 Materials..... | 35 |
| 2.3.2 Instrumentation..... | 36 |
| 2.3.3 Synthesis..... | 36 |
| 2.4 Results and Discussion..... | 37 |
| 2.4.1 Overview of the Synthesis..... | 37 |
| 2.4.2 Chemical Characterization..... | 51 |
| 2.4.2.1 ¹ H NMR..... | 51 |
| 2.4.2.2 FTIR..... | 60 |
| 2.4.2.3 MALDI-TOF and SEC-MALLS..... | 67 |
| 2.5 Summary and Conclusions..... | 69 |
| 2.6 References..... | 73 |

| | |
|--|---------|
| Chapter 3 – Solution Behavior of the Linear-Dendritic Rod Diblock Copolymers..... | 79 |
| 3.1 Introduction..... | 79 |
| 3.2 Background..... | 80 |
| 3.2.1 Spherical Dendritic Homopolymers..... | 80 |
| 3.2.2 Dendritic Rods and Hyperbranched Polymers..... | 87 |
| 3.2.3 Hybrid-Linear Dendritic Diblock Copolymers..... | 89 |
| 3.2.4 Rod-Coil Diblock Copolymers..... | 92 |
| 3.3 Theory..... | 94 |
| 3.3.1 Dynamic Light Scattering..... | 94 |
| 3.3.2 Intrinsic Viscosity..... | 96 |
| 3.4 Experimental..... | 102 |
| 3.4.1 Materials..... | 102 |
| 3.4.2 Dynamic Light Scattering..... | 102 |
| 3.4.3 Intrinsic Viscosity..... | 103 |
| 3.5 Results and Discussion..... | 104 |
| 3.5.1 Dynamic Light Scattering..... | 104 |
| 3.5.2 Intrinsic Viscosity..... | 109 |
| 3.5.2.1 Determination of the Intrinsic Viscosity..... | 109 |
| 3.5.2.2 Intrinsic Viscosity as a Function of Generation and End Group..... | 118 |
| 3.5.2.3 Determination of Size..... | 127 |
| 3.6 Summary and Conclusions..... | 132 |
| 3.7 References..... | 136 |
| Chapter 4 – Langmuir Films of the Linear-Dendritic Rod Diblock Copolymers..... | 143 |
| 4.1 Introduction..... | 143 |
| 4.2 Background..... | 145 |
| 4.2.1 Spherical Dendritic Homopolymers..... | 145 |
| 4.2.2 Dendritic Rods..... | 149 |
| 4.2.3 Hybrid-Linear Dendritic Diblock Copolymers..... | 149 |
| 4.2.4 Rod-Coil Diblock Copolymers..... | 150 |

| | | |
|-------|--|-----|
| 4.3 | Experimental..... | 151 |
| 4.3.1 | Materials..... | 151 |
| 4.3.2 | Instrumentation..... | 153 |
| 4.3.3 | Methods..... | 153 |
| 4.4 | Results and Discussion..... | 154 |
| 4.4.1 | Pressure-Area Isotherms for the Polymers..... | 154 |
| 4.4.2 | Surface Pressure..... | 161 |
| 4.4.3 | Surface Area per Molecule..... | 168 |
| 4.4.4 | Compressibility of the Polymers..... | 173 |
| 4.4.5 | Reversibility and Reproducibility of the Pressure/Area Isotherms..... | 176 |
| 4.4.6 | Possible Surface Structures..... | 182 |
| 4.5 | Summary and Conclusions..... | 197 |
| 4.6 | References..... | 200 |

Chapter 5 – Bulk Characterization and Morphology of the Linear-Dendritic Rod Diblock

| | | |
|---------|---|-----|
| | Copolymers..... | 207 |
| 5.1 | Introduction..... | 207 |
| 5.2 | Background..... | 208 |
| 5.2.1 | Spherical Dendritic Homopolymers..... | 208 |
| 5.2.1.1 | Glass Transition Temperature and Liquid Crystalline Properties..... | 208 |
| 5.2.1.2 | Imaging of the Dendrimers..... | 215 |
| 5.2.2 | Dendritic Rods..... | 220 |
| 5.2.3 | Hybrid-Linear Dendritic Diblock Copolymers..... | 224 |
| 5.2.4 | Rod-Coil and Comb-Coil Diblock Copolymers..... | 228 |
| 5.3 | Experimental..... | 229 |
| 5.3.1 | Differential Scanning Calorimetry (DSC)..... | 229 |
| 5.3.2 | Small Angle X-ray Scattering (SAXS) and Wide Angle X-ray Diffraction (WAXD)..... | 230 |
| 5.3.3 | Transmission Electron Microscopy (TEM)..... | 231 |

| | | |
|--|--|-----|
| 5.3.4 | Optical Microscopy (OM)..... | 232 |
| 5.3.5 | Atomic Force Microscopy (AFM)..... | 232 |
| 5.4 | Results and Discussion..... | 233 |
| 5.4.1 | Differential Scanning Calorimetry (DSC) and Optical Microscopy (OM)..... | 233 |
| 5.4.2 | X-ray Scattering and Transmission Electron Microscopy (TEM)..... | 251 |
| 5.4.3 | Atomic Force Microscopy (AFM)..... | 263 |
| 5.5 | Summary and Conclusions..... | 267 |
| 5.6 | References..... | 270 |
| Chapter 6 – Conclusions and Future Work..... | | 279 |
| 6.1 | Conclusions..... | 279 |
| 6.2 | Future Work..... | 287 |
| 6.3 | References..... | 292 |
| Appendix 2.A – Synthetic Details..... | | 294 |
| 2.A.1 | Generational Synthesis..... | 294 |
| 2.A.1.1 | Linear Dendritic Rod Diblock Copolymers Consisting of a Polyethylene Oxide Block of 43 Repeats and a Dendritic Block of 97 Repeats..... | 294 |
| 2.A.1.2 | Linear Dendritic Rod Diblock Copolymers Consisting of a Polyethylene Oxide Block of 43 Repeats and a Dendritic Block of 178 Repeats..... | 301 |
| 2.A.2 | End Group Modification..... | 303 |
| 2.A.2.1 | Linear Dendritic Rod Diblock Copolymers Consisting of a Polyethylene Oxide Block of 43 Repeats and a Dendritic Block of 97 Repeats..... | 303 |
| 2.A.2.2 | Linear Dendritic Rod Diblock Copolymers Consisting of a Polyethylene Oxide Block of 43 Repeats and a Dendritic Block of 178 Repeats..... | 321 |

| | |
|--------------------------------------|-----|
| 2.A.3 References..... | 324 |
| Appendix 5.A – DSC Data..... | 325 |
| 5.A.1 Generational Polymers..... | 325 |
| 5.A.2 Alkyl Terminated Polymers..... | 325 |
| 5.A.2.1 Generation 1.0..... | 325 |
| 5.A.2.2 Generation 2.0..... | 326 |
| 5.A.2.3 Generation 3.0..... | 326 |
| 5.A.2.4 Generation 4.0..... | 326 |
| 5.A.2.5 Generation 5.0..... | 327 |

List of Figures

| | | |
|-------------|--|-----|
| Figure 1.1. | Graphical representation of a linear-dendritic rod diblock copolymer..... | 23 |
| Figure 2.1. | Synthetic scheme used to prepare the poly(ethylene oxide)-poly(ethylene imine) diblock copolymer backbone..... | 43 |
| Figure 2.2. | Synthetic scheme used to prepare the poly(ethylene oxide)-poly(ethylene imine)-poly(amido amine) linear-dendritic rod diblock copolymer..... | 44 |
| Figure 2.3. | Synthetic scheme used to functionalize the methyl ester chain end of the linear-dendritic rod diblock copolymers with alkyl groups..... | 45 |
| Figure 2.4. | ¹ H NMR of the poly(ethylene oxide)-poly(ethylene imine) diblock copolymer consisting of 43 repeats of poly(ethylene oxide) and 97 repeats of poly(ethylene imine)..... | 54 |
| Figure 2.5. | ¹ H NMR of the generation 4.5 linear-dendritic rod diblock copolymer..... | 56 |
| Figure 2.6. | ¹ H NMR of the generation 2.0-amine terminated linear-dendritic rod diblock copolymer..... | 57 |
| Figure 2.7. | ¹ H NMR of the generation 3.0-octyl terminated linear-dendritic rod diblock copolymer..... | 59 |
| Figure 2.8. | FTIR spectra of the poly(ethylene oxide)-poly(ethylene imine)-poly(amido amine) linear dendritic rod diblock copolymers..... | 65 |
| Figure 2.9. | FTIR spectra of the generation 3.0-alkyl terminated poly(ethylene oxide)-poly(ethylene imine)-poly(amido amine) linear dendritic rod diblock copolymers..... | 66 |
| Figure 3.1. | Average effective hydrodynamic radius of the polymers as a function of concentration determined in methanol at 25°C..... | 106 |
| Figure 3.2. | Average effective hydrodynamic radius of the polymers as a function of generation determined in methanol at 25°C..... | 108 |
| Figure 3.3. | Huggins and Kramer plots of the solution viscosity as a function of concentration for the poly(ethylene oxide)-poly(ethylene imine) diblock copolymer..... | 111 |

| | | |
|--------------|--|-----|
| Figure 3.4. | Huggins and Kramer plots of the solution viscosity as a function of concentration for the generation 2.5 linear-dendritic rod diblock copolymer..... | 112 |
| Figure 3.5. | Fuoss plot of the solution viscosity as a function of concentration for the generation 2.5 linear-dendritic rod diblock copolymer..... | 113 |
| Figure 3.6. | Fedors plot of the solution viscosity as a function of concentration for the generation 2.5 linear-dendritic rod diblock copolymer..... | 114 |
| Figure 3.7. | Fedors plots of the solution viscosity as a function of concentration for the poly(ethylene oxide)-poly(ethylene imine) diblock copolymer..... | 115 |
| Figure 3.8. | Intrinsic viscosity as a function of generation for the linear-dendritic rod diblock copolymers..... | 119 |
| Figure 3.9. | Graphical representation of the model for comb polymers in which the side chains are treated as spheres placed randomly around the polymer backbone (a). Graphical representation of the model for a dendritic rod polymer in which the dendrons are treated as hemispheres placed randomly around the polymer backbone (b)..... | 123 |
| Figure 3.10 | The estimated intrinsic viscosity as a function of generation for two different values of relative lengths of the branches to the monomer unit along the backbone..... | 125 |
| Figure 3.11. | The hydrodynamic and the viscometric radii of the polymers as a function of generation in methanol at 25°C and assuming a spherical shape..... | 132 |
| Figure 4.1. | A list of the polymers under investigation and the percent substitution of the alkyl chains on the polymer..... | 152 |
| Figure 4.2. | Pressure/area isotherms of the generation 1.0 linear-dendritic rod diblock copolymers which possessed a dendritic block length of 97 repeats..... | 155 |
| Figure 4.3. | Pressure/area isotherms of the generation 1.0 linear-dendritic rod diblock copolymers which possessed a dendritic block length of 178 repeats..... | 156 |
| Figure 4.4. | Pressure/area isotherms of the generation 2.0 linear-dendritic rod diblock copolymers which possessed a dendritic block length of 97 repeats..... | 157 |
| Figure 4.5. | Pressure/area isotherms of the generation 3.0 linear-dendritic rod diblock copolymers which possessed a dendritic block length of 97 repeats..... | 158 |

| | | |
|--------------|--|-----|
| Figure 4.6. | Pressure/area isotherms of the generation 4.0 linear-dendritic rod diblock copolymers which possessed a dendritic block length of 97 repeats..... | 159 |
| Figure 4.7. | Pressure/area isotherms of the generation 5.0 linear-dendritic rod diblock copolymers which possessed a dendritic block length of 97 repeats..... | 160 |
| Figure 4.8. | Surface pressure at collapse versus alkyl chain length of the linear-dendritic rod diblock copolymers..... | 167 |
| Figure 4.9. | Surface area per molecule versus alkyl chain length of the linear-dendritic rod diblock copolymers..... | 169 |
| Figure 4.10. | Compressibility versus surface pressure for the generation 2.0-octyl terminated linear-dendritic rod diblock copolymer..... | 174 |
| Figure 4.11. | Compressibility versus alkyl chain length of the linear-dendritic rod diblock copolymers..... | 175 |
| Figure 4.12. | First and second compression and decompression pressure/area isotherms of the generation 1.0 linear dendritic rod diblock copolymers which had a dendritic block length of 97 repeats..... | 178 |
| Figure 4.13. | First and second compression and decompression pressure/area isotherms of the generation 3.0 linear dendritic rod diblock copolymers which had a dendritic block length of 97 repeats..... | 180 |
| Figure 4.14. | First and second compression and decompression pressure/area isotherms of the generation 5.0 linear dendritic rod diblock copolymers which had a dendritic block length of 97 repeats..... | 181 |
| Figure 4.15. | Proposed models for the arrangement of the linear-dendritic rod diblock copolymers on the surface..... | 184 |
| Figure 5.1. | Examples of DSC traces for the amine and ester terminated linear-dendritic rod diblock copolymers: poly(ethylene oxide)-poly(ethylene imine) diblock copolymer backbone, generation 2.0 linear-dendritic rod diblock copolymer, generation 3.5 linear-dendritic rod diblock copolymer..... | 234 |
| Figure 5.2. | Variation of the melting point and the glass transition temperature with generation for the amine and ester terminated linear-dendritic rod diblock copolymers..... | 237 |
| Figure 5.3. | Examples of DSC traces for the alkyl terminated linear-dendritic rod diblock copolymers..... | 240 |

| | | |
|--------------|--|-----|
| Figure 5.4. | Variation of the poly(ethylene oxide) melting point with alkyl chain length and generation for the alkyl terminated linear-dendritic rod diblock copolymers..... | 241 |
| Figure 5.5. | Variation of the glass transition temperature with alkyl chain length and generation for the alkyl terminated linear-dendritic rod diblock copolymers..... | 242 |
| Figure 5.6. | Variation of the alkyl chain melting point with alkyl chain length and generation for the alkyl terminated linear-dendritic rod diblock copolymers..... | 247 |
| Figure 5.7. | Crystallization of the poly(ethylene oxide) block in the poly(ethylene oxide)-poly(ethylene imine)) generation 0.5 linear-dendritic rod diblock copolymer as indicated by the formation of the Maltese cross pattern..... | 248 |
| Figure 5.8. | Crystallization of the octadecyl chains in the poly(ethylene oxide)-poly(ethylene imine) generation 1.0-octadecyl linear-dendritic rod diblock copolymer..... | 250 |
| Figure 5.9. | Temperature dependent 1D SAXS profiles for the poly(ethylene oxide)-poly(ethylene imine) diblock copolymer backbone..... | 252 |
| Figure 5.10. | TEM image of the bulk morphology of the poly(ethylene oxide)-poly(ethylene imine) diblock copolymer backbone at room temperature..... | 253 |
| Figure 5.11. | Temperature dependent 1D SAXS profiles for the poly(ethylene oxide)-poly(ethylene imine) generation 0.5 linear-dendritic rod diblock copolymer | 254 |
| Figure 5.12. | TEM image of the bulk morphology of the poly(ethylene oxide)-poly(ethylene imine) generation 0.5 linear-dendritic rod diblock copolymer at room temperature..... | 255 |
| Figure 5.13. | Temperature dependent 1D SAXS profiles for the poly(ethylene oxide)-poly(ethylene imine) generation 4.5 linear-dendritic rod diblock copolymer..... | 256 |
| Figure 5.14. | TEM image of the bulk morphology of the poly(ethylene oxide)-poly(ethylene imine) generation 4.5 linear-dendritic rod diblock copolymer at room temperature..... | 257 |
| Figure 5.15. | Temperature dependent 1D SAXS profiles for the poly(ethylene oxide)-poly(ethylene imine) generation 1.0-dodecyl terminated linear-dendritic rod diblock copolymer..... | 259 |
| Figure 5.16. | TEM image of the bulk morphology of the poly(ethylene oxide)-poly(ethylene imine) generation 1.0-dodecyl terminated linear-dendritic rod diblock copolymer at room temperature..... | 259 |

| | | |
|--------------|--|-----|
| Figure 5.17 | Room temperature WAXD of the poly(ethylene oxide)-poly(ethylene imine) generation 1.0-dodecyl terminated linear-dendritic rod diblock copolymer..... | 260 |
| Figure 5.18. | Temperature dependent 1D SAXS profiles for the poly(ethylene oxide)-poly(ethylene imine) generation 4.0-dodecyl terminated linear-dendritic rod diblock copolymer..... | 262 |
| Figure 5.19. | TEM image of the bulk morphology of the poly(ethylene oxide)-poly(ethylene imine) generation 4.0-dodecyl terminated linear-dendritic rod diblock copolymer at room temperature..... | 262 |
| Figure 5.20. | Possible dimensions and arrangement of the poly(ethylene oxide)-poly(ethylene imine) generation 4.0-dodecyl terminated linear-dendritic rod diblock copolymers in the bulk..... | 263 |
| Figure 5.21. | AFM image of an individual poly(ethylene oxide)-poly(ethylene imine) generation 4.5 linear-dendritic rod diblock copolymer..... | 264 |
| Figure 5.22. | Lateral cross-section of an individual poly(ethylene oxide)-poly(ethylene imine) generation 4.5 linear-dendritic rod diblock copolymer..... | 264 |
| Figure 5.23. | Graphical representation relating the dimensions of the poly(ethylene oxide)-poly(ethylene imine) generation 4.5 linear-dendritic rod diblock copolymer to an approximate shape..... | 267 |
| Figure 6.1. | Preliminary TEM image of gold nanoparticles templated with the generation 3.0-amine terminated linear-dendritic rod diblock copolymers..... | 292 |

List of Tables

| | | |
|------------|---|-----|
| Table 2.1. | Molecular weight and polydispersity of a poly(ethylene oxide) “blank” which was subjected to the same weak acid hydrolysis conditions used in the formation of the poly(ethylene oxide)-poly(ethylene imine) diblock copolymer..... | 42 |
| Table 3.1. | Viscometric radius calculated as a function of aggregation number and its comparison to the hydrodynamic radii for all of the generations in methanol at 25°C..... | 130 |
| Table 4.1. | Experimentally determined and theoretically calculated surface areas as well as possible surface structures for the generation 1.0 linear-dendritic rod diblock copolymers..... | 185 |
| Table 4.2. | Experimentally determined and theoretically calculated surface areas as well as possible surface structures for the generation 2.0 linear-dendritic rod diblock copolymers..... | 185 |
| Table 4.3. | Experimentally determined and theoretically calculated surface areas as well as possible surface structures for the generation 3.0 linear-dendritic rod diblock copolymers..... | 186 |
| Table 4.4. | Experimentally determined and theoretically calculated surface areas as well as possible surface structures for the generation 4.0 linear-dendritic rod diblock copolymers..... | 186 |
| Table 4.5. | Experimentally determined and theoretically calculated surface areas as well as possible surface structures for the generation 5.0 linear-dendritic rod diblock copolymers..... | 187 |

Chapter 1

Introduction and Objectives

1.1 Introduction

Dendrimers are three-dimensional, hyperbranched macromolecules that possess a uniform size and shape.¹ These macromolecules derive their name from the Greek words *dendron* meaning tree and *mers* meaning parts, since each polymer is composed of many tree like parts.² For the same reason, these polymers have also been called “arborols”³ and “cascade” polymers.⁴ Dendrimers differ from conventional polymers in that they are synthesized in a stepwise manner, which allows for precise control over the number and the length of the branches, as well as the molecular weight.⁵ This stepwise synthesis also allows one to tailor the chemistry of the polymer in the core, in the interior branches, and most importantly on the surface where the chemistry can dramatically affect the properties of the polymer.⁶ While researchers have assembled a whole library of dendritic chemistries and architectures, their common characteristic is their unique, controlled, hyperbranched structure.

The first dendrimers that were prepared were spherical in shape, consisting of a small molecule core with three or four sites for dendron attachment,⁷ however, researchers have found that the shape of the dendrimer could be altered by modifying the number and the position of the branching points in the core. For example, rod shaped dendrimers have been synthesized by assembling the dendrons around each repeat unit of a linear polymer core,⁸⁻¹⁷ and dendritic mushrooms (hybrid-linear dendritic diblock copolymers) have been synthesized by attaching a single dendron to the end functional group of a linear polymer.¹⁸⁻³⁰ In general, the sizes of dendrimers are on the order of nanometers, but the particular size of a dendrimer can be tuned using not only the chemistry and the generation number for spherical dendrimers, but also the length of the linear polymer core for dendritic rods, and the length of the linear block for hybrid-linear dendritic diblock copolymers. The unique tree-like nature of dendrimers also allows for the formation of molecular cavities or pores in the interior area between the branches.⁶

Thus, due to their specific shape, a size that can be carefully programmed, and their ability to form molecular cavities, dendrimers offer an interesting approach to the formation of

nanomaterials.³¹ Nanomaterials are those materials that have length scales between 1 and 100 nanometers and that are also able to exhibit some function.³² Recently, there has been a large interest in the formation of nanomaterials as researchers have been trying to tailor the properties of materials down to the molecular level. In addition, researchers have been trying to make devices that are smaller, faster, and less expensive than current devices, which are micrometers in size, and as the devices have become smaller and faster, the techniques that have been used to make these devices have been approaching their limits of applicability.³³ Thus, there exists a need to find new methods and new materials to work at the nanoscale level.

Spherical dendrimers have already been used as nanomaterials for applications in solution, in thin interfacial films, and in the bulk. In solution, spherical dendrimers have been shown to absorb and release two different dye molecules upon the application of two different acidic conditions.^{34,35} Azobenzene terminated dendrimers have been shown to form photoresponsive Langmuir and Langmuir-Blodgett interfacial films.³⁴⁻³⁸ Finally, dendrimers have been used to template the formation of metal nanoparticles, creating unique nanoscopic composite materials in the bulk.³⁹⁻⁴⁴ For some applications, spherical dendritic homopolymers have proved to be sufficient, but for other applications, they have lacked the necessary organization and physical integrity. Thus, researchers have prepared hybrid-linear dendritic diblock copolymers in which the linear block adds not only physical integrity, but also a mechanism to induce assembly and organization of the dendritic block. For example, in solution, amphiphilic hybrid-linear dendritic diblock copolymers have been found to assemble into macromolecular micelles whose aggregation follows classic Isrealachvili behavior for small molecule surfactants in which the shape of the surfactant affects the type of aggregation.²³⁻²⁵ Similarly, in interfacial films, the linear block in amphiphilic hybrid-linear dendritic diblock copolymers has provided a cohesive layer to aid in the formation of multi-layer Langmuir-Blodgett films.^{23-25,45} Finally, in the bulk, the presence of the linear block has been shown to induce segregation of the dendritic and the linear block into domains due to unfavorable interactions between the two blocks.^{26,46}

While extensive research has focused on the synthesis and characterization of spherical dendrimers, the synthesis and properties of dendritic rods are only beginning to be developed and understood. Dendritic rods may find use in some nanomaterial applications where not only the size and the function are important, but also the shape. Nonetheless, it can be expected that these

dendritic rods will suffer from some of the same difficulties that impeded the use of spherical dendrimers in some nanomaterial applications, such as a lack of physical integrity as well as a mechanism of assembly and organization. A natural solution to these problems is to add a linear block to the dendritic rod, creating a linear-dendritic rod diblock copolymer; however, no one has yet reported doing so. Thus, the synthesis, characterization, and assembly behavior of linear-dendritic rod diblock copolymers are the subjects of this thesis.

1.2 Research Objectives and Scope

The objectives of this research were to design and synthesize a diblock copolymer possessing a linear-dendritic rod diblock copolymer architecture and then to study the assembly behavior of a series of these diblock copolymers in solution, at the air/water interface, and in the bulk. Of primary interest are the effects of dendritic generation and end group chemistry on the above properties. While dendrimers possessing a dendritic rod architecture and others possessing a hybrid-linear dendritic diblock copolymer have been prepared, those with a linear-dendritic rod diblock copolymer architecture proposed have not yet been reported. A graphical representation of this unique dendritic architecture is presented in Figure 1.1. This architecture was of interest as the polymers possessed not only a rod block, which is a nanosized object, but also a linear block, which could add physical integrity and could drive the organization of these molecular objects through various assembly mechanisms.

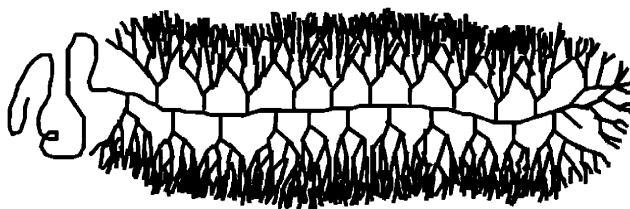


Figure 1.1. Graphical representation of a linear-dendritic rod diblock copolymer.

Specifically, the diblock copolymers under investigation consisted of a linear poly(ethylene oxide)-poly(ethylene imine) diblock copolymer around which poly(amido amine) branches were divergently synthesized. The dendritic branches were terminated with amine and ester groups, which were formed during the generational synthesis; however, the ester groups were also converted to alkyl groups of various lengths allowing one to “tune” the hydrophilic/hydrophobic nature of the dendritic block, and thus, the amphiphilic nature of the diblock copolymer. Poly(ethylene oxide) was chosen as the linear block because it was a commercially available, hydrophilic linear polymer that was soluble in both water and organic solvents, thus decreasing solvent compatibility issues during the synthesis.

In the remainder of this thesis, the following topics will be presented. Chapter Two will focus on the design and synthesis of two series of linear-dendritic rod diblock copolymers, one consisting of a dendritic block of approximately 97 repeats and a poly(ethylene oxide) block of 43 repeats and the other consisting of a dendritic block of approximately 178 repeats and a poly(ethylene oxide) block of approximately 43 repeats. Functionalization of the dendritic end groups with various lengths of alkyl chains will also be discussed. Finally, the chemical characterization of all of the polymers will be presented. In Chapter Three, the solution behavior of these linear-dendritic rod diblock copolymers will be explored. This behavior will be examined using dynamic light scattering and intrinsic viscosity measurements in order to gain insight into the size and aggregation of the polymers as a function of generation and end group chemistry. The focus of Chapter Four will be the behavior of these linear-dendritic rod diblock copolymers as Langmuir films as determined from pressure/area isotherms. Of particular interest are the effects of generation number and alkyl chain length on the surface pressure, surface area, compressibility, reversibility, and reproducibility of the films. In addition, from the pressure/area isotherms, a model for the arrangement of the polymers in the films is presented. Chapter Five will concentrate on the thermal and morphological bulk properties of the polymers. The glass transition temperature and the melting point, as determined from differential scanning calorimetry, as well as the morphology, as characterized with x-ray scattering and transmission electron microscopy, will be presented and discussed with regard to the generation number and end group chemistry. Preliminary imaging of one of the polymers with tapping mode atomic force microscopy will also be shown. It should be noted that at the beginning of Chapters Two through Five, literature about dendrimers relevant to each chapter will be reviewed. Finally, in

Chapter Six all of the results will be summarized and conclusions will be drawn in light of the work presented. In addition, suggestions for future research directions will be offered.

1.3 References

- (1) de Brabander-van den Berg, E. M. M.; Meijer, E. W. "Poly(propylene imine) dendrimers-large-scale synthesis by heterogeneously catalyzed hydrogenations," *Angewandte Chemie-International Edition in English* **1993**, *32*, 1308-1311.
- (2) Tomalia, D. A.; Baker, H.; Dewald, J.; Hall, M.; Kallos, G.; Martin, S.; Roeck, J.; Ryder, J.; Smith, P. "Dendritic macromolecules - synthesis of starburst dendrimers," *Macromolecules* **1986**, *19*, 2466-2468.
- (3) Newkome, G. R.; Yao, Z. Q.; Baker, G. R.; Gupta, V. K. "Micelles 1. Cascade molecules-a new approach to micelles - a [27]-arborol," *Journal of Organic Chemistry* **1985**, *50*, 2003-2004.
- (4) Buhleier, E.; Wehner, W.; Vögtle, F. "Cascade-chain-like and nonskid-chain-like syntheses of molecular cavity topologies," *Synthesis* **1978**, 155-158.
- (5) Tomalia, D. A. "Dendrimer molecules," *Scientific American* **1995**, *272*, 62-66.
- (6) Tomalia, D. A.; Naylor, A. M.; Goddard, W. A. "Starburst dendrimers - molecular-level control of size, shape, surface-chemistry, topology, and flexibility from atoms to macroscopic matter," *Angewandte Chemie-International Edition in English* **1990**, *29*, 138-175.
- (7) Tomalia, D. A.; Durst, H. D. "Genealogically directed synthesis: Starburst*/cascade dendrimers and hyperbranched structures," *Topics in Current Chemistry* **1994**, *165*, 193-313.
- (8) Yin, R.; Zhu, Y.; Tomalia, D. A.; Ibuki, H. "Architectural copolymers: Rod-shaped, cylindrical dendrimers," *Journal of the American Chemical Society* **1998**, *120*, 2678-2679.
- (9) Percec, V.; Ahn, C. H.; Cho, W. D.; Jamieson, A. M.; Kim, J.; Leman, T.; Schmidt, M.; Gerle, M.; Möller, M.; Prokhorova, S. A.; Sheiko, S. S.; Cheng, S. Z. D.; Zhang, A.; Ungar, G.; Yeardley, D. J. P. "Visualizable cylindrical macromolecules with controlled stiffness from backbones containing libraries of self- assembling dendritic side groups," *Journal of the American Chemical Society* **1998**, *120*, 8619-8631.
- (10) Percec, V.; Ahn, C. H.; Ungar, G.; Yeardley, D. J. P.; Möller, M.; Sheiko, S. S. "Controlling polymer shape through the self-assembly of dendritic side-groups," *Nature* **1998**, *391*, 161-164.
- (11) Percec, V.; Cho, W. D.; Mosier, P. E.; Ungar, G.; Yeardley, D. J. P. "Structural analysis of cylindrical and spherical supramolecular dendrimers quantifies the concept of monodendron shape control by generation number," *Journal of the American Chemical Society* **1998**, *120*, 11061-11070.
- (12) Percec, V.; Holerca, M. N.; Magonov, S. N.; Yeardley, D. J. P.; Ungar, G.; Duan, H.; Hudson, S. D. "Poly(oxazolines)s with tapered minidendritic side groups. The simplest cylindrical models to investigate the formation of two-dimensional and three-dimensional order by direct visualization," *Biomacromolecules* **2001**, *2*, 706-728.

- (13) Neubert, I.; Amoulong-Kirstein, E.; Schlüter, A.-D.; Dautzenberg, H. "Polymerization of styrenes carrying dendrons of the first, second and third generation," *Macromolecular Rapid Communications* **1996**, *17*, 517-527.
- (14) Neubert, I.; Schlüter, A.-D. "Dendronized polystyrenes with hydroxy and amino groups in the periphery," *Macromolecules* **1998**, *31*, 9372-9378.
- (15) Stocker, W.; Schürmann, B. L.; Rabe, J. P.; Forster, S.; Lindner, P.; Neubert, I.; Schlüter, A.-D. "A dendritic nanocylinder: Shape control through implementation of steric strain," *Advanced Materials* **1998**, *10*, 793-797.
- (16) Shu, L. J.; Schlüter, A.-D.; Ecker, C.; Severin, N.; Rabe, J. P. "Extremely long dendronized polymers: Synthesis, quantification of structure perfection, individualization, and sfm manipulation," *Angewandte Chemie-International Edition* **2001**, *40*, 4666-4669.
- (17) Ouali, N.; Mery, S.; Skoulios, A.; Noirez, L. "Backbone stretching of wormlike carbosilane dendrimers," *Macromolecules* **2000**, *33*, 6185-6193.
- (18) Gitsov, I.; Fréchet, J. M. J. "Solution and solid-state properties of hybrid linear-dendritic block-copolymers," *Macromolecules* **1993**, *26*, 6536-6546.
- (19) Gitsov, I.; Fréchet, J. M. J. "Novel nanoscopic architectures - linear-globular aba copolymers with polyether dendrimers as a-blocks and polystyrene as b-block," *Macromolecules* **1994**, *27*, 7309-7315.
- (20) Gitsov, I.; Lambrych, K. R.; Remnant, V. A.; Pracitto, R. "Micelles with highly branched nanoporous interior: Solution properties and binding capabilities of amphiphilic copolymers with linear dendritic architecture," *Journal of Polymer Science Part A-Polymer Chemistry* **2000**, *38*, 2711-2727.
- (21) Gitsov, I.; Wooley, K. L.; Fréchet, J. M. J. "Novel polyether copolymers consisting of linear and dendritic blocks," *Angewandte Chemie-International Edition in English* **1992**, *31*, 1200-1202.
- (22) Gitsov, I.; Wooley, K. L.; Hawker, C. J.; Ivanova, P. T.; Fréchet, J. M. J. "Synthesis and properties of novel linear dendritic block-copolymers - reactivity of dendritic macromolecules toward linear-polymers," *Macromolecules* **1993**, *26*, 5621-5627.
- (23) van Hest, J. C. M.; Baars, M. W. P. L.; Elissen-Román, C.; van Genderen, M. H. P.; Meijer, E. W. "Acid-functionalized amphiphiles derived from polystyrene-poly(propylene imine) dendrimers, with a pH-dependent aggregation," *Macromolecules* **1995**, *28*, 6689-6691.
- (24) van Hest, J. C. M.; Delnoye, D. A. P.; Baars, M. W. P. L.; Elissen-Román, C.; van Genderen, M. H. P.; Meijer, E. W. "Polystyrene-poly(propylene imine) dendrimers: Synthesis, characterization, and association behavior of a new class of amphiphiles," *Chemistry-A European Journal* **1996**, *2*, 1616-1626.
- (25) van Hest, J. C. M.; Delnoye, D. A. P.; Baars, M. W. P. L.; van Genderen, M. H. P.; Meijer, E. W. "Polystyrene-dendrimer amphiphilic block-copolymers with a generation-dependent aggregation," *Science* **1995**, *268*, 1592-1595.
- (26) Román, C.; Fischer, H. R.; Meijer, E. W. "Microphase separation of diblock copolymers consisting of polystyrene and acid-functionalized poly(propylene imine) dendrimers," *Macromolecules* **1999**, *32*, 5525-5531.
- (27) Chang, Y.; Kwon, Y. C.; Lee, S. C.; Kim, C. "Amphiphilic linear peo-dendritic carbosilane block copolymers," *Macromolecules* **2000**, *33*, 4496-4500.

- (28) Chang, Y. Y.; Kim, C. "Synthesis and photophysical characterization of amphiphilic dendritic-linear-dendritic block copolymers," *Journal of Polymer Science Part a-Polymer Chemistry* **2001**, *39*, 918-926.
- (29) Chapman, T. M.; Hillyer, G. L.; Mahan, E. J.; Shaffer, K. A. "Hydraamphiphiles - novel linear dendritic block-copolymer surfactants," *Journal of the American Chemical Society* **1994**, *116*, 11195-11196.
- (30) Iyer, J.; Fleming, K.; Hammond, P. T. "Synthesis and solution properties of new linear-dendritic diblock copolymers," *Macromolecules* **1998**, *31*, 8757-8765.
- (31) Balagurusamy, V. S. K.; Ungar, G.; Percec, V.; Johansson, G. "Rational design of the first spherical supramolecular dendrimers self-organized in a novel thermotropic cubic liquid- crystalline phase and the determination of their shape by x-ray analysis," *Journal of the American Chemical Society* **1997**, *119*, 1539-1555.
- (32) Moriarty, P. "Nanostructured materials," *Reports on Progress in Physics* **2001**, *64*, 297-381.
- (33) Edelstein, A. S.; Murday, J. S.; Rath, B. B. "Challenges in nanomaterials design," *Progress in Materials Science* **1997**, *42*, 5-21.
- (34) Jansen, J. F. G. A.; de Brabander-van den Berg, E. M. M.; Meijer, E. W. "Encapsulation of guest molecules into a dendritic box," *Science* **1994**, *266*, 1226-1229.
- (35) Jansen, J. F. G. A.; Meijer, E. W.; de Brabander-van den Berg, E. M. M. "The dendritic box - shape-selective liberation of encapsulated guests," *Journal of the American Chemical Society* **1995**, *117*, 4417-4418.
- (36) Schenning, A. P. H. I.; Elissen-Román, C.; Weener, J. W.; Baars, M. W. P. L.; van der Gaast, S. J.; Meijer, E. W. "Amphiphilic dendrimers as building blocks in supramolecular assemblies," *Journal of the American Chemical Society* **1998**, *120*, 8199-8208.
- (37) Schenning, A. P. H. I.; Peeters, E.; Meijer, E. W. "Energy transfer in supramolecular assemblies of oligo(p- phenylene vinylene)s terminated poly(propylene imine) dendrimers," *Journal of the American Chemical Society* **2000**, *122*, 4489-4495.
- (38) Weener, J. W.; Meijer, E. W. "Photoresponsive dendritic monolayers," *Advanced Materials* **2000**, *12*, 741-746.
- (39) Balogh, L.; Tomalia, D. A. "Poly(amidoamine) dendrimer-templated nanocomposites. 1. Synthesis of zerovalent copper nanoclusters," *Journal of the American Chemical Society* **1998**, *120*, 7355-7356.
- (40) Zhao, M. Q.; Sun, L.; Crooks, R. M. "Preparation of cu nanoclusters within dendrimer templates," *Journal of the American Chemical Society* **1998**, *120*, 4877-4878.
- (41) Zhao, M. Q.; Crooks, R. M. "Dendrimer-encapsulated pt nanoparticles: Synthesis, characterization, and applications to catalysis," *Advanced Materials* **1999**, *11*, 217-+.
- (42) Crooks, R. M.; Lemon, B. I.; Sun, L.; Yeung, L. K.; Zhao, M. Q. In *Dendrimers iii: Design, dimension, function* 2001; Vol. 212, p 81-135.
- (43) Crooks, R. M.; Zhao, M. Q.; Sun, L.; Chechik, V.; Yeung, L. K. "Dendrimer-encapsulated metal nanoparticles: Synthesis, characterization, and applications to catalysis," *Accounts of Chemical Research* **2001**, *34*, 181-190.
- (44) Manna, A.; Imae, T.; Aoi, K.; Okada, M.; Yogo, T. "Synthesis of dendrimer-passivated noble metal nanoparticles in a polar medium: Comparison of size between silver and gold particles," *Chemistry of Materials* **2001**, *13*, 1674-1681.

- (45) Iyer, J.; Hammond, P. T. "Langmuir behavior and ultrathin films of new linear-dendritic diblock copolymers," *Langmuir* **1999**, *15*, 1299-1306.
- (46) Johnson, M. A. *Self-assembly of linear-dendritic diblock copolymers*; Ph.D. Dissertation, Department of Chemical Engineering, Massachusetts Institute of Technology, 2002.

Chapter 2

Synthesis and Chemical Characterization of the Linear-Dendritic Rod Diblock Copolymers

2.1 Introduction

For many years, one of the primary goals of those working in the dendrimer community was to synthesize as many different dendritic chemistries as possible so that a broad range of applications, which each had their own specific chemical needs, could take advantage of the unique properties offered by the dendritic structure.¹ In some cases, this meant developing an entirely new synthetic scheme such that the resulting polymers had unique interior functional groups and bonding configurations. In other cases, it meant tuning an existing chemistry by changing the chemical nature of the end functional group resulting in dendrimers that were amphiphilic.²⁻⁷ Over time, a huge library of chemistries had been compiled; however, almost all of these chemistries had been developed for traditional spherical dendrimers.⁸ Unfortunately, as research progressed, it was found that chemistry alone could not be used to tune all of the desired properties, and the spherical architecture limited the use of dendrimers in some applications.^{9,10} Thus, researchers began to turn their interest to dendritic architecture in order to examine the effect of architecture on properties. One way that this was done was to incorporate traditional polymers into their chemistries. They first prepared dendritic rods in which a linear polymer served as the dendritic core, with each repeat unit serving as a site for dendron attachment.^{9,11-19} Other groups used the end functional group of a linear polymer as the dendritic core, forming hybrid linear-dendritic diblock copolymers.²⁰⁻²⁵ When making these architectural changes, researchers attempted to keep the chemistry of the dendritic portion very similar to that which had been previously developed; however, it was found that the synthetic schemes developed for the spherical dendrimers were not always directly applicable to these new structures. Unfortunately, there were new problems that arose from the unique architecture involved. Luckily, researchers were able to overcome these problems and create the novel dendritic architectures with the desired chemistry; however, it was not as easy as originally expected.

Therefore, while several researchers have prepared dendritic homopolymers and others have prepared linear-dendritic diblock copolymers, no one has yet tried to combine the two architectures into a single polymer – a linear-dendritic rod diblock copolymer. Thus, the first goal in this project was to determine a suitable way to synthesize these polymers. The target chemistry of the linear-dendritic rod diblock copolymers consisted of a poly(amido amine) dendritic rod covalently linked to a linear poly(ethylene oxide) block. In order to make these diblock copolymers amphiphilic, the ends of the dendrimer were functionalized with hydrophobic groups since both the poly(ethylene oxide) and the poly(amido amine) dendrimer were naturally hydrophilic. While functionalization of the poly(amido amine) dendrimers with hydrophobic groups had been described in the literature, almost all of the chemistries introduced new functional groups or arrangements of functional groups in the interior branches. Thus, development of a method for dendritic end group functionalization that maintained the exact branch chemistry and that was applicable over several generations as well as a wide range of lengths of alkyl groups was also desired. The synthetic pathways that were developed to make these linear-dendritic rod diblock copolymers along with a chemical confirmation that the desired linear-dendritic rod diblock copolymers were prepared are the focus of this chapter. In the remainder of this chapter, Section 2.2 will present background information on the synthesis of spherical and rod-shaped dendritic polymers as well as hybrid-linear dendritic diblock copolymers. Section 2.3 will describe the materials, instrumentation, and outline the synthetic route for the linear-dendritic rod diblock copolymers and for the polymers that have been functionalized with n-alkyl chains. Section 2.4 discusses the design of the overall synthetic scheme as well as the successes/challenges encountered during the synthesis. In addition, an in-depth analysis of the ^1H NMR and FTIR data is presented. A chapter summary and concluding remarks are presented in Section 2.5, and the references in Section 2.6. Finally, the detailed synthetic procedures which were used for each of the polymers characterized in subsequent chapters as well as their structural verification by ^1H NMR and FTIR are given in Appendix 2.A. Two different series of block copolymers are described; one which is synthesized up to generation 4.5 and consists of a poly(ethylene oxide) block of 43 repeats and a dendritic block of approximately 97 repeats, and the other which is only synthesized as far as generation 1.0 and consists of a poly(ethylene oxide) block of 43 repeats and a dendritic block of approximately 178 repeats.

2.2 Background

2.2.1 Spherical Dendritic Homopolymers

The three most common and highly developed dendrimer chemistries are the poly(amido amine) (PAMAM) chemistry,²⁶ the poly(propylene imine) chemistry,²⁷ and the poly(benzyl ether) (Fréchet type) chemistry.²⁸ As researchers began to look at the effect of dendrimer architecture, they began by trying to make architectural analogues of these three systems. PAMAM dendrimers are divergently made by the exhaustive Michael addition of methyl acrylate to an ammonia or ethylenediamine core, followed by the exhaustive addition of ethylenediamine to the newly formed methyl ester branches.^{26,29} Similarly, the poly(propylene imine) dendrimers are divergently made by the exhaustive Michael addition of acrylonitrile to a 1,4-diaminobutane core, followed by the hydrogenation of the nitrile with a Raney-cobalt catalyst, regenerating the amine.²⁷ Conversely, the poly(benzyl ether) dendrimers are made in a convergent manner by the selective alkylation of phenolic hydroxyl groups with brominated exterior pieces, conversion of the remaining benzylic alcohol to a bromide, and coupling of these larger, brominated dendritic pieces by the repeated selective alkylation of phenolic hydroxyl groups.²⁸

Over the years, researchers have tried to “tune” the properties of these three dendritic chemistries by changing the chemical nature of the dendritic end functional groups. For example, hydrophilic PAMAM dendrimers have been made amphiphilic by the addition of hydrophobic groups to the amine terminated polymers. Sayed-Sweet *et al.* accomplished this by reacting the PAMAM amino end groups with various epoxyalkanes,⁴ and Sui *et al.* did this by reacting the PAMAM amino end groups with the N-hydroxysuccinimide ester of hydroxydodecanoic acid.^{6,7} Similarly, Aoi *et al.* reacted a methyl ester terminated generation 2.5 polymer with n-hexyl amine.²⁴ Dvornic *et al.* used a slightly different approach by adding hydrophobic organosilicon groups to the PAMAM amino groups using a Michael addition as well as haloalkylation.^{30,31} Finally, Iyer *et al.* functionalized the end groups of a poly(ethylene oxide)-poly(amido amine) hybrid-linear dendritic diblock copolymer using a DCC coupling of the amine terminated polymers with stearic acid.^{6,7,32} Hydrophilic poly(propylene imine) dendrimers have also been made amphiphilic by the addition of large hydrophobic groups to the surface of the polymer. Schenning *et al.* have reacted the amine terminated polymers with three

different reagents using three different chemistries.⁵ In the first, they reacted the dendrimer with palmitoyl chloride using simple acid chloride/amine chemistry; in the second, they reacted the dendrimer with pentafluorophenyl azo-ester using ester/amine chemistry; and in the third, they reacted the dendrimer with 1-succinimidoyl adamantane carboxylate using succinimide ester/amine chemistry. Finally, Hawker *et al.* found that they could make their hydrophobic poly(benzyl ether) dendrimers (Fréchet-type) amphiphilic by starting with exterior phenyl pieces that had been substituted with methyl ester groups, which could later be hydrolyzed to form hydrophilic carboxylic acid exterior surfaces.³³

2.2.2 Dendritic Rods

The first dendritic architecture that combined a linear polymer and a dendrimer was the dendritic rod. As early as 1987, Tomalia *et al.* reported the synthesis of a PAMAM dendritic rod;¹¹ however, inadequate analytical methodologies prevented the unequivocal characterization of this structure until 1998.¹² This polymer was prepared by the divergent addition of poly(amido amine) branches around a linear poly(ethylene imine) core. Unfortunately, there were several problems that were encountered during the synthesis of this architectural analog, which were not encountered in the synthesis of the spherical polymer. The primary problem was that during the ethylenediamine step, the polymer was found to crosslink unless huge excesses of ethylenediamine (1250 for generation 1.0 and 10,000 for generation 4.0) were used and unless the reaction was run at low temperatures (5°C) and for long times (5 days for generation 1.0 and 8 days for generation 4.0.) The excess ethylenediamine was needed so that the difunctional amine would only react at one end and would not react on the other end with neighboring methyl ester groups, thus resulting in the crosslinking. The low reaction temperatures were needed to slow the reaction down to ensure that unreacted ethylenediamine had time to diffuse to the unreacted methyl ester groups, and the long reaction times were needed to ensure complete conversion. These conditions were not needed for the spherical dendrimers since there were significantly fewer amine groups on the spherical polymers and their proximity to each other was not as close. Another problem with the PAMAM dendritic rod synthesis was that there were purification challenges that needed to be addressed for the dendritic rods, which did not need to be addressed for the spheres. Since the spherical PAMAM dendrimers were relatively small, the low generation polymers did not need to be purified after each reaction since the excess reagents

could be easily removed by vacuum distillation. However, the structure of the dendritic rods prevented the excess ethylenediamine from being easily removed. Not only were the dendritic rods bigger such that they could more easily physically trap the ethylenediamine, they also possessed a larger number of amine end groups that could more readily hydrogen bond with the excess ethylenediamine. Thus, Tomalia *et al.* found it necessary to purify the amine terminated polymer by dialysis since residual ethylene diamine resulted in the formation of spherical dendrimer impurities as well as imperfections in the branching. Ghosh *et al.* have used step growth polymerization to form side chain dendritic polyesters that possess an azobenzene backbone and poly(amido amine) dendritic side chains. Unfortunately, because preformed generation 3.5 methyl ester terminated poly(amido amine) dendrons were used, it was difficult to obtain a high degree of polymerization due to the steric constraints of the dendritic side groups.³⁴

Synthetic challenges were also encountered as researchers tried to prepare poly(benzyl ether) dendritic rods. Schlüter *et al.* have attached first and second generation poly(benzyl ether) dendrons to a rigid poly(para-phenylene) backbone; however, they found that the chemistry of the linking groups was very important to achieving a high degree of substitution.³⁵ They have also been able to attach third generation dendrons to this same backbone, but due to steric constraints from the large size of this dendron, complete substitution could not be achieved.¹ Hawker *et al.* had similar problems when they tried to attach preformed poly(benzyl ether) dendrons to a flexible, functionalized polystyrene backbone.¹⁰ As the size of the dendritic block increased, the degree of substitution of the dendrons on the backbone decreased, resulting in globular macromolecules instead of rigid rods. Other groups have attempted to synthesize rigid rod Fréchet type dendrimers by the polymerization of a dendritic macromonomer. Schlüter *et al.* have used free radical polymerization to polymerize first, second, and third generation functionalized polystyrene.^{14,16,17,19,36,37} They found that with increasing generation, both initiator concentration and temperature had to be increased in order to obtain polymers with high molecular weights. They also have used Suzuki cross-coupling to polymerize a third and fourth generation poly(benzyl ether) macrodendron; however, it took rigorous optimization of the reaction conditions and the monomer design in order to get the polymerization to occur.^{35,38} Percec *et al.* have been the most successful in polymerizing poly(benzyl ether) dendritic monomers into rod shaped structures.^{13-16,37} By adding alkyl groups to the dendritic end groups, the dendritic macromonomers have been found to self-assemble into various structures, such as

rods or spheres, depending on the generation number of the dendron as well as the placement of the alkyl groups on the dendron. Once these dendritic monomers had been self-assembled they were subsequently polymerized using a variety of techniques. For both dendritic rod chemistries discussed above, the synthetic challenges were found to arise primarily from the steric interactions caused by the large number of branches on the polymer, and optimization of the reaction conditions and reagents was needed to overcome these difficulties.

2.2.3 Hybrid-Linear Dendritic Diblock Copolymers

The other main dendritic architecture that combines a dendrimer and a linear polymer is the hybrid-linear dendritic diblock copolymer. While problems have also been encountered in the synthesis of these polymers, they have not been as serious as those found for the dendritic rods. Iyer *et al.*²³ found that they could synthesize a polyethylene oxide-PAMAM hybrid-linear dendritic diblock copolymer by the divergent addition of a PAMAM dendron to an amine terminated poly(ethylene oxide) linear polymer. Fortunately, the synthetic conditions used to make these polymers were almost identical to those used to make the spherical polymers; however, purification of the diblock copolymers was an important challenge that they needed to address. As previously mentioned, the spherical dendrimers do not need to be purified since the excess reagents are easily removed by vacuum distillation after every step. However, the presence of the poly(ethylene oxide) block made diffusion of the excess reagents difficult and trapped small amounts of them in the polymer during the vacuum distillation. Thus, it became necessary to precipitate the polymer into ether after each reaction step to ensure that residual reagents were removed and that imperfections did not occur.

Unfortunately, it was more difficult for van Hest *et al.*³⁹ to synthesize their polystyrene-poly(propylene imine) hybrid-linear dendritic diblock copolymers. These diblock copolymers were prepared by the divergent addition of a poly(propylene imine) dendron to a hydroxyl terminated polystyrene linear polymer. Since the polystyrene was hydrophobic and the poly(propylene imine) and its reagents were hydrophilic, it was necessary to develop a two-phase system with a phase-transfer catalyst for the cyanoethylation reaction to occur. In addition, a new solvent system, which dissolved the polystyrene block, needed to be derived for the hydrogenation reaction.

Nonetheless, Gitsov *et al.* found that they could easily prepare a poly(ethylene oxide)-poly(benzyl ether) dendrimer by the reaction of hydroxyl terminated PEO with NaH, forming the PEO-anion, and then reacting the PEO-anion with the dendritic bromide.^{40,41} Surprisingly, they found that the rate of this Williamson ether reaction actually increased as the size of the PEO and the dendritic block increased due to solvation and conformational issues. After purification of the diblock copolymer to remove small amounts of unreacted polymer, the PEO-poly(benzyl ether) dendritic diblock was obtained. Gitsov *et al.* had more difficulty preparing polystyrene-poly(benzyl ether) hybrid-linear dendritic diblock copolymers by coupling a living polystyrene chain end with a dendritic bromide.⁴² Unfortunately, side reactions of the polystyrene anion with the benzylic halomethyl groups occurred that had to be minimized and purification performed in order to achieve the desired polymer. Leduc *et al.*⁴³ were also able to prepare a polystyrene-poly(benzyl ether) hybrid-linear dendritic diblock copolymer by employing the benzylic halides in the dendritic core as macroinitiators for the controlled free radical polymerization of polystyrene. Unfortunately, purification of the diblock copolymer was needed to remove small amounts of unreacted dendrimer. In general, most of the synthetic challenges were found to be caused by polymer/solvent compatibility issues as well as new purification needs to remove excess reagents or unreacted polymer blocks.

2.3 Experimental

2.3.1 Materials

Poly(ethylene glycol) monomethyl ether of molecular weight 1900g/mol from PolySciences was purified twice by precipitation from chloroform into a 10-fold excess of ethyl ether. It was then dried on a vacuum line for a day and then in a vacuum dessicator with P₂O₅ for another day. Tosyl chloride from Aldrich was recrystallized using a known procedure.⁴⁴ Triethyl amine, methylene chloride, benzene, and acetonitrile were predried with CaH₂ and distilled from P₂O₅. 2-ethyl-2-oxazoline was predried overnight with CaH₂ and distilled from fresh CaH₂. Pyridine was predried with KOH for one day and then distilled from KOH into KOH. Anhydrous ethyl ether, anhydrous ethyl alcohol, methanol, chloroform, and hexane were used as purchased. Methyl acrylate was washed two times with 5% NaOH, two times with 18Ω

Millipore water, and dried with MgSO_4 overnight to remove the inhibitor. Ethylenediamine was distilled prior to use. N-butyl amine, n-hexyl amine, and n-octyl amine were predried with MgSO_4 and distilled from CaH_2 into KOH. N-decyl amine was predried with MgSO_4 and vacuum distilled from CaH_2 , and n-dodecyl amine was only vacuum distilled prior to use. N-octadecyl amine was used as purchased. Aqueous acid and base solutions were prepared in 18Ω Millipore water. Millipore BIOMAX Polyethersulfone 5000 NMWL and Millipore PLBC regenerated cellulose 3000 NMWL ultrafiltration membranes were flushed first with water and then with methanol prior to use to remove the glycerin and azide with which they were pretreated.

2.3.2 Instrumentation

NMR analysis were performed on a Bruker 400 (400 MHz) instrument using the solvents $\text{DMSO}-d_6$, CDCl_3 , and $\text{MeOH}-d_4$ as indicated. FTIR spectra were collected on a Nicolet Magna-IR 550 spectrometer from thin, solution cast films of the polymers on KBr plates. Gel permeation chromatography (GPC) in THF was performed on a Waters system though Styragel HT3 and HT4 columns. Size exclusion chromatography-multi-angle laser light scattering (SEC-MALLS) was performed using a 0.1M citric acid buffer through two TosoHaas TSK-gel columns in series, G6000PW and G4000PW, and one Waters ultrahydrogel 250 columns in our lab. The SEC-MALLS system consisted of a Waters Model 150C which was connected to a Wyatt Dawn Model F multi-angle light scattering detector. In addition, these measurements were taken using a 1.0M acetic acid/1.0M sodium nitrate/0.25% sodium azide buffer solution which was passed through TosoHaas G6000PW, G3000PW, T0116, and G1000PW columns at the Michigan Molecular Institute. Their system consisted of a Waters 510 pump which was connected to a Water 410 differential refractive index detector and a Wyatt Dawn DSP-F multi-angle light scattering detector.

2.3.3 Synthesis

The synthetic scheme used to prepare the desired linear-dendritic rod diblock copolymers is outlined in Figures 2.1 and 2.2. Figure 2.1 shows the synthesis of the diblock copolymer backbone while Figure 2.2 shows the addition of the dendritic branches to the diblock copolymer backbone. These polymers were made amphiphilic by the addition of alkyl chains of varying

lengths to the half-generation methyl ester terminated branches of the dendritic block as shown in Figure 2.3. The synthetic details for each of the polymers, as well as their chemical verification by ^1H NMR and FTIR are given in appendix 2.A at the end of this thesis.

2.4 Results and Discussion

2.4.1 Overview of the Synthesis

The target linear-dendritic rod diblock copolymers consisted of a linear poly(ethylene oxide)-poly(ethylene imine) diblock copolymer around which poly(amido amine) branches were divergently synthesized. The poly(amido amine) chemistry was chosen since this chemistry had been well characterized,^{26,29,45-48} and the synthesis of poly(amido amine) dendritic rod homopolymers have been reported in the literature,¹² providing a good starting point for the synthesis. Also, the properties of the previously synthesized homopolymers and these new linear-dendritic rod diblock copolymers could be compared to study the effect of architecture and the addition of the linear block on their behavior. The end functional groups of the dendritic branches were amine and ester groups, which were formed during the generational synthesis; however, the ester groups were also converted to alkyl groups of various lengths in order to increase the hydrophobicity of the dendritic block and thus, the amphiphilic nature of the diblock copolymer. Linear poly(ethylene imine) was chosen as the dendritic block core since it has secondary amines in each repeat unit, which could be used to form branches by the Michael addition of methyl acrylate. In addition, it was the only polyamine that allowed for the same branch length and chemistry in every generation. (For example, poly(allyl amine) would also have allowed for the Michael addition of methyl acrylate but it would have resulted in a first generation branch that was only half of the length of the other branches and that would not have contained an amide group.) Poly(ethylene oxide) was chosen as the linear block because it was a hydrophilic linear polymer that was soluble in both water and organic solvents, thus decreasing solvent compatibility issues during the synthesis. In addition, poly(ethylene oxide) was a highly characterized polymer that was commercially available. Finally, since the synthesis and assembly behavior of poly(ethylene oxide)-poly(amido amine) hybrid linear-dendritic diblock copolymers had been previously examined,^{23,49,50} it was hoped that insight could be gained into

the effects of architecture and the number of dendritic end groups on the diblock copolymer behavior by comparing the two systems.

Once the poly(ethylene oxide)-poly(ethylene imine)-poly(amido amine) linear-dendritic rod diblock copolymer chemistry had been chosen, the individual reagents and the order and methods by which they would be combined needed to be determined. Poly(amido amine) dendrimers are traditionally synthesized by starting with a small molecule, multifunctional amine core, such as ammonia or ethylenediamine, and then divergently building the branches outward by the alternating addition of methyl acrylate and ethylenediamine.^{26,29} Thus, for the synthesis of the poly(amido amine) dendritic rod block, it was decided to start with a linear poly(ethylene imine) core and divergently add the poly(amido amine) branches in the same manner. The next question was at what point the PEO and the PEI blocks should be covalently linked together - should it be done before or after the PAMAM branches had been synthesized around the backbone? It was decided to link the PEO block and the PEI block before the synthesis of the PAMAM branches since there were concerns over whether a reactive terminal group on the PEO block would be able to find and react with a reactive end group of the PEI backbone if it was buried under a highly branched dendritic shell. In addition, since the methyl ester and amine groups were both highly reactive it would have been difficult to design a synthesis route in which the PEO group would have preferentially reacted with the PEI end group and not with the dendritic end groups without first protecting the dendritic end groups with a complicated protecting reaction. Finally, since PEO was known to be soluble in methanol⁵¹ and stable in the presence of ethylenediamine and methyl acrylate,²³ it was hypothesized that it should be possible to apply the same PAMAM reactions to a PEO-PEI backbone. Initially in this research, an attempt was made to couple preformed PEI and PEO blocks via the reaction of PEI-OH with NaH_2 forming $\text{PEI-O}^-\text{Na}^+$, followed by its reaction with PEO-tosylate.⁵² Another attempt was made to couple a preformed PEO block with a preformed poly(2-ethyl 2-oxazoline) (PEOX) block, which is the precursor polymer to linear PEI. In this case, a PEOX block which had been formed by the living cationic ring opening polymerization of 2-ethyl-2-oxazoline with methyl tosylate and was still terminated with the tosylate end group, was reacted with a PEO-NH₂ polymer since amines are known to react with tosylates.⁵³ Unfortunately, both of the methods described above were unsuccessful. Instead, it was found that the optimal method for forming the desired PEO-PEI backbone was to use a two-step PEO-tosylate macroinitiator approach. In

this approach, PEO-tosylate was used as a macroinitiator in the cationic ring opening polymerization of 2-ethyl-2-oxazoline forming an intermediate PEO-PEOX diblock copolymer, which could then be hydrolyzed to form the desired PEO-PEI diblock copolymer backbone,⁵⁴ as depicted in Figure 2.1. These reactions will be described in more detail in the following paragraphs. It should be noted that to form the linear PEI block, it was necessary to first form the PEOX block, which is its precursor. The monomer for PEI is aziridine, which is a highly reactive three membered ring. When this monomer is polymerized, it polymerizes so rapidly that it forms a highly branched polymer and not the desired linear polymer.⁵⁵ Thus, to form the linear PEI, it was necessary to form the PEOX intermediate.

The tosylation of PEO has been described several times in the literature with the general synthesis involving the reaction of a PEO-OH with tosyl chloride in the presence of an organic base, such as triethylamine or pyridine, to neutralize the acid which is formed during the reaction.^{54,56-58} Unfortunately, PEO has sometimes been found to degrade in the presence of triethylammonium chloride and pyridinium hydrochloride salts,⁵⁹ which form as a byproduct, such that much effort has been put into finding the right reaction conditions to prevent this degradation from occurring. Harris *et al.*⁵⁸ have developed a method for PEO tosylation that uses triethylamine as the base, and this method was applied successfully to form one of the series of polymers described in this work, the series in which the dendritic block consisted of 97 repeats. Maechling-Strasser *et al.*⁵⁶ have developed another method for PEO tosylation that uses pyridine as the base and this method was applied successfully to form the other series of polymers in this work, the series whose dendritic block consisted of 176 repeats. Both methods involved rigorous purification of the PEO-tosylate. From ¹H NMR analysis of the PEO-tosylate products, it appeared that the tosylation was close to 100% complete for both reactions. In addition, GPC of both series of polymers in THF before and after tosylation indicated no breakdown of the PEO block. As a side note, we found that SEC of the PEO-tosylate polymers in 0.05M NaNO₃/0.02% NaN₃ aqueous solution was not an effective method to determine whether or not degradation had occurred. While the PEO-OH polymer gave a well formed peak at the expected molecular weight, the PEO-OTs gave a skewed peak at molecular weights much less than expected. We believe that the tosylate end group was interacting with the columns and thus not eluting from the columns as it should since GPC of the same polymer in THF showed no degradation. Harris *et al.*⁵⁸ also reported using SEC with an aqueous eluent to verify that their

polymer had not degraded; however to do so, they hydrolyzed the tosylated polymer back to the PEO-OH form and did not characterize the PEO-tosylate polymer directly.

Polymerization of 2-ethyl-2-oxazoline,⁶⁰ as well as other 2-substituted oxazolines,^{54,56,61} with a PEO-tosylate macroinitiator has been successfully described in the literature. No one method was followed to form both series of our diblock copolymers; instead, elements of a few of the reactions were combined to form our PEO-PEOX diblock copolymers. From SEC, the polydispersity of the diblock copolymer consisting of the shorter oxazoline block was found to be approximately 1.2, and the diblock copolymer consisting of the longer oxazoline block was found to have a polydispersity of approximately 1.4. The structures of both polymers were verified with NMR and FTIR. Unfortunately, while the polymerization of 2-substituted oxazolines with poly(ethylene oxide)-tosylate has been found to be a living cationic polymerization such that all of the monomer is consumed, the rate of initiation is much slower than the rate of polymerization, such that the resulting polymers are somewhat polydisperse.^{60,62} This effect has not been observed in the polymerization of poly(2-ethyl-2-oxazoline) homopolymers that were initiated with methyl tosylate. Thus, it has been hypothesized that the lower rate of reactivity of the PEO tosylate is due to a combination of steric hindrance as well as an electron withdrawing effect of the β -alkoxy group.⁶⁰ For example, Litt *et al.* found the ratio of the rate of initiation to the rate of polymerization (k_i/k_p) to be 0.0070 for 2-isobutyl-2-oxazoline polymers that had been initiated with a PEO tosylate of molecular weight 3500g/mol, while they found this same ratio to be 0.22 for the same polymers that had been initiated with methyl tosylate. Similarly, Miyamoto *et al.* found k_i/k_p to be approximately 0.012 for 2-methyl-2-oxazoline polymers initiated with triethylene glycol di-methanesulphonate and 0.72 for the same polymers that had been initiated with methyl tosylate. Nonetheless, in the polymerization of 2-methyl-2-oxazoline with PEO tosylate, Overberger *et al.* found the polydispersity of the polymers to increase with increasing molecular weight of the oxazoline block, which is in good agreement with our results.⁵⁴ Attempts were made to decrease the polydispersity of our PEO-PEOX diblock copolymers by removing poly(ethylene oxide) homopolymer which had not initiated the polymerization of the PEOX block, as well as diblock copolymer which only possessed a very short PEOX block. To do this, the diblock copolymers were ultrafiltered through a regenerated cellulose ultrafiltration membrane which had a cutoff molecular weight of approximately 3000g/mol. Unfortunately this process did not produce the desired results, as the

GPC traces of the diblock copolymer before and after were virtually identical. Fortunately, it was found that the low molecular weight diblock copolymer as well as the unreacted homopolymer could be removed during the acid hydrolysis step, which will be discussed in the following paragraph.

Hydrolysis of the poly(ethylene oxide)-poly(2-ethyl-2-oxazoline) diblock copolymer to the poly(ethylene oxide)-poly(ethylene imine) diblock copolymer was accomplished using a weak acid. Initially, we were apprehensive about using an acid hydrolysis since PEO is known to be acid labile, so a basic hydrolysis was attempted. Unfortunately, we found that the use of base resulted in only approximately 50% hydrolysis of the amide groups before the polymer precipitated from solution. Fortunately, Overberger and Peng developed the acidic reaction conditions necessary for hydrolysis.⁵⁴ However, unlike Overberger and Peng who were unable to isolate the PEO-PEI diblock copolymer after neutralization of the PEO-PEI-H⁺Cl⁻ salt with base and thus had to resort to an ion exchange resin to neutralize the acidic salt, we found that the polymer did precipitate from solution once the pH had been adjusted well above 10, at which point all of the amines were deprotonated. The polymer was isolated from solution by a wash with chloroform, vacuum filtration, and recrystallization in water. (Uncharged linear poly(ethylene imine) is insoluble in cold water.) This process had the added benefit of removing PEO that had not initiated the polymerization of the second block or that only formed a short PEOX/PEI block such that the polymers were still soluble in water and chloroform. From ¹H NMR, it was found that approximately 100% of the amide groups were hydrolyzed. It was also found from ¹H NMR that there was a large increase in the (PEOX/PEI):PEO block integration ratios between the PEO-PEOX and the PEO-PEI diblock copolymers. For example, for the diblock copolymer that contained the shorter PEOX/PEI block, the initial PEOX:PEO ratio was 1.37, while after hydrolysis, the PEI/PEO ratio became 2.32. While we believed that this change was the result of removing the polymer chains that were predominately PEO, a PEO homopolymer “blank” was subjected to the same reaction conditions to alleviate our fear that change may have come about by degradation of the PEO in the acidic conditions. Aliquots of solution and polymer were taken at various times during the process, and the PEO homopolymer was then analyzed by SEC to determine the molecular weight and the polydispersity index. Even after seven days in the acidic conditions, the molecular weight of the polymer decreased by less than 50g/mol and the polydispersity of the PEO homopolymer was changed by less than 0.01,

both of which were within the experimental error of the instrument. A complete list of the molecular weights and the polydispersities of the PEO homopolymers collected at various times is given in Table 2.1. Thus, we believe using a weak acid hydrolysis was a safe and effective method to convert the PEOX block into the PEI block. Unfortunately, it was difficult to determine from SEC how effective the neutralization process and the subsequent purification had been at removing the polymers that were predominately PEO. During the hydrolysis process, the molecular weight of the polymer was decreased by approximately half, shifting the molecular weight much closer to that of the initial poly(ethylene oxide) block. In addition, in the acidic SEC eluent, which was necessary for solvation and elution of the polymer from the columns, the PEI block most likely took on an extended polyelectrolyte conformation, making accurate determination of the molecular weight and the polydispersity more difficult. Nonetheless, ^1H NMR of the isolated PEO-PEI diblock copolymer showed a polymer that was rich in PEI (the PEI:PEO ratio was 2.32) while ^1H NMR of the chloroform and water wash solutions showed a polymer which was rich in PEO but that did contain PEI (the PEI:PEO ratio was 0.33), indicating that the polymer chains that were removed were predominately PEO.

| Sample | Number Average Molecule Weight* | Weight Average Molecule Weight* | Polydispersity Index* |
|---|---------------------------------|---------------------------------|-----------------------|
| PEO-OH No acidic conditions | 2839 | 2949 | 1.039 |
| PEO-OH After 2 days of acid hydrolysis | 2824 | 2935 | 1.039 |
| PEO-OH After 2+3 days of acid hydrolysis | 2806 | 2928 | 1.043 |
| PEO-OH After 2+5 days of acid hydrolysis | 2796 | 2925 | 1.046 |

*The values are the average of two SEC runs.

Table 2.1. Molecular weight and polydispersity of a poly(ethylene oxide) “blank”, which was subjected to the same weak acid hydrolysis conditions used in the formation of the poly(ethylene oxide)-poly(ethylene imine) diblock copolymer.

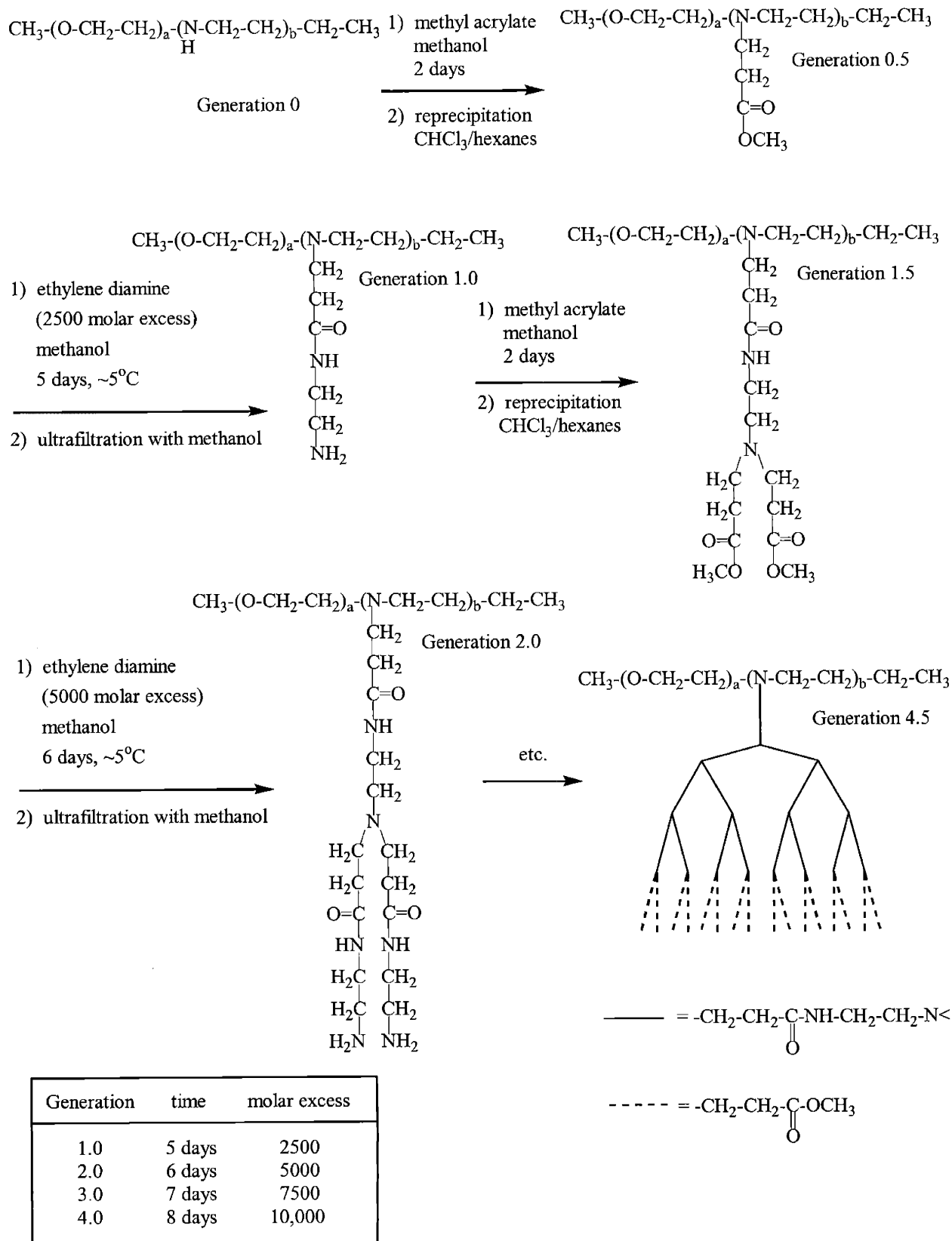


Figure 2.2. Synthetic scheme used to prepare the poly(ethylene oxide)-poly(ethylene imine)-poly(amido amine) linear-dendritic rod diblock copolymer.

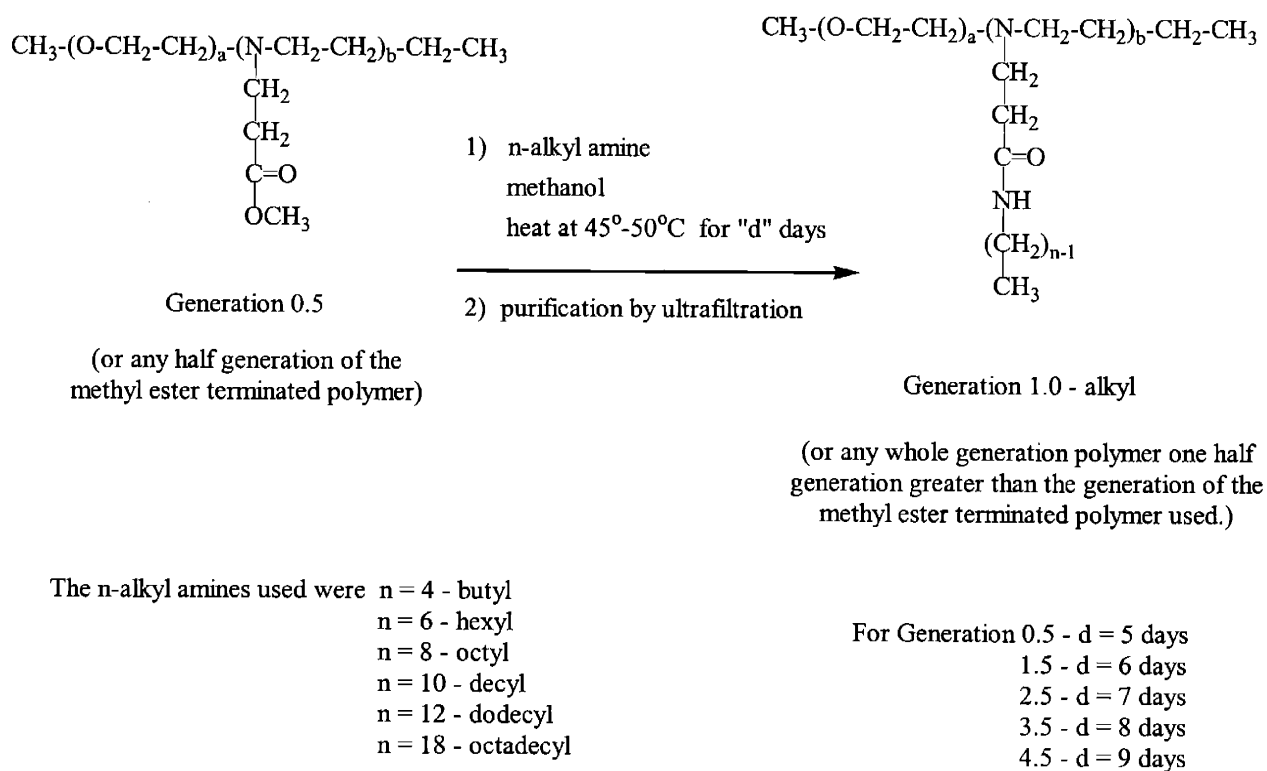


Figure 2.3. Synthetic scheme used to functionalize the methyl ester chain end of the linear-dendritic rod diblock copolymers with alkyl groups.

Formation of the methyl ester terminated half generation polymer proceeded as expected by the addition of methyl acrylate to the poly(ethylene oxide)-poly(ethylene imine) diblock copolymer backbone. Initially, the reaction solution was chilled to ensure that the reaction rate did not proceed too quickly, as the Michael addition of methyl acrylate to an amine is highly exothermic. After slowly warming to room temperature, the reaction was then allowed to proceed for another 48 hours to ensure complete addition of the methyl acrylate groups to the poly(ethylene imine) backbone. The reaction was run using a 2.7 molar excess of methyl acrylate in an approximately 5% by weight polymer solution. These reaction conditions were an adaptation of those described for the poly(amido amine) homopolymers in the patent by Tomalia *et al.*¹¹ and in the paper by Yin *et al.*¹² These two works described slightly different conditions for the formation of the homopolymer. There were two main differences between the two procedures. First, the patent ran the reaction using a larger excess of methyl acrylate, between a

1.67 and an 11 molar excess, but in very dilute conditions (an approximately 3-5% by weight solution.) Conversely, the paper ran the reaction using a much smaller excess of methyl acrylate, only 1.25 molar excess; however, the reaction was run in much more concentrated solutions (approximately 10% by weight polymer solutions.) Second, the patent ran the reaction for 48 hours, initially with the solution at 0°C and later allowing it to warm to room temperature. While the paper also started the reaction at 0°C, but it then heated it to 40°C to accelerate the reaction, as the reaction was only allowed to run for 24 hours. Nonetheless, neither synthetic scheme for the PAMAM homopolymers included a purification step for the methyl ester terminated polymers; however, one was added in the synthesis of the diblock copolymers to ensure that all of the excess methyl acrylate had been removed since the crude polymer exhibited the same strong odor associated with methyl acrylate. This purification step consisted of dissolving the polymer in chloroform and precipitating the polymer into hexanes. After being allowed to stir overnight, the hexane/chloroform solution was poured off and the polymer dried under vacuum, which removed the odor. Unfortunately, even after extensive drying, ¹H NMR of the polymer indicated that the hexanes were being trapped in the polymer. To remove the hexanes, the polymer was redissolved in methanol and the methanol and residual hexanes were removed by vacuum distillation. As the methanol was a fairly good solvent for the polymer, the dissolution of the polymer in methanol allowed the branches to “open up” to remove the hexane. The formation of the subsequent half generation polymers also proceeded as expected. The reaction conditions for these polymers were basically identical to those described above for the generation 0.5 polymer, the primary difference being the molar excess of methyl acrylate used in each reaction. As the generation number increased, so did the molar excess. For example, for the generation 1.5 diblock copolymer, a molar excess of 4.7 was employed, while for the generation 4.5 diblock copolymer, a molar excess of 7.6 was used. The structures of all of the half generation, methyl ester terminated polymers were confirmed with ¹H NMR and FTIR.

Unfortunately, the reaction of the methyl ester terminated polymers with ethylene diamine to form the whole generation, amine terminated polymers did not proceed nearly as easily. As was found in the case of the PAMAM dendritic homopolymers,¹² it was necessary to run the reaction with huge excesses of ethylenediamine (2500 for generation 1.0, 5000 for generation 2.0, 7500 for generation 3.0, and 10,000 for generation 4.0); at low temperatures (approximately 5°C); and for long times (5 days for generation 1.0, increasing to 8 days for

generation 4.0 polymer), in order to prevent the polymer from inter- and intramolecular crosslinking. It was also found that rigorous purification of both the ethylenediamine before the reaction and the amine terminated linear-dendritic rod copolymer after the reaction were necessary to prevent this crosslinking. Unless these steps were taken, the polymer formed an insoluble precipitate either initially, or shortly after the reaction was complete, making characterization impossible. In addition, the imperfections caused by not diligently following the above two steps also affected the formation of the methyl ester terminated polymers, such that they too crosslinked upon standing. Purification of the ethylenediamine by distillation from potassium hydroxide worked well to remove residual water. Two methods for purification of the amine terminated diblock copolymers were attempted. The first one involved dissolution of the crude polymer in methanol, followed by reprecipitation in ethyl ether. This method worked moderately well for removing trace amounts of ethylenediamine; however, it was very difficult to redissolve the purified polymer in methanol. Perhaps this occurred because the ethyl ether could not hydrogen bond with the amine groups, forcing the end groups to hydrogen bond with each other and the polymer to collapse upon itself. Afterward, breaking up these numerous hydrogen bonds with methanol proved extremely difficult. A second method for purification of the amine terminated polymers involved ultrafiltration of the crude polymer in methanol. This method also worked well for removing trace ethylenediamine; fortunately, the purified polymers were much easier to redissolve in methanol, perhaps because they contained traces of methanol, which prevented the amine groups from intra- and intermolecular hydrogen bonding. In order to obtain high yields of purified polymer using this method, it was necessary to use a regenerated cellulose NMWL 3000 ultrafiltration membrane. This membrane is usually not recommended for amines since it can hydrogen bond with the surface, thus easily fouling the membrane.⁶³ This was found to be the case for the amine terminated linear-dendritic rod diblock copolymers as the throughput time was greatly increased for these polymers over other non-amine polymers. Nonetheless, purified polymers were still obtained in this manner. Unfortunately, even though the fourth generation linear-dendritic rod diblock copolymer had been purified by ultrafiltration, it still took 36 hours of stirring as well as sonication for an additional four hours in order to redissolve it in methanol after it had been dried under vacuum between reaction steps. Again, this was probably due to the hydrogen bonding of the terminal amine groups. All of the purified amine terminated, whole generation polymers were stored in methanol after synthesis and before

characterization to prevent the polymers from crosslinking upon standing. Then, they were dried under vacuum immediately before characterization to remove the methanol from the polymer. ¹H NMR and FTIR confirmed that the desired amine terminated polymers had been formed.

In order to make the diblock copolymers amphiphilic, the end groups of the dendritic block were functionalized with alkyl groups. While functionalization of the poly(amido amine) spherical and hybrid-linear dendrimers had been previously accomplished using various methods,^{4,6,32,64-66} we developed a new synthetic scheme such that the exact chemistry of the polymer branches was maintained, and that no new functional groups were introduced, besides the alkyl groups. It was decided that the best way to accomplish this was by reacting the methyl ester terminated, half-generation polymers with various n-alkyl amines. Using this approach, the alkyl groups were connected to the dendrimers using amide bonds in the same position and the same bond order as had been used in the formation of the amine terminated polymers. Thus, the first challenge was to determine the best reaction conditions for the addition of the n-alkyl amines to the methyl ester groups. From experiment, the following factors were found to be important: the amount of excess n-alkyl amine used in the reaction, the concentration of polymer and reagent in the solution, the reaction temperature, the composition of the solvent, and the duration of the reaction.

Since intra- and intermolecular crosslinking reactions were not a threat for the addition of the n-alkyl amines to the methyl ester terminated polymers, as they had been for the addition of the ethylenediamine, the huge excesses of reagent were not needed. Nonetheless, in order to accelerate the reaction, excesses were still used, approximately 60 times for the butyl amine reactions, to approximately 20-30 times for the dodecyl amine reactions, but they were nowhere near the 2500-10,000 times excesses that were used for the ethylenediamine reactions. In general, the amount of excess n-alkyl amine used in the reaction decreased with increasing length of the alkyl chain. This was due to the very high boiling points the longer alkyl amines possessed, resulting in difficulty removing excess reagent by distillation. For example, the boiling point of n-butyl amine was only 78°C, while the boiling point of n-octadecyl amine was not accessible as its melting point was 55°C.⁶⁷ In addition, there were solubility issues during the purification process, which will be discussed below, that made use of large excesses of the longer alkyl amines, especially that of n-octadecyl amine, very difficult. Nonetheless, if too little excess n-alkyl amine was used, it was difficult to achieve as high of a degree of substitution on

the methyl ester groups. For example, for the generation 4.0-octadecyl terminated polymer, only a 1.22 molar excess of n-octadecyl amine was used in the reaction and the resulting polymer had only a 12% substitution. However, in the formation of the 3.0-octadecyl terminated polymer, an 11 molar excess of n-octadecyl amine was used and the substitution reached 33%. Similarly, for the generation 2.0-dodecyl terminated polymer, a 30 molar excess of dodecyl amine was used and over a 90% substitution was achieved. The concentration of the n-alkyl amine in the solution was also found to be important. For these reactions, the highest degree of substitution was observed when the concentration of the n-alkyl amine in the methanol was approximately 30% by weight. In initial experiments in which the concentration of n-alkyl amine was approximately 77% (the same concentration that was used in the ethylenediamine reactions) the degree of substitution was much less, approximately 66%, possibly due to the formation of n-alkyl amine micelles, which interfered with the molecule's ability to participate in the reaction.

Even though the concentration conditions had been optimized, it was still difficult to achieve high degrees of substitution for some of the longer n-alkyl amines on the methyl ester groups. To raise the degree of substitution, the solution was heated in order to increase the rate of reaction. For most of the reactions involving the butyl through the dodecyl alkyl chains, the reactions were performed at approximately 45-50°C. This temperature was chosen such that it was low enough to prevent transamidation and reverse Michael reactions,²⁹ but high enough to still yield a high degree of conversion. For the n-octadecyl terminated polymers, a higher temperature was used. From experiment, it was found that the n-octadecyl amine precipitated from solution as the reaction progressed if it was run at 45°C, but that increasing the temperature to 65°C was enough to drive the n-octadecyl amine back into solution. In addition, since large excesses of n-octadecyl amine could not be used in the reactions, it was hoped that the degree of substitution could be increased with heat instead. Nonetheless, it did not appear as if transamidation and reverse Michael reactions occurred at this temperature. A second method was attempted to increase the degree of substitution. This method involved not only increasing the reaction temperature, but also included adding chloroform as a co-solvent with methanol. It was hoped that the chloroform might be a better solvent for the n-alkyl amines and thus prevent them from forming unimolecular micelles in the reaction solution. Unfortunately, this method was not successful and it resulted in a mixture of products that could not be easily separated.

One final reaction parameter that should be noted is the duration of the reaction. For the reaction of the methyl ester groups with ethylenediamine, the reaction was allowed to proceed for five days for the generation 1.0 polymer, increasing to eight days for the generation 4.0 polymer. These same reaction times were used in the reaction with the n-alkyl amines in order to give the n-alkyl amines and the methyl ester groups plenty of time to react to achieve high degrees of substitution.

One of the challenging aspects of the synthesis of the n-alkyl functionalized polymers was their purification to remove excess n-alkyl amine. For the polymers terminated with the shorter n-alkyl amines, most of the excess reagent could be removed by vacuum distillation; nonetheless, a small amount of residual n-alkyl amine remained. However, for the polymers terminated with the longer n-alkyl amines, it was even difficult to remove the majority of the excess reagent due to the extremely high boiling points of these molecules. In order to remove this residual reagent from both categories of polymers, a couple of approaches were tried. The first one involved reprecipitation of the polymer from chloroform into ethyl ether. While this method worked well for the polymers that were substituted with the shorter alkyl chains (butyl, hexyl, octyl), it did not work at all for the longer alkyl chains because the resulting functionalized polymers were soluble in the ether and the polymer could not be recovered. The second approach involved ultrafiltration of the polymer in methanol, as had been done for the amine terminated polymers. This method worked well for all of the alkyl terminated polymers, regardless of chain length, and thus was used to purify the majority of the polymers synthesized. The one drawback of this method was that some of the higher generation polymers that had been terminated with dodecyl and octadecyl groups and that had been soluble in methanol in their crude form, began to precipitate from the methanol solution during the purification process. It is possible that when the residual n-alkyl amine was present, the n-alkyl amine was able to coat the surface of the diblock copolymer, acting as a surfactant, and helping to dissolve it in solution. However, when this excess reagent was removed, the n-alkyl terminated polymers were chemically incompatible with the methanol such that the polymer precipitated from solution. Thus, it was difficult to achieve a high yield of these polymers. In addition, for the reactions involving n-octadecyl amine, after the reaction was complete, the n-octadecyl amine began to precipitate from solution. Unfortunately, this precipitation was very uncontrolled such that it made purification extremely difficult and precluded the use of large excesses of n-octadecyl

amine in the reaction solution. Methanol had been chosen as a solvent for the ultrafiltration of these polymers due to its compatibility with the ultrafiltration apparatus. In the future, it is recommended that the octadecyl polymers be ultrafiltered in a chloroform solution, which is a better solvent for the hydrophobic, functionalized polymers if solvent compatible ultrafiltration equipment is available.

It should be noted that Imae *et al.* have also reported the use of n-hexyl amine to functionalize the end groups of poly(amido amine) spherical⁶⁸ and hybrid-linear diblock copolymers.²⁴ However, in their work, they only used the hexyl version of the n-alkyl amines, and thus did not encounter or explore the challenges associated with using longer amines or with functionalization of the rod analogue of the poly(amido amine) chemistry.

2.4.2 Chemical Characterization

In order to verify that the desired polymers had been synthesized, the chemical structures of these poly(ethylene oxide)-poly(ethylene imine)-poly(amido amine) linear-dendritic rod diblock copolymers were verified using ¹H NMR (proton nuclear magnetic resonance) and FTIR (Fourier transform infrared) spectroscopy. MALDI-TOF (matrix assisted laser desorption ionization time of flight) mass spectroscopy as well as SEC-MALLS (size exclusion chromatography-multi angle laser light scattering) experiments were also attempted to determine the molecular weight and the molecular weight distributions of the polymers. A general overview of the results is presented below; however, spectral details for all of the polymers are given in appendix 2.A.

2.4.2.1 ¹H NMR

As its name implies, NMR uses a magnetic field to induce an energy difference between the two electron spin states in an atom. The size of this energy difference is dependent on not only the atom involved, but it is also influenced by neighboring atoms. By applying the correct energy frequency, the spin will flip from one state to the other; thus, by measuring the frequency required for a flip, one can gain insight into the nature and position of an atom and its neighbors. One of the advantages of ¹H NMR is that the amount of energy absorbed at each resonance frequency is proportional to the number of hydrogen nuclei that are absorbing energy at that

frequency. Thus, in ^1H NMR, by measuring the areas under each of the resonance peaks, one may determine the relative number of each of the different kinds of hydrogen in the molecule.^{69,70}

The first step in the preparation of the linear-dendritic rod diblock copolymers was the formation of the poly(ethylene oxide)-tosylate macroinitiator. Unfortunately, it is often difficult to determine the end group chemistry on a polymer because such a small percentage of the protons in the spectra correspond to the end group protons. Fortunately, Dust *et al.* have found that by using DMSO as the NMR solvent, the end group chemistry for poly(ethylene oxide) can be determined quantitatively for molecular weights less than 12,000g/mol.⁵⁸ Thus, we have also used DMSO in our NMR analysis of the tosylation reaction. As previously mentioned, ^1H NMR of the tosylated poly(ethylene oxide) indicated that close to 100% of the hydroxyl groups had been converted to tosylate groups. The peak due to protons on the hydroxyl group, which appeared at 4.56ppm, completely disappeared and were replaced by peaks at 7.78, 7.48, 4.11, and 2.42ppm, corresponding to the two sets of benzyl protons, the CH_2 next to the tosylate, and the CH_3 on the end of the tosylate, respectively, in good agreement with the results of others.^{58,71}

Formation of the poly(ethylene oxide)-poly(2-ethyl-2-oxazoline) diblock copolymer was confirmed by ^1H NMR in CDCl_3 . The main peak for the poly(ethylene oxide) block remained at 3.66ppm, while the peaks for the poly(2-ethyl-2-oxazoline) block appeared at 3.47ppm ($-\text{N}-\text{CH}_2-\text{CH}_2-$), 2.42 and 2.33ppm ($-\text{CO}-\text{CH}_2-\text{CH}_3$), and 1.14ppm ($-\text{CO}-\text{CH}_2-\text{CH}_3$). Surprisingly, two separate peaks showed up for the protons associated with the CH_2 's of the side chain; however, only one peak appeared for these same protons when the NMR was performed in $\text{DMSO}-d_6$ and D_2O . (The extra peak was real and not just due to splitting of the original peak caused by neighboring protons.) Perhaps this indicated that the CH_2 's were able to adopt two slightly different conformations in CDCl_3 , but that they were not in the other solvents due to their interactions with the polymer. Nonetheless, the values for the NMR peaks corresponded well to those found for other poly(2-ethyl-2-oxazoline) homopolymers and diblock copolymers.^{60,72,73} Since ^1H NMR is not only qualitative, but also quantitative, we were also able to determine the relative length of the poly(2-ethyl-2-oxazoline) block to the poly(ethylene oxide) block by comparing the number of protons associated with each. From there, the length of the poly(2-ethyl-2-oxazoline) block was determined since the length of the poly(ethylene oxide) block was known.

Weak acid hydrolysis of the poly(ethylene oxide)-poly(2-ethyl-2-oxazoline) diblock copolymer to the poly(ethylene oxide)-poly(ethylene imine) diblock copolymer resulted in almost complete hydrolysis of the pendant acyl groups to the desired secondary amines, as indicated by ^1H NMR in Figure 2.4. The peak due to the poly(2-ethyl-2-oxazoline) main chain at 3.47ppm almost completely disappeared and was replaced by a peak at 2.75ppm due to the poly(ethylene imine) main chain, while the peak due to the poly(ethylene oxide) protons remained virtually unchanged at 3.65ppm. The proton on the secondary amine of the poly(ethylene imine) block was not observed in ^1H NMR, perhaps due to exchange of the proton with the deuterated methanol. It is very common for protons on amines to be exchanged with deuterons in their NMR solvents, especially if the deuterons are easily dissociated.⁷⁰ Similar results have been observed for poly(ethylene imine) homopolymers.⁷⁴ The length of the poly(ethylene imine) block was determined by integration of the protons associated with each of the blocks. For both sets of polymers synthesized, the ratio of the polyimine block to the poly(ethylene oxide) block determined for the poly(ethylene oxide)-poly(2-ethyl-2-oxazoline) diblock copolymers was much smaller than that determined for the poly(ethylene oxide)-poly(ethylene imine) diblock copolymers, as discussed in the preceding section. The ratio determined for the poly(ethylene oxide)-poly(ethylene imine) block copolymers was that which was used to determine the molecular weight of each of the polymers, as it did not vary greatly during the synthesis of subsequent generations.

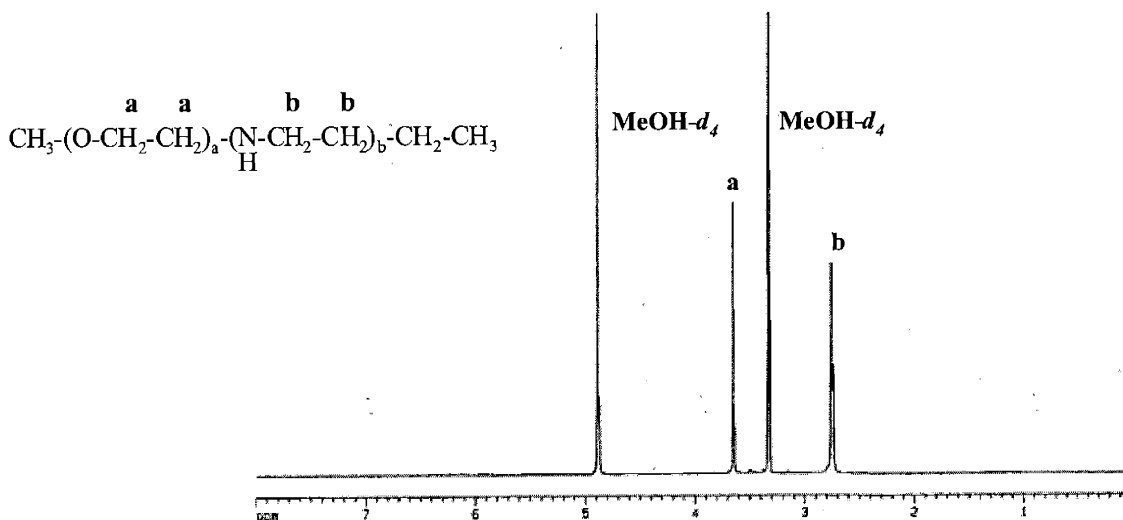


Figure 2.4. ^1H NMR of the poly(ethylene oxide)-poly(ethylene imine) diblock copolymer consisting of 43 repeats of poly(ethylene oxide) and 97 repeats of poly(ethylene imine).

Addition of methyl acrylate to the poly(ethylene oxide)-poly(ethylene imine) diblock copolymer backbone resulted in the formation of the 0.5 generation, methyl ester terminated polymer. The chemical structure of this polymer was confirmed by the addition of peaks at 3.69ppm ($-\text{CH}_2-\text{CH}_2-\text{CO}-\text{OCH}_3$), 2.85ppm ($-\text{CH}_2-\text{CH}_2-\text{CO}-\text{OCH}_3$), and 2.53ppm ($-\text{CH}_2-\text{CH}_2-\text{CO}-\text{OCH}_3$), as well as a shift in the poly(ethylene imine) backbone protons to 2.61ppm ($-\text{N}-\text{CH}_2-\text{CH}_2-$). The poly(ethylene oxide) peak remained unchanged at 3.65ppm. $\text{MeOH}-d_4$ was chosen as the NMR solvent for this and all subsequent half generation polymers as it was not only a good solvent for both blocks, but it also gave a greater resolution than CDCl_3 between the peak at 3.69ppm of the methyl ester protons and the peak at 3.65ppm of the poly(ethylene oxide) protons. The NMR's for the subsequent half generation polymers were much more complex, as they contained not only the protons from the exterior half branches, but also the interior whole branches. The NMR's of all of the half generation polymers gave peaks at approximately the same positions because the chemistry remained the same between generations and can be represented by the generation 4.5 polymer in Figure 2.5. The peaks for the methyl ester terminated branches shifted slightly to 3.69ppm ($-\text{CH}_2-\text{CH}_2-\text{CO}-\text{OCH}_3$), 2.79ppm ($-\text{CH}_2-\text{CH}_2-$

CO-OCH₃), and 2.49ppm (-CH₂-CH₂-CO-OCH₃), while the peaks for the interior whole branches appeared at 3.28ppm (-CO-NH-CH₂-CH₂-N<), 2.84ppm (-CH₂-CH₂-CO-NH-), 2.64ppm (-N-CH₂-CH₂-) and (-CO-NH-CH₂-CH₂-N<) next to a whole branch, 2.58ppm (-CO-NH-CH₂-CH₂-N<) next to a half branch, and 2.40ppm (-CH₂-CH₂-CO-NH-). The poly(ethylene oxide) peak remained virtually unchanged at 3.65ppm. While the peak positions remained virtually unchanged between generations, the integration ratios of some of the peaks did change. For example, one set of ratios that changed was that of the protons of the poly(amido amine) dendritic branches, (-CH₂-CH₂-CO-NH-CH₂-CH₂-N<) and (-CH₂-CH₂-CO-OCH₃), to that of the poly(ethylene oxide) (-O-CH₂-CH₂-). This change was expected as the number of branches in the dendritic poly(amido amine) block multiplied with increasing generation, while the poly(ethylene oxide) block remained the same size. (It should be noted that the integration ratio of the backbone poly(ethylene imine) protons to the poly(ethylene oxide) protons remained constant, and the increase in the branch protons occurred proportionally.) Another set of ratios that changed with increasing generation was the set of ratios from the peaks due to the exterior branches (-CH₂-CH₂-CO-OCH₃) to that of the interior branches (-CH₂-CH₂-CO-NH-CH₂-CH₂-N<). These ratios were found to decrease with increasing generation as expected. For example, for the generation 1.5 polymers, the ratio was 2:1 = 2, while for the generation 3.5 polymers, the ratio was 8:7 = 1.14.

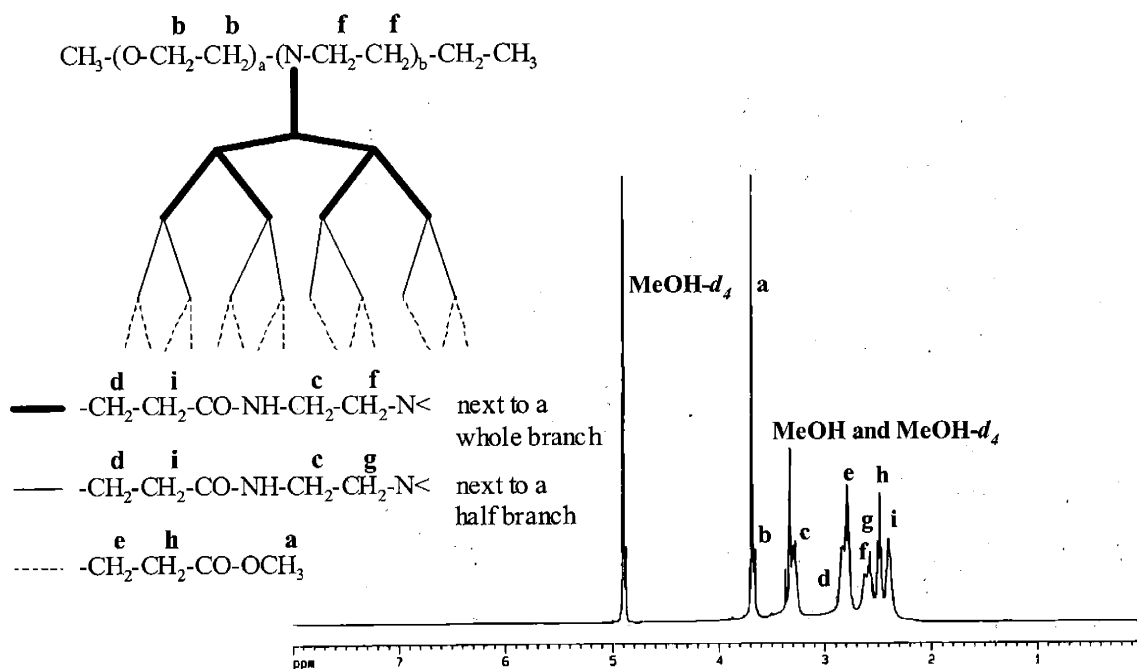


Figure 2.5. ^1H NMR of the generation 4.5 linear-dendritic rod diblock copolymer.

Similarly, the ^1H NMR spectra of all of the amine terminated polymers can essentially be represented by one spectra because the branch chemistry remained identical with increasing generation. The ^1H NMR spectra of the generation 2.0 polymer in $\text{MeOH}-d_4$ is shown in Figure 2.6. $\text{MeOH}-d_4$ was chosen over D_2O as the solvent, so that there would be consistency between the NMRs of the half and the whole generation polymers. The peak from the poly(ethylene oxide) remained unchanged at 3.65ppm, while the peaks for the whole branches were found at 3.28ppm ($-\text{CO}-\text{NH}-\text{CH}_2-\text{CH}_2-\text{N}<$), 2.82ppm ($-\text{CH}_2-\text{CH}_2-\text{CO}-\text{NH}-$), 2.77ppm ($-\text{CO}-\text{NH}-\text{CH}_2-\text{CH}_2-\text{NH}_2$), 2.62ppm ($-\text{N}-\text{CH}_2-\text{CH}_2-$) and ($-\text{CO}-\text{NH}-\text{CH}_2-\text{CH}_2-\text{N}<$), and 2.40ppm ($-\text{CH}_2-\text{CH}_2-\text{CO}-\text{NH}-$), similar to those found for the interior branches of the methyl ester terminated polymers. As was the case of the ester terminated polymers, the main difference between the low generation and the high generation spectra for the amine polymers was the integration ratio of the protons in the dendritic branches to those in the poly(ethylene oxide) block, which increased proportionally with increasing generation, as well as a decrease in the ratio of the interior to exterior branch protons. The primary difference in peaks between the interior and the

exterior branches of the whole generation polymers is that due to the protons on the carbon adjacent to the amine. For the interior tertiary amine (-CO-NH-CH₂-CH₂-N<), they overlap with the poly(ethylene imine) backbone protons at approximately 2.62ppm, while for the exterior primary amine (-CO-NH-CH₂-CH₂-NH₂), they appear at approximately 2.77ppm.

Integration of the NMR peaks for both the half and whole generation polymers, as well as a complete disappearance of the methyl ester protons at 3.69ppm during the formation of the whole generation polymers, indicate that close to 100% substitution occurred at each generation. The proton of the amide group did not appear in the spectra for either the half or the whole generation polymers, probably due to exchange of the proton with the deuterated methanol. The peak positions for both the amine and the methyl ester terminated polymers were in good agreement with those found for the poly(amido amine) spherical^{26,29,72,73} and hybrid-linear dendritic diblock copolymers.²³ Finally, not surprisingly, the length of the dendritic block did not affect the proton peak positions; its only effect was on the integration ratios of the dendritic block to the poly(ethylene oxide) block.

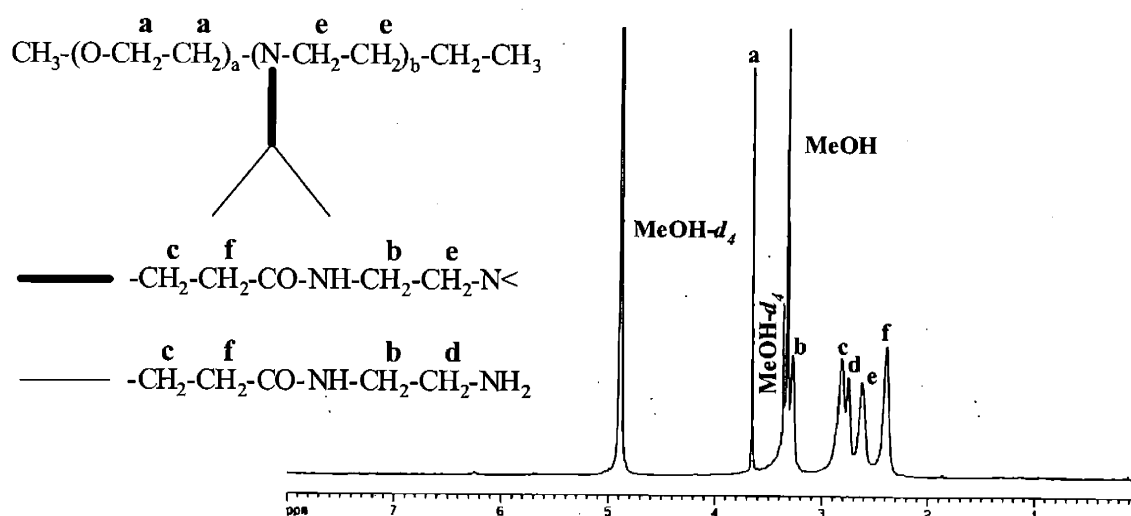


Figure 2.6. ¹H NMR of the generation 2.0-amine terminated linear-dendritic rod diblock copolymer.

^1H NMR was also used to verify the structures of the whole generation polymers that had been functionalized with alkyl groups. $\text{MeOH-}d_4$ was chosen as the solvent for the polymers substituted with the butyl through the decyl group since it resulted in good separation between the poly(ethylene oxide) protons at 3.65ppm and the residual methyl ester protons at 3.69ppm, while CDCl_3 was chosen as the solvent for most of the dodecyl and octadecyl terminated polymers as the purified versions of these polymers were mostly insoluble in methanol. For the generation 1.0-alkyl polymers, addition of the alkyl groups was confirmed by the addition of peaks at approximately 3.20ppm ($-\text{CO-NH-CH}_2\text{-CH}_2\text{-(CH}_2\text{)}_{n-3}\text{-CH}_3$), 1.51ppm ($-\text{CO-NH-CH}_2\text{-CH}_2\text{-(CH}_2\text{)}_{n-3}\text{-CH}_3$), 1.38ppm ($-\text{CO-NH-CH}_2\text{-CH}_2\text{-(CH}_2\text{)}_{n-3}\text{-CH}_3$), and 0.94ppm ($-\text{CO-NH-CH}_2\text{-CH}_2\text{-(CH}_2\text{)}_{n-3}\text{-CH}_3$), all from the alkyl protons. In addition, the peak from the protons on the carbon next to the amide shifted slightly upfield to 2.38ppm ($-\text{CH}_2\text{-CH}_2\text{-CO-NH-}$) while the protons peaks from the poly(ethylene oxide), poly(ethylene imine) backbone, and the most interior carbon, ($-\text{CH}_2\text{-CH}_2\text{-CO-NH-}$), remained virtually unchanged. The generation 2.0, 3.0, 4.0, and 5.0-alkyl terminated polymers gave similar spectra; however, they also contain peaks from the interior poly(amido amine) whole branches. As an example, the spectra of the generation 3.0-octyl terminated polymer, which is very representative of all of the alkyl terminated polymers, is given in Figure 2.7. In general, for the alkyl terminated polymers, the peak at 3.65ppm of the poly(ethylene oxide) remained virtually unchanged, the protons from the interior poly(amido amine) branches fell at 3.28ppm ($-\text{CO-NH-CH}_2\text{-CH}_2\text{-N<}$), 2.84ppm ($-\text{CH}_2\text{-CH}_2\text{-CO-NH-CH}_2\text{-CH}_2\text{-N<}$), 2.61ppm ($-\text{N-CH}_2\text{-CH}_2\text{-}$) and ($-\text{CO-NH-CH}_2\text{-CH}_2\text{-N<}$), 2.40ppm ($-\text{CH}_2\text{-CH}_2\text{-CO-NH-CH}_2\text{-CH}_2\text{-N<}$), while the new peaks from the exterior alkyl groups came in at 3.18ppm ($-\text{CO-NH-CH}_2\text{-CH}_2\text{-(CH}_2\text{)}_{n-3}\text{-CH}_3$), 2.81ppm ($-\text{CH}_2\text{-CH}_2\text{-CO-NH-CH}_2\text{-CH}_2\text{-(CH}_2\text{)}_{n-3}\text{-CH}_3$), 2.36ppm ($-\text{CH}_2\text{-CH}_2\text{-CO-NH-CH}_2\text{-CH}_2\text{-(CH}_2\text{)}_{n-3}\text{-CH}_3$), 1.52ppm ($-\text{CO-NH-CH}_2\text{-CH}_2\text{-(CH}_2\text{)}_{n-3}\text{-CH}_3$), 1.34ppm ($-\text{CO-NH-CH}_2\text{-CH}_2\text{-(CH}_2\text{)}_{n-3}\text{-CH}_3$), and 0.93ppm ($-\text{CO-NH-CH}_2\text{-CH}_2\text{-(CH}_2\text{)}_{n-3}\text{-CH}_3$). Unfortunately, for most of the polymers, not all of the methyl ester groups reacted to form the alkyl groups as indicated by residual protons at 3.69ppm ($-\text{CH}_2\text{-CH}_2\text{-CO-OCH}_3$), 2.76ppm ($-\text{CH}_2\text{-CH}_2\text{-CO-OCH}_3$), and 2.50ppm ($-\text{CH}_2\text{-CH}_2\text{-CO-OCH}_3$). The only significant differences between the generation 2.0, 3.0, 4.0, and 5.0 polymers were the integration ratios between the dendritic block and the poly(ethylene oxide) block, as well as those between the interior and exterior dendritic branches, which had also been observed for the ester and the amine terminated polymers.

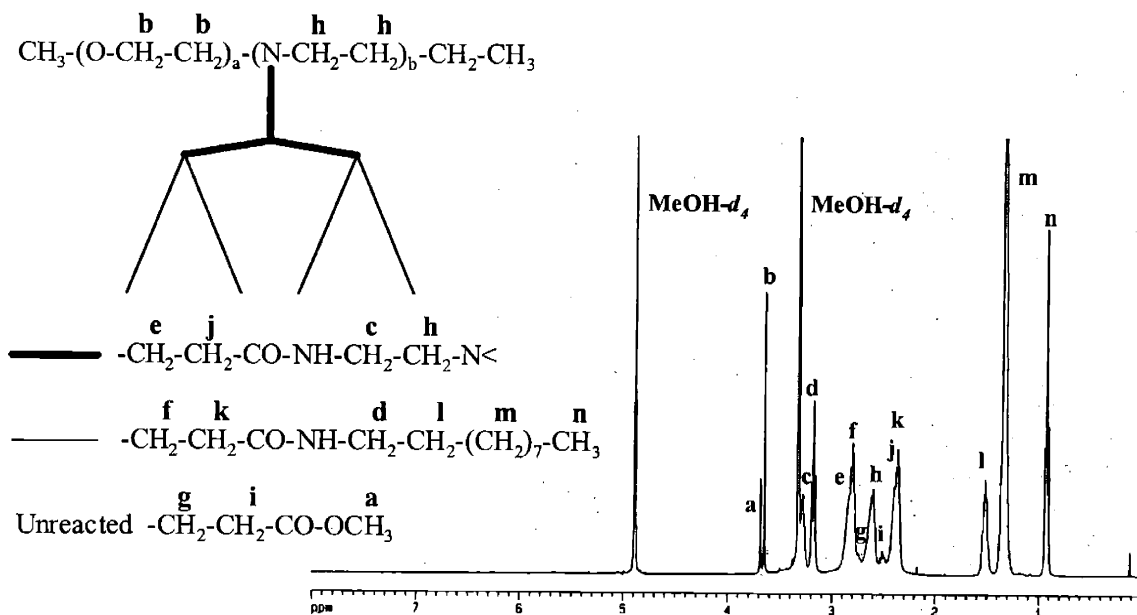


Figure 2.7. ^1H NMR of the generation 3.0-octyl terminated linear-dendritic rod diblock copolymer.

Within the same generation, the NMR spectra did not appear much different from one alkyl chain length to the next, the main difference being the ratio of the integration value obtained for the CH_2 next to the terminal CH_3 , ($-\text{CO}-\text{NH}-\text{CH}_2-\text{CH}_2-(\text{CH}_2)_{n-3}-\text{CH}_3$), to that of the other protons in the polymer. Not surprisingly, as the length of the alkyl chain increased, the relative integration value from this peak increased accordingly. For example, for the butyl terminated polymers, the ratio of the protons on the CH_2 next to the terminal CH_3 to those of the terminal CH_3 was 2:3, for the octyl terminated polymers it was 10:3, and for the dodecyl terminated polymers it was 18:3. As the length of the alkyl chain increased, the chemical environment experienced by these additional protons was very similar to that of the other protons already present in CH_2 groups which were at least three carbons from the amide group. Thus, these protons did not appear as new peaks in the NMR spectrum, instead they appeared as multiplication of the CH_2 peaks which appeared for the shorter alkyl chains.

In addition to being used to verify the chemical structure of the polymers, ^1H NMR was also used to determine the percent substitution of the n-alkyl amines on the ester terminated

polymers by comparing the integration values of peaks attributed to functionalized and non-functionalized repeat units. Specifically, the integration value from the non-functionalized methyl ester group, (-CH₂-CH₂-CO-OCH₃) which appeared around 3.69ppm, was compared to the integration values from the CH₂ adjacent to the newly formed amide group (-CO-NH-CH₂-CH₂-(CH₂)_n-CH₃), which appeared at 3.18ppm, and the terminal methyl group of the alkyl chain (-CO-NH-CH₂-CH₂-(CH₂)_{n-3}-CH₃), which appeared at 0.92ppm. The two equations that were used to determine the percent substitution are given below in Equations 2.1 and 2.2. The two values that were calculated from these equations were very consistent, almost always within one to two percent of each other.

$$\text{percent substitution} = \frac{\text{CH}_2 \text{ next to amide}}{\text{CH}_2 \text{ next to amide} + \frac{2}{3} \text{OCH}_3 \text{ of ester}} \times 100\% \quad (2.1)$$

$$\text{percent substitution} = \frac{\text{CH}_3 \text{ of alkyl group}}{\text{CH}_3 \text{ of alkyl group} + \text{OCH}_3 \text{ of ester}} \times 100\% \quad (2.2)$$

2.4.2.2 FTIR

In FTIR, infrared radiation is directed at a sample, the material absorbs the energy and then converts it into the energy of molecular stretching and bending vibrations. The wavelength of the absorbed energy depends on the types and geometries of the atoms present as well as the length of the bonds between them.⁷⁵ Most of the common functional groups give rise to characteristic absorption bands in different regions of the infrared range. Thus, by measuring the spectra of light absorbed, usually by measuring that which is transmitted, one can determine the presence or absence of absorption bands, and thus, the presence or absence of functional groups.⁷⁶ Unfortunately, it is much more difficult to acquire quantitative information about the relative numbers of functional groups present from FTIR than it is from NMR; nonetheless, FTIR provides a good qualitative measure of the types of functional groups present in a material.

FTIR was also used to verify the chemical structures of all of the linear-dendritic rod diblock copolymers synthesized by identifying the functional groups present. Tosylation of the hydroxyl group on the poly(ethylene oxide) was confirmed by the complete loss of the O-H stretching band at approximately 3450cm⁻¹ and the addition of bands at approximately 1170cm⁻¹

from the S=O sulfonate ester stretching, and at 810cm^{-1} and 750cm^{-1} from the C-H bending of the aromatic groups. Unfortunately, because the fraction of the tosylate group in the polymer was so small, the magnitude of the absorbance of these peaks in comparison to those due to the poly(ethylene oxide) block was also small such that the addition and subtraction of these peaks did not produce a large change in the spectra. Nonetheless, the spectra from the tosylate polymer compared well with that observed by others for the same polymer.^{54,61}

Polymerization of 2-ethyl-2-oxazoline with the poly(ethylene oxide) tosylate macroinitiator to form the desired diblock copolymer produced a much more dramatic effect on the FTIR spectra. The 2-ethyl-2-oxazoline block added strong peaks at 1646cm^{-1} for the C=O stretching and at 1426cm^{-1} for the C-N stretching, while the characteristic C-O-C stretching peak of the poly(ethylene oxide) block remained at approximately 1111cm^{-1} . The C-H stretching peaks also shifted to slightly larger wavenumbers, most likely due to the addition of the CH_3 group on the poly(2-ethyl-2-oxazoline) side chain. These results were in good agreement with those found for poly(2-ethyl-2-oxazoline) homopolymers⁷⁷ and other poly(ethylene oxide)-poly(acyl-oxazoline) diblock copolymers.^{54,60}

Weak acid hydrolysis of the poly(ethylene oxide)-poly(2-ethyl-2-oxazoline) diblock copolymer to the desired poly(ethylene oxide)-poly(ethylene imine) diblock copolymer was confirmed by the almost complete disappearance of the C=O stretching band and the C-N stretching band of the tertiary amine in the poly(2-ethyl-2-oxazoline) block as well as the addition of the N-H stretching band at approximately 3219cm^{-1} and the C-N stretching band at approximately 1135cm^{-1} , both due to the secondary amines on the poly(ethylene imine). In addition, the C-H stretching peaks shifted back to slight lower wavenumbers probably due to the loss of the CH_3 group on the poly(2-ethyl-2-oxazoline) side chain. Through this all, the C-O-C stretching peak of the poly(ethylene oxide) remained constant at approximately 1111cm^{-1} . Saegusa *et al.* have observed similar FTIR bands for linear poly(ethylene imine) homopolymers⁷⁴ as well as poly(ethylene oxide)-poly(ethylene imine) diblock copolymers which contained residual 2-methyl-2-oxazoline groups.⁶⁰

FTIR confirmed the formation of the generation 0.5 linear-dendritic rod diblock copolymer, whose spectra is shown in Figure 2.8. As can be seen, the N-H stretching band of the poly(ethylene imine) block completely disappeared and was replaced by a very strong C=O stretching peak, characteristic of the methyl ester groups at 1733cm^{-1} . In addition, new bands

were observed at 1196 and 1038 cm^{-1} due to stretching of the C-C(=O)-O and O-C-C bonds in the ester, respectively. The FTIRs of the higher generation methyl ester terminated half generation polymers also exhibited these characteristic peaks due to the terminal methyl ester groups on the branch ends; however, they also possessed adsorption bands from the interior branches which contained amide groups. The N-H stretching of the amide produced two bands at approximately 3300 and 3070 cm^{-1} , while the C=O stretching of the amide fell at approximately 1650 cm^{-1} , and the N-H bending absorbed at approximately 1540 cm^{-1} . It was not surprising that all of the higher generation polymers exhibited these same absorption peaks as they all possessed the same functional groups. Nonetheless, the relative intensities of these peaks did vary from generation to generation, as can be seen in Figure 2.8. While it is difficult to quantitatively determine the fractions of each of the groups present, qualitatively, one can gain some insight into the relative numbers of groups present from the relative intensities of the peaks. For these half generation polymers, the most obvious change in the peak intensity ratios that occurred was that between the C=O stretching peak of the methyl ester group and the C=O stretching peak of the amide group. At generation 1.5, the ester carbonyl peak was approximately twice as large as the amide carbonyl peak; however, at higher generations, this ratio decreased dramatically, and at generation 4.5, the amide carbonyl peak was slightly larger than that of the ester carbonyl. This result was consistent with the relative numbers of each of the functional groups present. For example, for the generation 1.5 polymer, there were two exterior methyl ester groups for every one interior amide group, while for generation 4.5, there were sixteen exterior methyl ester groups for every fifteen interior amide groups. The fact that the amide carbonyl peak was slightly larger than the ester carbonyl peak most likely occurred because each of the functional groups did not absorb the same intensity of light, which speaks to the difficulty in obtaining quantitative information from FTIR. A second set of relative peak intensities that changed were the ratios of the poly(ethylene oxide) C-O-C stretching band at approximately 1115 cm^{-1} to that of the other functional groups. In the generation 0.5 polymer, a small, yet noticeable absorption band can be observed; however, as the generation number increases, the relative intensity of this band decreases, such that by generation 3.5 it is hard to detect the presence of this band at all. From ^1H NMR, we know that the poly(ethylene oxide) block was still present, but by generation 3.5 its weight fraction in the entire polymer was so small that the absorption peaks from the dendritic block were able to dominate it.

The spectra of the amine terminated, whole generation linear-dendritic rod diblock copolymers all exhibited the same characteristic absorption bands regardless of generation, as they all possessed the same functional groups. A representative spectra, that of the generation 3.0 polymer is given at the bottom of Figure 2.8. The most characteristic feature marking the transition from the methyl ester groups to the amine groups was the complete disappearance of the C=O stretching band at approximately 1740cm^{-1} found in the ester terminated polymers. In addition, the amine spectra exhibited N-H stretching bands at approximately 3260 and 3058cm^{-1} as well as C=O stretching bands at approximately 1654cm^{-1} , and N-H bending bands at approximately 1470cm^{-1} due to the amine and amide groups. Unfortunately, for the amine terminated polymers, it was difficult to differentiate between the N-H stretching and bending peaks of the interior amide and the exterior amine groups; thus, qualitative conclusions about the relative sizes of those peaks with respect to the number of each of the groups present could not be drawn. However, qualitative insight was still gained from the relative sizes of the absorption bands of the dendritic block to that of the poly(ethylene oxide) block. As had been observed for the methyl ester terminated polymers, the C-O-C stretching absorption band of the poly(ethylene oxide) block all but disappeared at approximately generation 3.0, due to its relative small weight percent in the polymer.

The absorption bands for both the amine and the methyl ester terminated polymers were in good agreement with those found for the poly(amido amine) hybrid-linear dendritic diblock copolymers.^{23,24} The length of the dendritic block did not affect the position of the absorption bands of the linear-dendritic rod diblock copolymers. It's only effect was on the relative intensity of the poly(ethylene oxide) C-O-C stretching band at approximately 1115cm^{-1} to that of the other dendritic peaks in the spectra. Not surprisingly, as the length of the dendritic block increased, the relative intensity of the poly(ethylene oxide) block to the dendritic block decreased.

The FTIR spectra for all of the alkyl terminated polymers exhibited the same characteristic peaks for a given length of alkyl chain substitution. This observation was not surprising since all of the polymers possessed the same characteristic functional groups. These spectra can be represented by the spectra for the generation 3.0-alkyl terminated polymers shown in Figure 2.9. The modes of adsorption and the functional groups associated with them are also given in the figure. There is only one subtle difference between the spectra as the generation

number increased – the somewhat weak C-O-C stretching peak from the PEO at approximately 1115cm^{-1} decreased in intensity with increasing generation and disappeared altogether for the generation 3.0-substituted polymers. This result was consistent with that which was observed for the ester and amine terminated polymers as well as the fact that the percentage of PEO decreased dramatically with increasing generation. Surprisingly, more dramatic changes in the FTIR spectra were seen as a function of the length of the alkyl chain with which the polymer was substituted. The spectra from the generation 3.0-series as shown in figure 2.9 was representative of the changes in the spectra that were observed. For the generation 3.0-butyl substituted polymer, the absorption peaks from the C-H stretching of the methylene groups in the poly(amido amine) portion at 2960 and 2821cm^{-1} , are of approximate equal intensity as those adsorption peaks from the C-H stretching of the alkyl methylene groups at 2933 and 2869cm^{-1} . However, as the length of the alkyl chain with which the polymer was substituted increased, the C-H stretching peaks in the alkyl portion grew dramatically in intensity relative to the C-H stretching peaks in the poly(amido amine) portion as well as to the absorption peaks attributed to other groups in the poly(amido amine) portion, such as the amide C=O stretching peak at 1640cm^{-1} . For the generation 3.0-octyl substituted polymer, the alkyl C-H stretching peaks were approximately twice as large as the poly(amido amine) C-H stretching peaks, and for the generation 3.0-octadecyl substituted polymer, the alkyl C-H stretching peaks were so big that they almost engulfed the poly(amido amine) C-H stretching peaks. Fortunately, these results were consistent with an increasing percentage of alkyl CH_2 in the polymer as the length of the alkyl chain with which the polymer was substituted was increased.

Qualitatively, FTIR also offered insight into the degree of substitution of the n-alkyl amines on the ester terminated groups. The methyl ester group had a characteristic strong absorption peak at 1743cm^{-1} due to C=O stretching. For polymers in which almost 100% substitution of the alkyl groups had been achieved, this peak all but disappeared; however, in polymers in which the percent substitution was much less, this peak remained, but became much less intense than it had been for the pure methyl ester terminated half generation polymers. Thus, one could qualitatively compare these results with those from the ^1H NMR spectra for consistency.

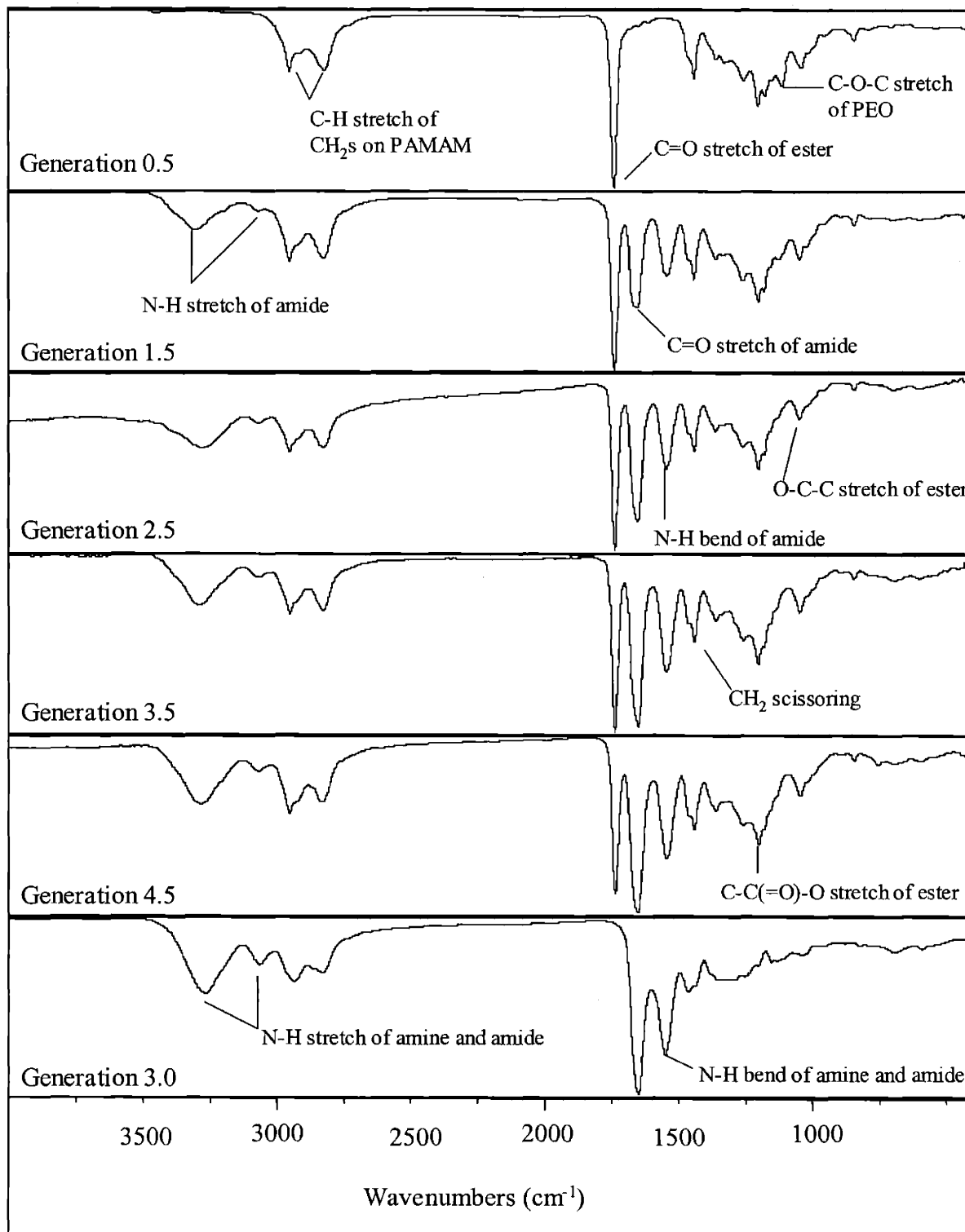


Figure 2.8. FTIR spectra of the poly(ethylene oxide)-poly(ethylene imine)-poly(amido amine) linear dendritic rod diblock copolymers.

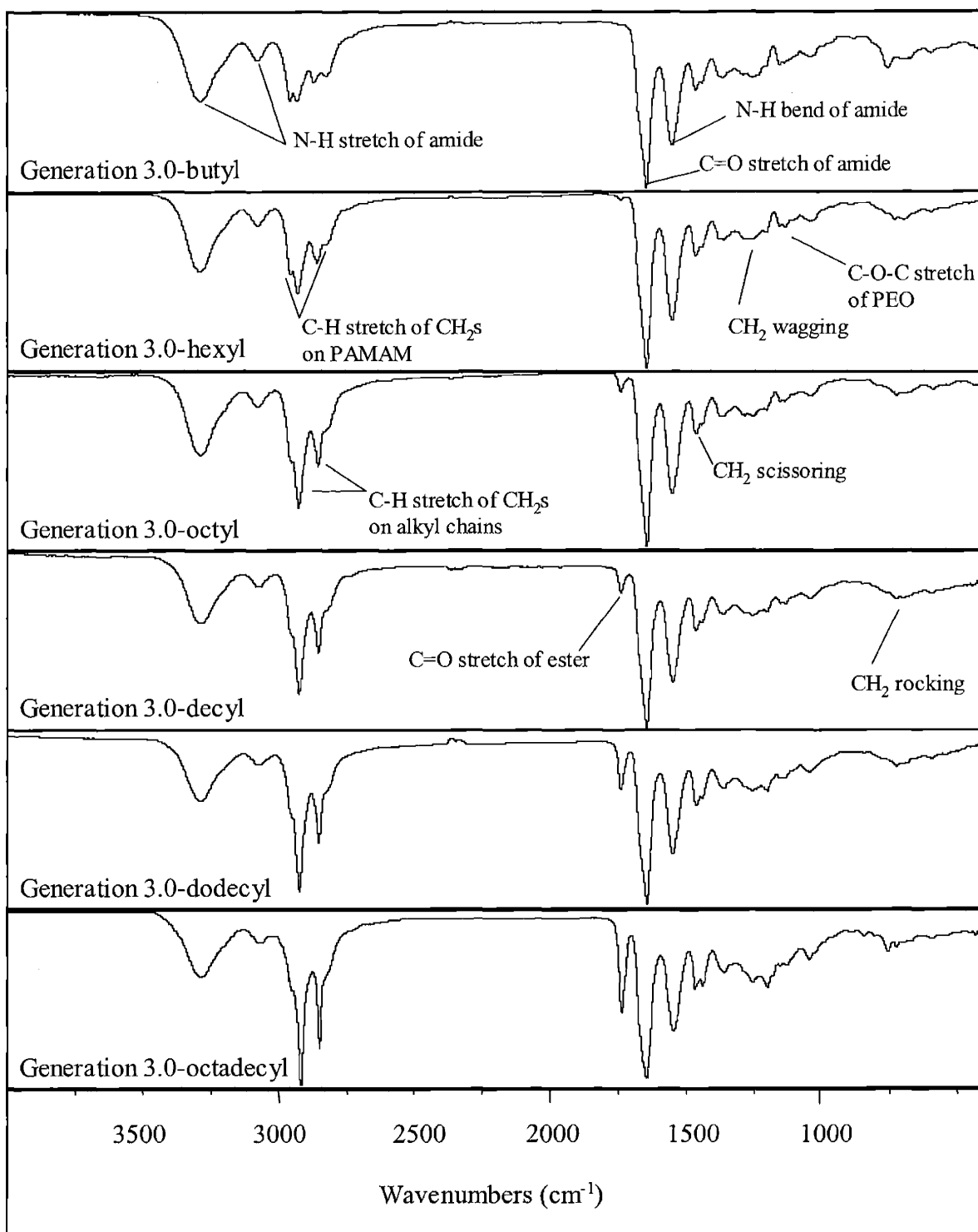


Figure 2.9. FTIR spectra of the generation 3.0-alkyl terminated poly(ethylene oxide)-poly(ethylene imine)-poly(amido amine) linear dendritic rod diblock copolymers.

2.4.2.3 MALDI-TOF and SEC-MALLS

Since spherical dendrimers and their hybrid-linear dendritic diblock copolymers are extremely monodisperse, MALDI-TOF (matrix-assisted laser desorption ionization time of flight) spectrometry has become a popular technique to characterize the molecular weight of these polymers.^{6,23,25,78} In traditional time of flight mass spectrometry, the molecular weights of small molecules are determined by first ionizing the molecules in the gas phase. Then, these ionized molecules travel, “fly”, a given distance where they are separated by their size with the lighter molecules traveling faster. Finally, these ionized molecules are collected and their m/z (mass/charge) values are determined.⁷⁹ For several years, polymeric molecules could not be examined in this manner because of difficulties in effectively ionizing them. However, in MALDI-TOF, a sample is embedded in small, highly absorbing organic compounds which induce an efficient transfer of the laser-pulse energy to the sample and a soft desorption process, causing the molecules to “fly” down the spectrometer tube.⁸⁰ Unfortunately, as the molecular weight and the polydispersity of a samples increases, MALDI-TOF analysis of the molecular weight becomes less reliable as the entire molecular weight distribution will not travel equally down the tube since the different molecular weights present will require differing amounts of energy to ionize and desorb them.⁷⁸ Usually the best results are obtained for polymers with a polydispersity of less than 1.2.⁸¹ Attempts were made to characterize our poly(ethylene oxide)-poly(2-ethyl-2-oxazoline) as well as our poly(ethylene oxide)-poly(ethylene imine) diblock copolymers by MALDI-TOF. Unfortunately, these polymers did not meet the stringent monodispersity requirements for MALDI-TOF and did not give good results; thus, none will be reported in this thesis.

Characterization of the molecular weight and the molecular weight distribution was also attempted using SEC-MALLS (size exclusion chromatography-multi angle laser light scattering.) In SEC-MALLS, a polymer sample is passed through a series of columns which separates the polymer molecules by size. The weight average molecular weight of each polymer fraction is then determined as it passes through a multi-angle laser light scattering using Debye’s equation in the limit of small concentration.⁸² The benefit of using SEC-MALLS is that it doesn’t rely on standards and can in theory, give an absolute molecular weight of the polymer. Unfortunately, reproducible results could not be obtained for these linear-dendritic rod diblock copolymers, and the molecular weight were often much smaller than expected. The polymers were examined

using the SEC-MALLS instrument in our lab with several different solvent systems as well as by the chromatography team at the Michigan Molecular Institute, which specializes in dendritic systems. Most likely, there were several factors that contributed to these observations. The most significant factor was probably the polydispersity of the polymers. The poly(ethylene oxide)-poly(ethylene imine) diblock copolymer backbone started with a polydispersity of approximately 1.2-1.4. This polydispersity was expected to rise dramatically with increasing generation as the molecular weight of the dendritic block increased with generation while that of the poly(ethylene oxide) did not. Thus, it was possible that during each injection, a slightly different molecular weight distribution was sampled resulting in values that were difficult to reproduce. Another factor may have been the dn/dc (change in refractive index/change in concentration) used in the molecular weight calculations. At the Michigan Molecular Institute, they employed an *in situ* process to determine this value for each of the polymers. However, for polymers that are composed of more than one block and which possess a wide range of molecular weights, and thus compositions of the two blocks, that value can vary with molecular weight. Thus using a value that had been calculated for the entire sample may not have been accurate.⁸² Nonetheless, this factor was probably not nearly as important as the polydispersity in the polymers. One last factor that may have affected the SEC-MALLS results was the shape of the polymers under investigation. Percec *et al.* have also reported anomalous behavior in SEC-MALLS for some of their higher molecular weight dendritic rods.¹⁴ Usually in SEC, the highest molecular weight polymers elute at the lowest elution volume and the molecular weight decreases with increasing elution volume in a linear fashion. Similarly, the radius of gyration increases with molecular weight in a linear fashion. However, Percec *et al.* found that the higher molecular weight polymers eluted at both normal and at larger than normal elution volumes resulting in two different values of the elution volume and the radius of gyration for the same molecular weight. They hypothesized that the extremely high molecular weight fraction interacted with the columns and eluted at a higher elution volume than expected based on pure size exclusion.¹⁴ Thus, at small elution volumes, the normal size distribution mechanism prevailed and the polydispersity of the eluting species was fairly small. However, at larger elution volumes, both normally eluting small molecules as well as retarded high molecular weight polymers eluted such that the polydispersity within an elution slice was greater than 100. This unusual behavior has also been reported for styrene microgels and other branched polymers;^{82,83} nonetheless, Percec *et al.* did

not necessarily believe that their polymers contained branched structures or aggregates. Since Percec's paper, Gerle *et al.* have also reported similar anomalous elution behavior for high molecular weight cylindrical brushes based on methacrylol end functionalized oligo methacrylates.⁸⁴ For the linear-dendritic rod diblock copolymers under investigation in this thesis, an upturn in the molecular weight versus elution volume graph was also observed for many of the polymers, and it was especially prevalent for the generation 4.0 diblock copolymers, which also exhibited a strong upturn radius of gyration versus elution time graph. Ideally, the molecular weight determined from SEC-MALLS should not have been affected by the phenomena described above, as it does not rely on standards and it allows one to measure the molecular weight at each elution slice. Nonetheless, the above phenomena may have affected the determination of the molecular weight by SEC-MALLS in ways not yet completely understood.

2.5 Summary and Conclusions

The synthetic scheme for a series of linear-dendritic rod diblock copolymers consisting of a poly(ethylene oxide)-poly(ethylene imine) diblock copolymer backbone and poly(amido amine) dendritic branches has been successfully developed. The linear-dendritic rod diblock copolymers were also made amphiphilic by the reaction of various n-alkyl amines with the methyl ester terminated, half-generation polymers. The chemical structures of all of the polymers were confirmed using ¹H NMR and FTIR.

The first step in the synthesis of the linear-dendritic rod diblock copolymers was the formation of the poly(ethylene oxide)-poly(ethylene imine) diblock copolymer backbone. This was accomplished by tosylation of a hydroxyl terminated poly(ethylene oxide) homopolymer to form a poly(ethylene oxide) macroinitiator using tosyl chloride. This macroinitiator was then used in the cationic ring opening polymerization of 2-ethyl-2-oxazoline to form a poly(ethylene oxide)-poly(2-ethyl-2-oxazoline) diblock copolymer. Since the rate of polymerization of the 2-ethyl-2-oxazoline block was much larger than the rate of its initiation with poly(ethylene oxide) tosylate, the polymers possessed a polydispersity between 1.2 and 1.4. The poly(2-ethyl-2-oxazoline) block of the diblock copolymer was then hydrolyzed, using a weak acid hydrolysis, to form the desired poly(ethylene oxide)-poly(ethylene imine) diblock copolymer backbone.

Formation of the methyl ester terminated half generation polymer proceeded as expected by the addition of methyl acrylate to the poly(ethylene oxide)-poly(ethylene imine) diblock copolymer backbone. The reaction was performed using a 2.7 molar excess of methyl acrylate in an approximately 5% by weight polymer solution. During the addition of the methyl acrylate, the reaction solution was chilled, it was then allowed to slowly warm to room temperature, and finally to react for another 48 hours to ensure complete addition of the methyl acrylate groups to the poly(ethylene imine) backbone. Unfortunately, after removal of all of the methanol and methyl acrylate by vacuum distillation, the polymer still exhibited the same strong odor associated with methyl acrylate. To eliminate this residual methyl acrylate, the polymer was purified by dissolution in chloroform and precipitation into hexanes to obtain the desired diblock copolymer. The synthesis of the subsequent half-generation polymers of higher generation was conducted using similar reaction conditions.

Reaction of the half generation methyl ester terminated polymers with ethylenediamine to form the whole generation, amine terminated polymers proved to be more difficult. It was found that these polymers were susceptible to intra- and intermolecular crosslinking and that the only way to avoid this crosslinking was to conduct the amidation reactions with huge excesses of ethylenediamine (2500 for generation 1.0, 5000 for generation 2.0, 7500 for generation 3.0, and 10,000 for generation 4.0); at low temperatures (approximately 5°C); and for long times (5 days for generation 1.0 increasing to 8 days for generation 4.0 polymer). It was also found that rigorous purification of both the ethylenediamine before the reaction and the amine terminated linear-dendritic rod copolymer after the reaction were necessary to prevent this crosslinking. Unless these steps were taken, the polymer formed an insoluble precipitate either initially, or shortly after the reaction was complete, making characterization impossible. In addition, the imperfections caused by not being diligent with the above two steps also affected the formation of the methyl ester terminated polymers, such that they too crosslinked upon standing. Nonetheless, once these precautions were taken, the whole generation, amine terminated polymers were synthesized. Once prepared, it was found that the best way to purify the polymers and remove any residual ethylenediamine was ultrafiltration in methanol.

Formation of the amphiphilic diblock copolymers by functionalization of the methyl ester end groups with n-alkyl amines proceeded much more smoothly. This method of functionalization was chosen so that the same chemistry and bond order that was used in the

formation of the whole generation, amine terminated polymers was maintained. The generation 0.5, 1.5, 2.5, and 3.5 polymers were functionalized with butyl, hexyl, octyl, decyl, dodecyl, and octadecyl groups, while the generation 4.5 polymer was functionalized with dodecyl and octadecyl groups. From experiment, it was found that the best reaction conditions to achieve a high degree of substitution for the butyl through the dodecyl terminated polymers consisted of the following: use of an approximately 50 molar excess of n-alkyl amine; use of an approximately 30% by weight n-alkyl amine in methanol solution; and heating of the reaction solution to approximately 45-50°C for five to eight days depending on the generation. The majority of the excess n-alkyl amine and methanol were then removed by vacuum distillation and the polymer purified by ultrafiltration in methanol. Due to the extremely high boiling point of the n-octadecyl amine, the large excesses of reagent could not be used in the formation of the octadecyl terminated polymers as it was very difficult to remove the excess reagent and to purify the crude polymers. In addition, the reaction solution needed to be heated at 65°C in order to prevent the n-octadecyl amine from precipitating from solution. Unfortunately, it was very difficult to achieve a high degree of substitution for the octadecyl terminated polymers.

Once synthesized, the chemical structures of the diblock copolymers were confirmed using ^1H NMR. In addition, ^1H NMR was also used to determine the length and the molecular weight of the dendritic block by integration of the areas under each of the peaks and comparison of the areas attribute to the dendritic block to those of the poly(ethylene oxide) block, whose length was known. The NMRs of all of the half generation, methyl ester terminated polymers all contained the desired peaks from the methyl ester terminated half-branches. In addition, the methyl ester terminated polymers of generation 1.5 and larger also contained peaks due to the interior full branches. Not surprisingly, these characteristic peaks all fell at the same peak positions regardless of generation because the dendritic chemistry remained unchanged with the addition of new branches at higher generations. Similarly, the NMRs of all of the amine terminated, whole generation polymers also exhibited peaks at the same peak positions, yet different from the ester terminated polymers. Between generations, the primary differences in the NMRs of the diblock copolymers were the ratio of the integration areas of the interior and the exterior branches. For the alkyl terminated, whole generation polymers, these same two observations were also found to be true. In addition, within the same generation, the NMR spectra did not appear much different from one alkyl chain length to the next, the main

difference being the ratio of the integration value obtained from the CH₂ next to the terminal CH₃, (-CO-NH-CH₂-CH₂-(CH₂)_{n-3}-CH₃), to that of the other protons in the polymer. Not surprisingly, as the length of the alkyl chain increased, the relative integration value from this peak increased accordingly. Finally, ¹H NMR was used to determine the percent substitution of the n-alkyl groups on the methyl ester terminated polymers by comparison of the areas of the peaks attributed to the alkyl groups to those of the unfunctionalized methyl ester groups.

FTIR was also used to gain insight into the chemical structures of the linear-dendritic rod diblock copolymers by identifying the functional groups present. All of the half-generation polymers could be easily identified by the presence of an absorption band at approximately 1740cm⁻¹ due to the carbonyl stretching of the methyl ester group. In addition, as had been seen in the NMRs, the spectra of the generation 0.5 polymer was slightly different than that of all of the other half-generation polymers whose spectra possessed the same peaks. The generation 0.5 polymer lacked the absorbance bands of the amide carbonyls at approximately 1650cm⁻¹, which were created during the formation of the full branches. Nonetheless, as the generation number increased, the ratio of the intensity of the carbonyl peak of the methyl ester group to that of the carbonyl peak of the amide group decreased as the ratio of the exterior to the interior branches decreased. All of the amine terminated, whole generation polymers also possessed the same peaks in the FTIR spectra. The addition of ethylenediamine to the methyl ester end groups was marked by the virtual disappearance of the methyl ester carbonyl peak. Unfortunately, since it was difficult to differentiate between the N-H stretching and bending peaks of the interior amide and the exterior amine groups, a correlation between the number of interior to exterior branches could not be made. Functionalization of the methyl ester end groups with n-alkyl amines resulted in the appearance of C-H stretching peaks at approximately 2930 and 2870cm⁻¹ whose relative intensity increased with increasing length of the alkyl chain. In addition, FTIR also offered qualitative insight into the degree of substitution of the n-alkyl amines on the methyl ester terminated groups. For polymers in which close to 100% substitution of the alkyl groups had been achieved, the carbonyl stretching peak of the methyl ester groups all but disappeared; however, in polymers in which the percent substitution was much less, this peak remained, but was much weaker than had been for the pure methyl ester terminated half generation polymers. Nonetheless, for all of the linear-dendritic rod diblock copolymers regardless of end group functionalization, the fraction of the poly(ethylene oxide) in the total polymer after

approximately generation 3.0 became so small that its characteristic C-O-C stretching band virtually disappeared even though the presence of the poly(ethylene oxide) block could still be detected through NMR characterization.

Neither MALDI-TOF nor SEC-MALLS proved to be reliable techniques for measuring the molecular weight and the molecular weight distributions of these linear-dendritic rod diblock copolymers. Most likely, one of the main reasons that they were not effective in making these measurements was the polydispersity in the PEO-PEI diblock copolymer backbone that multiplied with increasing generation. In addition, it was also possible that the highly branched nature and the shape of the polymers contributed to the anomalous SEC-MALLS results. Nonetheless, ¹H NMR proved to be the best method for determining the molecular weights of the polymers.

2.6 References

- (1) Karakaya, B.; Claussen, W.; Gessler, K.; Saenger, W.; Schlüter, A.-D. "Toward dendrimers with cylindrical shape in solution," *Journal of the American Chemical Society* **1997**, *119*, 3296-3301.
- (2) Newkome, G. R.; Moorefield, C. N.; Baker, G. R.; Johnson, A. L.; Behera, R. K. "Chemistry of micelles .11. Alkane cascade polymers possessing micellar topology - micellanoic acid-derivatives," *Angewandte Chemie-International Edition in English* **1991**, *30*, 1176-1178.
- (3) Jansen, J. F. G. A.; de Brabander-van den Berg, E. M. M.; Meijer, E. W. "Encapsulation of guest molecules into a dendritic box," *Science* **1994**, *266*, 1226-1229.
- (4) Sayed-Sweet, Y.; Hedstrand, D. M.; Spinder, R.; Tomalia, D. A. "Hydrophobically modified poly(amidoamine) (PAMAM) dendrimers: Their properties at the air-water interface and use as nanoscopic container molecules," *Journal of Materials Chemistry* **1997**, *7*, 1199-1205.
- (5) Schenning, A. P. H. I.; Elissen-Román, C.; Weener, J. W.; Baars, M. W. P. L.; van der Gaast, S. J.; Meijer, E. W. "Amphiphilic dendrimers as building blocks in supramolecular assemblies," *Journal of the American Chemical Society* **1998**, *120*, 8199-8208.
- (6) Sui, G.; Micic, M.; Huo, Q.; Leblanc, R. M. "Studies of a novel polymerizable amphiphilic dendrimer," *Colloids and Surfaces A-Physicochemical and Engineering Aspects* **2000**, *171*, 185-197.
- (7) Sui, G. D.; Micic, M.; Huo, Q.; Leblanc, R. M. "Synthesis and surface chemistry study of a new amphiphilic pamam dendrimer," *Langmuir* **2000**, *16*, 7847-7851.
- (8) Newkome, G. R.; Moorefield, C. N.; Vögtle, F. *Dendritic molecules. Concepts, Synthesis, Perspectives*; VCH: Weinheim, 1996.

- (9) Jahromi, S.; Coussens, B.; Meijerink, N.; Braam, A. W. M. "Side chain dendritic polymers: Synthesis and physical properties," *Journal of the American Chemical Society* **1998**, *120*, 9753-9762.
- (10) Desai, A.; Atkinson, N.; Rivera, F.; Devonport, W.; Rees, I.; Branz, S. E.; Hawker, C. J. "Hybrid dendritic-linear graft copolymers: Steric considerations in "coupling to" approach," *Journal of Polymer Science Part A-Polymer Chemistry* **2000**, *38*, 1033-1044.
- (11) Tomalia, D. A.; Kirchoff, P. M. "Rod-Shaped Dendrimer," The Dow Chemical Company: United States Patent #4,694,064, 1987.
- (12) Yin, R.; Zhu, Y.; Tomalia, D. A.; Ibuki, H. "Architectural copolymers: Rod-shaped, cylindrical dendrimers," *Journal of the American Chemical Society* **1998**, *120*, 2678-2679.
- (13) Percec, V.; Ahn, C. H.; Barboiu, B. "Self-encapsulation, acceleration and control in the radical polymerization of monodendritic monomers via self-assembly," *Journal of the American Chemical Society* **1997**, *119*, 12978-12979.
- (14) Percec, V.; Ahn, C. H.; Cho, W. D.; Jamieson, A. M.; Kim, J.; Leman, T.; Schmidt, M.; Gerle, M.; Möller, M.; Prokhorova, S. A.; Sheiko, S. S.; Cheng, S. Z. D.; Zhang, A.; Ungar, G.; Yearley, D. J. P. "Visualizable cylindrical macromolecules with controlled stiffness from backbones containing libraries of self- assembling dendritic side groups," *Journal of the American Chemical Society* **1998**, *120*, 8619-8631.
- (15) Percec, V.; Ahn, C. H.; Ungar, G.; Yearley, D. J. P.; Möller, M.; Sheiko, S. S. "Controlling polymer shape through the self-assembly of dendritic side-groups," *Nature* **1998**, *391*, 161-164.
- (16) Percec, V.; Cho, W. D.; Mosier, P. E.; Ungar, G.; Yearley, D. J. P. "Structural analysis of cylindrical and spherical supramolecular dendrimers quantifies the concept of monodendron shape control by generation number," *Journal of the American Chemical Society* **1998**, *120*, 11061-11070.
- (17) Neubert, I.; Amoulong-Kirstein, E.; Schlüter, A.-D.; Dautzenberg, H. "Polymerization of styrenes carrying dendrons of the first, second and third generation," *Macromolecular Rapid Communications* **1996**, *17*, 517-527.
- (18) Neubert, I.; Schlüter, A.-D. "Dendronized polystyrenes with hydroxy and amino groups in the periphery," *Macromolecules* **1998**, *31*, 9372-9378.
- (19) Stocker, W.; Schürmann, B. L.; Rabe, J. P.; Forster, S.; Lindner, P.; Neubert, I.; Schlüter, A.-D. "A dendritic nanocylinder: Shape control through implementation of steric strain," *Advanced Materials* **1998**, *10*, 793-797.
- (20) Gitsov, I.; Wooley, K. L.; Hawker, C. J.; Ivanova, P. T.; Fréchet, J. M. J. "Synthesis and properties of novel linear dendritic block- copolymers - reactivity of dendritic macromolecules toward linear-polymers," *Macromolecules* **1993**, *26*, 5621-5627.
- (21) Chapman, T. M.; Hillyer, G. L.; Mahan, E. J.; Shaffer, K. A. "Hydraamphiphiles - novel linear dendritic block-copolymer surfactants," *Journal of the American Chemical Society* **1994**, *116*, 11195-11196.
- (22) van Hest, J. C. M.; Baars, M. W. P. L.; Elissen-Román, C.; van Genderen, M. H. P.; Meijer, E. W. "Acid-functionalized amphiphiles derived from polystyrene-poly(propylene imine) dendrimers, with a pH-dependent aggregation," *Macromolecules* **1995**, *28*, 6689-6691.
- (23) Iyer, J.; Fleming, K.; Hammond, P. T. "Synthesis and solution properties of new linear-dendritic diblock copolymers," *Macromolecules* **1998**, *31*, 8757-8765.

- (24) Aoi, K.; Motoda, A.; Ohno, M.; Tsutsumiuchi, K.; Okada, M.; Imae, T. "Synthesis and assembly of amphiphilic tadpole-shaped block copolymers based on poly(amido amine) dendrimer," *Polymer Journal* **1999**, *31*, 1071-1078.
- (25) Chang, Y.; Kwon, Y. C.; Lee, S. C.; Kim, C. "Amphiphilic linear PEO-dendritic carbosilane block copolymers," *Macromolecules* **2000**, *33*, 4496-4500.
- (26) Tomalia, D. A.; Baker, H.; Dewald, J.; Hall, M.; Kallos, G.; Martin, S.; Roeck, J.; Ryder, J.; Smith, P. "A new class of polymers - starburst-dendritic macromolecules," *Polymer Journal* **1985**, *17*, 117-132.
- (27) de Brabander-van den Berg, E. M. M.; Meijer, E. W. "Poly(propylene imine) dendrimers-large-scale synthesis by heterogeneously catalyzed hydrogenations," *Angewandte Chemie-International Edition in English* **1993**, *32*, 1308-1311.
- (28) Hawker, C. J.; Frechet, J. M. J. "Preparation of polymers with controlled molecular architecture - a new convergent approach to dendritic macromolecules," *Journal of the American Chemical Society* **1990**, *112*, 7638-7647.
- (29) Tomalia, D. A.; Baker, H.; Dewald, J.; Hall, M.; Kallos, G.; Martin, S.; Roeck, J.; Ryder, J.; Smith, P. "Dendritic macromolecules - synthesis of starburst dendrimers," *Macromolecules* **1986**, *19*, 2466-2468.
- (30) Dvornic, P. R.; de Leuze-Jallouli, A. M.; Owen, M. J.; Perz, S. V. "Radially layered poly(amidoamine-organosilicon) dendrimers," *Macromolecules* **2000**, *33*, 5366-5378.
- (31) Dvornic, P. R.; De Leuze-Jallouli, A. M.; Perz, S. V.; Owen, M. J. "Nanostructured materials from radially layered copolymeric amidoamine-organosilicon (pamamos) dendrimers," *Molecular Crystals and Liquid Crystals* **2000**, *353*, 223-236.
- (32) Iyer, J.; Hammond, P. T. "Langmuir behavior and ultrathin films of new linear-dendritic diblock copolymers," *Langmuir* **1999**, *15*, 1299-1306.
- (33) Hawker, C. J.; Wooley, K. L.; Frechet, J. M. J. "Unimolecular micelles and globular amphiphiles - dendritic macromolecules as novel recyclable solubilization agents," *Journal of the Chemical Society-Perkin Transactions 1* **1993**, 1287-1297.
- (34) Ghosh, S.; Banthia, A. K. "Photoswitchable architectural polymer: Toward azo-based polyamidoamine side-chain dendritic polyester," *Journal of Polymer Science Part A-Polymer Chemistry* **2001**, *39*, 4182-4188.
- (35) Karakaya, B.; Claussen, W.; Schafer, A.; Lehmann, A.; Schluter, A. D. "Full coverage of a hydroxy-substituted poly(para-phenylene) with first- and second-generation dendritic wedges having isocyanate focal points," *Acta Polymerica* **1996**, *47*, 79-84.
- (36) Percec, V.; Cho, W. D.; Möller, M.; Prokhorova, S. A.; Ungar, G.; Yeardley, D. J. P. "Design and structural analysis of the first spherical monodendron self-organizable in a cubic lattice," *Journal of the American Chemical Society* **2000**, *122*, 4249-4250.
- (37) Percec, V.; Cho, W. D.; Ungar, G.; Yeardley, D. J. P. "From molecular flat tapers, discs, and cones to supramolecular cylinders and spheres using frechet-type monodendrons modified on their periphery," *Angewandte Chemie-International Edition* **2000**, *39*, 1597-1602.
- (38) Bo, Z. S.; Schluter, A. D. "Entering a new level of use for suzuki cross-coupling: Poly(para-phenylene)s with fourth-generation dendrons," *Chemistry-A European Journal* **2000**, *6*, 3235-3241.
- (39) van Hest, J. C. M.; Delnoye, D. A. P.; Baars, M. W. P. L.; Elissen-Román, C.; van Genderen, M. H. P.; Meijer, E. W. "Polystyrene-poly(propylene imine) dendrimers:

- Synthesis, characterization, and association behavior of a new class of amphiphiles," *Chemistry-A European Journal* **1996**, *2*, 1616-1626.
- (40) Gitsov, I.; Wooley, K. L.; Fréchet, J. M. J. "Novel polyether copolymers consisting of linear and dendritic blocks," *Angewandte Chemie-International Edition in English* **1992**, *31*, 1200-1202.
- (41) Gitsov, I.; Fréchet, J. M. J. "Solution and solid-state properties of hybrid linear-dendritic block-copolymers," *Macromolecules* **1993**, *26*, 6536-6546.
- (42) Gitsov, I.; Fréchet, J. M. J. "Novel nanoscopic architectures - linear-globular aba copolymers with polyether dendrimers as a-blocks and polystyrene as b-block," *Macromolecules* **1994**, *27*, 7309-7315.
- (43) Leduc, M. R.; Hawker, C. J.; Dao, J.; Fréchet, J. M. J. "Dendritic initiators for "living" radical polymerizations: A versatile approach to the synthesis of dendritic-linear block copolymers," *Journal of the American Chemical Society* **1996**, *118*, 11111-11118.
- (44) Armarego, W. L. F.; Perrin, D. D. *Purification of Laboratory Chemicals*; Fourth ed.; Butterworth-Heinemann: Oxford, 1997.
- (45) Tomalia, D. A.; Durst, H. D. "Genealogically directed synthesis: Starburst*/cascade dendrimers and hyperbranched structures," *Topics in Current Chemistry* **1994**, *165*, 193-313.
- (46) Tomalia, D. A.; Naylor, A. M.; Goddard, W. A. "Starburst dendrimers - molecular-level control of size, shape, surface-chemistry, topology, and flexibility from atoms to macroscopic matter," *Angewandte Chemie-International Edition in English* **1990**, *29*, 138-175.
- (47) Topp, A.; Bauer, B. J.; Klimash, J. W.; Spindler, R.; Tomalia, D. A.; Amis, E. J. "Probing the location of the terminal groups of dendrimers in dilute solution," *Macromolecules* **1999**, *32*, 7226-7231.
- (48) Topp, A.; Bauer, B. J.; Tomalia, D. A.; Amis, E. J. "Effect of solvent quality on the molecular dimensions of pamam dendrimers," *Macromolecules* **1999**, *32*, 7232-7237.
- (49) Iyer, J. *Self assembly in linear-dendritic diblock copolymer films*; Ph.D. Dissertation, Department of Chemical Engineering, Massachusetts Institute of Technology, 1999.
- (50) Johnson, M. A. *Self-assembly of linear-dendritic diblock copolymers*; Ph.D. Dissertation, Department of Chemical Engineering, Massachusetts Institute of Technology, 2002.
- (51) Vandermiers, C.; Damman, P.; Dosiere, M. "Static and quasielastic light scattering from solutions of poly(ethyleneoxide) in methanol," *Polymer* **1998**, *39*, 5627-5631.
- (52) Harris, J. M.; Hundley, N. H.; Shannon, T. G.; Struck, E. C. "Poly(ethylene glycols) as soluble, recoverable, phase-transfer catalysts," *Journal of Organic Chemistry* **1982**, *47*, 4789-4791.
- (53) Kobayashi, S.; Uyama, H.; Higuchi, N.; Saegusa, T. "Synthesis of a nonionic polymer surfactant from cyclic imino ethers by the terminator method," *Macromolecules* **1990**, *23*, 54-59.
- (54) Overberger, C. G.; Peng, L. "Synthesis of poly(ethylene glycol methyl ether)-b-poly(ethylenimine) and its derivatives containing thymine and amino-acids as pendants," *Journal of Polymer Science Part A-Polymer Chemistry* **1986**, *24*, 2797-2813.
- (55) Tomalia, D. A. In *Handbook of Polymer Synthesis. Part A.*; Kricheldorf, H. R., Ed.; Marcel Dekker: New York, New York, 1992, p 743-805.
- (56) Maechling-Strasser, C.; De Jardin, P.; Galin, J. C.; Schmitt, A.; Housseferrari, V.; Sebille, B.; Mulvihill, J. N.; Cazenave, J. P. "Synthesis and adsorption of a poly(n-

- acetyleneimine)- polyethyleneoxide-poly (n-acetyleneimine) triblock-copolymer at a silica solution interface - influence of its preadsorption on platelet-adhesion and fibrinogen adsorption," *Journal of Biomedical Materials Research* **1989**, *23*, 1395-1410.
- (57) Harris, J. M.; Struck, E. C.; Case, M. G.; Paley, M. S.; Vanalstine, J. M.; Brooks, D. E. "Synthesis and characterization of poly(ethylene glycol) derivatives," *Journal of Polymer Science Part A-Polymer Chemistry* **1984**, *22*, 341-352.
- (58) Dust, J. M.; Fang, Z. H.; Harris, J. M. "Proton NMR characterization of poly(ethylene glycols) and derivatives," *Macromolecules* **1990**, *23*, 3742-3746.
- (59) Harris, J. M. "Laboratory synthesis of polyethylene glycol derivatives," *Journal of Macromolecular Science-Review. Macromolecular Chemistry and Physics* **1985**, *C25*, 325-373.
- (60) Miyamoto, M.; Sano, Y.; Saegusa, T.; Kobayashi, S. "Synthesis of poly[(n-acetyleneimine)-b-(ethylene oxide)] and its anti-electrostatic property," *European Polymer Journal* **1983**, *19*, 955-961.
- (61) Simionescu, C. I.; Rabia, I. "Triblock co-polymers of 2-substituted-2-oxazoline and poly(ethylene oxide)," *Polymer Bulletin* **1983**, *10*, 311-314.
- (62) Litt, M. H.; Swamikannu, A. X. In *Ring opening polymerization: Kinetics, Mechanisms, and Synthesis*; McGrath, J., Ed.; American Chemical Society: Washington, D.C., 1985; Vol. 286, p 231-243.
- (63) Waters Corporation, Ultrafiltration Instructions, Medford, Massachusetts, 1999.
- (64) Schmitzer, A.; Perez, E.; Rico-Lattes, I.; Lattes, A.; Rosca, S. "First example of supramolecular assemblies in water of new amphiphilic glucose-persubstituted poly(amidoamine) dendrimers," *Langmuir* **1999**, *15*, 4397-4403.
- (65) Wang, J. F.; Jia, X. R.; Zhong, H.; Wu, H. Z.; Li, Y. Y.; Xu, X. J.; Li, M. Q.; Wei, Y. "Cinnamoyl shell-modified poly(amidoamine) dendrimers," *Journal of Polymer Science Part a-Polymer Chemistry* **2000**, *38*, 4147-4153.
- (66) Baker, W. S.; Lemon, B. I.; Crooks, R. M. "Electrochemical and spectroscopic characterization of viologen- functionalized poly(amidoamine) dendrimers," *Journal of Physical Chemistry B* **2001**, *105*, 8885-8894.
- (67) *CRC Handbook of Chemistry and Physics*; Seventieth ed.; Weast, R. C.; Lide, D. R.; Astle, M. J.; Beyer, W. H., Eds.; CRC Press, Inc.: Boca Raton, Florida, 1990.
- (68) Imae, T.; Ito, M.; Aoi, K.; Tsutsumiuchi, K.; Noda, H.; Okada, M. "Formation of organized adsorption layers by amphiphilic dendrimers," *Colloids and Surfaces A-Physicochemical and Engineering Aspects* **2000**, *175*, 225-234.
- (69) Streitwieser, A.; Heathcock, C. H.; Kosower, E. M. In *Introduction to Organic Chemistry*; 4th ed.; Macmillan Publishing Company: New York, New York, 1992, p 322-329.
- (70) Silverstein, R. M.; Webster, F. X. In *Spectrometric Identification of Organic Compounds*; 6th ed.; John Wiley & Sons: New York, New York, 1998, p 144-179.
- (71) Devos, R. J.; Goethals, E. J. "Convenient synthesis of alpha-tosyl-omega-tosyloxypoly(oxyethylene)," *Makromolekulare Chemie-Rapid Communications* **1985**, *6*, 53-56.
- (72) Liu, Q.; Konas, M.; Riffle, J. S. "Investigations of 2-ethyl-2-oxazoline polymerizations in chlorobenzene," *Macromolecules* **1993**, *26*, 5572-5576.

- (73) Liu, Q.; Wilson, G. R.; Davis, R. M.; Riffle, J. S. "Preparation and properties of poly(dimethylsiloxane-2-ethyl-2-oxazoline) diblock copolymers," *Polymer* **1993**, *34*, 3030-3036.
- (74) Saegusa, T.; Ikeda, H.; Fujii, H. "Crystalline polyethyleneimine," *Macromolecules* **1972**, *5*, 108.
- (75) Silverstein, R. M.; Webster, F. X. In *Spectrometric Identification of Organic Compounds*; 6th ed.; John Wiley & Sons: New York, New York, 1998, p 71-72.
- (76) Streitwieser, A.; Heathcock, C. H.; Kosower, E. M. In *Introduction to Organic Chemistry*; 4th ed.; Macmillan Publishing Company: New York, New York, 1992, p 457-465.
- (77) Rivas, B. L.; Ananias, S. I. "Synthesis and characterization of poly(n-propionyl)iminoethylene," *Polymer Bulletin* **1992**, *28*, 3-8.
- (78) Yu, D.; Vladimirov, N.; Frechet, J. M. J. "MALDI-TOF in the characterizations of dendritic-linear block copolymers and stars," *Macromolecules* **1999**, *32*, 5186-5192.
- (79) Silverstein, R. M.; Webster, F. X. In *Spectrometric Identification of Organic Compounds*; 6th ed.; John Wiley & Sons: New York, New York, 1998, p 2-6.
- (80) Bahr, U.; Deppe, A.; Karas, M.; Hillenkamp, F.; Giessmann, U. "Mass-spectrometry of synthetic-polymers by UV matrix-assisted laser desorption ionization," *Analytical Chemistry* **1992**, *64*, 2866-2869.
- (81) McEwen, C. N.; Jackson, C.; Larsen, B. S. "Instrumental effects in the analysis of polymers of wide polydispersity by MALDI mass spectrometry," *International Journal of Mass Spectrometry and Ion Processes* **1997**, *160*, 387-394.
- (82) Wyatt, P. "Light scattering and the absolute characterization of macromolecules," *Analytical Chimie Acta* **1993**, *272*, 1-40.
- (83) Johann, C.; Kilz, P. "Copolymer characterization using conventional size exclusion and molar mass sensitive detection," *Journal of Applied Polymer Science: Applied Polymer Symposium* **1991**, *48*, 111-120.
- (84) Gerle, M.; Fischer, K.; Roos, S.; Muller, A. H. E.; Schmidt, M.; Sheiko, S. S.; Prokhorova, S.; Moller, M. "Main chain conformation and anomalous elution behavior of cylindrical brushes as revealed by GPC/MALLS, light scattering, and SFM," *Macromolecules* **1999**, *32*, 2629-2637.

Chapter 3

Solution Behavior of the Linear-Dendritic Rod Diblock Copolymers

3.1 Introduction

Since dendrimers were first introduced in the mid-1980's, the size, shape, and properties of these polymers have led to their comparison with traditional micelles.¹ Traditional micelles are formed by the aggregation of small amphiphilic molecules into complex structures such as spheres, rods, and bilayer sheets in solution.² These micelles organize such that the lyophobic (solvent hating) portions of the small molecules gather together in the center of the micelle and the lyophilic (solvent loving) portions of the small molecule assemble at the exterior of the micelle, exposed to the solvent. This arrangement leads to a minimization of the unfavorable interactions between the molecule and the solvent, and thus the free energy in the system.³ Typically, micelles range in size from just a few to several tens of nanometers, and they have often been used to solubilize molecules, such as hydrocarbons, in a solvent that has the opposite character, such as water.⁴ Traditional spherical dendrimers have often been called unimolecular micelles since they are composed of many small molecule units that are covalently bonded to a central core, they can be designed to have a lyophobic interior and a lyophilic exterior, they have sizes on the order of a few nanometers, and they have been used to sequester small molecules in their interior regions as guest/host systems.⁵ Dendrimers have the advantage over traditional micelles in that they are stable upon dilution, whereas traditional micelles fall apart once their concentration falls below their critical micelle concentration.⁶ The first studies of dendrimers in solution focused on the determination of their size, density profiles, and ability to encapsulate and release small molecules from their interior regions. However, as researchers began to change the dendrimer architecture by incorporating linear polymers into dendritic systems, they also began to look at the ability of these polymers to form more complex, multi-polymer micellar assemblies in solution. While the solution behavior of dendritic rods has not yet been extensively studied, the behavior of hybrid-linear dendritic diblock copolymers has been more closely examined as these polymers are often designed to look like macromolecular

amphiphilic, with a well-defined dendritic head that possesses either a hydrophobic or hydrophilic character, and a linear polymer tail that possesses the opposite character.^{7 8-10 11-17} Researchers were very interested in whether these hybrid linear-dendritic diblock copolymers would continue to exist simply as unimolecular micelles or whether they would assemble into larger, more complex micellar structures as do small molecule amphiphiles. It was found that either state could be achieved depending on the interactions between the polymer and the solvent.^{8-13,16,18}

Since the architecture of the poly(ethylene oxide)-poly(ethylene imine)-poly(amido amine) linear-dendritic rod diblock copolymers that we have synthesized is unique, the solution behavior of these diblock copolymers was studied in methanol in order to first determine the sizes of the polymers in dilute solution, and second, to determine whether or not the polymers formed unimolecular or multimolecular micelles under these conditions. Methanol was chosen as the solvent since it is a fairly good solvent for both the amine and the ester terminated polymers and thus might be expected to decrease the chances of polymer aggregation, simplifying the determination of the sizes of the polymers. The behavior of these diblock copolymers was examined using intrinsic viscosity and light scattering, both of which have been used to gain insight into the sizes and types of structures that polymers form in solution. Thus, an investigation into the solution behavior of the linear-dendritic rod diblock copolymers is the focus of this chapter. In the remainder of this chapter, Section 3.2 will present background information on the solution behavior of other dendritic and diblock copolymer systems, Section 3.3 will review intrinsic viscosity and light scattering theory, and Section 3.4 will describe the materials, instrumentation, and methods used for collecting the data. Section 3.5 will present, discuss, and compare the light scattering and intrinsic viscosity results. Finally, a chapter summary and concluding remarks are presented in Section 3.6 and the references in Section 3.7.

3.2 Background

3.2.1 Spherical Dendritic Homopolymers

For the spherical poly(amido amine) (PAMAM) dendrimers, one of the first solution properties that was examined was the intrinsic viscosity.¹⁹ The intrinsic viscosity is roughly a measure of the ratio of the size of a particle to its molecular weight, and it is commonly used to

determine the sizes of polymeric as well as micellar systems in solution. Since the PAMAM dendrimers under investigation were spherical, Tomalia *et al.* applied Einstein's relationships between the intrinsic viscosity of a sphere and its volume to determine the radius of the dendrimers at various generations in two different solvent systems, water and methanol. The sizes of the dendrimers that they calculated ranged from approximately 5.7 Å for the first generation polymers (ammonia core) which possessed three branches, up to 24.6 Å for the fifth generation polymers (ammonia core) which possessed 48 branches. In addition, they found that the amine terminated polymers exhibited a higher intrinsic viscosity than the ester terminated polymers that possessed the same degree of branching. They attributed this difference in the intrinsic viscosity to dendrimer aggregation caused by intermolecular hydrogen bonding of the amine end groups which was absent in the ester terminated polymers. For the amine terminated polymers up to generation 5.0, they calculated a Mark-Houwink equation in methanol of $[\eta] = 1.07 \times 10^{-2} M^{0.190}$, while for the ester terminated polymers, they found the equation to be $[\eta] = 5.25 \times 10^{-3} M^{0.200}$. In later experiments in which they examined the intrinsic viscosity of the polymers beyond generation 5.0, they found a maximum in the intrinsic viscosity which fell between generation 4.0 and 5.0, and which subsequently decreased with increasing generation.¹ These results were consistent with the definition of intrinsic viscosity and the way that the volume and molecular weight of dendrimers scale. For spherical dendritic systems, each generation contributes linearly to the radius. Thus, the volume of the dendrimer scales as g^3 , where g is the generation number. However, the molecular weight scales as B^{g-1} , where B is the branch multiplicity. Thus, a maximum in the intrinsic viscosity is reached at generation $3/\ln(B)$, or it falls between generations 4.0 and 5.0.^{20 6} In addition, Tomalia *et al.* also found that the density and refractive index of dendrimers were minimized between generations 4 and 5 due to the exponential accumulation of surface groups as a function of generation. They concluded that these results were consistent with the polymer behaving as an Einstein spheroid after generation 4.0. In order to determine the location of the amine terminal groups in methanol solution, Topp *et al.* conducted small angle neutron scattering (SANS) experiments on deuterated versions of the generation 7.0 polymer.²¹ They found that the branch ends were located very near the periphery for this high generation dendrimer in methanol, which is a good solvent for the dendrimer. They also found that the interior region appeared to have a uniform density and not a density gradient as had been predicted by others. Topp *et al.* have also used SANS to determine

the effect of solvent quality on the radius of gyration of generation 5.0 and 8.0 dendrimers.²² The radius of gyration was found to decrease as the number of methylene groups in various alkyl alcohol solvents increased. However, the radius of gyration was not found to be influenced by the addition of acetone (a non-solvent for the polymer) to methanol over the acetone/methanol composition range in which the polymer was soluble. Finally, temperature did not appear to affect the radius of gyration of the polymers in methanol over the range -10°C to 50°C . One very interesting phenomena that Topp *et al.* observed in both sets of SANS experiments was that the radius of gyration of the dendrimers increased with decreasing concentration of the solutions. They attributed this phenomena to the scattering structure factor and they did not believe that this represented real changes in the dimensions of the dendrimer in solution.

By changing the chemistry of the functional groups on the surface of the dendrimer, the solubility of the dendrimer as well as its ability to form unimolecular or multimolecular aggregates in solution can be tuned.²³ For example, Dvornic *et al.* found that hydrophilic PAMAM dendrimers could be functionalized with hydrophobic organosilane end groups. As the number of carbosilane end groups increased, the solubility of the polymer slowly shifted from water soluble to water insoluble.²⁴ Similarly, Sayed-Sweet *et al.* functionalized the end groups of hydrophilic PAMAM dendrimers with various hydrophobic epoxy-alkanes in order to create inverse unimolecular micelles in organic solvents.²⁵ In order to demonstrate that they had in fact prepared inverse unimolecular micelles, they dissolved these alkyl terminated dendrimers in organic solvents and found that they were able to extract copper sulfate from aqueous solutions into the organic phase, as indicated by the formation of a blue color in the organic phase. The copper ions were not able to transfer into the organic phase without the presence of the alkyl terminated dendrimers. In another example of dendrimers being able to solubilize and stabilize small molecules in their interior regions, Schmitzer *et al.* were able to solubilize pyrene molecules in the interior regions of glucose persubstituted generation 1.0, 2.0, and 3.0 PAMAM dendrimers in aqueous solutions.²⁶ These “filled” polymers also were able to assemble into larger aggregates due to hydrogen bonding of the glucose end groups. In a slightly different system, Sui *et al.* functionalized the end groups of PAMAM dendrimers with hydrophobic 10,12-pentacosadynoic groups, which contained polymerizable diacetylene bonds.²⁷ In chloroform, these functionalized polymers assembled into fiber-like structures which could be polymerized by UV radiation. Due to the geometry of the polymer, the triple bonds were not in close enough

proximity to polymerize with other groups on the same dendrimer, but rather, they were forced to polymerize with the groups on neighboring dendrimers, locking the assembled structure into place. Conversely, Wang *et al.* were able to design a system in which PAMAM dendrimers which had been functionalized with polymerizable cinnamoyl groups did not aggregate but rather remained as individual molecules in solution.²⁸ Intrinsic viscosity as well as GPC measurement confirmed that upon polymerization, these molecules formed individual polymers with a hard outer shell.

Intrinsic viscosity has also been used to examine the solution behavior of poly(benzyl ether) dendrimers. In THF, these dendrimers also exhibited a maximum in the intrinsic viscosity as a function of generation that was reached at generation three for the monodendrons and generation five for the tridendrons.²⁹ In addition, the refractive index increment of these dendrimers passed through a minimum, as had been observed for the PAMAM dendrimers. Finally, the hydrodynamic radius of these polymers was found to increase linearly with generation, consistent with the above observations. The effect of solvent quality on the intrinsic viscosity and size of generation three, four, and five poly(benzyl ether) dendrimers was also examined by Jeong *et al.*²⁰ In agreement with the results of other dendritic systems, the intrinsic viscosity, and thus the viscometric radii decreased with decreasing solvent quality. There was a difference of approximately a factor of two in the sizes of the dendrimers in good solvents compared with those in poor solvents, which was much larger change than had been observed for other dendritic systems. In addition, they found that the maximum in intrinsic viscosity as a function of generation observed for dendrimers in good solvents, disappeared for the dendrimers in poor solvents. In poor solvents, the intrinsic viscosity was almost constant, independent of generation, indicating that the dendrimer took on a very collapsed structure in these solvents. Finally, in some very interesting work, Matos *et al.* looked at the effect of core size and structure on the hydrodynamic properties of a series of dendrimers that consisted of a porphyrin core and poly(benzyl ether) dendrons.³⁰ They found that as the size of the core increased, the maximum in the intrinsic viscosity shifted to larger molecular weights and eventually disappeared. They attributed this shift to the increased flexibility that the larger cores imparted to the dendritic branches, resulting in the branches being able to adopt a larger number of conformations in solution and making them less likely to behave as hard spheres. Poly(benzyl ether) dendrimers have also been able to act as unimolecular micelles and sequester small hydrophobic molecules

in their interior regions. Fréchet *et al.* found that even in very dilute solution, poly(benzyl ether) dendrimers with surface acid groups were able to solubilize pyrene without exhibiting a cmc.⁶

The solution behavior of poly(propylene imine) dendrimers has also been examined. As had been seen for the PAMAM dendrimers, de Brabander-van den Berg *et al.* observed that the poly(propylene imine) dendrimers with cyano end groups that were studied in methanol exhibited a maximum in the intrinsic viscosity at approximately generation four.³¹ From these experiments, they concluded that the polymer took on a spherical shape with a sterically hindered shell at the fifth generation. In later experiments in which the viscosity of poly(propylene imine) dendrimers was examined over a larger concentration range, Rietveld *et al.* found that the polymers showed soft-sphere behavior, as indicated by the value of the Huggins coefficient. Thus, the dendrimers did not interpenetrate, rather they deformed (collapsed) with increasing generation and concentration.³² Rietveld *et al.* have also used low angle laser light scattering³³ and pulsed field gradient spin echo NMR³⁴ to examine the solution behavior of poly(propylene imine) dendrimers in solution. The NMR experiments gave information about the diffusion coefficient, and thus the hydrodynamic radii of the dendrimers in solution, while the static light scattering allowed them to calculate the radii of gyration of the dendrimers. They found that the hydrodynamic radii ranged from 0.65nm for the generation 1.0 polymer to 1.98nm for the generation 5.0 polymer, while the radii of gyration ranged from 0.5nm to 1.59nm. Since the hydrodynamic and the viscometric radii were found to be approximately equal, while the radii of gyration followed the formula $R_g^2 = (3/5)R_\eta^2$ they concluded that the methanol was being solvated in the interior of the dendrimers, and that the dendrimers were behaving as non-draining hard spheres. Topp *et al.* used SANS to study the behavior of generation 4.0 and 5.0 poly(propylene imine) dendrimers in methanol as a function of concentration.³⁵ These results also confirmed that in the dilute solution regime, the dendrimers behaved as very open, soft spheres; however, at higher concentrations, the dendrimers were found to collapse into noninterpenetrating hard spheres. Bu *et al.* found that the solvent had an effect on the intrinsic viscosity, and thus the size of the dendrimers. In experiments in which the intrinsic viscosity of third, fourth, and fifth generation cyano terminated poly(propylene imine) dendrimers were examined in THF, no maximum in the intrinsic viscosity was observed, only a linear relationship with a very shallow slope. This behavior was very different from what had been previously observed about their behavior in methanol and water,³⁶ confirming the effect

that solvent has on the solution behavior of dendrimers. In addition to studying the intrinsic viscosity of poly(propylene imine) dendrimers, several groups have also looked at the ability of these polymers to encapsulate and release small molecules on demand. In some very interesting work, Meijer *et al.* were able to show that poly(propylene imine) dendritic unimolecular micelles functionalized with amino acid surface groups could store and release two different molecules based on size - Bengal Rose and p-nitro benzoic acid - in a controlled manner by selective hydrolysis of the amino acid groups.^{37,38} Since that time, Meijer *et al.* have functionalized the end groups of poly(propylene imine) dendrimers with other hydrophobic moieties such as oligo(*p*-phenylene vinylenes), and have shown that they can also extract anionic dye molecules into hydrophobic solvents.³⁷⁻³⁹ Conversely, Pan *et al.* have functionalized the end groups with both hydrophilic and hydrophobic moieties and have been able to solubilize lipophilic molecules in aqueous solutions.⁴⁰ In order to understand the way that these functionalized polymers assemble in solution, Schenning *et al.* have examined the aggregation behavior of these polymers in aqueous solutions.⁴¹ Surprisingly, they find that the polymers form bilayer structures in solution where the poly(propylene imine) flattens and the hydrophobic groups align “back to back” in order to shield themselves from water. This behavior was similar to that observed for the same polymers at the air/water interface. Finally, Grohn *et al.* have shown that the assembly behavior of hydrophilic poly(propylene imine) dendrimers which have been modified with stearate groups is strongly influenced by the nature of molecules that have been encapsulated within it.⁴² In toluene, these polymers do not aggregate and they take on spherical structure with a collapsed core; however, upon the addition of metal salt hydrides, the polymers aggregate forming cylindrical multi-dendrimer structures with a swollen, metal-salt filled core. Upon reduction of the metal salt, the polymers reform their original spherical, unaggregated structures.

The results of a couple of other spherical dendritic systems are worth mentioning. Merino *et al.* examined the solution behavior of a series of phosphorous based dendrimers, linear polymers, and hyperbranched polymers all with the same chemical composition.⁴³ They found that the dendritic polymers showed a maximum in the intrinsic viscosity as a function of generation which fell between generations three and four, while the linear polymers exhibited classic behavior in which the intrinsic viscosity increased linearly with molecular weight. However, the intrinsic viscosity of hyperbranched polymers did not show either behavior, but rather increased only very moderately with molecular mass. They concluded that the

hyperbranched polymers were densely packed macromolecules whose density remained approximately constant, independent of molecular weight. In addition, they found that both branched architectures were much more soluble than the linear polymers at the same temperature and concentration ranges and that their intrinsic viscosity was also much lower due to their highly packed nature. In some very different work, Aharoni *et al.* examined the intrinsic viscosity of poly(L-lysine) Denkewalter dendrimers in DMF.⁴⁴ They observed a constant value for the intrinsic viscosity of the dendrimers over several generations. Thus, they concluded that the densities of all of the polymers were approximately constant and that the volume and mass increased equally with generation. Nonetheless, it is important to remember that these dendrimers possessed an asymmetrical branching and therefore did not pack the same way that symmetrical dendrimers do. One final spherical dendritic system that is very interesting has been prepared by Newkome *et al.*^{45,46} This system is composed of an all hydrocarbon interior with ammonium carboxylate branch ends and has been called “Micellanoate” because it most closely resembles the chemistry of traditional micelles formed from classic small molecule surfactants. These polymers have been shown to behave as true unimolecular micelles as indicated by their ability to solubilize guest molecules in their interior regions as well as an absence of intermolecular aggregation in aqueous solutions.

Several groups have worked on modeling the behavior of dendrimers in solution.⁴⁷ The first to do so were de Gennes and Hervet who employed a self-consistent field model to look at the behavior of dendrimers with a trifunctional branching and long flexible spacers between junctions in an athermal solvent.⁴⁸ They predicted that the density of the dendrimer would minimize in the center and would increase linearly to the outer surface. Later, Lescanec and Muthukumar used a kinetic growth model for predicting the density profile and intrinsic viscosity of dendrimers. Unlike de Gennes, they found that the density of the dendrimer should be highest at the center and then decrease linearly to the edges of the molecule.⁴⁹ Lescanec’s model also predicted a maximum in the intrinsic viscosity as a function of generation, which has been found experimentally. Mansfield and Klushin have used this kinetic growth model to calculate the hydrodynamic radii of a poly(amido amine) dendritic system and found that the model calculations agreed well with experimental data.⁵⁰ Murat and Grest have used molecular dynamics simulations to study the properties of dendritic systems.⁵¹ They too found that the density of the dendrimer was highest at the core and decayed to the surface of the molecule. In

addition, they looked at the effects of solvent quality on the size of the dendrimer and found that the dendrimer took on a more compact structure as the quality of the solvent decreased. Similarly, Ganazzoli *et al.* have used a self-consistent free energy minimization model to study the expansion of dendrimers in good solvents.⁵² They found that the expansion of dendrimers in good solvents occurred primarily because of stretching of the core region. These observations were consistent with experimental results for several spherical dendritic systems. Finally, based on the work of Mansfield and Klushin, Aerts has developed a model to predict the intrinsic viscosity of dendrimers and hyperbranched polymers which have a varying number of linear spacers in the branches. Even incorporating a large fraction of linear spacers, they still predicted a maximum in the intrinsic viscosity as a function of generation.⁵³ Nonetheless, while the de Gennes model predicted that the ends of the branches would reside on the surface of the dendrimer, almost all of the other models have found that the branch ends should be distributed throughout the molecule.⁴⁷

3.2.2 Dendritic Rods and Hyperbranched Polymers

As researchers have been successfully synthesizing dendritic rod homopolymers, they have also been examining the behavior of these polymers in solution. The first to do so were Schlüter *et al.* who looked at the behavior of polystyrene jacketed with first, second, and third generation poly(benzyl ether) dendrons that were formed by polymerization of a dendritic macromonomer. Using a combination of static and dynamic light scattering, they determined the radius of gyration as well as the hydrodynamic radius of the first and second generation polymers.⁵⁴ Comparing these radii, they found that these polymers were not yet behaving as dendritic rods, but rather as Gaussian chains. However, when they examined the third generation polymers using small angle neutron scattering, they found that the polymers had gained enough steric hinderence from the bulky dendritic groups to elongate into rods.⁵⁵ They have also looked at the solution behavior of second generation polymers with amine groups at the periphery. These polymers were found to behave as polyelectrolytes as indicated by an increase in the reduced viscosity with decreasing concentration (polyelectrolyte effect).⁵⁶ Percec *et al.* have also examined the solution behavior of polystyrene as well as poly(methacrylate) which were jacketed with poly(benzyl ether) dendrons, although their dendrons possessed dodecyl groups on the surface.⁵⁷ They too used static and dynamic light scattering to determine the radius of

gyration as well as the hydrodynamic radii of the polymers. The radii that they measured for the “jacketed polymers” were much larger than those measured for unfunctionalized polystyrene or poly(methyl methacrylate); therefore, they concluded that the polymer was taking on an extended, rod-like configuration. From these measurements, they also fit the data to a worm-like chain model using the Wintermantle method, and determined the Kuhn statistical segment length, which varied from 20 to 103nm depending on the composition of the dendritic side chains. In another dendritic rod system based on poly(benzyl ether) dendrimers, Jahromi *et al.* examined the behavior of side chain poly(benzyl ether) dendritic polymers with a polyurethane backbone using a size exclusion chromatograph which had been equipped with a differential viscometer.⁵⁸ They prepared a variety of polymers with three different dendritic generations as well as well as with four different isocyanate groups. The intrinsic viscosity behavior of these polymers was plotted as a function of molecular weight and generation, but independent of isocyanate group. From this graph, they were able to determine the values of the Mark-Houwink parameters as a function of molecular weight and generation. For the generation two polymers, they found only one region of behavior whose Mark-Houwink parameter (“a” ~ 0.6) corresponded to the polymers behaving as spheres in solution. Thus, these polymers were not rigid enough to form rods. However, for the generation three and four polymers, two regions of behavior were observed, one for the low molecular weight polymers and the other for higher molecular weight polymers. Below approximately 50,000 g/mol (approximately 30 repeats for the third generation polymers and 15 for the fourth generation polymers), the polymers appeared to be behaving as spheres with an “a” value of less than 0.3. Conversely, above approximately 50,000g/mol the polymers appeared to be behaving as rods with an “a” value greater than one. Thus, they concluded that a minimum polymer length was needed to induce a rod-like structure. Unfortunately, they were not able to directly compare the absolute values of the intrinsic viscosity of the polymers as a function of generation since there was a lot of variance in the molecular weight with generation and with the type of isocyanate used. (In general, more flexible urethane spacers and lower generation dendritic groups gave higher molecular weight polymers.)

The intrinsic viscosity of hyperbranched polymers with a poly(amido amine) (PAMAM) chemistry has also been examined. These polymers were formed by the one-pot synthesis of aminoacrylate hydrochloride resulting in regularly hyperbranched polymers. When plotted

versus molecular weight, the intrinsic viscosity of these polymers also displayed a maximum as had been seen for purely spherical polymers; however, the maximum was found to appear at a lower molecular weight than had been observed for spherical polymers.⁵⁹ Thus, these polymers were able to display this unique property of dendrimers without requiring the laborious synthesis required of traditional dendrimers. In addition, in methanol, these polymers exhibited classic polyelectrolyte behavior with respect to solution viscosity which, was suppressed by the addition of 1% LiCl to the methanol solution.⁶⁰

3.2.3 Hybrid-Linear Dendritic Diblock Copolymers

The solution behavior of hybrid-linear dendritic diblock copolymers has also been examined. The first systems examined by Gitsov *et al.* consisted of poly(ethylene oxide)-poly(benzyl ether) linear-dendritic diblock as well as dendritic-linear-dendritic triblock copolymers.^{11,61} Using SEC and intrinsic viscosity measurements, they found that in dilute aqueous solution, the radius of gyration of the diblock copolymer was smaller than that of pure poly(ethylene oxide) homopolymer, indicating the formation of unimolecular micelles that consisted of a dendritic core and poly(ethylene oxide) corona. In more concentrated solution, these diblock copolymers formed multimolecular micelles composed of seven to eight polymer molecules. Similarly, the triblock copolymers formed unimolecular micelles in dilute solution, but they form multi-molecular micelles above a critical micelle concentration, whose value decreased with increasing generation. These multimolecular micelles consisted of a dendritic core and poly(ethylene oxide) corona that could solubilize hydrophobic molecules such as pyrene in the interior of the micelle as well as in the interior regions of the dendritic molecule. Thus, these dendritic micelles allowed for a much greater loading of guest molecules than traditional micelles as well as a loading of molecules with a larger size than had been possible with spherical dendrimers.^{13,62} The other system that Gitsov *et al.* examined consisted of polystyrene-poly(benzyl ether) dendritic-linear-dendritic triblock copolymers.¹² In THF, using GPC they found that the triblock copolymers underwent a transition from an unfolded coil to a more compact, globular shape as the polystyrene block started folding back into the polymer as its molecular weight, and the molecular weight of the entire polymer exceeded 50,000 g/mol. They concluded that the hybrid macromolecules were behaving as unimolecular micelles that possessed a density distribution which was not uniform throughout the entire polymer. Joeng *et*

al. have examined the intrinsic viscosity behavior of polystyrene-poly(benzyl ether) diblock copolymers in benzene and chloroform.²⁰ In benzene, which is a good solvent for both the polystyrene and the dendritic blocks, the intrinsic viscosity was found to increase with increasing molecular weight, but not to the same extent as pure polystyrene, due to the branched nature of the dendritic block. In chloroform, which is not a great solvent for either block, the intrinsic viscosity of the diblock copolymer was found to increase only moderately with molecular weight and corresponded more closely to that of pure polystyrene since both blocks adopted a more collapsed structure in this solvent. Nonetheless, in all three solvents, the maximum in the intrinsic viscosity with increasing molecular weight which has been observed for spherical polymers was absent for these di- and triblock copolymers, and the value of the intrinsic viscosity approached that of pure linear polystyrene as the size of the polystyrene block increased. In a very interesting study, Zhu *et al.* examined the solution behavior of a poly(acrylic acid)-poly(benzyl ether) hybrid-linear dendritic diblock copolymer to determine the effect of having a polyelectrolyte as the linear block.⁶³ They found that the poly(acrylic acid) block behaved very differently than the poly(ethylene oxide) block. Whereas the polyethylene oxide block formed a corona around the dendrimer, the poly(acrylic acid) block could not due to electrostatic repulsive forces between the acrylic acid repeats, resulting in the formation of a more expanded linear block around the dendrimer. Thus, for these diblock copolymers, the charged linear block was much less influenced by the presence of the dendritic block.

One of the best examples of how hybrid-linear dendritic diblock copolymers can aggregate into larger, more complex, well-defined micellar structures has been shown by van Hest *et al.* for their polystyrene-poly(propylene imine) diblock copolymers.¹⁰ These polymers exhibited classic Israelachvili behavior observed for small molecule surfactants in which the molecular shape affects the type of micellar aggregation. For these diblock copolymers, the generation affected the size and thus the shape of the diblock copolymer. They found that in aqueous solutions, the low generation amine terminated polymers formed inverted micelles, the polymers with eight dendritic end groups formed vesicles, those with sixteen dendritic end groups formed rod-like micelles, and those with thirty-two end groups formed spherical micelles. Many of these micellar structures remained stable upon dilution, which is not traditionally seen for small molecule amphiphiles. They hypothesized that this micellar stability was caused by electrostatic interactions between the amine head groups. Unlike many of the other hybrid-linear

dendritic diblock systems that solubilized hydrophobic molecules in the dendritic block, these polystyrene-poly(propylene imine) polymers solubilized pyrene in the hydrophobic polystyrene interiors of the micelles.⁹ van Hest *et al.* also examined the carboxylic acid functionalized derivatives of these same hybrid-linear dendritic diblock copolymers. In addition to size of the head group, they also found that pH affected the types of micellar structures that formed for these diblock copolymers.⁸ Thus, these polystyrene-poly(propylene imine) hybrid-linear dendritic diblock copolymers could very well be described as macromolecular surfactants.

There have primarily been two PAMAM hybrid-linear dendritic diblock copolymer systems whose solution behavior has been examined. Using intrinsic viscosity and size exclusion chromatography, Iyer *et al.* studied the effect of molecular weight, dendritic end group, and generation on the behavior of poly(ethylene oxide)-PAMAM hybrid-linear dendritic diblock copolymers in aqueous solution. Surprisingly, the polymers with the shorter poly(ethylene oxide) block (molecular weight of 2000g/mol) were found to follow the Mark-Houwink equation relating intrinsic viscosity to molecular weight, while the polymers with the longer poly(ethylene oxide) block (molecular weight 5000g/mol) were instead found to behave as unimolecular micelles, as indicated by the decrease in intrinsic viscosity of the linear polymer with the introduction of the dendrimer block.¹⁶ In addition, for the diblock copolymers with the larger poly(ethylene oxide) block, the end group chemistry, amine versus methyl ester, had a large effect on the measured intrinsic viscosity. These differences in the intrinsic viscosity behavior which were observed as a function of poly(ethylene oxide) block length were caused by the ability of the poly(ethylene oxide) to “wrap around” the dendrimer for the 5000g/mol series, and its not being large enough to do so for the 2000g/mol series. Poly(2-methyl-2-oxazoline)-PAMAM hybrid-linear dendritic diblock copolymers have been examined in aqueous solutions using SANS by Aoi *et al.*¹⁸ These diblock copolymers were found to form spherical structures that were much larger than the individual molecules, indicating that the polymers were aggregating together as individual globules within a larger spherical structure, and not as classic macromolecular amphiphiles. They also found that the critical micelle concentration (CMC) decreased as the generation number increased, most likely due to geometric constraints of the dendritic block.

In addition to examining the solution behavior of hybrid-linear dendritic diblock copolymers based on the most common dendritic chemistries, the behavior of a few other hybrid-

linear dendritic diblock copolymer systems based on less familiar dendritic chemistries have also been studied. One of the early hybrid-linear dendritic diblock copolymer systems examined consisted of a poly(L-lysine) dendritic block and a poly(ethylene oxide) linear block. Chapman *et al.* found that these copolymer surfactants formed micelles that were able to solubilize the hydrophobic dye orange-OT in the interior regions of the micelle. Unlike the results of Gitsov, these polymers did not absorb a dye below a critical micelle concentration, indicating that the dye was not solubilized in the interior regions of the dendritic block but only in the aggregated regions of the micelle. In addition, solutions of the diblock copolymers formed foams with temporal stability, similar to that observed for small molecule surfactants.⁷ More recently, Chang *et al.* have examined the behavior of amphiphilic linear-dendritic di- and triblock copolymers based on hydrophilic poly(ethylene oxide) and hydrophobic carbosilane dendrimers.^{14,15} Not surprisingly, the hydrophobicity of the polymer increased with increasing generation of the hydrophobic dendritic block such that the low generation polymers (generation one and two) were soluble in water but the third generation polymer was not. The lower generation polymers also formed micelles that were able to solubilize pyrene, and whose size and critical micelle concentration increased with increasing generation. In addition, they found that the critical micelle concentration of these polymeric surfactants was much lower than that of traditional micelles. In some very different work, Al-Muallem *et al.* examined the intrinsic viscosity behavior of hybrid-linear dendritic diblock copolymers in which low polydispersity hyperbranched polystyrene was used to initiate the polymerization of a second block of polystyrene. Since the chemistries of the two blocks were identical, they were able to look at the effect of dendritic architecture on the intrinsic viscosity of the polymer. They found that the intrinsic viscosity values were intermediate to that of pure linear polystyrene and that of pure hyperbranched dendritic polystyrene, indicating the influence of the two blocks on the resulting intrinsic viscosity.⁶⁴

3.2.4 Rod-Coil Diblock Copolymers

It is important to remember that the linear-dendritic rod diblock copolymers under investigation are not only dendrimers, but are also diblock copolymers, and their behavior in solution will also be controlled by their block copolymer nature. Over the years, the assembly and properties of several di- and multiblock copolymer systems have been investigated. Just a

few examples of block copolymers that have been examined include: polystyrene-poly(acrylic acid),⁶⁵ polystyrene-poly(vinyl pyridine),⁶⁶ polybutadiene-poly(ethylene oxide),⁶⁷ poly(ethylene oxide)-polydimethylsiloxane,⁶⁸ poly(ethylene-co-propylene)-b-poly(ethylene oxide),⁶⁹ and poly(ethylene oxide)-poly(propylene oxide) di and tri-block (Pluronics) copolymers.^{70,71} In general, it has been found that block copolymer amphiphiles self-assembled into aggregates in the presence of a selective solvent for one of the blocks. The character of the micellar aggregates is determined by a number of factors including the solvent composition, the relative and absolute lengths of each of the blocks, the presence of additives, and the temperature.⁶⁵ A few groups have looked more specifically at the solution behavior of rod-coil di- and multiblock copolymer systems and several different assembly behaviors have been observed. Tu *et al.* have examined the behavior of a poly(styrene-b-(2,5-bis[4-methoxyphenyl]oxycarbonyl)styrene) (PS-PMPCS) rod-coil diblock copolymer system in xylene, which is a poor solvent for the rigid PMPCS block at room temperature.⁷² They found that the diblock copolymer initially formed a micellar structure which consisted of a PMPCS core and a polystyrene corona. As more chains assembled into the micelle, the radius of the core remained constant, due to the rod-like nature of the PMPCS block; however, the polystyrene chains were forced to stretch to accommodate more diblock copolymer molecules in the micelle resulting in an increase in the thickness of the corona. As the density of chains increased, so did the elongation of the flexible chains. This stretching of the polystyrene chains in the micelle is similar to that observed for flexible chains grafted to a surface. The self-assembly behavior of an amphiphilic rod-coil multiblock copolymer consisting of rigid, polydisperse poly(methylphenylsilane) segments and poly(ethylene oxide) coil blocks has been studied by Sommerdijk *et al.*⁷³ They found that the composition of the solvent system influenced the packing of the rigid, conjugated polymer block as well as the molecular conformation of the silicon backbone in such a way that micellar, vesicular, and even helical superstructures were generated despite the polydisperse structure of the polymer. Finally, Jenekhe *et al.* have looked at the self-assembly behavior of amphiphilic poly(phenylquinoline)-polystyrene rod-coil diblock copolymers in mixed solvent systems that were good solvents for the rod block.⁷⁴ By adjusting the initial solvent composition as well as the relative and absolute lengths of the two blocks, several different micelle morphologies were observed whose size scale decreased with decreasing fraction of the rigid-rod block. These morphologies included hollow spheres, vesicles, hollow cylinders, and lamellae. These micellar

aggregates had dimensions that were about two times larger than traditional coil-coil copolymer micelles, and they consisted of over 10^8 polymer molecules. Unfortunately, not a lot of work has been done to examine the intrinsic viscosity behavior of rod-coil polymers in solution.

3.3 Theory

3.3.1 Dynamic Light Scattering

Dynamic, or quasielastic laser light scattering is a technique that has been used to measure the hydrodynamic radius of micelles and other colloidal polymer particles. Dynamic light scattering measures the fluctuations in the intensity of the scattered light from a particle in solution and is able to correlate these fluctuations to the size of the particle. As a particle scatters light, one can measure its intensity with a detector that is placed at a fixed angle and distance from the particle solution. However, since the particles is moving about randomly in the solution (Brownian motion) its distance from the detector, as well as the distance that the scattered light travels to the detector, change as a function of time. These differences in the distance that the light travels result in constructive and destructive interference in the intensity of the light which can be measured as a function of time. The frequencies of the fluctuations depend on the speed, and thus, the size of the particles. Smaller particles move faster and thus exhibit high frequency fluctuations, while large particles move much slower, and exhibit low frequency fluctuations. Thus, once the frequency of fluctuation has been determined, the size of the particle can be determined.⁷⁵

The fluctuations in the scattering intensity of a particle can be related to an autocorrelation function, $g(\tau)$, as a function of τ , the time between measurements. For a monodisperse suspension of particles, the function decays exponentially as:⁷⁶

$$g(\tau) = \exp(-\Gamma\tau) \quad (3.1)$$

where Γ is related to the relaxation of the fluctuations by:

$$\Gamma = Dq^2 \quad (3.2)$$

The value of q is calculated from the index of refraction of the suspending liquid (n), the wavelength of the laser light (λ_0), and the scattering angle (τ).^{75,77,78}

$$q = (4\pi n / \lambda_0) \sin(\theta / 2) \quad (3.3)$$

Since most particle solutions have a polydisperse size distribution, each size will contribute its own exponential to the autocorrelation function and the equation becomes:^{75 77,78}

$$g(\tau) = \int G(\Gamma) \exp(-\Gamma\tau) d\Gamma \quad (3.4)$$

The left hand side of the equation is the measured autocorrelation function, and the desired distribution information is contained in $G(\Gamma)$. Unfortunately, the solution to $G(\Gamma)$ is non-trivial, so a method of cumulant analysis is used to find an average Γ .⁷⁵ To do this, the equation is expanded as a Taylor's series about the mean value, and the series is integrated to give a polynomial in sample time τ . The first moment of the polynomial is the average and the second is the variance.⁷⁶

$$\ln g(\tau) = -\bar{\Gamma}\tau + \frac{\mu_2\tau^2}{2} + \frac{\mu_3\tau^3}{6} + \Lambda \quad (3.5)$$

Equation 3.2 then becomes:

$$\bar{\Gamma} = \bar{D}q^2 \quad (3.6)$$

Where \bar{D} is the average diffusion coefficient. The value of the diffusion coefficient is independent of shape and assumes only translational diffusion. It is only when the aspect ratio is less than 0.2 that a significant rotational term will appear in the diffusion equation.⁷⁵

The average diffusion coefficient of the particles is related to the particles' average frictional coefficient (\bar{f}) through the equation:

$$\bar{D} = \frac{k_B T}{\bar{f}} \quad (3.7)$$

where k_B is Boltzmann's constant and T is the absolute temperature. This equation is also independent of shape.⁷⁹ For spheres, Stokes determined the translational frictional coefficient to be $6\pi\eta r_H$, where r_H is the radius of an equivalent sphere, and η is the viscosity of the solvent. The equivalent sphere consists of the particle plus any solvent that is bound to it; thus, the radius that is determined is called the hydrodynamic radius of the particle and is calculated with the equation:⁷⁵

$$\bar{D} = \frac{k_B T}{6\pi\eta r_H} \quad (3.8)$$

For ellipsoids, the translational frictional coefficient can be written as $6\pi\eta r_E P(s)$, where r_E is the radius of the sphere with the same volume as the ellipsoid and is equal to $(ab^2)^{1/3}$, and s is the axial ratio defined as b/a where a is the semi-axis of revolution and b is the semi-equatorial

axis. (It should be noted that some scientists and engineers define the axial ratio as the reciprocal of this value.) For prolate ellipsoids ($s < 1$), Perrin found $P(s)$ to be:⁷⁹

$$P(s) = \frac{(1 - s^2)^{1/2}}{s^{2/3} \ln\left(\frac{1 + (1 - s^2)^{1/2}}{s}\right)} \quad (3.9)$$

So that \bar{D} becomes:

$$\bar{D} = \frac{k_B T s^{2/3} \ln\left(\frac{1 + (1 - s^2)^{1/2}}{s}\right)}{6\pi\eta r_E (1 - s^2)^{1/2}} \quad (3.10)$$

From dynamic light scattering one can determine the diffusion coefficient of the particle. Unfortunately, since there are two unknowns in equation 3.10, one cannot simultaneously measure the hydrodynamic radius of the sphere of equivalent volume and its axial ratio. (The diffusion coefficient allows one to calculate the radius of a sphere of equivalent frictional coefficient, but not equivalent hydrodynamic volume.) Dynamic light scattering can only give information into these properties if some other piece of information is known from other experiments or if it can be estimated.⁷⁵ Nonetheless, for spheroids with an axial ratio between 0.5 and 1, the hydrodynamic radius of a sphere of equivalent frictional coefficient is a good estimation of the hydrodynamic radius of the real particle, as this assumption will calculate a radius that is less than 4% larger than the true radius. However, the axial ratio, and thus the exact particle dimensions, cannot be calculated accurately in this manner.

3.3.2 Intrinsic Viscosity

Another common method that has been used to determine the sizes of polymers and other particles in solution is intrinsic viscosity. Intrinsic viscosity is defined as the viscosity of a particle in a solution at infinite dilution, and is dependent on the volume, mass, and shape of the particle. The equations used to relate the intrinsic viscosity to these parameters are derived from those used in traditional fluid mechanics.⁸⁰

As a pure solvent flows down a capillary tube, the velocity of the solvent at any point will be dependent on the distance of the solvent molecules from the side of the capillary wall. If a particle of a larger size is placed in the solution, the particle will experience this gradient in

solvent velocities causing the particle to rotate. This rotation distorts the established velocity gradient, resulting in a dissipation of energy around the particle, and the viscosity of the solution is increased. If the particle is non-spherical, then the particle will also tend to orient in the solvent; however, the degree of orientation will depend on the solvent velocity as well as the tendency of the polymer to prefer a random orientation.⁸⁰

The relative viscosity of a polymer solution is defined as the ratio of the viscosity of the polymer solution at a known concentration to the viscosity of the pure solvent. It is determined by measuring the ratio of the flow time of the polymer solution through a known volume to that of the pure solvent.⁸¹

$$\eta_{rel} = \frac{\eta}{\eta_o} = \frac{t}{t_o} \quad (3.11)$$

Where η is the viscosity of the polymer solution at a known concentration, η_o is the viscosity of the pure solvent, t is the flow time of the polymer solution through a known volume, and t_o is the flow time of the pure solvent through the same volume. Ideally, η_{rel} should be between 1.1 and 1.6.⁸² If η_{rel} is too small and the solution is too dilute, then the polymer will adsorb on the walls of the capillary.⁸¹ However, if η_{rel} is too large and the solution is too concentrated, then one is no longer working in the dilute solution regime and the equations described no longer apply since the effect of shear can no longer be neglected.⁸²

The specific viscosity is defined as ratio of the increase in the viscosity of the solvent containing the polymer to that of the pure solvent, and it represents the incremental increase in the viscosity attributed to the particle.⁸²

$$\eta_{sp} = \frac{\eta - \eta_o}{\eta_o} = \eta_{rel} - 1 \quad (3.12)$$

The amount of energy dissipated by the solution, and thus the change in the viscosity of the solution, will be dependent on the number of particles in the solution, or its concentration. In order to take into account the number of particles in the solution, the reduced viscosity (η_{red}) is defined.⁸⁰

$$\eta_{red} = \frac{\eta_{sp}}{c} \quad (3.13)$$

Where c is the concentration of the particles in the solution. At infinite dilution, one would expect that the motion of one particle would be independent of the motions of the other particles. Therefore, the intrinsic viscosity, $[\eta]$, is defined as the limiting value of the reduced viscosity at infinite dilution.^{80,81,83} The intrinsic viscosity is characteristic of a specific particle/solvent system.

$$[\eta]_0 = (\eta_{\text{red}})_{c \rightarrow 0} \quad (3.14)$$

Practically, the intrinsic viscosity is determined by measuring the viscosity of a series of polymer solutions at various concentrations, plotting the viscosity versus concentration, and then extrapolating the values to zero concentration. There are several equations which have been developed to plot the viscosity versus the concentration for this determination. The most common of these equations is the Huggins equation, which is known to work well for most uncharged polymer solutions.⁸¹

$$\frac{\eta_{\text{sp}}}{c} = [\eta] + k_H [\eta]^2 c \quad (3.15)$$

k_H is defined as the Huggins coefficient and its value depends on polymer architecture and molecular weight.⁸⁴ For traditional polymers, the value of k_H is usually approximately 0.35⁸³ and for hard spheres, its value approaches 0.99.⁸⁵

In dilute solutions, where the relative viscosity is just over unity, the following algebraic expansion is also used to determine the intrinsic viscosity.⁸²

$$\ln \eta_{\text{rel}} - 1 = \ln (\eta_{\text{sp}} + 1) \cong \eta_{\text{sp}} - \eta_{\text{sp}}^2 + \dots \quad (3.16)$$

Dividing η_{rel} by c and extrapolating to zero concentration also yields the intrinsic viscosity. This equation is called the Kramer equation and is usually used to verify the Huggins equation as the two should extrapolate to the same value.

$$\frac{\ln(\eta_{\text{rel}})}{c} = [\eta] - k_K [\eta]^2 c \quad (3.17)$$

k_K is called the Kramer parameter and for random coils its value is usually approximately -0.15 ⁸³ while for hard spheres, it usually has a value of approximately 0.5.^{85,86} For many polymers $k_H - k_K = 0.5$.

Unfortunately, not all polymer solutions display this same viscosity/concentration dependence. For example, the viscosity of a polyelectrolyte in aqueous solutions has been found

to increase with decreasing concentration (polyelectrolyte effect). This phenomena is caused by the disassociation of counterions from the backbone upon dilution, which result in an increase in the repulsive forces between adjacent charges along the backbone and an expansion of the polymer into a larger, possibly even rod-like, configuration.^{87,88} (It should be noted that in isoionic solutions, this disassociation does not occur upon dilution as the charge counter ion balance remains unchanged, and the polyelectrolyte viscosity/concentration dependence can be fit with the Huggins Equation.)⁸⁹

Thus, other equations have been developed to determine the intrinsic viscosity of these solutions. The most commonly used equation is the Fuoss equation which applies to polyelectrolytes in low salt solutions which have concentrations greater than $2 \cdot 5 \times 10^{-3}$ g/dl.⁹⁰

$$\frac{\eta_{sp}}{c} = \frac{[\eta]}{(1 + Bc^{1/2})} \quad (3.18)$$

This empirical equation has been found to give straight lines when c/η_{sp} is plotted versus $c^{1/2}$ and B is taken to be a constant.⁹¹

Another equation that has been applied to aqueous polyelectrolyte solutions but that also works well for describing the viscosity of dilute to moderately concentrated non-charged polymer solutions is the Fedors equation.^{92,93} The Fedors equation was derived as a rearrangement of Eiler's equation which describes the viscosity of Newtonian suspensions of rigid particles. This equation, originally proposed by van Dijck, but applied by Eilers, takes into account the fluctuations in size and velocity that the particles may experience in very concentrated conditions.⁹⁴ Eiler's equation is given by:

$$\eta_r = \left(1 + \frac{1.25\phi}{1 - \frac{\phi}{\phi_m}} \right)^2 \quad (3.19)$$

where ϕ is the volume fraction of suspended particles and ϕ_m is the maximum volume fraction to which the particles can pack. If it is assumed that ϕ is proportional to the polymer concentration ($\phi = kc$, where k is a constant of proportionality) then:

$$\eta_r = \left(1 + \frac{1.25kc}{1 - \frac{c}{c_m}} \right)^2 \quad (3.20)$$

where c_m is a polymer concentration parameter and corresponds to ϕ_m . For small c , equation 3.19 reduces to $\eta_r = 1 + 2.5kc$, or $[\eta] = 2.5k$. Using this result:

$$\eta_r = \left(1 + \frac{[\eta]_c}{2\left(1 - \frac{c}{c_m}\right)} \right)^2 \quad (3.21)$$

which can be arranged to the Fedor's Equation shown below.

$$\frac{1}{2(\eta_r^{1/2} - 1)} = \frac{1}{[\eta]c} - \frac{1}{[\eta]c_m} \quad (3.22)$$

Applying this equation, $1/2(\eta_r^{1/2} - 1)$ is plotted versus $1/c$ where c_m is a polymer concentration parameter. The intrinsic viscosity is simply the reciprocal of the slope of the line that forms. A more thorough investigation into the physical basis of this equation is currently in progress.

Once the intrinsic viscosity of the polymer solution has been determined, then the intrinsic viscosity can be related to the volume, mass, and shape of the particle under investigation. The most general equation relating these parameters is:⁸⁰

$$[\eta] = \frac{N_A v v}{M} \quad (3.23)$$

where N_A is Avagardo's number, v is the volume of the particle, M is its mass, and v is a factor that depends only on the shape of the particle. The shape of the particle is important since different shapes will dissipate the energy and slow the solvent velocity in different ways by exhibiting shape dependent translational and rotational diffusion coefficients. For spheres, Einstein found that the value of the shape parameter was $v = 5/2$, giving:⁸⁰

$$[\eta] = \frac{5vN_A}{2M} \quad (3.24)$$

Substituting $4\pi r_v^3/3$ for the volume of a sphere allows one to calculate the viscometric radius of the particle.

$$[\eta] = \frac{10\pi r_v^3 N_A}{3M} \quad (3.25)$$

For ellipsoids of revolution, the value of ν is highly dependent on the axial ratio of the particle, $s = b/a$, where b is the length of the semi-equatorial axis and a is the length of the axis of revolution. For prolate ellipsoids (rod-like particles), $s < 1$, while for oblate ellipsoids (disk-like particles), $s > 1$. For prolate ellipsoids of any axial ratio, Simha found ν to be:⁸⁰

$$\nu = \frac{2(1-s^2)^2}{15s^2} \left[\frac{\left\{ 2 - 41s^2 + \frac{3s^2(8+5s^2)}{s^{2/3}P(s)} \right\}}{\left\{ 2 - 5s^2 + \frac{3s^{10/3}}{P(s)} \right\} \left\{ \frac{(2+s)}{s^{2/3}P(s)} - 3 \right\}} + \frac{3 \left\{ 1 - 2s^2 + \frac{s^{10/3}}{P(s)} \right\}}{\left\{ \frac{2(2-s^2)}{s^{2/3}P(s)} - 1 \right\} \left\{ 1 + 2s^2 - \frac{3s^{10/3}}{P(s)} \right\}} \right] \quad (3.26)$$

where $P(s)$ is Perrin's factor. (This is the same factor used to calculate the diffusion coefficient of ellipsoids in dynamic light scattering.)

$$P(s) = \frac{(1-s^2)^{1/2}}{s^{2/3} \ln \left(\frac{1+(1-s^2)^{1/2}}{s} \right)} \quad (3.27)$$

For prolate ellipsoids in which $(1/15) \leq s \leq 1$, the following empirical approximation for ν has been made:⁹⁵

$$\nu = 2.5 + 0.407 \left(\frac{1}{s} - 1 \right)^{1.508} \quad (3.28)$$

For prolate ellipsoids in which $s < (1/15)$, ν can be estimated as:⁹⁵

$$\nu = \frac{24}{15} + \frac{1}{15s^2} \left[\frac{1}{(\ln(2/s)) - 1.5} + \frac{3}{(\ln(2/s)) - 0.5} \right] \quad (3.29)$$

As in the case of dynamic light scattering, one cannot simultaneously measure the viscometric particle volume and the particle axial ratio, since there are two unknowns and one equation. Therefore, in order to be able to determine these quantities, some other piece of information must be known or be able to be estimated. Nonetheless, for particles with aspect ratios between 0.5 and one, a spherical approximation to determine the viscometric volume is reasonable since it will only overestimate the calculated viscometric volume by a factor of less than 1.2 (20%) and the viscometric radius of a sphere of equal volume by a factor of less than 1.06 (6%).

3.4 Experimental

3.4.1 Materials

The linear-dendritic rod diblock copolymers under investigation consisted of a poly(ethylene oxide) block length of approximately 43 repeats and a dendritic block length of approximately 97 repeats. The half generation polymers were terminated with ester groups while the whole generation polymers were terminated with amine groups. (The solution behavior of the alkyl terminated polymers was not examined in this thesis.) The synthesis and characterization of these polymers are described in Chapter 2. The polymer solutions were prepared in methanol, which was used as received from Mallinckrodt.

3.4.2 Dynamic Light Scattering

Dynamic light scattering measurements were performed using a Brookhaven Instruments BI-200SM system equipped with an automatic goniometer, a digital autocorrelator (model BI-9000AT), and a 488nm argon ion laser. The measurements were collected at a scattering angle $\theta=90^\circ$ and at a temperature of $25\pm 0.1^\circ\text{C}$, which was maintained by a circulating ethylene glycol bath. The polymer solutions were prepared in methanol over a concentration range of 0.75-30mg/ml, as indicated in the results, in order to mimic the concentration range used in the intrinsic viscosity experiments. The low generation polymer samples were allowed to equilibrate at least twenty minutes before use, while the higher generation polymers samples were prepared the day before in order to assure complete solubilization of the polymer. In order to minimize the effect of dust, the polymer solutions were filtered five times through a $0.22\mu\text{m}$ PTFE syringe filter into borosilicate sample cells that had been cleaned with compressed air. The diffusion coefficient, D , was extracted from the measured autocorrelation function using the cumulants analysis method with a quadratic fit. The effective hydrodynamic radius was then calculated from the diffusion coefficient assuming a spherical particle shape. At each concentration, four measurements of the effective radius were made which were then averaged to give the value reported for that concentration. At each generation, all of the measurements at all of the concentrations were averaged in order to give the value reported for that generation. The error bars were calculated assuming one standard deviation from the mean of the values at each concentration. In order to determine whether there was a statistical difference between the

hydrodynamic radii measured as a function of concentration for polymers of the same generation, all of the measurements at all of the concentrations were inputted into a linear regression analysis and a “p-value” was calculated. A statistical difference was noted if the “p-value” was less than 0.05, a value which is traditionally used as the cutoff for statistical significance.⁹⁶

3.4.3 Intrinsic Viscosity

Intrinsic viscosity measurements were made in methanol at 25°C using a size 25 Cannon-Ubbelohde capillary viscometer which was immersed in a circulating water bath to maintain the desired temperature. The size (diameter) of the capillary viscometer was chosen such that the pure solvent would have a flow time above 200s in order to avoid the need for kinetic energy corrections. The solution concentration range was determined so that the relative viscosity of the polymers ranged from 1.6 to 1.0. This ensured that the concentration was not too low such that there were wall effects nor too high such that the effect of shear could no longer be neglected. The low generation polymer solutions were allowed to equilibrate at least twenty minutes after preparation, while the higher generation polymer samples were prepared the day before in order to assure complete solubilization of the polymer. All solutions were filtered through a 0.22µm PTFE syringe filter prior to use in order to remove dust. The polymer solutions were placed in the viscometer with a 1ml glass pipet, and the viscometer and solution were immersed in the water bath for at least 20 minutes before taking measurements to allow the solution to come to thermal equilibrium. Dilutions were prepared directly in the viscometer and after each dilution, the sample solution was thoroughly mixed and immersed in the water bath for at least another 20 minutes to allow the solution to regain thermal equilibrium. The viscosity at each concentration was measured at least three times such that the difference between flow times was no greater than one second and in most cases was no greater than a half a second. The viscosity reported at each concentration was an average of these values. The solution viscosity was determined at five different concentrations and was plotted using Huggin’s, Kramer’s, as well as Fedor’s equation in order to determine the intrinsic viscosity of the polymer. The error in the value of the intrinsic viscosity was estimated from the standard error calculated from linear regression of the above equations. The viscometric radii were then calculated from the intrinsic viscosity assuming a spherical particle shape. The error in the radii was calculated with the differential method

assuming a variance in the molecular weight of the polymer based on 2.3 repeat units (from NMR). The equation used for this calculation was:

$$dr = r \left(\frac{d[\eta]}{\eta} + \frac{dM}{M} \right)^{1/3} \quad (3.30)$$

3.5 Results and Discussion

3.5.1 Dynamic Light Scattering

Dynamic light scattering has often been used to measure the hydrodynamic radius of polymers in solution. Given the unique chemistry and architecture of these poly(ethylene oxide)-poly(ethylene imine)-poly(amido amine) linear-dendritic rod diblock copolymers under investigation in this thesis, the hydrodynamic radii of the polymers were determined in methanol in order to understand how the hydrodynamic radii were affected by the chemistry of the end group as well as the generation number of the dendritic block and the concentration of the polymer solution. Finally, by comparing the results from dynamic light scattering with those from intrinsic viscosity, we hoped to gain insight into the size and aggregation of these linear-dendritic rod diblock copolymers in solution.

As discussed in the theory section, the hydrodynamic radius of a particle is calculated from its measured diffusion coefficient, which is influenced by its shape. For particles that are spherical in shape, the hydrodynamic radius can be simply calculated using equation 3.8. However, most particles are not spherical in shape, most are ellipsoidal such that a more accurate calculation of their hydrodynamic radius can be made with equation 3.10. Unfortunately, application of equation 3.10 is extremely difficult as it contains two unknowns, the hydrodynamic radius of a sphere of equivalent volume and the axial ratio of the particle. This equation can only be used if one of the variables can be accurately determined or estimated using an independent technique, which is not always possible.⁷⁵ Nonetheless, for most polymer systems, the reported hydrodynamic radius is that assuming a spherical shape. For axial ratios greater than 0.5, this value is a fairly good approximation as it will over estimate the real radius by less than 4%. However, the axial ratio, and thus the particle dimensions, cannot be calculated accurately in this manner. The size of the other dendritic rod systems that have been examined using dynamic light scattering, those by Percec⁵⁷ and by Schlüter,⁵⁴ were also simply reported as

the hydrodynamic radius assuming a spherical shape. Since most of our linear-dendritic rod diblock copolymers, especially those of low generation, can be expected to take on a spherical shape or an ellipsoidal one with an axial ratio between 0.5 and 1, we too will report the effective hydrodynamic radius assuming a spherical shape for all generations of the diblock copolymers.

The hydrodynamic radius of each of the polymers under investigation was measured as a function of concentration and the results are presented in Figure 3.1. The effect of concentration on the hydrodynamic radius was examined for two reasons. First, we wanted to determine if there was obvious aggregation of the polymer, which would appear as a dramatic increase in the size of the polymer once its concentration exceeded that of its critical micelle concentration. Second, it is common practice when determining the diffusion coefficient, which is used to calculate the hydrodynamic radius, to take measurements at several different concentrations and then to extrapolate to zero concentration to obtain the self-diffusion coefficient of an isolated polymer, since at any given concentration the diffusion coefficient also includes the effects of interparticle interactions.⁷⁵ Depending on the system, neighboring particles may increase or decrease the overall diffusion of the particle, and thus decrease or increase its effective radius.⁷⁶

As can be seen, all of the polymers exhibited a very small, yet noticeable increase in the hydrodynamic radius with decreasing concentration. (In order to determine whether there was a statistical difference between the hydrodynamic radii measured as a function of concentration for polymers of the same generation, all of the measurements at all of the concentrations were inputted into a linear regression analysis and a “p-value” was calculated, as described in the experimental section. A statistical difference was noted if the “p-value” was less than 0.05, a value which is traditionally used as the cutoff for statistical significance.⁹⁶) For the generation 1.5, 2.5, and 4.5 polymers, this increase appeared to be statistical as reflected in “p-values” of 4.99×10^{-9} , 0.03, and 0.018, respectively. For the generation 1.0 polymer, the “p-value” was 0.056, indicating that the increase was almost statistical, but for the other polymers the difference was not statistically significant.) Since polymer aggregation and the formation of micellar structures usually occur with an increase in the hydrodynamic radius with increasing concentration as well as a much larger total increase in the hydrodynamic radius, usually at least an approximate doubling, it does not appear as if aggregates formed over the concentration range which was investigated, or if they did form, the critical micellar concentration was either well above or well below the concentration range studied. The formation of micellar structures will

be discussed in greater detail when these results are compared with those from the intrinsic viscosity measurements.

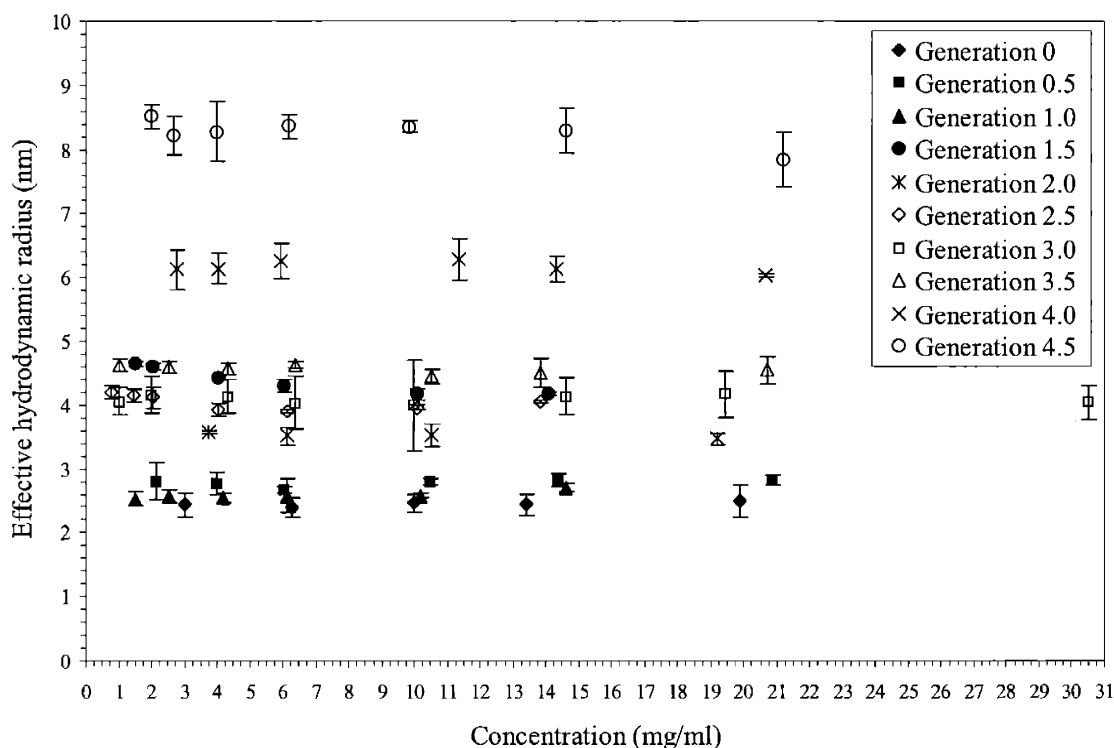


Figure 3.1. Average effective hydrodynamic radius of the polymers as a function of concentration determined in methanol at 25°C.

Therefore, the increase in hydrodynamic radius with decreasing concentration must have been due to some other effect. One possible explanation is that these linear-dendritic rod diblock copolymers were behaving as polyelectrolytes. It is known that the measured diffusion coefficient for polyelectrolytes in low salt solutions increases with increasing polymer concentration, resulting in a decrease in the measured effective radius.⁹⁷ For example, Koene *et al.* have found this to be true for poly(styrenesulfonate),⁹⁸ Forester *et al.* for quaternized poly(2-vinyl pyridine),⁹⁹ and Smits *et al.* for linear poly(ethylene imine).^{100,101} This increase in the effective hydrodynamic radius with decreasing concentration is due to solvation and dissociation of the counter ions away from the polyelectrolyte, resulting in a greater effective charge for the polymer. This charge causes the polymer to expand in order to decrease these self-repulsive

interactions. In isoionic solution, this dissociation does not occur as the balance between charges does not change with dilution.^{87,88} While ideally, our linear-dendritic rod diblock copolymers should not have behaved as polyelectrolytes, since they should not have been charged, it is not surprising that they might have become charged upon exposure to traces of water in the reagents as well as in the environment. More evidence supporting the behavior of these linear-dendritic rod diblock copolymers as polyelectrolytes will be presented when the intrinsic viscosity results are discussed.

The measured hydrodynamic radius was also plotted as a function of generation and end group and the results are given in Figure 3.2. The measured value of approximately 2.5nm for the radius of the poly(ethylene oxide)-poly(ethylene imine) diblock copolymer backbone was in good agreement with that measured for the poly(ethylene oxide) block by itself in water, approximately 1.35nm.¹⁶ For the other linear-dendritic rod diblock copolymers, a slow, yet noticeable increase in the effective radius with generation can be seen up to generation 3.5 at which point the effective radius begins to increase more dramatically. For these diblock copolymers, the value of the effective hydrodynamic radius depends primarily on the length and the stiffness of the polymer backbone. Since the dimensions of a polymer do not grow linearly with the addition of branches, but rather much more slowly, so too will their effective radius increase as the number of branches along the backbone and thus, its stiffness, increases. Therefore, at low generations where the stiffness gradually increases, one might expect the hydrodynamic radii to increase gradually as well. However, above generation 3.5 there are a couple of possible explanations for the dramatic increase in the hydrodynamic radius above generation 3.5. First, it is possible that the polymers were forming aggregates; although for reasons discussed in the intrinsic viscosity section, we do not believe this to be the case. A second possible explanation was that the polymers experienced a large increase in their hydrodynamic volume due to a change in the shape of the polymer and a breakdown of the spherical approximation as the polymer elongated into a rod-like shape. As the axial ratio of a polymer increases, the measured hydrodynamic radius assuming a spherical shape will overestimate the value of the real hydrodynamic radius by an increasingly larger amount, depending on the value of Perrin's factor $P(s)$, equation 3.9. As an example, for an axial ratio of 0.2, which is reasonable for the generation 4.5 polymers, the spherical approximation will measure a hydrodynamic radius approximately 25% larger than the real hydrodynamic radius.

Thus, the measured hydrodynamic radius of approximately 8nm for the generation 4.5 polymer would give a real effective hydrodynamic radius of approximately 6nm, which fits into the trend for the hydrodynamic radii much more nicely. Therefore, we believe that at generation 4.0, the steric hindrance induced by the dendritic branches was large enough to cause the polymer backbone to unwind, and take on an elongated, rod-like shape.

These results are in good agreement with those observed by Tomalia *et al.* for the poly(amido amine) homopolymer using transmission electron microscopy (TEM). They found that the poly(amido amine) dendritic rod homopolymers adopted a rod-like configuration at generation 4.5.¹⁰² However, the technique that they used to “stain” their dendritic rods consisted of base hydrolysis of the methyl ester groups to form the sodium carboxylate salts. It is possible that their dendritic polymers also began to elongate at generation 4.0, but from their paper, it did not appear as if the generation 4.0 polymer had also been examined by TEM.

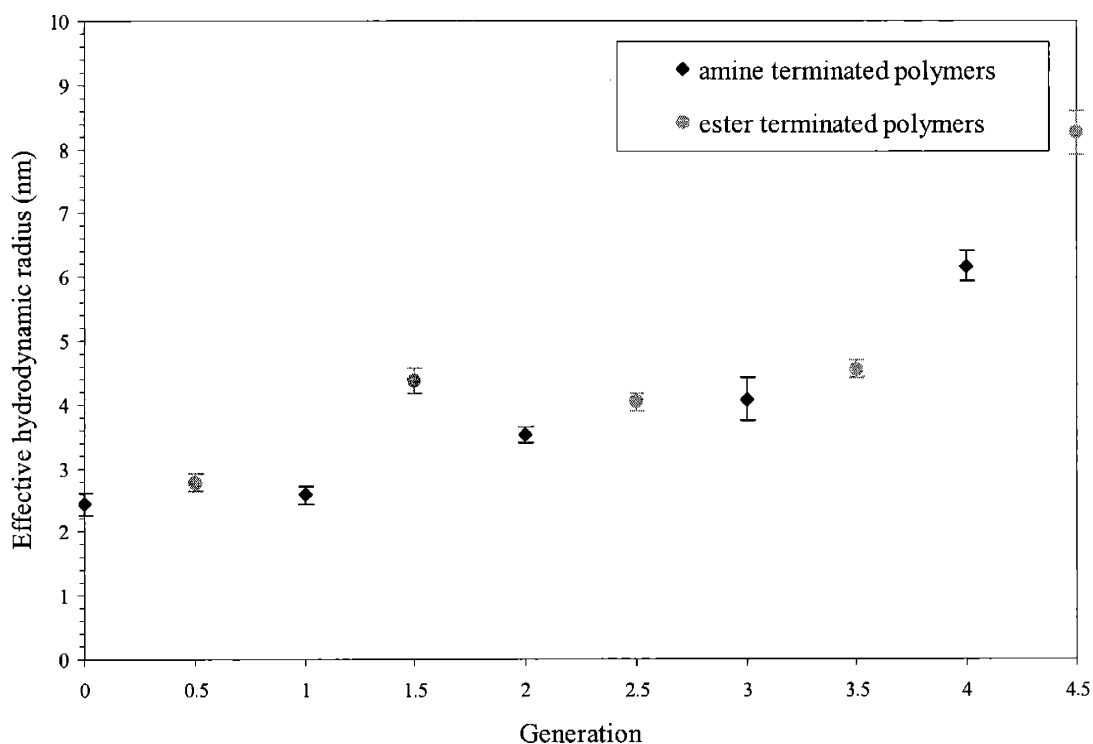


Figure 3.2. Average effective hydrodynamic radius of the polymers as a function of generation determined in methanol at 25°C.

Overall, it did not appear as if the end group had a large effect on the measured hydrodynamic radii of these linear-dendritic rod diblock copolymers. The hydrodynamic radii of both the amine and the ester terminated polymers seemed to follow the same trends of increasing hydrodynamic radii with increasing generation. Nonetheless, small differences in the sizes of the polymers caused by their interaction with solvent could not be measured due to the inherent error in the experiments. The one polymer that was not consistent with the trend of increasing size with increasing generation trend was that of the generation 1.5 diblock copolymer. Its value was slightly higher than one would have expected given the sizes of polymers of similar generations. In general, the behavior of this polymer in the light scattering sample solutions was quite different from that of the others. When the sample solutions were originally prepared, the value measured for the hydrodynamic radius was approximately twice what was expected, and twice what the final value turned out to be. However, after allowing the polymer/methanol solution to sit for approximately one month and then remeasuring the hydrodynamic radius, the value of the hydrodynamic radius decreased to one which was much more reasonable but one which was still slightly larger than one would have expected it to be. This was true of all the sample solutions for the entire range of the concentrations examined, so that we know that the polymer was not just above its critical micelle concentration. One possible explanation for this phenomena was that the polymer initially formed an aggregated structure that disassociated over time, but the exact nature of that structure or the reasons for its initial formation and later disassociation are still unknown. Thus, the slightly higher value reported for the hydrodynamic radius may have occurred because some of the polymers were still in their aggregated form. As this did not occur for any of the other polymers, including those that possessed a similar chemistry, we do not believe that this decrease was due to a breakdown of the structure of the polymer.

3.5.2 Intrinsic Viscosity

3.5.2.1 Determination of the Intrinsic Viscosity

Intrinsic viscosity is a common technique that has been used to examine the behavior of dendrimers in solution. Since the architecture of the poly(ethylene oxide)-poly(ethylene imine)-poly(amido amine) linear-dendritic rod diblock copolymers under investigation in this thesis was unique, the solution behavior of these diblock copolymers was studied in methanol in order to

gain insight into how the intrinsic viscosity was affected by the generation number (molecular weight) and the chemistry of the end group. We wanted to determine whether the polymers would behave as traditional spherical dendrimers, showing a maximum in the intrinsic viscosity as a function of generation (molecular weight), as hyperbranched polymers, exhibiting little to no dependence on the molecular weight, or as traditional linear polymers, in which the intrinsic viscosity increases with increasing molecular weight. In addition, we wanted to use the information collected from the intrinsic viscosity experiments to gain insight into the size, density, elongation, and aggregation of the polymers in solution and compare these results with those obtained from dynamic light scattering.

For each of the polymers under investigation, the viscosity was determined as a function of concentration and the results were plotted to obtain the intrinsic viscosity of the polymer. The results were first plotted using the Huggins (equation 3.15) and Kraemer (equation 3.17) equations, which are commonly used for traditional polymer systems. While these equations worked well for a few of the low generation amine terminated polymers, they did not for the ester terminated or the higher generation amine terminated polymers. The Huggins and the Kramer plots of the poly(ethylene oxide)-poly(ethylene imine) diblock copolymer backbone as well as the generation 2.5, methyl ester terminated linear-dendritic rod diblock copolymer are shown in Figures 3.3 and 3.4, respectively, as examples. The plots of the poly(ethylene oxide)-poly(ethylene imine) diblock copolymer showed the expected linear relationships and both extrapolated to the same value for the intrinsic viscosity at 0.238ml/mg. Unfortunately, for the generation 2.5 polymer, neither the Huggins nor the Kramer plots exhibited a nice linear relationship, but instead they gave plots that had an upward curvature.

In order to determine a more accurate value for the intrinsic viscosity, the solution viscosity was plotted with other equations that have been used to determine the intrinsic viscosity of polymer systems under different conditions. One of the equations that has been found to work well for polyelectrolytes in aqueous solutions is the Fuoss equation (equation 3.18). In general, when polyelectrolytes are diluted with nonionic aqueous solvents, the reduced viscosity will increase upon dilution, and a maximum can be observed before the reduced viscosity heads for its value at infinite dilution. This increase in the reduced viscosity is known as the polyelectrolyte effect. In spite of this unusual behavior, the Fuoss equation has been able to derive a linear relationship between viscosity and concentration so as to be able to obtain the

intrinsic viscosity.⁹¹ Thus, the Fuoss equation was applied to the linear-dendritic rod diblock polymers which exhibited an upward curvature in the Huggins and Kramer plots. As an example, the results for the generation 2.5 polymer are presented in Figure 3.5. Unfortunately, this equation also did not give a linear relationship for these polymers.

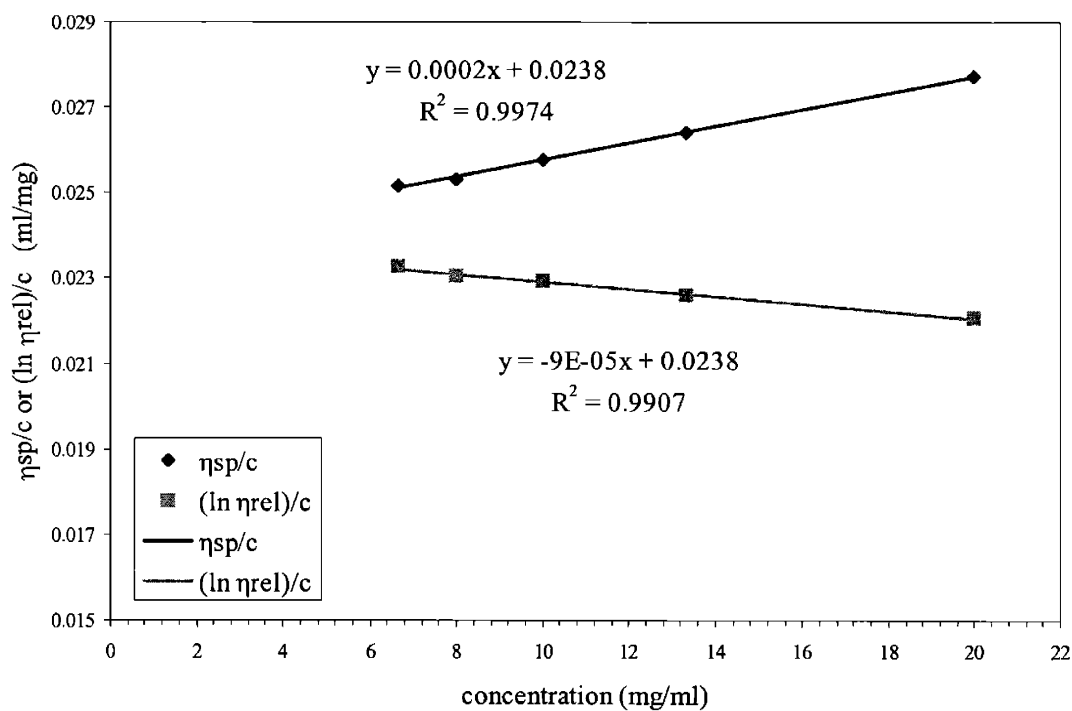


Figure 3.3. Huggins and Kramer plots of the solution viscosity as a function of concentration for the poly(ethylene oxide)-poly(ethylene imine) diblock copolymer.

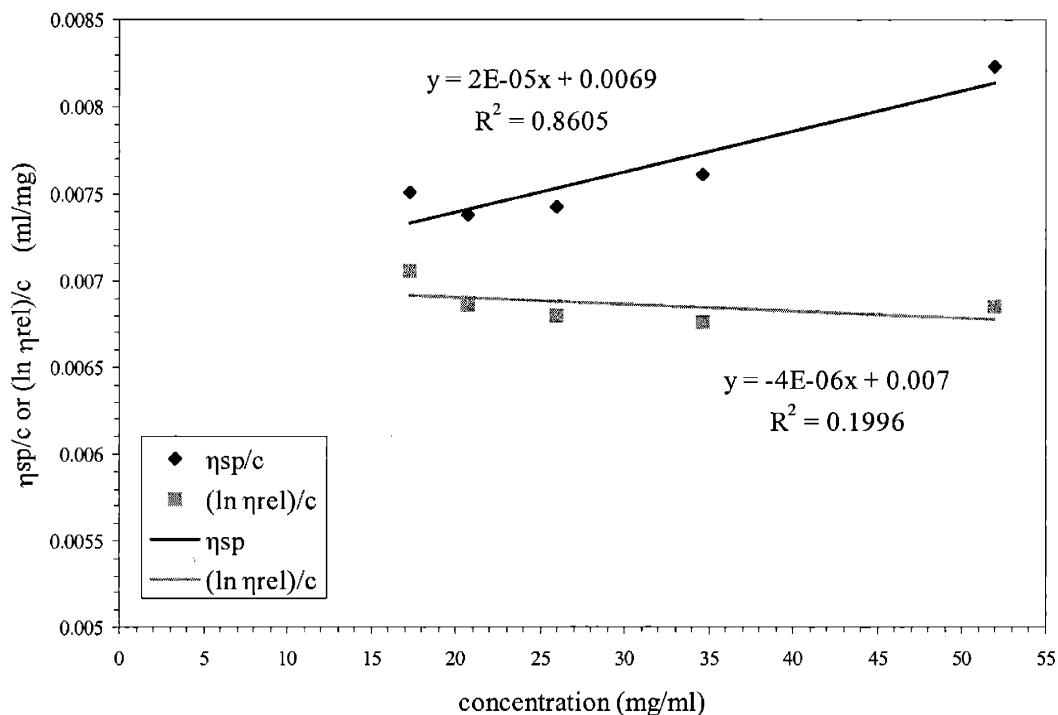


Figure 3.4. Huggins and Kramer plots of the solution viscosity as a function of concentration for the generation 2.5 linear-dendritic rod diblock copolymer.

Another lesser known equation that has been applied to various dilute and moderately concentrated polymer as well as polyelectrolyte solutions is Fedors equation (equation 3.22).⁹² The Fedors equation was derived as a rearrangement of Eiler's equation which describes the viscosity of Newtonian suspensions of rigid particles. This equation, originally proposed by van Dijck, but applied by Eilers, takes into account the fluctuations in size and velocity that the particles may experience in very concentrated conditions. This equation has been found to work exceptionally well for concentrated polymer solutions where the concentration of the solution passes into the semi-dilute regime, and the polymer chains are overlapping. For example, Ioan *et al.* have found that Fedors equation is very effective at calculating the intrinsic viscosity of dilute to moderately concentrated high molecular weight poly(butyl methacrylate) polymer solutions,¹⁰³ and Ghimici *et al.* have found that Fedor's equation does a better job of calculating the intrinsic viscosity of hydrophobically modified polyelectrolytes than Fuoss's equation.^{88,93} Fedors equation was applied to our linear-dendritic rod diblock copolymer systems which exhibited an

upward curvature in the Huggins and Kramer equations, and it surprisingly gave a very good linear correlation. The results of the generation 2.5 polymers are shown in Figure 3.6 as an example. The Fedors equation also could be applied to the low generation amine terminated polymers which had originally obeyed the Huggins and the Kramer equations. The Fedors plot of the viscosity data as a function of concentration for the poly(ethylene oxide)-poly(ethylene imine) diblock copolymers is shown in Figure 3.7. As can be seen, a nice linear relationship was obtained for this polymer as well. Thus, since the Fedors equation was able to give linear viscosity data for all of the polymers under investigation, the intrinsic viscosity of all of the polymers was determined using this equation. A plot showing the intrinsic viscosity as a function of generation and end group is shown in Figure 3.8 for the linear-dendritic rod diblock copolymers under investigation.

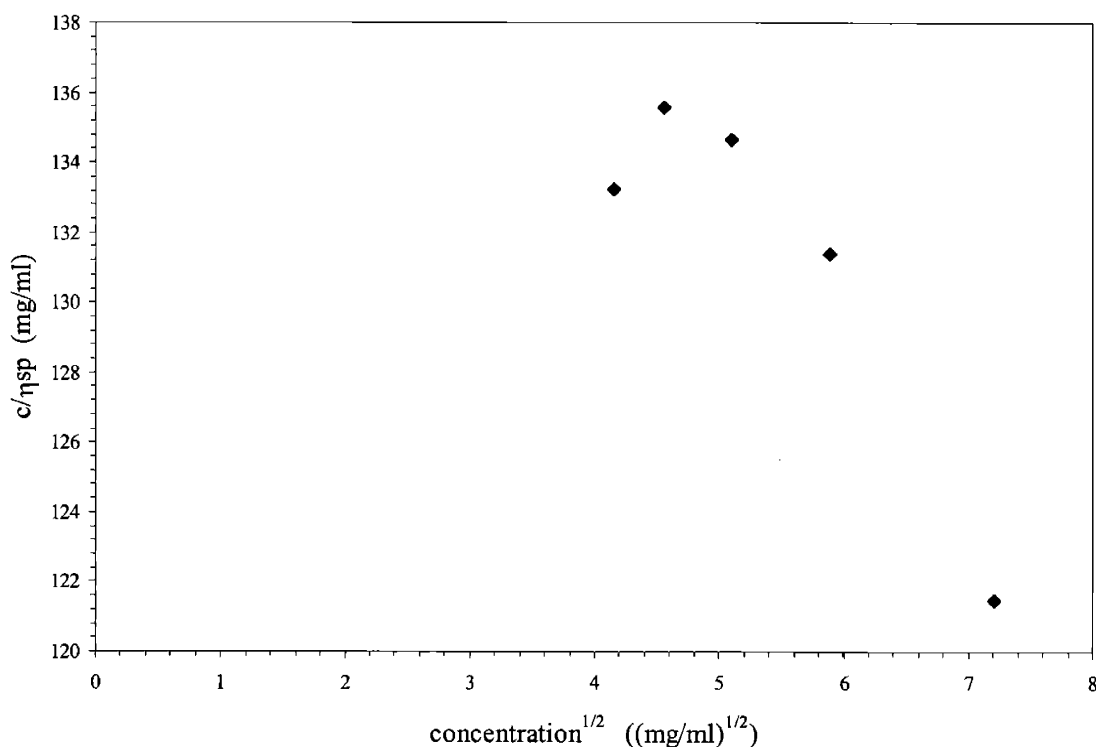


Figure 3.5. Fuoss plot of the solution viscosity as a function of concentration for the generation 2.5 linear-dendritic rod diblock copolymer.

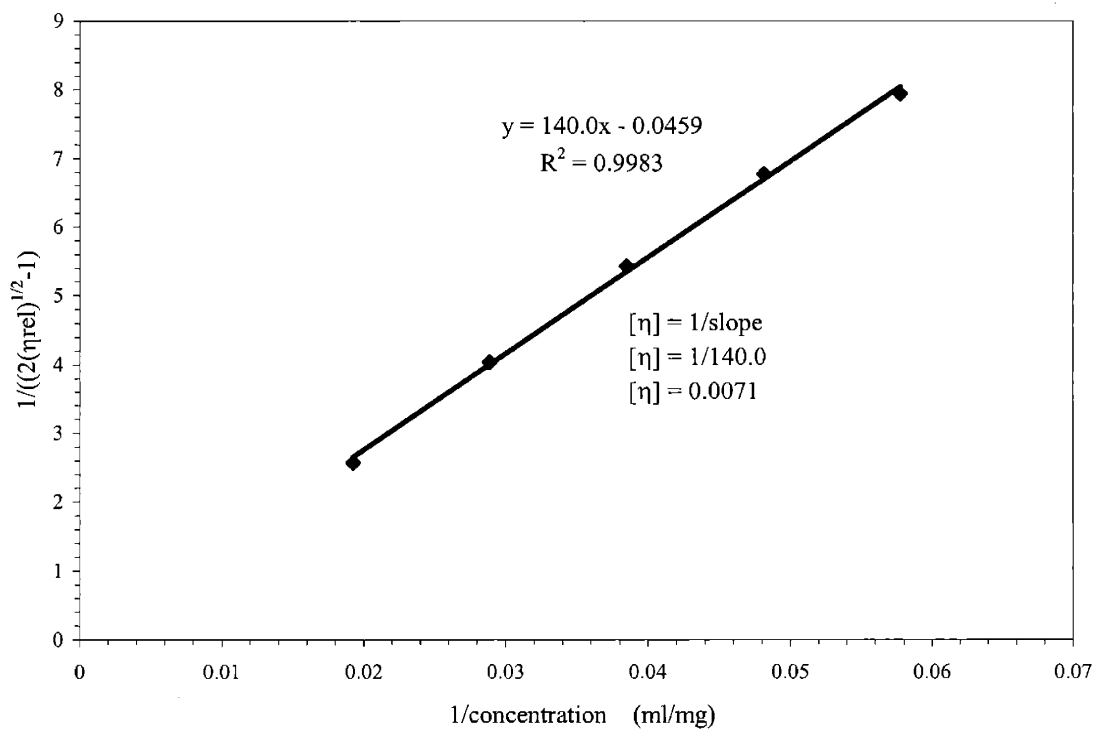


Figure 3.6. Fedors plot of the solution viscosity as a function of concentration for the generation 2.5 linear-dendritic rod diblock copolymer.

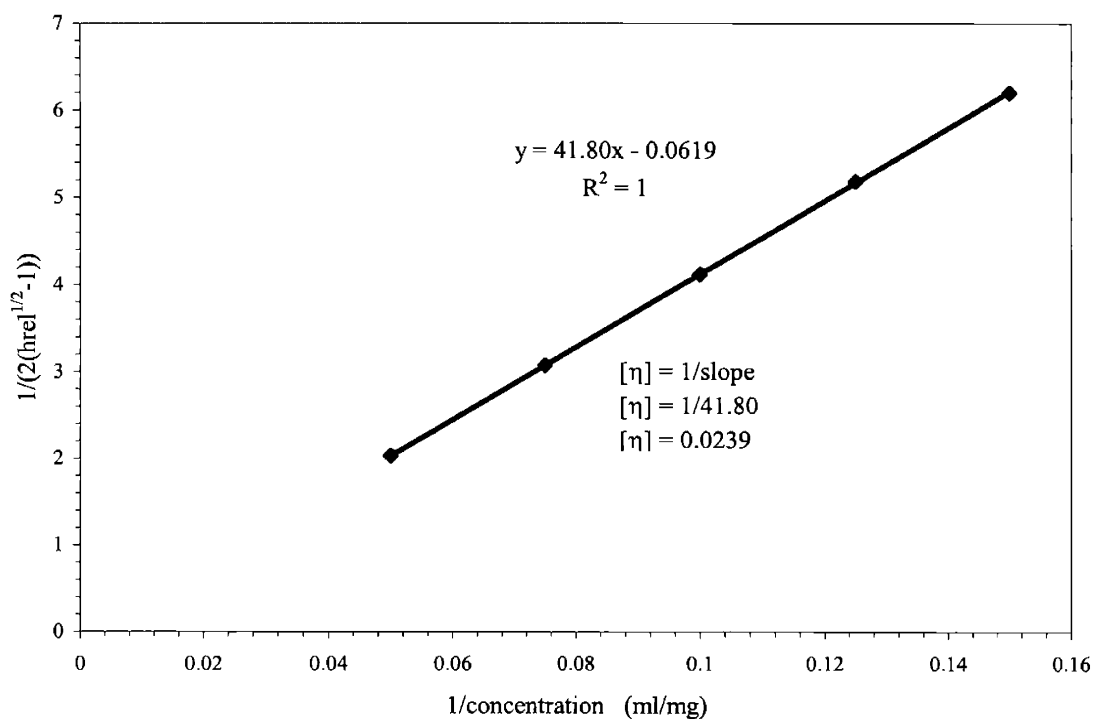


Figure 3.7. Fedors plots of the solution viscosity as a function of concentration for the poly(ethylene oxide)-poly(ethylene imine) diblock copolymer.

In order to understand the nature of the curvature in the Huggins and Kramer plots we examined a couple of possible explanations. Initially, we had thought that that the minimum in the Huggins and Kramer plots might be attributed to the polymer going from an aggregated to an unaggregated state. However, from dynamic light scattering studies, this did not appear to be the case as the hydrodynamic radius remained fairly constant, independent of concentration over the entire concentration range examined in the intrinsic viscosity experiments. Similarly, we were concerned that the minimum could be attributed to an initial solution concentration which was too large, since the Fedors equation fit the data very well, but the Fuoss equation did not. In the past, either a deviation from linearity in polymer solutions or a minimum in the viscosity of polyelectrolytes from the Huggins equation has been indicative of the solution passing from the dilute to the semi-dilute regime.⁸⁴ This transition concentration, c^* , has been calculated as $1/[\eta]$, as well as by determining the concentration in which the flow time through the capillary viscometer is twice that of the solvent.⁸⁸ However, for the generation 2.5 diblock copolymer, as well as the other linear-dendritic rod diblock copolymers which exhibited a minimum in the Huggins's plot, this did not appear to be the case. If one calculates the c^* for this polymer based

on the intrinsic viscosity determined from the Fedors equation, one obtains a c^* of $1/(0.00754 \text{ ml/mg})$, or 132.6 mg/ml , which is well above the concentration regime in which the measurements were obtained. Thus, it appears as if the minimum obtained in the Huggins plot of these linear-dendritic rod diblock copolymers was not an effect of concentration, but instead must be due to some other phenomenon.

Finally, we propose that the polymers were in fact behaving as polyelectrolytes but that in less polar solvents such as methanol, they did not exhibit the traditional polyelectrolyte effect. Kawaguchi *et al.* have examined the counterion binding and ionomer-like behavior of partially quaternized poly(4-vinyl pyridine) in aqueous alcohols.¹⁰⁴ They found that the reduced viscosity of poly(4-vinyl pyridine) in water monotonically increased with decreasing polymer concentration, typical of the behavior of polyelectrolytes in the absence of added salt, the polyelectrolyte effect. On the other hand, in 80% ethanol/water solutions, the reduced viscosity of the polymer first decreased and then increased with decreasing concentration, which is very similar to that which was observed for our linear-dendritic rod diblock copolymers. They believed that the less polar solvent was more effective in stabilizing the condensed polyelectrolyte counterion pair, which resulted in the formation of collapsed, ionomer-like chains at high concentration. However, upon sufficient dilution, the methanol was able to break apart the counterion pairs, resulting in more traditional polyelectrolyte behavior. Similarly, Ghimici *et al.* have examined the viscosity behavior of cationic polyelectrolytes in methanol and found that the strength of binding between the counterion and the polyelectrolyte is dependent on the structure of the polycation, the type of counterion, and the nature of the solvent. For their polymers, there was a strong association between the counterion and the polyelectrolyte chain owing to the poor solvation of the counterion in methanol.¹⁰⁵ Finally, this effect is seen and exploited in the anionic polymerization of some polymers. By careful choice of the solvent, counterion, and concentration, the speed of the polymerization reaction can be increased or decreased to give the desired polymer. For example, the polymerization of dienes in polar solvents, such as THF, leads to unacceptably high 1,2 and 3,4 unit contents, while the 1,4 placement is essential for applications as elastomers and can be achieved by polymerization in nonpolar pentane using a lithium counterion.¹⁰⁶

Thus, for our linear-dendritic rod diblock copolymers, we believe that the polymers are behaving as polyelectrolytes in methanol. At high polymer concentrations, there was a strong

association between the counterions and the polymer, such that the diblock copolymers were behaving as traditional polymers, exhibiting a decrease in the reduced viscosity as a function of generation. However, upon dilution, the solution eventually reached a concentration (based on the dissociation constant of the ion pair) such that the counterions were no longer bound to the diblock copolymer and they began to dissociate, causing an increase in the effective polymer charge and an increase in the chain dimensions. This conclusion was consistent with the results obtained from dynamic light scattering as a function of concentration. While a large change in the chain dimensions was not observed for the polymers as a function of concentration, a more subtle one was. The effective diameter of the polymers increased slightly with decreasing concentration, up to one to one and a half nanometers, consistent with the diblock copolymer behaving as a polyelectrolyte, with the diblock copolymer taking on slightly larger chain dimensions as the counterions were dissociated away from the polymer. Hobson and Feast have found that their poly(amido amine) hyperbranched polymers made with a one-pot synthesis exhibited the traditional polyelectrolyte effect in methanol.⁵⁹ We believe that the reason that they observed a very strong, traditional polyelectrolyte effect, while we observed only a more subtle one, was that they used aminoacrylate hydrochloride to make their polymer. Thus, they knew for sure that the amines were protonated and that counterions were present, while for our linear-dendritic rod diblock copolymers, there was a much smaller percentage of groups that were protonated, since any protonation of the amines was unintentional, as steps were taken to remove water and to avoid protonated solvents.

Nonetheless, it should be noted that to our knowledge, this is the first application of the Fedors equation to polyelectrolytes in non-aqueous solutions that show a minimum in the reduced viscosity as a function of concentration and whose behavior cannot be described adequately using the Fuoss equation. We believe that the Fedors equation is able to take into account the effect of polyelectrolyte counterion dissociation, which the Fuoss equation cannot; however, a more thorough investigation into the physical basis of the Fedors equation is currently in progress. An extensive search of the literature did not yield another system that gave similar results.

3.5.2.2 Intrinsic Viscosity as a Function of Generation and End Group

Once the intrinsic viscosity had been determined for all of the polymers, it was plotted as a function of generation as shown in Figure 3.8. As can be seen, at low generation, the intrinsic viscosity of the amine and ester terminated polymers appeared to follow two different trends, with the intrinsic viscosity of the amine polymers being greater than that of the ester terminated polymers, but as the generation number increased, the intrinsic viscosity of the two almost merged into one curve. In order to appreciate this phenomenon, it is important to remember that the intrinsic viscosity is a ratio of the polymer's volume and shape to its molecular weight. Thus, a polymer with a higher intrinsic viscosity doesn't necessarily mean that the polymer is bigger, it just means that the polymer is more expanded and/or possibly more elongated with respect to its molecular weight as reflected in equation 3.23. The dendritic block backbone, linear poly(ethylene imine) is known to take on a very extended, almost rigid conformation in methanol due to hydrogen bonding, resulting in a fairly high intrinsic viscosity.¹⁰⁷ Similarly, the other amine terminated linear-dendritic rod diblock copolymers were also expected to have very favorable interactions with the methanol due to hydrogen bonding and thus, it was likely that they too would take on more extended conformations and/or a larger hydrodynamic volume with respect to their molecular weights. The ester groups were slightly more hydrophobic and did not have the same hydrogen bonding capability, thus they would not be expected to have as favorable interactions with the solvent. In addition, at low generation, the backbone of the dendritic block was very flexible and could easily expand and contract upon changes in the dendritic end group, thus, the chemistry of the end group and its interaction with the solvent were important. However, at higher generations, the backbone was much more constrained by the dendritic groups such that it could not easily undergo conformational changes, and the dendritic nature of the diblock copolymer was more significant than the end group, as was reflected in the intrinsic viscosity results.

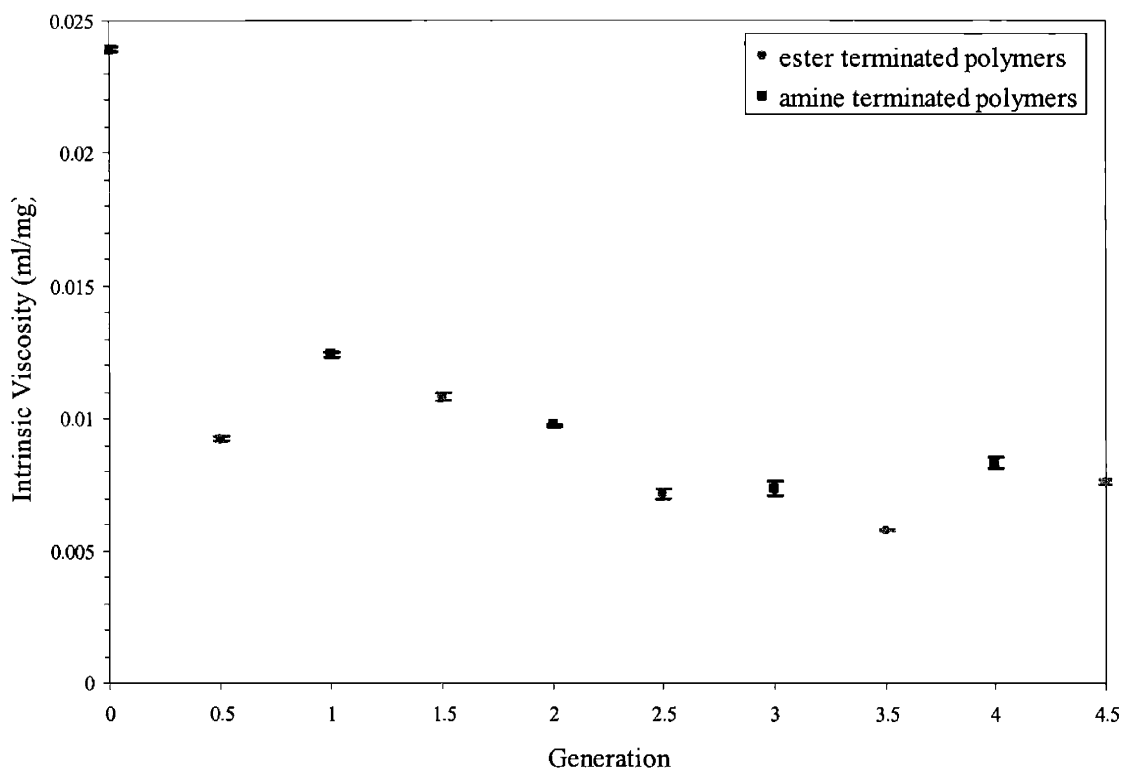


Figure 3.8. Intrinsic viscosity as a function of generation for the linear-dendritic rod diblock copolymers.

Tomalia *et al.* also observed slightly larger values for the intrinsic viscosity of the amine terminated spherical poly(amido amine) dendrimers than for the ester terminated polymers.¹⁹ They hypothesized that this difference was due to aggregation of the amine groups in solution caused by hydrogen bonding; although, they did not have any additional evidence of aggregation to support their claim. As discussed below, we do not believe that aggregation is occurring, but instead propose that amine terminated polymers are taking on more expanded configurations due to favorable interactions between the methanol and the amine groups. An end group dependence on the intrinsic viscosity was also observed by Iyer *et al.* who looked at the intrinsic viscosity of poly(ethylene oxide)(molecular weight 5000g/mol)-poly(amido amine) hybrid-linear dendritic diblock copolymers.¹⁶ Two very different trends in the intrinsic viscosity were observed for the amine and the ester terminated polymers that depended not only on the interaction of the dendritic block with the solvent, but also its interaction with the poly(ethylene oxide) block. For

the ester terminated polymers, the poly(ethylene oxide) block was able to form a corona around the dendrimer, shielding it from the solvent; however, for the amine terminated polymers, it was proposed that the poly(ethylene oxide) block was hydrogen bonding with the amine groups, creating a more compact structure. Nonetheless, for both end groups, the poly(ethylene oxide) block eventually became too short with respect to the dendrimer as the generation number of the dendrimer increased such that its presence did not have as great of an influence on the intrinsic viscosity results. Gitsov *et al.* also observed that the relative length of the poly(ethylene oxide) block had a profound effect on the intrinsic viscosity of their poly(ethylene oxide)-poly(benzyl ether) hybrid linear-dendritic diblock copolymers.⁶¹ In order for the dendritic block to be soluble in water, a minimum length of the poly(ethylene oxide) block was needed whose size increased as the generation number increased. In addition, the diblock copolymer formed a unimolecular micelle in solution with the poly(ethylene oxide) block forming a corona around the dendritic block as indicated by a decrease in the intrinsic viscosity as well as the hydrodynamic radius relative to the poly(ethylene oxide) homopolymer. In our linear-dendritic rod diblock copolymers we did not appear to observe a noticeable effect of the poly(ethylene oxide) block on the intrinsic viscosity. While the intrinsic viscosity of the higher generation polymers did decrease relative to the poly(ethylene oxide)-poly(ethylene imine) backbone, the resulting hydrodynamic radius (as calculated below) did not. It is possible that for our polymers, the poly(ethylene oxide) block was too small relative to the dendritic block, and its capacity to shield the dendritic block from the solvent as well as its ability to interact with the dendritic block was negligible.

For our methyl ester terminated linear-dendritic rod diblock copolymers, a maximum in the intrinsic viscosity was observed with increasing generation, which is similar to that reported for a number of traditional spherical dendrimers in good solvents. For example, Tomalia *et al.* have observed this maximum between generations four and five for their spherical poly(amido amine) dendrimers in methanol,¹ de Brabander-van den Berg *et al.* have observed this maximum at generation four for their cyano terminated poly(propylene imine) dendrimers in methanol,³¹ and Mourey *et al.* have observed this maximum at generation 3.0 for their poly(benzyl ether) dendrimers in THF.²⁹ Iyer *et al.* have also reported a maximum in the intrinsic viscosity of their ester terminated poly(ethylene oxide)-poly(amido amine) hybrid-linear dendritic diblock copolymers at generation 2.5.¹⁶ Hobson and Feast have even reported this maximum in the

intrinsic viscosity of hyperbranched poly(amido amine) polymers prepared using a one-pot synthesis.⁶⁰ This maximum occurs when the molecular weight of the polymer begins to increase more rapidly than its size due to the multiplicity of the dendritic branches. For spherical dendritic systems, each generation contributes linearly to the effective viscometric radius such that the volume of the dendrimer scales as g^3 where g is the generation number. However, the molecular weight scales as B^{g-1} , where N is the branch multiplicity. Thus, the generation at which a maximum in the intrinsic viscosity is reached can be determined from g^3/B^{g-1} , or at generation $3/\ln(B)$.^{6,20} For our linear dendritic rod diblock copolymers, the effective viscometric radius does not grow linearly with generation. Instead, its value is primarily determined by the length and the flexibility of the polymer backbone. Since the dimensions of a polymer do not grow linearly with the addition of branches, but rather much slower, so too will the effective radius of the linear-dendritic rod diblock copolymers as the number of branches along the backbone and thus, its stiffness, increases. However, the molecular weight of the linear-dendritic rod diblock copolymer will continue to scale approximately as $(B^g - 1)$. Therefore, since the size of the linear-dendritic rod diblock copolymers increases more slowly than that of spherical dendrimers, but the molecular weight scales approximately the same, it can be expected that the maximum in the intrinsic viscosity of the linear dendritic rod diblock copolymers would be reached at a lower generation than that of the spherical dendrimers. The reason for this maximum in the intrinsic viscosity of the ester terminated dendrimers is also related to the reason for the decrease in the intrinsic viscosity of the amine terminated dendrimers. For the amine terminated polymers, there are two factors that contribute to the intrinsic viscosity. The first is the nature of the end group and its interaction with the solvent and the second is the dendritic nature of the diblock copolymer. As previously mentioned, at low generation, the favorable interactions between the amine groups and the methanol will cause the polymer to expand and elongate, creating a less dense polymer. However, as the generation number increases, so does the degree of branching, and thus, the flexibility of the polymer backbone to expand and contract, as well as to elongate decreases. At these higher generations, the dendritic nature of the polymer becomes more important, and thus the ratio of the volume to the molecular weight as described above, dominates the value of the intrinsic viscosity resulting in polymers that have a higher density and a lower intrinsic viscosity than polymers of a lower generation.

In order to confirm that a maximum in the intrinsic viscosity would be expected at generation 1.5, a simple scaling relationship for the intrinsic viscosity has been developed, similar to that developed for spherical dendrimers. The molecular weight of the linear-dendritic rod diblock copolymer can be expected to scale approximately with that of the dendritic block, which scales as $(2^g - 1)$, or the number of branches. This scaling is slightly different than that observed for the spherical dendrimers, as the spherical dendrimers are growing in two directions whereas the dendron on the dendritic rod is only growing in one.

To determine the volume for these linear-dendritic rod diblock copolymers, scaling relationships developed for comb polymers were applied, due to the similarity of the comb polymer architecture to that of the dendritic rod block. Using a mean-field Flory-type of approach, the free energy of comb polymers has been estimated and minimized to find the radius of gyration of the polymers.^{108,109} In these calculations, the comb polymers consisted of N backbone monomers, M monomer units in each side chain, and σ side chains per backbone monomer units. It was also assumed that $N \gg M \gg 1$, and that all of the monomers and the solvent molecules occupied the same volume a^3 . Depending on the coverage of the side chains on the monomer units, σ , the comb polymer was expected to adopt either a flexible (coil-like) or an extended (rod-like) configuration. The coil-like configuration was assumed for relatively low coverage numbers, or when $\sigma \ll M^{3/5}$, in which case the average spacing of side chains along the backbone exceeded the Flory radius of the side chains, $R_m \sim aM^{3/5}$, where R_m is the radius of a sphere used to estimate the volume of the side chains. For these low aggregation numbers, the radius of the side chain was essentially unchanged by attachment to the backbone. However, when $\sigma \gg M^{3/5}$, the side chains were stretched perpendicular to the backbone due to steric crowding, and the comb polymer adopted a more rigid, bottle-brush structure. Models of these two configurations took two very different forms.

In the case of the low coverage, or a coil-like configuration, the free energy has been estimated by treating the side chains as spheres randomly placed along the backbone as illustrated in Figure 3.9 (a). The expression for the free energy is:

$$F_c = \frac{R_c^2}{Na^2} + a^3 \frac{N^2}{R_c^3} + R_m^3 \frac{(\sigma N)^2}{R_c^3} \quad (3.31)$$

where F is the free energy of the system and R_c is the radius of gyration of the comb polymer. The first term on the right hand side of this equation describes the elastic energy (configurational entropy) of deformation for a radius R_c . The second term describes the excluded volume associated with the N backbone monomers each of volume a^3 , and the third term describes the excluded volume of the σN side chains each of volume R_m^3 . To find the minimum in the equation, the derivative is taken with respect to R_c and set equal to zero, resulting in the following:

$$0 = \frac{2R_c}{Na^2} + -3a^3 \frac{N^2}{R_c^4} + -3R_m^3 \frac{(\sigma N)^2}{R_c^4} \quad (3.32)$$

Thus, the radius of gyration of a comb polymer is:

$$R_c = \left(\frac{3N^3 a^2 (a^3 + R_m^3 \sigma^2)}{2} \right)^{1/5} \quad (3.33)$$

or

$$R_c \propto N^{3/5} a^{2/5} (a^3 + R_m^3 \sigma^2)^{1/5} \quad (3.34)$$

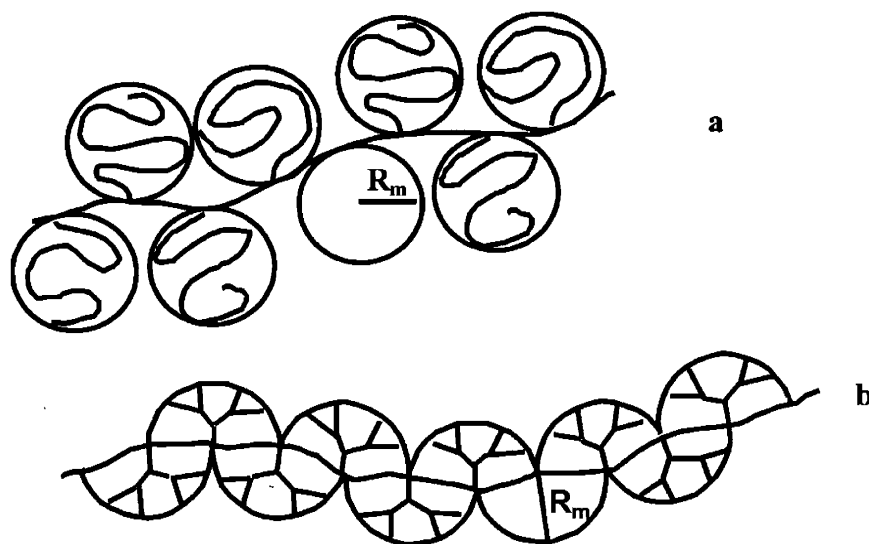


Figure 3.9. Graphical representation of the model for comb polymers in which the side chains are treated as spheres placed randomly around the polymer backbone (a). Graphical representation of the model for a dendritic rod polymer in which the dendrons are treated as hemispheres placed randomly around the polymer backbone (b).

For the high coverage limit, the bottle-brush polymer has been modeled as a wormlike chain, and the equations used to calculate the elastic constants of deformed monolayers and bilayers in surfactant and block copolymer systems have been applied. Nonetheless, for the linear-dendritic rod diblock copolymers under investigation, the low-coverage limit is the better model to apply and modify. For almost all of the generations of polymer examined, the dendritic block has been shown experimentally to adopt a coil-like shape. It is only between generations 4.0 and 4.5 that the dendritic block has been found to adopt a rod-like configuration. Thus, as the maximum in the intrinsic viscosity has been observed at low generations, and it is verification of this observation which is the motivation for determining scaling relationships for the radius of gyration, the coil-like model will be used.

As previously mentioned, R_m^3 represents the excluded volume of the side chains modeled as spheres in the coil-like model. For the dendritic rod diblock, one would not expect the dendrons to behave as spheres. A better model would be to treat them as hemispheres attached randomly along the polymer backbone, as illustrated in Figure 3.9 (b), with the radius of the hemisphere scaling linearly with the generation. Thus, R_m^3 can be replaced by the excluded volume of these hemispheres, which is $\frac{1}{2}(gan)^3$, where g is the generation number, a is the dimension of a backbone monomer unit and n is the ratio of the length of a branch to that of a backbone monomer unit. Thus, the radius of gyration of the dendritic block can be expected to scale as:

$$R_d \propto N^{3/5} a^{2/5} (a^3 + \frac{1}{2}(gan)^3)^{1/5} \quad (3.35)$$

or

$$R_d \propto N^{3/5} a (1 + \frac{1}{2} g^3 n^3)^{1/5} \quad (3.36)$$

The volume of the dendritic block can be expected to scale as:

$$V_d \propto \left[N^{3/5} a (1 + \frac{1}{2} g^3 n^3)^{1/5} \right]^3 \quad (3.37)$$

In order to simplify the problem, one can assume that the dendritic block will be the primary contributor to the radius of gyration of the entire polymer, such that the poly(ethylene oxide) block can be neglected. Therefore, the intrinsic viscosity of the linear-dendritic rod diblock copolymer can be expected to scale as:

$$[\eta] \propto \frac{[N^{3/5} a (1 + \frac{1}{2} g^3 n^3)^{1/5}]^3}{2^g - 1} \quad (3.38)$$

This maximum in the intrinsic viscosity is dependent on the relative length of the dendritic branch to that of the backbone repeat unit, n . Taking n to be 1, the maximum is found at generation one; however, taking n to be 2, the maximum is found at generation two as observed in Figure 3.10. For these poly(amido amine) dendrimers, the relative length of the branch will be dependent on the end group and its interaction with the solvent and the backbone. Thus, it is not surprising that the maximum in the intrinsic viscosity of the methyl ester terminated polymer was found at generation 1.5 (two end groups), while the intrinsic viscosity of the generation 1.0 amine-terminated polymer was higher than that of the generation 2.0 (two end groups) amine terminated polymers.

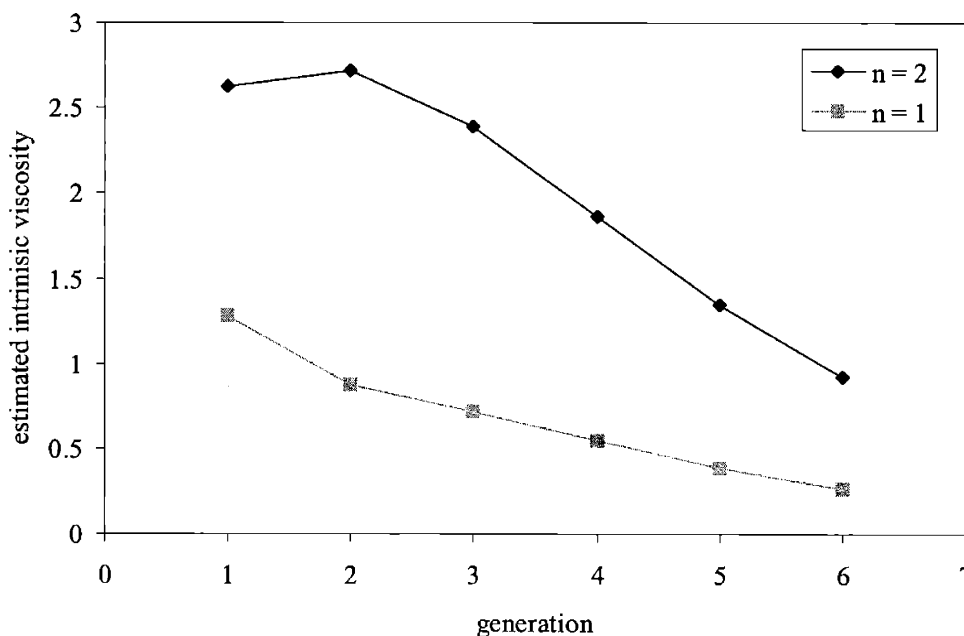


Figure 3.10. The estimated intrinsic viscosity as a function of generation for two different values of relative lengths of the branches to the monomer unit along the backbone.

Surprisingly, a minimum in the intrinsic viscosity was observed for both the amine and the ester terminated polymers at generations 3.0 and 3.5, respectively. We believe that this minimum corresponds to a transition from the polymers adopting a globular shape at lower generations, to an extended, rod-like shape at higher generations. Since the dendritic block of the linear-dendritic rod diblock copolymers possesses a flexible polymer core, it has the unique ability to undergo a shape change to a rod-like configuration at high generation when the steric crowding becomes too great. As discussed above, the intrinsic viscosity is a ratio of the volume and shape of the polymer to its molecular weight (equation 3.20). If the diblock copolymer were to continue to be spherical, one would have expected the intrinsic viscosity to continue to decrease due to its increasing density; however, this was not observed. Even if we were to assume that addition of these new branches would have caused the volume to increase such that the density remained constant, the value of the intrinsic viscosity also would have remained constant, as is seen for hyperbranched polymers. This too was not the case. In order for the intrinsic viscosity to have increased, a dramatic change in the hydrodynamic volume and/or the shape (and the shape factor, ν) of the polymer needed to occur. As can be seen in equations 2.28 and 2.29, for a prolate ellipsoid (rod) of any axial ratio, the value of the shape factor, ν , will always be greater than 2.5, which is the value of a sphere. For example, for an axial ratio of 0.8, the value of the shape factor will be 2.55, for 0.5, it will be 2.91, and for 0.2, it will be 5.79. Thus, if one had two particles of equivalent hydrodynamic volumes, the particle that was an ellipsoid would have a larger intrinsic viscosity than the particle that was a sphere. Since the increase in the intrinsic viscosity was so large, we do not believe that it could be accounted for solely by an increase in the hydrodynamic volume, but that it was also accompanied by an elongation of the dendritic block into a rod-like shape. These results are in good agreement with the dynamic light scattering results for which a dramatic increase in the hydrodynamic volume began to occur at generation 4.0, which also indicated the transition to a rod-like configuration.

As a quick aside, it is interesting to look at the absolute value of the intrinsic viscosity obtained from experiment for the poly(ethylene oxide)-poly(ethylene imine) diblock copolymer backbone with that predicted using a diblock copolymer model. Since this thesis is one of the first to report the synthesis of this diblock copolymer, molecular weight-intrinsic viscosity relationships have not yet been determined; however, information about each of the two

individual blocks is available. Weyes *et al.* have determined the Mark-Howink equation for linear poly(ethylene imine) in methanol at 25°C and found the relationship $[\eta] = 1.04 \times 10^{-2} M^{0.95}$.¹⁰⁷ (Linear poly(ethylene imine) is known to take on a helical conformation due to intramolecular hydrogen bonding, and the high value of the “a” parameter is a reflection of the stiffness of the polymer.) For a poly(ethylene imine) block of molecular weight of approximately 4400g/mol, this corresponds to an intrinsic viscosity of approximately 0.0301ml/mg. The intrinsic viscosity of poly(ethylene oxide) of molecular weight 1900g/mol has been found to be approximately 0.0077ml/mg in water at 30°C.¹⁶ One simple model that has been used to determine the intrinsic viscosity of diblock copolymers assumes that the hydrodynamic volumes of each of the blocks are additive, resulting in the relationship:

$$[\eta] = w_1 [\eta]_1 + w_2 [\eta]_2 \quad (3.39)$$

where w_1 and w_2 are the weight fractions of each of the blocks.²⁰ Applying this model and using the information for each of the two blocks gives:

$$[\eta] = \frac{4400}{6300} (0.0301 \text{ ml/mg}) + \frac{1900}{6300} (0.0077 \text{ ml/mg}) = 0.0233 \text{ ml/mg}$$

This predicted value for the intrinsic viscosity of the poly(ethylene oxide)-poly(ethylene imine) diblock copolymer corresponds well to the actual value of 0.0238ml/mg determined from experiment. Unfortunately, the intrinsic viscosity of poly(amido amine) rod homopolymers is not known, so a similar analysis can not be made for the higher generation diblock copolymers.

3.5.2.3 Determination of Size

Once the value of the intrinsic viscosity had been obtained for each of the linear-dendritic rod diblock copolymers, it was used to try to determine the dimension of each of the polymers. As in the case of the dynamic light scattering, the intrinsic viscosity of a particle is influenced by both the size and the shape of the particle. For particles that are spherical in shape, a viscometric radius can be calculated using equation 3.25. However, most particles are not spherical, most are ellipsoidal such that a more accurate calculation of their dimension can be made using equations 3.23 and 3.29. Unfortunately, application of these equations is extremely difficult as they contain two unknowns, the volume and the axial ratio of the particle. These equations can only be used if one of the variables can be accurately determined or estimated using some other technique, which isn't always possible. Nonetheless, for particles with aspect ratios between 0.5

and 1, a spherical approximation to determine the viscometric volume is reasonable since it will only overestimate the calculated viscometric volume by a factor of less than 1.2 and the viscometric radius of a sphere of equal volume by a factor of less than 1.06. However, the axial ratio, and thus the other particle dimensions cannot be extracted accurately from this information. Since most of our linear-dendritic rod diblock copolymers, especially those of low generation, can be expected to take on a spherical shape or an ellipsoidal one with an axial ratio between 0.5 and 1, the spherical approximation should be a good one for most of our polymers. It is only at high generation that it might break down, but it should offer a good basis for comparison between generations. In addition, since a spherical approximation was made in order to determine the hydrodynamic radii of the polymer using dynamic light scattering, a spherical approximation for the viscometric radius offers consistency between the two experiments. Thus, the viscometric radius of a sphere of equivalent volume will be determined for each of our linear-dendritic rod diblock copolymers from the intrinsic viscosity data.

Another important consideration when determining the size of the polymers was whether they were behaving as isolated polymers in solution or whether they had aggregated into more complex micellar structures. The viscometric radius of any particle, an individual polymer or an entire micelle, can be calculated using equation 3.25, $R_v = \{3[\eta]M/(4*2.5\pi N_A)\}^{1/3}$, which is dependent on both the intrinsic viscosity and the molecular weight, M , of the particle. For an isolated polymer in solution, the molecular weight is simply that of the individual polymer; however, for micelles, the molecular weight is that of the entire micelle,¹¹⁰ which is the molecular weight of one of the molecules in the micelle times the number of molecules in the micelle. Thus, for a given particle with a given intrinsic viscosity, the radius calculated assuming a micelle of n molecules will be $(n^{1/3})$ times greater than that calculated assuming just one molecule. For example, a dimer of a molecule will have a calculated radius approximately 1.26 times greater than that assuming a unimolecular micelle, and a micelle made up of eight molecules will have a calculated radius two times that of the monomer. Thus, by comparing the viscometric radius calculated assuming different aggregation numbers with the measured hydrodynamic radius, one might be able to obtain some insight into whether or not the polymers were aggregating in solution.

The viscometric radii of each of the polymers has been calculated and tabulated in Table 3.1 assuming that the polymer was as an individual particle, as well as if it were to have

aggregated into dimers, trimers, and octamers in solution. Also included in this table are the hydrodynamic radii determined from dynamic light scattering as well as the ratios of the viscometric to the hydrodynamic radii assuming these different aggregation numbers.

In general, it has been found that the ratio of the viscometric radius to the hydrodynamic radius of linear polymers is approximately 1.1, while that of branched polymers approaches 1.0 as the degree of branching increases. For example, Bauer *et al.* found this to be the case for linear and star versions of polyisoprene,⁸⁵ and Roovers and Toporowski found the ratio to be near unity for a wide variety of polystyrene branching architectures.¹¹¹ For spherical micelles of diblock copolymers, the ratio of the viscometric to the hydrodynamic radii has also been found to be approximately 1.0.^{112,113}

Therefore, in order to determine whether the linear-dendritic rod diblock copolymers were acting as individual polymers or had formed larger aggregates in solution under these conditions, the number of polymers in the particle was chosen such that the ratio of the viscometric to the hydrodynamic radii was approximately 1.0-1.1. For all of the polymers investigated, it appears as if the assumption that the linear-dendritic rod diblock copolymers under investigation form unimolecular micelles, or at the most dimers, is the best fit. Since there is some intrinsic error in the experiments, a more complex analysis of the data will not be made as it may only lead to incorrect conclusions. Nonetheless, it can be easily ruled out that the polymer formed huge micelles with aggregation numbers above ten, as an aggregation number of eight already gave a viscometric size that would be approximately twice that which was expected based on the measured hydrodynamic volume. It is not surprising that the polymers did not appear to aggregate in solution as methanol is a good solvent for both the poly(amido amine)²² as well as the poly(ethylene oxide) chemistry.¹¹⁴ In the first paper published about the poly(amido amine) spherical dendrimers, Tomalia *et al.* hypothesized that the reason that the amine terminated polymers exhibited larger intrinsic viscosities than the ester terminated polymers was that the amine polymers were aggregating in solution due to hydrogen bonding; however, they did not offer any additional evidence to support their claim. Nonetheless, after an extensive search of the literature, we have not been able to find other papers that mention the aggregation of either the amine or the ester terminated polymers in methanol solutions, and methanol has commonly been used to study the dimensions of isolated dendrimers in solution.^{21,22}

| Generation | Hydrodynamic radius R_H (nm) | Viscometric radius R_V (nm) (molecules in micelle) | Ratio of R_V/R_H (molecules in micelle) |
|------------|-----------------------------------|--|--|
| 0 | 2.44 | (1) 2.88 (2) 3.63 (3) 4.15 (8) 5.76 | (1) 1.18 (2) 1.49 (3) 1.70 (8) 2.36 |
| 0.5 | 2.78 | (1) 2.76 (2) 3.48 (3) 3.98 (8) 5.52 | (1) 0.99 (2) 1.25 (3) 1.43 (8) 1.99 |
| 1.0 | 2.58 | (1) 3.22 (2) 4.06 (3) 4.64 (8) 6.44 | (1) 1.25 (2) 1.57 (3) 1.80 (8) 2.50 |
| 1.5 | 4.38 | (1) 3.86 (2) 4.86 (3) 5.57 (8) 7.72 | (1) 0.88 (2) 1.11 (3) 1.27 (8) 1.76 |
| 2.0 | 3.52 | (1) 3.92 (2) 4.94 (3) 5.65 (8) 7.84 | (1) 1.11 (2) 1.40 (3) 1.61 (8) 2.23 |
| 2.5 | 4.04 | (1) 4.41 (2) 5.56 (3) 6.36 (8) 8.82 | (1) 1.09 (2) 1.38 (3) 1.57 (8) 2.18 |
| 3.0 | 4.09 | (1) 4.57 (2) 5.76 (3) 6.59 (8) 9.14 | (1) 1.12 (2) 1.41 (3) 1.61 (8) 2.23 |
| 3.5 | 4.56 | (1) 5.15 (2) 6.49 (3) 7.43 (8) 10.3 | (1) 1.13 (2) 1.42 (3) 1.63 (8) 2.26 |
| 4.0 | 6.15 | (1) 6.05 (2) 7.62 (3) 8.73 (8) 12.1 | (1) 0.98 (2) 1.24 (3) 1.42 (8) 1.97 |
| 4.5 | 8.25 | (1) 7.10 (2) 8.95 (3) 10.2 (8) 14.2 | (1) 0.86 (2) 1.09 (3) 1.24 (8) 1.72 |

Table 3.1. Viscometric radius calculated as a function of aggregation number and its comparison to the hydrodynamic radii for all of the generations in methanol at 25°C.

The calculated viscometric radius for the linear dendritic rod diblock copolymers assuming isolated polymers in solution is plotted as a function of generation in Figure 3.11. For comparison, the measured hydrodynamic radii of the polymers are also shown in that figure. As can be seen, there is good agreement between the radii calculated from the two experiments. Just as in the case of the hydrodynamic radii, the viscometric radii were found to slowly increase with generation up to generation 3.5, at which point the viscometric radii began to grow at a much larger rate. The reasons for the slow rate of growth for the lower generation polymers are explained in the previous section with the light scattering data. The large increase in the viscometric radii for the generation 4.0 and 4.5 polymers was most likely due to an elongation of the polymer into a more rod-like configuration. The possibility of the large increase being caused by aggregation has been ruled out based on the analysis described in the previous paragraph. As in the case of the hydrodynamic radii, the error in the viscometric radii assuming a spherical configuration increases as the axial ratio of the polymer approaches zero, as can be seen from equations 3.23 and 3.26. For an axial ratio of 0.2, which is a reasonable estimation for the generation 4.5 polymers, the value for the measured viscometric radius assuming a spherical shape will be approximately 1.32 times that of the real viscometric radius. Thus, for the generation 4.5 polymer, the measured viscometric radius of approximately 7.1nm would give a real effective radius of approximately 5.4nm, which fits more neatly into the trend for the viscometric radii calculated for the lower generation polymers. Thus, as we found from the light scattering results, we believe that at approximately generation 4.0, the steric interactions caused by the dendritic side groups cause the dendritic block to adopt a rod-like configuration.

The large error bars in the viscometric radii data are worth mentioning. Using the differential method, as calculated in equation 3.30, it was found that the factor that contributed the most to the possible error was the molecular weight of the polymer. The molecular weight was estimated from NMR experiments by comparing the number of protons from the poly(ethylene oxide), whose length was known, with those from the dendritic block. As integration is not always perfect, an error of 2.3 repeats out of approximately 97, or approximately 2.3%, was used. This percentage is probably an overestimation of the error in the molecular weight, but was used to err on the side of caution.

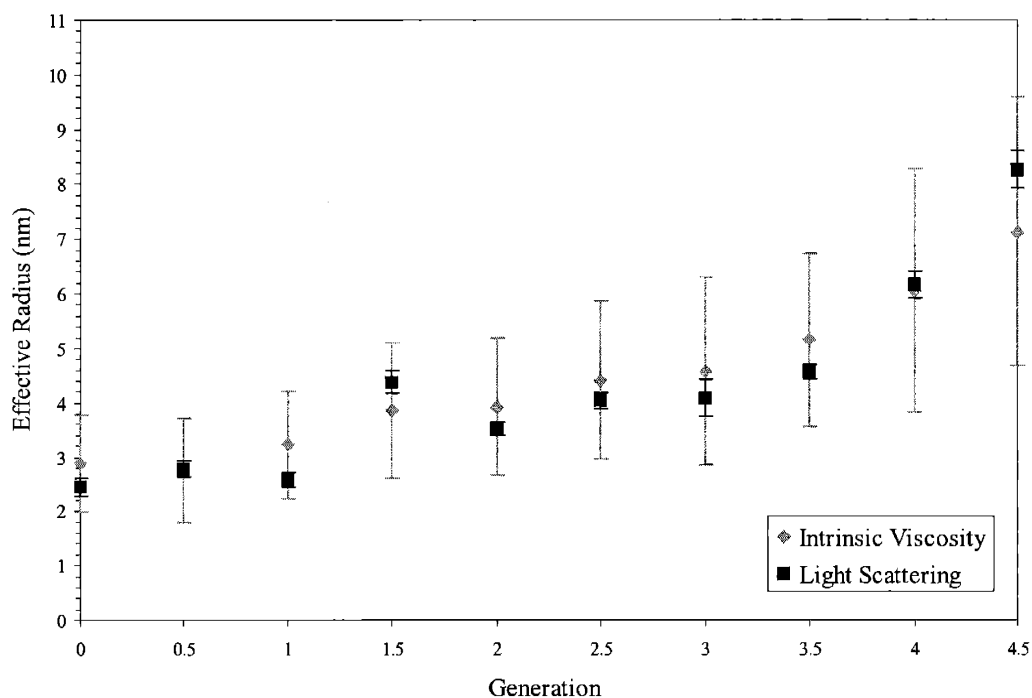


Figure 3.11. The hydrodynamic and the viscometric radii of the polymers as a function of generation in methanol at 25°C and assuming a spherical shape.

3.6 Summary and Conclusions

The solution behavior of a series of poly(ethylene oxide)-poly(ethylene imine) linear-dendritic rod diblock copolymers was examined in methanol at 25°C using the techniques of dynamic light scattering and viscometry. From dynamic light scattering, the hydrodynamic radii of the polymers were measured as a function of polymer concentration, end group chemistry, and generation. Similarly, viscometry was used to determine the intrinsic viscosity and the viscometric radii of the polymers as a function of end group chemistry and generation. By comparing the results of these two experiments, we not only were able to determine the sizes of the polymers in solution, but we were also able to gain insight into the effect these parameters on the aggregation and shape of the polymers in solution.

Dynamic light scattering was used to determine the hydrodynamic radii of the polymers using a spherical approximation. A spherical approximation was employed as it was nearly

impossible to accurately extract the dimensions of the polymer assuming an ellipsoid, since the necessary equation contained more than one unknown variable. The hydrodynamic radii of the polymers were found to increase slowly with increasing generation up to generation 3.5; however, after generation 3.5, the hydrodynamic radii were found to increase very rapidly. This rapid increase in the hydrodynamic radii can be explained by an elongation of the dendritic block into a more rod-like configuration due to the steric hinderance of the dendritic side groups. This elongation would result in not only a larger hydrodynamic volume but also a breakdown of the spherical approximation, resulting in an overestimation of the hydrodynamic radii. The generation number that we have determined for the transition to a rod-like configuration is in good agreement with that reported for the poly(amido amine) dendritic rod homopolymers. Nonetheless, the chemistry of the end group did not seem to have a large effect on the measured hydrodynamic radii. Finally, for all of the polymers, the hydrodynamic radii were found to increase slightly with decreasing concentration indicating that the polymers were behaving as polyelectrolytes in solution. This behavior also indicated that the polymers were not forming aggregates over the concentration range that was examined or that the critical micelle concentration was well below that which was examined.

Viscometry was used to determine the intrinsic viscosity of the polymers, and from that, their viscometric radii using a spherical approximation. As in the case of dynamic light scattering, the intrinsic viscosity of a particle is dependent on not only its size but also its shape. Unfortunately, the determination of the dimensions of the polymer using an ellipsoidal model was extremely difficult as there was more than one unknown in the equation relating the intrinsic viscosity to the polymer dimensions. For ease and consistency with the dynamic light scattering results, a spherical approximation was also made when calculating the viscometric radius. In order to determine the intrinsic viscosity of the polymers, their reduced viscosity was first plotted as a function of concentration using the Huggins and Kramer equations. While the low generation amine terminated polymers obeyed these equations, giving a linear relationship, the low generation ester terminated polymers as well as the higher generation polymers did not, as their application resulted in lines which had an upward curvature. Attempts were also made to fit the data to the Fuoss equation which has been used for traditional polyelectrolytes, but this too was unsuccessful. However, the data from all of the polymers could be successfully plotted using the Fedors equation, and thus this equation was used to determine the intrinsic viscosity of

all of the polymers. Previously, the Fedors equation had been applied to polymers in the dilute to semi-dilute regime as well as to aqueous solutions of polyelectrolytes whose data could also be fitted using the Fuoss equation. Since the concentration range employed in the viscosity experiments was well below that of semi-dilute regime, we believe that these linear-dendritic rod diblock copolymers were in fact behaving as polyelectrolytes, but that the traditional polyelectrolyte effect was being muted by the nature of the solvent and its interaction with the polyelectrolyte counterions. At higher polymer concentrations, the polyelectrolyte and the counterion were forming stable ion pairs (counter ion condensation), resulting in traditional polymer behavior for the viscosity. However, in more dilute polymer solutions, dissociation of the counterions from the polyelectrolyte occurred as the methanol was better able to solvate the counterions away from the polyelectrolyte giving rise to more traditional polyelectrolyte behavior. These results were in good agreement with those obtained from dynamic light scattering. Nonetheless, to our knowledge, this thesis is the first to report the use of the Fedors equation for polyelectrolytes in less polar solvents whose behavior could not be described by either the Huggins or the Fuoss equations.

The intrinsic viscosity of the amine and ester terminated polymers was found to follow two different trends at low generation that merged into one trend at higher generations. At low generations, the chemistry of the end groups and its interaction with the solvent were found to be more important, while at higher generations, the highly branched nature of the dendritic block was the more important factor. For the half generation ester terminated polymers, a maximum in the intrinsic viscosity occurred which is similar to that seen in traditional spherical dendrimers. This maximum occurred at the generation where the molecular weight of the dendritic block was beginning to grow more rapidly than its size due to its highly branched nature. The decrease in the intrinsic viscosity of the amine terminated polymers with increasing generation can be related to this same effect. In order to confirm the generation at which the maximum in the intrinsic viscosity would be expected, a simple scaling relationship for the intrinsic viscosity has been developed. The molecular weight of the diblock copolymers was found to scale as $2^g - 1$. To find a scaling relationship for the volume, the equations used to scale the radius of gyration of a comb polymer were applied; however, instead of treating the side chains as spheres, as is done for comb polymers, the dendrons were treated as hemispheres, resulting in the volume scaling as $V \sim [N^{3/5} a(1 + 1/2g^3 n^3)^{1/5}]^3$. Thus, the volume was dependent on both the generation number, g ,

and the relative length of the dendritic branch to that of the backbone monomer unit to which it was attached, n . Thus, the maximum in the intrinsic viscosity was found to occur with either one branch end or with two branch ends, depending on the value of n . For these poly(amido amine) dendrimers, the relative length of the branch will be dependent on the end group and its interaction with the solvent and the backbone. Thus, it is not surprising that the maximum in the intrinsic viscosity of the methyl ester terminated polymer was found at generation 1.5 (two end groups), while the intrinsic viscosity of the generation 1.0 amine-terminated polymer was higher than that of the generation 2.0 (two end groups) amine terminated polymers. Nonetheless, a minimum in the intrinsic viscosity was observed for both the amine and the ester terminated polymers at generation 3.5, which can be attributed to an elongation of the polymers into a more rod-like shape. This increase in the intrinsic viscosity above generation 3.5 resulted from the polymer not only adopting a larger viscometric radius because of its shape, but also because of the increased influence of the shape factor on the intrinsic viscosity that occurs with rod-like structures.

Finally, the hydrodynamic radii measured from dynamic light scattering were compared to the viscometric radii determined from viscometry assuming various aggregation numbers in order to gain insight into the aggregation behavior of the polymers in solution. For all of the generations of the polymers, it appeared as if they were behaving as isolated polymers in solution, or at most, aggregates of two or three, but that they were not aggregating into larger micellar structures with aggregation numbers of four or more. The viscometric radii assuming an isolated polymer in solution was found to follow the same generation dependence as that of the hydrodynamic radii, with a large increase in the radii observed after generation 3.5, which was most likely caused by an elongation of the polymer into a rod-like shape.

One thing that is important to remember is that the solution behavior of a polymer is very dependent on conditions of the experiment. Thus, it is very important to specify the conditions when describing the behavior. Therefore, these linear-dendritic rod diblock copolymers may be able to form more complex micellar structures by changing the solvent, end group, and even temperature of the experiment.

3.7 References

- (1) Tomalia, D. A.; Naylor, A. M.; Goddard, W. A. "Starburst dendrimers - molecular-level control of size, shape, surface-chemistry, topology, and flexibility from atoms to macroscopic matter," *Angewandte Chemie-International Edition in English* **1990**, *29*, 138-175.
- (2) Jönsson, B.; Lindman, B.; Holmberg, K.; Kronberg, B. In *Surfactants and Polymers in Aqueous Solution*; John Wiley & Sons: Chichester, England, 1998, p 35.
- (3) Atkins, P. W. In *Physical Chemistry*; Fourth ed.; W. H. Freeman and Company: New York, 1990, p 708.
- (4) Jönsson, B.; Lindman, B.; Holmberg, K.; Kronberg, B. In *Surfactants and Polymers in Aqueous Solution*; John Wiley & Sons: Chichester, England, 1998, p 51-52.
- (5) Hawker, C. J.; Wooley, K. L.; Fréchet, J. M. J. "Unimolecular micelles and globular amphiphiles - dendritic macromolecules as novel recyclable solubilization agents," *Journal of the Chemical Society-Perkin Transactions 1* **1993**, 1287-1297.
- (6) Fréchet, J. M. J.; Hawker, C. J.; Wooley, K. L. "The convergent route to globular dendritic macromolecules - a versatile approach to precisely functionalized 3-dimensional polymers and novel block-copolymers," *Journal of Macromolecular Science-Pure and Applied Chemistry* **1994**, *A31*, 1627-1645.
- (7) Chapman, T. M.; Hillyer, G. L.; Mahan, E. J.; Shaffer, K. A. "Hydraamphiphiles - novel linear dendritic block-copolymer surfactants," *Journal of the American Chemical Society* **1994**, *116*, 11195-11196.
- (8) van Hest, J. C. M.; Baars, M. W. P. L.; Elissen-Román, C.; van Genderen, M. H. P.; Meijer, E. W. "Acid-functionalized amphiphiles derived from polystyrene-poly(propylene imine) dendrimers, with a pH-dependent aggregation," *Macromolecules* **1995**, *28*, 6689-6691.
- (9) van Hest, J. C. M.; Delnoye, D. A. P.; Baars, M. W. P. L.; Elissen-Román, C.; van Genderen, M. H. P.; Meijer, E. W. "Polystyrene-poly(propylene imine) dendrimers: Synthesis, characterization, and association behavior of a new class of amphiphiles," *Chemistry-A European Journal* **1996**, *2*, 1616-1626.
- (10) van Hest, J. C. M.; Delnoye, D. A. P.; Baars, M. W. P. L.; van Genderen, M. H. P.; Meijer, E. W. "Polystyrene-dendrimer amphiphilic block-copolymers with a generation-dependent aggregation," *Science* **1995**, *268*, 1592-1595.
- (11) Gitsov, I.; Fréchet, J. M. J. "Solution and solid-state properties of hybrid linear-dendritic block-copolymers," *Macromolecules* **1993**, *26*, 6536-6546.
- (12) Gitsov, I.; Fréchet, J. M. J. "Novel nanoscopic architectures - linear-globular aba copolymers with polyether dendrimers as A-blocks and polystyrene as B-block," *Macromolecules* **1994**, *27*, 7309-7315.
- (13) Gitsov, I.; Lambrych, K. R.; Remnant, V. A.; Pracitto, R. "Micelles with highly branched nanoporous interior: Solution properties and binding capabilities of amphiphilic copolymers with linear dendritic architecture," *Journal of Polymer Science Part A-Polymer Chemistry* **2000**, *38*, 2711-2727.
- (14) Chang, Y.; Kwon, Y. C.; Lee, S. C.; Kim, C. "Amphiphilic linear PEO-dendritic carbosilane block copolymers," *Macromolecules* **2000**, *33*, 4496-4500.

- (15) Chang, Y. Y.; Kim, C. "Synthesis and photophysical characterization of amphiphilic dendritic-linear-dendritic block copolymers," *Journal of Polymer Science Part A-Polymer Chemistry* **2001**, *39*, 918-926.
- (16) Iyer, J.; Fleming, K.; Hammond, P. T. "Synthesis and solution properties of new linear-dendritic diblock copolymers," *Macromolecules* **1998**, *31*, 8757-8765.
- (17) Johnson, M. A. *Self-assembly of linear-dendritic diblock copolymers*; Ph.D. Dissertation, Department of Chemical Engineering, Massachusetts Institute of Technology, 2002.
- (18) Aoi, K.; Motoda, A.; Ohno, M.; Tsutsumiuchi, K.; Okada, M.; Imae, T. "Synthesis and assembly of amphiphilic tadpole-shaped block copolymers based on poly(amido amine) dendrimer," *Polymer Journal* **1999**, *31*, 1071-1078.
- (19) Tomalia, D. A.; Baker, H.; Dewald, J.; Hall, M.; Kallos, G.; Martin, S.; Roeck, J.; Ryder, J.; Smith, P. "A new class of polymers - starburst-dendritic macromolecules," *Polymer Journal* **1985**, *17*, 117-132.
- (20) Jeong, M.; Mackay, M. E.; Vestberg, R.; Hawker, C. J. "Intrinsic viscosity variation in different solvents for dendrimers and their hybrid copolymers with linear polymers," *Macromolecules* **2001**, *34*, 4927-4936.
- (21) Topp, A.; Bauer, B. J.; Klimash, J. W.; Spindler, R.; Tomalia, D. A.; Amis, E. J. "Probing the location of the terminal groups of dendrimers in dilute solution," *Macromolecules* **1999**, *32*, 7226-7231.
- (22) Topp, A.; Bauer, B. J.; Tomalia, D. A.; Amis, E. J. "Effect of solvent quality on the molecular dimensions of PAMAM dendrimers," *Macromolecules* **1999**, *32*, 7232-7237.
- (23) Dvornic, P. R.; Tomalia, D. A. "Starburst(r) dendrimers - a conceptual-approach to nanoscopic chemistry and architecture," *Macromolecular Symposia* **1994**, *88*, 123-148.
- (24) Dvornic, P. R.; de Leuze-Jallouli, A. M.; Owen, M. J.; Perz, S. V. "Radially layered poly(amidoamine-organosilicon) dendrimers," *Macromolecules* **2000**, *33*, 5366-5378.
- (25) Sayed-Sweet, Y.; Hedstrand, D. M.; Spinder, R.; Tomalia, D. A. "Hydrophobically modified poly(amidoamine) (PAMAM) dendrimers: Their properties at the air-water interface and use as nanoscopic container molecules," *Journal of Materials Chemistry* **1997**, *7*, 1199-1205.
- (26) Schmitzer, A.; Perez, E.; Rico-Lattes, I.; Lattes, A.; Rosca, S. "First example of supramolecular assemblies in water of new amphiphilic glucose-persubstituted poly(amidoamine) dendrimers," *Langmuir* **1999**, *15*, 4397-4403.
- (27) Sui, G.; Micic, M.; Huo, Q.; Leblanc, R. M. "Studies of a novel polymerizable amphiphilic dendrimer," *Colloids and Surfaces A-Physicochemical and Engineering Aspects* **2000**, *171*, 185-197.
- (28) Wang, J. F.; Jia, X. R.; Zhong, H.; Wu, H. Z.; Li, Y. Y.; Xu, X. J.; Li, M. Q.; Wei, Y. "Cinnamoyl shell-modified poly(amidoamine) dendrimers," *Journal of Polymer Science Part A-Polymer Chemistry* **2000**, *38*, 4147-4153.
- (29) Mourey, T. H.; Turner, S. R.; Rubinstein, M.; Frechet, J. M. J.; Hawker, C. J.; Wooley, K. L. "Unique behavior of dendritic macromolecules - intrinsic- viscosity of polyether dendrimers," *Macromolecules* **1992**, *25*, 2401-2406.
- (30) Matos, M. S.; Hofkens, J.; Verheijen, W.; De Schryver, F. C.; Hecht, S.; Pollak, K. W.; Fréchet, J. M. J.; Forier, B.; Dehaen, W. "Effect of core structure on photophysical and hydrodynamic properties of porphyrin dendrimers," *Macromolecules* **2000**, *33*, 2967-2973.

- (31) de Brabander-van den Berg, E. M. M.; Meijer, E. W. "Poly(propylene imine) dendrimers - large-scale synthesis by heterogeneously catalyzed hydrogenations," *Angewandte Chemie-International Edition in English* **1993**, *32*, 1308-1311.
- (32) Rietveld, I. B.; Bedeaux, D. "The viscosity of solutions of poly(propylene imine) dendrimers in methanol," *Journal of Colloid and Interface Science* **2001**, *235*, 89-92.
- (33) Rietveld, I. B.; Smit, J. A. M. "Colligative and viscosity properties of poly(propylene imine) dendrimers in methanol," *Macromolecules* **1999**, *32*, 4608-4614.
- (34) Rietveld, I. B.; Bedeaux, D. "Self-diffusion of poly(propylene imine) dendrimers in methanol," *Macromolecules* **2000**, *33*, 7912-7917.
- (35) Topp, A.; Bauer, B. J.; Prosa, T. J.; Scherrenberg, R.; Amis, E. J. "Size change of dendrimers in concentrated solution," *Macromolecules* **1999**, *32*, 8923-8931.
- (36) Bu, L. J.; Nonidez, W. K.; Mays, J. W.; Tan, N. B. "MALDI/TOF/MS and SEC study of astromol dendrimers having cyano end groups," *Macromolecules* **2000**, *33*, 4445-4452.
- (37) Jansen, J. F. G. A.; de Brabander-van den Berg, E. M. M.; Meijer, E. W. "Encapsulation of guest molecules into a dendritic box," *Science* **1994**, *266*, 1226-1229.
- (38) Jansen, J. F. G. A.; Meijer, E. W.; de Brabander-van den Berg, E. M. M. "The dendritic box - shape-selective liberation of encapsulated guests," *Journal of the American Chemical Society* **1995**, *117*, 4417-4418.
- (39) Schenning, A. P. H. I.; Peeters, E.; Meijer, E. W. "Energy transfer in supramolecular assemblies of oligo(*p*- phenylene vinylene)s terminated poly(propylene imine) dendrimers," *Journal of the American Chemical Society* **2000**, *122*, 4489-4495.
- (40) Pan, Y. J.; Ford, W. T. "Amphiphilic dendrimers with both octyl and triethylenoxy methyl ether chain ends," *Macromolecules* **2000**, *33*, 3731-3738.
- (41) Schenning, A. P. H. I.; Elissen-Román, C.; Weener, J. W.; Baars, M. W. P. L.; van der Gaast, S. J.; Meijer, E. W. "Amphiphilic dendrimers as building blocks in supramolecular assemblies," *Journal of the American Chemical Society* **1998**, *120*, 8199-8208.
- (42) Grohn, F.; Bauer, B. J.; Amis, E. J. "Hydrophobically modified dendrimers as inverse micelles: Formation of cylindrical multidendrimer nanostructures," *Macromolecules* **2001**, *34*, 6701-6707.
- (43) Merino, S.; Brauge, L.; Caminade, A. M.; Majoral, J. P.; Taton, D.; Gnanou, Y. "Synthesis and characterization of linear, hyperbranched, and dendrimer-like polymers constituted of the same repeating unit," *Chemistry-A European Journal* **2001**, *7*, 3095-3105.
- (44) Aharoni, S. M.; Crosby, C. R.; Walsh, E. K. "Size and solution properties of globular tert-butyloxycarbonyl- poly(alpha,xi-L-lysine)," *Macromolecules* **1982**, *15*, 1093-1098.
- (45) Newkome, G. R.; Moorefield, C. N.; Baker, G. R.; Johnson, A. L.; Behera, R. K. "Chemistry of micelles .11. Alkane cascade polymers possessing micellar topology - micellanoic acid-derivatives," *Angewandte Chemie-International Edition in English* **1991**, *30*, 1176-1178.
- (46) Newkome, G. R.; Moorefield, C. N.; Baker, G. R.; Saunders, M. J.; Grossman, S. H. "Chemistry of micelles .13. Unimolecular micelles," *Angewandte Chemie-International Edition in English* **1991**, *30*, 1178-1180.
- (47) Boris, D.; Rubinstein, M. "A self-consistent mean field model of a starburst dendrimer: Dense core vs. dense shell," *Macromolecules* **1996**, *29*, 7251-7260.
- (48) Degennes, P. G.; Hervet, H. "Statistics of starburst polymers," *Journal de Physique Lettres* **1983**, *44*, L351-L360.

- (49) Lescanec, R. L.; Muthukumar, M. "Configurational characteristics and scaling behavior of starburst molecules - a computational study," *Macromolecules* **1990**, *23*, 2280-2288.
- (50) Mansfield, M. L.; Klushin, L. I. "Monte-carlo studies of dendrimer macromolecules," *Macromolecules* **1993**, *26*, 4262-4268.
- (51) Murat, M.; Grest, G. S. "Molecular dynamics study of dendrimer molecules in solvents of varying quality," *Macromolecules* **1996**, *29*, 1278-1285.
- (52) Ganazzoli, F.; La Ferla, R.; Terragni, G. "Conformational properties and intrinsic viscosity of dendrimers under excluded-volume conditions," *Macromolecules* **2000**, *33*, 6611-6620.
- (53) Aerts, J. "Prediction of intrinsic viscosities of mixed hyperbranched- linear polymers," *Computational and Theoretical Polymer Science* **2000**, *10*, 73-81.
- (54) Neubert, I.; Amoulong-Kirstein, E.; Schlüter, A.-D.; Dautzenberg, H. "Polymerization of styrenes carrying dendrons of the first, second and third generation," *Macromolecular Rapid Communications* **1996**, *17*, 517-527.
- (55) Stocker, W.; Schürmann, B. L.; Rabe, J. P.; Forster, S.; Lindner, P.; Neubert, I.; Schlüter, A.-D. "A dendritic nanocylinder: Shape control through implementation of steric strain," *Advanced Materials* **1998**, *10*, 793-797.
- (56) Neubert, I.; Schlüter, A.-D. "Dendronized polystyrenes with hydroxy and amino groups in the periphery," *Macromolecules* **1998**, *31*, 9372-9378.
- (57) Percec, V.; Ahn, C. H.; Cho, W. D.; Jamieson, A. M.; Kim, J.; Leman, T.; Schmidt, M.; Gerle, M.; Möller, M.; Prokhorova, S. A.; Sheiko, S. S.; Cheng, S. Z. D.; Zhang, A.; Ungar, G.; Yeardley, D. J. P. "Visualizable cylindrical macromolecules with controlled stiffness from backbones containing libraries of self- assembling dendritic side groups," *Journal of the American Chemical Society* **1998**, *120*, 8619-8631.
- (58) Jahromi, S.; Coussens, B.; Meijerink, N.; Braam, A. W. M. "Side chain dendritic polymers: Synthesis and physical properties," *Journal of the American Chemical Society* **1998**, *120*, 9753-9762.
- (59) Hobson, L. J.; Feast, W. J. "Poly(amidoamine) hyperbranched systems: Synthesis, structure and characterization," *Polymer* **1999**, *40*, 1279-1297.
- (60) Hobson, L. J.; Kenwright, A. M.; Feast, W. J. "A simple 'one pot' route to the hyperbranched analogues of tomalia's poly(amidoamine) dendrimers," *Chemical Communications* **1997**, 1877-1878.
- (61) Gitsov, I.; Wooley, K. L.; Fréchet, J. M. J. "Novel polyether copolymers consisting of linear and dendritic blocks," *Angewandte Chemie-International Edition in English* **1992**, *31*, 1200-1202.
- (62) Fréchet, J. M. J.; Gitsov, I.; Monteil, T.; Rochat, S.; Sassi, J. F.; Vergelati, C.; Yu, D. "Modification of surfaces and interfaces by non-covalent assembly of hybrid linear-dendritic block copolymers: Poly(benzyl ether) dendrons as anchors for poly(ethylene glycol) chains on cellulose or polyester," *Chemistry of Materials* **1999**, *11*, 1267-1274.
- (63) Zhu, L. Y.; Tong, X. F.; Li, M. Z.; Wang, E. J. "Synthesis and solution properties of anionic linear-dendritic block amphiphiles," *Journal of Polymer Science Part A-Polymer Chemistry* **2000**, *38*, 4282-4288.
- (64) Al-Muallem, H. A.; Knauss, D. M. "Synthesis of hybrid dendritic-linear block copolymers with dendritic initiators prepared by convergent living anionic polymerization," *Journal of Polymer Science Part A-Polymer Chemistry* **2001**, *39*, 152-161.

- (65) Burke, S. E.; Eisenberg, A. "Effect of sodium dodecyl sulfate on the morphology of polystyrene-b-poly(acrylic acid) aggregates in dioxane-water mixtures," *Langmuir* **2001**, *17*, 8341-8347.
- (66) Burke, S.; Eisenberg, A. "Physico-chemical investigation of multiple asymmetric amphiphilic diblock copolymer morphologies in solution," *High Performance Polymers* **2000**, *12*, 535-542.
- (67) Won, Y. Y.; Paso, K.; Davis, H. T.; Bates, F. S. "Comparison of original and cross-linked wormlike micelles of poly(ethylene oxide-b-butadiene) in water: Rheological properties and effects of poly(ethylene oxide) addition," *Journal of Physical Chemistry B* **2001**, *105*, 8302-8311.
- (68) Kunieda, H.; Uddin, M. H.; Furukawa, H.; Harashima, A. "Phase behavior of a mixture of poly(oxyethylene)- poly(dimethylsiloxane) copolymer and nonionic surfactant in water," *Macromolecules* **2001**, *34*, 9093-9099.
- (69) Poppe, A.; Willner, L.; Allgaier, J.; Stellbrink, J.; Richter, D. "Structural investigation of micelles formed by an amphiphilic PEP-PEO block copolymer in water," *Macromolecules* **1997**, *30*, 7462-7471.
- (70) Nagarajan, R.; Ganesh, K. "Comparison of solubilization of hydrocarbons in (PEO-PPO) diblock versus (PEO-PPO-PEO) triblock copolymer micelles," *Journal of Colloid and Interface Science* **1996**, *184*, 489-499.
- (71) Goldmints, I.; Holzwarth, J. F.; Smith, K. A.; Hatton, T. A. "Micellar dynamics in aqueous solutions of PEO-PPO-PEO block copolymers," *Langmuir* **1997**, *13*, 6130-6134.
- (72) Tu, Y. F.; Wan, X. H.; Zhang, D.; Zhou, Q. F.; Wu, C. "Self-assembled nanostructure of a novel coil-rod diblock copolymer in dilute solution," *Journal of the American Chemical Society* **2000**, *122*, 10201-10205.
- (73) Sommerdijk, N.; Holder, S. J.; Hiorns, R. C.; Jones, R. G.; Nolte, R. J. M. "Self-assembled structures from an amphiphilic multiblock copolymer containing rigid semiconductor segments," *Macromolecules* **2000**, *33*, 8289-8294.
- (74) Jenekhe, S. A.; Chen, X. L. "Self-assembled aggregates of rod-coil block copolymers and their solubilization and encapsulation of fullerenes," *Science* **1998**, *279*, 1903-1907.
- (75) In *BI-9000AT autocorrelator instrument manual*; Brookhaven Instruments Corporation: Holtsville, New York, p A-1-D-7.
- (76) Yen, D. R. *Synthesis and characterization of poly(ethylene oxide) star molecules for biological and medical applications*, Department of Chemical Engineering, Massachusetts Institute of Technology, 1998.
- (77) Yamamoto, H.; Tomatsu, I.; Hashidzume, A.; Morishima, Y. "Associative properties in water of copolymers of sodium 2- (acrylamido)-2-methylpropanesulfonate and methacrylamides substituted with alkyl groups of varying lengths," *Macromolecules* **2000**, *33*, 7852-7861.
- (78) Bezot, P.; Hessebezot, C.; Elmakoudi, B.; Constans, B.; Faure, D.; Hoornaert, P. "Comparison of hydrodynamic and rheological properties of dilute-solutions of a styrene-hydrogenated butadiene copolymer in aliphatic solvents by light-scattering and viscometric techniques," *Journal of Applied Polymer Science* **1994**, *51*, 1715-1725.
- (79) Biddle, D.; Walldal, C.; Wall, S. "Characterisation of colloidal silica particles with respect to size and shape by means of viscosity and dynamic light scattering measurements," *Colloids and Surfaces A-Physicochemical and Engineering Aspects* **1996**, *118*, 89-95.

- (80) Richards, E. G. In *An Introduction to the Physical Properties of Large Molecules in Solution*; Cambridge University Press: Cambridge, England, 1980, p 157-159.
- (81) Rudin, A. In *The Elements of Polymer Science and Engineering*; 2nd ed.; Academic Press: New York, New York, 1982, p 99-100.
- (82) Flory, P. J. In *Principles of Polymer Chemistry*; Cornell University Press: Ithaca, New York, 1953, p 309-310.
- (83) Sperling, L. H. In *Introduction to Physical Polymer Science*; 2nd ed.; John Wiley & Sons: New York, New York, 1992, p 101-106.
- (84) Antonietti, M.; Briel, A.; Forster, S. "Quantitative description of the intrinsic viscosity of branched polyelectrolytes," *Macromolecules* **1997**, *30*, 2700-2704.
- (85) Bauer, B. J.; Fetters, L. J.; Graessley, W. W.; Hadjichristidis, N.; Quack, G. F. "Chain dimensions in dilute polymer-solutions - a light-scattering and viscometric study of multiarmed polyisoprene stars in good and theta-solvents," *Macromolecules* **1989**, *22*, 2337-2347.
- (86) Roovers, J.; Zhou, L. L.; Toporowski, P. M.; Vanderzwan, M.; Iatrou, H.; Hadjichristidis, N. "Regular star polymers with 64 and 128 arms - models for polymeric micelles," *Macromolecules* **1993**, *26*, 4324-4331.
- (87) Elias, H.-G. In *An Introduction to Polymer Science*; 1st ed.; VCH: Weinheim, 1997, p 202-211.
- (88) Dragan, S.; Ghimici, L. "Viscometric behaviour of some hydrophobically modified cationic polyelectrolytes," *Polymer* **2001**, *42*, 2887-2891.
- (89) Ullner, M.; Staikos, G.; Theodorou, D. N. "Monte carlo simulations of a single polyelectrolyte in solution: Activity coefficients of the simple ions and application to viscosity measurements," *Macromolecules* **1998**, *31*, 7921-7933.
- (90) Ng, W. K.; Tam, K. C.; Jenkins, R. D. "Evaluation of intrinsic viscosity measurements of hydrophobically modified polyelectrolyte solutions," *European Polymer Journal* **1999**, *35*, 1245-1252.
- (91) Flory, P. J. In *Principles of Polymer Chemistry*; Cornell University Press: Ithaca. New York, 1953, p 635-636.
- (92) Fedors, R. F. "Equation suitable for describing the viscosity of dilute to moderately concentrated polymer-solutions," *Polymer* **1979**, *20*, 225-228.
- (93) Ghimici, L.; Popescu, F. "Determination of intrinsic viscosity for some cationic polyelectrolytes by fedors method," *European Polymer Journal* **1998**, *34*, 13-16.
- (94) Eilers, V. H. "Die viskosität von emulsionen hochviskoser stoffe als funktion der konzentration," *Kolloid-Zeitschrift* **1941**, *97*, 313-321.
- (95) Nagarajan, R. "Are large micelles rigid or flexible a reinterpretation of viscosity data for micellar solutions," *Journal of Colloid and Interface Science* **1982**, *90*, 477-486.
- (96) Hopkins, W. G.; "A new view of statistics," Internet Society for Sport Science: 2000; <http://www.sportssci.org/resources/stats/>.
- (97) Chitanu, G. C.; Skouri, M.; Schosseler, F.; Munch, J. P.; Carpov, A.; Candaua, S. J. "Static and dynamic light scattering of maleic acid copolymers," *Polymer* **2000**, *41*, 3683-3692.
- (98) Koene, R. S.; Mandel, M. "Scaling relations for aqueous poly-electrolyte salt-solutions .1. Quasi-elastic light-scattering as a function of poly- electrolyte concentration and molar mass," *Macromolecules* **1983**, *16*, 220-227.

- (99) Forster, S.; Schmidt, M.; Antonietti, M. "Static and dynamic light-scattering by aqueous polyelectrolyte solutions - effect of molecular-weight, charge-density and added salt," *Polymer* **1990**, *31*, 781-792.
- (100) Smits, R. G.; Kuil, M. E.; Mandel, M. "Molar-mass and ionic-strength dependence of the apparent diffusion-coefficient of a flexible polyelectrolyte at dilute and semidilute concentrations - linear poly(ethylenimine)," *Macromolecules* **1993**, *26*, 6808-6816.
- (101) Smits, R. G.; Kuil, M. E.; Mandel, M. "Quasi-elastic light-scattering study on solutions of linear flexible polyelectrolytes at low ionic strengths," *Macromolecules* **1994**, *27*, 5599-5608.
- (102) Yin, R.; Zhu, Y.; Tomalia, D. A.; Ibuki, H. "Architectural copolymers: Rod-shaped, cylindrical dendrimers," *Journal of the American Chemical Society* **1998**, *120*, 2678-2679.
- (103) Ioan, S.; Simionescu, B. C.; Neamtu, I.; Simionescu, C. I. "Solution properties of ultrahigh molecular-weight polymers .10. Viscosity of dilute to moderately concentrated poly(butyl methacrylate) solutions," *Polymer Communications* **1986**, *27*, 113-116.
- (104) Kawaguchi, D.; Kawauchi, S.; Satoh, M.; Komiyama, J. "Counterion binding and ionomer-like behaviour of partially quaternized poly(4-vinyl pyridine) in aqueous alcohols," *Polymer* **1998**, *39*, 1387-1392.
- (105) Ghimici, L.; Dragan, S. "Behaviour of cationic polyelectrolytes upon binding of electrolytes: Effects of polycation structure, counterions and nature of the solvent," *Colloid and Polymer Science* **2002**, *280*, 130-134.
- (106) Rempp, P.; Merrill, E. W. In *Polymer Synthesis*; 2nd, revised ed.; Hüthig & Wepf: Basel, Switzerland, 1991, p 131.
- (107) Weyts, K. F.; Goethals, E. J.; Bunge, W. M.; Vantreslong, C. J. B. "A new Mark-Houwink equation for linear poly(ethylene imine)," *European Polymer Journal* **1990**, *26*, 445-447.
- (108) Fredrickson, G. H. "Surfactant-induced lyotropic behavior of flexible polymer-solutions," *Macromolecules* **1993**, *26*, 2825-2831.
- (109) Rouault, Y.; Borisov, O. V. "Comb-branched polymers: Monte carlo simulation and scaling," *Macromolecules* **1996**, *29*, 2605-2611.
- (110) Quintana, J. R.; Villacampa, M.; Katime, I. A. "Micellization of a polystyrene-b-poly(ethylene propylene) block copolymer in n-dodecane 1,4-dioxane mixtures .2. Structure and dimensions of micelles," *Macromolecules* **1993**, *26*, 606-611.
- (111) Roovers, J.; Toporowski, P. M. "Hydrodynamic studies on model branched polystyrenes," *Journal of Polymer Science Part B-Polymer Physics* **1980**, *18*, 1907-1917.
- (112) Schillen, K.; Yekta, A.; Ni, S. R.; Farinha, J. P. S.; Winnik, M. A. "Characterization of polyisoprene-b-poly(methyl methacrylate) diblock copolymer micelles in acetonitrile," *Journal of Physical Chemistry B* **1999**, *103*, 9090-9103.
- (113) Pispas, S.; Hadjichristidis, N.; Potemkin, I.; Khokhlov, A. "Effect of architecture on the micellization properties of block copolymers: A(2)_b miktoarm stars vs ab diblocks," *Macromolecules* **2000**, *33*, 1741-1746.
- (114) Vandermiers, C.; Damman, P.; Dosiere, M. "Static and quasielastic light scattering from solutions of poly(ethyleneoxide) in methanol," *Polymer* **1998**, *39*, 5627-5631.

Chapter 4

Langmuir Films of the Linear-Dendritic Rod Diblock Copolymers

4.1 Introduction

Due to their uniformly hyperbranched structure, large number of end groups, nanoporous interior, and controlled chemistry in both the interior and exterior regions, dendrimers have been proposed and examined as functional surfaces and interfacial materials for such applications as sensing, separations, catalysis, microelectronics, and adhesion promotion and inhibition.¹ However, for many of these surface applications, only the outermost layer of dendrimers or a very thin multilayer of dendrimers are needed to achieve the desired effect or response. Since researchers have found that dendrimers can be difficult and expensive to prepare, those working in the area have investigated ways to attach dendrimers to the surfaces of other materials in a controlled and organized manner, instead of preparing devices composed completely of dendrimers. In addition, substrates made of other materials are able to provide properties, such as strength and/or function, which cannot be provided for by a dendrimer substrate. Thus, the challenge has been to find ways in which dendrimers can be either physically adsorbed or chemically bonded to substrates in a controlled and organized manner that preserves or enhances the desirable properties of the dendritic structure. Four main approaches have been investigated for the formation of thin, ordered dendritic films on substrates. The first involves the covalent attachment of dendrimers to self-assembled monolayers;²⁻¹¹ the second involves the buildup of dendritic multilayers using coordination chemistry,¹² reactive functional groups,¹³⁻¹⁵ electrostatic assembly,¹⁶⁻²⁰ or hydrophilic/hydrophobic interactions;²¹ the third involves drop- and spin-casting dendrimers from dilute solution;²²⁻³⁶ finally, the fourth involves the formation of ordered Langmuir films of amphiphilic dendrimers or their block copolymer derivatives at the air/water interface, and the subsequent transfer of these ordered films to solid substrates using the Langmuir-Blodgett technique.³⁷⁻⁴⁴ Of these methods, only the Langmuir-Blodgett technique offers the advantage of controlling both the thickness of the dendritic film as well as the orientation of the dendrimers within the film. However, before an amphiphilic dendrimer can be

transferred to a solid substrate, the behavior and organization of that polymer at the air/water interface needs to be well understood as that organization will determine whether a Langmuir-Blodgett film can be formed, and if it can, will be indicative of the organization within the transferred film. In addition, the study of Langmuir films of these amphiphilic dendrimers can be used to probe such properties of the dendrimers as their shape, compressibility, and localization of the end groups.¹ Up to this point, almost all of the research in the study of dendritic films at the air/water interface has focused on the study of amphiphilic spherical dendrimers or their diblock copolymer derivatives, which possess only three or four dendrons radiating out from a central core. Only one study has been done to examine the behavior of dendritic rod homopolymers at the air/water interface.^{45,46} However, a much better understanding of the effect of dendritic architecture on the Langmuir behavior is needed because architecturally unique dendritic systems, such as dendritic rods, may exhibit a different ordering at the air/water interface due to their geometry.

Thus, since the architecture of the linear-dendritic rod diblock copolymers prepared in this thesis is completely unique, an investigation of the behavior of these polymers at the air/water interface will be the focus of this chapter. These diblock copolymers are of interest because they may exhibit a unique organization at the air/water interface as their assembly will not only be governed by their dendritic nature but also by their diblock copolymer nature. In addition, while several different dendritic chemistries have been functionalized with alkyl chains, no one has yet conducted a comprehensive study on the effect that the alkyl chain length has on the surface pressure, the surface area, and the arrangement of the polymers in the films formed. (Other groups have only looked at one, two, or three alkyl chain lengths and they have been over a very small alkyl chain length range.) In the remainder of this chapter, Section 4.2 will provide background information on the behavior of other dendritic and diblock copolymer systems at the air/water interface, and Section 4.3 will describe the materials, instrumentation, and experimental procedure used to study the behavior of these linear-dendritic rod diblock copolymers at the air/water interface. Section 4.4.1 presents the pressure/area isotherms that were collected for the various polymers examined. An in-depth discussion of the effect of the length of the terminal alkyl chain, the generation number, and the length of the dendritic block on the surface pressure and area are given in Sections 4.4.2 and 4.4.3. Section 4.4.4 talks about the compressibility of the films, and Section 4.4.5 the reversibility and reproducibility of the isotherms as a function of

these same parameters. Based on the pressure/area isotherms, a model for the arrangement of the polymers in the films is presented in Section 4.4.6. Finally, a chapter summary and concluding remarks are presented in Section 4.5, and the references in Section 4.6.

4.2 Background

4.2.1 Spherical Dendritic Homopolymers

The first type of dendrimers that were examined at the air/water interface were the poly(benzyl ether) (Fréchet type) dendrimers. Saville *et al.* studied the behavior of a series of poly(benzyl ether) dendrons at the air/water interface as a function of generation.^{47,48} These dendrons consisted of a hydrophilic hydroxymethyl group at the core and hydrophobic benzyl ether chain ends. Within this series, they found that the generation two through four dendrons exhibited surfactant-like behavior, but that the larger, generation five and six dendrons did not as the hydroxymethyl core became sterically shielded from the water by the branches of the larger dendrons. From neutron reflectivity, they also found that as the amphiphilic dendrons were compressed, they were squeezed from a spherical to a prolate shape at the air/water interface before they eventually collapsed to form multilayers. Kirton *et al.* later examined the effect of chain end chemistry on the behavior of poly(benzyl ether) dendrons at the air/water interface.⁴⁹ The dendrons employed in their work were the same as those used in the Saville work, except that they were substituted with either a methyl ester or a cyano group at the para position of the peripheral benzyl ether groups. They found that the slightly more hydrophilic methyl ester and cyano groups formed more stable bilayers and led to larger cross-sectional area for the polymers. This was due to flattening of the polymers at the air/water interface caused by the favorable interactions between the hydrophilic groups and the water surface. They also found that upon compression, the polymers with the methyl ester and cyano groups were more likely to become dissolved in the water than to form bilayers as the unsubstituted polymers did. Inspired by the work of Saville *et al.* in which the relative size of the dendron focal point to the overall dendron size was found to be important in the behavior of the dendrons at the air/water interface, Kampf *et al.* studied the effect of dendron focal point size and chemistry on poly(benzyl ether) dendrons terminated with benzyl ether end groups by adding oligo(ethylene glycol) chains of varying length to the focal point of the dendron.⁵⁰ They found that the stability of the monolayers increased with increasing length of the oligo(ethylene glycol units) as the longer oligo(ethylene

glycol) chains were able to interact more strongly with the water subphase; however, the amount of this increase was influenced to a larger extent by the relative sizes of the dendron and the oligo(ethylene glycol) core than the absolute size of the oligo(ethylene glycol) core. Finally, they concluded that the higher generation dendrons produce more stable monolayer films as the dispersive interactions between the neighboring hydrophobic groups were increased by the larger size of the dendrons. Similarly, Pao *et al.* examined poly(benzyl ether) dendrons functionalized with hydrophobic dodecyl chains at the periphery, and hydrophilic crown ether and oligo(ethylene glycol) units at the core.⁵¹ Using X-ray reflectivity, they found that the hydrophilic cores ground the dendrons to the surface of the water, the benzyl ether dendrons formed a high density region just above the surface, and the alkyl chains extended upward, perpendicular to the surface. In another closely related study, Sidorenko *et al.* examined the behavior of poly(benzyl ether) dendrimers with dodecyl chain ends and an azobenzene crown ether core.⁵² They also found that upon compression, the dodecyl chains were aligned perpendicular to the surface at lower generations; however, at higher generations, generation two and three, the dodecyl chains were oriented radially due to the curvature of the dendritic portion. Due to their orientation, the alkyl chains did not crystallize. In addition, photoswitching of the azobenzene core resulted in a mechanical response for the entire dendritic film in the generation one and two polymers as indicated by an increase in the surface area of the polymer. However, the films formed from the higher generation polymers did not show this response, as the dendritic block was too big. Finally, Cui *et al.* have been able to prepare an amphiphilic dendron, which in essence is the reverse of the Pao dendron, and have looked at its behavior at the air/water interface.³⁹ These amphiphilic dendrons consisted of a hydrophobic dodecyloxyphenol core to which poly(benzyl ether) dendrons were attached. The dendrons were functionalized with hydrophilic carboxylic acid groups in the para position of the peripheral benzyl ether groups creating a dendron with multi-hydrophilic head groups and a single hydrophobic tail group. They found that these amphiphilic dendrons were also able to form stable monolayers at the air/water interface with the area per molecule determined by the size of the hydrophilic dendritic group and not the hydrophobic alkyl group. They have also been able to transfer these films to glass and mica substrates producing Langmuir-Blodgett monolayers which exhibited a periodic intralayer ordering.

Researchers have also looked at the ordering of poly(amido amine) (PAMAM) dendrimers at the air/water interface. Sayed-Sweet *et al.* were the first to examine hydrophilic PAMAM amine terminated dendrimers, which were functionalized with various hydrophobic epoxyalkanes (hexane, octane, and dodecane) at the ends of the dendrimer.⁵³ They found that changing the length of the hydrophobic alkyl chain on the periphery of the dendrimer did not have a significant effect on the surface area occupied by the polymer even at the collapse point and that this area per molecule was found to be larger than the value obtained from size exclusion chromatography (SEC). Thus, they proposed a model in which the hydrophilic PAMAM interior flattened and interacted with the water surface and the hydrophobic chain ends extended outward, perpendicular to the air/water interface. (This model was somewhat different from that proposed by Saville *et al.* for poly(benzyl ether) dendrimers, as the poly(benzyl ether) dendrimers were found to elongate vertically upon pressure whereas the poly(amido amine) dendrimers were found to elongate laterally upon compression.) They also implied, but did not state outright, that the collapse pressure of approximately 46-48mN/m was independent of alkyl chain length. However, they did state that the addition of sulfuric acid to the subphase increased the collapse pressure 10-15% and that the incorporation of copper nanoparticles into the dendrimer structure also slightly increased the collapse pressure. Sui *et al.* have looked at the functionalization of PAMAM dendrimers with other hydrophobic groups. They have attached 10, 12 pentacosadiynoic acid to the end groups of second and third generation PAMAM dendrimers.⁵⁴ These hydrophobic groups contained acetylene triple bonds which could be polymerized by UV radiation. Upon compression, the amphiphilic dendrimers arranged themselves in a manner similar to that observed by Sayed-Sweet in which the PAMAM dendrimers interfaced with the water and the hydrophobic chains extended up into the air perpendicular to the surface. They were then able to polymerize the acetylene groups to form a highly branched polymerized macromolecule at the air/water interface. By tuning the size of the dendrimer and the nature of the hydrophobic substituent, Sui *et al.* have also been able to change the orientation of the PAMAM dendrimers at the air/water interface.⁴² As previously mentioned, the preferred orientation of amphiphilic PAMAM dendrimers at the air/water interface is in a “face-on” configuration, with the hydrophilic dendrimer lying flat, or almost flat, on the surface of the water, and the hydrophobic substituents extending up into the air, perpendicular to the interface. However, by attaching 12-hydroxyldodecanoic acid chains, which have a terminal

hydroxyl group, to the chain ends of a fourth generation PAMAM dendrimer, they found that the dendrimer preferred to adopt an “edge on” configuration upon compression. In this configuration, both the hydroxydodecane chains and the dendrimer lie perpendicular to the air/water interface, with the hydroxydodecane chains interacting with both the air and the water and the dendrimer sandwiched between the two. They believe that the hydroxy end groups led to an increase in hydrogen bonding between the chains ends and thus a flattening of the dendrimer structure. In addition, the increased size of the dendrimer employed led to increased core-core interactions and thus the likelihood of the “edge on” configuration. Transfer of the films to hydrophilic mica resulted in the formation of a new hydrophilic surface, which was only possible with an “edge on” configuration.

Schenning *et al.* have examined the behavior of amphiphilic poly(propylene imine) dendrimers at the air/water interface.^{41,55} For the dendrimers which were terminated with palmitoyl, alkyl azobenzene, and oligo(*p*-phenylene vinylene) groups, they found that the surface area per molecule of the polymer was directly proportional to the number of hydrophobic end groups. Thus, for these systems, they proposed a model in which the poly(propylene imine) dendrimers were lying flat on the surface - anchoring the polymer to the surface, and the hydrophobic groups were extended perpendicular to the surface. However, they found that dendrimers which had been terminated with adamantane groups did not fit this model. The adamantane groups were too bulky to be able to pack perpendicular to the surface and they distorted the dendrimer from its flat arrangement at the surface. These polymers did not behave as amphiphiles but rather formed multilayers upon compression. They also found that the surface pressure of the polymer was highly dependent on the type of hydrophobic group with which the dendrimers were terminated, and it exhibited very little dependence on the generation number of the dendrimer. In addition, they found that they were able to transfer the palmitoyl, azobenzene, and oligo(*p*-phenylene vinylene) terminated dendrimers to solid substrates and that the azobenzene and oligo(*p*-phenylene vinylene) terminated dendrimers exhibited a blue shift in UV-vis spectrometry due to the parallel packed arrangement of the hydrophobic groups. Finally, the azobenzene derivatives were also able to form photoresponsive Langmuir and Langmuir-Blodgett films when illuminated with UV and IR light, as indicated by changes in the surface area of the polymer at constant pressure.^{41,43,55}

4.2.2 Dendritic Rods

The only research into the behavior of dendritic rod homopolymers at the air/water interface has been conducted by Bo *et al.*^{45,46} They have examined the behavior of three different amphiphilic rod systems which possessed a poly(*p*-phenylene) backbone, poly(benzyl ether) dendritic branches, and a lengthwise (not block-wise) amphiphilic nature. The first system consisted of two dendrons on each repeat of the backbone, one which was a hydrophobic benzyl ether terminated dendron and the other which was a hydrophilic dendron which had been end-capped with oligo(ethylene glycol). The second system consisted of one hydrophobic poly(benzyl ether) terminated dendron and a hydrophilic linear chain of oligo(ethylene glycol) on each repeat of the backbone, and the third system consisted of one hydrophilic dendron which has been end-capped with oligo(ethylene glycol) and one hydrophobic dodecane chain on each repeat of the backbone. Only the two polymer systems which possessed a hydrophobic dendron along the backbone formed reproducible, stable monolayers at the air/water interface. In these monolayers, the polymer backbone was oriented parallel to the air/water interface and the oligo(ethylene glycol) chains of the dendron perpendicular to the interface. Unfortunately, they did not offer any explanation as to why the polymer with the hydrophobic dendron and the hydrophilic oligo(ethylene glycol) chains did not form a reproducible monolayer; however, it can be hypothesized that it was caused by the very large imbalance of hydrophobic and hydrophilic components in the system.

4.2.3 Hybrid-Linear Dendritic Diblock Copolymers

While several hybrid-linear dendritic diblock copolymers have been prepared, only a few of these polymers have been examined at the air/water interface. The first group to look at these polymers at the air/water interface was van Hest *et al.* who studied the interfacial behavior of amphiphilic polystyrene-poly(propylene imine) dendrimers.⁵⁶ They found that the polymers arranged such that the hydrophilic poly(propylene imine) dendrimers were attracted to the interface and the hydrophobic polystyrene rested in the air above the dendrimer. At low generations, solid polystyrene films formed whose interactions were dominated by the polystyrene block; however, at high generations (8 and 16 end groups), the dendritic block was large enough so that the interactions between these blocks began to govern the areas occupied by the diblock copolymers and the type of films that formed. Iyer *et al.* have looked at the

interfacial behavior of amphiphilic hybrid-linear dendritic diblock copolymers systems which have a hydrophilic poly(ethylene oxide) block and a hydrophobic stearate terminated poly(amido amine) block.^{40,57} Not surprisingly, these polymers were found to arrange at the air/water interface in the opposite manner to those of the polystyrene-poly(propylene imine) dendrimers since the amphiphilic nature of the diblock copolymer was reversed. From pressure/area isotherms and neutron reflectivity measurements, they found that the low generation polymers arranged such that the poly(ethylene oxide) block formed a segregated layer just below the surface of the water, the poly(amido amine) branches formed a layer above the poly(ethylene oxide), and the stearate groups arranged themselves perpendicular to the air/water interface above the PAMAM branches. As Sayed-Sweet and Schenning found, the surface area occupied by the polymers was directly proportional to the number of stearate groups. For polymers at high generation, generation four and above, they found that the poly(ethylene oxide) formed a separate layer with the PAMAM dendrimer and stearate groups lying above it. However, the poly(amido amine) layer was smaller than predicted for all of the stearate groups implying compression and mixing between the poly(amido amine) interior and the stearate exterior. Iyer *et al.* were able to transfer these linear-dendritic diblock copolymers to solid substrates and prepare bi- and multilayers. While the bilayers readily formed the multilayers did not. Since poly(ethylene oxide) by itself is known to be self-repulsive, the multi-layers were only formed when poly(methacrylic acid) was added to the subphase forming a hydrogen bonding adhesive between the layers. Aoi *et al.* have looked at another amphiphilic poly(amido amine) based linear-dendritic diblock copolymer at the air/water interface.⁵⁸ Their diblock copolymer consisted of a hydrophobic PAMAM dendrimer functionalized with hexyl groups attached to a linear, hydrophilic polysarcosine polymer. From surface tension measurements, they found that the polymer was arranged such that the hydrophilic polysarcosine chain was dissolved in the water, the poly(amido amine) branches formed a layer at the air/water interface, and the hexyl chains were arranged above and perpendicular to the interface.

4.2.4 Rod-Coil Diblock Copolymers

As previously mentioned, it is important to remember that the linear-dendritic rod diblock copolymer under investigation is not only a dendrimer, but also a diblock copolymer and its behavior at the air/water interface will also be controlled by block copolymer segregation. A few

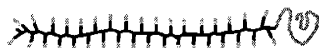
groups have examined the behavior of rod-coil di- and multiblock copolymer systems at the air/water interface. Higashi *et al.* have prepared an amphiphilic poly(γ -benzyl-L-glutamate)-b-poly(L-glutamic acid) (PBLG-b-PLGA) copolyptide where the PBLG block formed a rigid rod hydrophobic helical structure and the PLGA a less rigid hydrophilic helical structure.⁵⁹ Since the PBLG block was more rigid and possessed a larger cross-sectional area, upon compression it prevented both polypeptides from forming beta sheets and allowed each of the blocks to maintain their helical conformations. These diblock copolymers were found to orient perpendicular to the air/water interface and had a tilt angle of 33° when transferred to solid surfaces. Toyotama *et al.* have looked at a similar system which consisted of a poly(γ -methyl-L-glutamate)-b-poly(ethylene glycol) diblock copolymer.⁶⁰ They too found that the more rigid poly(γ -methyl-L-glutamate) polypeptide block oriented itself perpendicular to the air/water interface and the poly(ethylene glycol) served as the interface between the water and the polypeptide. Finally, Sommerdijk *et al.* have examined multiblock copolymers consisting of hydrophilic poly(ethylene oxide) segments and rigid, hydrophobic poly(methylphenylsilane) (PMPS) segments.⁶¹ From the pressure/area isotherms and Brewster angle microscopy, they found that the rigid PMPS segments aligned perpendicular to the air/water interface and the hydrophilic poly(ethylene oxide) segments formed interfaces with both the air above and the water below the PMPS segments.

4.3 Experimental

4.3.1 Materials

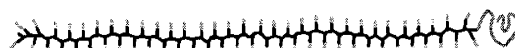
The synthesis and characterization of all of the polymers examined in this chapter are described in chapter 2. A graphical summary of the polymers is given in Figure 4.1. The polymer solutions were prepared in chloroform at a concentration of 0.75-1.75mg/ml. The chloroform was used as received from Mallinckrodt. The solutions were filtered through a 0.45 μ m PTFE filter prior to use to remove dust. The subphase studied in all of the experiments consisted of freshly purified Millipore water (18.2m Ω). 50 μ l Hamilton microsyringes were employed to spread the polymer solutions at the air/water interface and they too were used as received.

Generation 1.0
PEO = 43, Dendrimer = 97



| n-alkyl group | substitution |
|---------------|--------------|
| butyl | 98% |
| hexyl | 95% |
| octyl | 87% |
| decyl | 93% |
| dodecyl | 90% |
| octadecyl | 95% |

Generation 1.0
PEO = 43, Dendrimer = 178



| n-alkyl group | substitution |
|---------------|--------------|
| butyl | 92% |
| hexyl | 66% |
| octyl | 72% |
| decyl | 58% |
| dodecyl | 89% |
| octadecyl | 73% |

Generation 2.0
PEO = 43, Dendrimer = 97



| n-alkyl group | substitution |
|---------------|--------------|
| butyl | 82% |
| hexyl | 98% |
| octyl | 96% |
| decyl | 76% |
| dodecyl | 95% |
| octadecyl | 27% |

Generation 3.0
PEO = 43, Dendrimer = 97



| n-alkyl group | substitution |
|---------------|--------------|
| butyl | 99% |
| hexyl | 97% |
| octyl | 89% |
| decyl | 84% |
| dodecyl | 66% |
| octadecyl | 33% |

Generation 4.0
PEO = 43, Dendrimer = 97



| n-alkyl group | substitution |
|---------------|--------------|
| butyl | 99% |
| hexyl | 97% |
| octyl | 94% |
| decyl | 90% |
| dodecyl | 99% |
| octadecyl | 12% |

Generation 5.0
PEO = 43, Dendrimer = 97



| n-alkyl group | substitution |
|---------------|--------------|
| dodecyl | 92% |
| octadecyl | 13% |

Figure 4.1. A list of the polymers under investigation and the percent substitution of the alkyl chains on the polymer. (Please note that the graphical representations of the polymers are meant only to illustrate the differences in the length of the dendritic block and the number of branches in each generation and are not meant to indicate the conformation of the polymer.)

4.3.2 Instrumentation

The Langmuir experiments were conducted on a Teflon lined Lauda FW-2 trough possessing a total surface area of 927cm^2 and a subphase volume of 1.3L. The surface pressure of the polymer film was determined using a pressure transducer, which was connected to a float via a set of transducer pins. The surface area was compressed using an automated Teflon coated movable barrier. The temperature of the subphase was maintained at 20°C using a Neslab RTE-111 refrigerated recirculating water bath.

4.3.3 Methods

In all of the experiments, the trough was first filled with Millipore water, and the water level was automatically aspirated to a consistent height by the instrument. A baseline of the clean water surface was collected to ensure that there were no impurities on the surface, which could bias the results. 0.5mN/m was the maximum acceptable surface pressure in the baseline measurement and the trough was cleaned again if this condition was not met. 25-50 μl of the polymer/chloroform solution were carefully placed dropwise at the air/water interface using a 50 μl Hamiltonian syringe. (In general, smaller amounts of lower concentration polymer solution were needed for the lower generation polymers terminated with short alkyl chains; however, as the generation number and the alkyl chain length increased, larger amounts of higher concentration polymer solution were needed for accurate isotherms.) A minimum of twenty minutes was allowed for evaporation of the solvent and for spreading of the monolayer before compression was initiated. Pressure-area isotherms were collected at compression and decompression rates of $45\text{cm}^2/\text{minute}$. Second compression and decompression pressure-area isotherms were collected after completion of the original isotherms to examine the reproducibility and stability of the polymer films. For each polymer, a minimum of three original compression and decompression isotherms were collected from two different polymer castings solutions in order to reduce the error incurred during the weighing and measuring process. The most representative of the three isotherms is reported.

4.4 Results and Discussion

4.4.1 Pressure-Area Isotherms for the Polymers

Once the diblock copolymers had been prepared, we wanted to look at their behavior at the air/water interface to determine what conditions, if any, would allow us to obtain stable, ordered films, preferentially with the dendritic rod lying perpendicular to the air/water interface. Originally, it was hoped that the methyl ester terminated polymers might be able to form stable, ordered films, since the methyl ester group was known to be slightly hydrophobic, but the polymers were also terminated with alkyl chains of varying length to determine the effect of the alkyl chain length, and thus the hydrophobic nature of the dendritic block on the resulting film isotherms. It was also hoped that even if a methyl ester terminated polymer or one substituted with short alkyl chains may not be able to form the desired ordered films at a lower generation, it may at a higher generation due to the multiplication of the number of end groups that occurs at higher generations. Similarly, it was hoped that by increasing the length of the dendritic block, and thus the fraction of the hydrophobic component, methyl ester terminated polymers or those substituted with shorter alkyl chains may be able to form the desired ordered films whereas they may not have been able to when the fraction of the hydrophobic component was lower. Thus, the effects of the end group as well as the generation number and the length of the dendritic block on the surface pressure and surface area of the Langmuir films that formed were examined.

The pressure/area isotherms that were collected for the polymers are presented in Figures 4.2 through 4.7. Figure 4.2 shows the isotherms collected for the generation 0.5 and 1.0 polymers which were terminated with varying lengths of alkyl groups and which have a poly(ethylene oxide) block length of approximately 43 repeats and a dendritic block length of approximately 97 repeats. Figure 4.3 shows a similar graph except for a polymer which has a poly(ethylene oxide) block length of approximately 43 repeats and a dendritic block length of approximately 178 repeats, and thus allows us to look at the effect of dendritic block length on the Langmuir films that form. Figures 4.4, 4.5, 4.6, and 4.7 also show the pressure/area isotherms for the polymers as a function of alkyl chain length; however they are given for generation 1.5 and 2.0, generation 2.5 and 3.0, generation 3.5 and 4.0, and generation 4.5 and 5.0, respectively. For these studies, all of the polymers possessed a poly(ethylene oxide) block length of approximately 43 repeats and a dendritic block length of approximately 97 repeats in order to examine the effect of generation number on the Langmuir films that formed.

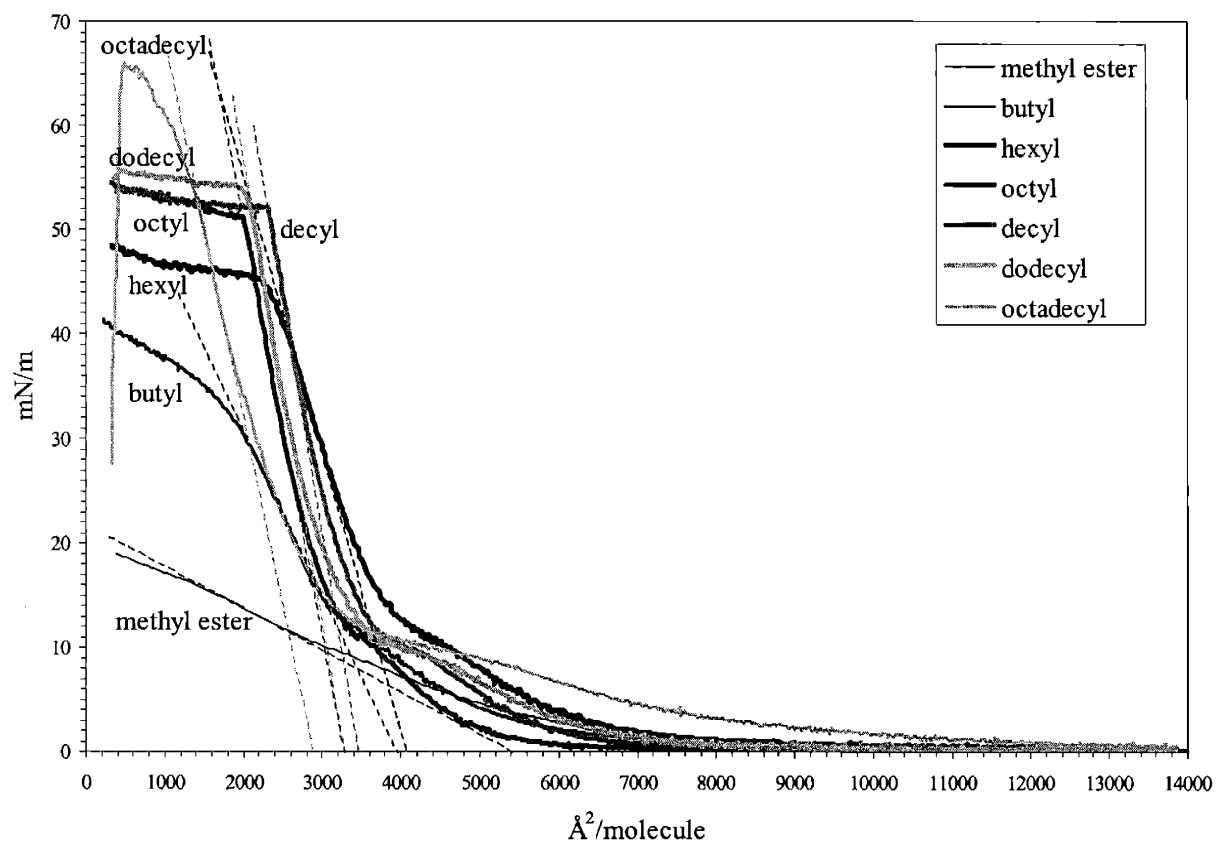


Figure 4.2. Pressure/area isotherms of the generation 1.0 linear-dendritic rod diblock copolymers which possessed a dendritic block length of 97 repeats.

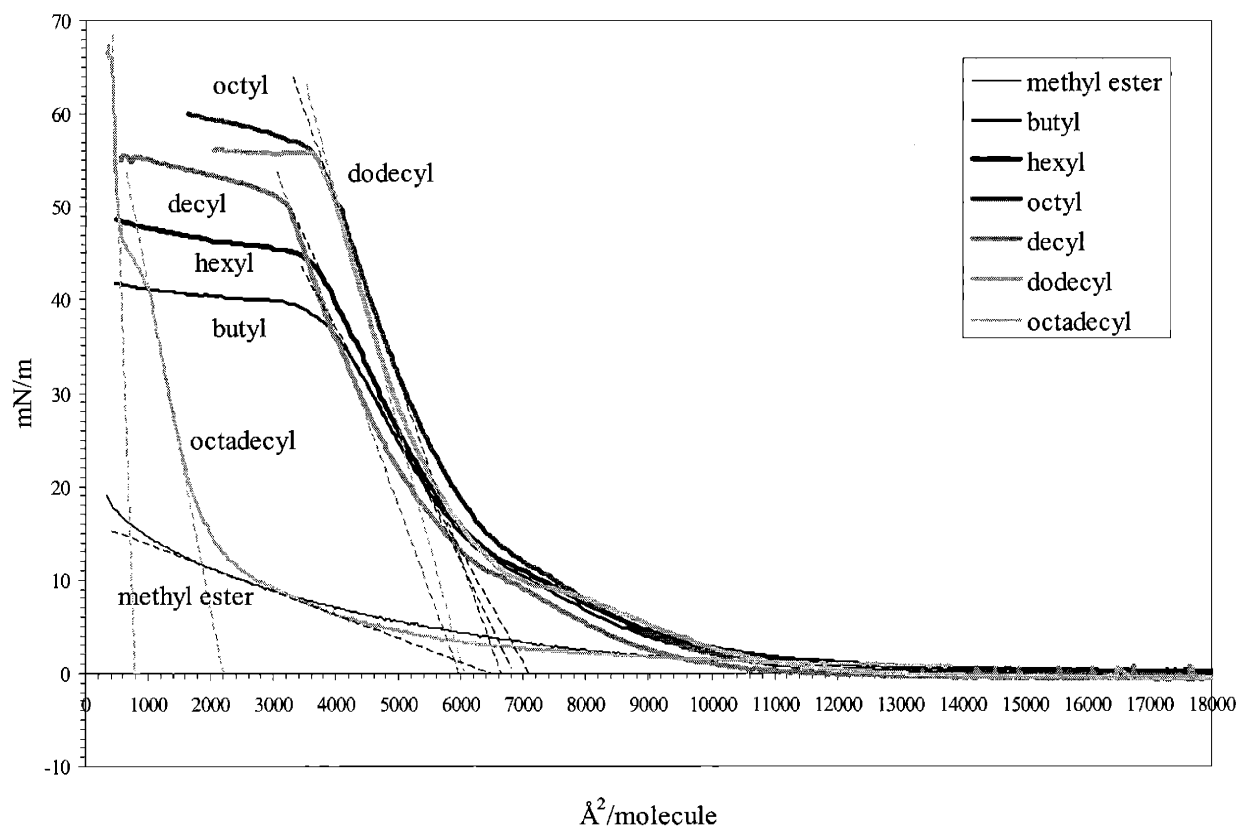


Figure 4.3. Pressure/area isotherms of the generation 1.0 linear-dendritic rod diblock copolymers which possessed a dendritic block length of 178 repeats.

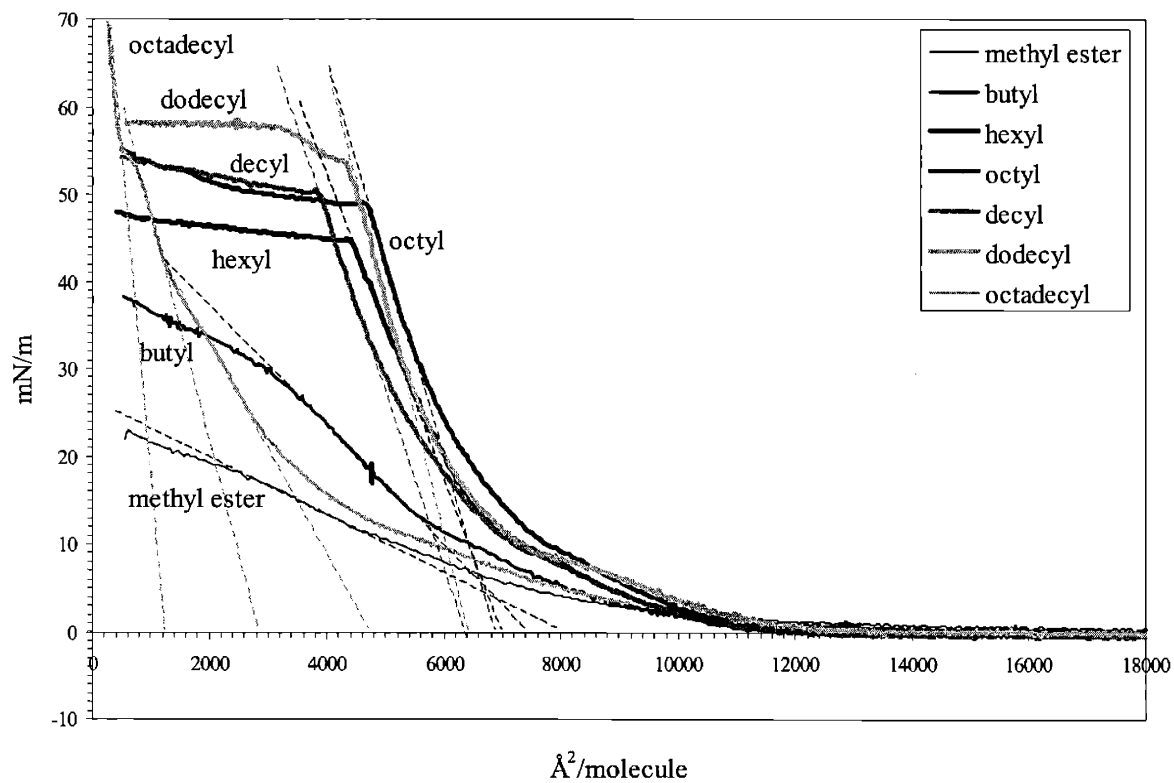


Figure 4.4. Pressure/area isotherms of the generation 2.0 linear-dendritic rod diblock copolymers which possessed a dendritic block length of 97 repeats.

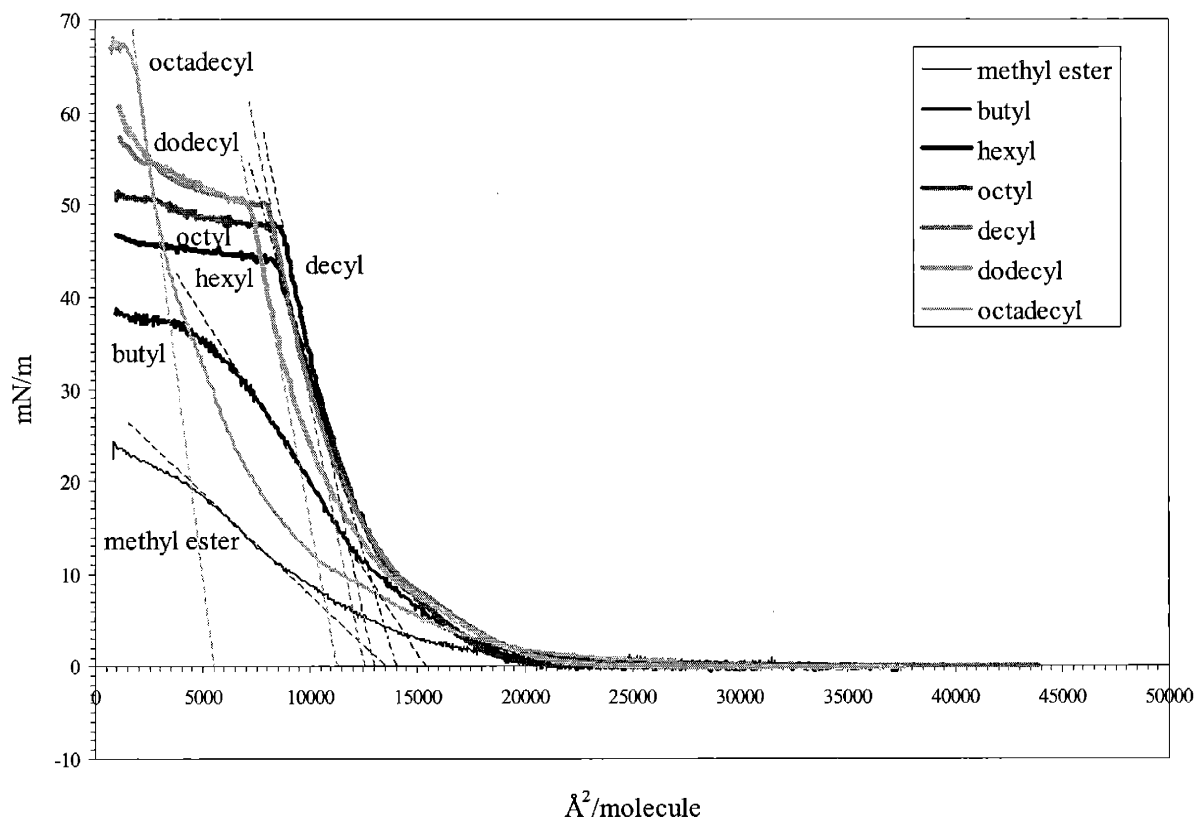


Figure 4.5. Pressure/area isotherms of the generation 3.0 linear-dendritic rod diblock copolymers which possessed a dendritic block length of 97 repeats.

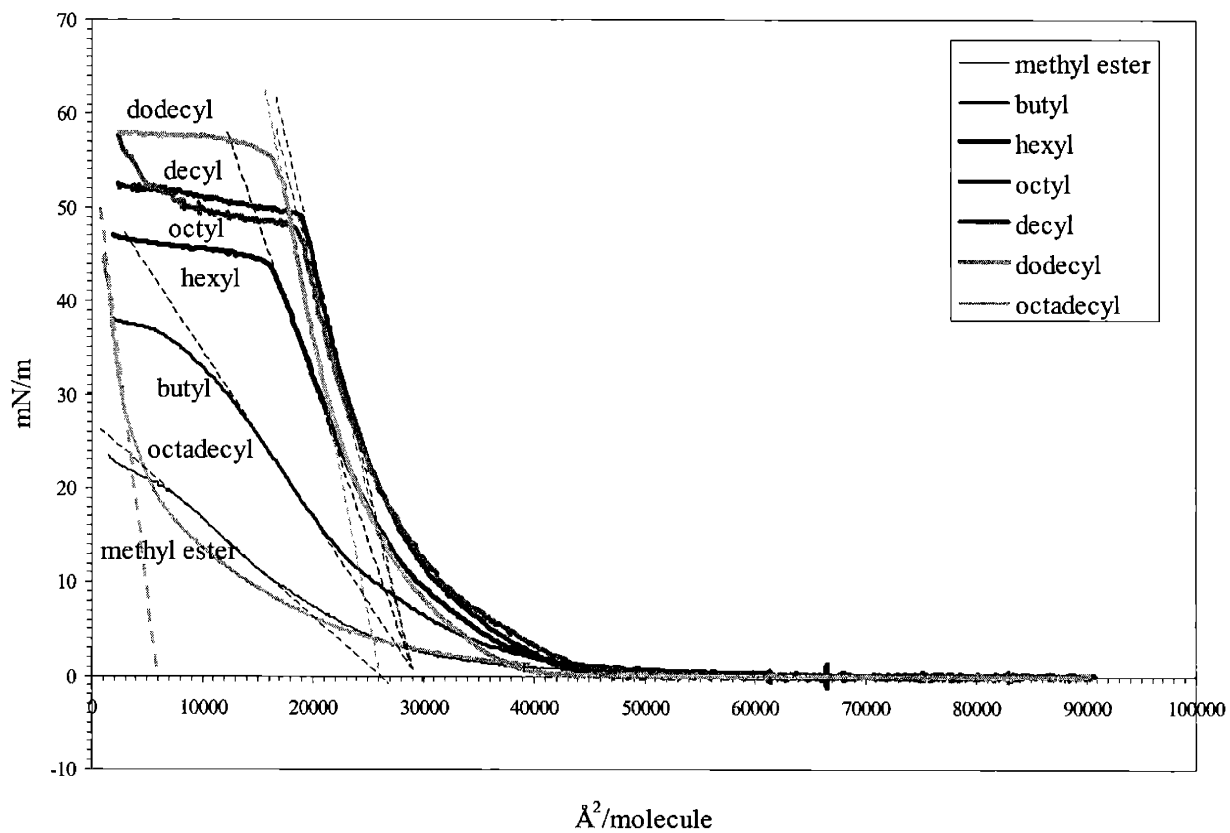


Figure 4.6. Pressure/area isotherms of the generation 4.0 linear-dendritic rod diblock copolymers which possessed a dendritic block length of 97 repeats.

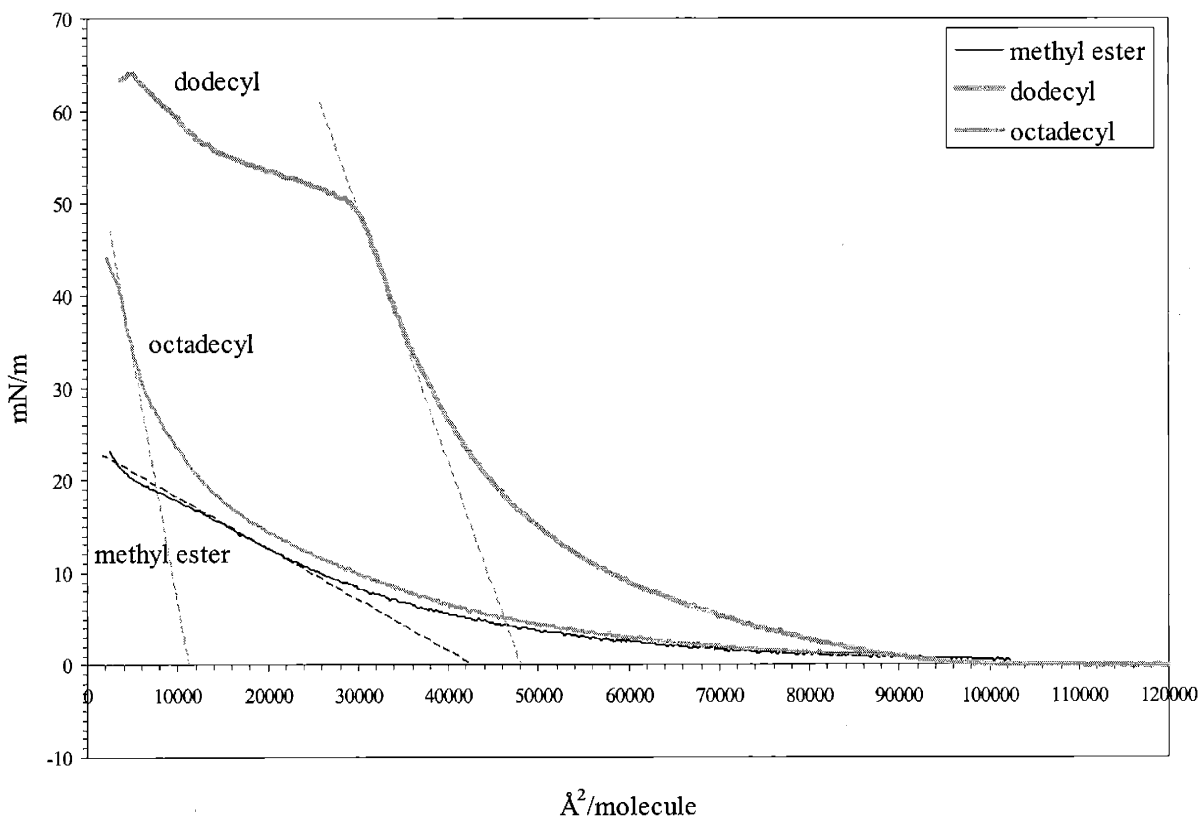


Figure 4.7. Pressure/area isotherms of the generation 5.0 linear-dendritic rod diblock copolymers which possessed a dendritic block length of 97 repeats.

4.4.2 Surface Pressure

Once the pressure/area isotherms for the polymers had been collected as a function of alkyl chain length, generation number, and length of the dendritic block, the effect that each of these parameters contributed to the properties of the isotherms could be studied. One property from the isotherms was examined was the surface pressure. As a quick reminder, the surface pressure (π) is defined as the difference between the surface pressure of the pure liquid (γ_0) and that of the film covered liquid (γ), or $\pi = \gamma_0 - \gamma$.⁶² At large areas where the molecules do not interact and cannot cover the surface, the surface pressure is zero. Upon compression, the molecules begin to interact and exhibit a surface pressure, which in general, increases with decreasing surface area; however, at some point, the molecules become so compressed that the monolayer collapses and forms a multi-layer. This transition from a mono- to a multilayer is usually indicated by a sudden drop-off or a plateau in the pressure/area isotherm.⁶³ (Although a plateau in the isotherm does not always mean that a collapse in the monolayer has occurred and could be indicative of another transition.)⁶⁴ In general, the higher the surface pressure of a monolayer before collapse, the more condensed and close packed the molecules in the monolayer will be, resulting in the formation of a more stable monolayer.⁶⁵ In addition, molecules which are subsequently transferred to solid substrates tend to form more coherent films if they can be transferred at higher pressures.⁶⁶

One of the first features of the surface pressure that was observed for the isotherms as the surface area was decreased was the formation of a broad plateau in the surface pressure at approximately 10-12mN/m for the series of generation 1.0 polymers which possessed a dendritic block length of 97 repeats (Figure 4.2). At the same pressure, a much smaller plateau could be seen for the generation 1.0 polymers composed of a dendritic block length of 178 repeats as well as the generation 2.0 polymers, but the plateau all but disappeared for the generation 3.0, 4.0 and 5.0 isotherms. This plateau can be attributed to the interactions of the poly(ethylene oxide) block with the water as well as with the poly(ethylene oxide) blocks on neighboring polymers. As the linear-dendritic rod diblock copolymer grows in generation, the weight and volume ratios of the dendritic block to the poly(ethylene oxide) block not only grew, but also the geometric ratio of the hydrodynamic size of the dendritic block to the poly(ethylene oxide) block grew as the radius of the dendritic block became larger, especially when functionalized with a long alkyl chain, while that of the random coil of hydrated poly(ethylene oxide) remained the same. Thus, as the

generation of the dendrimer increased, not only was it more difficult for the poly(ethylene oxide) to interact with the interface due to competing interactions with the growing dendritic block, but it was also more difficult for the poly(ethylene oxide) to physically reach the interface, resulting in a disappearance of the poly(ethylene oxide) plateau. Faure, Cox, and Bijsterbosch have all observed a similar plateau at the approximately the same pressure when they examined the behavior of polystyrene-poly(ethylene oxide) diblock copolymers at the air/water interface and have attributed this plateau to the poly(ethylene oxide) block.⁶⁷⁻⁷⁰ Faure also found that the length of the plateau decreased with decreasing length of the poly(ethylene oxide) block. For several years, researchers have known that poly(ethylene oxide) is itself an amphiphilic polymer that can be compressed and expanded reversibly when spread at the air/water interface.⁷¹ The polymer forms a very hydrated layer just below the interface and as it is compressed, begins to extend down into the subphase, while maintaining a constant surface concentration in the hydrated layer.^{72,73} Poly(ethylene oxide) homopolymers reach a maximum surface pressure of approximately 10mN/m at 25°C, which corresponds well with the surface pressure which has been observed in the plateau region of the diblock copolymers.⁷² Iyer *et al.* did not directly observe a plateau for their poly(ethylene oxide)-poly(amido amine) linear-dendritic diblock copolymers at the air/water interface, but they did find that it was difficult to achieve a non-zero surface pressure at low surface concentrations for their low generation polymers, and they attributed this non-zero surface pressure to the presence of the poly(ethylene oxide) block and its interactions at the interface.⁴⁰

Continued compression of the monolayers resulted in the formation of a second and a third plateau in the surface pressure, in some cases, and a slope change in others. As previously mentioned, the formation of a plateau sometimes indicates collapse of the monolayer into bi- or multilayer structures; although, it may also indicate another transition such as rearrangement of the polymers on the surface or reorganization of the pendent alkyl groups.⁶⁴ For the linear-dendritic rod diblock copolymers, we believe that the plateau at the highest surface pressure is attributed to the collapse of the monolayer while any intermediate plateaus, besides the one at approximately 10mN/m, can be attributed to the rearrangement of the polymer backbone and/or the pendent alkyl chains. Riou *et al.* have studied the behavior of a “hairy rod” co-polyglutamate [poly(γ -methyl-L-glutamate-co- γ -n-octadecyl-L-glutamate)] which possessed long alkyl side chains.⁷⁴ Upon compression, this polymer formed multiple transitions, and the organization of

the alkyl chains during these transitions was monitored by an *in situ* FTIR experiment. During the intermediate plateau regions, the ratio of the gauche to the trans conformation states in the alkyl chains decreased dramatically as the alkyl chains were pushed to order into the more compact trans arrangement. In addition, Gargallo *et al.* have looked at the behavior of Langmuir films of poly(4-vinyl pyridine) which have been quaternized with various n-alkyl bromides.⁷⁵ These polymers also formed intermediate plateau regions upon compression and the behavior of the film was monitored by Brewster angle microscopy. They found that the Brewster angle images did not vary greatly during the intermediate plateau regions but a definite collapse in the monolayer was seen for the highest plateau. Thus, they also believe that reorganization of the polymer and the alkyl chains were the cause of the intermediate plateaus. These results were in good agreement with those observed by Li *et al.*, who used X-ray reflectivity to study the Langmuir behavior of similar polystyrene-alkylated poly(vinyl pyridine) diblock copolymers.⁷⁶ Another diblock copolymer system which exhibited a plateau attributed to rearrangement of the hydrophobic block was observed by Yamamoto *et al.*⁷⁷ They reported that in the plateau region, diblock copolymers consisting of a hydrophobic poly(isobutyl vinyl ether) block and a hydrophilic glucose vinyl ether block underwent a transition from a state in which the hydrophobic block was lying flat on the interface to one in which the hydrophobic block was pushed from the interface into the air. One final example of a diblock copolymer which exhibited a rearrangement of the polymer, and a corresponding plateau, is the poly(γ -benzyl-L-glutamate)-poly(L-glutamic acid) (PBLG-PLGA) diblock copolymer studied by Higashi *et al.*⁵⁹ They too found that the polymer rearranged from a structure in which the rigid PBLG block was lying horizontally on the surface to one in which it was lying almost normal to the surface during the plateau region.

While not all of the alkyl terminated linear dendritic rod diblock copolymers under investigation exhibited intermediate plateaus, those that were terminated with longer alkyl chains were more likely to display them. First of all, the longer alkyl chains needed to pass through more conformation states on the way to forming ordered films, resulting in more pronounced changes in ordering of the polymer and the surface pressure. The consequence of these changes was the formation of a plateau. In addition, Kang has investigated the lateral diffusion of several long alkyl chain amphiphilic derivatives and found that the longer alkyl chain amphiphiles exhibited smaller immersion depths and thus larger diffusion constants of lateral mobility than

the shorter alkyl chain amphiphiles did.⁷⁸ Thus, for the linear dendritic rod diblock copolymers under investigation, the polymers terminated with the longer alkyl chains may not have been as deeply immersed in the water and may have been more likely to undergo rearrangement of the entire dendritic block, whereas the short alkyl terminated polymers were grounded more firmly at the interface and could not undergo this type of rearrangement.

The plateau that formed at the highest pressure for each of the linear-dendritic rod diblock copolymers is most likely attributed to collapse of the monolayer film. This collapse pressure was found to be highly dependent on the length of the alkyl chain with which the polymers were functionalized and only weakly dependent on the generation number and length of the dendritic block. A graph which illustrates this point is presented in Figure 4.8. In this graph, the surface pressure of the isotherm at the highest plateau was plotted versus the alkyl chain length. In general, as the length of the alkyl chain increased, the surface pressure of the polymers at their highest plateau increased. The polymers which were terminated with methyl ester groups ($n=1$) all exhibited a plateau surface pressure of approximately 19-22mN/m. This value was very comparable to the plateau surface pressure of poly(methyl acrylate) homopolymers which have a plateau pressure of approximately 20mN/m at 25°C.⁷⁹ The plateau surface pressure of the butyl terminated polymers increased to 33-39mN/m, the hexyl terminated polymers to 43-46mN/m, and the octyl to 51-56mN/m. Between the octyl and the dodecyl terminated polymers, the surface pressure increased only slightly to 51-55mN/m for the decyl and to 54-64mN/m for the dodecyl terminated polymers. The octadecyl polymers exhibited two very different values for the surface pressure depending on the generation, one at 65-70mN/m and the other at 44-45mN/m. The reasons for these two very different values observed for the octadecyl polymers will be explained in the next paragraph. This overall trend of increasing surface pressure with increasing alkyl chain length can be explained by the increase in the hydrophobic nature of the end groups as well as the increase in the overall size of the dendrimer as the alkyl chain length is increased. It has been well established that for small molecule amphiphiles such as fatty acids, the surface pressure and the stability of the film increases with increasing alkyl chain length due to the larger dispersive interactions which form between larger hydrophobic groups. Kobayashi *et al.* have observed a similar relationship between the alkyl group and the collapse pressure for cyclodextrin which had been substituted at the C-6 position with hexyl, decyl, tetradecyl, and octadecyl chains.⁸⁰ They found that the collapse pressure was

highly dependent on the alkyl chain length and that it increased with increasing alkyl chain length. This trend was also reported by Gargallo *et al.* for their alkylated poly(vinyl pyridine) polymers.⁷⁵ With regard to dendritic systems, Schenning found that for poly(propylene imine) dendrimers which had been substituted with three different alkylated functional groups, palmitoyl chains, alkyl/azobenzene chromophores, and adamantane groups, the surface pressure was highly dependent on the alkyl group with which the polymer had been substituted.⁵⁵ In addition, they found that the surface pressure for their dendrimers that had been substituted with palmitoyl chains (15 carbons) was 55-65mN/m, which fits well within the trend that we observed. Conversely, Sayed-Sweet *et al.* did not report a dependence of the surface pressure on the length of the alkyl group with which their PAMAM dendrimers were terminated.⁵³ However, it is important to keep in mind that in their study, only three different alkyl groups were examined, the hexyl, octyl, and dodecyl groups, three groups which all fell within the range of alkyl groups in our study where only a slight change in surface pressure was noticed. (The surface pressures which they found for these end groups were in the range of 45-48mN/m, which corresponds well with the range that we found for the hexyl through dodecyl terminated polymers.)

Two very different trends in the surface pressure of the octadecyl terminated linear-dendritic rod diblock copolymers were found. For the lower generation polymers, generation 1.0 through 3.0, the octadecyl terminated polymers all exhibited a compressed surface pressure of between 65-70mN/m; however, the higher generation, generation 4.0 and 5.0, polymers exhibited a compressed surface pressure of 44-45mN/m. The most obvious explanation for these two different values is that the higher generation polymers had a much lower degree of substitution of octadecyl chains than the lower generation polymers did. (The lower generation polymers all possessed at least 27% substitution, while the substitution on the higher generation polymers was only approximately 13%.) Unfortunately, this difference in the degree of substitution resulted from difficulties encountered during the synthesis of the octadecyl polymers, particularly that as the dendrimer generation and number of end groups grew, it became harder and harder to push the reaction of the large and bulky octadecyl groups onto the larger number of chain ends due to steric constraints. The result was that the higher generation polymers did not have nearly the same ratio of hydrophobic to hydrophilic components in the polymer. Without a large enough component of hydrophobic groups, the polymer was not stable

at high pressures, and at these high pressures the polymers were pushed into the subphase. Bo *et al.* found that for poly(benzyl ether) dendritic rod systems, the ratio of hydrophobic to hydrophilic components was an important factor in whether or not the polymers produced reproducible, stable films.⁴⁶ An alternate explanation for the difference in surface pressures observed for the high generation and the low generation octadecyl-terminated polymers might be that even though the higher generation polymers did not have as high a degree of substitution of octadecyl chains, it was still enough such that the alkyl groups were able to completely cover the underlying PAMAM with a hydrophobic shield such that the polymer lost its surfactant-like nature. Saville *et al.* found this to be the case for their high generation hydrophobic poly(benzyl ether) dendrimers which possessed a single hydrophilic group at the core to anchor the polymers to the water.⁴⁸ However, Saville *et al.* also found that when this transition from surfactant to non-surfactant behavior occurred, it resulted in featureless isotherms which recorded a very high surface pressure at zero area at the barrier, as had previously been observed for polystyrene with a single hydrophilic terminal hydroxyl group. Since a lower surface pressure was measured for the generation 4.0 and 5.0 octadecyl terminated polymers in our system, a more likely scenario was that this value was caused by the low degree of substitution of octadecyl groups and not by the loss of surfactant-like behavior. Thus, it appears as though there is a minimum degree of substitution necessary to result in the formation of stable octadecyl terminated polymers. The polymers that were found to be stable were substituted with at least 30% of octadecyl chains. Mabuchi *et al.* have prepared poly(γ -methyl-L-glutamate)-co-(γ -octadecyl-L-glutamate) copolymers and reported that in order to form stable films at the air/water interface, the content of the octadecyl units needed to be at least 30 percent,⁸¹ which is in good agreement with our results.

Besides the length of the alkyl chains with which the polymers were substituted, the other parameters which were examined to observe their effect on the surface pressure were the generation number and the length of the dendritic block. From our experiments, it appeared that the generation number had very influence on the surface pressure of the polymers at high compression. If there was any effect it was very small. Since the surface pressures, as a function of generation, of the butyl through the dodecyl terminated polymers all had approximately the same value, the slight variation in the degree of substitution of the alkyl chains on these polymers made it difficult to decouple these two parameters to notice any small differences that

may have been caused by the generation number alone. These results were consistent with those reported by Sayed-Sweet and Schenning who found that the generation did not influence the collapse pressure of the dendrimer.^{53,55} It also appeared as if the length of the dendritic block made a very small contribution to the surface pressures of the polymers. As the length of the dendritic block increased, the surface pressure of the polymers appeared to slightly increase. Again, since the degree of substitution on the polymers varied, it was difficult to quantify the change. It would not be surprising if the slight increase were real, since larger molecules are known to produce more stable films due to the increased dispersive interactions between the hydrophobic groups.⁵⁰ Nonetheless, any increase in the surface pressure due to the length of the dendritic block was minor in comparison to the effect of the length of the terminal alkyl chain.

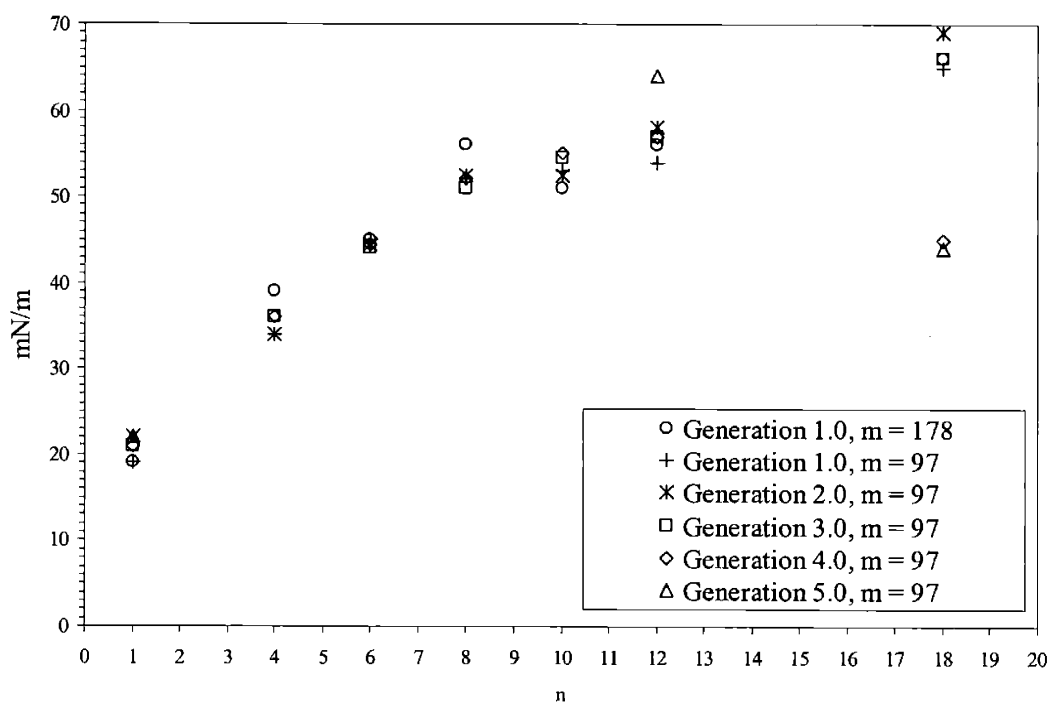


Figure 4.8. Surface pressure at collapse versus alkyl chain length for the linear-dendritic rod diblock copolymers.

4.4.3 Surface Area per Molecule

Another feature from the pressure/area isotherms that was examined was the surface area per molecule. The surface area per molecule is the area that one molecule occupies on the surface when it is in its most condensed state. As previously mentioned, the surface area per molecule was determined by extrapolation of the steepest portion of the isotherm to zero pressure.⁶⁶ The steepest portion of the isotherm was used since the polymer is least compressible at this point, and thus it represents the minimum area that the molecule can occupy. Extrapolation of the steepest portion of the isotherm to zero pressure was done for each of the linear-dendritic rod diblock copolymers and is represented by the dotted lines in Figures 4.2 through 4.7. For two of the octadecyl terminated polymers, the generation 1.0 polymer which consisted of a dendritic block of 178 repeats and the generation 2.0 polymer, extrapolation to zero pressure was performed at more than one point along the isotherm since there appeared to be more than one dominant transition for these polymers in their condensed state. A graph that presents the surface area per molecule that was measured for each of the polymers is shown in Figure 4.9.

For the linear-dendritic rod diblock copolymers that were terminated with methyl ester through dodecyl groups, the surface area per molecule was found to increase with increasing generation number as well as increasing length of the dendritic block. This observation was not surprising since the volume and thus the surface area occupied by the polymer increased with both of these parameters. From the graph, it appears that the surface area approximately doubled as each polymer grew by one generation. In addition, an approximate doubling of the surface area was seen as the length of the dendritic block roughly doubled. This effect of increasing surface area per molecule with increasing dendritic generation has been seen by many groups. Sayed-Sweet also found that the surface area approximately doubled with increasing generation for amphiphilic spherical polyamidoamine dendrimers.⁵³ Increases in the surface area per molecule with increasing generation were also seen by Schenning *et al.* for amphiphilic polypropyleneimine dendrimers,⁵⁵ Sidorenko *et al.* for amphiphilic polybenzyl ether dendrimers,⁵² Mulders *et al.* for amphiphilic spherical amino acid dendrimers,⁸² and Iyer *et al.* for poly(ethylene oxide)-polyamidoamine hybrid-linear dendritic diblock copolymers.⁸³ Unfortunately, all of the work with dendritic rod systems has been focused on making stable monolayers and none of it has focused on the effect of the length of the dendritic block on the

properties of the isotherm such as the surface area per molecule, thus there is no previous literature in this area. However, others have found that for traditional linear diblock copolymers, there is an increase in the surface area per molecule with increasing length of the hydrophobic block. For example, this effect was seen in polystyrene-poly(ethylene oxide) and polystyrene-poly(ethyl acrylate) diblock copolymers when the length of the polystyrene block was increased.⁸⁴⁻⁸⁶ Since the effect of dendritic block length was only examined for the generation 1.0-alkyl terminated linear-dendritic rod diblock polymers, one can only say that this effect held true for the low generation polymers and one not say for sure that this effect would hold true for the higher generation polymers as well.

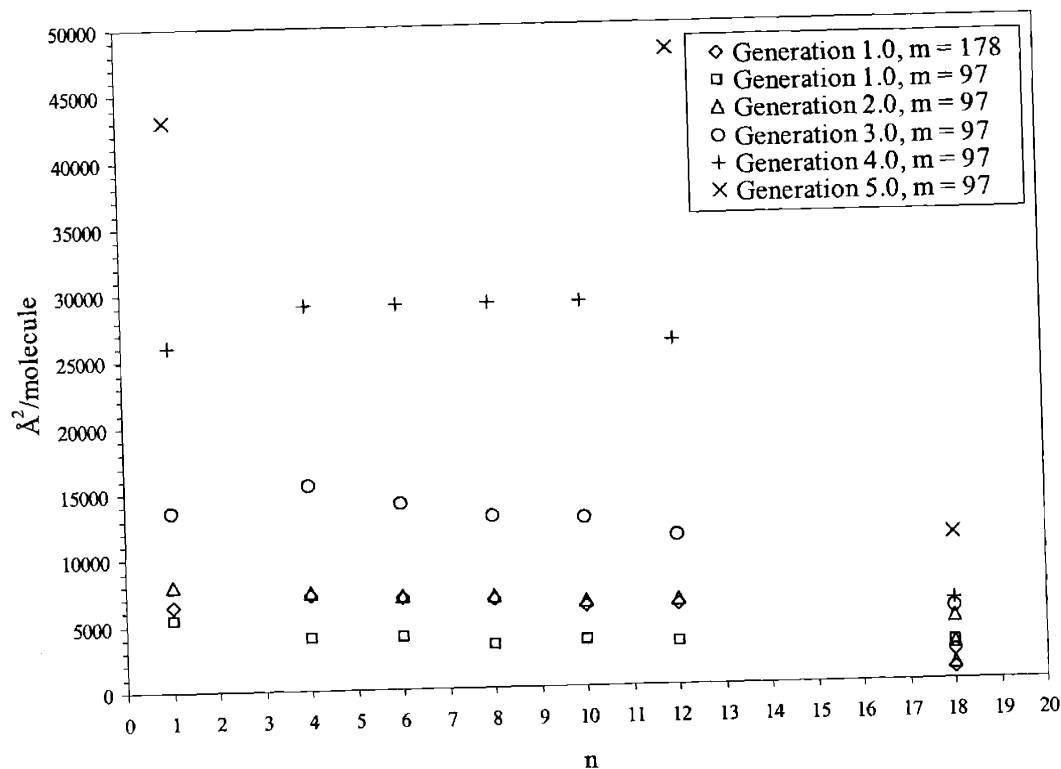


Figure 4.9. Surface area per molecule versus alkyl chain length of the linear-dendritic rod diblock copolymers

For the linear-dendritic rod diblock copolymers that were terminated with methyl ester through dodecyl groups, the surface area per molecule was found to increase with increasing generation number as well as increasing length of the dendritic block. This observation was not surprising since the volume, and thus the surface area occupied by the polymer increased with both of these parameters. From the graph, it appeared that the surface area approximately doubled as each polymer grew by one generation. In addition, an approximate doubling of the surface area was observed as the length of the dendritic block roughly doubled. This effect of increasing surface area per molecule with increasing dendritic generation has been seen by many groups. Sayed-Sweet also found that the surface area approximately doubled with increasing generation for amphiphilic spherical poly(amido amine) dendrimers.⁵³ Increases in the surface area per molecule with increasing generation were also observed by Schenning *et al.* for amphiphilic poly(propylene imine) dendrimers,⁵⁵ Sidorenko *et al.* for amphiphilic poly(benzyl ether) dendrimers,⁵² Mulders *et al.* for amphiphilic spherical amino acid dendrimers,⁸² and Iyer *et al.* for poly(ethylene oxide)-poly(amido amine) hybrid-linear dendritic diblock copolymers.⁸³ Unfortunately, all of the work with dendritic rod systems has been focused on preparing stable monolayers and none of it has focused on the effect of the length of the dendritic block on the properties of the isotherm, such as the surface area per molecule, thus there is no previous literature in this area. However, others have found that for traditional linear diblock copolymers, there is an increase in the surface area per molecule with increasing length of the hydrophobic block. For example, this effect was seen in polystyrene-poly(ethylene oxide) and polystyrene-poly(ethyl acrylate) diblock copolymers when the length of the polystyrene block was increased.⁸⁴⁻⁸⁶ Since the effect of dendritic block length was only examined for the generation 1.0-alkyl terminated linear-dendritic rod diblock polymers, one can only say that this effect held true for the low generation polymers and one can not say for sure that this effect would hold true for the higher generation polymers as well.

The effect of the length of the alkyl chain on the surface area per molecule was found to be much more complex and very generation dependent for the polymers that were terminated with methyl ester through dodecyl groups. In general, for both series of generation 1.0 polymers, the generation 2.0 polymers, and the generation 3.0 polymers, the surface area per molecule was found to decrease with increasing length of the alkyl chain. These results were in contrast to those observed by Sayed-Sweet *et al.* for spherical amphiphilic poly(amido amine) polymers

where they found that the surface area per molecule remained approximately constant, independent of alkyl chain length.⁵³ These results were also in contrast to those seen by Kobayashi *et al.* for “hairy rod” cyclodextrin derivatives that had been substituted with alkyl chains of various lengths.⁸⁰ They too observed that the surface area per molecule remained approximately constant, independent of alkyl chain length. However, it is important to remember that in both of these systems, the hydrophilic portion of the polymer that was used to stabilize the polymer at the surface was very closely connected to the alkyl chains and thus bound them very closely to the surface. On the other hand, for the linear-dendritic rod diblock copolymers under investigation, the poly(ethylene oxide) block could be used to anchor the diblock copolymer to the surface such that the more hydrophobic dendritic blocks were free to form various random coil structures above the surface. These random coil structures could then elongate away from the surface as the length of the alkyl block was increased in order to minimize the interactions of the hydrophobic groups with the water, resulting in a decrease in the surface area of the polymer. Thus, these polymers were more flexible and able to take on more configurations than the polymers studied by Sayed-Sweet and Kobayashi. Unfortunately, no one has yet examined the behavior of poly(ethylene oxide)-poly(alkyl acrylates) as a function of alkyl chain length to see how the behavior of the polymer is influenced by the length of the alkyl chain. These polymers would probably be the most analogous to the low generation linear-dendritic rod diblock copolymers that were examined in this study. Nonetheless, in contrast, the surface area per molecule of the generation 4.0 linear dendritic-rod diblock copolymers was found to remain approximately constant, independent of alkyl chain length. This difference indicated that a change in the ordering and conformation of the polymers at the surface had occurred. Most likely, these higher generation polymers had become too stiff to be able to adopt various random coil configurations on the surface such that they were all adopting a very similar configuration on the surface. This is not surprising as the stiffness of the dendritic branches is known to increase with increasing generation.⁸⁷ Possible surface structures for all of these linear-dendritic rod diblock copolymers at the air/water interface as well as their reasons for their formation will be discussed in more detail in section 4.4.6.

For the linear-dendritic rod diblock copolymers that were terminated with octadecyl groups, two of the trends described above for the polymers terminated with shorter alkyl chains held true, but the third did not. The first trend that held true was that the surface area decreased

with increasing length of the alkyl chains, while the second was that the surface area of the polymer increased with increasing generation of the polymer. The trend that did not hold true was that the surface area of the octadecyl terminated polymers was found to be independent of the length of the dendritic block while the surface area of the polymers terminated with the shorter alkyl chains increased with increasing length of the dendritic block. As previously mentioned, the decrease in surface area per molecule with increasing alkyl chain length was most likely due to an elongation of the polymer away from the surface to minimize the unfavorable interactions between the alkyl chains and the water. The even more hydrophobic octadecyl chains would have even more reason to distance themselves from the water surface than the short alkyl chains, and thus probably adopted an even more vertically extended conformation, resulting in an even further decrease in the surface area. With regard to the increasing surface area per molecule with increasing generation, it was not surprising that an increase in the surface area was observed since the volume of the polymer increased dramatically with increased generation, and thus its overall surface areas also increased, as described for the shorter alkyl terminated polymers. The big difference in the behavior of the polymers that were terminated with the shorter alkyl chains and those that were terminated with the octadecyl chains was that the polymers terminated with octadecyl chains appeared to have a surface area that was independent of length of the dendritic block. If one examines the surface area for the generation 1.0 polymer of 97 repeats and the surface area for the first transition of the generation 1.0 polymer with 178 repeats one finds that they are approximately constant. In order for the surface area to be dependent on the generation number but independent of the length of the dendritic block, the polymer needs to adopt a vertical or vertically extended conformation where the surface area is primarily determined by the radius of the dendritic block. Toyotama *et al.* also reported an independence of the surface area on the length of the rod-like block for vertically aligned poly(γ -methyl-L-glutamate)-poly(ethylene oxide) rod-coil diblock copolymers at the air/water interface.⁶⁰ (Since the effect of dendritic block length was only examined for the generation 1.0-alkyl terminated linear-dendritic rod diblock polymers, one can only say that this effect held true for the low generation polymers and one not say for sure that this effect would hold true for the higher generation polymers as well.) The formation of a second transition for the generation 1.0-octadecyl terminated polymer with 178 repeats as well as the second and third transitions for the generation 2.0-octadecyl terminated polymer was mostly likely the result of

the polymers having a lower degree of substitution, and thus not being as rigid. Consequently, the polymers would be more likely to be able to be compressed into a more tightly packed configuration, possibly one in which the alkyl chains were able to fold in and/or interdigitate with those from neighboring polymer molecules. A more detailed discussion of the possible surface structures that the polymers formed as well as reasons for their formation will be discussed in section 4.4.6.

4.4.4 Compressibility of the Polymers

In addition to providing information about the surface area per molecule, the slope of the surface pressure/area isotherm was also able to give information about the compressibility of the films.⁸⁸ This calculation is analogous to the compressibility of bulk materials in three dimensions, which is calculated from the slope of the pressure versus volume isotherm.⁸⁹ In general, at large surface areas the molecules are very disperse such that the films that form are very compressible as indicated by a very shallow slope of the pressure/area isotherm. However, as the molecules begin to interact with one another, the film can no longer be as easily compressed and the slope of the pressure/area isotherm increases. Finally, when the molecules are tightly packed and there is very little room for further compression, the slope of the isotherm increases dramatically and the molecules are considered to be in a solid, or condensed state.⁹⁰ Usually, the same factors that lead to an increase in the stability and the collapse pressure of the films, such as an increase in the hydrophobic nature of the hydrophobic block, also lead to a decrease in the compressibility of the films in the condensed state, resulting in the formation of more tightly packed monolayers. In general, more tightly packed, condensed monolayers are able to form more coherent films when transferred to solid substrates.⁶⁶ The compressibility of the linear-dendritic rod diblock copolymer films was calculated using the equation $C = (-1/A)(\partial A/\partial \pi)_T$, where C is the compressibility, A is the area, and π is the surface pressure for each point along the isotherm.⁸⁸ The compressibility was then plotted versus the surface pressure to determine the range of surface pressures that gave the minimum compressibility. The compressibility of each polymer was then calculated by averaging the compressibility values over the small range of surface pressures that had been determined. As an example, the plot of the compressibility versus surface pressure is shown in Figure 4.10 for the generation 2.0-octyl terminated linear-dendritic rod diblock copolymer. The compressibility of this polymer was

calculated by averaging over the pressure range of 40-47mN/m. The compressibilities of all of the linear-dendritic rod diblock copolymers in their most condensed states are plotted as a functional of alkyl chain length in Figure 4.11.

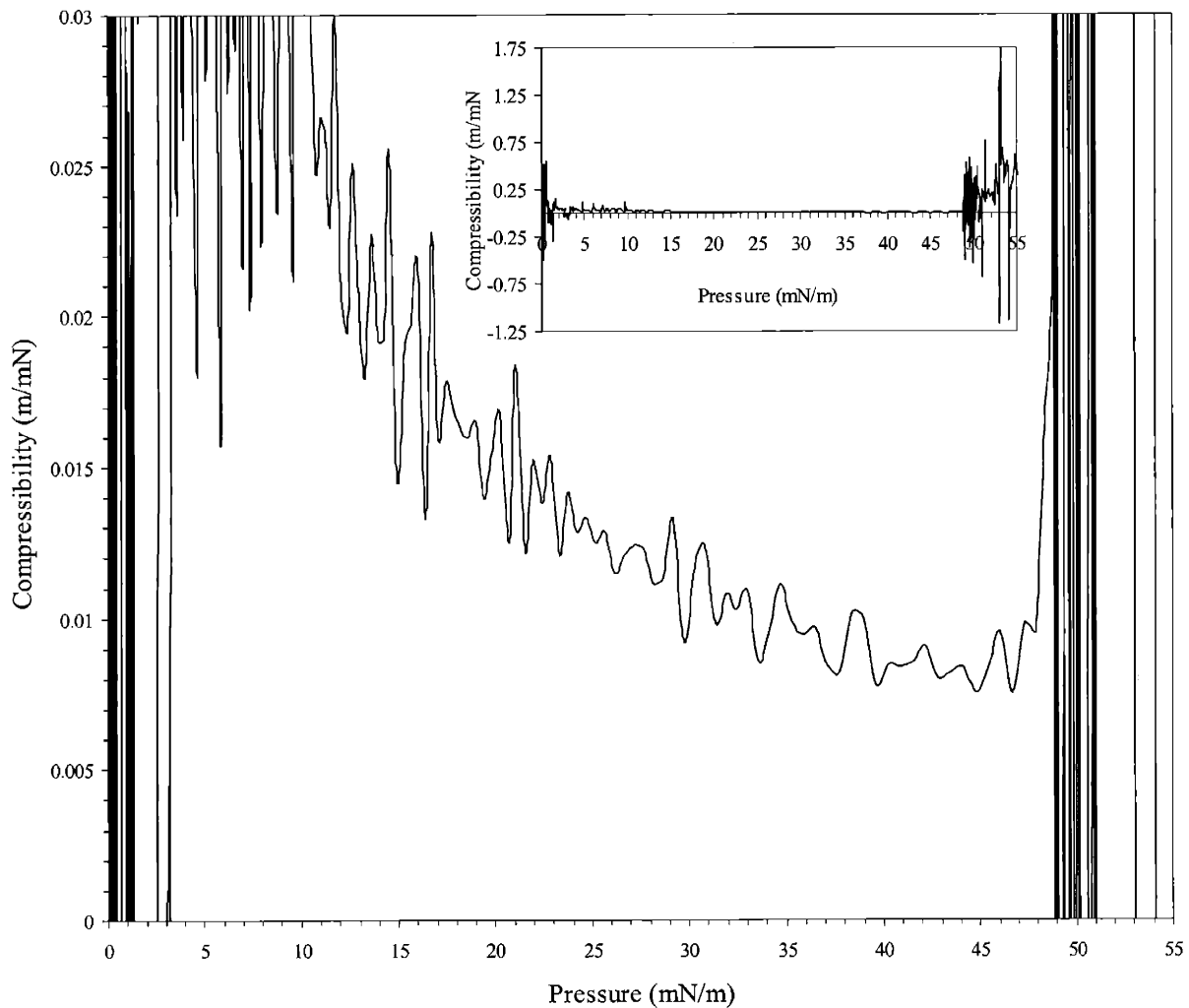


Figure 4.10. Compressibility versus surface pressure for the generation 2.0-octyl terminated linear-dendritic rod diblock copolymer. The larger graph is a blow up of the desired compressibility range while the insert shows the entire graph. The compressibility of this polymer in the condensed phase was calculated by averaging over the pressure range of 40-47mN/m.

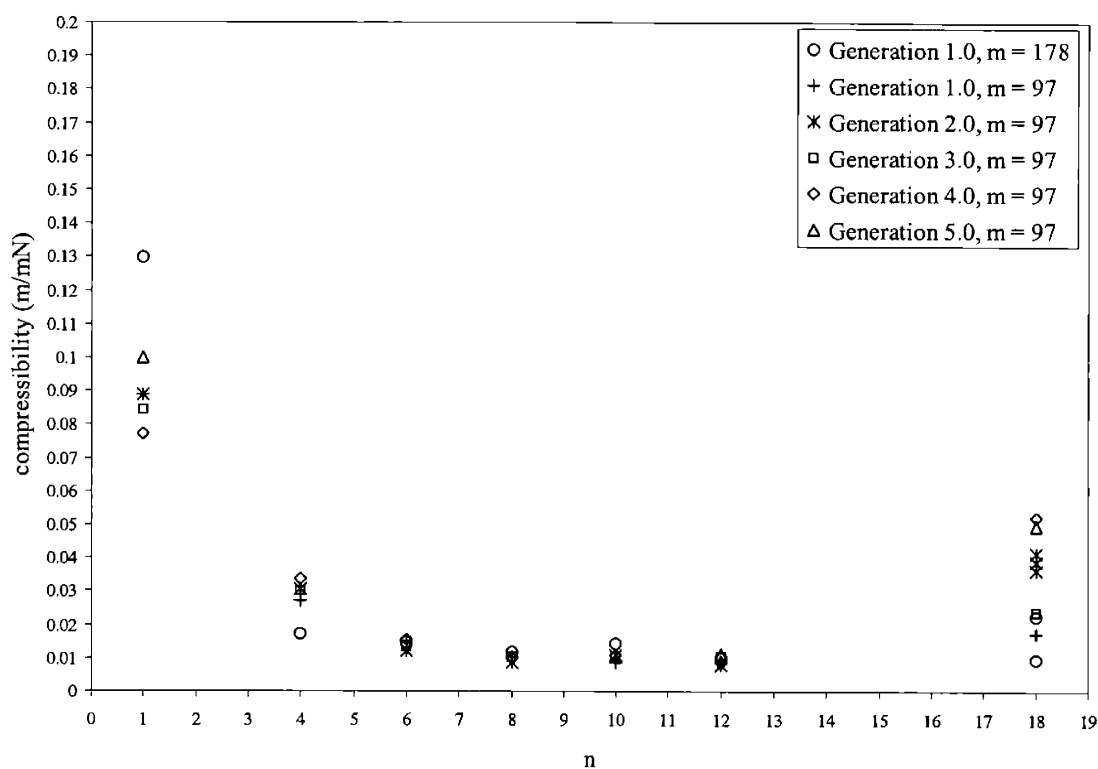


Figure 4.11. Compressibility versus alkyl chain length of the linear-dendritic rod diblock copolymers.

The pressure/area isotherms of the linear-dendritic rod diblock copolymers exhibited the traditional increase in slope and thus decrease in compressibility as the surface area was decreased. However, it appeared as if the slope of the isotherm at its steepest point, and thus the compressibility of the condensed monolayer, was highly dependent on the length of the alkyl chain with which the polymer was functionalized and was much less dependent on the generation number and length of the dendritic block. From the pressure/area isotherms, all of the methyl ester terminated polymers had very shallow slopes at their steepest positions. Thus, these polymers were all very compressible even at high generations, indicating that they were very flexible and/or did not form very stable monolayers at the air/water interface. It was difficult to determine whether the generation number and length of the dendritic block affected the compressibility of these polymers as the compressibilities calculated at various points along the graph were not very consistent and the error surrounding the averaged value was large. The compressibilities of the alkyl terminated linear-dendritic rod diblock copolymers in their most

condensed state decreased as the length of the alkyl chain increased, with the largest decrease in compressibility occurring between the methyl ester and the butyl groups. As the length of the alkyl chain was further increased, the compressibility continued to decrease, but not to as great of an extent, and there was very little to no decrease in compressibility between the octyl, decyl, and dodecyl alkyl groups. Thus, in general, the polymers terminated with the shorter alkyl chains formed more compressible films, while the polymers terminated with longer alkyl chains formed more tightly packed, less compressible films. The compressibilities were independent of both generation number and length of the dendritic block. Somewhat surprisingly, the octadecyl terminated polymers seemed to be more compressible than the dodecyl terminated polymers. This increase in the compressibility could have been due to several factors such as the octadecyl polymers adopting different configurations on the surface or the octadecyl polymers possessing a much lower degree of substitution of alkyl chains. Unfortunately, it was difficult to determine if the compressibility of the octadecyl polymers were dependent on the generation number or length of the dendritic block as there were also differences in the degrees of substitution of the octadecyl chains on each of the polymers. Nonetheless, the generation 1.0-octadecyl terminated polymers which had 178 repeats and the generation 2.0-octadecyl terminated polymers which had 97 repeats, both showed more than one transition during the formation of the condensed state. In general, as these transitions occurred, the compressibility of the films decreased, indicating that the polymers were able to arrange themselves into new configurations that were more tightly packed and less compressible than the previous state. Unfortunately, there is not a lot of literature which discusses the relative compressibility of stable Langmuir films prepared from small molecule amphiphiles as most research focus only on the ability to form stable films. This is also true for dendritic and diblock copolymer systems, so there not any other similar systems to which the results can be compared.

4.4.5 Reversibility and Reproducibility of the Pressure/Area Isotherms

In addition to the information that can be extracted from an amphiphile's first Langmuir compression isotherm, there is also information that can be learned from its decompression isotherm as well as from a second compression isotherm of the same material. For example, the decompression isotherm can give insight into the reversibility and the presence of hysteresis in the film, and thus its reordering upon decompression, and the second isotherm can give

information as to whether the film is stable enough to undergo multiple compression/decompression cycles or if permanent reordering takes place.³⁷ Unfortunately, the primary interest of most research is in the first compression of the film such that decompression and second isotherms are not always reported and are usually only discussed to the extent as to whether or not hysteresis is present and whether the film is reproducible. If hysteresis is present in a system, its causes are generally not discussed in great detail.

The reversibility and the reproducibility of the isotherms of the linear-dendritic rod diblock copolymers were mostly dependent on the generation number and the length of the alkyl group with which they were substituted. The degree of substitution also played a role, but the length of the dendritic block did not seem to be very important. For both series of generation 1.0 polymers, the polymers that were terminated with butyl through octyl groups exhibited a great deal of hysteresis upon decompression and were not able to form reproducible isotherms upon recompression. This behavior suggests the formation of stable aggregates of the diblock copolymers, probably due to entanglement of the dendritic blocks, and/or solubilization of the polymer in the water. Thus, the original configuration of the polymer in the monolayer that formed was not very stable. Similar behavior was observed by da Silva *et al.* who examined the hysteresis in polystyrene-poly(ethylene oxide) diblock copolymers and who attributed the observed hysteresis to the entanglement of the polymers.^{91,92} The generation 1.0 polymers that were terminated with decyl through octadecyl groups also exhibited some hysteresis, but not to the same extent as was seen for the polymers terminated with shorter alkyl chains. In addition, the decyl through octadecyl polymers were able to form somewhat more reproducible isotherms upon recompression, with only some loss of area and little loss of surface pressure. Since these polymers also did exhibit some hysteresis, they too probably formed aggregates due to entanglement of the polymer chains, but not to as great of an extent. This is not surprising since the longer alkyl chains are more rigid and thus less prone to entanglement, especially at very high degrees of substitution. In addition, the longer alkyl chains made them more hydrophobic and less soluble in water. Hence, these polymers were able to produce more stable initial films, but films that were kinetically hindered from completely reforming their original arrangement. The first and second compression and expansion isotherms for the generation 1.0-butyl and decyl terminated polymers are presented in Figure 4.12.

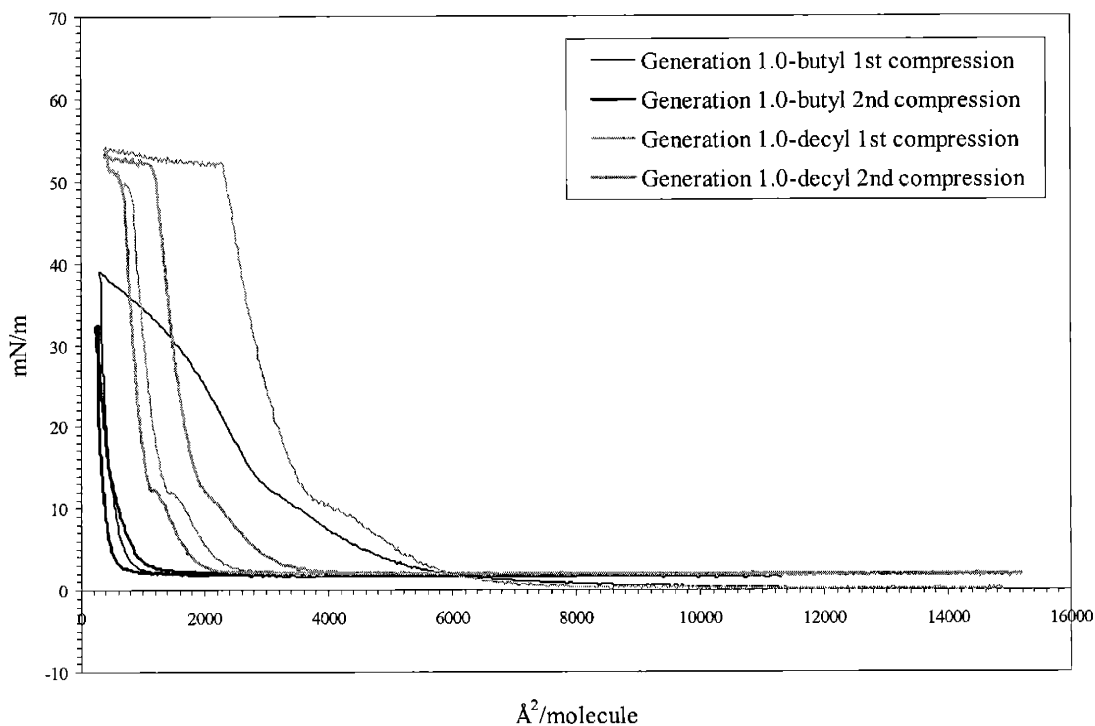


Figure 4.12. First and second compression and decompression pressure/area isotherms of the generation 1.0 linear-dendritic rod diblock copolymers which had a dendritic block length of 97 repeats.

Not surprisingly, the reversibility and the reproducibility of the isotherms seemed to improve with increasing generation. While the generation 2.0-butyl terminated polymer exhibited behavior that was very similar to the generation 1.0-butyl terminated polymer and did not form stable films, the generation 3.0 and 4.0-butyl terminated polymers exhibited a decrease in the hysteresis and were able to form somewhat more reproducible films upon recompression, indicating an increase in the stability of these films. Most likely, this was due to the more highly branched nature of the higher generation polymers that prevented entanglements from forming between the polymers, and thus their aggregation on the surface. Dendritic systems are known to have limited entanglements between individual molecules due to their short branch length and high density.⁹³ The first and second compression and expansion isotherms of the generation 3.0-butyl terminated polymer are presented in Figure 4.13 and can be compared to those of generation 1.0. The generation 2.0 and larger polymers that were terminated with hexyl through

decyl groups exhibited much less hysteresis than the butyl terminated polymers of the same generation and only a small loss of area upon recompression. (This increased reversibility and reproducibility of the isotherms improved slightly with increasing generation.) As previously mentioned, this small amount of hysteresis and loss of area can be attributed to the formation of aggregates that were kinetically hindered from dispersing. However, the formation of the aggregates in these polymer monolayers were probably hindered by both the more highly branched nature of the polymer as well as by the longer, more rigid alkyl chains. Thus, these polymers seemed to form much more stable films on the surface. The first and second compression and expansion isotherms for the generation 3.0 and 5.0-decyl terminated polymers can be seen in Figures 4.13 and 4.14, respectively. Surprisingly, at low surface areas, the decompression isotherms of all of the higher generation dodecyl and octadecyl terminated polymers exhibited more hysteresis than the shorter alkyl chains; however, at higher surface areas, the amount of hysteresis was approximately equal, sometimes resulting in the formation of “bumps” in the isotherm. This effect can be seen by comparing the first and second compression and decompression isotherms of the generation 3.0-decyl and octadecyl terminated polymers in Figure 4.13 as well as the first and second compression and decompression isotherms of the generation 5.0-decyl and dodecyl terminated polymers in Figure 4.14. As the length of the alkyl chains increased, the size of the dendritic block also increased, resulting in larger dispersive forces between polymers on the surface. Thus, the larger polymers were more likely to aggregate on the surface and required more time to dissipate upon decompression, resulting in the formation of a metastable “overexpanded” state. Ariga *et al.* have observed a similar effect for a dendritic amphiphile that they studied at the air/water interface.⁹⁴ The low generation polymers that they examined exhibited very little hysteresis upon decompression; however, the higher generation polymers exhibited a large hysteresis at low surface areas that slowly disappeared as the surface area increased. They attributed this unusual behavior of the hysteresis to the larger dispersive forces in the higher generation dendrimer which induced aggregation that kinetically hindered the reformation of the monolayer. Unfortunately, the generation 4.0 and 5.0-octadecyl terminated polymers did not fit the trends observed for the reversibility and the reproducibility of the isotherms that have been described. However, both of these polymers had a very low degree of substitution of the octadecyl groups on the methyl ester chains, which resulted in their inability to form stable films, and thus their inability to form reversible and

reproducible isotherms. The first and second compression and decompression isotherms of the generation 5.0-octadecyl terminated polymer are presented in Figure 4.14.

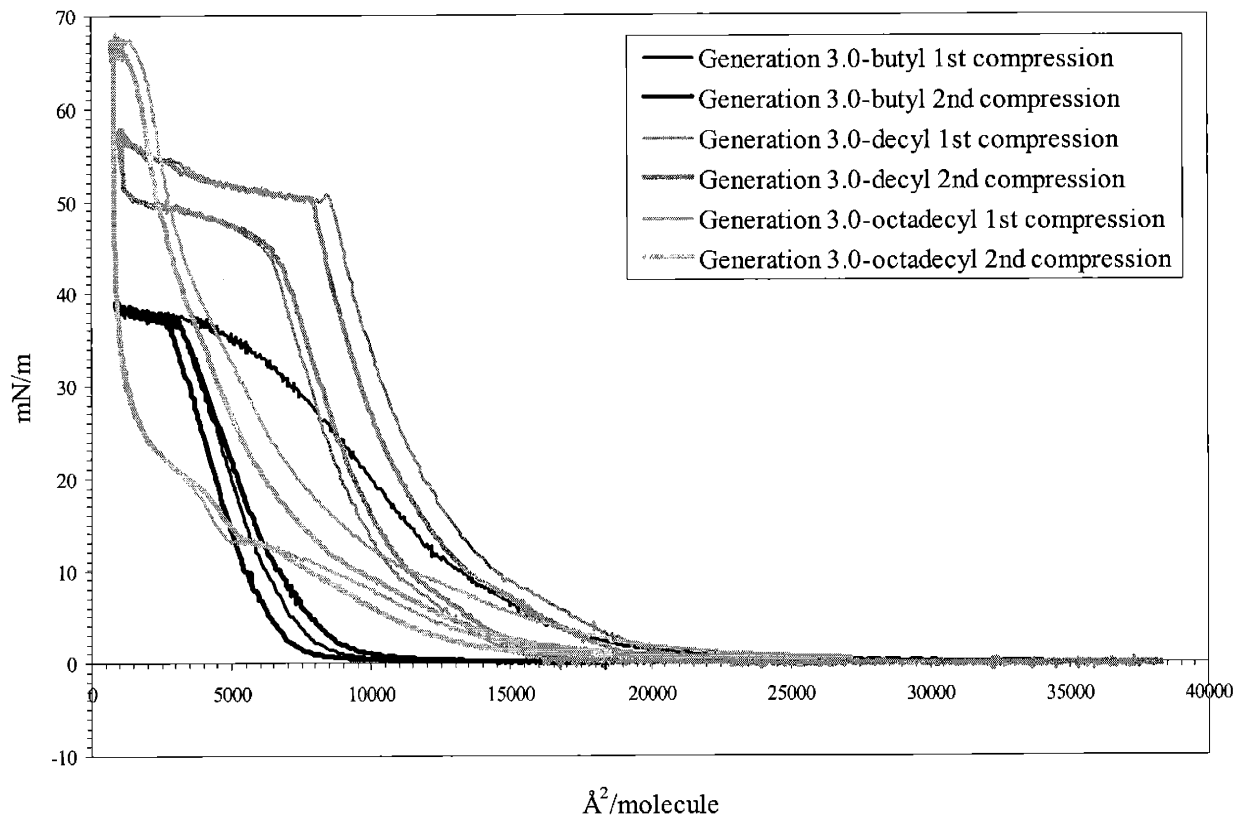


Figure 4.13. First and second compression and decompression pressure/area isotherms of the generation 3.0 linear-dendritic rod diblock copolymers which had a dendritic block length of 97 repeats.

Regardless of generation, all of the methyl ester terminated polymers exhibited a great deal of hysteresis and none of them formed reproducible isotherms. This was most likely the result of the formation of aggregates due to entanglements and the solubilization of the polymer in the subphase, since methyl ester terminated polymers are much more hydrophilic than the other alkyl terminated polymers. Thus, these polymers were not able to form stable films at high compression. The first and second compression and decompression isotherms of the generation 4.5 polymers are presented in Figure 4.14. These isotherms are representative of those collected for all of the methyl ester terminated polymers.

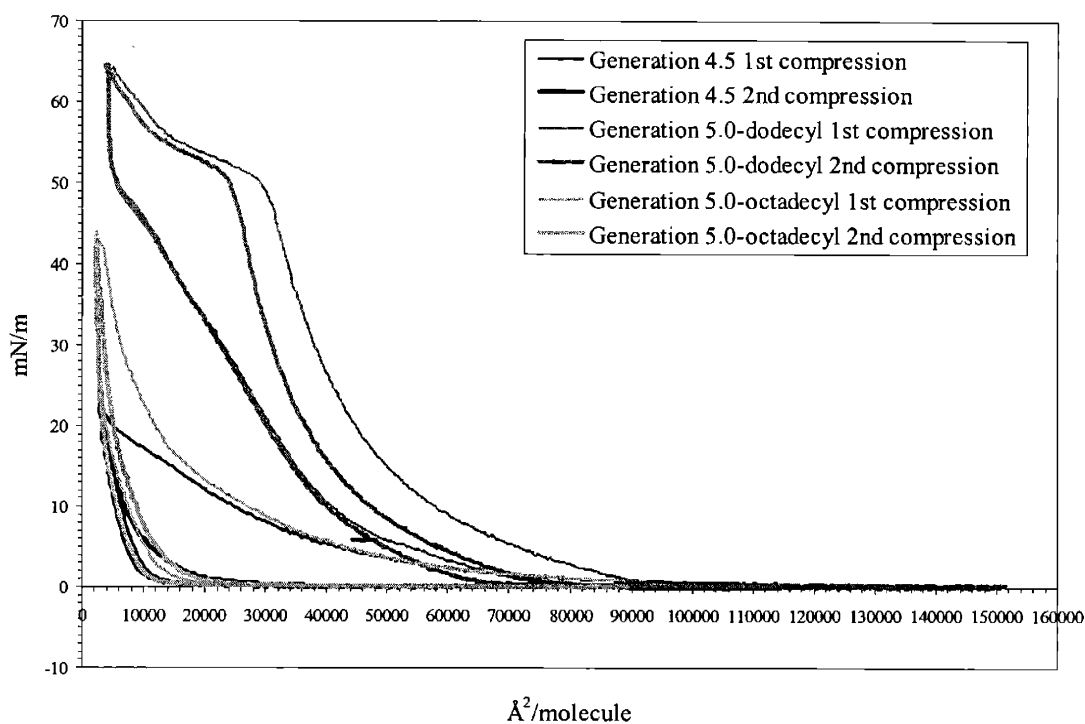


Figure 4.14. First and second compression and decompression pressure/area isotherms of the generation 5.0 linear-dendritic rod diblock copolymers which had a dendritic block length of 97 repeats.

From the decompression isotherms, there was one very interesting feature that was observed. The generation 1.0-alkyl substituted polymers from both series returned to a fully expanded pressure of 2-3mN/m upon expansion even though their initial pressures before compression were zero. This effect can be seen for the generation 1.0-butyl and decyl terminated polymers in Figure 4.12. As previously mentioned, the generation 1.0 polymers seemed to form monolayers in which the polymer arranged differently at the surface before compression and after expansion, possibly due to the formation of aggregates upon compression. Since poly(ethylene oxide) is known to be surface active and exhibits small surface pressures even at large areas,⁴⁰ it is possible that the aggregates that formed allowed the poly(ethylene oxide) block to rearrange itself on the surface upon decompression, and thus contribute more to the surface behavior of the polymer at low surface concentrations. This behavior was not observed for the higher generation polymers, possibly since the higher generation polymers were not as likely to form aggregates upon compression. In addition, the higher generation polymers

were composed of a smaller fraction of poly(ethylene oxide), and its effect on the surface pressure would have been much more limited.

4.4.6 Possible Surface Structures

Now that we have examined the pressure/area isotherms to understand the effects of alkyl chain length, generation number, and length of the dendritic block on the surface pressure, surface area, compressibility, and reversibility and reproducibility of the isotherms, we used this information to try to get an idea of how the polymers might have arranged themselves at the air/water interface. To do this, we proposed three possible models of how the polymer may be arranged, have estimated values for the fully extended (all trans conformation) radius and length of the polymer, and have calculated the surface areas that the polymer might occupy if it were arranged in each of the three models. From there, we compared the true surface area per molecule with the areas calculated using each of the models, and we have attempted to draw some conclusions as to how the polymer might be arranged at the air/water interface. The fully extended, all trans conformation was chosen for calculation of the radius and the length of the polymer for two reasons. First of all, if the alkyl chains were fully substituted and perfectly aligned in a crystalline manner they should exhibit this conformation. Secondly, when the polymer is rigid enough to behave as a rod, the polymer backbone should take on an all trans conformation. While these values are probably an overestimation of the behavior of the polymer, especially at low generation, they give a maximum bound to begin the analysis.

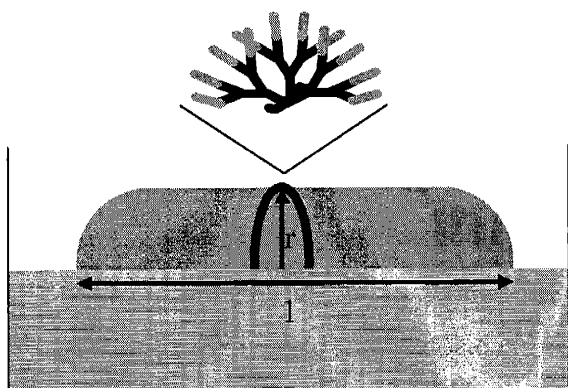
The first model that was proposed was one in which a fully extended, rod shaped polymer was lying flat on the surface, with all of the alkyl chains extended radially around the backbone. The surface area of the polymer for this case was calculated assuming a surface plane cut through the center of the rod parallel to the long axis of the rod: $A = 2rl$, where r was the radius of the rod and l was the length of the rod. (This model would also apply if the hydrophilic portion of the dendrimer was lying flat on the surface and the hydrophobic alkyl chains were extended radially in a hemi-rod away from the surface.) The second model that was proposed was one in which a fully extended rod shaped polymer was lying perpendicular to the surface, with all of the alkyl chains extended radially around the backbone. For this model, the surface area of the polymer was calculated from the area of the base of the rod: $A = \pi r^2$, where r is the radius of the rod. Finally, the third model that was proposed was one in which the poly(amido

amine) dendrimer was lying flat on the surface and all of the alkyl chains were extended vertically from the surface such that the area of the polymer was determined solely by the area occupied by the alkyl chains: $A = 20\text{\AA}^2 a$ where a is the number of alkyl chains with which the polymer had been substituted. This has been the model proposed by Sayed-Sweet for PAMAM homopolymers,⁵³ Schenning for poly(propylene imine) homopolymers,⁵⁵ and Iyer for PAMAM linear-dendritic rod diblock copolymers.⁴⁰ 20\AA^2 is the experimentally determined area that fully compressed alkyl chains are known to occupy.⁶⁵ For the model calculations, it was assumed that only the chains ends that were substituted with alkyl groups would contribute to the limiting area and that those which had not been substituted with alkyl chains would bury themselves into the PAMAM interior, due to phase segregation, and would not contribute to limiting area. Thus, n was determined by multiplying the number of chain ends by the percent substitution of the alkyl groups on the chain ends. Unfortunately, this may have been somewhat of an underestimation of the area occupied by the polymer since it did not take into account all of the monomer units; however, if one wanted to consider the situation where all of the chain ends contributed to the area, whether substituted or not, one only need to refer back to the value obtained for the methyl ester case, where it was assumed that 100 percent substitution of the functional group on the chain ends had occurred. The true value was most likely a value between these two extremes. Graphical representations of the three models are presented in Figure 4.15.

For analysis, values for the experimentally determined surface area and the theoretically determined surface areas assuming each of these models are presented in Tables 4.1, 4.2, 4.3, 4.4, and 4.5. These tables are organized such that each table represents a different generation and the effects of alkyl chain length and dendritic block length for a given generation are listed in the same table. Using this information, we tried to predict how the polymers were organizing themselves at the air/water interface and have illustrated this arrangement using graphical representations in each of the tables. By coincidence, the table number corresponds to the generation number that it models. In each of the representations, the poly(amido amine) portion of the dendrimer are shown in black, the alkyl chains are shown in light gray, and the poly(ethylene oxide) block is shown in medium gray. A cross-section of how the components may have arranged themselves within the polymer is also included.

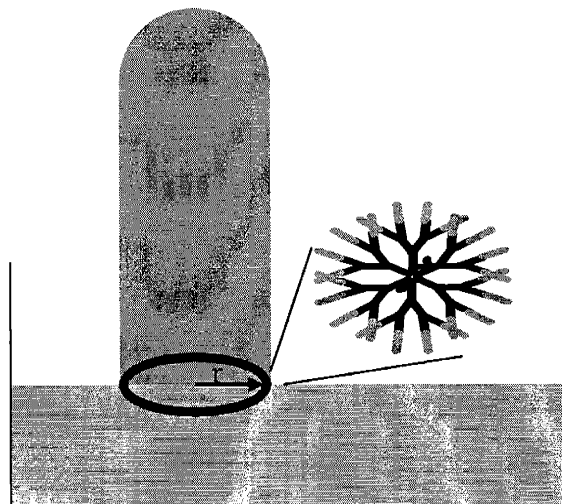
Horizontal Rod Model

$$\text{Area} = 2rl$$



Vertical Rod Model

$$\text{Area} = \pi r^2$$



All Alkyl Chain Model

$$\text{Area} = 20\text{\AA}^2 a$$

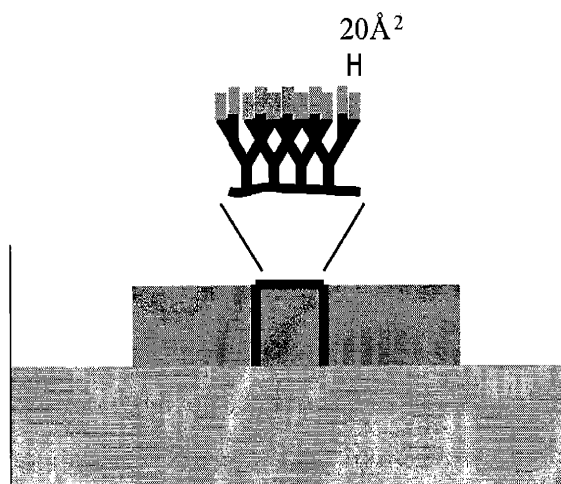


Figure 4.15. Proposed models for the arrangement of the linear-dendritic rod diblock copolymers on the surface.

| Polymer | ester | butyl | hexyl | octyl | decyl | dodecyl | octadecyl |
|--|--------------|----------------|----------------|------------------|------------------|------------------|-------------------|
| Isotherm surface area ($\text{\AA}^2/\text{molecule}$) m = 97 m = 178 | 5400 6400 | 4000 7100 | 4000 6900 | 3300 6600 | 3500 6000 | 3300 6000 | 2900 800, 2200 |
| Predicted fully extended radius (\AA) | 6.15 | 9.84 | 12.4 | 14.9 | 17.5 | 20.0 | 27.7 |
| Predicted fully extended length (\AA) m = 97 m = 178 dendrimer backbone plus 2r | 380 689 | 387 696 | 393 701 | 398 706 | 403 711 | 408 716 | 423 731 |
| Predicted surface area – horizontal rod ($\text{\AA}^2/\text{molecule}$) 2rl – surface plane m = 97 m = 178 | 4674 8474 | 7616 13,697 | 9746 17,384 | 11,860 21,039 | 14,105 24,885 | 16,320 28,640 | 23,434 40,497 |
| Predicted surface area – vertical rod ($\text{\AA}^2/\text{molecule}$) πr^2 – base of rod | 118 | 304 | 483 | 697 | 962 | 1257 | 2410 |
| Predicted surface area – alkyl groups ($\text{\AA}^2/\text{molecule}$) m = 97 m = 178 $20\text{\AA}^2 a$ – where a = # of alkyl chains | 1940 3560 | 1901 3275 | 1843 2350 | 1688 2563 | 1804 2064 | 1746 3168 | 1843 2599 |
| Possible surface structure | | | | | | | |

Table 4.1. Experimentally determined and theoretically calculated surface areas as well as possible surface structures for the generation 1.0 linear-dendritic rod diblock copolymers.

| Polymer | ester | butyl | hexyl | octyl | decyl | dodecyl | octadecyl |
|---|--------|--------|--------|--------|--------|---------|---------------|
| Isotherm surface area ($\text{\AA}^2/\text{molecule}$) m = 97 | 8000 | 7400 | 7000 | 6900 | 6400 | 6400 | 1200, 1800 |
| Predicted fully extended radius (\AA) | 14.4 | 18.3 | 20.9 | 23.4 | 26.0 | 28.6 | 36.3 |
| Predicted fully extended length (\AA) m = 97 dendrimer backbone plus 2r | 397 | 405 | 410 | 415 | 420 | 425 | 441 |
| Predicted surface area – horizontal rod ($\text{\AA}^2/\text{molecule}$) 2rl – surface plane m = 97 | 11,433 | 14,823 | 17,138 | 19,422 | 21,840 | 24,310 | 32,016 |
| Predicted surface area – vertical rod ($\text{\AA}^2/\text{molecule}$) πr^2 – base of rod | 651 | 1052 | 1372 | 1720 | 2123 | 2570 | 4139 |
| Predicted surface area – alkyl groups ($\text{\AA}^2/\text{molecule}$) m = 97 $20\text{\AA}^2 a$ – where a = # of alkyl chains | 3880 | 3182 | 3802 | 3725 | 2949 | 3686 | 1048 |
| Possible surface structure | | | | | | | |

Table 4.2. Experimentally determined and theoretically calculated surface areas as well as possible surface structures for the generation 2.0 linear-dendritic rod diblock copolymers.

| Polymer | ester | butyl | hexyl | octyl | decyl | dodecyl | octadecyl |
|--|--------|--------|--------|--------|--------|---------|-----------|
| Isotherm surface area ($\text{\AA}^2/\text{molecule}$) $m = 97$ | 13,500 | 15,500 | 14,000 | 13,000 | 12,750 | 11,250 | 5500 |
| Predicted fully extended radius (\AA) | 22.9 | 26.9 | 29.5 | 31.9 | 34.5 | 37.0 | 44.7 |
| Predicted fully extended length (\AA) $m = 97$ dendrimer backbone plus $2r$ | 414 | 422 | 427 | 432 | 437 | 442 | 457 |
| Predicted surface area – horizontal rod ($\text{\AA}^2/\text{molecule}$) $2rl$ – surface plane $m = 97$ | 18,961 | 22,703 | 25,193 | 27,562 | 30,153 | 32,708 | 40,856 |
| Predicted surface area – vertical rod ($\text{\AA}^2/\text{molecule}$) πr^2 – base of rod | 1647 | 2273 | 2733 | 3196 | 3739 | 4300 | 6277 |
| Predicted surface area – alkyl groups ($\text{\AA}^2/\text{molecule}$) $m = 97$ $20\text{\AA}^2 a$ – where $a = \#$ of alkyl chains | 7760 | 7682 | 7527 | 6906 | 6518 | 5122 | 2560 |
| Possible surface structure | | | | | | | |

Table 4.3. Experimentally determined and theoretically calculated surface areas as well as possible surface structures for the generation 3.0 linear-dendritic rod diblock copolymers.

| Polymer | ester | butyl | hexyl | octyl | decyl | dodecyl | octadecyl |
|--|--------|--------|--------|--------|--------|---------|-----------|
| Isotherm surface area ($\text{\AA}^2/\text{molecule}$) $m = 97$ | 26,000 | 29,000 | 29,000 | 29,000 | 29,000 | 26,000 | 6000 |
| Predicted fully extended radius (\AA) | 31.5 | 35.4 | 38.1 | 40.6 | 43.1 | 45.6 | 53.3 |
| Predicted fully extended length (\AA) $m = 97$ dendrimer backbone plus $2r$ | 430 | 438 | 444 | 449 | 454 | 460 | 475 |
| Predicted surface area – horizontal rod ($\text{\AA}^2/\text{molecule}$) $2rl$ – surface plane $m = 97$ | 27,090 | 31,010 | 33,833 | 36,459 | 39,125 | 41,952 | 50,635 |
| Predicted surface area – vertical rod ($\text{\AA}^2/\text{molecule}$) πr^2 – base of rod | 3117 | 3937 | 4560 | 5178 | 5836 | 6532 | 8925 |
| Predicted surface area – alkyl groups ($\text{\AA}^2/\text{molecule}$) $m = 97$ $20\text{\AA}^2 a$ – where $a = \#$ of alkyl chains | 15,520 | 15,365 | 15,054 | 14,589 | 13,969 | 15,365 | 1862 |
| Possible surface structure | | | | | | | |

Table 4.4. Experimentally determined and theoretically calculated surface areas as well as possible surface structures for the generation 4.0 linear-dendritic rod diblock copolymers.

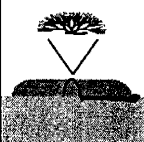

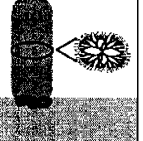
| Polymer | ester | dodecyl | octadecyl |
|--|---|--|---|
| Isotherm surface area ($\text{\AA}^2/\text{molecule}$) $m = 97$ | 43,000 | 48,000 | 11,000 |
| Predicted fully extended radius (\AA) | 40.0 | 54.1 | 61.8 |
| Predicted fully extended length (\AA) $m = 97$ dendrimer backbone plus $2r$ | 449 | 477 | 493 |
| Predicted surface area – horizontal rod ($\text{\AA}^2/\text{molecule}$) $2rl$ – surface plane $m = 97$ | 35,920 | 51,611 | 60,935 |
| Predicted surface area – vertical rod ($\text{\AA}^2/\text{molecule}$) πr^2 – base of rod | 5026 | 9194 | 11,998 |
| Predicted surface area – alkyl groups ($\text{\AA}^2/\text{molecule}$) $m = 97$ $20\text{\AA}^2 a$ – where $a = \#$ of alkyl chains | 31,040 | 28,557 | 4035 |
| Possible surface structure |  |  |  |

Table 4.5. Experimentally determined and theoretically calculated surface areas as well as possible surface structures for the generation 5.0 linear-dendritic rod diblock copolymers.

For all of the methyl ester terminated polymers, it appeared as if the model for the fully extended horizontal rod was the best fit for the dendritic block. The areas determined from this model were very close to the areas determined experimentally, and for the highest generation polymer, was smaller than the area determined experimentally. From AFM experiments, poly(amido amine) dendrimers are known to spread and flatten on hydrophilic surfaces such as mica, thus it would not be surprising if the methyl ester terminated polymers also would have spread and flattened on the water surface.²⁹ As previously mentioned, it was difficult to determine from the model if the dendritic branches were radiating from the backbone such that a full rod or a hemi-rod formed on the surface. It can be hypothesized that especially at low generations where the arms had much more flexibility, the arms were probably radiating out as a hemi-rod in order to minimize the interactions between the slightly hydrophobic methyl ester ends and the water. For the higher generation polymers which had much less flexibility, either situation seemed likely. Poly(amido amine) dendrimers are known to be able to contort themselves to lie flat on the surface to minimize unfavorable interactions, leading one to believe

that the hemi-rod was the most probable conformation for these polymers. On the other hand, the methyl ester groups were small enough that it may have been possible for them to bury themselves in the interior of the dendrimer to shield them from the water, resulting in the dendritic block still being able to behave as an almost complete rod but where the unfavorable interactions were also minimized. A combination of these situations might also have been the case, where the poly(amido amine) dendrimer was able to flatten itself partially, but not completely on the surface.

Now that a model has been set forth for the behavior of the dendritic block of the methyl ester terminated linear-dendritic rod diblock copolymers, a model for the behavior of the poly(ethylene oxide) block will be proposed. For the low generation polymers, generation 1.0 and 2.0, a plateau in the pressure/area isotherms was observed that was attributed to the presence of the poly(ethylene oxide) block. Thus, for these polymers, the poly(ethylene oxide) block was definitely active at the interface during the formation of the monolayers. While this plateau was not nearly as visible for the higher generation polymers, the poly(ethylene oxide) block was still probably contributing to the ordering of the polymers at the surface. Using x-ray reflectivity, Johnson *et al.* recently examined the ordering of stearate terminated poly(ethylene oxide)-poly(amido amine) hybrid-linear dendritic diblock copolymers at the air/water interface.⁵⁷ They found that for the generation 3.0 and 4.0 polymers, the poly(ethylene oxide) block formed an interfacial layer between the water and the dendritic block. Surprisingly, they did not find that the poly(ethylene oxide) block dissolved in the water to form a brush-like structure, but rather formed a very hydrated layer just below the surface of the water. Similar results were observed by Cox *et al.* who looked at the behavior of polystyrene-poly(ethylene oxide) diblock copolymers at the air/water interface.^{69,70} They found that the polystyrene block formed islands on a thin layer of hydrated poly(ethylene oxide) resulting in the formation of well-defined surface aggregates. Finally, Richards *et al.* have also found that the poly(ethylene oxide) block in poly(methyl methacrylate)-poly(ethylene oxide) diblock copolymers did not form a brush like structure upon compression but rather formed a thin hydrated layer just below the surface of the water. They also found that over 90 percent of the poly(ethylene) oxide resided just below the air/water interface and only the remaining 10 percent protruded into the bulk water.^{73,95} Thus, for the methyl ester terminated linear-dendritic rod diblock copolymers under investigation, it was very likely that the poly(ethylene oxide) block also formed a very hydrated layer at the

air/water interface and did not form a brush like structure upon compression. For the low generation polymers, where the fraction and sizes of the dendritic and poly(ethylene oxide) blocks were more comparable, the two blocks most likely formed a mixed poly(ethylene oxide)/dendritic block layer that was more rich in poly(ethylene oxide) near the water and more rich in dendritic block near the air. Since the methyl ester dendritic block was more hydrophilic than the other types of blocks that had been investigated, the poly(ethylene oxide) block was probably not able to form a discreet interfacial layer between the dendritic block and the water and thus formed this mixed layer. For the higher generation polymers, where the fraction and size of the methyl ester dendritic block was so much greater than the poly(ethylene oxide) block, and where it appeared as if the methyl ester dendritic block was lying as a horizontal rod on the surface, the poly(ethylene oxide) block was probably not able cover the entire interfacial area between the dendritic block and the water. Thus, portions of the interfacial area probably consisted of a mixed poly(ethylene oxide)/dendritic block layer, while the other portions consisted of only a dendritic layer. This situation was probably one to which the dendritic block was very amenable. As previously mentioned, Sayed-Sweet has examined the interfacial behavior of poly(amido amine) spherical dendrimers which were terminated with hydrophobic alkyl chains and found that the hydrophilic dendrimer was very happy residing at the air/water interface with the alkyl chains arranged perpendicular to the surface.⁵³

The surface structures for the butyl through the dodecyl terminated linear-dendritic rod diblock polymers seemed to be very dependent on the generation of the polymer as well as the length of the alkyl chains with which they were substituted. For both series of the generation 1.0-butyl through dodecyl terminated polymers, there did not appear to be one model that predicted the surface area per molecule. While the horizontal rod model was an overestimation, the vertical rod and the all alkyl chain models were underestimations; thus, the real arrangement was probably a combination of the models. As previously mentioned, the surface area per molecule of these polymers decreased with increasing alkyl chain length such that the vertical rod model or the all alkyl chain models appeared to become better fits as the alkyl chain length increased. However, if the all alkyl model were the dominant model, one would have expected that all, or almost all of the polymers would have exhibited the same surface area per molecule independent of alkyl chain length. Sayed-Sweet and Aoi reported the all alkyl model for PAMAM spherical dendrimers and their diblock copolymer derivatives that had been terminated

with alkyl chains as short as hexyl groups.^{53,58} As this was not observed for the generation 1.0 linear-dendritic rod diblock copolymers under investigation, the most likely arrangement of the polymers on the surface was one in which the dendritic blocks were behaving as random coils on the surface that tended to elongate away from the surface as the alkyl chain length was increased, as illustrated in table 4.1. Unlike the spherical dendrimers and their linear-dendritic rod diblock copolymer derivatives where the entire PAMAM portion was tethered to the surface and the alkyl chains had no other option than to extend away from the surface in order to be able to segregate and minimize their free energy, the dendritic block of the generation 1.0-alkyl terminated linear-dendritic diblock copolymers had much more flexibility and could behave as a random coil on the surface due to its length. This arrangement also allowed the alkyl chains of the dendritic block to minimize their free energy by forming domains within the dendritic coils. Other researchers have found that for amphiphilic diblock copolymers of polystyrene-poly(ethylene oxide) and poly(methyl methacrylate)-poly(ethylene oxide), the hydrophobic block tends to form a random coil structure on top of a thin poly(ethylene oxide) layer.^{68-70,95} Thus, for the generation 1.0-butyl through dodecyl terminated polymers, the arrangement of the polymers seemed to be governed more by their diblock copolymer nature than by their dendritic nature. It was also very reasonable to assume that the decrease in surface area per molecule was due to an elongation of the dendritic coils with increasing alkyl chain length. As the length of the alkyl chain, and thus its hydrophobic nature increased, the unfavorable interactions between the water and the alkyl chains also increased such that the alkyl chains preferred to distance themselves as much as possible from the surface of the water by elongated the dendritic backbone away from the interface. In addition, as previously mentioned, Kang *et al.* have investigated the lateral diffusion of several long alkyl chain amphiphilic derivatives, and they reported that longer alkyl chain amphiphiles exhibited smaller immersion depths and thus larger diffusion constants of lateral mobility than the shorter alkyl chain amphiphilics did due to their more hydrophobic nature.⁷⁸ Thus, the polymers terminated with the longer alkyl chains probably had more mobility on the surface and could more readily rearrange themselves into more elongated structures upon compression. Finally, from the compression data, it was found that the linear-dendritic rod diblock copolymers terminated with the longer alkyl chains formed more tightly packed, less compressible films than the polymers terminated with the shorter alkyl chains, such that the polymers terminated with the longer alkyl chains could be pushed into more

elongated structures while still maintaining a stable film. The poly(ethylene oxide) block in these generation 1.0-butyl through dodecyl terminated linear-dendritic rod diblock copolymers was most likely behaving in a similar manner to that observed for the low generation methyl ester terminated polymers described in the previous paragraph. The poly(ethylene oxide) block most likely attempted to form a very hydrated layer near the surface of the water. For the polymers terminated with the shorter alkyl chains, the poly(ethylene oxide) and the dendritic block probably formed a mixed layer than was more rich in poly(ethylene oxide) near the water and more rich in dendritic block near the air. However, as the length of the alkyl chain increased, the mixing between the two blocks probably decreased such that a more well-defined poly(ethylene oxide) interfacial layer formed with the dendritic block residing on top of it and the alkyl chains forming domains within the dendritic block, as illustrated in table 4.1.

The generation 2.0 and 3.0-butyl through dodecyl terminated polymers exhibited a similar behavior to that of the generation 1.0 terminated polymers - there was no one single model that fit the data and the actual arrangement was probably a combination of the models. As for the generation 1.0 polymers, the generation 2.0 and 3.0 polymers were probably behaving as random coils on the surface that tended to elongate away from the surface as the alkyl chain length increased, as illustrated in tables 4.2 and 4.3. The reasons for this arrangement are the same as those discussed above for the generation 1.0 polymers. While the dendritic blocks of the generation 2.0 and 3.0 polymers were much more branched and thus did not have the same degree of flexibility as the generation 1.0 polymers, they could still take on, at least somewhat, a random coil or extended random coil configuration. Yin *et al.* have found that poly(amido amine) dendritic rod homopolymers did not possess the degree of branching and stiffness necessary to form a rod-shaped structure until generation 4.5.⁸⁷ The poly(ethylene oxide) block in these generation 2.0 and 3.0-butyl through dodecyl terminated linear-dendritic rod diblock copolymers was probably trying to arrange itself in a manner similar to that observed for the generation 1.0-butyl through dodecyl terminated diblock copolymers described in the previous paragraph. However, as the generation number of the dendritic block increased, it probably became more difficult for the poly(ethylene oxide) block to cover the entire interfacial area between the dendritic block and the water. Thus, as in the case of the higher generation methyl ester terminated polymers, portions of the interfacial area probably consisted of a mixed poly(ethylene oxide)/dendritic block layer, while the other portions consisted of only a dendritic

layer. As in the case of the generation 1-butyl through dodecyl terminated polymers, in the places where the poly(ethylene oxide) was able to cover the surface, the polymers terminated with the shorter alkyl chains most likely formed a mixed poly(ethylene oxide)/poly(amido amine)/alkyl chain layer that was more rich in poly(ethylene oxide) near the water and more rich in alkyl chains near the air, while those terminated with the longer alkyl chains probably formed more discrete layers with the poly(ethylene oxide) layer near the water and the dendritic block residing on top of it. In the places where the poly(ethylene oxide) was not able to cover the surface, the polymers terminated with the shorter alkyl chains probably formed a mixed interfacial layer which was more rich in poly(amido amine) near the water and more rich in alkyl chains near the air, while the polymers terminated with the longer alkyl chains probably formed more discrete layers in which the poly(amido amine) interior shielded the alkyl chains from the water. Thus, the hydrophilic poly(amido amine) interior probably also helped to stabilize the linear-dendritic rod diblock copolymers on the surface.

When the generation 4.0 polymers were examined, all of the polymers that were terminated with butyl through dodecyl groups seemed to fit very closely to one model – a model in which the polymers were lying as near horizontal rods on the surface and where the alkyl groups exhibited some alignment perpendicular to the surface. For the butyl terminated polymers, the surface area predicted for a horizontal rod was in very good agreement with that from experiment. However, as the length of the alkyl chain increased, the surface area per molecule predicted for the horizontal rod began to overestimate the value from experiment, even though the value from experiment seemed to remain almost constant. This was because the predicted surface area per molecule was calculated assuming the alkyl chains were lying parallel to the surface, and thus the addition of more carbons increased the radius and the area of the rod. If instead, only the poly(amido amine) portion of the dendrimer was lying parallel to the surface and the alkyl chains were trying to align themselves perpendicular to the surface, then the addition of more carbons to the alkyl chains would not have resulted in an increase in the surface area per molecule and the surface area per molecule would have appeared to be independent of alkyl chain length. While some alignment of the alkyl chains was likely, an all alkyl model was not, as it greatly underestimated the value of the surface area. Thus, for the generation 4.0 polymers it appeared as if the polymer had reached a size and stiffness that prevented it from forming a random coil on the surface and instead caused it to take on a rod-like configuration.

This was not surprising when one considers that Yin found that the PAMAM rod homopolymers did not form rods at generation 3.5, but did at generation 4.5.⁸⁷ Since the addition of alkyl groups led to an increase in the size and thus the steric interactions around the dendrimer, plus the alkyl groups could align to order the branches and increase the stiffness of the dendritic block, it was not unreasonable to assume that these two factors had the same effect as the addition of another generation, and pushed the dendritic block to adopt a rod-like configuration. This increase in stiffness and curvature for the high generation polymers also probably prevented the alkyl chains from being able to align themselves completely perpendicular to the interface. These results were in good agreement with what had been observed for other dendritic systems at high generation. Iyer *et al.* found that for their generation 1.0 through 3.0 stearate terminated poly(ethylene oxide)-PAMAM hybrid-linear dendritic diblock copolymers, the polymers arranged such that the surface area per molecule was determined by the stearate groups; however, the generation 4.0 stearate terminated polymers did not follow this model as the curvature of the dendrimer was too great and did not allow for the complete alignment of the alkyl groups.⁴⁰ Similarly, when Sidorenko *et al.* examined poly(benzyl ether) dendrimers terminated with dodecyl groups and possessing an azobenzene crown ether core, they found that at low generation, the dodecyl chains were aligned perpendicular to the interface; however, at higher generations they were oriented radially due to the curvature of the dendritic portion.⁵² Now that the behavior of the dendritic block of the linear-dendritic rod diblock copolymer has been discussed, the behavior of the poly(ethylene oxide) block needs to be examined. At generation 4.0 of the diblock copolymers, the relative size and fraction of the poly(ethylene oxide) block to the dendritic block was very small. Since it appeared as if the dendritic portion was lying as a vertical rod on the surface, the poly(ethylene oxide) block was probably not large enough to provide a complete interfacial layer between the dendritic block and the water. While it probably was partially able to form a layer to cover the water, the hydrophilic poly(amido amine) interior portion of the dendritic block also probably contributed to the interface with the water and helped to stabilize the diblock copolymer on the surface as described above for the generation 2.0 and 3.0-butyl through dodecyl terminated polymers.

For all of the octadecyl terminated polymers, the model for the vertical rod, or a near vertical rod, appeared to be the best fit for the dendritic block. First of all, the surface areas determined experimentally seemed to correspond most closely with those of the vertical rod

model. Secondly, while the surface areas of the all alkyl model were also in the same range as the experimental determined areas, one would have expected that if this were the dominant model, all or almost all of the polymers would have exhibited the same surface area per molecule independent of alkyl chain, and this was not observed. (Even taking into account differences in the degree of substitution, the surface areas were not constant.) Finally, for the generation 1.0 polymers, the surface area per molecule was found to be independent of dendritic block length. This would only have been possible if the surface area of the polymer was determined primarily by the radius of the dendritic block, which is the case for the vertical rod model. For the generation 1.0 polymer with the shorter dendritic block ($m = 97$), the area reported at $2900\text{\AA}^2/\text{molecule}$ was in very good agreement with the vertical rod model. For the generation 1.0 polymer with the longer dendritic block ($m = 178$), two areas were reported since there appeared to be two dominant transitions. The first transition area, at approximately, $2200\text{\AA}^2/\text{molecule}$, was in good agreement with the vertical rod model, while the second transition area, at approximately $800\text{\AA}^2/\text{molecule}$, was a little less than half of it. The formation of a second transition for the polymer with 178 repeats was mostly likely the result of the polymer possessing a lower degree of substitution, and thus not being as rigid. As a result, the polymer could be more easily compressed to a more tightly packed configuration, possibly one in which the alkyl chains were able to fold in and/or interdigitate with those from neighboring polymer molecules. As a consequence, the polymer would have been able to rearrange to a smaller area on the surface. (It should be noted that the surface area of the polymer with the longer dendritic block in its most compressed state was still greater than the surface area of a vertical rod of a polymer of the same generation which had been substituted with at least octyl groups, indicating that the polymer did not compress to a state of unreasonable area, but one in which the alkyl chains were not adopting an all trans, non-interdigitating configuration.) A similar situation was observed for the generation 2.0-octadecyl terminated polymer. In this case, three dominant transitions were seen, one at approximately $4600\text{\AA}^2/\text{molecule}$, a second at approximately $1800\text{\AA}^2/\text{molecule}$, and a third at approximately $1200\text{\AA}^2/\text{molecule}$. The first transition, at approximately $4600\text{\AA}^2/\text{molecule}$ was in fairly good agreement with the model for a vertical rod, while the other two transitions were most likely due to folding in and/or interdigitation of the alkyl chains upon further compression due to their low degree of substitution. (Again it should be noted that the surface area of the polymer in its most

compressed state was still greater than the surface area of a vertical rod of a polymer of the same generation which had been substituted with at least butyl groups, indicating that the polymer did not compress to an unreasonable area.) The generation 3.0-octadecyl terminated polymer exhibited one transition, at approximately $5500\text{\AA}^2/\text{molecule}$, in good agreement with the value predicted for a vertical rod. While this polymer also possessed a somewhat low degree of substitution, approximately 33%, it appears as if it were rigid enough to prevent further folding or interdigitation. This isn't completely surprising when one considers that the generation 3.0 polymer had four branches per repeat, corresponding to an average of approximately 1.2 octadecyl chains per repeat plus a stiffer poly(amido amine) interior. However, the generation 1.0 polymer with the longer dendritic block had only 0.73 octadecyl groups per repeat and the generation 2.0 polymer had only 0.54 octadecyl groups per repeat plus in addition to a less rigid poly(amido amine) interior for both polymers. For the generation 4.0 and 5.0-octadecyl terminated polymers, the surface area per molecule was also most consistent with the polymer behaving as a vertical rod on the surface. Unfortunately, as previously mentioned, these polymers did not appear to be very stable on the surface, possibly due to the extremely low degree of substitution of the octadecyl groups. Thus, even if the polymers were able to adopt a vertical rod-like configuration, it would have been difficult to transfer them to prepare coherent Langmuir-Blodgett films due to their lack of stability. It is not unreasonable to find that the octadecyl terminated polymers were able to behave as vertical rods on the surface while the others were not. First of all, as previously mentioned, it has been found that longer alkyl chain amphiphiles exhibit smaller immersion depths and thus larger diffusion constants of lateral mobility than shorter alkyl chains do.⁷⁸ Thus, for the linear-dendritic rod diblock copolymers under investigation, the polymers terminated with the longer alkyl chains may not have been immersed as deeply in the water and have been more likely to undergo rearrangement of the entire dendritic block, whereas the short alkyl terminated polymers were ground more firmly at the interface and could not undergo this type of rearrangement. Second, the octadecyl chains were much longer and able to form stronger crystalline domains than the shorter alkyl chains, as illustrated by a higher melting point for the alkyl chains from DSC. The melting point of the other shorter chains was approximately 20°C , while that of the octadecyl chains was approximately 50°C . (For more detailed information about the melting and glass transition temperatures of the polymers, please see Section 5.4.1.) Even at room temperature, the

octadecyl chains still maintained their crystalline state while the shorter alkyl chains did not. Thus, the octadecyl terminated polymers were stiffer and more able to adopt a rod-like configuration. As previously mentioned, the ability of a rod-coil diblock copolymer to adopt an arrangement where the rod was aligned vertical to the surface has been observed by other groups. Amphiphilic poly(γ -benzyl-L-glutamate)-b-poly(L-glutamic acid) (PBLG-b-PLGA) copolypeptides, poly(γ -methyl-L-glutamate)-b-poly(ethylene glycol) diblock copolymers, and poly(ethylene oxide)-poly(methylphenylsilane) multiblock copolymers are all examples of polymers where the rigid portion was able to adopt a conformation perpendicular to the surface.⁵⁹⁻⁶¹

The poly(ethylene oxide) block in the octadecyl terminated linear-dendritic rod diblock copolymers most likely formed a surface layer at the air/water interface as had been observed for the other diblock copolymers. However, since it appeared that the octadecyl terminated polymers were behaving as vertical rods on the surface, the poly(ethylene oxide) was probably able to form a very discreet interfacial layer between the water and the dendritic block, and thus served as the primary hydrophilic anchor of the hydrophobic dendritic block to the surface. For the low generation octadecyl terminated polymers, the poly(ethylene oxide) block most likely covered the entire interfacial area, while for the higher generation polymers, it probably covered as much as it could, leaving a small area of poly(amido amine) interior to fill up the uncovered areas, but shielding the alkyl chains from the surface.

In the future, it would be very interesting to examine a linear-dendritic rod diblock copolymer system in which the poly(ethylene oxide) block was large enough to completely cover the water interface below a generation 4.0-alkyl terminated polymer. (The length of the poly(ethylene oxide) block was originally chosen such that it would be large enough to cover the base of a generation 4.5 methyl ester terminated diblock copolymer that was behaving as a vertical rod on the surface. Since it has been found that the methyl ester terminated polymers will not arrange in this manner, the poly(ethylene oxide) block was not large enough to be able to do this.) Since the alkyl terminated polymers were behaving as rods at this generation and since it appeared as if the polymers were somewhat anchored to the surface by the poly(amido amine) interior, if the poly(ethylene oxide) block were large enough to cover the poly(amido amine)/water interface and provide a very strong hydrophilic anchor and interfacial layer,

perhaps it would give the generation 4.0 polymers terminated with the longer alkyl chains enough mobility to break free from the surface and form vertical rods on the surface.

4.5 Summary and Conclusions

The behavior of amphiphilic linear-dendritic rod diblock copolymers at the air/water interface has been examined using pressure/area isotherms of the polymers collected on the surface of a Langmuir-Blodgett trough. A comprehensive study of the behavior which looked at the effects of alkyl chain length, generation number, and the length of the dendritic block was undertaken in order to gain information as to how these parameters affected the surface pressure, surface area, compressibility, and reversibility and reproducibility of the films. From this information, an arrangement of polymers on surface has been proposed.

The low generation polymers were found to form small plateaus in the surface pressure at approximately 20mN/m due to the presence of the poly(ethylene oxide) block on the surface. As the generation number and length of the dendritic block increased, this plateau all but disappeared as the fraction of the poly(ethylene oxide) in the polymers decreased. Other intermediate plateaus in the surface pressure were also found for the polymers terminated with the longer alkyl chains due to rearrangements of the alkyl chains as well as the polymers themselves on the surface. The plateaus that formed at the highest surface pressure were attributed to collapse of the polymer monolayer. The surface pressure at collapse was most highly dependent on the length of the alkyl group with which the polymers were functionalized and was independent of the generation number and length of the dendritic block. Especially for the octadecyl terminated polymers, the degree of substitution was also important, as polymers substituted with less than approximately 30% of octadecyl chains did not form stable films on the surface.

The surface area of the polymers in their most condensed state was found to increase with increasing generation and length of the dendritic block, except for the octadecyl terminated polymers where the surface area was found to be independent of dendritic block length. In addition, for the generation 1.0, 2.0, and 3.0 polymers, the surface area was found to decrease with increasing length of the alkyl chain, most likely due to elongation of the dendritic block backbone away from the surface in order to minimize the unfavorable interactions between the

longer, more hydrophobic alkyl chains and the water. For the generation 4.0 and 5.0 butyl through dodecyl terminated polymers, the surface area was found to remain approximately constant as the polymers became too large and too stiff to be able to elongate from the surface. For the generation 4.0 and 5.0 octadecyl terminated polymers, the surface area was found to decrease dramatically from the other, shorter alkyl chains. It is possible that the polymers terminated with longer alkyl chains were able to adopt a different conformation on the surface as amphiphilicities with longer alkyl chains are known to have greater diffusion constants and thus greater mobility on the surface. Although the low substitution of the octadecyl chains on these polymers may also have been a factor.

The compressibility of the polymers was found to be most dependent on the length of the alkyl chain with which the polymers were substituted and was mostly independent of the generation number and the length of the dendritic block. In general, the compressibility decreased with increasing length of the alkyl chains with the largest decrease occurring between the methyl ester and the butyl groups and little to no decrease occurring for the octyl through dodecyl groups. Surprisingly, the octadecyl polymers were found to be more compressible than the dodecyl terminated polymers, possibly due to a change in the conformation of the polymer on the surface or a lower degree of substitution of alkyl chains on the octadecyl terminated polymers.

In general, the reversibility and reproducibility of the isotherms improved as the generation number increased. As the generation number increased, the polymer became more densely packed, and thus it became more difficult for the polymers to entangle and form aggregates that remained somewhat intact upon decompression. In addition, the reversibility and reproducibility of the isotherms tended to be better for the polymers terminated with hexyl, octyl, and decyl groups than with shorter or longer alkyl chains. While it was more difficult for the polymers terminated with the shorter alkyl groups to form stable films due to their lack of hydrophobicity, the polymers terminated with the longer alkyl chains were more likely to form aggregates that did not disassociate as easily due to the increased dispersive forces between the polymers.

The arrangement of the polymers at the air/water interface was very different than what had been hypothesized at the beginning of the project. Originally, it had been hoped that the methyl ester terminated polymers might be able to form stable, ordered films with the dendritic portion aligned perpendicular to the surface. It was also hoped that even if a methyl ester

terminated polymer or one substituted with short alkyl chains may not be able to form the desired ordered films at a lower generation, it may at a higher generation due to the multiplication of the number of end groups that occurs at higher generations. Similarly, it was hoped that by increasing the length of the dendritic block and thus the fraction of the hydrophobic component, methyl ester terminated polymers or those substituted with shorter alkyl chains may be able to form the desired ordered films whereas they may not have been able to when the fraction of the hydrophobic component was less. None of these things were found to be true. Instead, it was found that all of the methyl ester terminated polymers formed fairly instable films at the air/water interface, and that the polymers were found to orient as horizontal rods on the surface. In addition, for the generation 1.0, 2.0, and 3.0 polymers that were terminated with butyl through dodecyl groups, the surface area per molecule decreased as the length of the polymer increased due to an elongation of dendritic block backbone away from the surface in order to minimize the unfavorable interactions between the alkyl chains and the surface of the water. Thus, for these low generation linear-dendritic diblock copolymers, the diblock copolymer nature of the polymer was found to be more important to the arrangement of the polymers in the films than the dendritic nature of the polymer. However, for the generation 4.0 butyl through dodecyl terminated polymers, it appeared as if the polymers had become too bulky and stiff to be able to form elongated random coils on the surface and thus oriented themselves as horizontal rods in which the alkyl chains tried to align themselves perpendicular to the surface, but could not because of the curvature of the dendritic branches. Thus, the dendritic nature of the diblock copolymer became important in the alignment of these higher generation polymers on the surface. Nonetheless, all of the octadecyl terminated polymers appeared to form vertical rods on the surface. This change in arrangement may have resulted from the stiffer octadecyl chains which caused the polymer to adopt a more rod-like nature, or by the higher diffusion constants that amphiphiles substituted with longer alkyl chains are known to possess. It is not unreasonable to think that the octadecyl terminated linear-dendritic rod diblock copolymers studied were able to orient as vertical rods on the surface, as this type of orientation has been reported for other rod-coil diblock copolymer systems. The poly(ethylene oxide) block in all of these linear-dendritic rod diblock copolymers appeared to form a very hydrated interfacial layer near the surface of the water. For the lower generation polymers, the poly(ethylene oxide) block was probably able to cover most of the interfacial area between the water and the dendritic block. The polymers that

were terminated with shorter alkyl chains most likely formed a mixed layer with the poly(ethylene oxide) that was more rich in poly(ethylene oxide) near the water and more rich in alkyl chains near the air, while the polymers that were terminated with longer alkyl chains most likely formed a more discrete poly(ethylene oxide) interfacial layer with the dendritic block forming a more distinct layer above it. For the higher generation polymers in which the poly(ethylene oxide) block was too small to be able to cover the entire interfacial area between the dendritic block and the water, the poly(ethylene oxide) block most likely formed a partial layer to cover the water, and the hydrophilic poly(amido amine) interior portion of the dendritic block also formed an interface with the water and helped to stabilize the diblock copolymer on the surface.

In conclusion, in order to form stable films at the air/water interface where the dendritic block is aligned perpendicular to the interface, it appears as if the poly(ethylene oxide)-poly(ethylene imine)-poly(amido amine) linear-dendritic rod diblock copolymers need to be substituted with octadecyl groups on the ends of the dendritic branches in order to give the dendritic block the stiffness and mobility that it needs on the surface. The poly(ethylene oxide) component of the linear-dendritic rod diblock copolymer was also necessary in order to form a hydrophilic anchor of the dendritic block to the surface. Without the poly(ethylene oxide) block, the hydrophilic poly(amido amine) interior bound the polymer and the alkyl chains to the surface and prevented them from elongated away from the surface, as has been observed for poly(octadecyl acrylate) polymers at the air/water interface.⁷⁴

4.6 References

- (1) Tully, D. C.; Fréchet, J. M. J. "Dendrimers at surfaces and interfaces: Chemistry and applications," *Chemical Communications* **2001**, 1229-1239.
- (2) Wells, M.; Crooks, R. M. "Interactions between organized, surface-confined monolayers and vapor-phase probe molecules .10. Preparation and properties of chemically sensitive dendrimer surfaces," *Journal of the American Chemical Society* **1996**, *118*, 3988-3989.
- (3) Gorman, C. B.; Miller, R. L.; Chen, K. Y.; Bishop, A. R.; Haasch, R. T.; Nuzzo, R. G. "Semipermeable, chemisorbed adlayers of focally-substituted organothiol dendrons on gold," *Langmuir* **1998**, *14*, 3312-3319.
- (4) Hierlemann, A.; Campbell, J. K.; Baker, L. A.; Crooks, R. M.; Ricco, A. J. "Structural distortion of dendrimers on gold surfaces: A tapping-mode AFM investigation," *Journal of the American Chemical Society* **1998**, *120*, 5323-5324.

- (5) Tokuhisa, H.; Zhao, M. Q.; Baker, L. A.; Phan, V. T.; Dermody, D. L.; Garcia, M. E.; Peez, R. F.; Crooks, R. M.; Mayer, T. M. "Preparation and characterization of dendrimer monolayers and dendrimer-alkanethiol mixed monolayers adsorbed to gold," *Journal of the American Chemical Society* **1998**, *120*, 4492-4501.
- (6) Chechik, V.; Crooks, R. M. "Monolayers of thiol-terminated dendrimers on the surface of planar and colloidal gold," *Langmuir* **1999**, *15*, 6364-6369.
- (7) Lackowski, W. M.; Campbell, J. K.; Edwards, G.; Chechik, V.; Crooks, R. M. "Time-dependent phase segregation of dendrimer/n-alkylthiol mixed-monolayers on Au(111): An atomic force microscopy study," *Langmuir* **1999**, *15*, 7632-7638.
- (8) Tully, D. C.; Wilder, K.; Fréchet, J. M. J.; Trimble, A. R.; Quate, C. F. "Dendrimer-based self-assembled monolayers as resists for scanning probe lithography," *Advanced Materials* **1999**, *11*, 314-318.
- (9) Tully, D. C.; Trimble, A. R.; Fréchet, J. M. J.; Wilder, K.; Quate, C. F. "Synthesis and preparation of ionically bound dendrimer monolayers and application toward scanning probe lithography," *Chemistry of Materials* **1999**, *11*, 2892-2898.
- (10) Yoon, H. C.; Hong, M. Y.; Kim, H. S. "Affinity biosensor for avidin using a double functionalized dendrimer monolayer on a gold electrode," *Analytical Biochemistry* **2000**, *282*, 121-128.
- (11) Yoon, H. C.; Hong, M. Y.; Kim, H. S. "Reversible association/dissociation reaction of avidin on the dendrimer monolayer functionalized with a biotin analogue for a regenerable affinity-sensing surface," *Langmuir* **2001**, *17*, 1234-1239.
- (12) Watanabe, S.; Regen, S. L. "Dendrimers as building-blocks for multilayer construction," *Journal of the American Chemical Society* **1994**, *116*, 8855-8856.
- (13) Liu, Y. L.; Bruening, M. L.; Bergbreiter, D. E.; Crooks, R. M. "Multilayer dendrimer-polyanhydride composite films on glass, silicon, and gold wafers," *Angewandte Chemie-International Edition in English* **1997**, *36*, 2114-2116.
- (14) Zhao, M. Q.; Liu, Y. L.; Crooks, R. M.; Bergbreiter, D. E. "Preparation of highly impermeable hyperbranched polymer thin- film coatings using dendrimers first as building blocks and then as in situ thermosetting agents," *Journal of the American Chemical Society* **1999**, *121*, 923-930.
- (15) Ghosh, P.; Lackowski, W. M.; Crooks, R. M. "Two new approaches for patterning polymer films using templates prepared by microcontact printing," *Macromolecules* **2001**, *34*, 1230-1236.
- (16) Tsukruk, V. V.; Rinderspacher, F.; Bliznyuk, V. N. "Self-assembled multilayer films from dendrimers," *Langmuir* **1997**, *13*, 2171-2176.
- (17) Bliznyuk, V. N.; Rinderspacher, F.; Tsukruk, V. V. "On the structure of polyamidoamine dendrimer monolayers," *Polymer* **1998**, *39*, 5249-5252.
- (18) Anzai, J.; Kobayashi, Y.; Nakamura, N.; Nishimura, M.; Hoshi, T. "Layer-by-layer construction of multilayer thin films composed of avidin and biotin-labeled poly(amine)s," *Langmuir* **1999**, *15*, 221-226.
- (19) He, J. A.; Valluzzi, R.; Yang, K.; Dolukhanyan, T.; Sung, C. M.; Kumar, J.; Tripathy, S. K.; Samuelson, L.; Balogh, L.; Tomalia, D. A. "Electrostatic multilayer deposition of a gold-dendrimer nanocomposite," *Chemistry of Materials* **1999**, *11*, 3268-3274.
- (20) Yoon, H. C.; Kim, H. S. "Multilayered assembly of dendrimers with enzymes on gold: Thickness-controlled biosensing interface," *Analytical Chemistry* **2000**, *72*, 922-926.

- (21) Imae, T.; Ito, M.; Aoi, K.; Tsutsumiuchi, K.; Noda, H.; Okada, M. "Formation of organized adsorption layers by amphiphilic dendrimers," *Colloids and Surfaces a-Physicochemical and Engineering Aspects* **2000**, *175*, 225-234.
- (22) Coen, M. C.; Lorenz, K.; Kressler, J.; Frey, H.; Mülhaupt, R. "Mono- and multilayers of mesogen-substituted carbosilane dendrimers on mica," *Macromolecules* **1996**, *29*, 8069-8076.
- (23) Sheiko, S. S.; Eckert, G.; Ignateva, G.; Muzafarov, A. M.; Spickermann, J.; Rader, H. J.; Möller, M. "Solid-like states of a dendrimer liquid displayed by scanning force microscopy," *Macromolecular Rapid Communications* **1996**, *17*, 283-297.
- (24) Wang, P. W.; Liu, Y. J.; Devadoss, C.; Bharathi, P.; Moore, J. S. "Electroluminescent diodes from a single-component emitting layer of dendritic macromolecules," *Advanced Materials* **1996**, *8*, 237-241.
- (25) Evenson, S. A.; Badyal, J. P. S. "Self-assembled pamam dendrimer films," *Advanced Materials* **1997**, *9*, 1097-1099.
- (26) Sheiko, S. S.; Muzafarov, A. M.; Winkler, R. G.; Getmanova, E. V.; Eckert, G.; Reineker, P. "Contact angle microscopy on a carbosilane dendrimer with hydroxyl end groups: Method for mesoscopic characterization of the surface structure," *Langmuir* **1997**, *13*, 4172-4181.
- (27) Miller, L. L.; Kunugi, Y.; Canavesi, A.; Rigaut, S.; Moorefield, C. N.; Newkome, G. R. "Vapoconductivity". Sorption of organic vapors causes large increases in the conductivity of a dendrimer," *Chemistry of Materials* **1998**, *10*, 1751-+.
- (28) Liu, M. J.; Fréchet, J. M. J. "Preparation, MALDI-TOF analysis, and micelle-like behavior of alkyl-modified poly(propylene imine) dendrimers," *Polymer Bulletin* **1999**, *43*, 379-386.
- (29) Li, J.; Piehler, L. T.; Qin, D.; Baker, J. R.; Tomalia, D. A.; Meier, D. J. "Visualization and characterization of poly(amidoamine) dendrimers by atomic force microscopy," *Langmuir* **2000**, *16*, 5613-5616.
- (30) Miller, L. L.; Bankers, J. S.; Schmidt, A. J.; Boyd, D. C. "Organic vapors, organic polymers and electrical conductivity," *Journal of Physical Organic Chemistry* **2000**, *13*, 808-815.
- (31) Tully, D. C.; Trimble, A. R.; Fréchet, J. M. J. "Dendrimers with thermally labile end groups: An alternative approach to chemically amplified resist materials designed for sub-100 nm lithography," *Advanced Materials* **2000**, *12*, 1118-1122.
- (32) Zhang, H.; Grim, P. C. M.; Foubert, P.; Vosch, T.; Vanoppen, P.; Wiesler, U. M.; Berresheim, A. J.; Mullen, K.; De Schryver, F. C. "Properties of single dendrimer molecules studied by atomic force microscopy," *Langmuir* **2000**, *16*, 9009-9014.
- (33) Zhang, H.; Grim, P. C. M.; Vosch, T.; Wiesler, U. M.; Berresheim, A. J.; Mullen, K.; De Schryver, F. C. "Discrimination of dendrimer aggregates on mica based on adhesion force: A pulsed force mode atomic force microscopy study," *Langmuir* **2000**, *16*, 9294-9298.
- (34) Zhang, X. Y.; Wilhelm, M.; Klein, J.; Pfaadt, M.; Meijer, E. W. "Modification of surface interactions and friction by adsorbed dendrimers: 1. Low surface-energy fifth-generation amino acid- modified poly(propyleneimine) dendrimers," *Langmuir* **2000**, *16*, 3884-3892.
- (35) Zhang, X. Y.; Klein, J.; Sheiko, S. S.; Muzafarov, A. M. "Modification of surface interactions and friction by adsorbed dendrimers: 2. High surface-energy -oh-terminated carbosilane dendrimers," *Langmuir* **2000**, *16*, 3893-3901.

- (36) Betley, T. A.; Holl, M. M. B.; Orr, B. G.; Swanson, D. R.; Tomalia, D. A.; Baker, J. R. "Tapping mode atomic force microscopy investigation of poly(amidoamine) dendrimers: Effects of substrate and pH on dendrimer deformation," *Langmuir* **2001**, *17*, 2768-2773.
- (37) Cardullo, F.; Diederich, F.; Echegoyen, L.; Habicher, T.; Jayaraman, N.; Leblanc, R. M.; Stoddart, J. F.; Wang, S. P. "Stable langmuir and langmuir-blodgett films of fullerene-glycodendron conjugates," *Langmuir* **1998**, *14*, 1955-1959.
- (38) Yokoyama, S.; Nakahama, T.; Otomo, A.; Mashiko, S. "Second harmonic generation of dipolar dendrons in the assembled thin films," *Thin Solid Films* **1998**, *331*, 248-253.
- (39) Cui, G. L.; Xu, Y.; Liu, M. Z.; Ji, T.; Chen, Y. M.; Li, Y. F. "Highly ordered assemblies of dendritic molecules bearing multi-hydrophilic head groups," *Macromolecular Rapid Communications* **1999**, *20*, 71-76.
- (40) Iyer, J.; Hammond, P. T. "Langmuir behavior and ultrathin films of new linear-dendritic diblock copolymers," *Langmuir* **1999**, *15*, 1299-1306.
- (41) Schenning, A. P. H. I.; Peeters, E.; Meijer, E. W. "Energy transfer in supramolecular assemblies of oligo(p-phenylene vinylene)s terminated poly(propylene imine) dendrimers," *Journal of the American Chemical Society* **2000**, *122*, 4489-4495.
- (42) Sui, G. D.; Micic, M.; Huo, Q.; Leblanc, R. M. "Synthesis and surface chemistry study of a new amphiphilic pamam dendrimer," *Langmuir* **2000**, *16*, 7847-7851.
- (43) Weener, J. W.; Meijer, E. W. "Photoresponsive dendritic monolayers," *Advanced Materials* **2000**, *12*, 741-746.
- (44) Li, F. Y.; Zhu, L. Y.; Huang, C. H.; Jin, L. P.; Zheng, J.; Shi, M.; Guo, J. Q.; Wang, E. J. "Photoelectric conversion of a novel photoresponsive dendritic dye in 1b monolayer films," *Applied Surface Science* **2001**, *172*, 323-330.
- (45) Bo, Z. S.; Rabe, J. P.; Schluter, A. D. "A poly(para-phenylene) with hydrophobic and hydrophilic dendrons: Prototype of an amphiphilic cylinder with the potential to segregate lengthwise," *Angewandte Chemie-International Edition* **1999**, *38*, 2370-2372.
- (46) Bo, Z. S.; Zhang, C. M.; Severin, N.; Rabe, J. P.; Schluter, A. D. "Synthesis of amphiphilic poly(p-phenylene)s with pendant dendrons and linear chains," *Macromolecules* **2000**, *33*, 2688-2694.
- (47) Saville, P. M.; White, J. W.; Hawker, C. J.; Wooley, K. L.; Frechet, J. M. J. "Dendrimer and polystyrene surfactant structure at the air-water-interface," *Journal of Physical Chemistry* **1993**, *97*, 293-294.
- (48) Saville, P. M.; Reynolds, P. A.; White, J. W.; Hawker, C. J.; Frechet, J. M. J.; Wooley, K. L.; Penfold, J.; Webster, J. R. P. "Neutron reflectivity and structure of polyether dendrimers as langmuir films," *Journal of Physical Chemistry* **1995**, *99*, 8283-8289.
- (49) Kirton, G. F.; Brown, A. S.; Hawker, C. J.; Reynolds, P. A.; White, J. W. "Surface activity of modified dendrimers at high compression," *Physica B* **1998**, *248*, 184-190.
- (50) Kampf, J. P.; Frank, C. W.; Malmstrom, E. E.; Hawker, C. J. "Stability and molecular conformation of poly(benzyl ether) monodendrons with oligo(ethylene glycol) tails at the air-water interface," *Langmuir* **1999**, *15*, 227-233.
- (51) Pao, W. J.; Stetzer, M. R.; Heiney, P. A.; Cho, W. D.; Percec, V. "X-ray reflectivity study of Langmuir films of amphiphilic monodendrons," *Journal of Physical Chemistry B* **2001**, *105*, 2170-2176.
- (52) Sidorenko, A.; Houphouet-Boigny, C.; Villavicencio, O.; Hashemzadeh, M.; McGrath, D. V.; Tsukruk, V. V. "Photoresponsive langmuir monolayers from azobenzene-containing dendrons," *Langmuir* **2000**, *16*, 10569-10572.

- (53) SayedSweet, Y.; Hedstrand, D. M.; Spinder, R.; Tomalia, D. A. "Hydrophobically modified poly(amidoamine) (PAMAM) dendrimers: Their properties at the air-water interface and use as nanoscopic container molecules," *Journal of Materials Chemistry* **1997**, *7*, 1199-1205.
- (54) Sui, G.; Micic, M.; Huo, Q.; Leblanc, R. M. "Studies of a novel polymerizable amphiphilic dendrimer," *Colloids and Surfaces A-Physicochemical and Engineering Aspects* **2000**, *171*, 185-197.
- (55) Schenning, A. P. H. I.; Elissen-Román, C.; Weener, J. W.; Baars, M. W. P. L.; van der Gaast, S. J.; Meijer, E. W. "Amphiphilic dendrimers as building blocks in supramolecular assemblies," *Journal of the American Chemical Society* **1998**, *120*, 8199-8208.
- (56) van Hest, J. C. M.; Delnoye, D. A. P.; Baars, M. W. P. L.; Elissen-Román, C.; van Genderen, M. H. P.; Meijer, E. W. "Polystyrene-poly(propylene imine) dendrimers: Synthesis, characterization, and association behavior of a new class of amphiphiles," *Chemistry-A European Journal* **1996**, *2*, 1616-1626.
- (57) Johnson, M. A.; Santini, C. M. B.; Iyer, J.; Satija, S.; Ivkov, R.; Hammond, P. T. "Neutron reflectivity of linear-dendritic diblock copolymer monolayers," *Macromolecules* **2002**, *35*, 231-238.
- (58) Aoi, K.; Motoda, A.; Ohno, M.; Tsutsumiuchi, K.; Okada, M.; Imae, T. "Synthesis and assembly of amphiphilic tadpole-shaped block copolymers based on poly(amido amine) dendrimer," *Polymer Journal* **1999**, *31*, 1071-1078.
- (59) Higashi, N.; Koga, T.; Niwa, M. "Helical superstructures from a poly(γ -benzyl-L-glutamate)-poly(L-glutamic acid) amphiphilic diblock copolymer: Monolayer formation on water and its specific binding of amino acids," *Langmuir* **2000**, *16*, 3482-3486.
- (60) Toyotama, A.; Kugimiya, S.; Yonese, M.; Kinoshita, T.; Tsujita, Y. "Controllable orientation of the peptide-based surfactant at air-water interface," *Chemistry Letters* **1997**, 443-444.
- (61) Sommerdijk, N.; Holder, S. J.; Hiorns, R. C.; Jones, R. G.; Nolte, R. J. M. "Self-assembled structures from an amphiphilic multiblock copolymer containing rigid semiconductor segments," *Macromolecules* **2000**, *33*, 8289-8294.
- (62) Gaines, G. L. In *Insoluble monolayers at liquid-gas interfaces*; John Wiley & Sons: New York, New York, 1966, p 14.
- (63) Ulman, A. In *An introduction to ultrathin organic films: From Langmuir-Blodgett to self-assembly*; Academic Press, Inc.: San Diego, CA, 1991, p 115.
- (64) Fischer, P.; Brooks, C. F.; Fuller, G. G.; Ritcey, A. M.; Xiao, Y. F.; Rahem, T. "Phase behavior and flow properties of "hairy-rod" monolayers," *Langmuir* **2000**, *16*, 726-734.
- (65) Gaines, G. L. In *Insoluble monolayers at liquid-gas interfaces*; John Wiley & Sons: New York, New York, 1966, p 162-167.
- (66) Gaines, G. L. In *Insoluble monolayers at liquid-gas interfaces*; John Wiley & Sons: New York, New York, 1966, p 328-331.
- (67) Bijsterbosch, H. D.; Dehaan, V. O.; Degraaf, A. W.; Mellema, M.; Leermakers, F. A. M.; Stuart, M. A. C.; Vanwell, A. A. "Tethered adsorbing chains - neutron reflectivity and surface pressure of spread diblock copolymer monolayers," *Langmuir* **1995**, *11*, 4467-4473.
- (68) Faure, M. C.; Bassereau, P.; Carignano, M. A.; Szleifer, I.; Gallot, Y.; Andelman, D. "Monolayers of diblock copolymer at the air-water interface: The attractive monomer-surface case," *European Physical Journal B* **1998**, *3*, 365-375.

- (69) Cox, J. K.; Yu, K.; Constantine, B.; Eisenberg, A.; Lennox, R. B. "Polystyrene-poly(ethylene oxide) diblock copolymers form well- defined surface aggregates at the air/water interface," *Langmuir* **1999**, *15*, 7714-7718.
- (70) Cox, J. K.; Yu, K.; Eisenberg, A.; Lennox, R. B. "Compression of polystyrene-poly(ethylene oxide) surface aggregates at the air/water interface," *Physical Chemistry Chemical Physics* **1999**, *1*, 4417-4421.
- (71) Shuler, R. L.; Zisman, W. A. "A study of the behavior of polyoxyethylene at the air-water interface by wave damping and other methods," *Journal of Physical Chemistry* **1970**, *74*, 1523-1534.
- (72) Henderson, J. A.; Richards, R. W.; Penfold, J.; Thomas, R. K.; Lu, J. R. "Organization of poly(ethylene oxide) monolayers at the air- water-interface," *Macromolecules* **1993**, *26*, 4591-4600.
- (73) Lu, J. R.; Su, T. J.; Thomas, R. K.; Penfold, J.; Richards, R. W. "The determination of segment density profiles of polyethylene oxide layers adsorbed at the air-water interface," *Polymer* **1996**, *37*, 109-114.
- (74) Riou, S. A.; Chien, B. T.; Hsu, S. L.; Stidham, H. D. "A spectroscopic study of polymers containing long flexible side chains at an air-liquid interface," *Journal of Polymer Science Part B-Polymer Physics* **1997**, *35*, 2843-2855.
- (75) Gargallo, L.; Miranda, B.; Rios, H.; Gonzalez-Nilo, F.; Radic, D. "Surface characterization and study of Langmuir films of poly(4- vinylpyridine) quaternized with n-alkylbromide," *Polymer International* **2001**, *50*, 858-862.
- (76) Li, Z.; Zhao, M. W.; Quinn, J.; Rafailovich, M. H.; Sokolov, J.; Lennox, R. B.; Eisenberg, A.; Wu, X. Z.; Kim, M. W.; Sinha, S. K.; Tolan, M. "X-ray reflectivity of diblock copolymer monolayers at the air/water interface," *Langmuir* **1995**, *11*, 4785-4792.
- (77) Yamamoto, S.; Tsujii, Y.; Yamada, K.; Fukuda, T.; Miyamoto, T.; Ito, S. "Langmuir-Blodgett films of a glucose residue-carrying amphiphilic block copolymer studied by surface plasmons and transmission electron microscopy," *Langmuir* **1996**, *12*, 3671-3674.
- (78) Kang, Y. S.; Majda, M. "Headgroup immersion depth and its effect on the lateral diffusion of amphiphiles at the air/water interface," *Journal of Physical Chemistry B* **2000**, *104*, 2082-2089.
- (79) Kawaguchi, M.; Suzuki, S.; Imae, T.; Kato, T. "Surface morphology of Langmuir-Blodgett blend films of poly(vinyl acetate) poly(methyl acrylate)," *Langmuir* **1997**, *13*, 3794-3799.
- (80) Kobayashi, K.; Kajikawa, K.; Sasabe, H.; Knoll, W. "Monomolecular layer formation of amphiphilic cyclodextrin derivatives at the air water interface," *Thin Solid Films* **1999**, *349*, 244-249.
- (81) Mabuchi, M.; Kobata, S.; Ito, S.; Yamamoto, M.; Schmidt, A.; Knoll, W. "Preparation and characterization of the Langmuir-Blodgett films made of hairy-rod polyglutamates bearing various chromophores in the side chain," *Langmuir* **1998**, *14*, 7260-7266.
- (82) Mulders, S. J. E.; Brouwer, A. J.; Kimkes, P.; Sudholter, E. J. R.; Liskamp, R. M. J. "Sizing of amino acid based dendrimers in Langmuir monolayers," *Journal of the Chemical Society-Perkin Transactions 2* **1998**, 1535-1538.
- (83) Iyer, J.; Fleming, K.; Hammond, P. T. "Synthesis and solution properties of new linear-dendritic diblock copolymers," *Macromolecules* **1998**, *31*, 8757-8765.
- (84) Niwa, M.; Katsurada, N.; Higashi, N. "Formation of a surface monolayer and a built-up multilayer from a well-defined amphiphilic block copolymer," *Macromolecules* **1988**, *21*, 1878-1880.

- (85) Niwa, M.; Higashi, N. "Reversible interpolymer complexation between poly(oxyethylene)-based amphiphilic block polymer and poly(acrylic acid) at the air water interface," *Macromolecules* **1989**, *22*, 1000-1002.
- (86) Rother, G.; Findenegg, G. H. "Monolayer films of PS-b-PEO diblock copolymers at the air/water- and an oil/water-interface," *Colloid and Polymer Science* **1998**, *276*, 496-502.
- (87) Yin, R.; Zhu, Y.; Tomalia, D. A.; Ibuki, H. "Architectural copolymers: Rod-shaped, cylindrical dendrimers," *Journal of the American Chemical Society* **1998**, *120*, 2678-2679.
- (88) Gaines, G. L. In *Insoluble monolayers at liquid-gas interfaces*; John Wiley & Sons: New York, New York, 1966, p 24.
- (89) Lupis, C. H. P. In *Chemical thermodynamics of materials*; Prentice Hall: Englewood Cliffs, New Jersey, 1983, p 5.
- (90) Gaines, G. L. In *Insoluble monolayers at liquid-gas interfaces*; John Wiley & Sons: New York, New York, 1966, p 186-188.
- (91) daSilva, A. M. G.; Filipe, E. J. M.; dOliveira, J. M. R.; Martinho, J. M. G. "Interfacial behavior of poly(styrene)-poly(ethylene oxide) diblock copolymer monolayers at the air-water interface. Hydrophilic block chain length and temperature influence," *Langmuir* **1996**, *12*, 6547-6553.
- (92) da Silva, A. M. G.; Gamboa, A. L. S.; Martinho, J. M. G. "Aggregation of poly(styrene)-poly(ethylene oxide) diblock copolymer monolayers at the air-water interface," *Langmuir* **1998**, *14*, 5327-5330.
- (93) Tomalia, D. A.; Durst, H. D. "Genealogically directed synthesis: Starburst*/cascade dendrimers and hyperbranched structures," *Topics in Current Chemistry* **1994**, *165*, 193-313.
- (94) Ariga, K.; Urakawa, T.; Michiue, A.; Sasaki, Y.; Kikuchi, J. "Dendritic amphiphiles: Dendrimers having an amphiphile structure in each unit," *Langmuir* **2000**, *16*, 9147-9150.
- (95) Richards, R. W.; Rochford, B. R.; Webster, J. R. P. "Surface phase separation in an amphiphilic block copolymer monolayer at the air-water interface," *Polymer* **1997**, *38*, 1169-1177.

Chapter 5

Bulk Characterization and Morphology of the Linear-Dendritic Rod Diblock Copolymers

5.1 Introduction

One of the features of dendrimers that makes them unique is the ability to design these polymers with a fairly specific shape. For example, spherical dendrimers have been prepared by attaching three or four monodendrons to a small molecule core, while dendritic rods have been prepared by attaching several dendrons to each repeat of a linear polymer core. The dimensions of these dendrimers can be tuned not only using the chemistry and the generation number for spherical dendrimers, but also the length of the core for rod-like systems. Unlike traditional polymers whose size and shape are highly dependent on their environment, dendritic systems possess sizes and shapes that are much more robust due to their congested, hyperbranched structure that prevents large fluctuations in these parameters. Thus, these dendritic polymers offer an interesting approach to preparing molecular objects.¹ For example, rigid dendrimers based on polyphenylene chemistry² as well as those based on poly(benzyl ether) chemistry³ have been proposed as molecular ball-bearings, and fluorinated dendrimers have been used as molecular lubricants.⁴ In addition, Schenning *et al.* have proposed rigid poly(triacetylene) and poly(pentaacetylene) linear polymers covered with poly(benzyl ether) dendrimers as “insulated molecular wires”.^{5,6} This ability to prepare molecular objects has become of increasing importance as researchers have begun assembling nanoscale devices, as devices of this size cannot be prepared using conventional techniques. Nonetheless, if dendritic systems are to be used in nanodevice fabrication, it is important to have a good understanding of their material properties such as their glass transition temperature and their melting point, as well as their ability to form liquid crystals, as these properties will determine the applications for which a particular dendritic system can be used.⁷ In addition, it is important to be able to image the polymers so that the dimensions of the polymer can be well characterized before their use in a particular application.⁸ Finally, it is important to have a mechanism that can be used to assemble the polymers in the desired position, as the object will be of no use if it cannot be placed where it is needed.

Due to the unique architecture of the poly(ethylene oxide)-poly(ethylene imine)-poly(amido amine) linear-dendritic rod diblock copolymers which have been synthesized in this thesis, a preliminary investigation into the thermal, liquid crystalline, and morphological, properties of the polymers was initiated in order to gain insight into the effects of generation, end group, and architecture on these properties. Differential scanning calorimetry (DSC) was used to determine the thermal transitions of the polymers, and polarized optical microscopy coupled with DSC were used to determine whether or not the polymers possessed a liquid crystalline nature, as some dendritic rod systems, as well as some other radially substituted linear polymers, such as the poly(*n*-alkyl glutamates),⁹ poly(dialkylsilanes),^{10,11} and cellulose trialkanoates,¹² have all been found to exhibit hexagonal columnar mesophases. Small angle x-ray scattering (SAXS), wide angle x-ray diffraction (WAXD), and transmission electron microscopy (TEM) were used to gain insight into the morphology of the polymers. Finally, preliminary imaging of the polymers was accomplished using tapping mode atomic force microscopy (AFM). In the remainder of this chapter, section 5.2 will present background information on the thermal and liquid crystalline properties, morphology, and imaging of other dendritic homopolymers, dendritic rods, hybrid-linear dendritic diblock copolymers, as well as more traditional comb-coil and rod-coil diblock copolymer systems. Section 5.3 describes the materials, instrumentation, and methods used in the experiments. The results of the above experiments will be presented and discussed in section 5.4. Finally, a chapter summary and concluding remarks are presented in section 5.5 and the references in section 5.6.

5.2 Background

5.2.1 Spherical Dendritic Homopolymers

5.2.1.1 Glass Transition Temperature and Liquid Crystalline Properties

Of the dendritic systems, the thermal properties and liquid crystalline behavior of the poly(benzyl ether) dendrimers have been most closely examined. Wooley *et al.* were one of the first to report on the effects of molecular weight, end group chemistry, and interior branch composition on the glass transition temperature of dendritic systems.¹³ They found that the glass transition temperature increased with increasing molecular weight up to a point and then leveled

off as the polymers became more globular and did not have as many opportunities for entanglements, one of the factors that has been known to increase the glass transition temperature of a polymer. In addition, upon increasing the polarity of the dendritic end group by changing it from hydrogen to bromo to cyano, they also observed an increase in the glass transition temperature due to the stronger association between the more polar end groups. Finally for dendrimers which consisted of two very different and incompatible chain ends, two glass transition temperatures were observed indicating phase segregation of the different end groups. The glass transition temperature of these poly(benzyl ether) mono- and tri-dendrons has been found to range from 255 to 315K depending on the end group chemistry and the generation number.¹⁴ In general, this variation in the glass transition temperature with the molecular weight and the end group composition obeyed a modified version of the chain-end free volume theory.¹⁵ Hay *et al.* have also compared the thermal properties of the poly(benzyl ether) dendrimers with their linear analogues to examine the effect of architecture on these transitions.¹⁶ They observed a crystalline state for the low generation dendrimers as well as the linear analogues of the higher generation dendrimers, but not for dendrimers of the third generation and larger due to their highly branched nature, indicating the importance of not only chemistry, but also architecture on the thermal properties of polymers. In order to induce liquid crystalline behavior in these poly(benzyl ether) dendrimers, two main approaches have been investigated. The first is by Percec *et al.* who have thoroughly examined the self-assembly behavior of poly(benzyl ether) dendrons which have been functionalized with long alkyl groups.¹⁷⁻²² By tuning the number, placement, and length of the alkyl groups on the terminal benzene rings, these dendrons assembled into hexagonal columnar mesophases as well as body centered cubic liquid crystalline phases as indicated by polarized optical microscopy as well as SAXS. Since Percec *et al.* have also proceeded to polymerize these self-assembled structures to make “dendron jacketed polymers” (a.k.a. dendritic rods), their properties will be discussed in more detail in section 5.2.2. Brewis *et al.* attempted a second approach to liquid crystalline poly(benzyl ether) dendrimers by covalently bonding one of these dendrons to a rigid phthalocyanine core, producing a material whose properties were dominated by both the columnar self-association of the phthalocyanine core as well as the glass-forming character of the poly(benzyl ether) dendrons.^{23,24} In polarized optical microscopy, textures characteristic of a hexagonal columnar mesophase were observed which were also verified with SAXS.

For the poly(amido amine) dendrimers, research has focused much more on examining the thermal behavior of functionalized as well as liquid crystalline derivatives than on the native polymers themselves. Nonetheless, for the amine terminated polymers, Dvornic *et al.* have reported a glass transition temperature of 11°C for the third generation polymer, 14°C for the fourth generation polymer, and 14°C for the fifth generation polymer.²⁵ Thus, even though there are a limited number of data points, it appears as if the glass transition temperature for these dendrimers increased with increasing generation and then approximately leveled off with further increases in generation. Functionalization of the dendrimer branch ends with one generation of organosilane groups also caused a slight increase in the glass transition temperature; however, functionalization with two generations of organosilane groups caused a dramatic decrease in the glass transition temperature, most likely due to the flexible organosilane groups that were then large enough to act independent of the poly(amido amine) core. From thermal gravimetric analysis (TGA) experiments, the dendrimers were found to degrade at approximately 150°C, most likely due to a series of retro-Michael reactions. In contrast Balogh *et al.* have found that the addition of more rigid polyacetylene groups to the chain ends of poly(amido amine) dendrimers cause an increase in the glass transition temperature of approximately 20°C for the third generation dendrimer and 28-30°C for the fourth generation dendrimer.²⁶ Suzuki *et al.* attempted to prepare liquid crystalline dendrimers by functionalization of poly(amido amine) chain ends with cyanobiphenyl groups. While these polymers did not exhibit thermotropic liquid crystalline behavior, they did exhibit a nematic, lyotropic liquid crystalline behavior in 80 weight percent solutions of DMF that contained lithium bromide. In general, the formation of liquid crystalline structures requires the mesogen units to possess a high degree of mobility. Therefore, they felt that the inter- and intramolecular hydrogen bonds between the poly(amido amine) amide groups restricted the mobility of the dendritic branches, and thus the terminal mesogen units.²⁷ However, Barberá *et al.* found that they could prepare thermotropic poly(amido amine) liquid crystalline dendrimers by functionalization of the dendrimer end groups with 4-(4'-decyloxybenzoyloxy)salicylaldehyde.²⁸ Nonetheless, formation of the smectic A mesophase was only observed after the polymer had been heated above its isotropization temperature and then slowly cooled. From x-ray diffraction studies, they proposed a model in which the mesogen units aligned perpendicular to one another on both sides of a poly(amido amine) core, which distorted to allow for alignment of the mesogen groups. The thickness of the

layered structure indicated that the mesogen units from neighboring polymers were not interdigitating but were rather meeting tip to tip. While the generation one polymer also possessed a crystalline melting point at 112°C, the other polymers did not. All of the polymers exhibited a glass transition temperature between 62 and 67°C and an isotropization of approximately 137°C for the generation one polymer and approximately 170-180°C for the higher generation polymers.

As was observed for the poly(amido amine) dendrimers, the thermal properties of functionalized as well as liquid crystalline poly(propylene imine) dendrimers have been examined more closely than those of the native polymers. DeBrabander-van den Berg *et al.* examined the glass transition temperature of the native polymers and they observed two trends, both which have been observed by other researchers.²⁹ First, the glass transition temperature was found to increase with increasing molecular weight; and second, the glass transition temperature was highly dependent on the end group chemistry with the nitrile terminated polymers exhibiting a higher glass transition temperature than the amine terminated polymers, most likely due to the stronger dipole interactions of the nitrile groups. The glass transition temperatures that they observed for both polymers were fairly low, -45°C for the nitrile terminated polymer and -65°C for the amine terminated polymer, indicating that the dendrimers possessed a high degree of conformational flexibility. Due to this high degree of flexibility, several groups have attempted to make liquid crystalline systems based on these dendrimers. The first to do so were Latterman *et al.* who attached a known mesogen, which consisted of a phenyl ring with two dodecyl chains radiating from it, onto a poly(propylene imine) scaffold.³⁰ The generation one through four polymers exhibited a hexagonal columnar mesophase with the dendrimer adopting a predominately flat conformation such that the columns consist of a poly(propylene imine) core surrounded by a mesogenic coat. The fifth generation dendrimer did not show this behavior as the poly(propylene imine) was too highly branched to be able to adopt this flattened conformation, and the mesogen units were not able to align and take on a liquid crystalline state. Similarly, Baars *et al.* have examined the thermal behavior of poly(propylene imine) dendrimers of generation one, two, and three that had been functionalized with pentyloxycyanodiphenyl or decyloxycyanodiphenyl groups.³¹ While all of the polymers exhibited a smectic A phase, the temperature range over which the mesophases existed was highly dependent on the length of the alkyl spacer between the dendrimer and the mesogen. From x-ray diffraction, the smectic

spacing for both alkyl chain lengths was found to be independent of generation, indicating that the dendritic core was completely distorted in the liquid crystalline phase. Yonetake *et al.* have examined a similar system, one which consists of a poly(propylene imine) dendritic core surrounded by cyanobiphenyl mesogen units; however, their mesogen were attached to the dendrimer via ester linkages as opposed to the amide linkages reported by Baars.³² Comparing the two linkages, they found that the glass transition temperature of the ester linkage was much lower than that of the amide linkage, which is a fairly rigid linkage due to hydrogen bonding of the amide groups. They have also compared the effect of the dendritic scaffold, poly(propylene imine) versus poly(amido amine), and found that the poly(propylene imine) scaffold was much more flexible and susceptible to liquid crystalline formation. Finally, Barbera *et al.* have examined liquid crystalline poly(propylene imine) dendrimers which have been functionalized with alkoxybenzoyloxy groups. Taking advantage of the ability of dendrimers to encapsulate nanoparticles, they have found that even these dendromesogens containing copper were able to exhibit liquid crystalline properties.³³

Since the flexibility of the dendrimer is important in producing liquid crystalline dendrimers which have terminal mesogen units, there has been a lot of work done with carbosilane dendrimers which are known to be very flexible and have a low glass transition temperature of below -30°C .³⁴ One of the first to do so were Coen *et al.* who examined carbosilane dendrimers which had been functionalized with cholesterol mesogen units on the periphery.³⁵ While the generation one and two polymers were able to form smectic liquid crystalline phases, the third generation polymer did not, most likely due to the increased spherical geometry of the dendrimer which prevented the mesogen-mesogen interactions necessary for a liquid crystalline state. Shortly thereafter, Frey *et al.* examined the liquid crystalline behavior of second generation carbosilane dendrimers whose end groups had been substituted with cyanobiphenyl mesogens.³⁶ They found that these dendrimers also formed smectic A liquid crystalline phases by deformation of the carbosilane interior into a layered structure. These observations have been corroborated by Ponomarenko *et al.* who have also examined the behavior of cyanobiphenyl terminated carbosilane dendrimers.³⁷ Frey *et al.* then went on to examine the behavior of carbosilane dendrimers which had been functionalized with perfluoroalkyl end groups.³⁸ They found that the first generation polymer formed a smectic mesophase between -15 and -30°C while the second and third generation dendrimers did not;

however, these generations did form a hexagonally packed array of columns. They noted that for traditional side chain liquid crystalline polymers, the development of smectic phases is initiated at different parts of the chain, independent of one another; however, in dendritic liquid crystals, the dendrimer must move as a whole to assembly into a layered structure, which is much harder to do. Thus, in order to obtain liquid crystalline behavior in dendritic systems, appropriate choice of the dendritic scaffold as well as the length of the spacer between the dendrimer and the mesogen are extremely important. Finally, they noted that the glass transition temperature of the fluorinated dendrimer decreased with increasing generation in contrast to that of the alkyl terminated polymer which increased with increasing generation. More recently, perfluorinated carbosilane dendrimers have also been examined by Stark *et al.* as well as by Omotowa *et al.* who observed similar phenomena.^{34,39}

Other interesting families of dendrimers whose thermal properties have been studied are the poly(ether imides) and the poly(ether amides). Leu *et al.* have examined a series of dendritic poly(ether imides) and observed similar trends to those discussed previously.⁴⁰ They found that the glass transition temperature was highly dependent on the internal monomer units as well as the polarity and the number of end groups, and that the glass transition temperature increased with increasing molecular weight. Wu *et al.* have examined hyperbranched aromatic poly(ether imides) which have been functionalized with various lengths of alkyl chains, ranging from one to seventeen carbons.⁴¹ As the length of the alkyl chain increased, the glass transition temperature of the polymers decreased. For the very long alkyl chains, they did not observe crystallization of alkyl groups, and thus an increase in the glass transition temperature, as had been observed by others. The rigid aromatic unit in the interior of the polymer most likely decreased the tendency for side chain crystallization. Conversely, Wei *et al.* prepared semicrystalline dendritic polymers from a second generation poly(ether amine) dendrimer that had been functionalized with myristoyl, pamitoyl, and octadecyl groups.⁴² Surprisingly, as the length of the alkyl chain increased, so did the glass transition temperature, which is in contrast to the trends observed for most other polymers. Nonetheless, the addition of the alkyl chains increased the tendency for crystallization in the dendrimer and the melting point depended only slightly on the length of the alkyl chain. However, the length of the alkyl chain did influence the rate of crystallization, the crystallization enthalpy, and the crystal size, all which increased with increasing chain length. These alkyl functionalized dendrimers did not exhibit liquid crystalline behavior.

The thermal properties of hyperbranched polyester polymers have also been studied by Malmström *et al.*^{43,44} While these polymers are not pure dendrimers, they represent a very similar architecture; thus, the trends in their thermal properties have often been noted by those studying more traditional dendritic systems. Malmström have primarily focused on the effect of end group chemistry on the transition temperatures and relaxation processes in these hyperbranched systems. In their early work, they looked at the effect of end group chemistry on the glass transition temperature of the polymers.⁴³ They too found that the polarity of the end groups had a large effect on the glass transition temperature with the hydroxy terminated polymers exhibiting the highest glass transition temperature, followed by the benzoate groups, and the acetate groups were found to have the lowest. The benzoate polymers were also found to crystallize upon standing. In their later work, a hyperbranched hydroxyfunctional polyester was end capped with five different alkyl chlorides, ranging in length from the three to sixteen carbons.⁴⁴ In general, the glass transition temperature of the polymers decreased with increasing length of alkyl chain. For the hydroxyl terminated polymers, the glass transition temperature was approximately 30°C, while for the longer alkyl chains, it fell well below zero. In addition, the polymers that were terminated with twelve carbons and longer tended to crystallize, adopting several different crystalline phases, as indicated by DSC.

A theoretical treatment of the glass transition temperature of dendritic polymers has also been undertaken by Stutz.⁷ Comparing his results with the experiments of others, Stutz drew several conclusions. First, the glass transition temperature is expected to increase with generation up to a point and then level off; however, this transition point is not dependent on the molecular weight of the dendrimers, but is much more highly dependent on the degree of branching. Second, the end group chemistry is expected to have a large impact on the glass transition temperature, with the introduction of more polar groups shifting the whole glass transition temperature versus generation curve to higher temperatures. Third, the initiator core does not appear to have a large impact on the glass transition temperature, as it is mostly buried beneath the dendritic groups. Fourth, the branch chemistry strongly influences the glass transition temperature with that of the siloxane dendrimers being much lower than that of the aryletherketone dendrimers being much less than that of the phenylene dendrimers.

The ability of a few other dendritic systems to exhibit a liquid crystalline phase are worth mentioning. Moore *et al.* have attached flexible oligoethylene glycol units to a rigid dendritic

phenylacetylene core.⁴⁵ Even though the dendritic core was very rigid, these polymers deformed into a pancake-like structure and assembled into columnar discotic liquid crystalline phases, as indicated by electron microscopy and diffraction measurements. The shape anisotropy in these polymers led to the formation of the liquid crystalline phase. Using the more traditional approach of adding mesogen units to a preformed dendrimer, Saez *et al.* have functionalized silsesquioxane dendrimers with a (S)-4'-octyloxybiphenyl-4-yl 4-[4-(2-methylbutoxy)-2-(pent-4-enyloxy)benzoyl]benzoate mesogen resulting in dendromesogens that exhibited chiral nematic phases and a glass transition temperature below room temperature.^{46,47} Similarly, Meier *et al.* have attached tris(dodecyl-oxy)phenyl mesogens to the periphery of stilbenoid dendrimers. The generation one and two polymers displayed two different discotic liquid crystalline phases; however, the generation three polymer did not as the steric hindrance between the mesogens in the periphery was too great to achieve good alignment of the mesogen units.⁴⁸

5.2.1.2 Imaging of the Dendrimers

In order to verify that the dendrimers were exhibiting the desired shape, researchers have imaged dendritic systems using atomic force microscopy (AFM) and transmission electron microscopy (TEM). In addition, AFM has also been used to gain information about other material properties of dendrimers such as their rigidity and their interaction with various substrates.

The dendrimers that have been most highly characterized with AFM and TEM are the poly(amido amine) spherical dendrimers. Originally, these dendrimers were imaged with TEM by functionalization of the end groups with sodium and potassium ions through hydrolysis of the methyl ester end groups with the corresponding metal hydroxides. The presence of the metal ions provided the necessary contrast to image the dendrimers as the native dendrimers were of such low molecular weight and composed of such light atoms that they were virtually transparent. From TEM, the diameter of the generation 4.5/sodium salt polymer was found to be approximately 88Å, while CPK measurement of the polymer would have estimated the diameter to be 78Å.^{49,50} In later TEM experiments, generation seven to ten poly(amido amine) spherical dendrimers were imaged with TEM by staining with aqueous sodium phosphotungstate, while the generation ten polymer was also imaged by cryo-TEM of aqueous solutions of the polymer.⁵¹ All of these experiments indicated that the polymer was in fact adopting a spherical

conformation. Unfortunately, it was difficult to visualize the dendrimers below generation six using the phosphotungstate stain because the grain of the carbon substrate was very close to the size of the molecules and it became difficult to delineate the edges of the dendrimer. Schmitzer *et al.* have also examined poly(amido amine) dendrimers which had been amphiphilic by the addition of glucose substituents at their periphery. From TEM, they were able to verify the aggregation of the dendrimers due to the presence of the glucose end groups.⁵² Similarly, Balogh *et al.* have used TEM to image individual, as well as aggregates of dendrimers which possess a poly(amido amine) core and polyacetylene chain ends.²⁶ Due to the differences in the electron densities of the two components, the dendrimers could be observed without additional stain. In addition to imaging individual dendrimers, TEM has also been used to image metal nanoparticles which have been templated in poly(amido amine) dendritic matrices. For example, He *et al.* have imaged gold/dendrimer nanocomposites,⁵³ Zhao have imaged platinum/dendrimer nanocomposites,⁵⁴ and Kéki *et al.* have imaged silver/dendrimer nanocomposites.⁵⁵ Kéki *et al.* also found that the nanoparticles formed from the amine terminated polymers were approximately the same size as the dendrimer, while those formed from the carboxylate terminated polymers were much larger, indicating that aggregation was occurring during their formation. In all of these cases, the metal nanoparticle was able to provide the necessary contrast in TEM to distinguish it from the dendritic matrix and no additional stain was necessary. Finally, in some very interesting work, Grohn *et al.* used TEM as well as SAXS to image gold, copper, and platinum nanoparticles that had been prepared in a poly(amido amine) dendrimer-poly(2-hydroxyethyl methacrylate) matrix. By selectively staining the poly(amido amine) dendrimers with phosphotungstic acid such that the dendrimers appeared gray, and using the inherent contrast of the metal particles which made them appear black, they were able to determine not only the size and shape of the individual nanoparticles and the dendrimers, but also the position of the nanoparticles with respect to the dendrimers.⁵⁶

More recently, several groups have imaged poly(amido amine) dendrimers with AFM. The first to do so were Tsukruk *et al.* who imaged dendrimers that had been adsorbed onto silica surfaces as well as dendrimers that were deposited in polyelectrolyte layer by layer films.⁵⁷ In both cases, they found that the thickness of the dendritic layer was much smaller than the diameter of the same dendrimer measured in solution, indicating that the dendrimers were not only collapsing, but also flattening along the surface normal. Shortly thereafter, Hierlemann *et*

al. used AFM to examine generation four and eight amine terminated dendrimers which had been adsorbed onto gold substrates.⁵⁸ They too found that the dendrimers had flattened on the surface, and that the measured diameter of an individual molecule was much larger than had been expected, even for a flattened dendrimer. They attributed this overestimation in the lateral dimensions to convolution of the surface due to tip effects as the size of the feature approached that of the tip, an effect which should not have affected the measured height. For example, for a generation eight dendrimer, the diameter measured from AFM was found to be approximately 20nm and its height was found to be approximately 3.5-4nm, while its ideal spherical diameter was 9.7nm. Similarly, for the generation 4 polymers, the ideal spherical diameter was 4.5nm, while the measured diameter was approximately 15nm, and its height was approximately 0.5-0.8nm. This flattening was attributed partially to the bonds that formed between the amine end groups and the gold surface, and was more pronounced for isolated dendrimers than for dendrimers with nearest neighbors, as the neighbors helped to prevent the polymer from flattening as they provided additional sites for bonding with the gold. To prove this point, *n*-alkane thiols were added to surfaces that had been covered in dendrimers. As the thiols were added, it was found that the shape of the dendrimer evolved from oblate to prolate as the thiols displaced the amine groups from the surface. Li *et al.* have also imaged individual poly(amido amine) dendrimers of generation five through ten.⁵⁹ They prepared their samples by spin coating extremely dilute (0.001% by weight) solutions of dendrimer onto mica surfaces. They too found that the dendrimers flattened on the high energy mica surface. Between generation five and generation nine, the diameter of the dendrimers was found to increase slowly with generation, eventually leveling off at around generation ten. In contrast, between generation five and eight, the height of the dendrimers was found to increase slowly with generation, but then for the generation nine and ten polymers, it was found to increase very rapidly indicating that the molecular rigidity of the polymers also increase dramatically, such that they were not as susceptible to deformation. In a follow-up paper, Li *et al.* examined the packing of generation nine poly(amido amine) dendrimers on mica surfaces under various conditions.⁶⁰ When the dendrimers were deposited such that they formed a monolayer, they packed into a hexagonal array; however, as the amount of dendrimer on the surface decreased, the dendrimers began to form an interconnected pattern with open spaces in between the dendrimer regions. Only a few isolated dendrimers were found in these open spaces. Nonetheless, they too found that the size

of the dendrimer depended on its spatial relation to the other dendrimers. For example, for dendrimers all in a row, the dimensions were measured to be 12.8nm by 24.7nm by 4.92nm. For a dendrimer in the center of a circle of other dendrimers, the dimensions were measured to be 12.8nm by 12.8nm by 6.81nm, and for an isolated dendrimer, the dimensions were 25.3nm by 25.3nm by 3.63nm. The isolated dendrimers had the smallest height and the largest diameter, suggesting that the dendrimers were soft, spongy, and elastic, and that their shape could be controlled by application of very small flow forces. Finally, Betley *et al.* have used AFM to examine the effect of the substrate and the pH on the sizes and shapes of various poly(amido amine) dendrimers.⁶¹ They found that as the dendrimer substrate became more hydrophobic, the measured height and diameter of the dendrimers began to approach ideal sphere dimensions as the favorable interactions between the dendrimer and the substrate were decreased. In addition, acidification of the dendrimer resulted in an increase in the dendrimer dimensions as the charges helped to increase the rigidity, and thus the dimensions of the polymers. In order to decrease the effect of tip convolution and to obtain topological information about the individual dendrimers, a carbon nanotube, which had a diameter of 3-4nm, was used as the AFM tip in these experiments.

Not nearly as much attention has focused on imaging the poly(propylene imine) or the poly(benzyl ether) spherical dendrimers. Schenning *et al.* have used TEM to image aggregates of poly(propylene imine) dendrimers which have been cast onto TEM grids and subsequently stained using a uranyl acetate stain (negative stain) or a platinum shadowing technique (positive stain). Cryo-TEM was also used to image these same dendrimer aggregates. Nonetheless, in all of these cases, the aggregates were the dominate features and it was difficult to distinguish the individual dendrimers and their sizes.⁶² Takada *et al.* have used tapping mode AFM to visualize poly(propylene imine) dendrimers which have been functionalized with cobaltocenium end groups.⁶³ As had been observed for the poly(amido amine) dendrimers, they found a measured diameter of 7.8nm, which was much larger than the expected diameter of 4.4nm. They too attributed this larger than expected size to flattening of the dendrimer on the surface as well as tip convolution. Flattening of the dendrimer on the surface was also observed for poly(benzyl ether) dendrimers which were coupled to a gold surface via an alkyl sulfide group which radiated from the core. In these experiments, Friggeri *et al.* used the self-assembly process to coat the surface of gold with an alkane thiol layer.⁶⁴ Then the dendritic sulfide was introduced and the sulfide group was able to displace some of the alkane thiol groups, covalently bonding the

dendrimer to the gold surface and resting on top of the neighboring alkyl groups. These poly(benzyl ether) dendrimers were found to have a height of approximately 18nm and a width of approximately 18nm, which was an overestimation that they attributed to tip convolution effects.

Carbosilane dendrimers have also been imaged with AFM. Sheiko *et al.* examined carbosilane dendrimers which possessed methyl as well as hydroxyl end groups on mica surfaces.⁶⁵ While the methyl terminated polymers formed globular structures on the surface, the hydroxyl terminated polymers deformed as the dendrimer flattened on the surface adopting an axial ratio of 3:1, due to the favorable interactions of the hydroxyl groups with the surface. Liquid crystalline dendrimers formed by the termination of carbosilane dendrimers with cyanobiphenyl groups have also been studied by Ponomarenko *et al.*³⁷ On silica surfaces, they found that the polymer formed a network of aggregates when there was not sufficient dendrimer to completely cover the surface. In addition, they found that the height of an individual dendrimer was approximately 3nm, while the distance between dendrimers in the aggregates was 5.5nm, in good agreement with the diameter of a single dendrimer in solution, as determined from x-ray scattering. Finally, they felt that the reduction in the measured height was caused by a distortion of the dendrimer with the AFM tip.

Using AFM, Zhang *et al.* have examined the behavior of polyphenylene dendrimers which were spin coated onto mica surfaces.^{66,67} In their initial experiments, they were able to image individual dendrimers which had been terminated with phenyl groups, and they found that the observed height was in good agreement with the size of an individual dendrimer molecules as obtained by molecular dynamics simulations, indicating that these dendrimers were “stiffer” than those of other chemistries, such as the poly(amido amine) chemistry. Nonetheless, they too observed an overestimation in the measured diameter of the dendrimer, most likely due to tip effects.⁶⁶ In later experiments, Zhang *et al.* used pulsed force AFM to study the stiffness and adhesion properties of both phenyl as well as carboxylic acid terminated dendrimers. Using a hydrophilic tip, they were able to discriminate between the two different types of dendrimers on a surface which was covered with both, based solely on their different adhesion strengths. In addition, they found that the carboxylic acid terminated dendrimers were more likely to aggregate on the mica surface than the polyphenylene dendrimers due to the hydrogen bonding capability of the acid terminated polymers.⁶⁷

Nonetheless, even before several groups observed flattening of dendrimers on the surface, Mansfield predicted this phenomena using molecular dynamics simulations of dendrimers which had been adsorbed onto surfaces at different interaction strengths.⁶⁸ From these simulations, he reached two conclusions. One, dendrimers will flatten and spread on surfaces even at intermediate interactions strengths; and two, an increase in the dendrimer generation or the interaction strength of the surface will increase the flattening of the molecules on the surface.

5.2.2 Dendritic Rods

Percec *et al.* have extensively examined the thermal, morphological, and liquid crystalline properties of “dendron jacketed linear polymers”, or dendritic rods.^{1,17-19,21,69-72} While various backbone chemistries have been employed, the dendritic portion has always consisted of poly(benzyl ether) (Fréchet type) chemistry. By the addition of alkyl or fluoroalkyl groups, usually dodecyl chains, to the exterior benzyl ether groups of the monodendron, they found that the monodendrons would assemble into thermotropic liquid crystalline phases as indicated by x-ray diffraction and optical microscopy. In addition, by tuning the position and number of alkyl groups, the generation number, and the backbone chemistry, either hexagonally packed columnar mesophases or body centered cubic spherical mesophases could be achieved. In general, the higher generation monodendrons as well as those composed of more high highly substituted benzyl units tended to form spherical mesophases while those monodendrons that were of lower generation and that were not as highly substituted preferred to adopt a cylindrical morphology.²¹ For example, for the monodendrons based on 3,4,5-trihydroxybenzoate, the first two generations of the polymer self-assembled into cylindrical supramolecular dendrimers with each dendron occupying a quarter to a half a disk, for the first and second generation polymers, respectively. The third generation monodendrons self-assembled into spherical structures with each monodendron occupying a sixth of that sphere.²¹ Finally, they found that by placing a polymerizable group at the core of the dendrons, such as styrene, methacrylate, or oxazoline groups, the dendrons could be polymerized into permanent spherical or cylindrical structures that could be imaged using scanning force microscopy. For polymers with a low degree of polymerization, less than 20 repeat units, spherical shapes were observed while for polymers with a much higher degree of polymerization, cylindrical structures resulted, which is the

opposite behavior observed for traditional linear polymers which form extended conformations at low degrees of polymerization and spherical, coiled conformations at higher degrees of polymerization.^{17,19} The first series of polymerized monodendrons that they examined possessed a poly(methyl methacrylate) backbone. These polymers formed a hexagonal liquid crystalline phase that disappeared above 70°C, the melting point of the alkyl tails. Upon heating, these hexagonal columns were found to elongate and narrow.⁷³ A series of polymers with polystyrene backbones have also been prepared; however, they did not display contour lengths which were as large as those based on the poly(methyl methacrylate) backbones. For both series of polymers, an increase in the isotropitization temperature was induced by increasing the molecular weight, diameter, and rigidity of the polymer. For the rods based poly(oxazoline) linear polymers, the diameters were found to be approximately 33-44Å at room temperature, which also decreased with increasing temperature as the initially helical poly(ethylene imine) backbone began to unwind.⁷² These polymers exhibited a glass transition temperature which increased with increasing degree of polymerization and then leveled off after a degree of polymerization of 100-200. In addition, the glass transition temperature was found to be dependent on the length of the alkyl groups which were attached to the terminal benzyl units, exhibiting a maximum for the decyl groups and then decreasing with the addition of longer alkyl chains. The isotropitization temperature was also found to be dependent on the degree of polymerization, but the melting and the crystallization temperatures were not. At high degrees of polymerization, these polymers formed cylindrical structures that assembled into a hexagonal columnar lattice in the bulk; however, for polymers with a degree of polymerization of less than twenty, an “inverse micellar” or “water in oil” thermotropic body centered cubic liquid crystalline phase formed, with the poly(ethylene imine) backbone serving as the “water” and the dendrons serving as the “oil”.⁸ To prove the existence of the cylindrical structures, Percec *et al.* have very successfully imaged the polymers using SFM and STM. They found that optimal sample preparation was necessary to obtain good images; thus, highly oriented pyrolytic graphite chosen as the substrate to induce alignment of the cylindrical polymers through the interactions of the alkyl groups with the surface. If the substitution of the alkoxy groups on the monodendrons was too dense, regular adsorption of the alkyl tails was impeded and clear images could not be obtained. These cylindrical molecules appeared as wormlike chains that were slightly flattened on the surface and whose length was consistent with the backbone adopting an all-trans conformation.^{70,71} It should

be noted that while the dendrons that Percec *et al.* employed were based on poly(benzyl ether) chemistry, the addition of the dodecyl groups to the surface caused this chemistry to strongly resemble that of 3,4,5-tris[(p-dodecyloxy)benzyl]oxy]benzoyl (DOBOB), which has previously been shown to be a “columnarogen” that has been used to induce the formation of hexagonal columnar liquid crystalline phases.⁷⁴

Similarly, Seitz *et al.* have attached 3,4-bis(alkyloxy)benzyl side groups to linear and branched poly(ethylene imine) and found that the polymers formed hexagonal, columnar mesophases. The structure of the side groups was found to be very important, as substitution of the polymers with similar, yet slightly different benzyl groups did not result in the formation of liquid crystalline polymers - some of the polymers were highly crystalline while others were completely amorphous. Nonetheless, the linear poly(ethylene imine) was found to stabilize the formation of the mesophases.⁷⁴

Another group that has very successfully prepared and imaged dendritic rods based on poly(benzyl ether) dendrimer chemistry are Schlüter *et al.*⁷⁵ In their original work, Schlüter *et al.* polymerized a third generation preformed poly(benzyl ether) monodendron that possessed a styrene monomer at the core. These polymers differed from those prepared by Percec *et al.* in two important respects. One, they were not functionalized with dodecyl groups at their periphery, thus, they did not self-assemble into columnar liquid crystalline phases before polymerization. Two, they were of higher generation than the rod-like polymers that Percec prepared, as most of Percec's monomers self-assembled into spheres and not cylinders at the third generation. Nonetheless, these polymers were also imaged by scanning force microscopy of samples that had been prepared by solvent casting extremely dilute polymer solutions onto highly oriented pyrolytic graphite. The polymers appeared as closed packed, highly oriented, molecular cylinders on the surface. Unfortunately, Schlüter *et al.* have found that by synthesizing the polymers convergently - by polymerization of the monodendrons - the length of the polymer that could be achieved was limited. Thus, more recently they have prepared extremely long dendronized polymers by the divergent addition of protected benzyl ester groups to a preformed, generation one dendronized polystyrene using amine/succinic ester chemistry, which is known to be an efficient coupling method.⁷⁶ This backbone consisted of approximately 460 repeats of polystyrene, and the dendrons were functionalized with dodecyl groups in order to impart rigidity to the polymer. The polymers were imaged with tapping mode SFM on samples that had

been prepared by spin coating extremely dilute solutions of polymer onto highly oriented pyrolytic surfaces. SFM images revealed extended, rod-like conformations, but also those in which the polymer was coiled up like yarn. These polymers could be moved large distances around the surface of the graphite with the SFM tip. Nonetheless, the thermal and liquid crystalline properties of these polymers were not reported.

Side chain dendritic polyurethanes based on poly(benzyl ether) monodendrons have been prepared by Jahromi *et al.*^{77,78} The polymers which possessed a degree of polymerization of six assembled into a cubic lattice, as indicated by x-ray diffraction studies, consistent with Percec's observation relating the degree of polymerization to the type of structure formed. In addition, the glass transition temperature was found to increase with increasing generation, and polymerization of the monodendron resulted in only a minor increase in the glass transition temperature. The magnitude of that increase depended on the nature and rigidity of the polyurethane backbone. Finally, these polymers did not possess a liquid crystalline nature.

Tomalia *et al.* have successfully imaged their poly(amido amine) dendritic rods using TEM.⁷⁹ In order to provide contrast, the methyl ester terminated polymers were hydrolyzed with sodium hydroxide, forming rods with sodium ions at their periphery, as had been done for the spherical polymers. Dilute solutions of the polymers, 5×10^{-4} weight percent, were then solvent cast onto beryllium grids for imaging of the individual polymers. Rod-like behavior was noted at generation 4.5, with the diameter of the rods ranging from 25-32Å, and their length from 500 to 3000Å, corresponding to a degree of polymerization of 100-500. Preliminary modeling of the rods predicted a diameter of 35-45Å. In addition, while they reported the use of AFM to image these dendritic rods as a function of pH, no images were published. Similarly, no thermal or morphological data have been reported for these polymers. Percec *et al.* have noted that they believe that these poly(amido amine) dendritic rods do not possess the long range order needed to pack into a lattice that can be characterized with x-ray diffraction.^{18,21}

The thermal and morphological properties of wormlike carbosilane dendrimers have also been investigated by Ouali *et al.*⁸⁰ These dendritic rods consisted of propylsilane branches which were divergently added to a linear poly(methylhydrosiloxane) core and were found to take on a wormlike nature at generation 2, much sooner than the poly(amido amine) dendrimers. While these polymers have not been directly imaged, their extended conformation was verified with neutron scattering of the polymers in solution. The glass transition temperature of the

polymers was found to increase with increasing generation; however, no liquid crystalline properties were observed when the polymers were analyzed with polarized optical microscopy and x-ray diffraction. The absence of liquid crystallinity was attributed to the flexibility of the propylsilane branches.

Two last dendritic rod systems are worth mentioning. Setayesh *et al.* have attached polyphenylene monodendrons to a rigid polyfluorene backbone in order to suppress the aggregation of the polymers, while retaining their light emitting quality.⁸¹ While the polymers substituted with linear alkyl chains retained their liquid crystalline nature, those with the monodendron side chains did not, resulting in amorphous polymers, as determined from x-ray diffraction. In addition, when this dendron substituted polymer was examined with AFM, beautiful rods were not observed, instead, only nondescript blobs were seen, perhaps due to the short length of the polymer backbone (25 repeats). Similarly, Masuo *et al.* have attached poly(benzyl ether) monodendrons to a poly(phenyleneethynylene) core resulting in fluorescent, wire type polymers.⁸² When examined with AFM, these polymers sometimes appeared as string, but other times they adopted a donut-like configuration or they appeared as single particles, depending on the conditions of sample preparation.

5.2.3 Hybrid-Linear Dendritic Diblock Copolymers

The first group to conduct a preliminary investigation into the thermal and morphological properties of hybrid-linear dendritic diblock copolymers were Gitsov *et al.* who examined AB and ABA block copolymers consisting of an A block of either poly(ethylene oxide) or polystyrene and a B block of a poly(benzyl ether) dendrimer.⁸³⁻⁸⁵ For the poly(ethylene oxide)-poly(benzyl ether) di- and triblock copolymers, they found that when the mass of the poly(ethylene oxide) block was equal to or larger than that of the dendritic block, microphase segregation occurred, as indicated by the presence of a melting point associated with the crystalline poly(ethylene oxide) block and a glass transition temperature attributed to the dendritic blocks. However, when the dendritic blocks were the majority blocks, no poly(ethylene oxide) melting point was observed due to phase mixing of the blocks and a loss of crystallinity in the poly(ethylene oxide).⁸³ In addition, for these polymers, the casting solvent and the thermal treatment were found to have a large effect on the resulting morphology. When cast from chloroform and THF solutions, the poly(ethylene oxide) homopolymers formed

spherulites that were visualized as a Maltese cross pattern in polarized optical microscopy. As the fraction of dendrimer in the block copolymers increased, the ability of the poly(ethylene oxide) to crystallize and form these patterns decreased. In addition, in 1:1 methanol/water solutions, a very different crystalline pattern was observed as the solvent was not a good solvent for the dendritic block. Finally, when films cast from methanol/water solutions were examined with x-ray diffraction, they exhibited either no peaks, or just one peak attributed to the poly(ethylene oxide) block, when both blocks should have been crystalline. For the polystyrene-poly(benzyl ether) di- and triblock copolymers, the glass transition temperature was found to increase with increasing molecular weight of the polystyrene block. Since the glass transition temperature of the poly(benzyl ether) di-dendrons, without the middle polystyrene block, was found to be mostly independent of generation, the effect of generation on the di- and triblock copolymers was not examined. Since a physical mixture of polystyrene homopolymer and poly(benzyl ether) homopolymer produced two glass transition temperatures but the block copolymers produced one, the block copolymers can be considered to have formed a mixed phase. Over the molecular weight range of 10,000-60,000, the glass transition temperature of the block copolymers was very close to the equation, $\ln T_g = m_1 \ln T_{g1} + m_2 \ln T_{g2}$, where m_1 and m_2 are the weight fractions of each of the blocks and T_{g1} and T_{g2} are the glass transition temperatures of each of the blocks.

More recently, Chang *et al.* have examined the thermal behavior of poly(ethylene oxide)-dendritic carbosilane hybrid-linear diblock copolymers as well as dendritic carbosilane-poly(ethylene oxide)-dendritic carbosilane triblock copolymers. For the diblock copolymers, the melting point was found to decrease with increasing generation. In addition, the glass transition temperature was also found to decrease with increasing generation and then level off, which is in contrast to the results observed by Iyer *et al.*, as described below. No explanation for this behavior was given.⁸⁶ For the triblock copolymers, the melting point of the poly(ethylene oxide) block was also found to decrease with increasing generation. The glass transition temperature of these polymers was not reported.⁸⁷

Román *et al.* conducted a more in-depth morphological characterization of a hybrid-linear dendritic diblock copolymer system.⁸⁸ Using TEM and SAXS they examined the microphase segregation of diblock copolymers consisting of a polystyrene block and a carboxylic acid functionalized poly(propylene imine) dendrimer. These asymmetric diblock

copolymers did not display the aggregation behavior typically observed for diblock copolymers consisting of two linear blocks, but rather they exhibited a generation dependent aggregation that qualitatively followed Isrealachvili's theory on the relationship between molecular weight and aggregation form, commonly applied to surfactant systems. The generation one polymers formed hexagonally packed cylinders of dendrimer in a polystyrene matrix. At this volume fraction of dendrimer, approximately 0.1, spherical aggregates traditionally form; however due to the branching in the dendritic block, the interface between the dendritic block and the polystyrene block was forced to curve toward the polystyrene, facilitating the formation of cylinders. The higher generation diblock copolymers all adopt a lamellar morphology whose thickness decreased with increasing generation, indicating that the polystyrene was adopting a conformation such that it "filled in" the area behind the dendrimer. As the generation increased, so did this area, such that the polystyrene needed to decrease its thickness in order to maintain its volume. Surprisingly, they found that the long range order of the morphology decreased with increasing generation, as indicated by less defined first order peaks as well as a loss of the second order peaks in SAXS. In addition, this loss in order was also directly observed with TEM. Finally, they noted that the presence of the carboxylic acid groups was instrumental in driving the morphology as the analogous amine terminated polymers did not exhibit phase segregation. The poly(propylene imine) dendrimers themselves were very compatible with polystyrene as indicated by their "chi" parameters.

The hybrid-linear dendritic diblock copolymer systems whose thermal and morphological properties have been the most extensively studied are the poly(ethylene oxide)-poly(amido amine) diblock copolymers. Iyer *et al.* examined two series of polymers, one which consisted of a poly(ethylene oxide) block that possessed a molecular weight of 2000g/mol and the other which possessed a molecular weight of 5000g/mol.⁸⁹ In both series, a poly(ethylene oxide) melting point was observed for all of the generations of dendrimer examined; however, the temperature of this melting point was found to decrease with increasing generation. This melting point depression was greater for the 2000 molecular weight series, as the percentage of the dendritic block was much higher in these polymers. In addition, while the normalized enthalpy of crystallization for the 5000 molecular weight series remained approximately constant, indicating a constant degree of crystallinity, it decreased with increasing generation for the 2000 molecular weight series, indicating a decreasing crystalline PEO content, most likely due to

phase mixing. As had been observed for the spherical homopolymers, the glass transition temperature of the poly(ethylene oxide)-poly(amido amine) hybrid-linear dendritic diblock copolymers was found to be very dependent on the end group chemistry and it increased with increasing generation. For the 5000 molecular weight series, a glass transition temperature was not observed until generation 3.0, as it most likely fell below the temperature range of the DSC detector for the lower generation polymers. Nonetheless, for the generation 3.0 amine terminated polymer, the glass transition temperature was approximately 0°C, which then increased to approximately 10°C for the generation 4.0 polymer, while for the ester terminated half generation polymers, the glass transition temperature was much lower, approximately -30°C for the generation 3.5 polymer and increasing to approximately -20°C for the generation 4.5 polymer. Similarly, for the 2000 molecular weight amine terminated polymers, a glass transition temperature was reported for the polymers of generation 2.0 and higher, which was found to increase with increasing generation. The glass transition temperatures of the corresponding ester terminated polymers were not reported. The ester terminated polymers from the 2000 molecular weight series were subsequently functionalized with stearate groups. The presence of the stearate groups caused further suppression of the melting point of the poly(ethylene oxide) block. In addition, for these polymers, a second and third melting point appeared above 100°C, which Iyer *et al.* attributed to crystallization of the stearate groups. Looking at these stearate terminated polymers in the polarized optical microscope, they observed birefringence reminiscent of that seen for poly(ethylene oxide) homopolymer, indicating phase segregation. Johnson *et al.* continued this work examining the effect of temperature on the resulting morphology of the 2000 molecular weight series using SAXS, WAXS, and TEM.⁹⁰ For all generations of the amine terminated polymers, they found that the crystallinity of the poly(ethylene oxide) block drove the resulting morphology. Below the melting point of the poly(ethylene oxide) block, this crystallinity was “softly confined” by the amorphous poly(amido amine) block, such that it was able to disrupt the presence of any morphology. Above the melting point, the diblock copolymer morphology was driven by traditional phase segregation, resulting in two different morphologies above and below the melting point. Nonetheless, all of these polymers exhibited a segregated melt state at temperatures above the melting point of poly(ethylene oxide). In general, in this melt state the poly(amido amine) domains appeared as elongated worms or globules, whose domains on average were one dendron wide and five dendrons long. For all of the generations of

the stearate terminated polymers, the crystalline stearate groups prevented the poly(ethylene oxide) block from driving the morphology by isolating the poly(ethylene oxide) block through a “hard confinement”. In general, these polymers also exhibited a lamellar morphology and were segregated in the melt state.

To our knowledge, no one has yet imaged an individual, isolated hybrid-linear dendritic diblock copolymer. Thus far, all of the imaging has been done in the bulk, as discussed in the previous paragraphs. While Choi *et al.* have used AFM to image the complex of plasmid DNA with a barbell-like poly(L-lysine) dendrimer-poly(ethylene oxide)-poly(L-lysine) dendrimer triblock copolymer, imaging of the triblock copolymer itself has not been reported.⁹¹ In addition, research that examines the possible liquid crystalline behavior of native or functionalized hybrid-linear dendritic diblock copolymers has not yet been found.

5.2.4 Rod-Coil and Comb-Coil Diblock Copolymers

In addition to possessing a dendritic nature, the linear-dendritic rod diblock copolymers under investigation in this thesis also possess a diblock copolymer nature, so it is important to look at a few other diblock copolymer systems that possess a similar architecture, such as rod-coil diblock copolymers and comb-coil diblock copolymers. One of the first rod-coil diblock copolymer systems whose morphology was examined was based on polypeptide rod blocks.⁹² These polymers were found to assemble into a lamellar morphology with the rod blocks tilted within their domains. Since then, Chen *et al.* have reported previously unseen morphologies for poly(hexyl isocyanate)-polystyrene rod-coil diblock copolymers. Polymers with rod fractions less than 0.42 assembled into wavy lamellar, while those with rod fractions of 0.73-0.9 formed a zigzag morphology with the poly(hexyl isocyanate) rods interpenetrating and tilting with respect to the polystyrene interface. Finally, for rod fractions of 0.98, the polystyrene formed an arrowhead pattern within a matrix of poly(hexyl isocyanate).^{93,94} These morphologies formed as a result of the competition between phase segregation and crystallization. For rod-coil diblock copolymers, the stiffness of the rod and the asymmetry of the polymer cause an increase in the Flory-Huggins chi parameter in comparison with traditional coil-coil diblock copolymer systems, such that phase segregation occurs at much lower molecular weights.⁹⁵ Thus, there has also been a lot of interest in rod-coil oligomers. Stupp *et al.* have found that rod-coil systems composed of an oligo(biphenyl ester) rod and a polystyrene-polyisoprene coil assemble into mushroom

structures with the rods aggregating to form the stem and the coils composing the head.⁹⁶ In addition, these mushroom aggregates assemble into larger three-dimension structures in which the mushrooms pack head to stem. In contrast, rod-coil oligomers based on poly(isocyanodipeptide)-polystyrene⁹⁷ chemistry as well as those based on poly(*para*-phenylethylene)-poly(dimethylsiloxane)⁹⁸ chemistry have been found to assemble into micrometer long fibers.

Recently, the morphology of comb-coil diblock copolymers has also generated a lot of interest. Ruokolainen *et al.* have examined comb-coil diblock copolymers which consist of 3-n-pentadecylphenol (PDP) arms hydrogen bonded to a polystyrene-poly(4-vinyl pyridine) backbone, and found that they phase segregated on two length scales, a “block copolymer” length scale and a much smaller “nanoscale”.⁹⁹⁻¹⁰¹ On the “block copolymer” scale, the polystyrene and the poly(vinyl pyridine)-PDP blocks are phase segregated, with the morphology transitioning from spherical to hexagonal to lamellar with the amount of the PDP present. The poly(vinyl pyridine)-PDP domains were further nanaseparated into lamellar structures due to incompatibility of the poly(vinyl pyridine) and the PDP. Similarly, several groups have examined the morphology of liquid crystalline rod-coil diblock copolymers and found segregation on two length scales for these polymers as well.¹⁰²⁻¹⁰⁹ In addition to the microphase segregated lamellar, cylindrical, and spherical structures observed at the 10-100nm length scale, the smectic order was observed on a much smaller scale in these polymers.

5.3 Experimental

5.3.1 Differential Scanning Calorimetry (DSC)

Differential scanning calorimetry measurements were recorded using a Perkin Elmer DSC7 calorimeter equipped with a compressed air sample dry box and a Perkin Elmer refridgerated cooling system. The polymers that were studied consisted of a poly(ethylene oxide) block length of 43 repeats and a dendritic block length of approximately 97 repeats. The thermal behavior of poly(ethylene oxide)-poly(ethylene imine) backbone, as well as the half generation methyl ester terminated, and the whole generation amine and alkyl terminated polymers were examined. The polymer samples were prepared in aluminum pans and each sample consisted of approximately 4-8mg of polymer. Each sample was heated and cooled at a

rate of 10°C/minutes. In order to detect any major changes in material behavior upon an initial heat treatment, each sample was subjected to two heating/cooling cycles. The melting points and glass transition temperatures were calculated from the first heating/cooling cycle as there were generally no differences between the results of the two cycles. The glass transition temperature was calculated using the half-height method, which used the midpoint of the inflection tangent. The melting point was calculated based on the mean of the area under the melting point.

5.3.2 Small Angle X-ray Scattering (SAXS) and Wide Angle X-ray Diffraction (WAXD)

Small angle x-ray experiments were performed under vacuum using a Siemens computer-controlled system with a rotating anode that produced Cu K α radiation ($\lambda=1.54\text{\AA}$) at 40kV and 30mA. The polymers that were examined were the following: the poly(ethylene oxide)-poly(ethylene imine) diblock copolymer backbone, the methyl ester terminated half generation polymers, and the whole generation dodecyl terminated polymers, all of which possessed a poly(ethylene oxide) block length of 43 repeats and a dendritic block length of approximately 97 repeats. Samples for analysis were prepared by dissolving the polymer in a minimum of solvent and then casting the polymer solution onto a glass slide that was coated with Teflon tape. The glass slide was then placed under a crystallization dish along with a small beaker of casting solvent in order to maintain equilibrium during the evaporation process. After two days, the majority of the casting solvent had been removed. All of the polymer samples were cast from methanol except the generation 4.0-dodecyl polymer, which was cast from chloroform, as this polymer was not completely soluble in methanol. The polymer, which was coated on the glass slide, was then placed in a vacuum oven and was annealed under vacuum for a minimum of two days at a temperature right below the highest melting point. For the poly(ethylene oxide)-poly(ethylene imine) polymer this temperature was 53°C, while for the other polymers, this temperature was approximately 37-42°C. The cast films were then carefully transferred to thin walled glass capillary tubes, which were used in the SAXS instrument. As some of the polymers were viscous liquids that were difficult to transfer, these polymers were dipped into liquid nitrogen, such that the sample temperature approached that of the glass transition of the polymer, causing the polymer to become more rigid and easier to place in the capillary tubes. The filled capillary tubes were then placed into a custom-built copper sample holder, which fit into an

Instec hotstage (model HS250 modified for vacuum operation) such that the samples were suspended vertically in the beam's path, 63.4cm away from the detector. An Instec model STC200 temperature controller was used to control the temperature of the sample. This setup allowed SAXS measurements to be taken at elevated temperatures. Data were collected at various temperatures, starting at room temperature and increasing incrementally, usually in 5-10°C intervals, until it surpassed the temperature at which the last transition was observed in DSC. The data were acquired using a detector consisting of a pressurized xenon chamber with a wire grid assembly that enabled direct imaging of the diffraction patterns, and it was plotted as scattered x-ray intensity as a function of temperature and the scattering vector \mathbf{q} . ($\mathbf{q} = (4\pi \sin \theta)/\lambda$, where θ was one half of the scattering angle.)

Wide angle x-ray diffraction experiments were conducted on the poly(ethylene oxide)-poly(ethylene imine) generation 1.0-dodecyl terminated polymer. The sample was prepared in the same manner as it had been for the DSC experiments. The experiments were performed on a Rigaku 250 XRD diffractometer with nickel-filtered Cu K α radiation ($\lambda=1.54\text{\AA}$). Measurements were made under three conditions: at room temperature, after having been chilled in liquid nitrogen, and after having rewarmed to room temperature.

5.3.3 Transmission Electron Microscopy (TEM)

TEM images were captured on JEOL JEM 2000 FX and JEOL JEM 2010 electron microscopes. The polymers whose morphology was imaged consisted of the following: the poly(ethylene oxide)-poly(ethylene imine) diblock copolymer backbone, the methyl ester terminated half generation polymers, and the whole generation dodecyl terminated polymers, all of which possessed a poly(ethylene oxide) block length of 43 repeats and a dendritic block length of approximately 97 repeats. For consistency, polymer samples for both TEM and SAXS were taken from the same cast film; therefore, conditions for polymer sample preparation are identical to those described above for the SAXS experiments. Ultrathin films were prepared by cryotomizing the polymer samples at -40°C using a RMC MTX microtome with a diamond knife. Sections were transferred dry from the diamond knife surface onto copper grids and then stained for 60 minutes with RuO $_4$ vapor, which selectively stained the poly(amido amine) dark, to provide contrast for the electron imaging.

5.3.4 Optical Microscopy (OM)

Polarized optical microscopy images were captured with a CCD camera, which was attached to a Leitz polarized optical microscope. The polymers that were investigated included the following: the poly(ethylene oxide)-poly(ethylene imine) diblock copolymer backbone, the generation 0.5-3.5 methyl ester terminated polymer, all of the generation 1.0-alkyl terminated polymers, and the generation 3.0-octadecyl terminated polymer. All of these polymers possessed a poly(ethylene oxide) block of 43 repeats and a dendritic block of approximately 97 repeats. Samples for the optical studies were prepared by casting very thin polymer solutions, which had been prepared in either methanol or chloroform (concentration 10-15mg/ml), onto glass slides. The glass slides were then placed under a crystallization dish along with a small beaker of casting solvent in order to maintain equilibrium during the evaporation process. After two days, the glass slides were removed from the crystallization dish and the polymer films were covered with a cover slip. The polymer coated glass slides were then placed into a Mettler FP-90 hot stage for analysis. The polymer films were heated at a rate of 10°C/minute, and images were taken with no polarization as well as with a 90° polarization as phase transitions appeared to be occurring. Image analysis was accomplished using Adobe Photoshop software.

5.3.5 Atomic Force Microscopy (AFM)

AFM images were collected using a Digital Instruments Multi-Mode AFM in the tapping mode. The only polymer imaged was the generation 4.5 linear-dendritic rod diblock copolymer consisting of 43 repeats of poly(ethylene oxide) and approximately 97 repeats of dendritic block, as this was one of the few polymers expected to take on a rod-like shape. Samples for AFM were prepared by spin-casting (2000 rpm, 2 minutes) 0.02 mg/ml generation 4.5 polymer solutions onto mica substrates that had been freshly cleaved with tape. The extremely dilute solution was used for imaging individual polymers. Images were collected using both standard (tip radius better than 10nm) and super sharp (tip radius better than 5nm) AFM probes from Molecular Imaging.

5.4 Results and Discussion

5.4.1 Differential Scanning Calorimetry (DSC) and Optical Microscopy (OM)

Differential scanning calorimetry has often been used to identify the thermal transitions in polymer systems. One of the thermal transitions that has been extensively studied in dendritic systems is the glass transition temperature. Researchers have not only been concerned with determining absolute values for a given family of dendrimers, but they have also been interested in how its value is affected by the generation number, interior chemistry, and exterior functionality of the dendrimer. Due to their hyperbranched nature, most dendrimers are amorphous and they possess a glass transition temperature but not a melting point. However, as researchers have begun to examine the thermal properties in hybrid-linear dendritic diblock copolymer systems, many of which possess a linear block that is semicrystalline, the effect of the dendrimer generation number and chemistry on the melting point of the linear block has also been examined. Finally, since some dendritic systems have been found to exhibit a liquid crystalline nature, either because of functionalization of the native polymers with mesogen units or because the dendrimer branches were themselves mesogenic, the transition temperatures over which these dendrimers exhibited the liquid crystalline phase have been identified. Thus, given the unique chemistry and architecture of the poly(ethylene oxide)-poly(ethylene imine) linear-dendritic rod diblock copolymers, the thermal transitions of the polymers were examined in order to determine the effect of dendritic block generation and exterior chemistry on the glass transition temperature as well as the melting point of the polymers. In addition, the DSC traces and the images from polarized optical microscopy were examined for evidence of the diblock copolymers displaying liquid crystalline behavior.

The thermal transitions of each of the linear-dendritic rod diblock copolymers were measured with DSC and their absolute values are reported in Appendix 5.A. Examples of DSC traces for the poly(ethylene oxide)-poly(ethylene imine) backbone polymer as well as the generation 2.0 amine terminated, and the generation 3.5 ester terminated linear-dendritic rod diblock copolymers are presented in Figure 5.1. The thermal transitions for the amine and ester polymers formed during the generational synthesis are summarized in Figure 5.2.

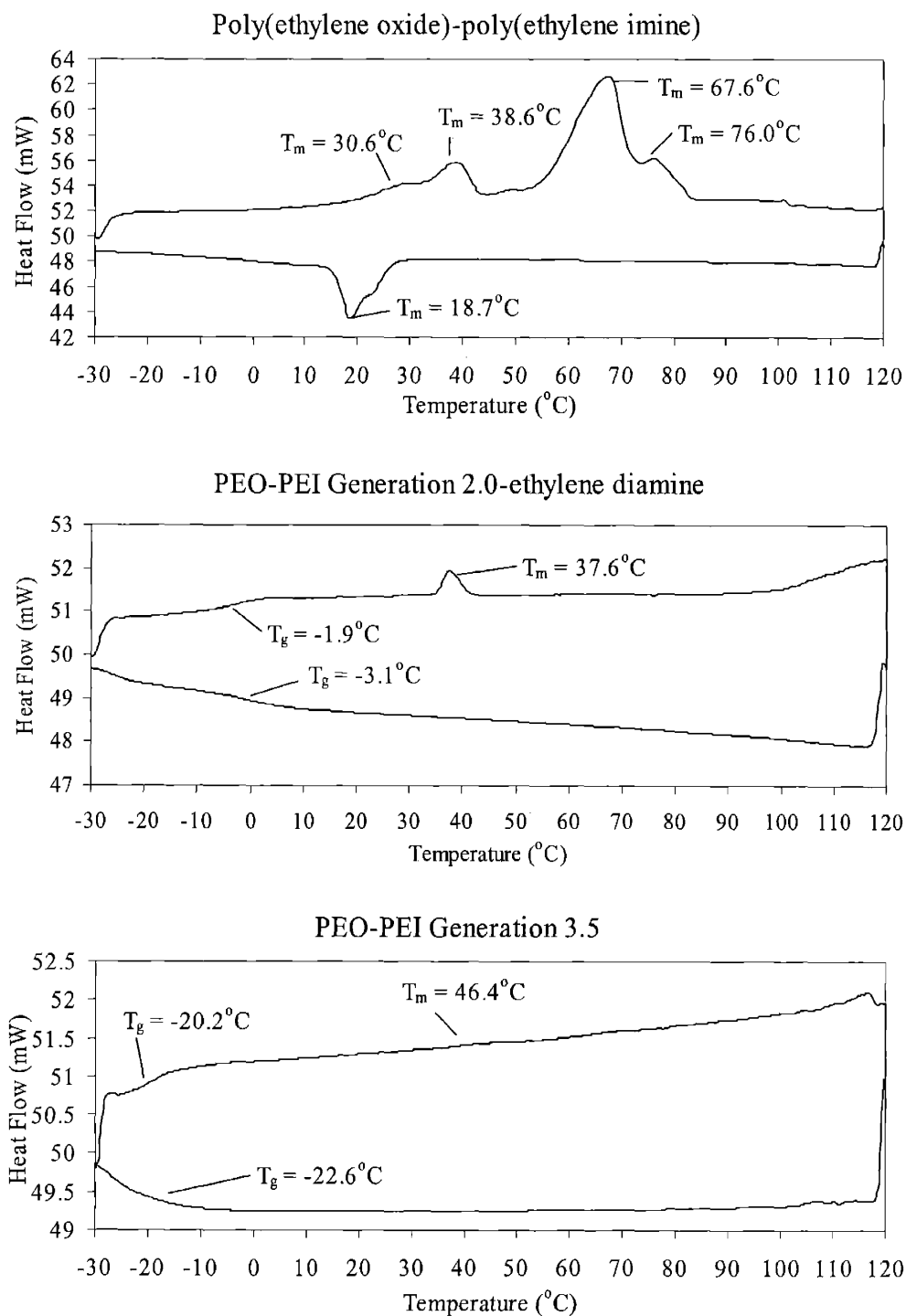


Figure 5.1. Examples of DSC traces for the amine and ester terminated linear-dendritic rod diblock copolymers: poly(ethylene oxide)-poly(ethylene imine) diblock copolymer backbone, generation 2.0 linear-dendritic rod diblock copolymer, generation 3.5 linear-dendritic rod diblock copolymer.

As can be seen, the poly(ethylene oxide)-poly(ethylene imine) diblock copolymer consisted of two crystalline blocks with each block exhibiting more than one melting point. The melting points for the poly(ethylene oxide) block were found to be 30.6°C and 38.6°C, while those for the poly(ethylene imine) block were found to be 67.6°C and 76.0°C. The melting point of pure poly(ethylene oxide) of molecular weight 2000g/mol is known to be approximately 54°C.¹¹⁰ Thus, the presence of the poly(ethylene imine) block resulted in a reduction of the poly(ethylene oxide) melting point, most likely due to a combination of destabilization of poly(ethylene oxide) crystals as well as phase mixing of the poly(ethylene oxide) and the poly(ethylene imine) blocks. The formation of two melting points most likely indicated that two different crystal structures were present, perhaps one in which the poly(ethylene oxide) block co-crystallized with or was plasticized by the poly(ethylene imine) block resulting in a lower melting point, and one in which the poly(ethylene oxide) was segregated from the poly(ethylene imine) block resulting in a slightly higher melting point. Iyer *et al.* have also observed a reduction in the melting point of the poly(ethylene oxide) block in poly(ethylene oxide)-poly(amido amine) hybrid-linear dendritic diblock copolymer systems.¹¹⁰ In these systems, the melting point was found to decrease with increasing generation, such that its value was approximately 40°C for the generation 4.0 amine terminated polymer. Similarly, two different melting points were observed that could be attributed to the poly(ethylene imine) block of the poly(ethylene oxide)-poly(ethylene imine) diblock copolymer. Linear poly(ethylene imine) homopolymer is known to exhibit two different melting points depending on the degree of hydration of the polymer. The anhydrous polymer has a melting point of 58.5°C, while the hydrated polymer has a melting point of 78.5°C.¹¹¹⁻¹¹³ From x-ray diffraction, the hydrated polymer has been found to adopt a helical conformation with the water molecules serving as hydrogen-bonded crosslinks that hold the crystalline structure in place, resulting in a higher melting point for the hydrated polymer. The exact crystal structure depends on the number of water molecules present, as this number will affect the dimensions of the crystalline lattice. Thus, for the poly(ethylene oxide)-poly(ethylene imine) diblock copolymer, the melting point at 76.0°C can be attributed to hydrated poly(ethylene imine). The melting point at 67.6°C is fairly broad, thus, it can most likely be attributed to a combination of several factors including poly(ethylene imine) which is anhydrous or only very lightly hydrated, as well as poly(ethylene imine) which has co-crystallized with the poly(ethylene oxide) block. Unfortunately, no glass

transition temperatures were detected for the poly(ethylene oxide)-poly(ethylene imine) diblock copolymer. The glass transition temperature of the poly(ethylene oxide) block is known to be approximately -51°C ,¹¹⁴ while that of the poly(ethylene imine) block has been found to be approximately -25°C .^{113,115} It is possible that no glass transition temperatures were detected for the diblock copolymer because they either fell below the detection range of the instrument or their intensity was too small, relative to the melting points of the polymer, such that they were lost in the baseline.

The addition of dendritic branches to the poly(ethylene imine) block resulted in a loss of crystallinity of this block for the amine and ester terminated diblock copolymers formed during the generational synthesis; thus, these linear-dendritic rod diblock copolymers appeared to consist of an amorphous poly(amido amine) dendritic block and a crystalline poly(ethylene oxide) block. The melting point of the poly(ethylene oxide) block and the glass transition temperature of the dendritic block have been plotted in Figure 5.2 as a function of generation. As can be seen, the melting point of the poly(ethylene oxide) block remained constant, at approximately 40°C , independent of generation and all but disappeared above generation 2.0. As the generation number increased, the weight fraction of poly(ethylene oxide) decreased such that by generation 2.5, the fraction of poly(ethylene oxide) in the diblock copolymer was approximately 2.5%. Thus, it was difficult to determine whether this decrease in the intensity of the melting point was caused by difficulty visualizing the melting point due to its relatively minor contribution or if it was caused by a loss in the crystallizability of the poly(ethylene oxide) block due to extensive phase mixing of the two blocks, since accurate enthalpy measurements of the melting point could not be made. Nonetheless, the melting point of the poly(ethylene oxide) block appeared to remain approximately constant, indicating that the type of crystalline structures that did form were very similar from generation to generation. These crystalline structures most likely consisted of poly(ethylene oxide) which had been plasticized by the dendritic block as indicated by a lowering of the melting point of the poly(ethylene oxide) block to approximately 40°C from that of approximately 54°C for the poly(ethylene oxide) homopolymer, as had been observed for the poly(ethylene oxide)-poly(ethylene imine) diblock copolymer. These results are somewhat different than those which had been observed for hybrid-linear dendritic diblock copolymer systems. Iyer *et al.* have found that for the poly(ethylene oxide)-poly(amido amine) hybrid-linear dendritic diblock copolymers, the melting

point of the poly(ethylene oxide) block decreased only slightly with increasing generation for the low generation polymers; however, as the molecular weight of the dendritic block approached that of the poly(ethylene oxide) block, the temperature of the melting point decreased much more rapidly as there was a much higher degree of phase mixing between the poly(amido amine) block and the poly(ethylene oxide) block.¹¹⁰ Similarly, Gitsov *et al.* have found that the poly(ethylene oxide) block does not exhibit any melting point when the molecular weight of the dendritic block is larger than that of the poly(ethylene oxide) block in their poly(ethylene oxide)-poly(benzyl ether) hybrid-linear dendritic diblock copolymers.⁸³

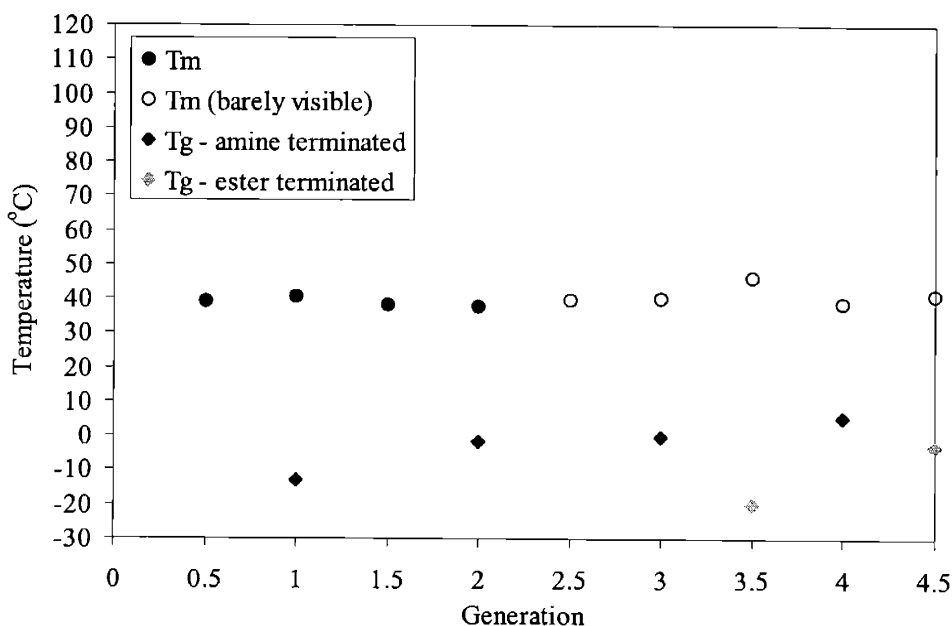


Figure 5.2. Variation of the melting point and the glass transition temperature with generation for the amine and ester terminated linear-dendritic rod diblock copolymers.

A glass transition temperature was observed for some of the linear-dendritic rod diblock copolymers that was attributed to the dendritic block due to its dependence on the end group chemistry as well as the generation number of the dendritic block, as can be seen in Figure 5.2. This glass transition temperature was observed for all of the amine terminated polymers; however, it was only observed for the generation 3.5 and 4.5 ester terminated polymers. The value of this glass transition temperature was always higher for the more polar amine terminated

polymers than for the ester terminated polymers of the same degree of branching, most likely due to the stronger interactions between the more polar groups which inhibited segmental motion. In addition, this glass transition temperature was found to increase with increasing generation, most likely due to the increased stiffness of the branches, as well as the increased size of the dendrimer, and thus the dispersive forces between the dendrimers, all which also would have increased the energy necessary for segmental motion. Thus, the reason that a glass transition temperature was not observed for the low generation methyl ester terminated polymers was most likely because it fell below the range of the detector. This dependence of the glass transition temperature of the dendrimer on the dendrimer end group chemistry and generation number has been observed for several other dendritic systems. Wooley *et al.* first observed this behavior for poly(benzyl ether) dendrimers.¹³ Dendrimers that were terminated with cyano groups exhibited a higher glass transition temperature than those that were terminated with less polar benzyl groups. They also found that the glass transition temperature increased with increasing molecular weight up to a point and then leveled off as the polymers became more globular and did not have as many opportunities for entanglements, one of the factors that has been known to increase the glass transition temperature of a polymer. Similarly, de Brabander-van den Berg *et al.* have measured a higher glass transition temperature for their cyano terminated poly(propylene imine) dendrimers than for their amine terminated polymers, and they too found that the glass transition temperature increased with increasing molecular weight.²⁹ Malmström *et al.* have also reported an influence of the end group chemistry on the glass transition temperature as they observed a higher glass transition temperature for hydroxyl terminated hyperbranched polyesters than for the benzoate and acetate terminated polymers.⁴³ These trends have also been observed in hybrid-linear dendritic diblock copolymer systems as Iyer *et al.* measured a glass transition temperature for their amine terminated poly(ethylene oxide)-poly(amido amine) hybrid linear-dendritic diblock copolymers that was 30°C higher than that of the ester terminated polymers of the same degree of branching.¹¹⁰ In addition, they too found that the glass transition temperature increased with increasing generation; however, they also found that the glass transition temperature was affected by the length of the poly(ethylene oxide) block, with the polymers possessing a longer poly(ethylene oxide) block exhibiting a higher glass transition temperature, consistent with the results of linear polymers. The above observations have been theoretically predicted by Stutz *et al.* as well.⁷ Finally, it should be noted that the glass transition

temperature measured for the dendritic block of the amine and methyl ester terminated linear-dendritic rod diblock copolymers under investigation in this thesis was in good agreement with that measured for other poly(amido amine) dendritic systems. For the diblock copolymers under investigation, the glass transition temperature was found to range from approximately -15°C to 5°C for the generation one through four amine terminated polymers, while it was found to range from approximately -20°C to -3°C for the generation 3.5 and 4.5 methyl ester terminated polymers and no glass transition temperature was observed for lower generation methyl ester terminated polymers. In comparison, Dvornic *et al.* measured the glass transition temperature of the third, fourth, and fifth generation amine terminated poly(amido amine) spherical dendrimers and found that it ranged from 11°C to 14°C .²⁵ Similarly, Iyer *et al.* found the glass transition temperature of the poly(ethylene oxide)-poly(amido amine) hybrid-linear dendritic diblock copolymers ranged from approximately -20°C to 10°C for the second through the fourth generation amine terminated polymers, while the glass transition temperature ranged from -30°C to -25°C for the generation 3.5 and 4.5 methyl ester terminated polymers and no glass transition temperature was measured for any of the lower generation methyl ester terminated polymers.¹¹⁰

Functionalization of the dendritic block terminal branches with alkyl groups in the linear-dendritic rod diblock copolymers added crystallinity to the dendritic block as indicated by the addition of an alkyl chain melting point to the thermal transitions of these polymers. These functionalized polymers also maintained the dendritic block glass transition temperature and the poly(ethylene oxide) melting point that had been observed in the unfunctionalized polymers. The thermal transitions of each of these alkylated linear-dendritic rod diblock copolymers were measured with DSC and their absolute values are reported in Appendix 5.A. Example DSC traces, which illustrate these three transitions are reported in Figure 5.3. The three examples traces are for the generation 4.0-hexyl, 3.0-octadecyl, and 1.0-dodecyl linear-dendritic rod diblock copolymers. The thermal transitions are summarized in Figures 5.4, 5.5, and 5.6, which plot the poly(ethylene oxide) melting point, the dendritic glass transition temperature, and the alkyl chain melting point, respectively, as a function of alkyl chain length and generation.

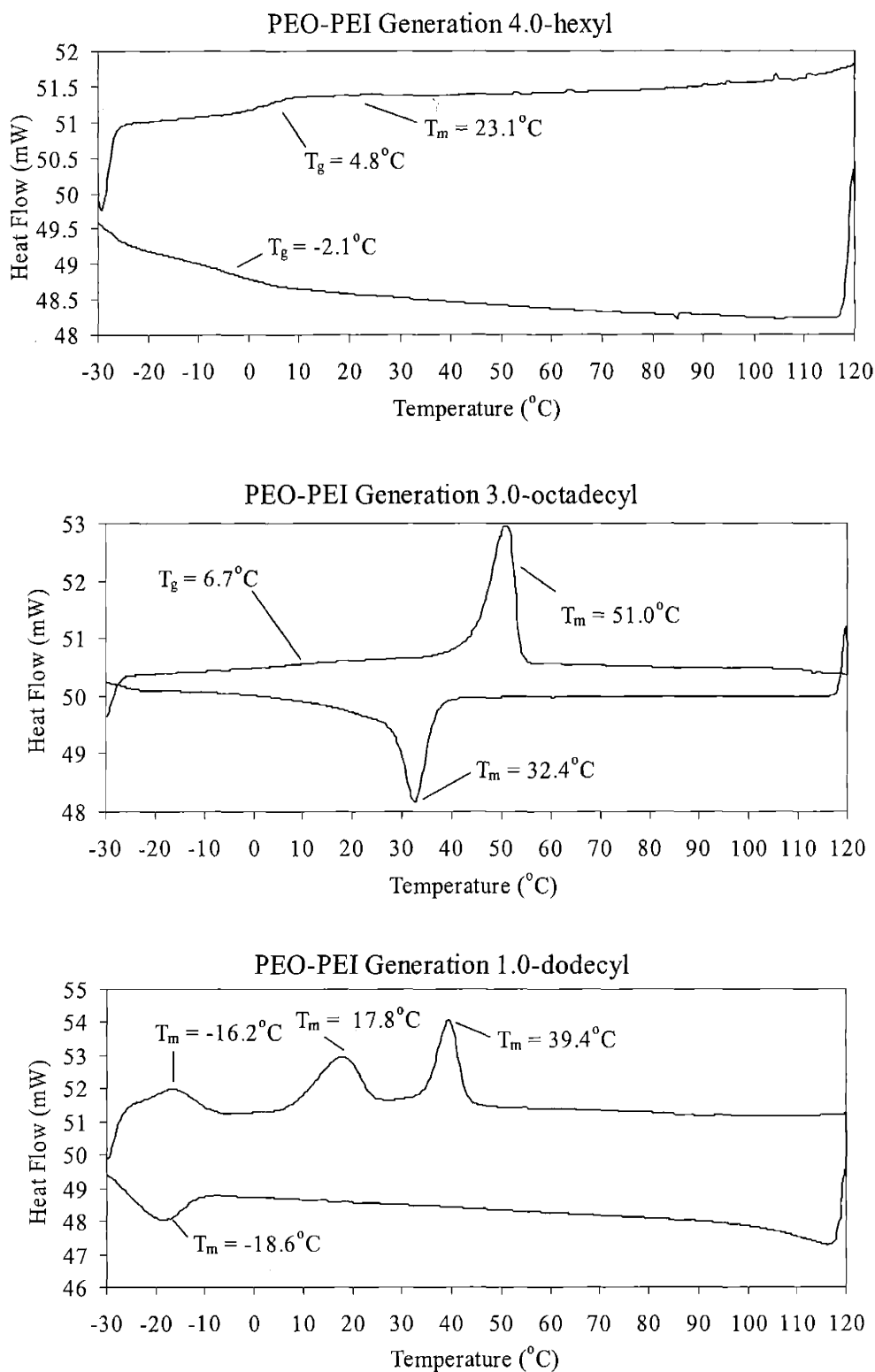


Figure 5.3. Examples of DSC traces for the alkyl terminated linear-dendritic rod diblock copolymers.

For these alkyl terminated linear-dendritic rod diblock copolymers, the melting point of the poly(ethylene oxide) block remained approximately constant, independent of alkyl chain length and generation, as can be seen in Figure 5.4. In addition, the melting point all but disappeared above generation two. These results were consistent with those observed for the methyl ester and the amine terminated polymers. Since the value of the melting point of the poly(ethylene oxide) block in the alkyl terminated diblock copolymers was approximately 40°C, in good agreement with that observed for the methyl ester and the amine terminated polymers, the crystal structure of the poly(ethylene oxide) in the alkyl terminated diblock copolymers was most likely very similar to that in the amine and ester terminated polymers - the poly(ethylene oxide) block was most likely plasticized by the dendritic block, resulting in a depression of the poly(ethylene oxide) melting point from its homopolymer value of 54°C. In addition, since the fraction of the poly(ethylene oxide) in the diblock copolymer was very small above generation 2.0, it was difficult to determine whether the almost complete disappearance of the poly(ethylene oxide) melting point was caused by difficulty visualizing it due to its relatively small magnitude or if it was caused by a loss in the crystalline nature of the poly(ethylene oxide) due to phase mixing.

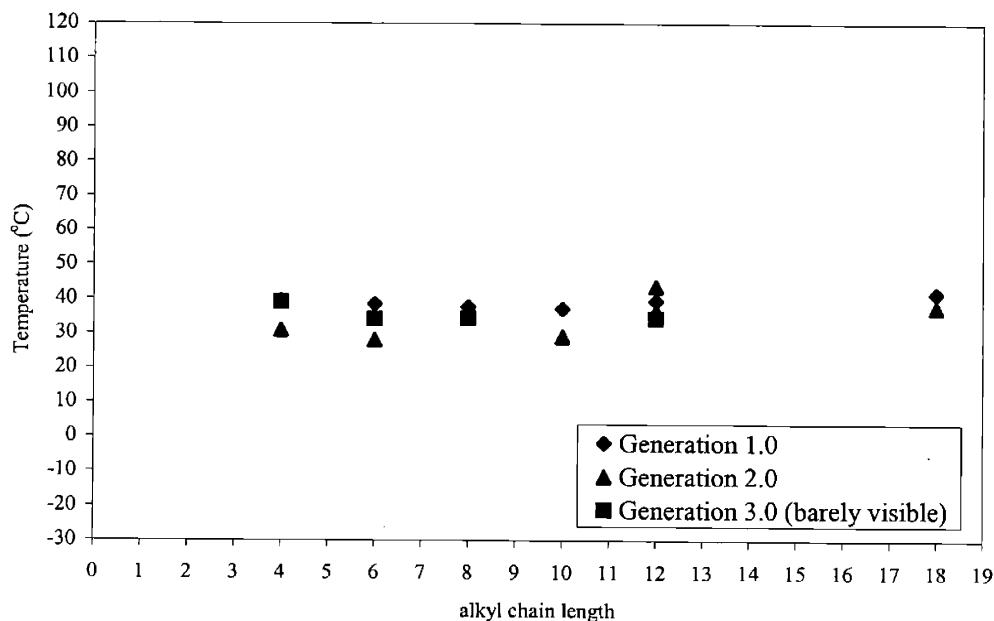


Figure 5.4. Variation of the poly(ethylene oxide) melting point with alkyl chain length and generation for the alkyl terminated linear-dendritic rod diblock copolymers.

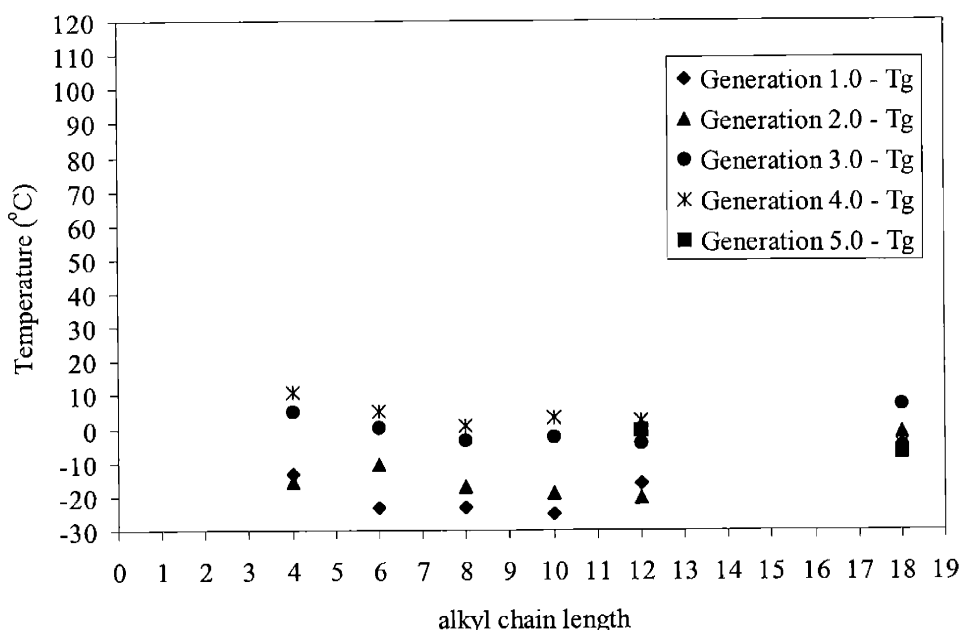


Figure 5.5. Variation of the glass transition temperature with alkyl chain length and generation for the alkyl terminated linear-dendritic rod diblock copolymers.

As had been observed for the methyl ester and the amine terminated linear-dendritic rod diblock copolymers, the glass transition temperature of the alkyl terminated diblock copolymers was found to be dependent not only on the generation number of the dendritic block, but also the end group chemistry of the dendritic block, or more specifically for the alkyl terminated polymers, the length of the alkyl chain. The glass transition temperature for the alkyl terminated polymers as a function of alkyl chain length and generation are plotted in Figure 5.5. In general, the glass transition temperature of the dendritic block was found to increase with increasing generation, which was the same trend as that observed for the amine and the ester terminated polymers. Within each generation, the effect of the alkyl chain length on the glass transition temperature varied from generation to generation. For the generation 1.0 alkyl terminated polymers, the glass transition temperature decreased from approximately -13.4°C for the generation 1.0-butyl terminated polymer to -25.3°C for the generation 1.0-decyl terminated polymer; however, it then increased to -16.2°C for the generation 1.0-dodecyl polymer. It should be noted that the glass transition temperature for the generation 1.0-dodecyl polymer took the form of a melting point; however, characterization of the transition as a glass transition was

more reasonable. (The crystalline nature of this diblock copolymer will be discussed in greater detail in the Section 5.4.2, which includes x-ray analysis of this polymer.) For the generation 1.0-octadecyl terminated polymer, no noticeable glass transition temperature was observed, most likely because of the predominance of the alkyl chain melting point for this polymer, which made other transitions difficult to visualize. This general decrease in the glass transition temperature with increasing alkyl chain length for the butyl through the decyl terminated polymers has been previously observed for poly(alkyl acrylates) as well as hyperbranched polymers that have been end capped with various alkyl groups. It is well known that for poly(alkyl acrylates), the glass transition temperature decreases with increasing chain length due to internal plastization of the long alkyl chains.¹¹⁶ For example, the glass transition temperature of poly(methyl acrylate) is approximately 18°C, while that of poly(decyl acrylate) is less than –70°C. In addition, Malström *et al.* have examined a series of hyperbranched polyesters that were end capped with five different alkyl chlorides, ranging in length from the three to sixteen carbons.⁴⁴ In general, they found that the glass transition temperature of the polymers decreased with increasing length of alkyl chain. They also found that the polymers that were terminated with twelve carbons and more tended to crystallize, adopting several different crystalline phases, as indicated by DSC. Similarly, Wu *et al.* have examined hyperbranched aromatic poly(ether imides) which have been functionalized with various lengths of alkyl chains, ranging from one to seventeen carbons and found that in general, as the length of the alkyl chain increased, the glass transition temperature of the polymers decreased.⁴¹ Nonetheless, the increase in the glass transition temperature observed for the generation 1.0-dodecyl terminated diblock copolymer can also be explained. In general, it has been found that polymers terminated with alkyl chains that possess twelve or more carbons have a higher degree of crystallinity than those possessing less than twelve carbons. Thus, the alkyl chains in the dodecyl terminated polymer were most likely crystalline and were more effective in inhibiting the motion of the underlying branches than those terminated with the shorter alkyl chains. Wei *et al.* found this to be the case when they examined semicrystalline dendritic polymers formed from a second generation poly(ether amine) dendrimers that had been functionalized with myristoyl, pamitoyl, and octadecyl groups.⁴² As the length of the alkyl chain increased, so did the glass transition temperature as the introduction of longer alkyl chains increased the tendency for crystallization and the crystalline moiety forced the amorphous core into a more rigid structure. For the generation 2.0-alkyl terminated linear-

dendritic rod diblock copolymers, the same trend of decreasing glass transition temperature with increasing alkyl chain length was observed. However, in this case, the generation 2.0-dodecyl polymer also exhibited a glass transition temperature that decreased in comparison to the generation 2.0-decyl terminated polymer. It is possible that the more highly branched polymer decreased the ability of the dodecyl chains to crystallize, and thus, decreased the effect of the alkyl chains on the glass transition temperature. It should also be noted that while the glass transition temperature did decrease with increasing alkyl chain length, the magnitude of the decrease was not as large for the decyl and dodecyl polymers as it had been for the butyl, hexyl, and octyl polymers, such that the glass transition temperature almost appeared to level off, perhaps indicating the influence of the poly(amido amine) interior on its value. Nonetheless, the generation 2.0-octadecyl polymer did not fit the trend. While it exhibited a glass transition temperature, the value of the glass transition temperature was higher than that of the other generation 2.0-alkyl terminated polymers, even that of the generation 2.0-butyl and hexyl terminated polymers. The reason for this can mostly likely be explained by more crystalline octadecyl chains inhibiting the motion of the underlying poly(amido amine) interior. Nonetheless, it is important to consider that the degree of substitution of the octadecyl chains on the generation 2.0-octadecyl terminated polymer was only approximately 27%; thus, substitution effects may also have contributed to the observed difference. The third generation polymer exhibited behavior resembling that of the second generation polymer, with the glass transition temperature decreasing and then leveling off with increasing alkyl chain through the generation 3.0-dodecyl terminated polymer, and then increasing for the generation 3.0-octadecyl terminated polymer. The fourth and the fifth generation alkyl terminated polymers exhibited similar trends in the glass transition temperature. For these two series of polymers, the glass transition temperature was found to decrease and then level off with increasing alkyl chain length for all of the lengths of alkyl chains examined, including the polymers that were terminated with octadecyl groups. There are two possible explanations for the glass transition temperature not increasing for the octadecyl terminated polymers. One explanation is that the octadecyl groups were not able to crystallize to as large of an extent due to the highly branched nature of the polymers, which prevented perfect alignment of the alkyl chains. Thus, the octadecyl groups were not able to have as great of an influence on the behavior of the interior poly(amido amine) branches. Iyer *et al.* have examined the behavior of stearate terminated poly(ethylene oxide)-poly(amido amine)

hybrid-linear dendritic diblock copolymers at the air/water interface and found that while they were able to achieve perfect ordering of the stearate groups for the third generation polymer, they were not for the fourth generation polymer as the highly branched nature of the dendritic interior prevented alignment of the chains.¹¹⁷ A second explanation is that the low degree of substitution of the octadecyl groups on the generation 4.0 and 5.0-octadecyl terminated polymers, less than 20%, prevented them crystallizing to as large of an extent, and thus they were not able to impart more rigidity to the interior poly(amido amine) branches. Wei *et al.* have examined the influence of the degree of substitution of alkyl chains on the glass transition temperature of dendritic polyetheramides that had been functionalized with myristoyl, palmitoyl, and octadecyl groups.⁴² They found that the glass transition temperature increased with increasing degree of substitution as there was a larger degree of crystallinity in the polymers that were more highly substituted, which forced the amorphous dendrimer interior into a more rigid structure.

In addition to the poly(ethylene oxide) melting point and the poly(amido amine) dendritic glass transition temperature, the alkyl terminated linear-dendritic rod diblock copolymers also exhibited an alkyl chain melting point. The variation of the alkyl chain melting point with alkyl chain length and generation for these linear-dendritic rod diblock copolymers is summarized in Figure 5.6. The melting point of the alkyl chains was found to be independent of generation and was approximately constant for the butyl through the dodecyl terminated polymers. Only the octadecyl terminated polymers exhibited an alkyl chain melting point that was much higher than that of the polymers terminated with the shorter alkyl chains; nonetheless, its value was also found to be independent of generation. The constant alkyl chain melting point observed for the polymers terminated with the butyl through dodecyl groups was somewhat surprising, as the alkyl chain melting point is usually found to be very dependent on the alkyl chain length - increasing with increasing length - and usually not being observed until the dodecyl group.¹¹⁸ As had been observed for the glass transition temperature, it is possible that the poly(amido amine) interior was affecting the crystallinity of the alkyl chains, increasing the tendency for crystallization due to the interior amide groups which were capable of hydrogen bonding. Wei *et al.* have also observed an alkyl chain melting point which was independent of alkyl chain length for semicrystalline poly(ether amine) dendrimers that had been terminated with myristoyl, palmitoyl, and octadecyl groups.⁴² Nonetheless, the value of the melting point for the octadecyl terminated linear-dendritic rod diblock copolymers, approximately 50°C, was in good agreement

with that observed for poly(octadecyl acrylates) which also have a melting point of approximately 50°C¹¹⁹ and poly(L-glutamates) substituted with octadecyl side chains which have a melting point of 55°C.⁹ There are two possible explanations for the octadecyl terminated polymers exhibiting a higher melting point than the polymers terminated with the shorter alkyl chains. The first is that there were greater dispersive forces between the longer octadecyl chains, which required a larger energy input to disrupt, as reflected by a higher melting point for the octadecyl terminated polymers. A second possible explanation is that there was a much lower degree of substitution of octadecyl chains on the linear-dendritic rod diblock copolymers than there had been for the polymers terminated with the shorter alkyl chains, and the degree of substitution affected the resulting melting point of the alkyl chains. While this second explanation is possible, it is much less likely as the generation 1.0-octadecyl terminated polymer possessed a degree of substitution of approximately 95%, and it too exhibited the higher melting point for the octadecyl chains. Another observation that should be noted from the DSC scans was that the alkyl chain melting point decreased in relative intensity with increasing generation. Unlike the poly(ethylene oxide) block, the relative amount of alkyl chains increased with increasing generation, thus, the decrease in the intensity could not be attributed to the amount of alkyl groups present. Most likely, this decrease in the intensity is caused by the increased difficulty that the alkyl chains have to crystallize as the dendritic interior becomes more congested and less able to take on the conformations necessary for crystallization. As previously mentioned, Iyer *et al.* also observed disorganization of the alkyl chains in their fourth generation stearate terminated linear-dendritic diblock copolymers due to the highly branched interior which prevented alignment of the alkyl groups.¹¹⁷

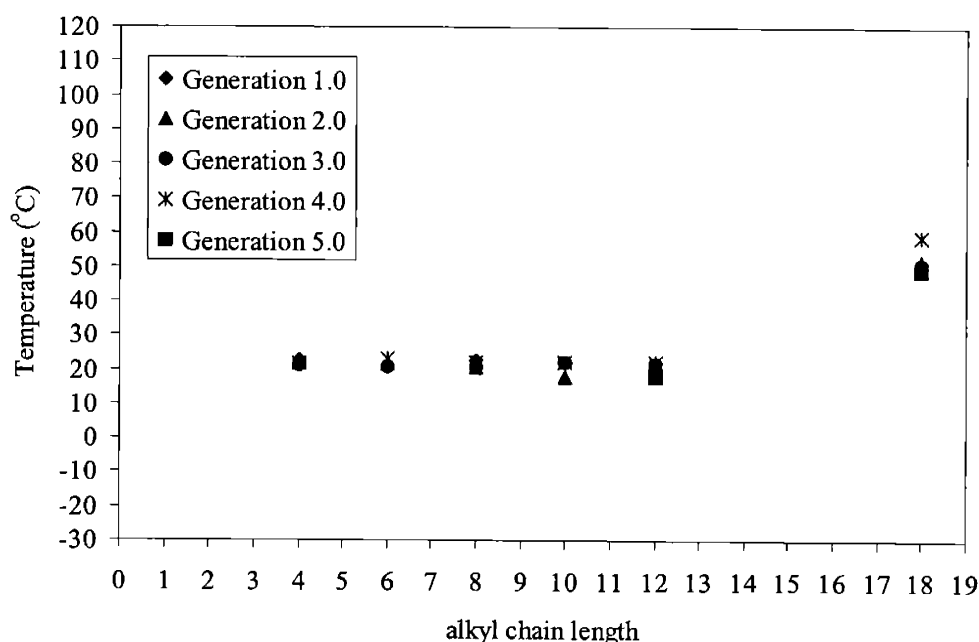


Figure 5.6. Variation of the alkyl chain melting point with alkyl chain length and generation for the alkyl terminated linear-dendritic rod diblock copolymers.

The thermal phase transitions of the polymers were also examined using polarized optical microscopy. The primary purpose of using polarized optical microscopy was to determine whether or not the polymers possessed any liquid crystalline nature since columnar mesophases have been found in other dendritic rod systems,^{1,17-19,21,69-72} as well as in other radially substituted linear polymers, such as the poly(*n*-alkyl glutamates),⁹ poly(dialkylsilanes),^{10,11} and cellulose trialkanoates.¹² Nonetheless, polarized optical microscopy was also able to confirm the melting transitions of the polymers that were semicrystalline. One of the polymers that was examined with polarized optical microscopy was the poly(ethylene oxide)-poly(ethylene imine) diblock copolymer backbone which was found from DSC to consist of two crystalline blocks. In general, this polymer exhibited a very grainy structure without well-defined crystallites, most likely due to the competing crystallization processes of the two blocks which prevented the formation of an ordered structure. Nonetheless, the generation 0.5 poly(ethylene oxide)-poly(ethylene imine)-poly(amido amine) linear dendritic rod diblock copolymer exhibited a Maltese cross crystalline pattern under 90° polarizers indicative of the formation of spherulites as illustrated in Figure 5.7. This crystalline pattern can be attributed to the poly(ethylene oxide) block as the dendritic block was amorphous and allowed the poly(ethylene oxide) to crystallize

without interference. Unfortunately, these crystalline patterns were not initially reformed upon cooling, indicating the influence of the solvent on the crystalline structure. In addition, these spherulite patterns were only observed for the generation 0.5 polymer and not for the higher generation polymers, perhaps because the fraction of the poly(ethylene oxide) in the higher generation polymers was too low to allow for optimal crystallization and the dendritic block was amorphous. Maltese cross crystalline patterns have been observed for the poly(ethylene oxide) block in other hybrid-linear dendritic diblock copolymer systems. For example, Gitsov *et al.* found that spherulite crystalline patterns formed for their poly(ethylene oxide)-poly(benzyl ether) hybrid-linear dendritic diblock copolymers that possessed a low generation dendritic block, and that the ability of these spherulites to form decreased with increasing generation. Similarly, Iyer *et al.* observed these spherulite patterns in their low generation stearate terminated poly(ethylene oxide)-poly(amido amine) hybrid-linear dendritic diblock copolymers.

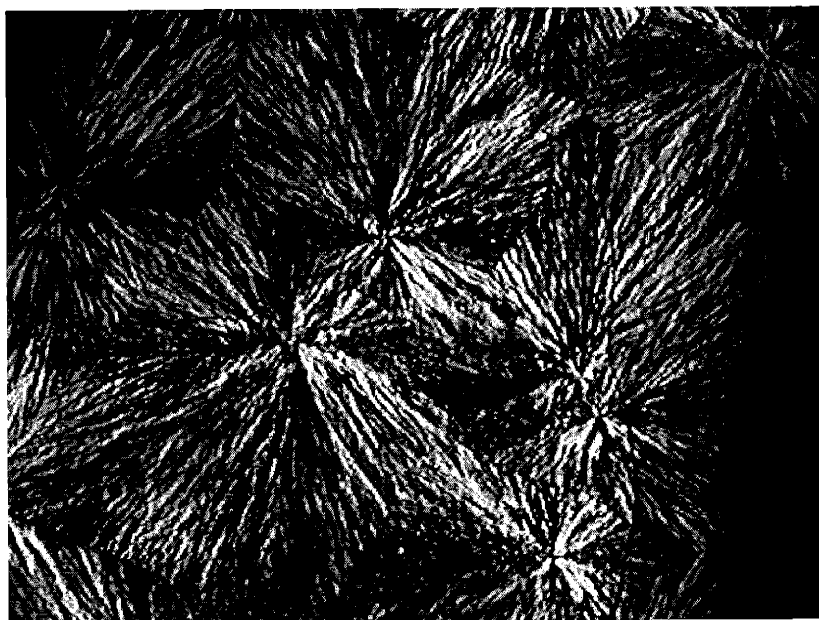


Figure 5.7. Crystallization of the poly(ethylene oxide) block in the poly(ethylene oxide)-poly(ethylene imine) generation 0.5 linear-dendritic rod diblock copolymer as indicated by the formation of the Maltese cross pattern. The image was taken with 90° polarizers at 50x magnification.

The alkyl terminated linear-dendritic rod diblock copolymers were also examined using polarized optical microscopy, focusing on those polymers that exhibited phase transitions in the DSC that might be attributed to the formation of mesophases as well as those polymers that might have adopted a rod-like configuration. One of the alkyl terminated polymers that was examined was the generation 1.0-dodecyl terminated polymer. Unfortunately, no optical textures were observed for this polymer, not even a crystalline pattern that might be attributed to the poly(ethylene oxide) block. Similarly, no optical textures were observed for the other generation 1.0-alkyl polymers that were terminated with shorter alkyl chains. Since the alkyl chain melting point of these polymers was approximately 20°C, and since the OM experiments were carried out between room temperature (approximately 25°C) and 100°C, it is possible that the alkyl chains were already in a melt state before the experiment was conducted, thus not exhibiting a crystalline texture. Also, the addition of the alkyl groups may have decreased the fraction of the poly(ethylene oxide) in the diblock copolymer to a point such that the formation of crystalline patterns was inhibited as discussed in the previous paragraph. Similar results were found for the higher generation polymers terminated with the butyl through the dodecyl groups. Conversely, the generation 1.0-octadecyl polymer exhibited a grainy crystalline texture in OM that was attributed to the octadecyl groups, as it disappeared between 50°C and 60°C, the melting point of the alkyl chains. This grainy crystalline texture was also observed for the higher generation octadecyl terminated polymers and is illustrated in Figure 5.8 for the generation 1.0-octadecyl polymer.

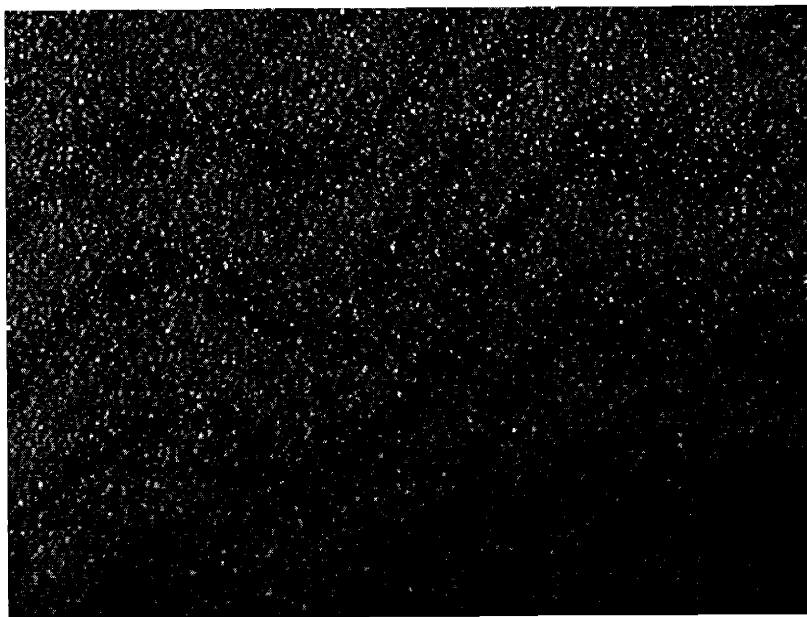


Figure 5.8. Crystallization of the octadecyl chains in the poly(ethylene oxide)-poly(ethylene imine) generation 1.0-octadecyl linear-dendritic rod diblock copolymer. The image was taken with 90° polarizers at 50x magnification.

Unfortunately, it did not appear as if any of the linear-dendritic rod diblock copolymers under investigation exhibited any liquid crystalline phases. While hexagonal liquid crystalline phases have been observed by Percec *et al.* for their “dendron jacketed polymers” composed of a polystyrene or poly(methyl methacrylate) backbone and poly(benzyl ether) dendrons which had been terminated with dodecyl groups,^{1,17-19,21,69-72} they have not been observed for other dendritic rod systems such as those based on carbosilane chemistry,⁸⁰ those composed of poly(benzyl ether) dendrons attached to a polyurethane backbone,^{77,78} and even those composed of poly(benzyl ether) attached to a polystyrene backbone which were not terminated with alkyl groups.^{75,76} Most likely, Percec’s use of 3,4,5-tris[(p-dodecyloxy)benzyl]oxy]benzoyl (DOBOB), a known columnarogen, as the terminal group induced the formation of the columnar liquid crystalline phase.⁷⁴

5.4.2 X-ray Scattering and Transmission Electron Microscopy (TEM)

The morphology of diblock copolymer systems is often characterized using a combination of small and wide angle x-ray scattering, (SAXS) and (WAXS), as well as transmission electron microscopy (TEM). From x-ray scattering one can determine the distance between periodic structures. In SAXS the structures are on the order of nanometers and they often represent the distance between polymer domains, while for WAXS the structures are on the order of angstroms and they are usually indicative of the size of the crystals in a semicrystalline polymer.¹²⁰ Unfortunately, it is often difficult to determine the exact morphology from x-ray data alone; thus, TEM is also used to be able to visualize the morphology of the systems, and assign the domains within that morphology.¹²¹ Since the linear-dendritic rod diblock copolymers under investigation in this thesis were also diblock copolymers, we wanted to determine whether or not the two blocks would phase segregate, and if so, what kind of morphology would form and how the morphology would be effected by the architecture of the polymer. In addition, we wanted to use TEM to image individual diblock copolymers, and thus be able to gain insight into the shape of the polymers at a particular generation.

The poly(ethylene oxide)-poly(ethylene imine) diblock copolymer backbone was the first polymer whose morphology was examined. The temperature dependent 1D SAXS profile for this polymer along with a TEM image of its morphology at room temperature are presented in Figures 5.9 and 5.10, respectively. From the SAXS profiles, one can see that no strong scattering peaks were recorded; however, a very weak scattering peak began to form above 50°C, with a d-spacing of approximately 15.5nm, which appeared to shift to a d-spacing of 12.4nm with increasing temperature. Unfortunately, due to its very weak signal, it was difficult to know if the peak was real; however, its formation above 50°C was consistent with melting of the poly(ethylene oxide) chains which would allow for rearrangement of the poly(ethylene imine) block into a more favorable crystal structure. In addition, the shift of the d-spacing was consistent with melting of the unhydrated poly(ethylene imine) crystals, whose melting point was approximately 67°C, leaving the hydrated poly(ethylene imine) crystals, which each have their own crystalline dimensions.¹²² While there are regions of segregated polymer domains, overall, there is a lack of long range order in the morphology, as confirmed by TEM, which is most likely due to the crystalline nature of each of the blocks. These results are consistent with those observed by Johnson *et al.* for poly(ethylene oxide)-poly(amido amine) hybrid-linear

dendritic diblock copolymers.⁹⁰ For their third generation polymer, they found that below 50°C, the poly(ethylene oxide) block was crystalline with no apparent phase segregation as the formation of the poly(ethylene oxide) crystals destroyed the morphology. However, above 50°C, a segregated melt state formed as the amorphous poly(ethylene oxide) could no longer dominate the morphology. Similarly, Quiram *et al.* reported that crystallization of the ethylene block in polyethylene-poly(3-methyl-1-butene) diblock copolymers completely disrupted the morphology when the blocks were weakly segregated.¹²³ Given that both the poly(ethylene oxide) and the poly(ethylene imine) blocks in the poly(ethylene oxide)-poly(ethylene imine) diblock copolymer were crystalline, long range order was most likely inhibited by the two competing crystalline states.

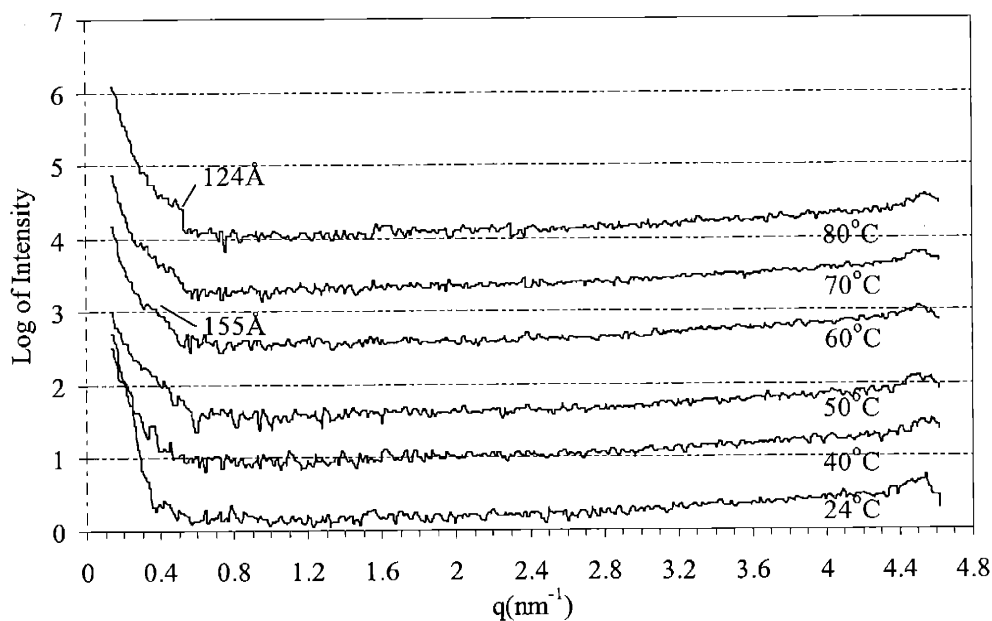


Figure 5.9. Temperature dependent 1D SAXS profiles for the poly(ethylene oxide)-poly(ethylene imine) diblock copolymer backbone.

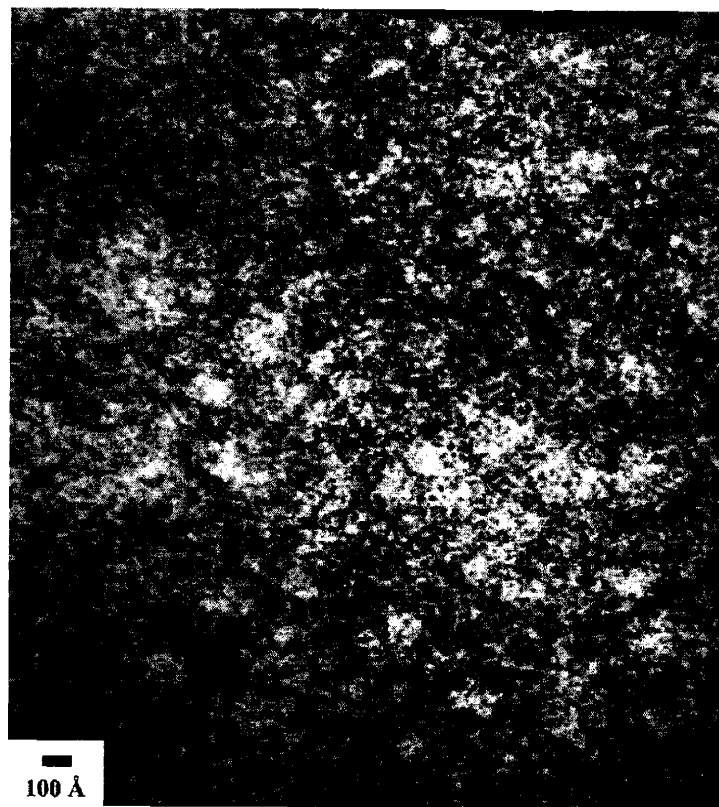


Figure 5.10. TEM image of the bulk morphology of the poly(ethylene oxide)-poly(ethylene imine) diblock copolymer backbone at room temperature. The poly(ethylene imine) block is stained black.

Similarly, no long range order was observed for the poly(ethylene oxide)-poly(ethylene imine) generation 0.5 linear-dendritic rod diblock copolymers. The 1D temperature dependent SAXS profile along with a TEM image of its room temperature morphology are presented in Figures 5.11 and 5.12, respectively. From the TEM image, it appeared as if the dendritic portion was forming spheres within a poly(ethylene oxide) matrix; however, no scattering peaks were observed in SAXS, indicating the absence of long range order. The absence of long range order was most likely due to crystallization of the poly(ethylene oxide) block which disrupted the morphology of the dendritic block as discussed in the previous paragraph. In addition, it is possible that the two blocks were miscible and there was not a driving force for segregation. Suvorova *et al.* have examined the morphology of poly(ethylene oxide)/poly(methyl acrylate) blends, and found that phase separation only occurred above the melting point of the poly(ethylene oxide) block when the weight fraction of poly(methyl acrylate) was between 0.5 and 0.8.¹²⁴ The weight fraction of the dendritic block in the linear-dendritic rod diblock

copolymer was 0.87. (Poly(methyl acrylate) has a similar chemical structure to that of the dendritic block.) Finally, it was somewhat surprising that the dendritic block appeared to form spheres within a poly(ethylene oxide) matrix, as the dendritic block is the major component and would have been expected to form the matrix based on traditional diblock copolymer theory. Nonetheless, casting solvent has been shown to have a large effect on diblock copolymer morphology⁸⁴ and it is possible that the methanol from which the diblock copolymer was cast, proved to be a better solvent for the poly(ethylene oxide) block than for the dendritic block, resulting in the formation of the poly(ethylene oxide) matrix.

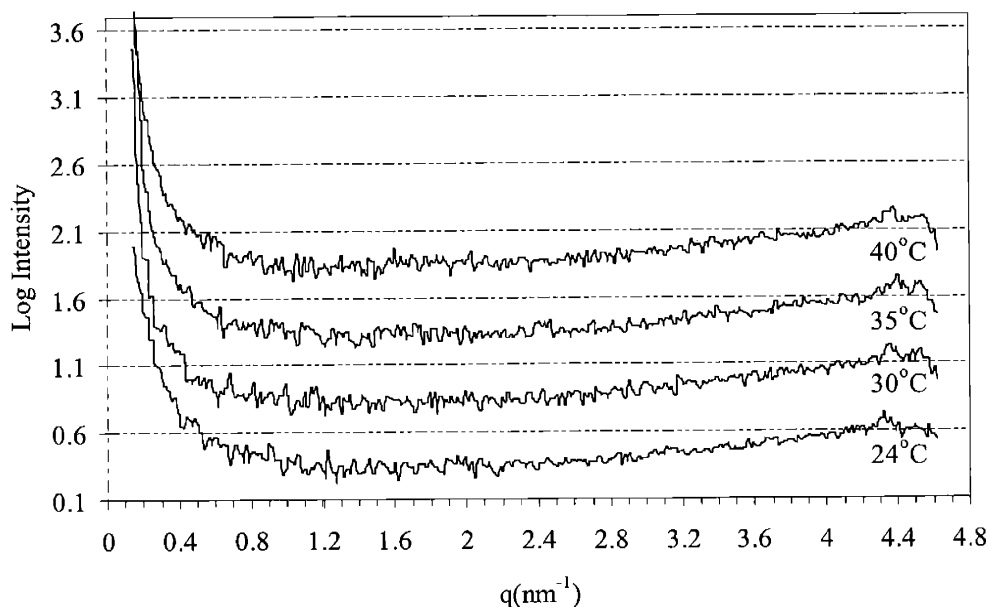


Figure 5.11. Temperature dependent 1D SAXS profiles for the poly(ethylene oxide)-poly(ethylene imine) generation 0.5 linear-dendritic rod diblock copolymer.

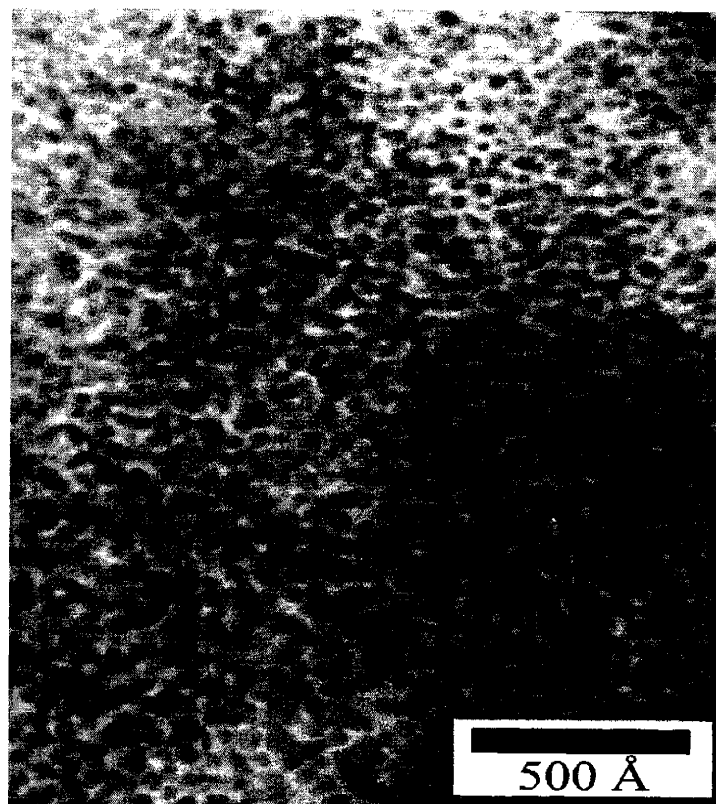


Figure 5.12. TEM image of the bulk morphology of the poly(ethylene oxide)-poly(ethylene imine) generation 0.5 linear-dendritic rod diblock copolymer at room temperature. The dendritic portion is stained black.

The morphology of the generation 4.5 poly(ethylene oxide)-poly(ethylene imine)-poly(amido amine) linear-dendritic rod diblock copolymer was also examined, and the 1D temperature dependent SAXS profile along with the TEM image of its room temperature morphology are presented in Figures 5.13 and 5.14, respectively. Unfortunately, there is also no long range order in this diblock copolymer system; although, probably not due to crystallization of the poly(ethylene oxide) block as described in the previous paragraphs. In this diblock copolymer, the fraction of the poly(ethylene oxide) block is extremely small, less than 1%, and its melting point is not obvious in the DSC traces, thus it is difficult to believe that its crystallization would disrupt the morphology. One more likely explanation is that the two blocks were chemically compatible such that there was no driving for segregation, as described above for poly(ethylene oxide)/poly(methyl acrylate) blends. A second is that the fraction of the poly(ethylene oxide) was too small to drive segregation, even if the polymer was amorphous.

Nonetheless, the morphology depicted in the TEM image is reminiscent of that observed for other comb polymer systems.¹²⁵ The length scale of the morphology is on the order of 2-3nm.

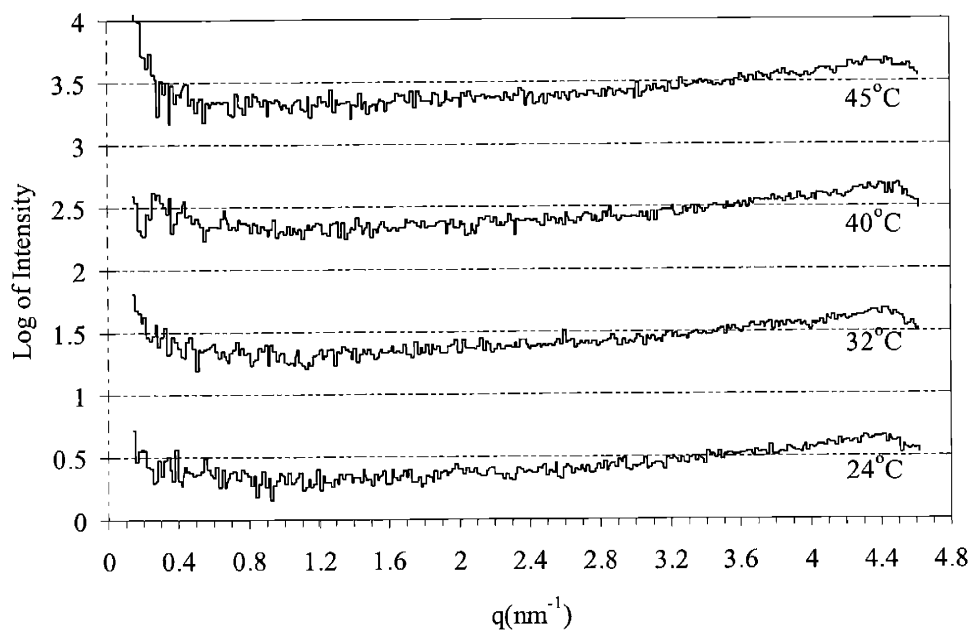


Figure 5.13. Temperature dependent 1D SAXS profiles for the poly(ethylene oxide)-poly(ethylene imine) generation 4.5 linear-dendritic rod diblock copolymer.

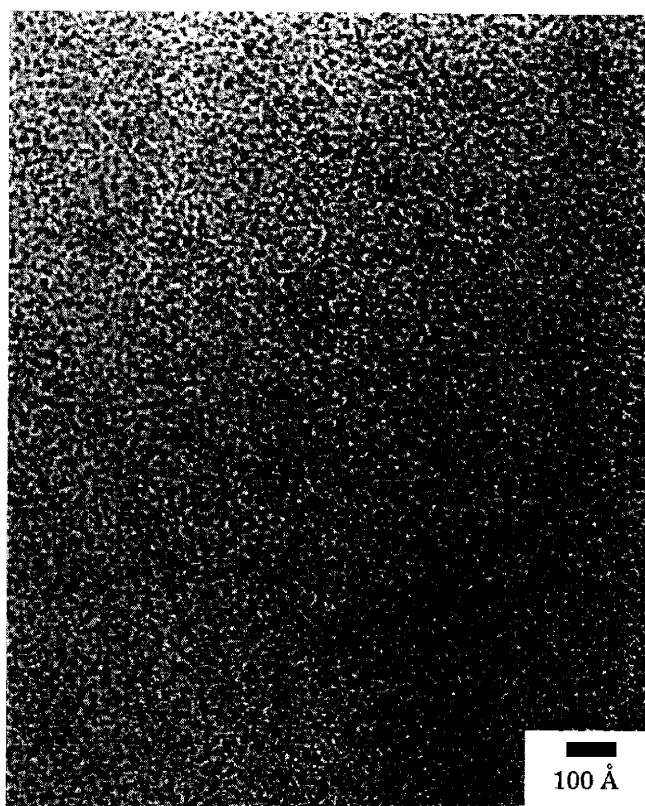


Figure 5.14. TEM image of the bulk morphology of the poly(ethylene oxide)-poly(ethylene imine) generation 4.5 linear-dendritic rod diblock copolymer at room temperature. The dendritic portion is stained black.

In the hopes that the presence of alkyl groups on the surface of the dendritic block might drive phase segregation, the morphology of the dodecyl terminated linear dendritic rod diblock copolymers were examined. For the generation 1.0, 2.0, and 3.0-dodecyl polymers, no long-range order was detected by SAXS and TEM. As an example, the temperature dependent 1D SAXS profile of the generation 1.0-dodecyl terminated diblock copolymer along with a TEM image of its morphology at room temperature are presented in Figures 5.15 and 5.16, respectively. The TEM image of this diblock copolymer is very similar to that observed for the generation 4.5 polymer, as well as other comb polymer systems. Given that the fraction of poly(ethylene oxide) in the diblock copolymer was 0.07, the morphology was most likely driven by the comb-like nature of the dendritic block, and not the crystallinity of the poly(ethylene oxide), as reflected in the TEM image. The length scale of the morphology was on the order of 2-3nm as well.

As mentioned in Section 5.4.1, the generation 1.0-dodecyl terminated linear-dendritic rod diblock copolymer exhibited three transitions in the DSC scan. Of particular interest was the transition at -16.2° , as a traditional glass transition temperature had been observed in the same temperature range for the other generation 1.0-alkyl terminated polymers, but this transition took the form of a melting point. In order to try to gain insight into the nature of this transition, wide-angle x-ray diffraction (WAXD) measurements were taken on the polymer to probe the types of crystalline structures present that might have led to the transition. The measurements were taken under three different conditions: at room temperature, after cooling with liquid nitrogen, and after rewarming to room temperature. Cooling the polymer with liquid nitrogen did not appear to have any effect on the resulting WAXD profile, as both room temperature profiles and the cooled profile were virtually identical. The room temperature WAXD profile is presented in Figure 5.17. There are two possible reasons for the similar profiles. One is that the peak at -16.2°C was a glass transition temperature and thus, no new crystalline peaks would have been expected to form. Glass transition temperatures taking the form of melting points have been observed for other polymer systems, such as urethanes. The second is that the polymer was not cooled, but rather quenched, such that the resulting morphology represented the quenched room temperature morphology. A better test would have been to slowly cool the polymer in a controlled manner. Unfortunately, the equipment necessary for such an experiment was not readily available. Nonetheless, as can be seen in Figure 5.17, the room temperature WAXD profile did exhibit several peaks, a sharp peak at 1.8nm^{-1} corresponding to a d-spacing of approximately 29.5\AA , and a broad peak with maxima at 13.8nm^{-1} (4.5\AA), 14.6nm^{-1} (4.3\AA), and 16.5nm^{-1} (3.7\AA). The broad peaks between 4.5\AA and 3.7\AA were the size expected for the poly(ethylene oxide) and the dodecyl chain crystals, in good agreement with that observed by Johnson *et al.* for the stearate terminated hybrid-linear dendritic diblock copolymers.⁹⁰ The peak at 29.5\AA most likely represented the polymer forming a smectic layer, as its value is approximately twice the branch length. The formation of this peak was somewhat surprising as it was not readily observed in SAXS, possibly due to differences in sample preparation. While the sample for SAXS had been solvent cast and annealed approximately two weeks before use, the sample for WAXS was taken directly from the purified polymer and had not been treated for over two years, perhaps allowing time for the formation of a more ordered structure.

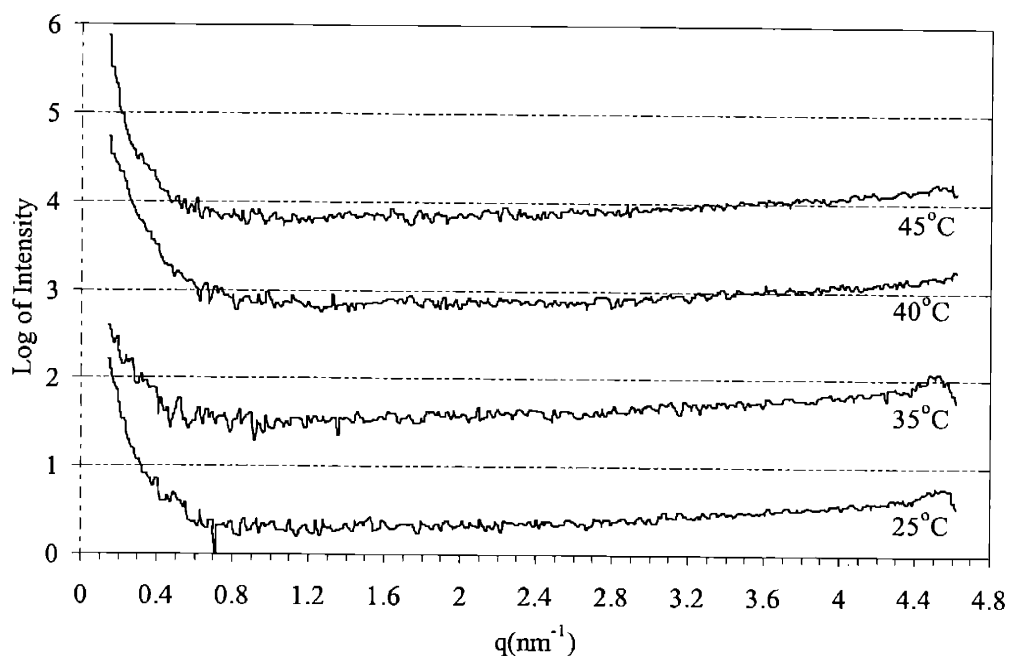


Figure 5.15. Temperature dependent 1D SAXS profiles for the poly(ethylene oxide)-poly(ethylene imine) generation 1.0-dodecyl terminated linear-dendritic rod diblock copolymer.

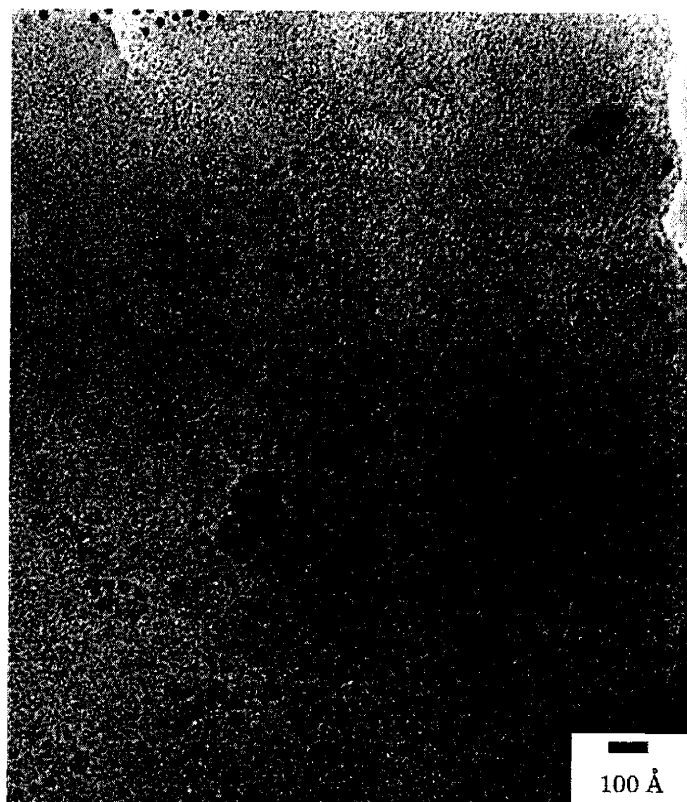


Figure 5.16. TEM image of the bulk morphology of the poly(ethylene oxide)-poly(ethylene imine) generation 1.0-dodecyl terminated linear-dendritic rod diblock copolymer at room temperature. The poly(amido amine) portion is stained black.

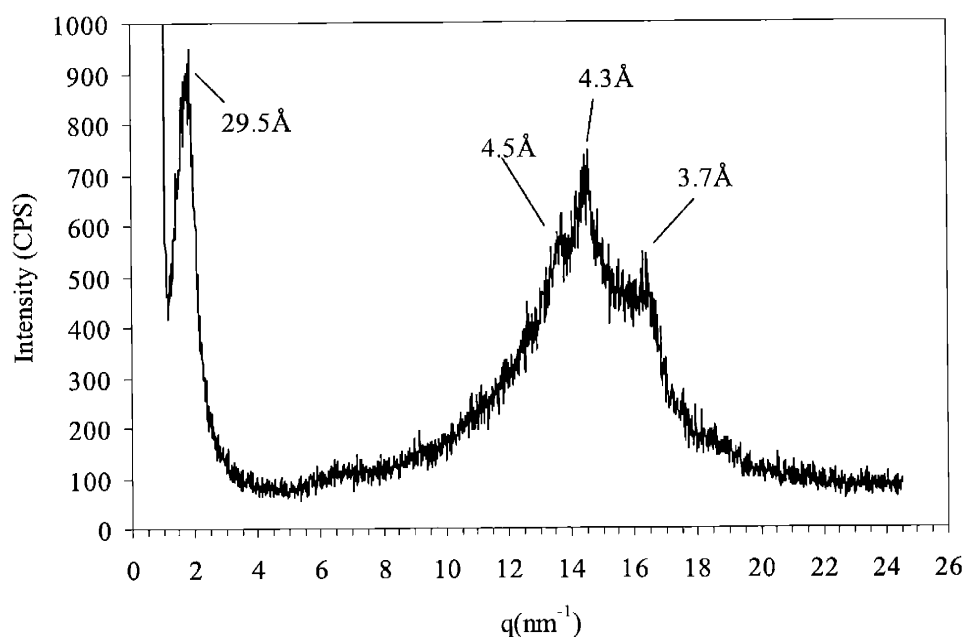


Figure 5.17. Room temperature WAXD of the poly(ethylene oxide)-poly(ethylene imine) generation 1.0-dodecyl terminated linear-dendritic rod diblock copolymer.

The only polymer that exhibited a predominate morphology was the poly(ethylene oxide)-poly(ethylene imine) generation 4.0-dodecyl linear-dendritic rod diblock copolymer. The 1D temperature dependent SAXS profile along with a TEM image of its room temperature morphology are presented in Figures 5.18 and 5.19, respectively. From the SAXS profiles, a strong scattering peak was observed at room temperature which corresponded to a d-spacing of approximately 4.1nm. This scattering peak decreased in intensity and eventually disappeared with increasing temperature, possibly due to melting of the alkyl chains, which were driving the phase segregation. Loss of the scattering peak occurred between 24°C and 30°C, which corresponded to the melting point of the alkyl chains as determined from DSC. As the scattering peak decreased in intensity with increasing temperature, it also shifted to slightly smaller d-spacings - the shift was from 4.1nm to 3.9nm. These results were consistent with the TEM images of the polymer, which revealed a worm-like morphology. In these images, the poly(amido amine) portion was stained dark, while the alkyl chains and the poly(ethylene oxide) block should have remained light. The value of the d-spacing determined for the fingerprint pattern within the larger, darker, globular domains was consistent with what might be expected

for the diameter of an individual dendritic rod and the size of the darker globular domains was approximately the length expected for a dendritic rod. Thus, it appeared as if the individual polymers were taking on a worm- or rod-like configuration. Based on bond lengths and angles, the length of an all-trans dodecyl chain is expected to be approximately 1.0-1.1 nm. Starting with a d-spacing of 4.1 nm and subtracting off 2.0 nm for two alkyl chains, as depicted in Figure 5.19, leaves 2.1 nm for the poly(amido amine) interior. This value is in good agreement with the diameter measured by Tomalia *et al.* for the generation 4.5 poly(amido amine) dendritic rod homopolymers that were terminated with sodium carboxylate groups. Using TEM, they measured a dendritic rod diameter of 2.5-3.2 nm for a polymer that was a full generation larger than the poly(amido amine) interior in these dodecyl terminated diblock copolymers.⁷⁹ The shift in the d-spacing for the linear-dendritic rod diblock copolymers was most likely due to melting of the crystalline alkyl chains into a less extended conformation. In addition, from the TEM images of the linear-dendritic rod diblock copolymers, the dark and the light regions within the larger, darker, globular domains appeared to have approximately the same dimensions, in good agreement with the model proposed for the dimension of these diblock copolymers. Nonetheless, if the poly(amido amine) interior had adopted an all trans conformation, the diameter of the interior would have been approximately 5.8 nm. Given that the measured diameter was much less than one assuming an all trans configuration, it appeared as if the poly(amido amine) interior was adopting a much more compact state, possibly due to incompatibility with the exterior alkyl chains. Overall, it appeared as if the individual worm-like polymers were assembling into domains with the alkyl chains on adjacent polymers meeting tip-to-tip as indicated in Figure 5.20. In addition, these diblock copolymer domains were large enough to accommodate the length of a dendritic rod leaving the poly(ethylene oxide) to fill in between the domains, as indicated by the very light regions in the TEM image.

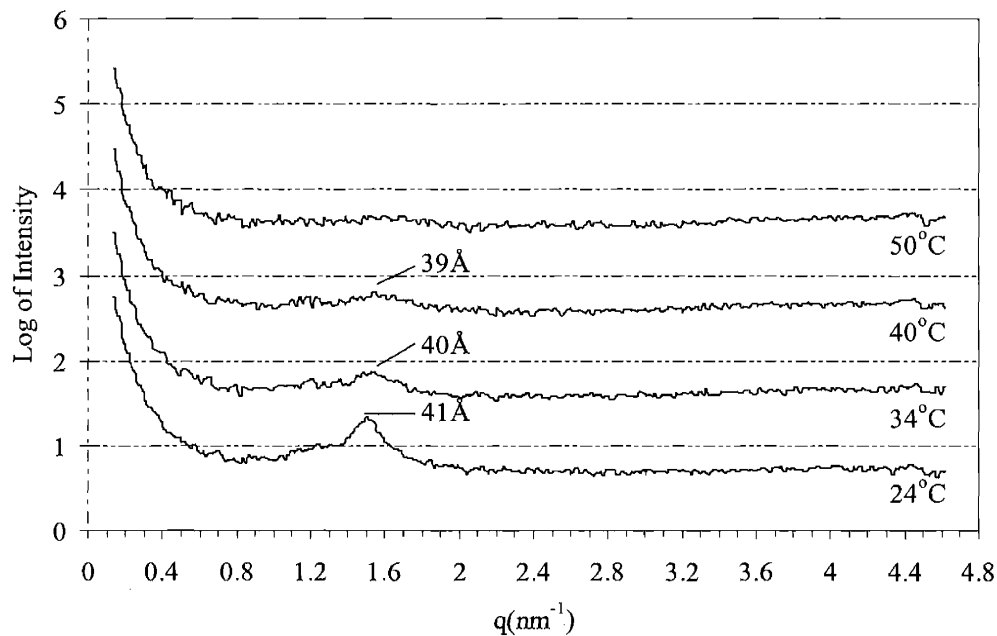


Figure 5.18. Temperature dependent 1D SAXS profiles for the poly(ethylene oxide)-poly(ethylene imine) generation 4.0-dodecyl terminated linear-dendritic rod diblock copolymer.

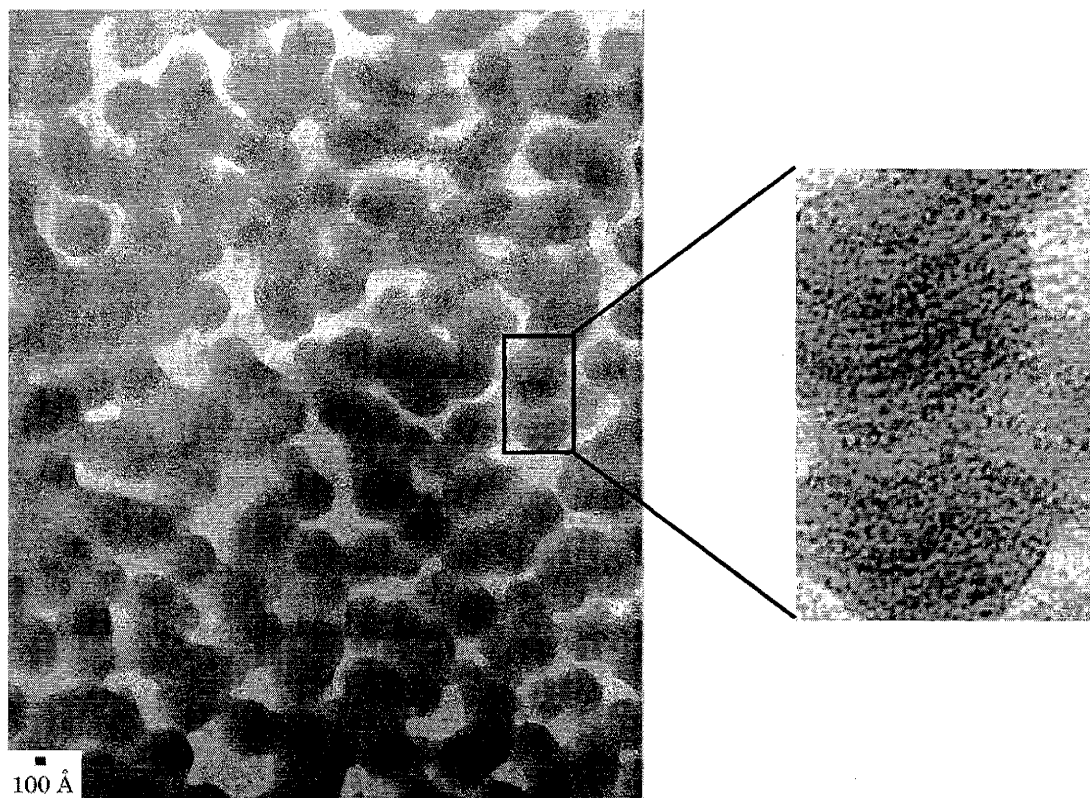


Figure 5.19. TEM image of the bulk morphology of the poly(ethylene oxide)-poly(ethylene imine) generation 4.0-dodecyl terminated linear-dendritic rod diblock copolymer at room temperature. The poly(amido amine) portion is stained black.

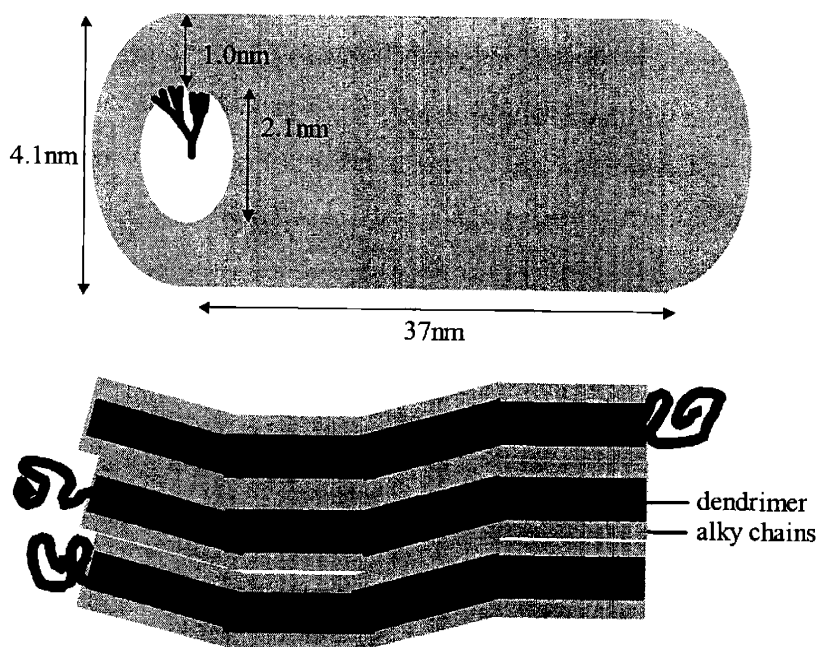


Figure 5.20. Possible dimensions and arrangement of the poly(ethylene oxide)-poly(ethylene imine) generation 4.0-dodecyl terminated linear-dendritic rod diblock copolymers in the bulk.

5.4.3 Atomic Force Microscopy (AFM)

Tapping mode AFM was used to image the individual linear-dendritic rod diblock copolymers. In AFM, a cantilever with a nanosize tip is rastered across a surface of interest and the deflections in the cantilever are used to measure the topography of that surface. Thus, if there is an object on a surface, the object can be imaged using AFM. AFM images of the generation 4.5 linear-dendritic rod diblock copolymer were taken in order to determine if the polymer was adopting a rod-like configuration.

A typical AFM image for the generation 4.5 linear-dendritic rod diblock copolymer, which had been spun cast from dilute solution onto mica is presented in Figure 5.21. Approximately eight individual polymers can be seen in the image, and these polymers appear as asymmetrical, elongated structures. Cross-sectional slices of the polymer images were taken in order to determine the dimensions of the polymer. As an example, a lateral cross-section of the polymer is shown in Figure 5.22. This cross-section reveals two different heights in the polymer, the taller height was found to be approximately 2.2nm, while the smaller height was

approximately 1.6nm. In addition, the total length of the polymer was found to be approximately 49nm. Similarly, the diameter of the polymer was measured to be approximately 22nm by taking a cross-section of the width of the polymer.

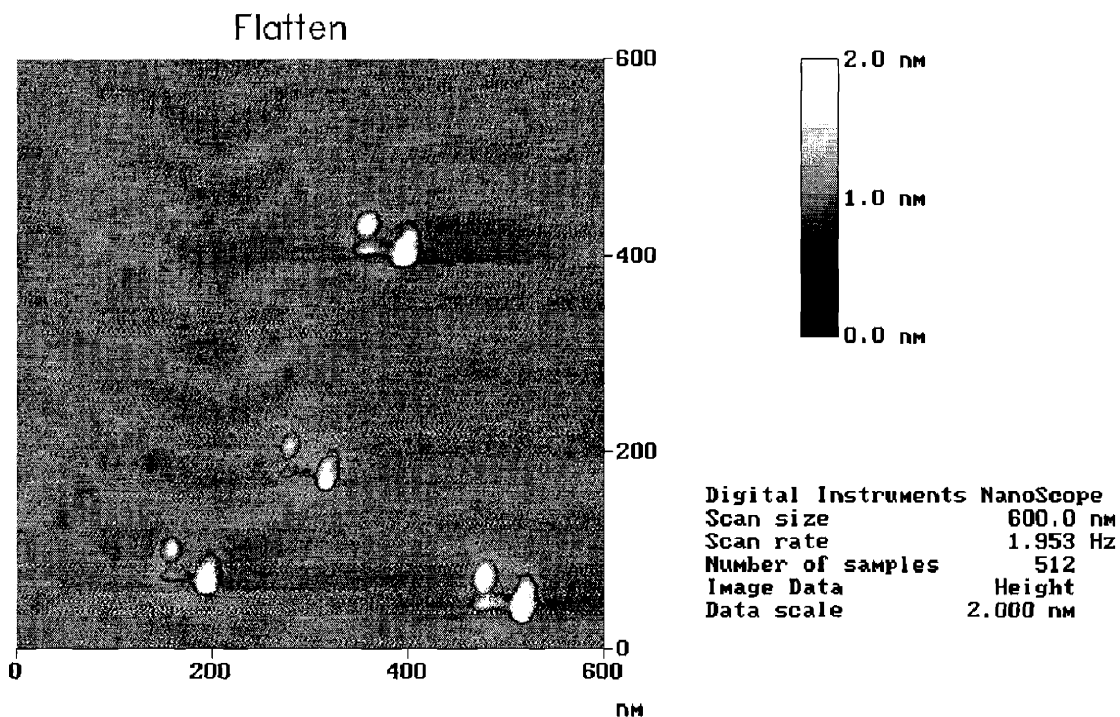


Figure 5.21. AFM image of an individual poly(ethylene oxide)-poly(ethylene imine) generation 4.5 linear-dendritic rod diblock copolymer.

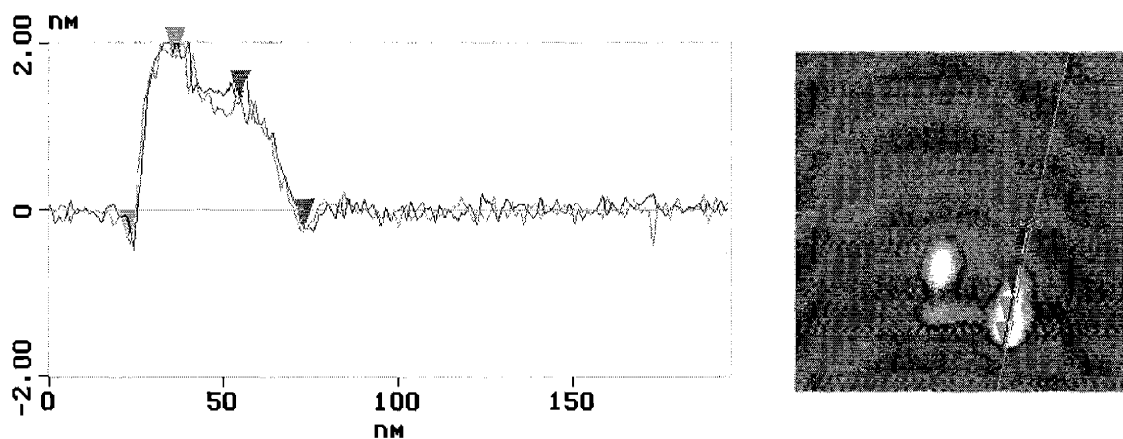


Figure 5.22. Lateral cross-section of an individual poly(ethylene oxide)-poly(ethylene imine) generation 4.5 linear-dendritic rod diblock copolymer.

One important consideration when looking at the dimensions of the diblock copolymer is that the measured dimensions for the length and the diameter will be exaggerated due to tip convolution; however, this tip convolution will not affect the measurement of the height. Tip convolution effects have been observed when imaging several other dendritic^{58,61,63,64,66} as well as comb polymer systems.¹²⁶ For example, Cheng *et al.* have used AFM to image an amphiphilic, cylindrical core-shell brush composed of an acrylate backbone and polystyrene/*t*-butyl acrylate diblock copolymer brushes. In order to take into account tip convolution effects, they subtracted 10nm from the measured length and diameter in order to compensate for the 10nm radius tip which was used in the experiments. It should be mentioned that when imaging the linear-dendritic rod diblock copolymers under investigation in their thesis, both regular AFM tips, which possessed a radius a tip radius of better than 10nm, as well as super sharp tips, which possessed a tip radius of better than 5nm, were used to measure the dimensions of the polymers; however, use of the super sharp tips did not affect the measured dimensions.

The measured dimensions reveal two important properties of the individual linear-dendritic rod diblock copolymers. The first is that the dendritic block of the diblock copolymer was flattening and spreading on the surface of the mica, as indicated by the two very different dimensions for the diameter and the height on the polymers. Even taking into account tip effects, the measured diameter was much larger than the measured height. This behavior has been observed for spherical poly(amido amine) dendrimers, which are known to flatten and spread on hydrophilic surfaces such as mica due to the favorable interactions between the dendrimer and the surface.⁵⁷⁻⁶¹ For example, Li *et al.* have imaged isolated generation nine poly(amido amine) dendrimers on mica surfaces and found that the diameter of the dendrimer was 25.3nm, while its height was found to be only 3.63nm.⁶⁰ From light scattering, the diameter of the dendrimer in solution was found to be 11.4nm. Similarly, they have imaged isolated generation seven dendrimers and found that the diameter of the dendrimer was 1.5nm while its height was 21nm.⁵⁹ The ability of these dendrimers to spread and flatten on the surface of the mica indicated that they were soft, spongy, and elastic, and that their shape could be controlled by application of very small flow forces. Nonetheless, Li *et al.* also found that the rigidity of the polymers increased with generation, such that the higher generation polymers were not as susceptible to deformation.⁵⁹ It should be noted that the dimensions of the linear-dendritic rod diblock

copolymers that were measured with AFM, a diameter of 22nm and a height of 1.6-2.2 are very reasonable when compared with the dimensions of spherical poly(amido amine) dendrimers.

The second property that was revealed was that the polymer was in fact a diblock copolymer, as indicated by its asymmetric shape and the two different heights measured. Most likely, the shorter portion of the polymer was the poly(ethylene oxide) block, which had segregated from the dendritic block due to steric crowding in the dendritic block; and the larger portion was the dendritic block itself. These dimensions of the polymer are reasonable if one allows for spreading and flattening of the dendritic block on the surface as well as tip convolution effects. Calculation of the dimensions of the polymer taking into account these effects is illustrated in Figure 5.23. This figure also presents a graphical representation of the approximate relative dimensions of the polymer. The radius of the poly(amido amine) branches assuming a fully extended, all-trans conformation is approximately 5nm, resulting in a diameter of 10nm. Adding 10nm to the diameter due to tip effects brings the total diameter of the polymer to approximately 20nm, in good agreement with the 23nm calculated. Similarly, the length of a fully extended poly(ethylene imine) backbone composed of 97 repeats is approximately 36nm. Adding 5nm for a fully extended poly(amido amine) branch which extends from one end, 3nm for the radius of gyration of the poly(ethylene oxide) block which extends from the other end, and 10nm due to tip effects, the entire length of the polymer can be estimated to be approximately 54nm, which is in good agreement with the 49nm measured. Thus, the axial ratio of the polymer can be calculated to be approximately 0.37, which would not be expected to appear as a long rod, but rather as an ellipsoid as depicted in Figure 5.23. Thus, the AFM image of the linear-dendritic rod diblock copolymer as an elongated, asymmetrical ellipsoid was reasonable, even if the polymer was adopting a rod-like configuration.

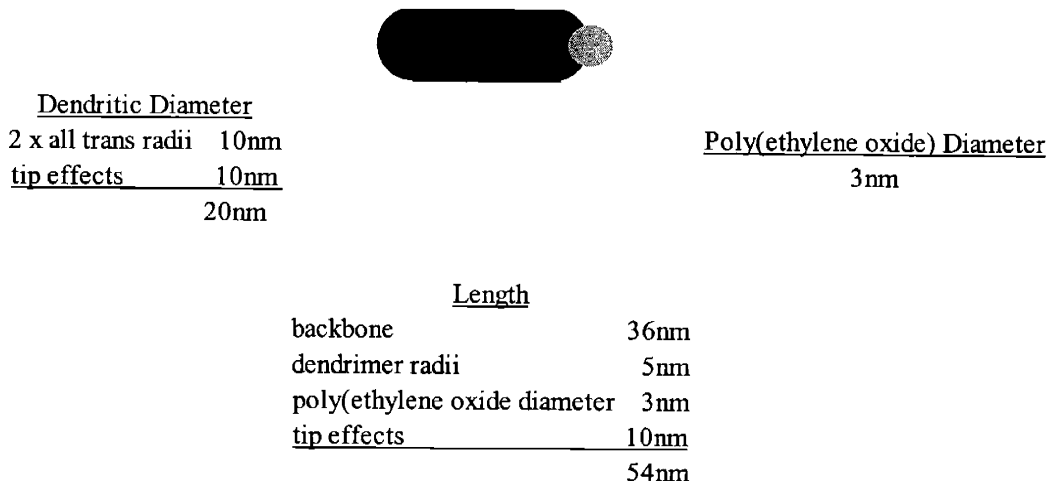


Figure 5.23. Graphical representation relating the dimensions of the poly(ethylene oxide)-poly(ethylene imine) generation 4.5 linear-dendritic rod diblock copolymer to an approximate shape.

5.5 Summary and Conclusions

A preliminary investigation into the thermal and morphological behavior of a series of poly(ethylene oxide)-poly(ethylene imine)-poly(amido amine) linear-dendritic rod diblock copolymers was conducted using differential scanning calorimetry (DSC), polarized optical microscopy (OM), x-ray scattering (SAXS and WAXS), transmission electron microscopy (TEM), and atomic force microscopy (AFM). The thermal phase transitions of the polymers were determined using DSC, and polarized optical microscopy coupled with DSC were used to determine whether or not the polymers possessed a liquid crystalline nature. Temperature dependent X-ray scattering was used to accurately determine the domain spacing in the diblock copolymer morphology and TEM provided an overall picture of the morphology. Finally, AFM was used to image individual linear-dendritic rod diblock copolymers on mica surfaces.

DSC was employed to examine the effect of dendritic block end group and generation number on the melting point of the poly(ethylene oxide) block, the glass transition temperature of the dendritic block, and the melting point of the alkyl chains. For all of the linear-dendritic rod diblock copolymers, the melting point of the poly(ethylene oxide) was found to remain approximately constant, independent of end group and generation, indicating that the crystals that formed were composed of similar structures from generation to generation. These

crystalline structures most likely consisted of poly(ethylene oxide) which had been plasticized by the dendritic block, as indicated by a lowering of the melting point of the poly(ethylene oxide) block to approximately 40°C from that of approximately 54°C for the poly(ethylene oxide) homopolymer. Nonetheless, the relative intensity of the melting point decreased with increasing generation, such that it virtually disappeared above generation 2.0. Unfortunately, since the weight fraction of poly(ethylene oxide) in the diblock copolymer decreased dramatically with increasing generation, it was difficult to determine whether the virtual disappearance of the melting point at higher generations was caused by a loss in the crystalline nature of the poly(ethylene oxide) or if it simply could not be observed due to its extremely minor contribution to the behavior of the polymer, such that it became lost in the baseline. A glass transition temperature was observed for some of the linear-dendritic rod diblock copolymers that was attributed to the dendritic block, due to its dependence on the end group chemistry as well as the generation number of the dendritic block. This glass transition temperature was observed for all of the amine and alkyl terminated polymers; however, it was only observed for the generation 3.5 and 4.5 ester terminated polymers. The value of this glass transition temperature was always higher for the more polar amine terminated polymers than for the ester terminated polymers of the same degree of branching, most likely due to the stronger interactions between the more polar groups, which inhibited segmental motion. The glass transition temperature of the alkyl terminated polymers was very dependent on the length of the alkyl chain. For the shorter alkyl chain, plastization of the alkyl groups caused a decrease in the glass transition temperature with increasing alkyl chain length. However, for the dodecyl and octadecyl terminated polymers, crystallization of the alkyl groups induced an increase in the glass transition temperature as the crystalline end groups were more effective in inhibiting the motion of the underlying branches than those terminated with the shorter alkyl chains. The glass transition temperature of the dendritic block was also found to increase with increasing generation, most likely due to the increased stiffness of the branches, as well as the increased size of the dendrimer, and thus the dispersive forces between the dendrimers, all which also would have increased the energy necessary for segmental motion. In addition to the poly(ethylene oxide) melting point and the poly(amido amine) dendritic glass transition temperature, the alkyl terminated linear-dendritic rod diblock copolymers also exhibited an alkyl chain melting point. The melting point of the alky chains was found to be independent of generation and was constant for the butyl through the

dodecyl terminated polymers at approximately 20°C. It is possible that the poly(amido amine) interior was affecting the crystallinity of the alkyl chains, increasing the tendency for crystallization due to the interior amide groups which were capable of hydrogen bonding. Only the octadecyl terminated polymers exhibited an alkyl chain melting point that was much higher than that of the polymers terminated with the shorter alkyl chains; nonetheless, its value of approximately 50°C, was also found to be independent of generation, and in good agreement with that observed for poly(octadecyl) acrylates.

For most of the polymers no predominate morphology was observed. While the TEM images of the polymers revealed phase segregation, no long range order was observed, consistent with the absence of scattering peaks in SAXS. For the poly(ethylene oxide)-poly(ethylene imine) diblock copolymer backbone, long range order was most likely lost due to the crystallinity of the two blocks which dominated the morphology. Similarly, for the generation 0.5 methyl ester terminated polymer, crystallinity of the poly(ethylene oxide) block was most likely responsible for the absence of long range order; however, compatibility of the two block could also have been an issue. Nonetheless, the TEM images of the generation 4.5 methyl ester terminated diblock copolymer revealed a morphology reminiscent of that observed for other comb polymer systems. Unfortunately, poly(ethylene oxide) domains could not be readily observed, most likely due to the small fraction of the poly(ethylene oxide) in the diblock copolymer. The generation 1.0, 2.0, and 3.0-dodecyl terminated polymers exhibited morphologies similar to that of the generation 4.5 polymer. The only polymer that exhibited a predominate morphology was the poly(ethylene oxide)-poly(ethylene imine) generation 4.0-dodecyl linear-dendritic rod diblock copolymer. This polymer exhibited a strong SAXS scattering peak at a d-spacing of 4.1nm. TEM images of this polymer revealed a worm-like morphology in which the diameter of the worms was approximately 4nm, and the length was approximately 30-40nm. These dimensions were consistent with those of an individual polymer, indicating that the generation 4.0-dodecyl polymers were adopting a worm or rod-like conformation.

Tapping mode AFM was used to image individual generation 4.5 linear-dendritic rod diblock copolymers. The polymers appeared as asymmetrical ellipsoids which possessed two different heights, indicating the presence of the two blocks. The region with the smaller higher was most likely the poly(ethylene oxide) block, while the region with the larger height was most

likely the dendritic block. The heights of the polymers were much less than expected, while the diameter and the length of the polymer was much larger than expected, due to a combination of spreading and flattening of the dendritic block on the surface as well as tip convolution effects. Estimations of the dimensions of the diblock copolymer taking into account these effects would give the polymer an aspect ratio of approximately 0.37, causing the polymer to appear as an ellipsoid. Thus, the AFM image of the linear-dendritic rod diblock copolymer as an elongated, assymetrical ellipsoid was reasonable, even if the polymer was adopting a rod-like configuration.

5.6 References

- (1) Balagurusamy, V. S. K.; Ungar, G.; Percec, V.; Johansson, G. "Rational design of the first spherical supramolecular dendrimers self-organized in a novel thermotropic cubic liquid- crystalline phase and the determination of their shape by x-ray analysis," *Journal of the American Chemical Society* **1997**, *119*, 1539-1555.
- (2) Kim, Y. H.; Beckerbauer, R. "Role of end-groups on the glass-transition of hyperbranched polyphenylene and triphenylbenzene derivatives," *Macromolecules* **1994**, *27*, 1968-1971.
- (3) Hawker, C. J.; Farrington, P. J.; Mackay, M. E.; Wooley, K. L.; Fréchet, J. M. J. "Molecular ball-bearings - the unusual melt viscosity behavior of dendritic macromolecules," *Journal of the American Chemical Society* **1995**, *117*, 4409-4410.
- (4) Klug, C.; Kowalewski, T.; Schaefer, J.; Straw, T.; Tasaki, K.; Wooley, K. "Fluorine-containing dendrimers: Characterization of solid-state structure and tailoring of properties," *Abstracts of Papers of the American Chemical Society* **1997**, *214*, 71-PMSE.
- (5) Schenning, A.; Martin, R. E.; Ito, M.; Diederich, F.; Boudon, C.; Gisselbrecht, J. P.; Gross, M. "Dendritic rods with a poly(triacetylene) backbone: Insulated molecular wires," *Chemical Communications* **1998**, 1013-1014.
- (6) Schenning, A. P. H. I.; Peeters, E.; Meijer, E. W. "Energy transfer in supramolecular assemblies of oligo(*p*-phenylene vinylene)s terminated poly(propylene imine) dendrimers," *Journal of the American Chemical Society* **2000**, *122*, 4489-4495.
- (7) Stutz, H. "The glass temperature of dendritic polymers," *Journal of Polymer Science Part B-Polymer Physics* **1995**, *33*, 333-340.
- (8) Yeardley, D. J. P.; Ungar, G.; Percec, V.; Holerca, M. N.; Johansson, G. "Spherical supramolecular minidendrimers self-organized in an "inverse micellar"-like thermotropic body-centered cubic liquid crystalline phase," *Journal of the American Chemical Society* **2000**, *122*, 1684-1689.
- (9) Watanabe, J.; Takashina, Y. "Columnar liquid-crystals in polypeptides .1. A columnar hexagonal liquid-crystal observed in poly(gamma-octadecyl L-glutamate)," *Macromolecules* **1991**, *24*, 3423-3426.
- (10) Weber, P.; Guillon, D.; Skoulios, A.; Miller, R. D. "Liquid-crystalline behavior of a series of poly(di-n- alkylsilanes)," *Liquid Crystals* **1990**, *8*, 825-837.

- (11) Frey, H.; Matyjaszewski, K.; Möller, M.; Oelfin, D. "Crystallization and mesomorphic disordering of di-normal-hexylsilylene di-normal-pentylsilylene copolymers," *Colloid and Polymer Science* **1991**, *269*, 442-448.
- (12) Yamagishi, T.; Fukuda, T.; Miyamoto, T.; Yakoh, Y.; Takashina, Y.; Watanabe, J. "Thermotropic cellulose derivatives with flexible substituents .4. Columnar liquid-crystals from ester-type derivatives of cellulose," *Liquid Crystals* **1991**, *10*, 467-473.
- (13) Wooley, K. L.; Hawker, C. J.; Pochan, J. M.; Fréchet, J. M. J. "Physical-properties of dendritic macromolecules - a study of glass-transition temperature," *Macromolecules* **1993**, *26*, 1514-1519.
- (14) Farrington, P. J.; Hawker, C. J.; Fréchet, J. M. J.; Mackay, M. E. "The melt viscosity of dendritic poly(benzyl ether) macromolecules," *Macromolecules* **1998**, *31*, 5043-5050.
- (15) Fréchet, J. M. J.; Hawker, C. J.; Wooley, K. L. "The convergent route to globular dendritic macromolecules - a versatile approach to precisely functionalized 3-dimensional polymers and novel block-copolymers," *Journal of Macromolecular Science-Pure and Applied Chemistry* **1994**, *A31*, 1627-1645.
- (16) Hay, G.; Mackay, M. E.; Hawker, C. J. "Thermodynamic properties of dendrimers compared with linear polymers: General observations," *Journal of Polymer Science Part B-Polymer Physics* **2001**, *39*, 1766-1777.
- (17) Percec, V.; Ahn, C. H.; Barboiu, B. "Self-encapsulation, acceleration and control in the radical polymerization of monodendritic monomers via self-assembly," *Journal of the American Chemical Society* **1997**, *119*, 12978-12979.
- (18) Percec, V.; Ahn, C. H.; Cho, W. D.; Jamieson, A. M.; Kim, J.; Leman, T.; Schmidt, M.; Gerle, M.; Möller, M.; Prokhorova, S. A.; Sheiko, S. S.; Cheng, S. Z. D.; Zhang, A.; Ungar, G.; Yearley, D. J. P. "Visualizable cylindrical macromolecules with controlled stiffness from backbones containing libraries of self-assembling dendritic side groups," *Journal of the American Chemical Society* **1998**, *120*, 8619-8631.
- (19) Percec, V.; Ahn, C. H.; Ungar, G.; Yearley, D. J. P.; Möller, M.; Sheiko, S. S. "Controlling polymer shape through the self-assembly of dendritic side-groups," *Nature* **1998**, *391*, 161-164.
- (20) Percec, V.; Cho, W. D.; Möller, M.; Prokhorova, S. A.; Ungar, G.; Yearley, D. J. P. "Design and structural analysis of the first spherical monodendron self-organizable in a cubic lattice," *Journal of the American Chemical Society* **2000**, *122*, 4249-4250.
- (21) Percec, V.; Cho, W. D.; Mosier, P. E.; Ungar, G.; Yearley, D. J. P. "Structural analysis of cylindrical and spherical supramolecular dendrimers quantifies the concept of monodendron shape control by generation number," *Journal of the American Chemical Society* **1998**, *120*, 11061-11070.
- (22) Percec, V.; Cho, W. D.; Ungar, G.; Yearley, D. J. P. "From molecular flat tapers, discs, and cones to supramolecular cylinders and spheres using Fréchet-type monodendrons modified on their periphery," *Angewandte Chemie-International Edition* **2000**, *39*, 1597-1602.
- (23) Brewis, M.; Clarkson, G. J.; Helliwell, M.; Holder, A. M.; McKeown, N. B. "The synthesis and glass-forming properties of phthalocyanine-containing poly(aryl ether) dendrimers," *Chemistry-A European Journal* **2000**, *6*, 4630-4636.
- (24) Brewis, M.; Clarkson, G. J.; Holder, A. M.; McKeown, N. B. "Phthalocyanines substituted with dendritic wedges: Glass-forming columnar mesogens," *Chemical Communications* **1998**, 969-970.

- (25) Dvornic, P. R.; de Leuze-Jallouli, A. M.; Owen, M. J.; Perz, S. V. "Radially layered poly(amidoamine-organosilicon) dendrimers," *Macromolecules* **2000**, *33*, 5366-5378.
- (26) Balogh, L.; de Leuze-Jallouli, A.; Dvornic, P.; Kunugi, Y. T.; Blumstein, A.; Tomalia, D. A. "Architectural copolymers of pamam dendrimers and ionic polyacetylenes," *Macromolecules* **1999**, *32*, 1036-1042.
- (27) Suzuki, K.; Haba, O.; Nagahata, R.; Yonetake, K.; Ueda, M. "Synthesis and characterization of polyamidoamine-based liquid crystalline dendrimers," *High Performance Polymers* **1998**, *10*, 231-240.
- (28) Barberá, J.; Marcos, M.; Serrano, J. L. "Dendromesogens: Liquid crystal organizations versus starburst structures," *Chemistry-A European Journal* **1999**, *5*, 1834-1840.
- (29) de Brabander-van den Berg, E. M. M.; Meijer, E. W. "Poly(propylene imine) dendrimers - large-scale synthesis by *heterogeneously* catalyzed hydrogenations," *Angewandte Chemie-International Edition in English* **1993**, *32*, 1308-1311.
- (30) Cameron, J. H.; Facher, A.; Lattermann, G.; Diele, S. "Poly(propyleneimine) dendromesogens with hexagonal columnar mesophase," *Advanced Materials* **1997**, *9*, 398-403.
- (31) Baars, M.; Sontjens, S. H. M.; Fischer, H. M.; Peerlings, H. W. I.; Meijer, E. W. "Liquid-crystalline properties of poly(propylene imine) dendrimers functionalized with cyanobiphenyl mesogens at the periphery," *Chemistry-A European Journal* **1998**, *4*, 2456-2466.
- (32) Yonetake, K.; Suzuki, K.; Morishita, T.; Nagahata, R.; Ueda, M. "Synthesis and characterization of poly(propylene imine)-based liquid crystalline dendrimers," *High Performance Polymers* **1998**, *10*, 373-382.
- (33) Barberá, J.; Marcos, M.; Omenat, A.; Serrano, J. L.; Martínez, J. I.; Alonso, P. J. "Copper-containing dendromesogens: The influence of the metal on the mesomorphism," *Liquid Crystals* **2000**, *27*, 255-262.
- (34) Omotowa, B. A.; Keefer, K. D.; Kirchmeier, R. L.; Shreeve, J. M. "Preparation and characterization of nonpolar fluorinated carbosilane dendrimers by APCI mass spectrometry and small- angle x-ray scattering," *Journal of the American Chemical Society* **1999**, *121*, 11130-11138.
- (35) Coen, M. C.; Lorenz, K.; Kressler, J.; Frey, H.; Mülhaupt, R. "Mono- and multilayers of mesogen-substituted carbosilane dendrimers on mica," *Macromolecules* **1996**, *29*, 8069-8076.
- (36) Lorenz, K.; Hölter, D.; Stühn, B.; Mülhaupt, R.; Frey, H. "A mesogen-functionalized carbosilane dendrimer: A dendritic liquid crystalline polymer," *Advanced Materials* **1996**, *8*, 414-416.
- (37) Ponomarenko, S. A.; Boiko, N. I.; Shibaev, V. P.; Magonov, S. N. "Atomic force microscopy study of structural organization of carbosilane liquid crystalline dendrimer," *Langmuir* **2000**, *16*, 5487-5493.
- (38) Lorenz, K.; Frey, H.; Stühn, B.; Mülhaupt, R. "Carbosilane dendrimers with perfluoroalkyl end groups. Core-shell macromolecules with generation-dependent order," *Macromolecules* **1997**, *30*, 6860-6868.
- (39) Stark, B.; Stuhn, B.; Frey, H.; Lach, C.; Lorenz, K.; Frick, B. "Segmental dynamics in dendrimers with perfluorinated end groups: A study using quasielastic neutron scattering," *Macromolecules* **1998**, *31*, 5415-5423.

- (40) Leu, C. M.; Shu, C. F.; Teng, C. F.; Shiea, J. "Dendritic poly(ether-imide)s: Synthesis, characterization, and modification," *Polymer* **2001**, *42*, 2339-2348.
- (41) Wu, F. I.; Shu, C. F. "Hyperbranched aromatic poly(ether imide)s: Synthesis, characterization, and modification," *Journal of Polymer Science Part a-Polymer Chemistry* **2001**, *39*, 2536-2546.
- (42) Wei, H. Y.; Shi, W. F.; Nie, K. M.; Shen, X. F. "Thermal properties and crystallization behavior of dendritic polyetheramides," *Polymer* **2002**, *43*, 1969-1972.
- (43) Malmström, E.; Hult, A.; Gedde, U. W.; Liu, F.; Boyd, R. H. "Relaxation processes in hyperbranched polyesters: Influence of terminal groups," *Polymer* **1997**, *38*, 4873-4879.
- (44) Malmström, E.; Johansson, M.; Hult, A. "The effect of terminal alkyl chains on hyperbranched polyesters based on 2,2-bis(hydroxymethyl)propionic acid," *Macromolecular Chemistry and Physics* **1996**, *197*, 3199-3207.
- (45) Moore, J. S. "Shape-persistent molecular architectures of nanoscale dimension," *Accounts of Chemical Research* **1997**, *30*, 402-413.
- (46) Saez, I. M.; Goodby, J. W. "Supermolecular liquid crystal dendrimers based on the octasilsesquioxane core," *Liquid Crystals* **1999**, *26*, 1101-1105.
- (47) Saez, I. M.; Goodby, J. W.; Richardson, R. M. "A liquid-crystalline silsesquioxane dendrimer exhibiting chiral nematic and columnar mesophases," *Chemistry-a European Journal* **2001**, *7*, 2758-2764.
- (48) Meier, H.; Lehmann, M. "Stilbenoid dendrimers," *Angewandte Chemie-International Edition* **1998**, *37*, 643-645.
- (49) Tomalia, D. A.; Baker, H.; Dewald, J.; Hall, M.; Kallos, G.; Martin, S.; Roeck, J.; Ryder, J.; Smith, P. "A new class of polymers - starburst-dendritic macromolecules," *Polymer Journal* **1985**, *17*, 117-132.
- (50) Tomalia, D. A.; Baker, H.; Dewald, J.; Hall, M.; Kallos, G.; Martin, S.; Roeck, J.; Ryder, J.; Smith, P. "Dendritic macromolecules - synthesis of starburst dendrimers," *Macromolecules* **1986**, *19*, 2466-2468.
- (51) Jackson, C. L.; Chanzy, H. D.; Booy, F. P.; Drake, B. J.; Tomalia, D. A.; Bauer, B. J.; Amis, E. J. "Visualization of dendrimer molecules by transmission electron microscopy (TEM): Staining methods and cryo-TEM of vitrified solutions," *Macromolecules* **1998**, *31*, 6259-6265.
- (52) Schmitzer, A.; Perez, E.; Rico-Lattes, I.; Lattes, A.; Rosca, S. "First example of supramolecular assemblies in water of new amphiphilic glucose-persubstituted poly(amidoamine) dendrimers," *Langmuir* **1999**, *15*, 4397-4403.
- (53) He, J. A.; Valluzzi, R.; Yang, K.; Dolukhanyan, T.; Sung, C. M.; Kumar, J.; Tripathy, S. K.; Samuelson, L.; Balogh, L.; Tomalia, D. A. "Electrostatic multilayer deposition of a gold-dendrimer nanocomposite," *Chemistry of Materials* **1999**, *11*, 3268-3274.
- (54) Zhao, M. Q.; Crooks, R. M. "Dendrimer-encapsulated Pt nanoparticles: Synthesis, characterization, and applications to catalysis," *Advanced Materials* **1999**, *11*, 217-220.
- (55) Keki, S.; Torok, J.; Deak, G.; Daroczi, L.; Zsuga, M. "Silver nanoparticles by PAMAM-assisted photochemical reduction of Ag⁺," *Journal of Colloid and Interface Science* **2000**, *229*, 550-553.
- (56) Grohn, F.; Kim, G.; Bauer, A. J.; Amis, E. J. "Nanoparticle formation within dendrimer-containing polymer networks: Route to new organic-inorganic hybrid materials," *Macromolecules* **2001**, *34*, 2179-2185.

- (57) Tsukruk, V. V.; Rinderspacher, F.; Bliznyuk, V. N. "Self-assembled multilayer films from dendrimers," *Langmuir* **1997**, *13*, 2171-2176.
- (58) Hierlemann, A.; Campbell, J. K.; Baker, L. A.; Crooks, R. M.; Ricco, A. J. "Structural distortion of dendrimers on gold surfaces: A tapping-mode AFM investigation," *Journal of the American Chemical Society* **1998**, *120*, 5323-5324.
- (59) Li, J.; Piehler, L. T.; Qin, D.; Baker, J. R.; Tomalia, D. A.; Meier, D. J. "Visualization and characterization of poly(amidoamine) dendrimers by atomic force microscopy," *Langmuir* **2000**, *16*, 5613-5616.
- (60) Li, J.; Qin, D. J.; Baker, J. R.; Tomalia, D. A. "The characterization of high generation poly(amidoamine) g9 dendrimers by atomic force microscopy (AFM)," *Macromolecular Symposia* **2001**, *167*, 257-269.
- (61) Betley, T. A.; Holl, M. M. B.; Orr, B. G.; Swanson, D. R.; Tomalia, D. A.; Baker, J. R. "Tapping mode atomic force microscopy investigation of poly(amidoamine) dendrimers: Effects of substrate and pH on dendrimer deformation," *Langmuir* **2001**, *17*, 2768-2773.
- (62) Schenning, A. P. H. I.; Elissen-Román, C.; Weener, J. W.; Baars, M. W. P. L.; van der Gaast, S. J.; Meijer, E. W. "Amphiphilic dendrimers as building blocks in supramolecular assemblies," *Journal of the American Chemical Society* **1998**, *120*, 8199-8208.
- (63) Takada, K.; Diaz, D. J.; Abruna, H. D.; Cuadrado, I.; Gonzalez, B.; Casado, C. M.; Alonso, B.; Moran, M.; Losada, J. "Cobaltocenium-functionalized poly(propylene imine) dendrimers: Redox and electromicrogravimetric studies and afm imaging," *Chemistry-A European Journal* **2001**, *7*, 1109-1117.
- (64) Friggeri, A.; Schonherr, H.; van Manen, H. J.; Huisman, B. H.; Vancso, G. J.; Huskens, J.; van Veggel, F.; Reinhoudt, D. N. "Insertion of individual dendrimer molecules into self-assembled monolayers on gold: A mechanistic study," *Langmuir* **2000**, *16*, 7757-7763.
- (65) Sheiko, S. S.; Muzafarov, A. M.; Winkler, R. G.; Getmanova, E. V.; Eckert, G.; Reineker, P. "Contact angle microscopy on a carbosilane dendrimer with hydroxyl end groups: Method for mesoscopic characterization of the surface structure," *Langmuir* **1997**, *13*, 4172-4181.
- (66) Zhang, H.; Grim, P. C. M.; Foubert, P.; Vosch, T.; Vanoppen, P.; Wiesler, U. M.; Berresheim, A. J.; Mullen, K.; De Schryver, F. C. "Properties of single dendrimer molecules studied by atomic force microscopy," *Langmuir* **2000**, *16*, 9009-9014.
- (67) Zhang, H.; Grim, P. C. M.; Vosch, T.; Wiesler, U. M.; Berresheim, A. J.; Mullen, K.; De Schryver, F. C. "Discrimination of dendrimer aggregates on mica based on adhesion force: A pulsed force mode atomic force microscopy study," *Langmuir* **2000**, *16*, 9294-9298.
- (68) Mansfield, M. L. "Surface adsorption of model dendrimers," *Polymer* **1996**, *37*, 3835-3841.
- (69) Percec, V.; Johansson, G.; Ungar, G.; Zhou, J. P. "Fluorophobic effect induces the self-assembly of semifluorinated tapered monodendrons containing crown ethers into supramolecular columnar dendrimers which exhibit a homeotropic hexagonal columnar liquid crystalline phase," *Journal of the American Chemical Society* **1996**, *118*, 9855-9866.
- (70) Prokhorova, S. A.; Sheiko, S. S.; Ahn, C. H.; Percec, V.; Möller, M. "Molecular conformations of monodendron-jacketed polymers by scanning force microscopy," *Macromolecules* **1999**, *32*, 2653-2660.

- (71) Prokhorova, S. A.; Sheiko, S. S.; Mourran, A.; Azumi, R.; Beginn, U.; Zipp, G.; Ahn, C. H.; Holerca, M. N.; Percec, V.; Möller, M. "Epitaxial adsorption of monodendron-jacketed linear polymers on highly oriented pyrolytic graphite," *Langmuir* **2000**, *16*, 6862-6867.
- (72) Percec, V.; Holerca, M. N.; Magonov, S. N.; Yeardley, D. J. P.; Ungar, G.; Duan, H.; Hudson, S. D. "Poly(oxazolines)s with tapered minidendritic side groups. The simplest cylindrical models to investigate the formation of two-dimensional and three-dimensional order by direct visualization," *Biomacromolecules* **2001**, *2*, 706-728.
- (73) Ungar, G.; Percec, V.; Holerca, M. N.; Johansson, G.; Heck, J. A. "Heat-shrinking spherical and columnar supramolecular dendrimers: Their interconversion and dependence of their shape on molecular taper angle," *Chemistry-A European Journal* **2000**, *6*, 1258-1266.
- (74) Seitz, M.; Plesnivý, T.; Schimossek, K.; Edelmann, M.; Ringsdorf, H.; Fischer, H.; Uyama, H.; Kobayashi, S. "Formation of hexagonal columnar mesophases by linear and branched oligo- and polyamides," *Macromolecules* **1996**, *29*, 6560-6574.
- (75) Stocker, W.; Schürmann, B. L.; Rabe, J. P.; Forster, S.; Lindner, P.; Neubert, I.; Schlüter, A.-D. "A dendritic nanocylinder: Shape control through implementation of steric strain," *Advanced Materials* **1998**, *10*, 793-797.
- (76) Shu, L. J.; Schlüter, A.-D.; Ecker, C.; Severin, N.; Rabe, J. P. "Extremely long dendronized polymers: Synthesis, quantification of structure perfection, individualization, and sfm manipulation," *Angewandte Chemie-International Edition* **2001**, *40*, 4666-4669.
- (77) Jahromi, S.; Coussens, B.; Meijerink, N.; Braam, A. W. M. "Side chain dendritic polymers: Synthesis and physical properties," *Journal of the American Chemical Society* **1998**, *120*, 9753-9762.
- (78) Jahromi, S.; Palmen, J. H. M.; Steeman, P. A. M. "Rheology of side chain dendritic polymers," *Macromolecules* **2000**, *33*, 577-581.
- (79) Yin, R.; Zhu, Y.; Tomalia, D. A.; Ibuki, H. "Architectural copolymers: Rod-shaped, cylindrical dendrimers," *Journal of the American Chemical Society* **1998**, *120*, 2678-2679.
- (80) Ouali, N.; Mery, S.; Skoulios, A.; Noirez, L. "Backbone stretching of wormlike carbosilane dendrimers," *Macromolecules* **2000**, *33*, 6185-6193.
- (81) Setayesh, S.; Grimsdale, A. C.; Weil, T.; Enkelmann, V.; Mullen, K.; Meghdadi, F.; List, E. J. W.; Leising, G. "Polyfluorenes with polyphenylene dendron side chains: Toward non-aggregating, light-emitting polymers," *Journal of the American Chemical Society* **2001**, *123*, 946-953.
- (82) Masuo, S.; Yoshikawa, H.; Asahi, T.; Masuhara, H.; Sato, T.; Jiang, D. L.; Aida, T. "Fluorescent doughnut-like assembling of wire-type dendrimers depending on their generation numbers and degrees of polymerization," *Journal of Physical Chemistry B* **2001**, *105*, 2885-2889.
- (83) Gitsov, I.; Wooley, K. L.; Hawker, C. J.; Ivanova, P. T.; Fréchet, J. M. J. "Synthesis and properties of novel linear dendritic block- copolymers - reactivity of dendritic macromolecules toward linear-polymers," *Macromolecules* **1993**, *26*, 5621-5627.
- (84) Gitsov, I.; Fréchet, J. M. J. "Solution and solid-state properties of hybrid linear-dendritic block-copolymers," *Macromolecules* **1993**, *26*, 6536-6546.

- (85) Gitsov, I.; Fréchet, J. M. J. "Novel nanoscopic architectures - linear-globular ABA copolymers with polyether dendrimers as A-blocks and polystyrene as B- block," *Macromolecules* **1994**, *27*, 7309-7315.
- (86) Chang, Y.; Kwon, Y. C.; Lee, S. C.; Kim, C. "Amphiphilic linear PEO-dendritic carbosilane block copolymers," *Macromolecules* **2000**, *33*, 4496-4500.
- (87) Chang, Y. Y.; Kim, C. "Synthesis and photophysical characterization of amphiphilic dendritic-linear-dendritic block copolymers," *Journal of Polymer Science Part A-Polymer Chemistry* **2001**, *39*, 918-926.
- (88) Román, C.; Fischer, H. R.; Meijer, E. W. "Microphase separation of diblock copolymers consisting of polystyrene and acid-functionalized poly(propylene imine) dendrimers," *Macromolecules* **1999**, *32*, 5525-5531.
- (89) Iyer, J. *Self assembly in linear-dendritic diblock copolymer films*; Dissertation, Department of Chemical Engineering, Massachusetts Institute of Technology, 1999.
- (90) Johnson, M. A. *Self-assembly of linear-dendritic diblock copolymers*; Ph.D. Dissertation, Department of Chemical Engineering, Massachusetts Institute of Technology, 2002.
- (91) Choi, J. S.; Joo, D. K.; Kim, C. H.; Kim, K.; Park, J. S. "Synthesis of a barbell-like triblock copolymer, poly(L-lysine) dendrimer-block-poly(ethylene glycol)-block-poly(L-lysine) dendrimer, and its self-assembly with plasmid DNA," *Journal of the American Chemical Society* **2000**, *122*, 474-480.
- (92) Douy, A.; Gallot, B. "Amphiphilic block copolymers with .2. Polypeptide blocks - synthesis and structural study of poly(n-epsilon- trifluoroacetyl-l-lysine) polysarcosine copolymers," *Polymer* **1987**, *28*, 147-154.
- (93) Chen, J. T.; Thomas, E. L.; Ober, C. K.; Hwang, S. S. "Zigzag morphology of a poly(styrene-b-hexyl isocyanate) rod coil block-copolymer," *Macromolecules* **1995**, *28*, 1688-1697.
- (94) Chen, J. T.; Thomas, E. L.; Ober, C. K.; Mao, G. P. "Self-assembled smectic phases in rod-coil block copolymers," *Science* **1996**, *273*, 343-346.
- (95) Klok, H. A.; Lecommandoux, S. "Supramolecular materials via block copolymer self-assembly," *Advanced Materials* **2001**, *13*, 1217-1229.
- (96) Stupp, S. I.; LeBonheur, V.; Walker, K.; Li, L. S.; Huggins, K. E.; Keser, M.; Amstutz, A. "Supramolecular materials: Self-organized nanostructures," *Science* **1997**, *276*, 384-389.
- (97) Cornelissen, J.; Fischer, M.; Sommerdijk, N.; Nolte, R. J. M. "Helical superstructures from charged poly(styrene)- poly(isocyanodipeptide) block copolymers," *Science* **1998**, *280*, 1427-1430.
- (98) Leclere, P.; Calderone, A.; Marsitzky, D.; Francke, V.; Geerts, Y.; Mullen, K.; Bredas, J. L.; Lazzaroni, R. "Highly regular organization of conjugated polymer chains via block copolymer self-assembly," *Advanced Materials* **2000**, *12*, 1042-1046.
- (99) Polushkin, E.; van Ekenstein, G.; Knaapila, M.; Ruokolainen, J.; Torkkeli, M.; Serimaa, R.; Bras, W.; Dolbnya, I.; Ikkala, O.; ten Brinke, G. "Intermediate segregation type chain length dependence of the long period of lamellar microdomain structures of supramolecular comb-coil diblocks," *Macromolecules* **2001**, *34*, 4917-4922.
- (100) Ikkala, O.; Knaapila, M.; Ruokolainen, J.; Torkkeli, M.; Serimaa, R.; Jokela, K.; Horsburgh, L.; Monkman, A.; ten Brinke, G. "Self-organized liquid phase and co-crystallization of rod-like polymers hydrogen-bonded to amphiphilic molecules," *Advanced Materials* **1999**, *11*, 1206-1210.

- (101) Ruokolainen, J.; ten Brinke, G.; Ikkala, O. "Supramolecular polymeric materials with hierarchical structure- within-structure morphologies," *Advanced Materials* **1999**, *11*, 777-780.
- (102) Zheng, W. Y.; Hammond, P. T. "Phase behavior of new side chain smectic c* liquid crystalline block copolymers," *Macromolecules* **1998**, *31*, 711-721.
- (103) Anthamatten, M.; Wu, J. S.; Hammond, P. T. "Direct observation of a smectic bilayer microstructure in side- chain liquid crystalline diblock copolymers," *Macromolecules* **2001**, *34*, 8574-8579.
- (104) Anthamatten, M.; Zheng, W. Y.; Hammond, P. T. "A morphological study of well-defined smectic side-chain LC block copolymers," *Macromolecules* **1999**, *32*, 4838-4848.
- (105) Moment, A.; Hammond, P. T. "Block copolymers of polystyrene and side-chain liquid crystalline siloxanes: Morphology and thermal properties," *Polymer* **2001**, *42*, 6945-6959.
- (106) Fischer, H.; Arnold, M. "On the interaction of the morphological structure and the LC behaviour of LC side group block copolymers," *Macromolecular Symposia* **1996**, *102*, 293-299.
- (107) Fischer, H.; Poser, S.; Arnold, M. "On the interaction of the morphological structure and the LC behavior of LC side-group block-copolymers," *Liquid Crystals* **1995**, *18*, 503-509.
- (108) Poser, S.; Fischer, H.; Arnold, M. "Liquid crystalline side-group block copolymers with triblock structure: Investigations on the influence of the block arrangement on the morphology and the LC-phase behavior," *Journal of Polymer Science Part A-Polymer Chemistry* **1996**, *34*, 1733-1740.
- (109) Mao, G.; Ober, C. K. "Block copolymers containing liquid crystalline segments," *Acta Polymerica* **1997**, *48*, 405-422.
- (110) Iyer, J.; Fleming, K.; Hammond, P. T. "Synthesis and solution properties of new linear-dendritic diblock copolymers," *Macromolecules* **1998**, *31*, 8757-8765.
- (111) Saegusa, T.; Fujii, H.; Ikeda, H. United States, 1974.
- (112) Saegusa, T.; Ikeda, H.; Fujii, H. "Crystalline polyethyleneimine," *Macromolecules* **1972**, *5*, 108.
- (113) Goethals, E. J. In *Ring Opening Polymerization*; Ivin, K. J., Saegusa, T., Eds.; Elsevier Applied Science: 1984; Vol. 2, p 715-807.
- (114) Brandrup, J.; Immergut, E. H. *Polymer Handbook*; Third ed.; John Wiley & Sons: New York, New York, 1989.
- (115) Weyts, K. F.; Goethals, E. J. "New synthesis of linear polyethyleneimine," *Polymer Bulletin* **1988**, *19*, 13-19.
- (116) Mogri, Z.; Paul, D. R. "Membrane formation techniques for gas permeation measurements for side-chain crystalline polymers," *Journal of Membrane Science* **2000**, *175*, 253-265.
- (117) Iyer, J.; Hammond, P. T. "Langmuir behavior and ultrathin films of new linear-dendritic diblock copolymers," *Langmuir* **1999**, *15*, 1299-1306.
- (118) Mogri, Z.; Paul, D. R. "Gas sorption and transport in poly(alkyl (meth)acrylate)s. I. Permeation properties," *Polymer* **2001**, *42*, 7765-7780.
- (119) Mogri, Z.; Paul, D. R. "Water-vapor permeation in semicrystalline and molten poly(octadecyl acrylate)," *Journal of Polymer Science Part B-Polymer Physics* **2001**, *39*, 979-984.

- (120) Baltá-Calleja, F. J.; Vonk, C. G. *X-ray Scattering of Synthetic Polymers*; Elsevier: Amsterdam, 1989.
- (121) Goodhew, P. H.; Humphreys, J.; Beanland, R. *Electron Microscopy and Analysis*; Taylor & Francis: London, England, 2001.
- (122) Tomalia, D. A. In *Handbook of Polymer Synthesis. Part A.*; Kricheldorf, H. R., Ed.; Marcel Dekker: New York, New York, 1992, p 743-805.
- (123) Quiram, D. J.; Register, R. A.; Marchand, G. R.; Ryan, A. J. "Dynamics of structure formation and crystallization in asymmetric diblock copolymers," *Macromolecules* **1997**, *30*, 8338-8343.
- (124) Suvorova, A. I.; Hassanova, A. H.; Tujkova, I. S. "Phase equilibrium in blends of crystalline poly(ethylene oxide) amorphous poly(methyl acrylate) or poly(methyl methacrylate)," *Polymer International* **2000**, *49*, 1014-1016.
- (125) Mayes, A., Personal Communication.
- (126) Cheng, G. L.; Boker, A. A.; Zhang, M. F.; Krausch, G.; Muller, A. H. E. "Amphiphilic cylindrical core-shell brushes via a "grafting from" process using ATRP," *Macromolecules* **2001**, *34*, 6883-6888.

Chapter 6

Conclusions and Future Work

6.1 Conclusions

This thesis is the first to demonstrate the synthesis and characterization of a diblock copolymer possessing a novel linear-dendritic rod diblock copolymer architecture. These diblock copolymers consisted of a linear poly(ethylene oxide)-poly(ethylene imine) backbone around which poly(amido amine) dendrons were divergently added. The synthetic route used to prepare these polymers has been outlined and preliminary characterization and analysis of the solution, Langmuir film, thermal, and morphological properties has been performed.

The synthesis of these poly(ethylene oxide)-poly(ethylene imine)-poly(amido amine) diblock copolymers was accomplished using a repetitive, multi-step process, which is traditionally used in dendritic systems. To form the backbone, poly(ethylene oxide)-tosylate monomethyl ether homopolymer was used to initiate the cationic ring opening polymerization of 2-ethyl-2-oxazoline forming the poly(ethylene oxide)-poly(2-ethyl-2-oxazoline) diblock copolymer. This polymer was then hydrolyzed, using a weak acid hydrolysis, to form the desired poly(ethylene oxide)-poly(ethylene imine) diblock copolymer backbone. Poly(amido amine) dendritic branches were divergently added to the poly(ethylene imine) block by the repeated addition of methyl acrylate, forming the half generation polymers, and ethylene diamine, forming the whole generation polymers. Branching occurred when the methyl acrylate added to the two protons on the terminal amine of the whole generation polymers. In order to make these polymers amphiphilic, n-alkyl amines, ranging in length from four to eighteen carbons, were added to the methyl ester end groups at each of the generations. The chemical structures of all of the polymers were confirmed using ^1H NMR and FTIR.

Dynamic light scattering and intrinsic viscosity measurements were used to examine the solution behavior of these poly(ethylene oxide)-poly(ethylene imine)-poly(amido amine) linear-dendritic rod diblock copolymers in methanol at 25°C. In order to determine the intrinsic viscosity of the polymers, their reduced viscosity was first plotted as a function of concentration using the Huggins and Kramer equations. While the low generation amine terminated polymers

obeyed these equations, producing a linear relationship, the low generation ester terminated polymers as well as the higher generation polymers of both end group chemistries did not, as their application resulted in lines which had an upward curvature. Attempts were also made to fit the data to the Fuoss equation, which has been used for traditional polyelectrolyte systems, but this too was unsuccessful. However, the data from all of the polymers could be successfully plotted using the Fedors equation, which had been previously applied to polymers in the dilute to semi-dilute regime as well as to polyelectrolytes whose data could also be fitted using the Fuoss equation. Since the concentration range employed in the viscosity experiments was well below that of semi-dilute regime, we believe that these linear-dendritic rod diblock copolymers were in fact behaving as polyelectrolytes, but that the traditional polyelectrolyte effect was muted by the organic nature of the solvent and its interaction with the polyelectrolyte counterions. These results were in good agreement with those obtained by dynamic light scattering, in which a small increase in the hydrodynamic radii of the polymers were measured with decreasing concentration. Nonetheless, to our knowledge, this thesis is the first to report the use of the Fedors equation for polyelectrolytes in nonaqueous solutions whose behavior could not be described by either the Huggins or the Fuoss equations.

The intrinsic viscosity of the amine and ester terminated polymers was found to follow two different trends at low generations that merged into one trend at higher generations. At low generations, the chemistry of the end groups and their interaction with the solvent was found to be more important, while at higher generations, the highly branched nature of the dendritic block was the more important factor. For the half generation ester terminated polymers, a maximum in the intrinsic viscosity occurred which is similar to that observed for traditional spherical dendrimers as the molecular weight of the dendritic block began to grow more rapidly than its size due to its highly branched nature. The decrease in the intrinsic viscosity of the amine terminated polymers with increasing generation can be related to this same effect. In order to confirm the generation number at which the maximum in the intrinsic viscosity would be expected, a simple scaling relationship for the intrinsic viscosity has been developed. The molecular weight of the linear-dendritic rod diblock copolymers was found to scale as $2^g - 1$. To determine a scaling relationship for the volume, the equations used to scale the radius of gyration of comb polymers were applied. However, instead of treating the side chains as spheres, as is done for comb polymers, the dendrons were treated as hemispheres, resulting in the volume

scaling as $V \sim [N^{3/5}a(1 + 1/2g^3n^3)^{1/5}]^3$. Thus, the scaling of the volume was dependent on both the generation number, g , and the relative length of the dendritic branch to that of the monomer unit to which it was attached, n . Therefore, the maximum in the intrinsic viscosity was found to occur at either one branch end or two branch ends, depending on the value of n . A minimum in the intrinsic viscosity was observed for both the amine and the ester terminated polymers at generation 3.5, which can be attributed to an elongation of the polymers into a more rod-like shape.

From dynamic light scattering, the hydrodynamic radii of the polymers were found to increase slowly with increasing generation up to generation 3.5; however, above generation 3.5, the hydrodynamic radii were found to increase very rapidly. This rapid increase in the hydrodynamic radii can be explained by an elongation of the dendritic block into a more rod-like configuration due to the steric hindrance of the dendritic side groups. This elongation would result in not only a larger hydrodynamic volume but also a breakdown of the spherical approximation, resulting in an overestimation of the hydrodynamic radii. Similar results were also observed for the viscometric radii of the polymers determined from intrinsic viscosity. The hydrodynamic radii measured from dynamic light scattering were also compared to the viscometric radii determined from intrinsic viscosity measurements assuming various aggregation numbers in order to gain insight into the aggregation behavior of the polymers in solution. For all of the generations of polymers, it appeared as if the linear-dendritic rod diblock copolymers were behaving as isolated polymers in solution, or at most, aggregates of two or three, but that they were not aggregating into larger micellar structures with aggregation number of four or more.

The behavior of amphiphilic linear-dendritic rod diblock copolymers at the air/water interface in Langmuir films has been examined using pressure/area isotherms. From the pressure area/isotherms, it was found that the low generation polymers formed small plateaus in the surface pressure at approximately 20mN/m due to the presence of the poly(ethylene oxide) block on the surface. As the generation number and length of the dendritic block increased, this plateau all but disappeared as the fraction of the poly(ethylene oxide) in the polymers decreased. Other intermediate plateaus in the surface pressure were also observed for the polymers terminated with the longer alkyl chains due to rearrangements of the alkyl chains and the polymers on the surface. The plateaus that formed at the highest surface pressure were attributed

to collapse of the polymer monolayer. The surface pressure at collapse was most highly dependent on the length of the alkyl group with which the polymers were functionalized and was independent of the generation number and length of the dendritic block. Especially for the octadecyl terminated polymers, the degree of substitution was also an important parameter, as polymers substituted with less than approximately 30% of octadecyl chains did not form stable films on the surface.

The surface area of the polymers in their most condensed state was found to increase with increasing generation and length of the dendritic block, except for the octadecyl terminated polymers where the surface area was found to be independent of dendritic block length. In addition, for the generation 1.0, 2.0, and 3.0 polymers, the surface area was found to decrease with increasing length of the alkyl chain, most likely due to elongation of the dendritic block backbone away from the surface, which minimized the unfavorable interactions between the longer, more hydrophobic alkyl chains and the water. For the generation 4.0 and 5.0-butyl through dodecyl terminated polymers, the surface area was found to remain approximately constant as the polymers became too large and too stiff to be able to elongate from the surface. It is possible that the polymers terminated with longer alkyl chains were able to take on a different conformation on the surface as amphiphilics with longer alkyl chains are known to have greater diffusion constants, and thus greater mobility on the surface.

Comparing the area per molecule determined experimentally with that determined theoretically for various models of the polymer on the surface, the arrangement of the linear-dendritic rod diblock copolymers on the surface was predicted. Three models were examined: one in which the dendritic block was oriented horizontally on the surface with the alkyl chains radiating in three dimensions (horizontal rod model), one in which the dendritic block was oriented vertically on the surface with the alkyl chains radiating in three dimensions (vertical rod model), and one in which the dendritic block was oriented horizontally with the alkyl chains aligned perpendicular to the interface such that the surface area per molecule was governed by the number of alkyl chains in the polymer (alkyl model). It was found that all of the methyl ester terminated polymers formed fairly instable films at the air/water interface, and that the polymers appeared to orient as horizontal rods on the surface with the alkyl chains radiating in three dimensions, as indicated by the good agreement of the experimentally determined area per molecule with that calculated for a horizontal rod. For the generation 1.0, 2.0, and 3.0 polymers

that were terminated with butyl through dodecyl groups, the surface area per molecule decreased as the length of the alkyl chains increased, with the values determined experimentally falling between and shifting from those calculated theoretically for the horizontal rod models to those calculated for the vertical rod models. This decrease in the area per molecule with increasing alkyl chain length most likely occurred as the dendritic block backbone adopted a random coil configuration which elongated away from the surface in order to minimize the increasing larger unfavorable interactions between the alkyl chains and the surface of the water. Thus, for these low generation linear-dendritic diblock copolymers, the diblock copolymer nature of the polymer was found to be more important to the arrangement of the polymers in the films than the dendritic nature of the polymer. However, for the generation 4.0 butyl through dodecyl terminated polymers, it appeared as if the polymers had become too bulky and stiff to be able to form elongated random coils on the surface and thus oriented themselves as horizontal rods in which the alkyl chains attempted to align themselves perpendicular to the surface, but could not because of the curvature of the dendritic branches. (The experimentally determined surface areas were for these polymers were all in good agreement with those determined for the horizontal rod models.) Thus, the dendritic nature of the diblock copolymer became important in the alignment of these higher generation polymers on the surface. The poly(ethylene oxide) block in all of these linear-dendritic rod diblock copolymers appeared to form a very hydrated interfacial layer near the surface of the water. For the lower generation polymers, the poly(ethylene oxide) block was probably able to cover most of the interfacial area between the water and the dendritic block. Thus, the polymers that were terminated with shorter alkyl chains most likely formed a mixed poly(ethylene oxide)/dendritic layer that was more rich in poly(ethylene oxide) near the water and more rich in alkyl chains near the air, while the polymers that were terminated with longer alkyl chains most likely formed more a more discrete poly(ethylene oxide) interfacial layer with the dendritic block forming a discrete layer above it. For the higher generation polymers, in which the poly(ethylene oxide) block was too small to be able to cover the entire interfacial area between the dendritic block and the water, the poly(ethylene oxide) block probably formed a partial layer to cover the water, and the hydrophilic poly(amido amine) interior portion of the dendritic block probably also formed an interface with the water helping to stabilize the diblock copolymer on the surface.

Finally, a preliminary investigation into the thermal and morphological behavior of a series of poly(ethylene oxide)-poly(ethylene imine)-poly(amido amine) linear-dendritic rod diblock copolymers was undertaken. DSC was used to examine the effect of dendritic block end group and generation number on the melting point of the poly(ethylene oxide) block, the glass transition temperature of the dendritic block, and the melting point of the alkyl chains. For all of the linear-dendritic rod diblock copolymers under investigation, the melting point of the poly(ethylene oxide) was found to remain approximately constant, independent of end group and generation, indicating that the crystals that formed were composed of very similar from generation to generation. These crystalline structures most likely consisted of poly(ethylene oxide) which had been plasticized by the dendritic block as indicated by a lowering of the poly(ethylene oxide) block melting point to approximately 40°C from that of approximately 54°C for the poly(ethylene oxide) homopolymer. Nonetheless, the relative intensity of the melting point decreased with increasing generation, such that it virtually disappeared above generation 2.0. A glass transition temperature was observed for some of the linear-dendritic rod diblock copolymers that was attributed to the dendritic block, due to its dependence on the end group chemistry as well as the generation number of the dendritic block. This glass transition temperature was observed for all of the amine and alkyl terminated polymers; however, it was only observed for the generation 3.5 and 4.5 ester terminated polymers. The value of this glass transition temperature was higher for the more polar amine terminated polymers than for the ester terminated polymers of the same degree of branching, most likely due to the stronger interactions between the more polar groups which inhibited segmental motion. The glass transition temperature of the alkyl terminated polymers was very dependent on the length of the alkyl chain. For the polymers terminated with the shorter alkyl chains, plastization of the alkyl groups caused a decrease in the glass transition temperature with increasing alkyl chain length. However, for the dodecyl and octadecyl terminated polymers, crystallization of the alkyl groups induced an increase in the glass transition temperature as the crystalline end groups were more effective in inhibiting the motion of the underlying branches than those terminated with the shorter alkyl chains. A melting point for the alkyl chains was also observed and was found to be approximately constant at 20°C, independent of generation for the butyl through the dodecyl terminated polymers. Only the octadecyl terminated polymers exhibited an alkyl chain melting point that was much higher than that of the polymers terminated with the shorter alkyl chains;

nonetheless, its value of approximately 50°C was also found to be independent of generation, and in good agreement with that observed for poly(octadecyl) acrylates. It should be noted that most of the octadecyl terminated polymers possessed a degree of substitution that was less than 30%, which also may have influenced the thermal behavior of these polymers.

For almost all of the methyl ester and dodecyl terminated polymers of varying generation that were examined, no predominate morphology was observed in the bulk. While the TEM images of the polymers revealed phase segregation, no long-range order was observed consistent with the absence of scattering peaks in SAXS. For the poly(ethylene oxide)-poly(ethylene imine) diblock copolymer backbone, long range order was most likely lost due to the crystallinity of the two blocks, which dominated the morphology. Similarly, for the generation 0.5 methyl ester terminated polymer, crystallinity of the poly(ethylene oxide) block was most likely responsible for the absence of long range order; however, good chemical compatibility of the two block could also have been an issue. Nonetheless, the TEM images of the generation 4.5 methyl ester terminated diblock copolymer revealed a morphology reminiscent of that observed for other comb polymer systems. Unfortunately, poly(ethylene oxide) domains could not be readily observed, most likely due to the small fraction of the poly(ethylene oxide) in the diblock copolymer. The generation 1.0, 2.0, and 3.0-dodecyl terminated polymers exhibited morphologies similar to that of the generation 4.5 polymer. The only polymer that exhibited a predominate morphology was the poly(ethylene oxide)-poly(ethylene imine) generation 4.0-dodecyl linear-dendritic rod diblock copolymer. This polymer exhibited a strong SAXS scattering peak with a d-spacing of 4.1 nm. TEM images of this polymer revealed a worm-like morphology in which the diameter of the worms was approximately 4 nm, and the length was approximately 30-40 nm. These dimensions were consistent with those of an individual polymer, indicating that the generation 4.0-dodecyl polymers were adopting a worm or rod-like conformation in the bulk.

Overall, there are two important conclusions that can be drawn from this thesis. The first is that the polymers exhibited both their diblock copolymer nature as well as their dendritic nature. At low generations, the diblock copolymer nature was predominant, while at higher generations, the dendritic nature was more important, perhaps as the poly(ethylene oxide) became too small to be able to have a large effect on the properties of the dendritic block. For example, in solution, the intrinsic viscosity of the poly(ethylene oxide)-poly(ethylene imine)

backbone could be accurately predicted based on contributions from the two blocks. However, as the generation number increased, so did the hydrodynamic and viscometric radii due to the effect of the dendritic block. At the air/water interface, the low generation alkyl terminated polymers behaved as elongated, random coils resting on a thin layer of poly(ethylene oxide). This would not have been observed if only the dendritic block was present as analogous alkyl acrylates of all lengths have been found to rest horizontally on the surface. In addition, for the generation 4.0 and 5.0-alkyl terminated polymers, the polymers were found to lay flat on the surface as the dendritic block became too sterically crowded to allow it to adopt a coiled conformation. Finally, in the bulk, a melting point for the poly(ethylene oxide) block and a glass transition temperature for the dendritic block could be observed below generation 2.0; however, above generation 2.0, only the glass transition temperature of the dendritic block was detected. In addition, from TEM, the generation 0.5 polymer appeared to phase segregate into irregularly spaced spheres of the dendritic block in a matrix of poly(ethylene oxide), but at generation 4.5, only the hyperbranched nature of the polymer was observed.

The second important conclusion is that a fundamental change in the behavior of these linear-dendritic rod diblock copolymers occurred at generation 4.0, regardless of whether the polymers were terminated with amine or alkyl groups. This change could be correlated to the dendritic block of the diblock copolymer extending to adopt a rod-like configuration. For example, in solution, the hydrodynamic and viscometric radii were found to increase to a much greater extent than expected for the generation 4.0 and 4.5 polymers, most likely due to a breakdown of the spherical approximation as the dendritic block extended into a rod-like configuration causing the diblock copolymer to adopt an elongated shape. Similarly, at the air/water interface, the dendritic block of the generation 4.0-alkyl terminated polymers were all found to take on a horizontal rod configuration, while the dendritic block of the lower generation polymers adopted a random coil configuration, which elongated vertically with increasing length of the alkyl chain and that elongated horizontally with increasing generation. Finally, in the bulk, direct observation of the generation 4.0-dodecyl terminated linear-dendritic rod diblock copolymer with TEM indicated that the polymer was adopting a rod- or worm-like conformation, while for the lower generation dodecyl terminated polymers only traditional diblock copolymer or polymer brush behavior was observed.

6.2 Future Work

While this thesis has successfully demonstrated the ability to synthesize linear-dendritic rod diblock copolymers and has contributed to the understanding of the behavior of these polymers in solution, at the air/water interface, and in the bulk; as is true for all projects, more questions were raised and ideas generated during the course of the research than there was time to pursue. For this project, these ideas for future work were inspired by the findings that were reported in each of the four results chapters of this thesis, as well as by experiments conducted by others on different dendritic systems. A few of these ideas will be discussed in the subsequent paragraphs.

One of the commonly noted features of traditional, spherical dendrimers is their monodispersity, which arises from the repetitive, step-by-step process by which they are synthesized.¹ Even hybrid-linear dendritic diblock copolymers have been found to be monodisperse when the linear polymer to which the dendrimer is attached is monodisperse. Unfortunately, the poly(ethylene oxide)-poly(ethylene imine) diblock copolymer core of the linear-dendritic rod diblock copolymers was polydisperse, resulting in linear-dendritic rod diblock copolymers that were also polydisperse and whose polydispersity increased with increasing generation. This polydispersity arose from the use of the poly(ethylene oxide) tosylate macroinitiator which was used in the cationic ring-opening polymerization of the poly(2-ethyl-2-oxazoline) block.^{2,3} One way that the polydispersity might be decreased is to fractionate either the poly(ethylene oxide)-poly(2-ethyl-2-oxazoline) or the poly(ethylene oxide)-poly(ethylene imine) diblock copolymers by running them through preparative GPC columns. It may be easier to fractionate the poly(ethylene oxide)-poly(2-ethyl-2-oxazoline) diblock copolymer as it is soluble in a wider range of organic solvents than the poly(ethylene oxide)-poly(ethylene imine) diblock copolymer whose solubility is limited to methanol and low pH water. Nonetheless, if one did fractionate the poly(ethylene oxide)-poly(2-ethyl-2-oxazoline) polymer, one would need to recheck the polydispersity of the poly(ethylene oxide)-poly(ethylene imine) diblock copolymer after hydrolysis to verify that it had not changed.

A second area of synthetic work would be to develop a route which allows for a higher degree of substitution of octadecyl groups onto the methyl ester terminated linear-dendritic rod diblock copolymers. Due to purification issues, the substitution of the octadecyl amine on the higher generation methyl ester terminated polymers was poor. Unfortunately, it was difficult to

use the excesses of octadecyl amine necessary for high degrees of substitution, as removal of excess octadecylamine with ultrafiltration proved to be a headache as the octadecyl amine precipitated from the solution in an unpredictable manner. Since both the octadecyl amine and the octadecyl amine terminated polymers are readily soluble in chloroform, ultrafiltration in chloroform would be the ideal; however, ultrafiltration in chloroform requires the use of a chemically resistant ultrafiltration cell, which is currently unavailable in our lab. In addition, ultrafiltration of the other linear-dendritic rod diblock copolymers that are terminated with shorter alkyl groups, especially decyl and dodecyl groups, may prove to be more efficient in chloroform than in methanol. There are several reasons why highly substituted octadecyl terminated linear-dendritic rod diblock copolymers may be of interest. Preliminary investigations into the behavior of these polymers at the air/water interface indicated that their behavior was somewhat different than that of the polymers terminated with the shorter alkyl chains. For example, the generation 1.0 and 3.0-octadecyl terminated polymers, which possessed a higher degree of substitution, exhibited a much higher collapse pressure than that of the polymers terminated with shorter alkyl chains. In addition, these octadecyl terminated polymers appeared to be taking on a vertical rod-like nature at the air/water interface, but more work needs to be done to verify this conclusion. A second reason that the octadecyl terminated polymers may be of interest is that they may drive segregation of the linear and the dendritic blocks by providing "hard confinement" of the crystalline poly(ethylene oxide), resulting in a more defined diblock copolymer morphology. Johnson *et al.* found this to be the case when they examined poly(ethylene oxide)-poly(amido amine) hybrid-linear dendritic diblock copolymers terminated with amine and stearate groups.⁴ The crystalline stearate groups were able to confine the crystalline poly(ethylene oxide) but the amorphous amine groups were not.

One final area of synthetic work might be to prepare linear-dendritic rod diblock copolymers whose compositions of poly(ethylene oxide) and dendritic blocks varied both relatively and absolutely. Of greatest interest are those polymers which possessed a much larger poly(ethylene oxide) block. For the polymers under investigation in this thesis, the poly(ethylene oxide) block became very small relative to the dendritic block at high generations, such that it was difficult to observe its effect in Langmuir films as well as in the morphology of the generation 4.0-alkyl terminated linear-dendritic rod diblock copolymers. Thus, a larger relative and absolute poly(ethylene oxide) block might prove to be a better anchor for the diblock

copolymer at the air/water interface, possibly even shielding the interface enough so that the dendritic rod block might prefer to align perpendicular to the interface. In addition, a larger poly(ethylene oxide) block might be able to participate to a greater extent in the morphology of the diblock copolymers at higher generations. Nonetheless, use of a larger poly(ethylene oxide) block may offer some challenges synthetically as it may be more difficult to isolate and purify the poly(ethylene oxide)-poly(ethylene imine) diblock copolymer backbone from the water during the hydrolysis step if the diblock copolymer possessed a larger water soluble component. Initial calculation of the length of the poly(ethylene oxide) block needed to cover the diameter of the rod block was based on the radius of the generation 4.5 methyl ester terminated polymer, as it was hoped that this polymer would possess the rigidity and segregation necessary for assembly at the air/water interface and in the bulk. As this was not the case, and as it was found that the generation 4.0-dodecyl terminated polymer was able to provide these attributes, this previous calculation was an underestimation resulting in a poly(ethylene oxide) block that was too short. New calculations into the size of poly(ethylene oxide) based on the experimentally determined diameter of 4.1nm for the generation 4.0-dodecyl terminated rods indicates that a poly(ethylene oxide) block of 5000-6000g/mol would be necessary to cover the base of these rods. This calculation was performed with the following equation.

$$PEO = MW_r \left(\frac{\frac{d}{2} \sqrt{6}}{L} \right)^2 \quad (6.1)$$

Where PEO is the molecular weight of poly(ethylene oxide) needed; MW_r is the molecular weight of a repeat of poly(ethylene oxide) which is 43g/mol; d is the diameter of the rod block which is 2.1nm; and L is the length of a repeat of poly(ethylene oxide) which is approximately 0.43-0.45nm. This calculation of a molecular weight of 5000-6000g/mol to cover a rod diameter of 4.1nm is reasonable as Iyer et al. have reported the radius of gyration of 5000 g/mol poly(ethylene oxide) to be approximately 2.1-2.2nm in water.⁵

It would also be interesting to examine the solution and aggregation behavior of these linear-dendritic rod diblock copolymers varying the relative and absolute lengths of the two blocks. Varying the relative and absolute lengths of the polymers will alter the size and geometry of the diblock copolymers, which are important factors in determining whether

aggregates can form and the types of aggregates that do form. In addition to varying the lengths of the polymers, it would also be interesting to further examine the effect of end group chemistry on the solution behavior of the polymers. In this thesis, only the solution behavior of the amine and the methyl ester end groups were examined. However, other end groups, such as alkyl groups, may encourage aggregation behavior in methanol and other polar solvents resulting in the formation of macromolecular micelles. Finally, it would be of interest to look at the solution and aggregation behavior by varying the solvent, examining some solvents that are selective for the poly(amido amine) dendritic block and others that are selective for the poly(ethylene oxide) block. Thus far only methanol, which is a good solvent for both blocks, has been used as a solvent resulting in the absence of aggregation; however, the use of other solvents may encourage aggregation. Thus, it may be possible to tune the size and shape of the individual linear dendritic rod diblock copolymers as well as the macromolecular micelles that they form by adjusting the relative lengths of the two blocks, the dendritic block end group, and the solvent.

In addition to examining the size and aggregation behavior of the polymers in solution, better quantification of their shape and the shape change that occurs with increasing generation should be examined with neutron scattering. In addition to AFM and TEM, neutron scattering is the most commonly used technique to determine the shape of dendritic systems, including dendritic rod homopolymers.^{6,7} Thus, while all of the experiments in this thesis point to a shape change occurring at generation 4.0, verification with neutron scattering would prove beyond a reasonable doubt that dendritic rods had been formed, and it would also offer insight into the shapes that the lower generation polymers were adopting.

Similarly, another neutron technique, neutron reflectivity, would help to verify the arrangement of the alkyl terminated, amphiphilic linear-dendritic rod diblock copolymers at the air/water interface. While the pressure-area isotherms of the polymer have been used to predict the arrangement of these polymers at the interface, neutron reflectivity would also be able to offer insight into their arrangement by determining the chemical composition of the film as a function of distance from the interface, as well as the total thickness of the polymer film. Neutron reflectivity had previously been used to determine the behavior of dendritic homopolymers as well as hybrid-linear dendritic diblock copolymers at the air/water interface. Thus, verification of the dendritic block behaving as a random coil at low generations and either

a horizontal or a vertical rod at high generation could be made. In addition, the exact arrangement of the poly(ethylene oxide) in the film could be determined.

Transfer of the Langmuir films of the linear-dendritic rod diblock copolymers to solid substrates may also offer insight into the properties of these films and the ability to do this should also be explored. For example, by examining the effect of generation and alkyl group on the thickness of the transferred films, one might also be able to determine whether the polymers were behaving as random coils or as vertical or horizontal rods on the surface. In addition, since the ultimate goal of this project is not only to prepare linear-dendritic rod diblock copolymers, but also to find ways to direct the assembly of these polymers such that are useful materials, the ability to transfer the order in these films to solid substrates is a necessity. Of particular interest is the ability to transfer the generation 4.0-alkyl terminated linear-dendritic rod diblock copolymers as these polymers appear to be behaving as rods on the surface. It is this rodlike shape of the linear-dendritic rod diblock copolymers that brings novelty and interest to the project.

One last idea for future work is to examine the use of these polymers as templates in the formation of metal nanoparticles. Several groups have templated gold, silver, copper, and platinum nanoparticles in poly(amido amine) spherical homopolymer as well as hybrid-linear dendritic diblock copolymers.^{4,8-13} By judicious choice of the reaction parameters, nanoparticles have been directed to form within the interior regions of the dendrimers as well as on the surface of the dendrimer. Some preliminary work in this area has been performed with these linear-dendritic rod diblock copolymers; however none has been reported in this thesis. As can be seen in Figure 6.1, it is possible to template gold nanoparticles in these linear-dendritic rod diblock copolymers. Unfortunately, control over their size and position has not yet been achieved. Thus, experiments that work toward control of these parameters are needed. One possibility is to use alkyl terminated polymers for templating as these polymers might allow for the isolation of the nanoparticles within the interior of the dendrimer as exterior sites would not be capable of complexing with the metal ions. It would also be interesting to examine the effect of dendritic generation as well as length of the dendritic block on the particle formation.

Thus, while much has already been learned about these linear-dendritic rod diblock copolymers, there is still much more to learn. These polymers have been, and will continue to be an exciting area of exploration.

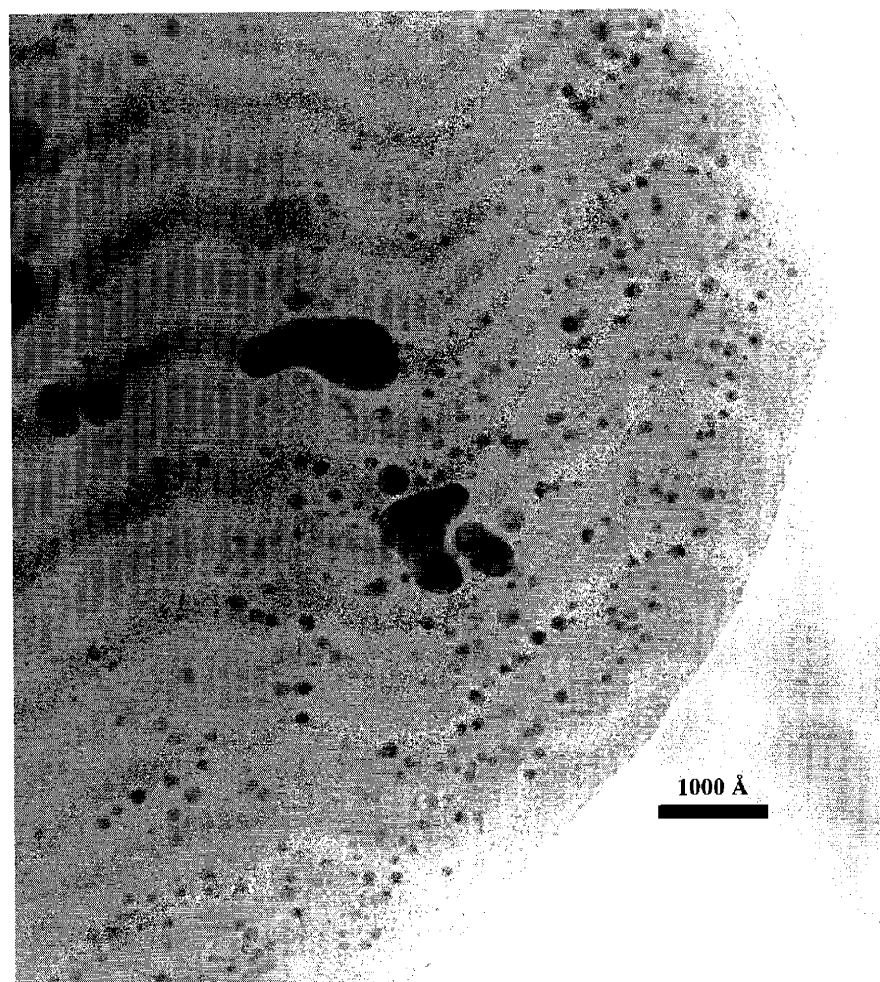


Figure 6.1. Preliminary TEM image of gold nanoparticles templated with the generation 3.0-amine terminated linear-dendritic rod diblock copolymers. The gold particles appear dark, while the diblock copolymer appears light.

6.3 References

- (1) Tomalia, D. A. "Dendrimer molecules," *Scientific American* **1995**, *272*, 62-66.
- (2) Litt, M. H.; Swamikannu, A. X. In *Ring Opening Polymerization: Kinetics, Mechanisms, and Synthesis*; McGrath, J., Ed.; American Chemical Society: Washington, D.C., 1985; Vol. 286, p 231-243.
- (3) Miyamoto, M.; Sano, Y.; Saegusa, T.; Kobayashi, S. "Synthesis of poly[(n-acylethylenimine)-b-(ethylene oxide)] and its anti-electrostatic property," *European Polymer Journal* **1983**, *19*, 955-961.
- (4) Johnson, M. A. *Self-assembly of linear-dendritic diblock copolymers*; Ph.D. Dissertation, Department of Chemical Engineering, Massachusetts Institute of Technology, 2002.

- (5) Iyer, J.; Fleming, K.; Hammond, P. T. "Synthesis and solution properties of new linear-dendritic diblock copolymers," *Macromolecules* **1998**, *31*, 8757-8765.
- (6) Neubert, I.; Amoulong-Kirstein, E.; Schlüter, A.-D.; Dautzenberg, H. "Polymerization of styrenes carrying dendrons of the first, second and third generation," *Macromolecular Rapid Communications* **1996**, *17*, 517-527.
- (7) Ouali, N.; Mery, S.; Skoulios, A.; Noirez, L. "Backbone stretching of wormlike carbosilane dendrimers," *Macromolecules* **2000**, *33*, 6185-6193.
- (8) Balogh, L.; Tomalia, D. A. "Poly(amidoamine) dendrimer-templated nanocomposites. 1. Synthesis of zerovalent copper nanoclusters," *Journal of the American Chemical Society* **1998**, *120*, 7355-7356.
- (9) Zhao, M. Q.; Crooks, R. M. "Intradendrimer exchange of metal nanoparticles," *Chemistry of Materials* **1999**, *11*, 3379-3385.
- (10) Zhao, M. Q.; Crooks, R. M. "Dendrimer-encapsulated Pt nanoparticles: Synthesis, characterization, and applications to catalysis," *Advanced Materials* **1999**, *11*, 217-+.
- (11) Zhao, M. Q.; Crooks, R. M. "Homogeneous hydrogenation catalysis with monodisperse, dendrimer-encapsulated Pd and Pt nanoparticles," *Angewandte Chemie-International Edition* **1999**, *38*, 364-366.
- (12) Crooks, R. M.; Lemon, B. I.; Sun, L.; Yeung, L. K.; Zhao, M. Q. In *Dendrimers III: Design, Dimension, Function* 2001; Vol. 212, p 81-135.
- (13) Crooks, R. M.; Zhao, M. Q.; Sun, L.; Chechik, V.; Yeung, L. K. "Dendrimer-encapsulated metal nanoparticles: Synthesis, characterization, and applications to catalysis," *Accounts of Chemical Research* **2001**, *34*, 181-190.

Appendix 2.A Synthetic Details

2.A.1 Generational Synthesis

2.A.1.1 Linear Dendritic Rod Diblock Copolymers Consisting of a Polyethylene Oxide Block of 43 Repeats and a Dendritic Block of 97 Repeats

Poly(ethylene oxide) monomethyl ether tosylate (PEO-OTs)

PEO-OTs was prepared using a known procedure.¹ All glassware were oven dried prior to use. A single neck, 100ml round bottom flask equipped with a glass stopper, a side arm vacuum adapter, and a stir bar in the bottom, was evacuated and filled with nitrogen. 14.23 g (0.00749 mol polymer and hydroxyl groups) of pre-dried m-PEO-OH were transferred to the round bottom flask through a solids funnel, which temporarily replaced the glass stopper. 30ml of methylene chloride were added to the m-PEO-OH and the two were stirred for five minutes while the m-PEO-OH dissolved. 3.1ml (0.0222 mol) of triethylamine were added to the flask, the flask was immersed in an ice bath, and the solution was stirred for another 20 minutes. 4.07 g (0.0213 mol) of tosyl chloride were added to the cold, stirring solution through a solids funnel, which temporarily replaced the glass stopper. The tosyl chloride slowly dissolved leaving a clear, colorless solution. The solution was allowed to slowly warm to room temperature. During the reaction process, an insoluble white precipitate formed from the creation of triethylammonium chloride salts. After 12 hours, the solution was filtered to remove the majority of this precipitate. The liquor was then transferred to a 100ml flask where it was concentrated by vacuum distillation. The resulting white solid was redissolved with approximately 50ml of benzene forming a faint yellow solution and more triethylammonium salt. This salt was also removed by filtration. The resulting faint yellow liquor was gently heated and stirred with Norit and silica gel to remove other impurities. The Norit and silica were removed by filtration through a Celite bed which had been packed in a size D glass filtration funnel. The liquor was then precipitated into 500ml of stirring ether forming a white precipitate, which was collected by filtration. This precipitate was purified twice more by reprecipitation in methylene chloride/ethyl ester, and the pure polymer was transferred to a pre-weighed 100ml airfree round bottom flask equipped with a side arm vacuum adapter and topped with a septum. The polymer was dried under vacuum for two days. The polymer was a powdery, white solid. Yield = 9.1961g. ¹H NMR in DMSO-*d*₆: 7.78 and 7.50 (CHs of aromatic ring), 4.11 (CH₂OTs), 3.51 (-O-CH₂-CH₂-), 3.24 (CH₃-O-), 2.43 (CH₃ of tosylate). FTIR, ν cm⁻¹: 2946, 2878, 2695, 1473, 1358, 1284, 1170, 1148, 1117, 1064, 949, 844, 810, 750.

Poly(ethylene oxide)-poly(2-ethyl 2-oxazoline) diblock copolymer (PEO-PEOX)

Polymerization of the PEO-PEOX diblock copolymer was performed in a manner similar to that of others. All glassware were oven dried prior to use. A two-necked, 250ml round bottom flask equipped with a condenser and vacuum adapter in the center arm, an addition funnel and glass stopper in the side arm, and a stirbar in the bottom, was evacuated and filled with nitrogen. 15ml (0.1490 mol) of 2-ethyl-2-oxazoline and 15ml of acetonitrile were placed in the reaction flask. 6.7838 g (0.00330 mol polymer and tosyl groups) of PEO-OTs were dissolved with 15ml of acetonitrile in the airfree flask and were transferred to the addition funnel with a syringe. The

PEO-OTs/acetonitrile solution was added to the reaction flask, and the addition funnel was rinsed with an additional 15ml of acetonitrile, which was then added to the reaction flask, for a total acetonitrile volume of 30ml. The reaction flask was heated at approximately 80°C for 48 hours. The reaction solution was then cooled in an ice bath after which time 2ml (0.0202 mol) of n-butyl amine were added to terminate the reaction. After 12 hours, the acetonitrile and excess n-butyl amine were removed by vacuum distillation. The resulting polymer was a colorless transparent solid. The polymer was dissolved in a minimum of chloroform and precipitated into 1000ml of ether. A white precipitate formed on the bottom of the flask and the liquid was removed by decantation. The polymer was purified a second time by reprecipitation in chloroform/ether and was dried under vacuum for 2 days. The polymer was a white solid. Yield = 21.21 g. ¹H NMR in CDCl₃: 3.66 (-O-CH₂-CH₂-), 3.47 (-N-CH₂-CH₂-), 2.42 and 2.33 (-CO-CH₂-CH₃), 1.14 (-CO-CH₂-CH₃). FTIR, ν cm⁻¹: 2972, 2936, 2878, 1646, 1473, 1426, 1379, 1200, 1111, 823.

Poly(ethylene oxide)-poly(ethylene imine) diblock copolymer (PEO-PEI)

Synthesis of the PEO-PEI diblock copolymer was accomplished by weak acid hydrolysis of the PEO-PEOX diblock copolymer using a modified procedure from Overberger and Peng.² 17.28g (0.00272 mol polymer, 0.1225 mol amide groups) of PEO-PEOX were placed in a single necked, 2000ml round bottom flask equipped with a condenser and vacuum adapter in the neck and a stirbar in the bottom. 350 ml of 6N HCl solution (2.1 mol) and 350 ml of methanol were added to the reaction flask and slowly dissolved the polymer. The solution was heated at 60°C for two days. After this time, the acidic solution was removed by vacuum distillation. The polymer was redissolved in 1000 ml of 3N HCl solution (3.0 mol) and the solution was again heated at 60°C for another three and a half days, at which time the polymer began to precipitate from solution. To ensure complete hydrolysis, the solution heated for another 24 hours at 60°C. After this time, the acidic solution was again removed by vacuum distillation. The resulting white PEO-PEI-H⁺Cl⁻ salt was dissolved with approximately 350 ml of water. After dissolution, a small amount of insoluble white precipitate formed, which was removed by vacuum filtration through a Büchner funnel fitted with standard filter paper. The acidic polymer solution was neutralized by the addition of approximately 150 ml of 10% NaOH solution, causing the polymer to precipitate from solution as fine white particles, which remained suspended in the aqueous solution. The pH of the solution was 14. The colloidal solution was vacuum filtered through a Büchner funnel fitted with standard filter paper to collect the polymer. The polymer was washed thoroughly with chloroform to remove unreacted PEO and low molecular weight diblock copolymer, and the chloroform/polymer suspension was vacuum filtered to recollect the polymer. This chloroform wash was repeated a second time. The polymer was recrystallized twice in water and was collected by vacuum filtration through a size D glass filtration funnel. The light yellow, solid polymer was transferred to a 200ml pear shaped flask where it was heated under vacuum at 110°C for six hours to remove residual water. After the polymer had stopped bubbling, the heat was removed and the polymer was dried at room temperature for another two days. The polymer was a clear, light yellow solid. Yield = 6.64g. ¹H NMR in MeOH-*d*: 3.65 (-O-CH₂-CH₂-), 2.75 (-NH-CH₂-CH₂-). FTIR, ν cm⁻¹: 3219, 2907, 2877, 2810, 2734, 1452, 1334, 1135, 1111, 803.

Poly(ethylene oxide)-poly(ethylene imine) dendritic diblock generation 0.5

All glassware were oven dried prior to use. A three-necked, 250ml round bottom flask equipped with a condenser and vacuum adapter in the center arm, an addition funnel and glass stopper in

one of the side arms, another glass stopper in the other side arm, and a stirbar in the bottom, was evacuated and filled with nitrogen. 5.2096g (8.531×10^{-4} mol polymer, 0.08275 mol amine groups) of PEO-PEI were dissolved in 40ml of methanol in a 50ml erlenmeyer flask. 20ml (0.222 mol) of methyl acrylate were added to the round bottom flask and were subsequently chilled in an ice bath for 15 minutes. All of the polymer/methanol solution was transferred to the addition funnel and was added dropwise over 35 minutes. The 50ml erlenmeyer flask and the addition funnel were rinsed with an additional 27ml of methanol, which were also added to the reaction flask, for a total methanol volume of 67ml. The reaction flask was covered with aluminum foil to prevent the polymer from yellowing, and the solution was allowed to warm to room temperature. After 48 hours, the majority of the methanol and the excess methyl acrylate were removed by vacuum distillation, and the polymer was left to dry under vacuum for two days. The polymer was dissolved in a minimum of chloroform and was purified by reprecipitation in approximately 475ml of hexanes. After stirring overnight, the polymer formed an opaque, yellow gne on the bottom of the flask. The chloroform and hexanes were removed by decantation, and the polymer was allowed to dry under vacuum for another two days. The polymer was a yellow, waxy solid. Yield = 11.90g. ^1H NMR in MeOH-*d*: 3.69 (-CH₂-CH₂-CO-OCH₃), 3.65 (-O-CH₂-CH₂-), 2.85 (-CH₂-CH₂-CO-OCH₃), 2.61 (-N-CH₂-CH₂-), 2.53 (-CH₂-CH₂-CO-OCH₃). FTIR, ν cm⁻¹: 2948, 2820, 1733, 1436, 1257, 1196, 1114, 1038, 844.

Poly(ethylene oxide)-poly(ethylene imine) dendritic diblock generation 1.0

All glassware were oven dried prior to use. Two three-necked round bottom flasks each equipped with an addition funnel and vacuum adapter in the center arm, a glass stopper in each of the two side arms, and a stir bar in the bottom, were evacuated and filled with nitrogen. 2550ml of ethylenediamine and 850ml of methanol were placed in each of the round bottom flasks, for a total ethylenediamine volume of 5100ml (76.3 mol) and a total methanol volume of 1700ml. The flasks and the ethylenediamine/methanol solution were chilled in an ice bath overnight. Two portions of PEO-PEI Generation 0.5 polymer, one of 2.1254g (1.471×10^{-4} mol polymer, 0.01427 mol ester groups) and the other of 2.1247g (1.470×10^{-4} mol polymer, 0.01426 mol ester groups), were each placed in a 50ml erlenmeyer flask and were each dissolved with 20ml of methanol. The two polymer/methanol solution portions were transferred to the two addition funnels, and the polymer/methanol solutions were added dropwise over 45-50 minutes. The total volume of polymer/methanol solution used in the reaction was 40ml (4.2501g polymer, 2.941×10^{-4} mol polymer, 0.0285 mol ester groups.) Each of the addition funnels was rinsed with an additional 10ml of methanol, for a total methanol volume of 1760ml. The two reaction flasks were covered with glass wool to keep the polymer from yellowing, and the solutions were stirred in ice baths for five days at temperatures between 5-12°C. After this time, the majority of methanol and excess ethylenedimaine were removed by vacuum distillation, and the polymer was left to dry under vacuum for two days. The polymer was redissolved in methanol and was purified by ultrafiltration in methanol through a BIOMAX polyethersulfone 5000 NMWL membrane. Unfortunately, some of the polymer had passed through the membrane, so the polymer/methanol solution which had passed through the membrane was concentrated by vacuum distillation, redissolved in methanol, and was purified by ultrafiltration in methanol through a BIOMAX polyethersulfone 5000 NMWL membrane again. The two pure polymer fractions from ultrafiltration were concentrated by vacuum distillation, and the polymer was again dried under vacuum for another day and a half. The polymer was a clear, light yellow, glassy solid. Yield = 4.16g. ^1H NMR in MeOH-*d*: 3.65 (-O-CH₂-CH₂-), 3.28 (-CO-NH-CH₂-

CH₂-NH₂), 2.85 (-N-CH₂-CH₂-CO-NH-), 2.75 (-CO-NH-CH₂-CH₂-NH₂), 2.62 (-N-CH₂-CH₂-), 2.41 (-N-CH₂-CH₂-CO-NH-). FTIR, ν cm⁻¹: 3255, 3058, 2935, 2830, 1654, 1555, 1475, 1346, 1112, 822.

Poly(ethylene oxide)-poly(ethylene imine) dendritic diblock generation 1.5

All glassware were oven dried prior to use. A three-necked, 250ml round bottom flask equipped with a condenser and vacuum adapter in the center arm, an addition funnel and glass stopper in one of the side arms, another glass stopper in the other side arm, and a stirbar in the bottom, was evacuated and filled with nitrogen. 4.16g (2.424×10^{-4} mol polymer, 0.02351 mol amine groups) of PEO-PEI generation 1.0 polymer were dissolved in 43ml of methanol. The polymer dissolved slowly over several hours. 10ml (0.111 mol) of methyl acrylate and 20ml of methanol were added to the round bottom flask and were subsequently chilled in an ice bath for 15 minutes. 37.5ml (3.63g polymer, 2.114×10^{-4} mol polymer, 0.02050 mol amine groups) of the polymer/methanol solution and 20ml of methanol were transferred to the addition funnel and were added dropwise over 40 minutes. The addition funnel was rinsed with an additional 13ml of methanol, which was then added to the reaction flask, for a total methanol volume of 90ml. The reaction flask was covered with aluminum foil to prevent the polymer from yellowing, and the solution was allowed to warm to room temperature. After 48 hours, the majority of the methanol and excess methyl acrylate were removed by vacuum distillation, and the polymer was left to dry under vacuum for four days. The polymer was dissolved in a minimum of chloroform and was purified by reprecipitation in approximately 475ml of hexanes. After stirring overnight, the polymer formed an opaque, golden yellow gunk on the bottom of the flask. The chloroform and hexanes were removed by decantation, and the polymer was allowed to dry under vacuum for another three days. The polymer was redissolved in approximately 50ml of methanol to free trapped hexanes, and the methanol was removed by vacuum distillation. The polymer was again left to dry under vacuum for another day and a half. The polymer was a yellow, viscous liquid. Yield = 5.91g. ¹H NMR in MeOH-*d*: 3.69 (-CH₂-CH₂-CO-OCH₃), 3.65 (-O-CH₂-CH₂-), 3.27 (-CO-NH-CH₂-CH₂-N<), 2.87 (-CH₂-CH₂-CO-NH-), 2.80 (-CH₂-CH₂-CO-OCH₃), 2.66 (-N-CH₂-CH₂-), 2.59 (-CO-NH-CH₂-CH₂-N<), 2.49 (-CH₂-CH₂-CO-OCH₃), 2.42 (-CH₂-CH₂-CO-NH-). FTIR, ν cm⁻¹: 3303, 3071, 2952, 2820, 1740, 1652, 1542, 1438, 1362, 1258, 1202, 1043, 847.

Poly(ethylene oxide)-poly(ethylene imine) dendritic diblock generation 2.0

All glassware were oven dried prior to use. Three three-necked 5000ml round bottom flasks, each equipped with an addition funnel and vacuum adapter in the center arm, a glass stopper in each of the two side arms, and a stir bar in the bottom, were evacuated and filled with nitrogen. 2780ml of ethylenediamine and 840ml of methanol were placed in each of the round bottom flasks, for a total ethylenediamine volume of 8340ml (124.8 mol) and a total methanol volume of 2520ml. The flasks and the ethylenediamine/methanol solutions were chilled in ice baths overnight. 3.78g (1.117×10^{-4} mol polymer, 0.02166 mol ester groups) of PEO-PEI Generation 1.5 polymer were dissolved in 60ml of methanol. A 20ml portion of the polymer/methanol solution was transferred to each of the three addition funnels, and the polymer/methanol solutions were added dropwise to the ethylenediamine/methanol solutions over 15-20 minutes. Each of the addition funnels was rinsed with an additional 5ml of methanol, which was then added to the reaction flasks, for a total methanol volume of 2595ml. The three reaction flasks were covered with glass wool to prevent the polymer from yellowing, and the solutions were stirred in ice baths for six days at temperatures between 5-12°C. After this time, the majority of

the excess ethylenediamine and methanol were removed by vacuum distillation, and the polymer was left to dry under vacuum overnight. The polymer was redissolved in methanol and was purified by ultrafiltration in methanol through a BIOMAX polyethersulfone 5000 NMWL membrane. Unfortunately, some of the polymer passed through the membrane, so the polymer/methanol solution which had passed through the membrane was concentrated by vacuum distillation, redissolved in methanol, and was purified by ultrafiltration in methanol through a PLBC regenerated cellulose 3000 NMWL membrane. The two pure polymer fractions from ultrafiltration were concentrated by vacuum distillation, and the polymer was again dried under vacuum for another day. The polymer was a clear, yellow, glassy solid. Yield = 3.9167g. ^1H NMR in MeOH-*d*: 3.65 (-O-CH₂-CH₂-), 3.28 (-CO-NH-CH₂-CH₂-N<) and (-CO-NH-CH₂-CH₂-NH₂), 2.82 (-CH₂-CH₂-CO-NH-), 2.77 (-CO-NH-CH₂-CH₂-NH₂), 2.62 (-N-CH₂-CH₂-) and (-CO-NH-CH₂-CH₂-N<), 2.40 (-CH₂-CH₂-CO-NH-). FTIR, ν cm⁻¹: 3261, 3058, 2938, 2823, 1652, 1548, 1466, 1334, 1252, 1110, 1039, 820.

Poly(ethylene oxide)-poly(ethylene imine) dendritic diblock generation 2.5

All glassware were oven dried prior to use. A two-necked, 250ml round bottom flask equipped with a condenser and vacuum adapter in the center arm, an addition funnel and glass stopper in the side arm, and a stir bar in the bottom, was evacuated and filled with nitrogen. 3.91g (9.95×10^{-5} mol polymer, 0.01931 mol amine groups) of PEO-PEI generation 2.0 polymer were dissolved in 80 ml of methanol. The polymer dissolved slowly over several hours. 10ml (0.111 mol) of methyl acrylate and 20ml of methanol were added to the round bottom flask and were subsequently chilled in an ice bath for 25 minutes. 71ml (3.47g polymer, 8.834×10^{-5} mol polymer, 0.01714 mol amine groups) of the polymer/methanol solution were transferred to the addition funnel and were added dropwise over 40 minutes. The addition funnel was rinsed with an additional 5ml of methanol, which was then added to the reaction flask, for a total methanol volume of 96ml. The reaction flask was covered with aluminum foil to prevent the polymer from yellowing, and the solution was allowed to warm to room temperature. After 48 hours, the majority of methanol and excess methyl acrylate were removed by vacuum distillation, and the polymer was left to dry under vacuum for four days. The polymer was dissolved in a minimum of chloroform and was purified by reprecipitation in approximately 700ml of hexanes. After stirring for two hours, the polymer formed an opaque, golden yellow glee on the bottom of the flask. The chloroform and hexanes were removed by decantation, and the polymer was allowed to dry under vacuum for another one and a half days. The polymer was redissolved in approximately 50ml of methanol to free trapped hexanes, and the methanol was removed by vacuum distillation. The polymer was again left to dry under vacuum for another four days. The polymer was a golden yellow, very viscous liquid. Yield = 5.29g. ^1H NMR in MeOH-*d*: 3.69 (-CH₂-CH₂-CO-OCH₃), 3.65 (-O-CH₂-CH₂-), 3.28 (-CO-NH-CH₂-CH₂-N<), 2.85 (-CH₂-CH₂-CO-NH), 2.79 (-CH₂-CH₂-CO-OCH₃), 2.64 (-N-CH₂-CH₂-) and (-CO-NH-CH₂-CH₂-N<) next to a whole branch, 2.58 (-CO-NH-CH₂-CH₂-N<) next to a half branch, 2.49 (-CH₂-CH₂-CO-OCH₃), 2.41 (-CH₂-CH₂-CO-NH-). FTIR, ν cm⁻¹: 3272, 3064, 2944, 2823, 1739, 1646, 1542, 1433, 1362, 1258, 1203, 1050, 842.

Poly(ethylene oxide)-poly(ethylene imine) dendritic diblock generation 3.0

All glassware were oven dried prior to use. Three three-necked, 5000ml round bottom flasks each equipped with an addition funnel and vacuum adapter in the center arm, a glass stopper in each of the two side arms, and a stir bar in the bottom, were evacuated and filled with nitrogen.

3000ml of ethylenediamine and 775ml of methanol were placed in each of the round bottoms flasks, for a total ethylenediamine volume of 9000ml (134.6 mol) and a total methanol volume of 2325ml. The flasks and the ethylenediamine/methanol solutions were chilled in ice baths overnight. 3.43g (4.721×10^{-5} mol polymer, 0.01832 mol ester groups) of PEO-PEI Generation 2.5 polymer were dissolved in 64ml of methanol. A 20ml portion of the polymer/methanol solution was transferred to each of the three addition funnels, and the polymer/methanol solutions were added dropwise to the ethylenediamine/methanol solutions over 40-45 minutes. The total volume of polymer/methanol solution used in the reaction was 60ml (3.22g polymer, 4.426×10^{-5} mol polymer, 0.01720 mol ester groups.) Each of the addition funnels was rinsed with an additional 10ml of methanol, which was then added to the reaction flasks, for a total methanol volume of 2415ml. The three reaction flasks were covered with glass wool to prevent the polymer from yellowing, and the solutions were stirred in ice baths for seven days at temperatures between 5-12°C. After this time, the majority of the methanol and excess ethylenediamine were removed by vacuum distillation, and the polymer was left to dry under vacuum for three and a half days. The polymer was redissolved in methanol and was purified by ultrafiltration in methanol through a BIOMAX polyethersulfone 5000 NMWL membrane. Unfortunately, some of the polymer passed through the membrane, so the polymer/methanol solution that had passed through the membrane was concentrated by vacuum distillation, redissolved in methanol, and was purified by ultrafiltration in methanol through a PLBC regenerated cellulose 3000 NMWL membrane. The two pure polymer fractions from ultrafiltration were combined, the methanol was removed by vacuum distillation, and the polymer was again dried under vacuum for another two days. The polymer was a clear, orange, glassy solid. Yield = 3.7995g. ^1H NMR in MeOH-*d*: 3.65 (-O-CH₂-CH₂-), 3.28 (-CO-NH-CH₂-CH₂-N<) and (-CO-NH-CH₂-CH₂-NH₂), 2.81 (-CH₂-CH₂-CO-NH-), 2.75 (-CO-NH-CH₂-CH₂-NH₂), 2.60 (-N-CH₂-CH₂-) and (-CO-NH-CH₂-CH₂-N<), 2.39 (-CH₂-CH₂-CO-NH-). FTIR, ν cm⁻¹: 3268, 3063, 2930, 2835, 1648, 1554, 1465, 1438, 1349, 1282, 1243, 1149, 1038, 689.

Poly(ethylene oxide)-poly(ethylene imine) dendritic diblock generation 3.5

All glassware were oven dried prior to use. A two-necked, 250ml round bottom flask equipped with a condenser and vacuum adapter in the center arm, an addition funnel and glass stopper in the side arm, and a stir bar in the bottom, was evacuated and filled with nitrogen. 3.7956g (4.545×10^{-5} mol polymer, 0.01763 mol amine groups) of PEO-PEI Generation 3.0 polymer were dissolved in 70ml of methanol. The polymer dissolved slowly over several hours. 10ml (0.111 mol) of methyl acrylate and 20ml of methanol were added to the round bottom flask and were subsequently chilled in an ice bath for 25 minutes. 60ml (3.2534g polymer, 3.896×10^{-5} mol polymer, 0.01512 mol amine groups) of the polymer/methanol solution were transferred to the addition funnel and were added dropwise to the methyl acrylate/methanol solution over 35 minutes. The addition funnel was rinsed with an additional 17ml of methanol, which was then added to the reaction flask, for a total methanol volume of 97ml. The reaction flask was covered with aluminum foil to prevent the polymer from yellowing, and the solution was allowed to warm to room temperature. After 60 hours, the majority of the methanol and excess methyl acrylate were removed by vacuum distillation, and the polymer was left to dry under vacuum for 52 hours. The polymer was dissolved in a minimum of chloroform and was purified by reprecipitation in approximately 900ml of hexanes. After stirring overnight, the polymer formed an opaque, orange glee on the bottom of the flask. The chloroform and hexanes were removed by decantation, and the polymer was allowed to dry under vacuum for another three days. The

polymer was redissolved in approximately 30ml of methanol to free trapped hexanes, and the methanol was removed by vacuum distillation. The polymer was again left to dry under vacuum for another two and a half days. The polymer was an orange, very viscous liquid. Yield = 4.89 g. ^1H NMR in MeOH-*d*: 3.69 (-CH₂-CH₂-CO-OCH₃), 3.65 (-O-CH₂-CH₂-), 3.28 (-CO-NH-CH₂-CH₂-N<), 2.85 (-CH₂-CH₂-CO-NH-), 2.79 (-CH₂-CH₂-CO-OCH₃), 2.64 (-N-CH₂-CH₂-) and (-CO-NH-CH₂-CH₂-N<) next to a whole branch, 2.58 (-CO-NH-CH₂-CH₂-N<) next to a half branch, 2.49 (-CH₂-CH₂-CO-OCH₃), 2.41 (-CH₂-CH₂-CO-NH-). FTIR, ν cm⁻¹: 3288, 3069, 2951, 2823, 1736, 1651, 1544, 1437, 1367, 1255, 1196, 1046, 843.

Poly(ethylene oxide)-poly(ethylene imine) dendritic diblock generation 4.0

All glassware were oven dried prior to use. Two three-necked, 5000ml round bottom flasks each equipped with an addition funnel and vacuum adapter in the center arm, a glass stopper in each of the two side arms, and a stir bar in the bottom, were evacuated and filled with nitrogen. 3530ml of ethylenediamine and 1000ml of methanol were placed in each of the round bottom flasks, for a total ethylenediamine volume of 7060ml (105.6 mol) and a total methanol volume of 2000ml. The flasks and the ethylenediamine/methanol solutions were chilled in ice baths overnight. 3.0239g (2.0126x10⁻⁵ mol polymer, 0.01562 mol ester groups) of PEO-PEI Generation 3.5 polymer were dissolved in 60ml of methanol. A 20ml portion of the polymer/methanol solution was transferred to each of the two addition funnels, and the polymer/methanol solutions were added dropwise to the ethylenediamine/methanol solutions over 70 minutes. The total volume of polymer/methanol solution used in the reaction was 40ml (2.0159g polymer, 1.338x10⁻⁵ mol polymer, 0.0104 mol ester groups.) Each of the addition funnels was rinsed with an additional 35ml of methanol, which was then added to the reaction flasks, for a total methanol volume of 2110ml. The two reaction flasks were covered with glass wool to prevent the polymer from yellowing, and the solutions were stirred in ice baths for eight days at temperatures between 5-12°C. After this time, the majority of the methanol and excess ethylenediamine were removed by vacuum distillation, and the polymer was left to dry under vacuum for three days. The polymer was redissolved in methanol and was purified by ultrafiltration in methanol through a BIOMAX polyethersulfone 5000 NMWL membrane. Unfortunately, some of the polymer passed through the membrane, so the polymer/methanol solution which had passed through the membrane was concentrated by vacuum distillation, redissolved in methanol, and was purified by ultrafiltration in methanol through a PLBC regenerated cellulose 3000 NMWL membrane. The two pure polymer fractions from ultrafiltration were combined, the methanol was removed by vacuum distillation, and the polymer was again dried under vacuum for another two days. The polymer was a clear, brown, glassy solid. Yield = 2.5820g. ^1H NMR in MeOH-*d*: 3.65 (-O-CH₂-CH₂-), 3.28 (-CO-NH-CH₂-CH₂-N<) and (-CO-NH-CH₂-CH₂-NH₂), 2.81 (-CH₂-CH₂-CO-NH), 2.75 (-CO-NH-CH₂-CH₂-NH₂), 2.60 (-N-CH₂-CH₂-) and (-CO-NH-CH₂-CH₂-N<), 2.39 (-CH₂-CH₂-CO-NH-). FTIR, ν cm⁻¹: 3257, 3057, 2930, 2819, 1648, 1543, 1460, 1432, 1349, 1243, 1149, 1033.

Poly(ethylene oxide)-poly(ethylene imine) dendritic diblock generation 4.5

All glassware were oven dried prior to use. A two-necked, 250ml round bottom flask equipped with a condenser and vacuum adapter in the center arm, an addition funnel and glass stopper in the side arm, and a stir bar in the bottom, was evacuated and filled with nitrogen. 2.5820g (1.5014x10⁻⁵ mol polymer, 0.01165 mol amine groups) of PEO-PEI Generation 4.0 polymer were dissolved in 80ml methanol. The polymer dissolved very slowly over 60 hours. During

this time, the polymer/methanol solution was sonicated a total of four hours to increase the dissolution rate. 5ml (0.0555 mol) of methyl acrylate and 10ml of methanol were added to the round bottom flask and were subsequently chilled in an ice bath for 25 minutes. 50ml (1.6138g polymer, 9.38×10^{-6} mol polymer, 0.00728 mol amine groups) of the polymer/methanol solution were transferred to the addition funnel and were added dropwise to the methyl acrylate/methanol solution over one and a half hours. The addition funnel was rinsed with an additional 5ml of methanol, which was then added to the reaction flask, for a total methanol volume of 65ml. The solution was allowed to warm to room temperature. After 60 hours, the majority of the methanol and excess methyl acrylate were removed by vacuum distillation, and the polymer was left to dry under vacuum for two days. The polymer was dissolved in a minimum of chloroform and was purified by reprecipitation in approximately 800ml of hexanes. After stirring overnight, the polymer formed a brown gne on the bottom of the flask. The chloroform and hexanes were removed by decantation, and the polymer was allowed to dry under vacuum for another two days. The polymer was redissolved in methanol to free trapped hexanes, and the methanol was removed by vacuum distillation. The polymer was again left to dry under vacuum for another two days. The polymer was a brown, soft, sticky solid. Yield = 3.2967g. $^1\text{H NMR}$ in MeOH-*d*: 3.69 (-CH₂-CH₂-CO-OCH₃), 3.65 (-O-CH₂-CH₂-), 3.28 (-CO-NH-CH₂-CH₂-N<), 2.84 (-CH₂-CH₂-CO-NH-), 2.79 (-CH₂-CH₂-CO-OCH₃), 2.64 (-N-CH₂-CH₂-) and (-CO-NH-CH₂-CH₂-N<) next to a whole branch, 2.58 (-CO-NH-CH₂-CH₂-N<) next to a half branch, 2.49 (-CH₂-CH₂-CO-OCH₃), 2.40 (-CH₂-CH₂-CO-NH-). FTIR, ν cm⁻¹: 3285, 3066, 2954, 2832, 1738, 1648, 1546, 1439, 1359, 1263, 1199, 1050, 847, 751.

2.A.1.2 Linear Dendritic Rod Diblock Copolymers Consisting of a Polyethylene Oxide Block of 43 Repeats and a Dendritic Block of 178 Repeats

Poly(ethylene oxide) monomethyl ether tosylate (PEO-OTs)

PEO-OTs was prepared using an adaptation of two known procedures. All glassware were oven dried prior to use. A single neck, 100ml round bottom flask equipped with an addition funnel and glass stopper, a side arm vacuum adapter, and a stir bar in the bottom, was evacuated and filled with nitrogen. 10.53g (0.00554 mol polymer and hydroxyl groups) of pre-dried m-PEO-OH were transferred to the round bottom flask through a solids funnel, which temporarily replaced the addition funnel. 30ml of pyridine were added to the flask, the flask was immersed in an ice bath, and the solution was stirred for 20 minutes. 5.0603g (0.0265 mol) of tosyl chloride were dissolved in 20ml of pyridine in a 50ml erlenmeyer flask. This tosyl chloride/pyridine solution was transferred to the addition funnel and was added dropwise to the chilled PEO-OH/pyridine solution over 10 minutes. The total volume of pyridine used was 50ml (0.6182 mol.) The reaction solution, which was a golden yellow color, was maintained at 0°C for 12 hours with the ice bath. The polymer was recovered by slow precipitation of the reaction solution into 750ml of cold, stirring anhydrous ethyl ether. The resulting precipitate was collected by vacuum filtration through a size D glass filtration funnel. The polymer was recrystallized five times in absolute ethanol by dissolution at 50°C, crystallization at 0°C, and collection by vacuum filtration. Finally, it was washed with 100ml of cold diethyl ether and collected by vacuum filtration. The pure polymer was transferred to a pre-weighed 100ml

airfree round bottom flask equipped with a side arm vacuum adapter and topped with a rubber septum. The polymer was dried under vacuum for two days. The polymer was a powdery, white solid. Yield = 6.71g. ^1H NMR in $\text{DMSO-}d_6$: 7.78 and 7.50 (CHs of aromatic ring), 4.11 (CH_2OTs), 3.51 ($-\text{O}-\text{CH}_2-\text{CH}_2-$), 3.24 ($\text{CH}_3-\text{O}-$), 2.43 (CH_3 of tosylate). FTIR, ν cm^{-1} : 2945, 2880, 2692, 1468, 1361, 1280, 1170, 1150, 1115, 1062, 947, 843, 810, 750

Poly(ethylene oxide)-poly(2-ethyl 2-oxazoline) diblock copolymer (PEO-PEOX)

Polymerization of the PEO-PEOX diblock copolymer was performed in a manner similar to that of others. All glassware were oven dried prior to use. A three-necked, 100ml round bottom flask equipped with a condenser and vacuum adapter in the center arm, and addition funnel and a rubber septum in one of the side arms, a glass stopper in the other side arm, and a stirbar in the bottom, was evacuated and filled with nitrogen. 9ml (0.0892 mol) of 2-ethyl-2-oxazoline and 10ml of acetonitrile were placed in the reaction flask. 6.71g (0.00327 mol polymer and tosyl groups) of PEO-OTs were dissolved with 30ml of acetonitrile in the airfree flask. 9ml (2.01g polymer, 9.79×10^{-4} mol polymer and tosyl groups) of the PEO-OTs/acetonitrile solution were transferred to the addition funnel with a syringe, and the solution was added to the reaction flask. The addition funnel was rinsed with an additional 7ml of acetonitrile, which was then added to the reaction flask, for a total acetonitrile volume of 25ml. The reaction flask was heated at approximately 80°C for 46 hours. The reaction solution was chilled in an ice bath for 30 minutes after which time 2ml (0.0202 mol) of n-butyl amine were added to terminate the reaction. After the solution was allowed to stir overnight, the acetonitrile and excess n-butyl amine were removed by vacuum distillation. The resulting polymer was a colorless transparent solid. The polymer was dissolved in a minimum of chloroform and precipitated into 1000ml of ether. A white precipitate formed on the bottom of the flask, and the liquid was removed by decantation. The polymer was purified a second time by reprecipitation in chloroform/ether and was dried under vacuum overnight. The polymer was a white solid. Yield = 10.77g. ^1H NMR in CDCl_3 : 3.67 ($-\text{O}-\text{CH}_2-\text{CH}_2-$), 3.47 ($-\text{N}-\text{CH}_2-\text{CH}_2-$), 2.43 and 2.33 ($-\text{CO}-\text{CH}_2-\text{CH}_3$), 1.14 ($-\text{CO}-\text{CH}_2-\text{CH}_3$). FTIR, ν cm^{-1} : 2977, 2936, 2881, 1645, 1474, 1426, 1380, 1247, 1199, 1110, 822.

Poly(ethylene oxide)-poly(ethylene imine) diblock copolymer (PEO-PEI)

Synthesis of the PEO-PEI diblock copolymer was accomplished by weak acid hydrolysis of the PEO-PEOX diblock copolymer using a modified procedure from Overberger and Peng. 10.2749g (9.388×10^{-4} mol of polymer, 0.08543 mol amide groups) of PEO-PEOX were placed in a single necked, 1000ml round bottom flask equipped with a condenser and vacuum adapter in the neck and a stirbar in the bottom. 205ml of 6N HCl solution (1.23 mol) and 205ml of methanol were added to the reaction flask. The solution was heated at 60°C for two days. After this time, the acidic solution was removed by vacuum distillation. The polymer was redissolved in 514ml of 3N HCl solution (1.54 mol), and the solution was once again heated at 60°C for another four days, at which time the polymer began to precipitate from solution. The acidic solution was again removed by vacuum distillation. To ensure complete hydrolysis, the polymer was once again redissolved in 514ml of 3N HCl solution (1.54 mol), and the solution was heated at 60°C overnight. This acidic solution was removed by vacuum distillation one last time. The resulting PEO-PEI-HCl salt was dissolved with approximately 200ml of water, and the solution was divided into two portions. Each portion was transferred to a 1000ml separatory funnel, and 400ml of chloroform were added to each portion at which point the polymer began to precipitate. The polymer was then neutralized in the separatory funnel by the addition of 10% NaOH until

the pH was 14. The chloroform was removed and the polymer solution was extracted four more times with approximately 400ml of chloroform to remove unreacted PEO and low molecular weight diblock copolymer. The polymer was collected by vacuum filtration through a size D glass filtration funnel. The polymer was purified by recrystallized in water and was collected by vacuum filtration through a size D glass filtration funnel. The light yellow, solid polymer was transferred to a 200ml pear shaped flask where it was heated under vacuum to remove residual water. After the polymer had stopped bubbling, the heat was removed and the polymer was dried at room temperature for a day. The polymer was a clear, light yellow solid. Yield = 4.00g. ^1H NMR in MeOH-*d*: 3.65 (-O-CH₂-CH₂-), 2.74 (-NH-CH₂-CH₂-). FTIR, ν cm⁻¹: 3251, 2880, 2816, 1468, 1404, 1356, 1287, 1107, 815.

Poly(ethylene oxide)-poly(ethylene imine) dendritic diblock generation 0.5

All glassware were oven dried prior to use. A three-necked, 100ml round bottom flask equipped with a condenser and vacuum adapter in the center arm, an additional funnel and glass stopper in one of the side arms, another glass stopper in the other side arm, and a stirbar in the bottom, was evacuated and filled with nitrogen. 3.0966g (3.2290×10^{-4} mol polymer, 0.05748 mol amine groups) of PEO-PEI were dissolved in 40ml of methanol in a 50ml Erlenmeyer flask. 14ml (0.1555 mol) of methyl acrylate were added to the round bottom flask and were subsequently chilled in an ice bath for 20 minutes. The polymer/methanol solution was transferred to the addition funnel and was added dropwise over 20 minutes. The 50ml erlenmeyer flask and the addition funnel were rinsed with an additional 10ml of methanol, which were also added to the reaction flask, for a total methanol volume of 50ml. The reaction flask was covered with aluminum foil to prevent the polymer from yellowing and the solution was allowed to warm to room temperature. After 48 hours, the majority of the methanol and the excess methyl acrylate were removed by vacuum distillation, and the polymer was left to dry under vacuum for two days. The polymer was a yellow, waxy solid. Yield = 7.5380g. ^1H NMR in MeOH-*d*: 3.69 (-CH₂-CH₂-CO-OCH₃), 3.65 (-O-CH₂-CH₂-), 2.85 (-CH₂-CH₂-CO-OCH₃), 2.60 (-N-CH₂-CH₂-), 2.52 (-CH₂-CH₂-CO-OCH₃). FTIR, ν cm⁻¹: 2954, 2816, 1738, 1436, 1255, 1202, 1181, 1123, 1038, 846.

2.A.2 End Group Modification

2.A.2.1 Linear Dendritic Diblock Copolymers Consisting of a Polyethylene Oxide Block of 43 Repeats and a Dendritic Block of 97 repeats

Poly(ethylene oxide)-poly(ethylene imine) dendritic diblock generation 1.0-butyl terminated

All glassware were oven dried prior to use. A two-necked, 250ml round bottom flask equipped with a condenser and vacuum adapter in the center arm, an addition funnel and glass stopper in the side arm, and a stir bar in the bottom, was evacuated and filled with nitrogen. 20ml (0.202 mol) of n-butyl amine and 20ml of methanol were added to the round bottom flask and were subsequently chilled in an ice bath for 5 minutes. 0.5026g (3.478×10^{-5} mol polymer, 0.00337 mol ester groups) of PEO-PEI generation 0.5 polymer were dissolved with 20 ml of methanol in a 50ml erlenmeyer flask. This polymer/methanol solution was transferred to the addition funnel and was added dropwise over 10 minutes. The 50ml erlenmeyer flask and the addition funnel

were rinsed with an additional 5ml of methanol, which was then added to the reaction flask, for a total methanol volume of 45ml. The reaction flask was covered with aluminum foil to prevent the polymer from yellowing, and the solution was allowed to warm to room temperature. After 24 hours, an oil bath was placed beneath the reaction flask and the solution was heated at 40°C. After four days of heating, the majority of the methanol and excess n-butyl amine were removed by vacuum distillation, and the polymer was left to dry under vacuum for two days. The polymer was purified twice by reprecipitation in chloroform/ethyl ether to remove traces of n-butyl amine. The polymer was again dried under vacuum for another two days. The polymer was a light yellow, very viscous liquid. Yield = 0.4651g. 98% substitution. ¹H NMR in MeOH-*d*: 3.69 (unreacted -CH₂-CH₂-CO-OCH₃), 3.65 (-O-CH₂-CH₂-), 3.20 (-CO-NH-CH₂-CH₂-CH₂-CH₃), 2.84 (-CH₂-CH₂-CO-NH-), 2.62 (-N-CH₂-CH₂-), 2.38 (-CH₂-CH₂-CO-NH-), 1.51 (-CO-NH-CH₂-CH₂-CH₂-CH₃), 1.38 (-CO-NH-CH₂-CH₂-CH₂-CH₃), 0.94 (-CO-NH-CH₂-CH₂-CH₂-CH₃). FTIR, ν cm⁻¹: 3280, 3065, 2958, 2928, 2866, 2810, 1738, 1646, 1554, 1467, 1115.

Poly(ethylene oxide)-poly(ethylene imine) dendritic diblock generation 1.0-hexyl terminated

All glassware were oven dried prior to use. A two-necked, 250ml round bottom flask equipped with a condenser and vacuum adapter in the center arm, an addition funnel and glass stopper in the side arm, and a stir bar in the bottom, was evacuated and filled with nitrogen. 25ml (0.189 mol) of n-hexyl amine and 20ml of methanol were added to the round bottom flask and were subsequently chilled in an ice bath for 10 minutes. 0.5042g (3.490x10⁻⁵ mol polymer, 0.00339 mol ester groups) of PEO-PEI generation 0.5 polymer were dissolved with 20 ml of methanol in a 50ml erlenmeyer flask. This polymer/methanol solution was transferred to the addition funnel and was added dropwise over 10 minutes. The 50ml erlenmeyer flask and the addition funnel were rinsed with an additional 11ml of methanol, which was then added to the reaction flask, for a total methanol volume of 51ml. The reaction flask was covered with aluminum foil to prevent the polymer from yellowing, and the solution was allowed to warm to room temperature. After 24 hours, an oil bath was placed beneath the reaction flask and the solution was heated at 40°C. After four days of heating, the majority of the methanol and excess n-hexyl amine were removed by vacuum distillation, and the polymer was left to dry under vacuum for two days. The polymer was purified twice by reprecipitation in chloroform/ethyl ether to remove traces of n-hexyl amine. The polymer was again dried under vacuum for another day. The polymer was a light yellow, very viscous liquid. Yield = 0.4529g. 95% substitution. ¹H NMR in MeOH-*d*: 3.69 (unreacted -CH₂-CH₂-CO-OCH₃), 3.65 (-O-CH₂-CH₂-), 3.19 (-CO-NH-CH₂-CH₂-(CH₂)₃-CH₃), 2.81 (-CH₂-CH₂-CO-NH-), 2.61 (-N-CH₂-CH₂-), 2.37 (-CH₂-CH₂-CO-NH-), 1.51 (-CO-NH-CH₂-CH₂-(CH₂)₃-CH₃), 1.34 (-CO-NH-CH₂-CH₂-(CH₂)₃-CH₃), 0.94 (-CO-NH-CH₂-CH₂-(CH₂)₃-CH₃). FTIR, ν cm⁻¹: 3285, 3071, 2953, 2922, 2856, 2815, 1743, 1651, 1549, 1462, 1115.

Poly(ethylene oxide)-poly(ethylene imine) dendritic diblock generation 1.0-octyl terminated

All glassware were oven dried prior to use. A two-necked, 250ml round bottom flask equipped with a condenser and vacuum adapter in the center arm, an addition funnel and glass stopper in the side arm, and a stir bar in the bottom, was evacuated and filled with nitrogen. 32ml (0.194 mol) of n-octyl amine and 20ml of methanol were added to the round bottom flask and were subsequently chilled in an ice bath for 10 minutes. 0.5051g (3.496x10⁻⁵ mol polymer, 0.00339 mol ester groups) of PEO-PEI generation 0.5 polymer were dissolved with 20 ml of methanol in

a 50ml erlenmeyer flask. This polymer/methanol solution was transferred to the addition funnel and was added dropwise over 10 minutes. The 50ml erlenmeyer flask and the addition funnel were rinsed with an additional 25ml of methanol, which was then added to the reaction flask, for a total methanol volume of 65ml. The reaction flask was covered with aluminum foil to prevent the polymer from yellowing, and the solution was allowed to warm to room temperature. After 24 hours, an oil bath was placed beneath the reaction flask and the solution was heated at 40°C. After four days of heating, the majority of the methanol and excess n-octyl amine were removed by vacuum distillation, and the polymer was left to dry under vacuum for two days. The polymer was purified twice by reprecipitation in chloroform/ethyl ether to remove traces of n-octyl amine. The polymer was again dried under vacuum for another two days. The polymer was a light yellow, very viscous liquid. Yield = 0.1804g. 87% substitution. ¹H NMR in MeOH-*d*: 3.70 (unreacted -CH₂-CH₂-CO-OCH₃), 3.65 (-O-CH₂-CH₂-), 3.19 (-CO-NH-CH₂-CH₂-(CH₂)₅-CH₃), 2.82 (-CH₂-CH₂-CO-NH-), 2.62 (-N-CH₂-CH₂-), 2.50 (unreacted -CH₂-CH₂-CO-OCH₃), 2.38 (-CH₂-CH₂-CO-NH-), 1.51 (-CO-NH-CH₂-CH₂-(CH₂)₅-CH₃), 1.34 (-CO-NH-CH₂-CH₂-(CH₂)₅-CH₃), 0.93 (-CO-NH-CH₂-CH₂-(CH₂)₅-CH₃). FTIR, ν cm⁻¹: 3280, 3071, 2950, 2922, 2856, 2815, 1743, 1646, 1554, 1462, 1115.

Poly(ethylene oxide)-poly(ethylene imine) dendritic diblock generation 1.0-decyl terminated

All glassware were oven dried prior to use. A two-necked, 250ml round bottom flask equipped with a condenser and vacuum adapter in the center arm, an addition funnel and glass stopper in the side arm, and a stir bar in the bottom, was evacuated and filled with nitrogen. 23ml (0.115 mol) of n-decyl amine and 20ml of methanol were added to the round bottom flask and were subsequently chilled in an ice bath for 20 minutes. 0.5000g (3.460×10^{-5} mol polymer, 0.00336 mol ester groups) of PEO-PEI generation 0.5 polymer were dissolved with 10 ml of methanol in a 50ml erlenmeyer flask. This polymer/methanol solution was transferred to the addition funnel and was added dropwise over 5 minutes. The 50ml erlenmeyer flask and the addition funnel were rinsed with an additional 16ml of methanol, which was added to the reaction flask, for a total methanol volume of 46ml. The reaction flask was covered with aluminum foil to prevent the polymer from yellowing, and the solution was allowed to warm to room temperature. After 24 hours, an oil bath was placed beneath the reaction flask and the solution was heated at 40°C. After four days of heating, the majority of the methanol and excess n-decyl amine were removed by vacuum distillation, and the polymer was left to dry under vacuum for a day. The polymer was redissolved in methanol and was purified by ultrafiltration in methanol through a PLBC regenerated cellulose 3000 NMWL membrane to remove traces of n-decyl amine. The pure polymer/methanol ultrafiltration solution was concentrated by vacuum distillation, and the polymer was again dried under vacuum for another day and a half. The polymer was a light yellow, very viscous liquid. Yield = 0.5175g. 93% substitution. ¹H NMR in MeOH-*d*: 3.70 (unreacted -CH₂-CH₂-CO-OCH₃), 3.65 (-O-CH₂-CH₂-), 3.19 (-CO-NH-CH₂-CH₂-(CH₂)₇-CH₃), 2.81 (-CH₂-CH₂-CO-NH-), 2.61 (-N-CH₂-CH₂-), 2.38 (-CH₂-CH₂-CO-NH-), 1.53 (-CO-NH-CH₂-CH₂-(CH₂)₇-CH₃), 1.32 (-CO-NH-CH₂-CH₂-(CH₂)₇-CH₃), 0.93 (-CO-NH-CH₂-CH₂-(CH₂)₇-CH₃). FTIR, ν cm⁻¹: 3285, 3071, 2952, 2922, 2856, 2815, 1743, 1646, 1549, 1462, 1355, 1115, 724.

Poly(ethylene oxide)-poly(ethylene imine) dendritic diblock generation 1.0-dodecyl terminated

All glassware were oven dried prior to use. A two-necked, 250ml round bottom flask equipped with a condenser and vacuum adapter in the center arm, an addition funnel and glass stopper in the side arm, and a stir bar in the bottom, was evacuated and filled with nitrogen. 13.7400g (0.0741 mol) of n-dodecyl amine were dissolved with 15ml of methanol in a 125ml erlenmeyer flask and were subsequently added to the round bottom flask. The solution was cooled in an ice bath for 15 minutes. 0.5063g (3.5040×10^{-5} mol polymer, 0.00340 mol ester groups) of PEO-PEI generation 0.5 polymer were dissolved with 10 ml of methanol in a 50ml erlenmeyer flask. This polymer/methanol solution was transferred to the addition funnel and was added dropwise over 5 minutes. The erlenmeyer flask and the addition funnel were rinsed with an additional 5ml of methanol, which was added to the reaction flask, for a total methanol volume of 30ml. The reaction flask was covered with aluminum foil to prevent the polymer from yellowing, and the solution was allowed to warm to room temperature. After 24 hours, an oil bath was placed beneath the reaction flask and the solution was heated at 40°C. After four days of heating, the majority of the methanol and excess n-dodecyl amine were removed by vacuum distillation, and the polymer was left to dry under vacuum for a day. The polymer was redissolved in methanol and was purified by ultrafiltration in methanol through a PLBC regenerated cellulose 3000 NMWL membrane to remove traces of n-dodecyl amine. The pure polymer/methanol ultrafiltration solution was concentrated by vacuum distillation, and the polymer was again dried under vacuum for another day. The polymer was a light yellow, soft solid. Yield = 0.5340g. 90% substitution. ¹H NMR in MeOH-d: 3.70 (unreacted -CH₂-CH₂-CO-OCH₃), 3.65 (-O-CH₂-CH₂-), 3.19 (-CO-NH-CH₂-CH₂-(CH₂)₉-CH₃), 2.79 (-CH₂-CH₂-CO-NH-), 2.61 (-N-CH₂-CH₂-), 2.37 (-CH₂-CH₂-CO-NH-), 1.53 (-CO-NH-CH₂-CH₂-(CH₂)₉-CH₃), 1.32 (-CO-NH-CH₂-CH₂-(CH₂)₉-CH₃), 0.93 (-CO-NH-CH₂-CH₂-(CH₂)₉-CH₃). FTIR, ν cm⁻¹: 3288, 3071, 2950, 2920, 2855, 2817, 1738, 1646, 1553, 1461, 1353, 1114, 724.

Poly(ethylene oxide)-poly(ethylene imine) dendritic diblock generation 1.0-octadecyl terminated

All glassware were oven dried prior to use. A two-necked, 100ml round bottom flask equipped with a condenser and vacuum adapter in the center arm, an addition funnel and glass stopper in the side arm, and a stir bar in the bottom, was evacuated and filled with nitrogen. 5.8814g (0.0218 mol) n-octadecyl amine and 20ml of methanol were placed in the round bottom flask. The n-octadecyl amine did not dissolve with stirring, so the flask was heated, which induced dissolution. The flask was allowed to cool to room temperature. A small amount of octadecyl amine fell back out of solution, as indicated by the formation of a white precipitate on the bottom of the flask; however, the majority of the n-octadecyl amine remained in solution. 0.4975g (3.443×10^{-5} mol polymer, 0.00334 mol ester groups) of PEO-PEI generation 0.5 polymer were dissolved with 5ml of methanol in a 25ml erlenmeyer flask. This polymer/methanol solution was transferred to the addition funnel and was added dropwise over 5 minutes at room temperature. The addition funnel was rinsed with an additional 5ml of methanol for a total methanol volume of 30ml. The reaction flask was covered with aluminum foil to prevent the polymer from yellowing, and the solution was allowed to react at room temperature. After 24 hours, an oil bath was placed beneath the reaction flask and the solution was heated at 40°C. After three days of heating at 40°C, the solution became cloudy. The reaction temperature was increased to 60°C, which induced dissolution, and the solution was left to stir at 60°C for another

two and a half days. The methanol was removed by removed by vacuum distillation and the polymer was left to dry under vacuum for a day. The polymer was redissolved in methanol and with time and exposure to air, the octadecyl amine fell out of solution as a white precipitate. The precipitate was removed by repeated vacuum filtration until no more precipitate appeared. The polymer/methanol solution was then purified by ultrafiltration in methanol through a PLBC regenerated cellulose 3000 NMWL membrane to remove traces of n-octadecyl amine. The pure polymer/methanol ultrafiltration solution was concentrated by vacuum distillation, and the polymer was again dried under vacuum for another day. The polymer was an off-white solid. Yield = 0.1892g. 95% substitution. $^1\text{H NMR}$ in CDCl_3 : 3.68 (unreacted $-\text{CH}_2-\text{CH}_2-\text{CO}-\text{OCH}_3$), 3.66 ($-\text{O}-\text{CH}_2-\text{CH}_2-$), 3.21 ($-\text{CO}-\text{NH}-\text{CH}_2-\text{CH}_2-(\text{CH}_2)_{15}-\text{CH}_3$), 2.76 ($-\text{CH}_2-\text{CH}_2-\text{CO}-\text{NH}-$), 2.64 ($-\text{N}-\text{CH}_2-\text{CH}_2-$), 2.33 ($-\text{CH}_2-\text{CH}_2-\text{CO}-\text{NH}-$), 1.50 ($-\text{CO}-\text{NH}-\text{CH}_2-\text{CH}_2-(\text{CH}_2)_{15}-\text{CH}_3$), 1.27 ($-\text{CO}-\text{NH}-\text{CH}_2-\text{CH}_2-(\text{CH}_2)_{15}-\text{CH}_3$), 0.90 ($-\text{CO}-\text{NH}-\text{CH}_2-\text{CH}_2-(\text{CH}_2)_{15}-\text{CH}_3$). FTIR, $\nu \text{ cm}^{-1}$: 3270, 3062, 2957, 2913, 2842, 2809, 1640, 1547, 1470, 1349, 1113, 751.

Poly(ethylene oxide)-poly(ethylene imine) dendritic diblock generation 2.0-butyl terminated

All glassware were oven dried prior to use. A two-necked, 100ml round bottom flask equipped with a condenser and vacuum adapter in the center arm, an addition funnel and glass stopper in the side arm, and a stir bar in the bottom, was evacuated and filled with nitrogen. 10ml (0.101 mol) of n-butyl amine and 10ml of methanol were added to the round bottom flask and were subsequently chilled in an ice bath for 10 minutes. 0.2929g (8.653×10^{-6} mol polymer, 0.00168 mol ester groups) of PEO-PEI generation 1.5 polymer were dissolved with 20ml of methanol in a 25ml erlenmeyer flask. This polymer/methanol solution was transferred to the addition funnel and was added dropwise over 5 minutes. The 25ml erlenmeyer flask and the addition funnel were rinsed with an additional 5ml of methanol, which was then added to the reaction flask, for a total methanol volume of 35ml. The reaction flask was covered with aluminum foil to prevent the polymer from yellowing, and the solution was allowed to warm to room temperature. After 18 hours, an oil bath was placed beneath the reaction flask and the solution was heated at 40°C . After four days of heating, the majority of the methanol and excess n-butyl amine were removed by vacuum distillation, and the polymer was left to dry under vacuum for a day and a half. The polymer was redissolved in methanol and was purified by ultrafiltration in methanol through a PLBC regenerated cellulose 3000 NMWL membrane to remove traces of n-butyl amine. The pure polymer/methanol ultrafiltration solution was concentrated by vacuum distillation, and the polymer was again dried under vacuum for another day and a half. The polymer was a yellow, very viscous liquid. Yield = 0.3222g. 82% substitution. $^1\text{H NMR}$ in $\text{MeOH}-d$: 3.69 (unreacted $-\text{CH}_2-\text{CH}_2-\text{CO}-\text{OCH}_3$), 3.65 ($-\text{O}-\text{CH}_2-\text{CH}_2-$), 3.28 ($-\text{CO}-\text{NH}-\text{CH}_2-\text{CH}_2-\text{N}<$), 3.19 ($-\text{CO}-\text{NH}-\text{CH}_2-\text{CH}_2-\text{CH}_2-\text{CH}_3$), 2.84 ($-\text{CH}_2-\text{CH}_2-\text{CO}-\text{NH}-\text{CH}_2-\text{CH}_2-\text{N}<$), 2.81 ($-\text{CH}_2-\text{CH}_2-\text{CO}-\text{NH}-\text{CH}_2-\text{CH}_2-\text{CH}_3$), 2.76 (unreacted $-\text{CH}_2-\text{CH}_2-\text{CO}-\text{OCH}_3$), 2.62 ($-\text{N}-\text{CH}_2-\text{CH}_2-$) and ($-\text{CO}-\text{NH}-\text{CH}_2-\text{CH}_2-\text{N}<$), 2.50 (unreacted $-\text{CH}_2-\text{CH}_2-\text{CO}-\text{OCH}_3$), 2.40 ($-\text{CH}_2-\text{CH}_2-\text{CO}-\text{NH}-\text{CH}_2-\text{CH}_2-\text{N}<$), 2.37 ($-\text{CH}_2-\text{CH}_2-\text{CO}-\text{NH}-\text{CH}_2-\text{CH}_2-\text{CH}_2-\text{CH}_3$), 1.51 ($-\text{CO}-\text{NH}-\text{CH}_2-\text{CH}_2-\text{CH}_2-\text{CH}_3$), 1.39 ($-\text{CO}-\text{NH}-\text{CH}_2-\text{CH}_2-\text{CH}_2-\text{CH}_3$), 0.96 ($-\text{CO}-\text{NH}-\text{CH}_2-\text{CH}_2-\text{CH}_2-\text{CH}_3$). FTIR, $\nu \text{ cm}^{-1}$: 3285, 3071, 2953, 2928, 2866, 2815, 1646, 1544, 1462, 1365, 1248, 1110, 752.

Poly(ethylene oxide)-poly(ethylene imine) dendritic diblock generation 2.0-hexyl terminated

All glassware were oven dried prior to use. A two-necked, 100ml round bottom flask equipped with a condenser and vacuum adapter in the center arm, an addition funnel and glass stopper in the side arm, and a stir bar in the bottom, was evacuated and filled with nitrogen. 25ml (0.189 mol) of n-hexyl amine and 25ml of methanol were added to the round bottom flask and were subsequently chilled in an ice bath for 10 minutes. 0.2909g (8.594×10^{-6} mol polymer, 0.00167 mol ester groups) of PEO-PEI generation 1.5 polymer were dissolved with 20ml of methanol in a 25ml erlenmeyer flask. This polymer/methanol solution was transferred to the addition funnel and was added dropwise over 10 minutes. The 25ml erlenmeyer flask and the addition funnel were rinsed with an additional 5ml of methanol, which was then added to the reaction flask, for a total methanol volume of 50ml. The reaction flask was covered with aluminum foil to prevent the polymer from yellowing, and the solution was allowed to warm to room temperature. After 18 hours, an oil bath was placed beneath the reaction flask and the solution was heated at 45°C. After five days of heating, the majority of the methanol and excess n-hexyl amine were removed by vacuum distillation, and the polymer was left to dry under vacuum for three and a half days. The polymer was redissolved in methanol and was purified by ultrafiltration in methanol through a PLBC regenerated cellulose 3000 NMWL membrane to remove traces of n-hexyl amine. The pure polymer/methanol ultrafiltration solution was concentrated by vacuum distillation, and the polymer was again dried under vacuum for another day and a half. The polymer was a yellow, very viscous liquid. Yield = 0.3426g. 98% substitution. $^1\text{H NMR}$ in MeOH-*d*: 3.69 (unreacted $-\text{CH}_2-\text{CH}_2-\text{CO}-\text{OCH}_3$), 3.65 ($-\text{O}-\text{CH}_2-\text{CH}_2-$), 3.28 ($-\text{CO}-\text{NH}-\text{CH}_2-\text{CH}_2-\text{N}<$), 3.18 ($-\text{CO}-\text{NH}-\text{CH}_2-\text{CH}_2-(\text{CH}_2)_3-\text{CH}_3$), 2.84 ($-\text{CH}_2-\text{CH}_2-\text{CO}-\text{NH}-\text{CH}_2-\text{CH}_2-\text{N}<$), 2.81 ($-\text{CH}_2-\text{CH}_2-\text{CO}-\text{NH}-\text{CH}_2-\text{CH}_2-(\text{CH}_2)_3-\text{CH}_3$), 2.76 (unreacted $-\text{CH}_2-\text{CH}_2-\text{CO}-\text{OCH}_3$), 2.62 ($-\text{N}-\text{CH}_2-\text{CH}_2-$) and ($-\text{CO}-\text{NH}-\text{CH}_2-\text{CH}_2-\text{N}<$), 2.50 (unreacted $-\text{CH}_2-\text{CH}_2-\text{CO}-\text{OCH}_3$), 2.40 ($-\text{CH}_2-\text{CH}_2-\text{CO}-\text{NH}-\text{CH}_2-\text{CH}_2-\text{N}<$), 2.36 ($-\text{CH}_2-\text{CH}_2-\text{CO}-\text{NH}-\text{CH}_2-\text{CH}_2-(\text{CH}_2)_3-\text{CH}_3$), 1.52 ($-\text{CO}-\text{NH}-\text{CH}_2-\text{CH}_2-(\text{CH}_2)_3-\text{CH}_3$), 1.34 ($-\text{CO}-\text{NH}-\text{CH}_2-\text{CH}_2-(\text{CH}_2)_3-\text{CH}_3$), 0.93 ($-\text{CO}-\text{NH}-\text{CH}_2-\text{CH}_2-(\text{CH}_2)_3-\text{CH}_3$). FTIR, $\nu \text{ cm}^{-1}$: 3281, 3073, 2957, 2920, 2853, 2820, 1739, 1646, 1547, 1459, 1364, 1248, 1119, 724, 685.

Poly(ethylene oxide)-poly(ethylene imine) dendritic diblock generation 2.0-octyl terminated

All glassware were oven dried prior to use. A two-necked, 250ml round bottom flask equipped with a condenser and vacuum adapter in the center arm, an addition funnel and glass stopper in the side arm, and a stir bar in the bottom, was evacuated and filled with nitrogen. 20ml (0.121 mol) of n-octyl amine and 20ml of methanol were added to the round bottom flask and were subsequently chilled in an ice bath for 10 minutes. 0.3050g (9.011×10^{-6} mol polymer, 0.00175 mol ester groups) of PEO-PEI generation 1.5 polymer were dissolved with 15ml of methanol in a 25ml erlenmeyer flask. This polymer/methanol solution was transferred to the addition funnel and was added dropwise over 10 minutes. The 25ml erlenmeyer flask and the addition funnel were rinsed with an additional 5ml of methanol, which was then added to the reaction flask, for a total methanol volume of 40ml. The reaction flask was covered with aluminum foil to prevent the polymer from yellowing, and the solution was allowed to warm to room temperature. After 18 hours, an oil bath was placed beneath the reaction flask and the solution was heated at 45°C. After five days of heating, the majority of the methanol and excess n-octyl amine were removed by vacuum distillation, and the polymer was left to dry under vacuum for three and a half days. The polymer was redissolved in methanol and was purified by ultrafiltration in methanol through a PLBC regenerated cellulose 3000 NMWL membrane to remove traces of n-octyl amine. The

pure polymer/methanol ultrafiltration solution was concentrated by vacuum distillation, and the polymer was again dried under vacuum for another day. The polymer was a yellow, very viscous liquid. Yield = 0.4349g. 96% substitution. ^1H NMR in MeOH-*d*: 3.69 (unreacted -CH₂-CH₂-CO-OCH₃), 3.65 (-O-CH₂-CH₂-), 3.28 (-CO-NH-CH₂-CH₂-N<), 3.18 (-CO-NH-CH₂-CH₂-(CH₂)₅-CH₃), 2.84 (-CH₂-CH₂-CO-NH-CH₂-CH₂-N<), 2.81 (-CH₂-CH₂-CO-NH-CH₂-CH₂-(CH₂)₅-CH₃), 2.76 (unreacted -CH₂-CH₂-CO-OCH₃), 2.62 (-N-CH₂-CH₂-) and (-CO-NH-CH₂-CH₂-N<), 2.50 (unreacted -CH₂-CH₂-CO-OCH₃), 2.40 (-CH₂-CH₂-CO-NH-CH₂-CH₂-N<), 2.36 (-CH₂-CH₂-CO-NH-CH₂-CH₂-(CH₂)₅-CH₃), 1.52 (-CO-NH-CH₂-CH₂-(CH₂)₅-CH₃), 1.34 (-CO-NH-CH₂-CH₂-(CH₂)₅-CH₃), 0.92 (-CO-NH-CH₂-CH₂-(CH₂)₅-CH₃). FTIR, ν cm⁻¹: 3280, 3071, 2954, 2922, 2856, 2817, 1738, 1641, 1548, 1460, 1356, 1279, 1245, 1120, 725.

Poly(ethylene oxide)-poly(ethylene imine) dendritic diblock generation 2.0-decyl terminated

All glassware were oven dried prior to use. A two-necked, 100ml round bottom flask equipped with a condenser and vacuum adapter in the center arm, an addition funnel and glass stopper in the side arm, and a stir bar in the bottom, was evacuated and filled with nitrogen. 8ml (0.0400 mol) of n-decyl amine and 4ml of methanol were added to the round bottom flask and were subsequently chilled in an ice bath for 10 minutes. 0.2188g (6.464x10⁻⁶ mol polymer, 0.00125 mol ester groups) of PEO-PEI generation 1.5 polymer were dissolved with 10ml of methanol in a 25ml erlenmeyer flask. This polymer/methanol solution was transferred to the addition funnel and was added dropwise over 10 minutes. The 25ml erlenmeyer flask and the addition funnel were rinsed with an additional 2ml of methanol, which was then added to the reaction flask, for a total methanol volume of 16ml. The reaction flask was covered with aluminum foil to prevent the polymer from yellowing, and the solution was allowed to warm to room temperature. After 18 hours, an oil bath was placed beneath the reaction flask and the solution was heated at 45°C. After five and a half days of heating, the majority of the methanol and excess n-decyl amine were removed by vacuum distillation and the polymer was left to dry under vacuum for three days. The polymer was redissolved in methanol and was purified by ultrafiltration in methanol through a PLBC regenerated cellulose 3000 NMWL membrane to remove traces of n-decyl amine. The pure polymer/methanol ultrafiltration solution was concentrated by vacuum distillation, and the polymer was again dried under vacuum for another day. The polymer was a clear, yellow solid. Yield = 0.2910g. 76% substitution. ^1H NMR in MeOH-*d*: 3.69 (unreacted -CH₂-CH₂-CO-OCH₃), 3.65 (-O-CH₂-CH₂-), 3.28 (-CO-NH-CH₂-CH₂-N<), 3.18 (-CO-NH-CH₂-CH₂-(CH₂)₇-CH₃), 2.85 (-CH₂-CH₂-CO-NH-CH₂-CH₂-N<), 2.80 (-CH₂-CH₂-CO-NH-CH₂-CH₂-(CH₂)₇-CH₃), 2.76 (unreacted -CH₂-CH₂-CO-OCH₃), 2.63 (-N-CH₂-CH₂-) and (-CO-NH-CH₂-CH₂-N<), 2.50 (unreacted -CH₂-CH₂-CO-OCH₃), 2.40 (-CH₂-CH₂-CO-NH-CH₂-CH₂-N<), 2.36 (-CH₂-CH₂-CO-NH-CH₂-CH₂-(CH₂)₇-CH₃), 1.52 (-CO-NH-CH₂-CH₂-(CH₂)₇-CH₃), 1.32 (-CO-NH-CH₂-CH₂-(CH₂)₇-CH₃), 0.92 (-CO-NH-CH₂-CH₂-(CH₂)₇-CH₃). FTIR, ν cm⁻¹: 3286, 3074, 2960, 2926, 2852, 2815, 1740, 1650, 1550, 1465, 1359, 1259, 1195, 1126, 1042, 724.

Poly(ethylene oxide)-poly(ethylene imine) dendritic diblock generation 2.0-dodecyl terminated

All glassware were oven dried prior to use. A three-necked, 100ml round bottom flask equipped with a condenser and vacuum adapter in the center arm, an addition funnel and glass stopper in one of the side arms, a glass stopper in the other side arm, and a stirbar in the bottom, was evacuated and filled with nitrogen. 8.7615g (0.0473 mol) of n-dodecyl amine were dissolved in 5ml of methanol in a 50ml Erlenmeyer flask and were subsequently added to the round bottom flask. The solution was chilled in an ice bath for 10 minutes. 0.2057g (6.077×10^{-6} mol polymer, 0.00118 mol ester groups) of PEO-PEI generation 1.5 polymer were dissolved with 10ml of methanol in a 25ml erlenmeyer flask. This polymer/methanol solution was transferred to the addition funnel and was added dropwise over 5 minutes. The 25ml erlenmeyer flask and the addition funnel was rinsed with an additional 2ml of methanol, which was then added to the reaction flask, for a total methanol volume of 17ml. The reaction flask was covered with aluminum foil to prevent the polymer from yellowing, and the solution was allowed to warm to room temperature. After 18 hours, an oil bath was placed beneath the reaction flask and the solution was heated at 45°C. After five and a half days of heating, the majority of the methanol and excess n-dodecyl amine were removed by vacuum distillation and the polymer was left to dry under vacuum for three days. The polymer was redissolved in methanol and was purified by ultrafiltration in methanol through a PLBC regenerated cellulose 3000 NMWL membrane to remove traces of n-dodecyl amine. The pure polymer/methanol ultrafiltration solution was concentrated by vacuum distillation, and the polymer was again dried under vacuum for another two and a half days. The polymer was a yellow, soft solid. Yield = 0.2311g. 95% substitution. ¹H NMR in CDCl₃: 3.68 (unreacted -CH₂-CH₂-CO-OCH₃), 3.66 (-O-CH₂-CH₂-), 3.33 (-CO-NH-CH₂-CH₂-N<), 3.18 (-CO-NH-CH₂-CH₂-(CH₂)₉-CH₃), 2.77 (-CH₂-CH₂-CO-NH-CH₂-CH₂-N<) and (-CH₂-CH₂-CO-NH-CH₂-CH₂-(CH₂)₉-CH₃), 2.55 (-N-CH₂-CH₂-) and (-CO-NH-CH₂-CH₂-N<), 2.36 (-CH₂-CH₂-CO-NH-CH₂-CH₂-N<) and (-CH₂-CH₂-CO-NH-CH₂-CH₂-(CH₂)₉-CH₃), 1.50 (-CO-NH-CH₂-CH₂-(CH₂)₉-CH₃), 1.27 (-CO-NH-CH₂-CH₂-(CH₂)₉-CH₃), 0.90 (-CO-NH-CH₂-CH₂-(CH₂)₉-CH₃). FTIR, ν cm⁻¹: 3287, 3073, 2963, 2924, 2848, 2815, 1739, 1640, 1552, 1465, 1360, 1256, 1102, 1026, 718.

Poly(ethylene oxide)-poly(ethylene imine) dendritic diblock generation 2.0-octadecyl terminated

All glassware were oven dried prior to use. A two-necked, 50ml round bottom flask equipped with a condenser and vacuum adapter in the center arm, an addition funnel and glass stopper in the side arm, and a stir bar in the bottom, was evacuated and filled with nitrogen. 1.2854g (0.00477 mol) n-octadecyl amine and 7ml of methanol were placed in a 50ml erlenmeyer flask. The n-octadecyl amine did not dissolve with stirring, so the flask was heated, which induced dissolution. The flask was allowed to cool to room temperature. A small amount octadecyl amine fell back out of solution, as indicated by the formation of a white precipitate on the bottom of the flask; however, the majority of the n-octadecyl amine remained in solution. The octadecyl amine/methanol solution was poured into the reaction flask through a glass funnel, which temporarily replaced the addition funnel. The 50ml erlenmeyer flask and the glass funnel were rinsed with an additional 3ml of methanol, which were also added to the reaction flask. 0.2417g (7.1405×10^{-6} mol polymer, 0.00139 mol ester groups) of PEO-PEI generation 1.5 polymer were dissolved with 10ml of methanol in a 25ml erlenmeyer flask. This polymer/methanol solution was transferred to the addition funnel and was added dropwise to the stirring octadecyl

amine/methanol solution over 5 minutes at room temperature. The 25ml erlenmeyer flask and the addition funnel were rinsed with an additional 5ml of methanol, which was then added to the reaction flask, for a total methanol volume of 25ml. The reaction flask was covered with aluminum foil to prevent the polymer from yellowing, and the solution was allowed to react at room temperature. After 17 hours, an oil bath was placed beneath the reaction flask and the solution was heated at 60°C for five days. After this time, the reaction solution was allowed to cool at which point some of the n-octadecyl amine fell out of solution as a precipitate. The precipitate was removed by vacuum filtration, the liquor was concentrated by vacuum distillation, and the polymer was left to dry under vacuum for a day. The polymer was redissolved in methanol and with time and exposure to air, more octadecyl amine fell out of solution as a white precipitate. The precipitate was removed by vacuum filtration until no more precipitate appeared. The polymer/methanol solution was then purified by ultrafiltration in methanol through a PLBC regenerated cellulose 3000 NMWL membrane to remove traces of n-octadecyl amine. The pure polymer/methanol ultrafiltration solution was concentrated by vacuum distillation, and the polymer was again dried under vacuum for another day. The polymer was a light yellow solid. Yield = 0.2083g. 27% substitution. ¹H NMR in CDCl₃: 3.68 (unreacted -CH₂-CH₂-CO-OCH₃), 3.66 (-O-CH₂-CH₂-), 3.31 (-CO-NH-CH₂-CH₂-N<), 3.18 (-CO-NH-CH₂-CH₂-(CH₂)₁₅-CH₃), 2.77 (-CH₂-CH₂-CO-NH-CH₂-CH₂-N<) and (-CH₂-CH₂-CO-NH-CH₂-CH₂-(CH₂)₁₅-CH₃), 2.56 (-N-CH₂-CH₂-) and (-CO-NH-CH₂-CH₂-N<), 2.45 (unreacted -CH₂-CH₂-CO-OCH₃), 2.37 (-CH₂-CH₂-CO-NH-CH₂-CH₂-N<) and (-CH₂-CH₂-CO-NH-CH₂-CH₂-(CH₂)₁₅-CH₃), 1.50 (-CO-NH-CH₂-CH₂-(CH₂)₁₅-CH₃), 1.27 (-CO-NH-CH₂-CH₂-(CH₂)₁₅-CH₃), 0.90 (-CO-NH-CH₂-CH₂-(CH₂)₁₅-CH₃). FTIR, ν cm⁻¹: 3277, 3067, 2959, 2921, 2851, 2813, 1740, 1648, 1551, 1470, 1438, 1362, 1254, 1200, 1125, 1044, 758.

Poly(ethylene oxide)-poly(ethylene imine) dendritic diblock generation 3.0-butyl terminated

All glassware were oven dried prior to use. A two-necked, 100ml round bottom flask equipped with a condenser and vacuum adapter in the center arm, an addition funnel and glass stopper in the side arm, and a stir bar in the bottom, was evacuated and filled with nitrogen. 10ml (0.101 mol) of n-butyl amine were added to the round bottom flask. 0.2602g (3.5816x10⁻⁶ mol polymer, 0.00139 mol ester groups) of PEO-PEI generation 2.5 polymer were dissolved with 15ml of methanol in a 25ml erlenmeyer flask. This polymer/methanol solution was transferred to the addition funnel and was added dropwise over 5 minutes to the stirring n-butyl amine at room temperature. As the polymer/methanol solution was being added, the reaction flask became slightly warm to the touch, but it gradually cooled to room temperature. The 25ml erlenmeyer flask and the addition funnel were rinsed with an additional 5ml of methanol, which was then added to the reaction flask, for a total methanol volume of 20ml. The reaction flask was covered with aluminum foil to prevent the polymer from yellowing. After 24 hours, an oil bath was placed beneath the reaction flask and the solution was heated at 47°C. After six days of heating, the majority of the methanol and excess n-butyl amine were removed by vacuum distillation, and the polymer was left to dry under vacuum for two days. The polymer was redissolved in methanol and was purified by ultrafiltration in methanol through a PLBC regenerated cellulose 3000 NMWL membrane to remove traces of n-butyl amine. The pure polymer/methanol ultrafiltration solution was concentrated by vacuum distillation, and the polymer was again dried under vacuum for another day and a half. The polymer was a clear, yellow solid. Yield = 0.2678g. 99% substitution. ¹H NMR in MeOH-*d*: 3.65 (-O-CH₂-CH₂-),

3.28 (-CO-NH-CH₂-CH₂-N<), 3.19 (-CO-NH-CH₂-CH₂-CH₂-CH₃), 2.84 (-CH₂-CH₂-CO-NH-CH₂-CH₂-N<), 2.81 (-CH₂-CH₂-CO-NH-CH₂-CH₂-CH₂-CH₃), 2.61 (-N-CH₂-CH₂-) and (-CO-NH-CH₂-CH₂-N<), 2.40 (-CH₂-CH₂-CO-NH-CH₂-CH₂-N<), 2.38 (-CH₂-CH₂-CO-NH-CH₂-CH₂-CH₂-CH₃), 1.50 (-CO-NH-CH₂-CH₂-CH₂-CH₃), 1.39 (-CO-NH-CH₂-CH₂-CH₂-CH₃), 0.96 (-CO-NH-CH₂-CH₂-CH₂-CH₃). FTIR, ν cm⁻¹: 3285, 3077, 2960, 2933, 2869, 2821, 1640, 1552, 1466, 1365, 1247, 1151, 1039, 757.

Poly(ethylene oxide)-poly(ethylene imine) dendritic diblock generation 3.0-hexyl terminated

All glassware were oven dried prior to use. A two-necked, 100ml round bottom flask equipped with a condenser and vacuum adapter in the center arm, an addition funnel and glass stopper in the side arm, and a stir bar in the bottom, was evacuated and filled with nitrogen. 10ml (0.0757 mol) of n-hexyl amine were added to the round bottom flask. 0.2504g (3.4467x10⁻⁶ mol polymer, 0.00134 mol ester groups) of PEO-PEI generation 2.5 polymer were dissolved with 15ml of methanol in a 25ml erlenmeyer flask. This polymer/methanol solution was transferred to the addition funnel and was added dropwise over 5 minutes to the stirring n-hexyl amine at room temperature. As the polymer/methanol solution was being added, the reaction flask became slightly warm to the touch, but it gradually cooled to room temperature. The 25ml erlenmeyer flask and the addition funnel were rinsed with an additional 5ml of methanol, which was then added to the reaction flask, for a total methanol volume of 20ml. The reaction flask was covered with aluminum foil to prevent the polymer from yellowing. After 24 hours, an oil bath was placed beneath the reaction flask and the solution was heated at 47°C. After six days of heating, the majority of the methanol and excess n-hexyl amine were removed by vacuum distillation, and the polymer was left to dry under vacuum for two days. The polymer was redissolved in methanol and was purified by ultrafiltration in methanol through a PLBC regenerated cellulose 3000 NMWL membrane to remove traces of n-hexyl amine. The pure polymer/methanol ultrafiltration solution was concentrated by vacuum distillation, and the polymer was again dried under vacuum for another four days. The polymer was a clear, yellow solid. Yield = 0.2754g. 97% substitution. ¹H NMR in MeOH-*d*: 3.69 (unreacted -CH₂-CH₂-CO-OCH₃), 3.65 (-O-CH₂-CH₂-), 3.28 (-CO-NH-CH₂-CH₂-N<), 3.18 (-CO-NH-CH₂-CH₂-(CH₂)₃-CH₃), 2.84 (-CH₂-CH₂-CO-NH-CH₂-CH₂-N<), 2.81 (-CH₂-CH₂-CO-NH-CH₂-CH₂-(CH₂)₃-CH₃), 2.76 (unreacted -CH₂-CH₂-CO-OCH₃), 2.62 (-N-CH₂-CH₂-) and (-CO-NH-CH₂-CH₂-N<), 2.50 (unreacted -CH₂-CH₂-CO-OCH₃), 2.40 (-CH₂-CH₂-CO-NH-CH₂-CH₂-N<), 2.36 (-CH₂-CH₂-CO-NH-CH₂-CH₂-(CH₂)₃-CH₃), 1.52 (-CO-NH-CH₂-CH₂-(CH₂)₃-CH₃), 1.34 (-CO-NH-CH₂-CH₂-(CH₂)₃-CH₃), 0.93 (-CO-NH-CH₂-CH₂-(CH₂)₃-CH₃). FTIR, ν cm⁻¹: 3289, 3072, 2956, 2928, 2856, 2820, 1743, 1645, 1552, 1464, 1361, 1284, 1248, 1155, 1129, 1037, 732, 691.

Poly(ethylene oxide)-poly(ethylene imine) dendritic diblock generation 3.0-octyl terminated

All glassware were oven dried prior to use. A two-necked, 100ml round bottom flask equipped with a condenser and vacuum adapter in the center arm, an addition funnel and glass stopper in the side arm, and a stir bar in the bottom, was evacuated and filled with nitrogen. 12ml (0.0726 mol) of n-octyl amine were added to the round bottom flask. 0.2303g (3.1700x10⁻⁶ mol polymer, 0.00123 mol ester groups) of PEO-PEI generation 2.5 polymer were dissolved with 15ml of methanol in a 25ml erlenmeyer flask. This polymer/methanol solution was transferred to the addition funnel and was added dropwise over 5 minutes to the stirring n-octyl amine at room temperature. As the polymer/methanol solution was being added, the reaction flask became

slightly warm to the touch, but it gradually cooled to room temperature. The 25ml erlenmeyer flask and the addition funnel were rinsed with an additional 9ml of methanol, which was then added to the reaction flask, for a total methanol volume of 24ml. The reaction flask was covered with aluminum foil to prevent the polymer from yellowing. After 24 hours, an oil bath was placed beneath the reaction flask and the solution was heated at 47°C. After six days of heating, the majority of the methanol and excess n-octyl amine were removed by vacuum distillation, and the polymer was left to dry under vacuum for two days. The polymer was redissolved in methanol and was purified by ultrafiltration in methanol through a PLBC regenerated cellulose 3000 NMWL membrane to remove traces of n-octyl amine. The pure polymer/methanol ultrafiltration solution was concentrated by vacuum distillation, and the polymer was again dried under vacuum for another day and a half. The polymer was a clear, yellow solid. Yield = 0.2701g. 89% substitution. ¹H NMR in MeOH-*d*: 3.69 (unreacted -CH₂-CH₂-CO-OCH₃), 3.65 (-O-CH₂-CH₂-), 3.28 (-CO-NH-CH₂-CH₂-N<), 3.18 (-CO-NH-CH₂-CH₂-(CH₂)₅-CH₃), 2.84 (-CH₂-CH₂-CO-NH-CH₂-CH₂-N<), 2.81 (-CH₂-CH₂-CO-NH-CH₂-CH₂-(CH₂)₅-CH₃), 2.76 (unreacted -CH₂-CH₂-CO-OCH₃), 2.61 (-N-CH₂-CH₂-) and (-CO-NH-CH₂-CH₂-N<), 2.50 (unreacted -CH₂-CH₂-CO-OCH₃), 2.40 (-CH₂-CH₂-CO-NH-CH₂-CH₂-N<), 2.36 (-CH₂-CH₂-CO-NH-CH₂-CH₂-(CH₂)₅-CH₃), 1.52 (-CO-NH-CH₂-CH₂-(CH₂)₅-CH₃), 1.34 (-CO-NH-CH₂-CH₂-(CH₂)₅-CH₃), 0.93 (-CO-NH-CH₂-CH₂-(CH₂)₅-CH₃). FTIR, ν cm⁻¹: 3289, 3072, 2959, 2923, 2856, 2820, 1743, 1640, 1547, 1464, 1372, 1284, 1248, 1155, 1134, 1037, 722.

Poly(ethylene oxide)-poly(ethylene imine) dendritic diblock generation 3.0-decyl terminated

All glassware were oven dried prior to use. A two-necked, 100ml round bottom flask equipped with a condenser and vacuum adapter in the center arm, an addition funnel and glass stopper in the side arm, and a stir bar in the bottom, was evacuated and filled with nitrogen. 7ml (0.0350 mol) of n-decyl amine were added to the round bottom flask. 0.2050g (2.8218x10⁻⁶ mol polymer, 0.00109 mol ester groups) of PEO-PEI generation 2.5 polymer were dissolved with 10ml of methanol in a 25ml erlenmeyer flask. This polymer/methanol solution was transferred to the addition funnel and was added dropwise over 5 minutes to the stirring n-decyl amine at room temperature. As the polymer/methanol solution was being added, the reaction flask became slightly warm to the touch, but it gradually cooled to room temperature. The 25ml erlenmeyer flask and the addition funnel were rinsed with an additional 5ml of methanol, which was then added to the reaction flask, for a total methanol volume of 15ml. The reaction flask was covered with aluminum foil to prevent the polymer from yellowing. After 17 hours, an oil bath was placed beneath the reaction flask and the solution was heated at 50°C. After six days of heating, the majority of the methanol and excess n-decyl amine were removed by vacuum distillation, and the polymer was left to dry under vacuum for five days. The polymer was redissolved in methanol and was purified by ultrafiltration in methanol through a PLBC regenerated cellulose 3000 NMWL membrane to remove traces of n-decyl amine. The pure polymer/methanol ultrafiltration solution was concentrated by vacuum distillation, and the polymer was again dried under vacuum for another four days. The polymer was a clear, yellow solid. Yield = 0.2622g. 84% substitution. ¹H NMR in MeOH-*d*: 3.69 (unreacted -CH₂-CH₂-CO-OCH₃), 3.65 (-O-CH₂-CH₂-), 3.28 (-CO-NH-CH₂-CH₂-N<), 3.18 (-CO-NH-CH₂-CH₂-(CH₂)₇-CH₃), 2.85 (-CH₂-CH₂-CO-NH-CH₂-CH₂-N<), 2.80 (-CH₂-CH₂-CO-NH-CH₂-CH₂-(CH₂)₇-CH₃), 2.76 (unreacted -CH₂-CH₂-CO-OCH₃), 2.63 (-N-CH₂-CH₂-) and (-CO-NH-CH₂-CH₂-N<), 2.50 (unreacted -CH₂-CH₂-CO-OCH₃), 2.40 (-CH₂-CH₂-CO-NH-CH₂-CH₂-N<), 2.36

(-CH₂-CH₂-CO-NH-CH₂-CH₂-(CH₂)₇-CH₃), 1.52 (-CO-NH-CH₂-CH₂-(CH₂)₇-CH₃), 1.32 (-CO-NH-CH₂-CH₂-(CH₂)₇-CH₃), 0.92 (-CO-NH-CH₂-CH₂-(CH₂)₇-CH₃). FTIR, ν cm⁻¹: 3285, 3073, 2956, 2923, 2856, 2815, 1737, 1644, 1551, 1463, 1359, 1256, 1199, 1152, 1132, 1049, 728.

Poly(ethylene oxide)-poly(ethylene imine) dendritic diblock generation 3.0-dodecyl terminated

All glassware were oven dried prior to use. A two-necked, 100ml round bottom flask equipped with a condenser and vacuum adapter in the center arm, an addition funnel and glass stopper in the side arm, and a stir bar in the bottom, was evacuated and filled with nitrogen. 7.2741g (0.03924 mol) of n-dodecyl amine were dissolved with 7ml of methanol in a 250ml erlenmeyer flask and were subsequently added to the round bottom flask. The 250ml erlenmeyer flask was rinsed with an additional 3ml of methanol which was also added to the reaction flask. 0.2000g (2.7530x10⁻⁶ mol polymer, 0.001068 mol ester groups) of PEO-PEI generation 2.5 polymer were dissolved with 10ml of methanol in a 25ml erlenmeyer flask. This polymer/methanol solution was transferred to the addition funnel and was added dropwise over 5 minutes to the stirring n-dodecyl amine/methanol solution at room temperature. As the polymer/methanol solution was being added, the reaction flask became slightly warm to the touch, but it gradually cooled to room temperature. The 25ml erlenmeyer flask and the addition funnel were rinsed with an additional 2ml of methanol, which was then added to the reaction flask, for a total methanol volume of 22ml. The reaction flask was covered with aluminum foil to prevent the polymer from yellowing. After 17 hours, an oil bath was placed beneath the reaction flask and the solution was heated at 50°C. After six days of heating, the majority of the methanol and excess n-dodecyl amine were removed by vacuum distillation, and the polymer was left to dry under vacuum for five days. The polymer was redissolved in methanol and was purified by ultrafiltration in methanol through a PLBC regenerated cellulose 3000 NMWL membrane to remove traces of n-dodecyl amine. The pure polymer/methanol ultrafiltration solution was concentrated by vacuum distillation, and the polymer was again dried under vacuum for another two days. The polymer was a clear, yellow solid. Yield = 0.2295g. 66% substitution. ¹H NMR in MeOH-*d*: 3.69 (unreacted -CH₂-CH₂-CO-OCH₃), 3.65 (-O-CH₂-CH₂-), 3.28 (-CO-NH-CH₂-CH₂-N<), 3.18 (-CO-NH-CH₂-CH₂-(CH₂)₉-CH₃), 2.85 (-CH₂-CH₂-CO-NH-CH₂-CH₂-N<), 2.80 (-CH₂-CH₂-CO-NH-CH₂-CH₂-(CH₂)₉-CH₃), 2.76 (unreacted -CH₂-CH₂-CO-OCH₃), 2.62 (-N-CH₂-CH₂-) and (-CO-NH-CH₂-CH₂-N<), 2.51 (unreacted -CH₂-CH₂-CO-OCH₃), 2.40 (-CH₂-CH₂-CO-NH-CH₂-CH₂-N<), 2.36 (-CH₂-CH₂-CO-NH-CH₂-CH₂-(CH₂)₉-CH₃), 1.52 (-CO-NH-CH₂-CH₂-(CH₂)₉-CH₃), 1.31 (-CO-NH-CH₂-CH₂-(CH₂)₉-CH₃), 0.92 (-CO-NH-CH₂-CH₂-(CH₂)₉-CH₃). FTIR, ν cm⁻¹: 3285, 3078, 2965, 2923, 2856, 2815, 1743, 1649, 1551, 1463, 1359, 1256, 1199, 1152, 1124, 1044, 722.

Poly(ethylene oxide)-poly(ethylene imine) dendritic diblock generation 3.0-octadecyl terminated

All glassware were oven dried prior to use. A two-necked, 100ml round bottom flask equipped with a condenser and vacuum adapter in the center arm, an addition funnel and glass stopper in the side arm, and a stir bar in the bottom, was evacuated and filled with nitrogen. 3.2358g (0.01203 mol) of n-octadecyl amine and 10ml of methanol were placed in a 50ml erlenmeyer flask. The n-octadecyl amine did not dissolve with stirring, so the flask was heated, which induced dissolution. The flask was allowed to cool to room temperature. A small amount octadecyl amine fell back out of solution, as indicated by the formation of a white precipitate on

the bottom of the flask; however, the majority of the n-octadecyl amine remained in solution. The octadecyl amine/methanol solution was poured into the reaction flask through a glass funnel, which temporarily replaced the addition funnel. The 50ml erlenmeyer flask and the glass funnel were rinsed with an additional 5ml of methanol, which were also added to the reaction flask. 0.1983g (2.7296×10^{-6} mol polymer, 0.001059 mol ester groups) of PEO-PEI generation 2.5 polymer were dissolved with 10ml of methanol in a 25ml erlenmeyer flask. This polymer/methanol solution was transferred to the addition funnel and was added dropwise to the stirring octadecyl amine/methanol solution over 5 minutes at room temperature. The 25ml erlenmeyer flask and the addition funnel were rinsed with an additional 10ml of methanol, which was then added to the reaction flask, for a total methanol volume of 35ml. A small amount of n-octadecyl amine began to fall out of solution, so the reaction solution was heated in order to redissolve the n-octadecyl amine. The reaction solution was heated at 60°C for seven days with an oil bath. The methanol was removed by removed by vacuum distillation and the polymer was left to dry under vacuum for five and a half days. The polymer was redissolved in methanol and with time and exposure to air, the octadecyl amine fell out of solution as a white precipitate. The precipitate was removed by repeated vacuum filtration until no more precipitate appeared. The polymer/methanol solution was then purified by ultrafiltration in methanol through a PLBC regenerated cellulose 3000 NMWL membrane to remove traces of n-octadecyl amine. The pure polymer/methanol ultrafiltration solution was concentrated by vacuum distillation, and the polymer was again dried under vacuum for another day. The polymer was a light yellow solid. Yield = 0.1567g. 33% substitution. ¹H NMR in CDCl₃: 3.69 (unreacted -CH₂-CH₂-CO-OCH₃), 3.67 (-O-CH₂-CH₂-), 3.29 (-CO-NH-CH₂-CH₂-N<), 3.20 (-CO-NH-CH₂-CH₂-(CH₂)₁₅-CH₃), 2.77 (-CH₂-CH₂-CO-NH-CH₂-CH₂-N<) and (-CH₂-CH₂-CO-NH-CH₂-CH₂-(CH₂)₁₅-CH₃), 2.56 (-N-CH₂-CH₂-) and (-CO-NH-CH₂-CH₂-N<), 2.45 (unreacted -CH₂-CH₂-CO-OCH₃), 2.38 (-CH₂-CH₂-CO-NH-CH₂-CH₂-N<) and (-CH₂-CH₂-CO-NH-CH₂-CH₂-(CH₂)₁₅-CH₃), 1.50 (-CO-NH-CH₂-CH₂-(CH₂)₁₅-CH₃), 1.27 (-CO-NH-CH₂-CH₂-(CH₂)₁₅-CH₃), 0.90 (-CO-NH-CH₂-CH₂-(CH₂)₁₅-CH₃). FTIR, ν cm⁻¹: 3284, 3069, 2961, 2919, 2849, 2817, 1736, 1645, 1549, 1469, 1437, 1362, 1260, 1201, 1153, 1132, 1046, 757, 725.

Poly(ethylene oxide)-poly(ethylene imine) dendritic diblock generation 4.0-butyl terminated

All glassware were oven dried prior to use. A two-necked, 100ml round bottom flask equipped with a condenser and vacuum adapter in the center arm, an addition funnel and glass stopper in the side arm, and a stir bar in the bottom, was evacuated and filled with nitrogen. 10ml (0.101 mol) of n-butyl amine were added to the round bottom flask. 0.2509g (0.00130 mol ester groups) of PEO-PEI generation 3.5 polymer were dissolved with 15ml of methanol in a 25ml erlenmeyer flask. This polymer/methanol solution was transferred to the addition funnel and was added dropwise over 5 minutes to the stirring n-butyl amine at room temperature. As the polymer/methanol solution was being added, the reaction flask became slightly warm to the touch, but it gradually cooled to room temperature. The 25ml erlenmeyer flask and the addition funnel were rinsed with an additional 5ml of methanol, which was then added to the reaction flask, for a total methanol volume of 20ml. The reaction flask was covered with aluminum foil to prevent the polymer from yellowing. After 24 hours, an oil bath was placed beneath the reaction flask and the solution was heated at 47°C. After seven days of heating, the majority of the methanol and excess n-butyl amine were removed by vacuum distillation, and the polymer was left to dry under vacuum for five days. The polymer was redissolved in methanol and was

purified by ultrafiltration in methanol through a PLBC regenerated cellulose 3000 NMWL membrane to remove traces of n-butyl amine. The pure polymer/methanol ultrafiltration solution was concentrated by vacuum distillation, and the polymer was again dried under vacuum for another four days. The polymer was a clear, yellow solid. Yield = 0.2652g. 99% substitution. ^1H NMR in MeOH-*d*: 3.65 (-O-CH₂-CH₂-), 3.28 (-CO-NH-CH₂-CH₂-N<), 3.19 (-CO-NH-CH₂-CH₂-CH₂-CH₃), 2.81 (-CH₂-CH₂-CO-NH-CH₂-CH₂-N<) and (-CH₂-CH₂-CO-NH-CH₂-CH₂-CH₂-CH₃), 2.61 (-N-CH₂-CH₂-) and (-CO-NH-CH₂-CH₂-N<), 2.38 (-CH₂-CH₂-CO-NH-CH₂-CH₂-N<) and (-CH₂-CH₂-CO-NH-CH₂-CH₂-CH₂-CH₃), 1.49 (-CO-NH-CH₂-CH₂-CH₂-CH₃), 1.37 (-CO-NH-CH₂-CH₂-CH₂-CH₃), 0.96 (-CO-NH-CH₂-CH₂-CH₂-CH₃). FTIR, ν cm⁻¹: 3283, 3074, 2956, 2930, 2871, 2817, 1645, 1554, 1463, 1437, 1356, 1233, 1153, 1041, 752, 693.

Poly(ethylene oxide)-poly(ethylene imine) dendritic diblock generation 4.0-hexyl terminated

All glassware were oven dried prior to use. A two-necked, 100ml round bottom flask equipped with a condenser and vacuum adapter in the center arm, an addition funnel and glass stopper in the side arm, and a stir bar in the bottom, was evacuated and filled with nitrogen. 10ml (0.0757 mol) of n-hexyl amine were added to the round bottom flask. 0.2450g (0.00127 mol ester groups) of PEO-PEI generation 3.5 polymer were dissolved with 15ml of methanol in a 25ml erlenmeyer flask. This polymer/methanol solution was transferred to the addition funnel and was added dropwise over 5 minutes to the stirring n-hexyl amine at room temperature. As the polymer/methanol solution was being added, the reaction flask became slightly warm to the touch, but it gradually cooled to room temperature. The 25ml erlenmeyer flask and the addition funnel were rinsed with an additional 5ml of methanol, which was then added to the reaction flask, for a total methanol volume of 20ml. The reaction flask was covered with aluminum foil to prevent the polymer from yellowing. After 24 hours, an oil bath was placed beneath the reaction flask and the solution was heated at 47°C. After seven days of heating, the majority of the methanol and excess n-hexyl amine were removed by vacuum distillation, and the polymer was left to dry under vacuum for two days. The polymer was redissolved in methanol and was purified by ultrafiltration in methanol through a PLBC regenerated cellulose 3000 NMWL membrane to remove traces of n-hexyl amine. The pure polymer/methanol ultrafiltration solution was concentrated by vacuum distillation, and the polymer was again dried under vacuum for another four days. The polymer was a clear, yellow solid. Yield = 0.2342g. 97% substitution. ^1H NMR in MeOH-*d*: 3.69 (unreacted -CH₂-CH₂-CO-OCH₃), 3.65 (-O-CH₂-CH₂-), 3.28 (-CO-NH-CH₂-CH₂-N<), 3.18 (-CO-NH-CH₂-CH₂-(CH₂)₃-CH₃), 2.81 (-CH₂-CH₂-CO-NH-CH₂-CH₂-N<) and (-CH₂-CH₂-CO-NH-CH₂-CH₂-(CH₂)₃-CH₃), 2.76 (unreacted -CH₂-CH₂-CO-OCH₃), 2.62 (-N-CH₂-CH₂-) and (-CO-NH-CH₂-CH₂-N<), 2.50 (unreacted -CH₂-CH₂-CO-OCH₃), 2.38 (-CH₂-CH₂-CO-NH-CH₂-CH₂-N<) and (-CH₂-CH₂-CO-NH-CH₂-CH₂-(CH₂)₃-CH₃), 1.52 (-CO-NH-CH₂-CH₂-(CH₂)₃-CH₃), 1.34 (-CO-NH-CH₂-CH₂-(CH₂)₃-CH₃), 0.93 (-CO-NH-CH₂-CH₂-(CH₂)₃-CH₃). FTIR, ν cm⁻¹: 3283, 3075, 2960, 2927, 2855, 2818, 1739, 1646, 1548, 1460, 1436, 1367, 1247, 1197, 1152, 1131, 1039, 762, 688.

Poly(ethylene oxide)-poly(ethylene imine) dendritic diblock generation 4.0-octyl terminated

All glassware were oven dried prior to use. A two-necked, 100ml round bottom flask equipped with a condenser and vacuum adapter in the center arm, an addition funnel and glass stopper in the side arm, and a stir bar in the bottom, was evacuated and filled with nitrogen. 12ml (0.0726 mol) of n-octyl amine were added to the round bottom flask. 0.2420g (0.00125 mol ester

groups) of PEO-PEI generation 3.5 polymer were dissolved with 15ml of methanol in a 25ml erlenmeyer flask. This polymer/methanol solution was transferred to the addition funnel and was added dropwise over 5 minutes to the stirring n-octyl amine at room temperature. As the polymer/methanol solution was being added, the reaction flask became slightly warm to the touch, but it gradually cooled to room temperature. The 25ml erlenmeyer flask and the addition funnel were rinsed with an additional 9ml of methanol, which was then added to the reaction flask, for a total methanol volume of 24ml. The reaction flask was covered with aluminum foil to prevent the polymer from yellowing. After 24 hours, an oil bath was placed beneath the reaction flask and the solution was heated at 47°C. After seven days of heating, the majority of the methanol and excess n-octyl amine were removed by vacuum distillation, and the polymer was left to dry under vacuum for four days. The polymer was redissolved in methanol and was purified by ultrafiltration in methanol through a PLBC regenerated cellulose 3000 NMWL membrane to remove traces of n-octyl amine. The pure polymer/methanol ultrafiltration solution was concentrated by vacuum distillation, and the polymer was again dried under vacuum for another four days. The polymer was a clear, yellow solid. Yield = 0.2835g. 94% substitution. ¹H NMR in MeOH-*d*: 3.69 (unreacted -CH₂-CH₂-CO-OCH₃), 3.65 (-O-CH₂-CH₂-), 3.28 (-CO-NH-CH₂-CH₂-N<), 3.17 (-CO-NH-CH₂-CH₂-(CH₂)₅-CH₃), 2.82 (-CH₂-CH₂-CO-NH-CH₂-CH₂-N<) and (-CH₂-CH₂-CO-NH-CH₂-CH₂-(CH₂)₅-CH₃), 2.76 (unreacted -CH₂-CH₂-CO-OCH₃), 2.60 (-N-CH₂-CH₂-) and (-CO-NH-CH₂-CH₂-N<), 2.50 (unreacted -CH₂-CH₂-CO-OCH₃), 2.38 (-CH₂-CH₂-CO-NH-CH₂-CH₂-N<) and (-CH₂-CH₂-CO-NH-CH₂-CH₂-(CH₂)₅-CH₃), 1.52 (-CO-NH-CH₂-CH₂-(CH₂)₅-CH₃), 1.34 (-CO-NH-CH₂-CH₂-(CH₂)₅-CH₃), 0.92 (-CO-NH-CH₂-CH₂-(CH₂)₅-CH₃). FTIR, ν cm⁻¹: 3285, 3077, 2953, 2922, 2853, 2820, 1744, 1642, 1552, 1461, 1440, 1365, 1285, 1247, 1157, 1039, 724, 684.

Poly(ethylene oxide)-poly(ethylene imine) dendritic diblock generation 4.0-decyl terminated

All glassware were oven dried prior to use. A two-necked, 100ml round bottom flask equipped with a condenser and vacuum adapter in the center arm, an addition funnel and glass stopper in the side arm, and a stir bar in the bottom, was evacuated and filled with nitrogen. 8ml (0.04002 mol) of n-decyl amine were added to the round bottom flask. 0.2496g (1.6612x10⁻⁶ mol polymer, 0.001289 mol ester groups) of PEO-PEI generation 3.5 polymer were dissolved with 10ml of methanol in a 25ml erlenmeyer flask. This polymer/methanol solution was transferred to the addition funnel and was added dropwise over 5 minutes to the stirring n-decyl amine at room temperature. As the polymer/methanol solution was being added, the reaction flask became slightly warm to the touch, but it gradually cooled to room temperature. The 25ml erlenmeyer flask and the addition funnel were rinsed with an additional 7ml of methanol, which was then added to the reaction flask, for a total methanol volume of 17ml. The reaction flask was covered with aluminum foil to prevent the polymer from yellowing. After 24 hours, an oil bath was placed beneath the reaction flask and the solution was heated at 50°C. After eight days of heating, the majority of the methanol and excess n-decyl amine were removed by vacuum distillation, and the polymer was left to dry under vacuum for two days. The polymer was redissolved in methanol and was purified by ultrafiltration in methanol through a PLBC regenerated cellulose 3000 NMWL membrane to remove traces of n-decyl amine. The pure polymer/methanol ultrafiltration solution was concentrated by vacuum distillation, and the polymer was again dried under vacuum for another three and a half days. The polymer was a clear, yellow solid. Yield = 0.3149g. 90% substitution. ¹H NMR in MeOH-*d*: 3.69 (unreacted -

CH₂-CH₂-CO-OCH₃), 3.65 (-O-CH₂-CH₂-), 3.28 (-CO-NH-CH₂-CH₂-N<), 3.18 (-CO-NH-CH₂-CH₂-(CH₂)₇-CH₃), 2.80 (-CH₂-CH₂-CO-NH-CH₂-CH₂-N<) and (-CH₂-CH₂-CO-NH-CH₂-CH₂-(CH₂)₇-CH₃), 2.60 (-N-CH₂-CH₂-) and (-CO-NH-CH₂-CH₂-N<), 2.50 (unreacted -CH₂-CH₂-CO-OCH₃), 2.36 (-CH₂-CH₂-CO-NH-CH₂-CH₂-N<) and (-CH₂-CH₂-CO-NH-CH₂-CH₂-(CH₂)₇-CH₃), 1.52 (-CO-NH-CH₂-CH₂-(CH₂)₇-CH₃), 1.32 (-CO-NH-CH₂-CH₂-(CH₂)₇-CH₃), 0.92 (-CO-NH-CH₂-CH₂-(CH₂)₇-CH₃). FTIR, ν cm⁻¹: 3288, 3074, 2959, 2925, 2854, 2818, 1739, 1645, 1550, 1467, 1440, 1362, 1289, 1252, 1200, 1153, 1037, 723.

Poly(ethylene oxide)-poly(ethylene imine) dendritic diblock generation 4.0-dodecyl terminated

All glassware were oven dried prior to use. A three-necked, 100ml round bottom flask equipped with a condenser and vacuum adapter in the center arm, an addition funnel and glass stopper in one of the side arms, a glass stopper in the other side arm, and a stir bar in the bottom, was evacuated and filled with nitrogen. 7.3791g (0.03981 mol) of n-dodecyl amine were dissolved with 7ml of methanol in a 125ml erlenmeyer flask and were subsequently added to the round bottom flask. The 250ml erlenmeyer flask was rinsed with an additional 3ml of methanol which was also added to the reaction flask. 0.2458g (1.6360x10⁻⁶ mol polymer, 0.001269 mol ester groups) of PEO-PEI generation 3.5 polymer were dissolved with 10ml of methanol in a 25ml erlenmeyer flask. This polymer/methanol solution was transferred to the addition funnel and was added dropwise over 5 minutes to the stirring n-dodecyl amine/methanol solution at room temperature. The 25ml erlenmeyer flask and the addition funnel were rinsed with an additional 3ml of methanol, which was then added to the reaction flask, for a total methanol volume of 23ml. The reaction flask was covered with aluminum foil to prevent the polymer from yellowing. After 24 hours, an oil bath was placed beneath the reaction flask and the solution was heated at 50°C. After eight days of heating, the majority of the methanol and excess n-dodecyl amine were removed by vacuum distillation, and the polymer was left to dry under vacuum for two days. Attempts were made to redissolve the polymer in methanol for purification. While some of the polymer did dissolve, some of it did not and instead formed a yellow gule on the bottom of the flask. The polymer that wouldn't dissolve was washed eight times with approximately 30ml of methanol to removed residual n-dodecyl amine, which is soluble in methanol. The methanol solution that was used to wash the polymer and which also contained a small amount of polymer was collected and was purified by ultrafiltration in methanol through a PLBC regenerated cellulose 3000 NMWL membrane to remove residual n-dodecyl amine. The two fractions were concentrated by vacuum distillation and the polymer was again dried under vacuum for another two days. The polymer was a clear, yellow solid. Yield = 0.2200g. 99% substitution. ¹H NMR in CDCl₃: 3.66 (-O-CH₂-CH₂-), 3.25 (-CO-NH-CH₂-CH₂-N<), 3.18 (-CO-NH-CH₂-CH₂-(CH₂)₉-CH₃), 2.75 (-CH₂-CH₂-CO-NH-CH₂-CH₂-N<) and (-CH₂-CH₂-CO-NH-CH₂-CH₂-(CH₂)₉-CH₃), 2.54 (-N-CH₂-CH₂-) and (-CO-NH-CH₂-CH₂-N<), 2.36 (-CH₂-CH₂-CO-NH-CH₂-CH₂-N<) and (-CH₂-CH₂-CO-NH-CH₂-CH₂-(CH₂)₉-CH₃), 1.50 (-CO-NH-CH₂-CH₂-(CH₂)₉-CH₃), 1.27 (-CO-NH-CH₂-CH₂-(CH₂)₉-CH₃), 0.89 (-CO-NH-CH₂-CH₂-(CH₂)₉-CH₃). FTIR, ν cm⁻¹: 3285, 3078, 2961, 1931, 2855, 2814, 1740, 1648, 1552, 1471, 1436, 1375, 1263, 1035, 807, 726.

Poly(ethylene oxide)-poly(ethylene imine) dendritic diblock generation 4.0-octadecyl terminated

All glassware were oven dried prior to use. A two-necked, 100ml round bottom flask equipped with a condenser and vacuum adapter in the center arm, an addition funnel and glass stopper in the side arm, and a stir bar in the bottom, was evacuated and filled with nitrogen. 0.3491g (0.001295 mol) n-octadecyl amine and 7ml of methanol were placed in a 50ml Erlenmeyer flask. The n-octadecyl amine did not dissolve with stirring, so the flask was heated, which induced dissolution, and the flask was allowed to cool to room temperature. This n-octadecyl amine/methanol solution was transferred to the reaction flask, and the 50ml Erlenmeyer flask was rinsed with an additional 5ml of methanol, which were also added to the reaction flask. 0.2055g (1.3677×10^{-6} mol polymer, 0.001061 mol ester groups) of PEO-PEI generation 3.5 polymer were dissolved with 10ml of methanol in a 25ml erlenmeyer flask. This polymer/methanol solution was transferred to the addition funnel and was added dropwise over 5 minutes at room temperature. The addition funnel was rinsed with an additional 5ml of methanol for a total methanol volume of 27ml. The reaction flask was covered with aluminum foil to prevent the polymer from yellowing, and the solution was allowed to react at room temperature. After 20 hours, an oil bath was placed beneath the reaction flask and the solution was heated at 60°C. After eight days of heating, the methanol was removed by removed by vacuum distillation and the polymer was left to dry under vacuum for a day. The polymer was redissolved in methanol and with time and exposure to air, the octadecyl amine fell out of solution as a white precipitate. The precipitate was removed by repeated vacuum filtration until no more precipitate appeared. The polymer/methanol solution was then purified by ultrafiltration in methanol through a PLBC regenerated cellulose 3000 NMWL membrane to remove traces of octadecyl amine. The pure polymer/methanol ultrafiltration solution was concentrated by vacuum distillation, and the polymer was again dried under vacuum for another two days. The polymer was a yellow solid. Yield = 0.1146g. 12% substitution. ¹H NMR in CDCl₃: 3.69 (unreacted -CH₂-CH₂-CO-OCH₃), 3.66 (-O-CH₂-CH₂-), 3.29 (-CO-NH-CH₂-CH₂-N<), 2.77 (-CH₂-CH₂-CO-NH-CH₂-CH₂-N<) and (-CH₂-CH₂-CO-NH-CH₂-CH₂-(CH₂)₁₅-CH₃), 2.56 (-N-CH₂-CH₂-) and (-CO-NH-CH₂-CH₂-N<), 2.45 (unreacted -CH₂-CH₂-CO-OCH₃), 2.38 (-CH₂-CH₂-CO-NH-CH₂-CH₂-N<) and (-CH₂-CH₂-CO-NH-CH₂-CH₂-(CH₂)₁₅-CH₃), 1.50 (-CO-NH-CH₂-CH₂-(CH₂)₁₅-CH₃), 1.27 (-CO-NH-CH₂-CH₂-(CH₂)₁₅-CH₃), 0.90 (-CO-NH-CH₂-CH₂-(CH₂)₁₅-CH₃). FTIR, ν cm⁻¹: 3287, 3073, 2963, 2922, 2853, 2815, 1740, 1653, 1543, 1467, 1438, 1363, 1259, 1203, 1044, 755, 662.

Poly(ethylene oxide)-poly(ethylene imine) dendritic diblock generation 5.0-dodecyl terminated

All glassware were oven dried prior to use. A two-necked, 100ml round bottom flask equipped with a condenser and vacuum adapter in the center arm, an addition funnel and glass stopper in the side arm, and a stir bar in the bottom, was evacuated and filled with nitrogen. 8.1875g (0.04417 mol) of n-dodecyl amine were dissolved with 8ml of methanol in a 250ml erlenmeyer flask and were subsequently added to the round bottom flask. The 250ml erlenmeyer flask was rinsed with an additional 5ml of methanol which was also added to the reaction flask. 0.2395g (7.8409×10^{-7} mol polymer, 0.001217 mol ester groups) of PEO-PEI generation 4.5 polymer were dissolved with 10ml of methanol in a 50ml erlenmeyer flask. This polymer/methanol solution was transferred to the addition funnel and was added dropwise over 5 minutes to the stirring n-dodecyl amine/methanol solution at room temperature. The 25ml erlenmeyer flask and the

addition funnel were rinsed with an additional 5ml of methanol, which was then added to the reaction flask, for a total methanol volume of 28ml. The reaction flask was covered with aluminum foil to prevent the polymer from yellowing. After 19 hours, an oil bath was placed beneath the reaction flask and the solution was heated at 60°C. After nine days of heating, the heat was removed and the reaction solution was allowed to cool. The crude polymer and reaction solution were purified by ultrafiltration in methanol through a PLBC regenerated cellulose 3000 NMWL membrane to remove the excess n-dodecyl amine. The pure polymer/methanol ultrafiltration solution was concentrated by vacuum distillation, and the polymer was again dried under vacuum for another three and a half days. The polymer was a clear, orange solid. Yield = 0.2479g. 92% substitution. ¹H NMR in CDCl₃: 3.68 (unreacted -CH₂-CH₂-CO-OCH₃), 3.66 (-O-CH₂-CH₂-), 3.25 (-CO-NH-CH₂-CH₂-N<), 3.19 (-CO-NH-CH₂-CH₂-(CH₂)₉-CH₃), 2.74 (-CH₂-CH₂-CO-NH-CH₂-CH₂-N<) and (-CH₂-CH₂-CO-NH-CH₂-CH₂-(CH₂)₉-CH₃), 2.56 (-N-CH₂-CH₂-) and (-CO-NH-CH₂-CH₂-N<), 2.35 (-CH₂-CH₂-CO-NH-CH₂-CH₂-N<) and (-CH₂-CH₂-CO-NH-CH₂-CH₂-(CH₂)₉-CH₃), 1.50 (-CO-NH-CH₂-CH₂-(CH₂)₉-CH₃), 1.27 (-CO-NH-CH₂-CH₂-(CH₂)₉-CH₃), 0.90 (-CO-NH-CH₂-CH₂-(CH₂)₉-CH₃). FTIR, ν cm⁻¹: 3284, 3066, 2957, 2923, 2854, 2819, 1736, 1645, 1547, 1461, 1438, 1370, 1249, 1192, 1140, 1032, 728.

Poly(ethylene oxide)-poly(ethylene imine) dendritic diblock generation 5.0-octadecyl terminated

All glassware were oven dried prior to use. A three-necked, 50ml round bottom flask equipped with a condenser and vacuum adapter in the center arm, an addition funnel and glass stopper in one of the side arms, a glass stopper in the other side arm, and a stir bar in the bottom, was evacuated and filled with nitrogen. 0.3349g (0.001243 mol) n-octadecyl amine and 7ml of methanol were placed in a 50ml Erlenmeyer flask. The n-octadecyl amine did not dissolve with stirring, so the flask was heated, which induced dissolution, and the flask was allowed to cool to room temperature. This n-octadecyl amine/methanol solution was transferred to the reaction flask, and the 50ml Erlenmeyer flask was rinsed with an additional 3ml of methanol, which were also added to the reaction flask. 0.2013g (6.5903⁻⁷ mol polymer, 0.001023 mol ester groups) of PEO-PEI generation 4.5 polymer were dissolved with 10ml of methanol in a 50ml erlenmeyer flask. This polymer/methanol solution was transferred to the addition funnel and was added dropwise over 5 minutes at room temperature. The addition funnel was rinsed with an additional 5ml of methanol for a total methanol volume of 25ml. The reaction flask was covered with aluminum foil to prevent the polymer from yellowing. After 19 hours, an oil bath was placed beneath the reaction flask and the solution was heated at 60°C. After nine days of heating, the heat was removed and the reaction solution was allowed to cool. A small amount of precipitate fell out of solution and was removed by vacuum filtration through a size D glass funnel. The crude polymer and reaction solution were purified by ultrafiltration in methanol in methanol through a PLBC regenerated cellulose 3000 NMWL membrane to remove the excess n-octadecyl amine. The pure polymer/methanol ultrafiltration solution was concentrated by vacuum distillation, and the polymer was again dried under vacuum for another two days. The polymer was an orange solid. Yield = 0.1173g. 13% substitution. ¹H NMR in CDCl₃: 3.69 (unreacted -CH₂-CH₂-CO-OCH₃), 3.66 (-O-CH₂-CH₂-), 3.30 (-CO-NH-CH₂-CH₂-N<), 2.77 (-CH₂-CH₂-CO-NH-CH₂-CH₂-N<) and (-CH₂-CH₂-CO-NH-CH₂-CH₂-(CH₂)₁₅-CH₃), 2.56 (-N-CH₂-CH₂-) and (-CO-NH-CH₂-CH₂-N<), 2.45 (unreacted -CH₂-CH₂-CO-OCH₃), 2.38 (-CH₂-CH₂-CO-NH-CH₂-CH₂-N<) and (-CH₂-CH₂-CO-NH-CH₂-CH₂-(CH₂)₁₅-CH₃), 1.50 (-CO-NH-CH₂-CH₂-(CH₂)₁₅-

CH₃), 1.27 (-CO-NH-CH₂-CH₂-(CH₂)₁₅-CH₃), 0.90 (-CO-NH-CH₂-CH₂-(CH₂)₁₅-CH₃). FTIR, ν cm⁻¹: 3279, 3065, 2950, 2915, 2852, 2812, 1733, 1652, 1542, 1438, 1358, 1254, 1196, 1040, 838, 758.

2.A.2.2 Linear Dendritic Rod Diblock Copolymers Consisting of a Polyethylene Oxide Block of 43 Repeats and a Dendritic Block of 178 Repeats

Poly(ethylene oxide)-poly(ethylene imine) dendritic diblock generation 1.0-butyl terminated

All glassware were oven dried prior to use. A two-necked, 100ml round bottom flask equipped with a condenser and vacuum adapter in the center arm, an addition funnel and glass stopper in the side arm, and a stir bar in the bottom, was evacuated and filled with nitrogen. 20ml (0.202 mol) of n-butyl amine and 15ml of methanol were added to the round bottom flask and were subsequently chilled in an ice bath for 5 minutes. 0.2767g (1.1112×10^{-5} mol polymer, 0.001978 mol ester groups) of PEO-PEI generation 0.5 polymer were dissolved with 20 ml of methanol in a 25ml erlenmeyer flask. This polymer/methanol solution was transferred to the addition funnel and was added dropwise over 15 minutes. The 50ml erlenmeyer flask and the addition funnel were rinsed with an additional 6ml of methanol, which was then added to the reaction flask, for a total methanol volume of 41ml. The reaction flask was covered with aluminum foil to prevent the polymer from yellowing, and the solution was allowed to warm to room temperature. After five days of stirring at room temperature, the majority of the methanol and excess n-decyl amine were removed by vacuum distillation, and the polymer was left to dry under vacuum for a day. The polymer was redissolved in methanol and was purified by ultrafiltration in methanol through a BIOMAX polyethersulfone 5000 NMWL membrane to remove traces of n-butyl amine. The pure polymer/methanol ultrafiltration solution was concentrated by vacuum distillation, and the polymer was again dried under vacuum overnight. The polymer was a light yellow, viscous liquid. Yield = 0.1721g. 92% substitution. ¹H NMR in MeOH-*d*: 3.69 (unreacted -CH₂-CH₂-CO-OCH₃), 3.65 (-O-CH₂-CH₂-), 3.20 (-CO-NH-CH₂-CH₂-CH₂-CH₃), 2.84 (-CH₂-CH₂-CO-NH-), 2.62 (-N-CH₂-CH₂-), 2.51 (unreacted -CH₂-CH₂-CO-OCH₃), 2.38 (-CH₂-CH₂-CO-NH-), 1.51 (-CO-NH-CH₂-CH₂-CH₂-CH₃), 1.39 (-CO-NH-CH₂-CH₂-CH₂-CH₃), 0.96 (-CO-NH-CH₂-CH₂-CH₂-CH₃). FTIR, ν cm⁻¹: 3269, 3066, 2955, 2930, 2869, 2814, 1732, 1646, 1554, 1461, 1363, 1289, 1111, 1031, 742.

Poly(ethylene oxide)-poly(ethylene imine) dendritic diblock generation 1.0-hexyl terminated

All glassware were oven dried prior to use. A two-necked, 250ml round bottom flask equipped with a condenser and vacuum adapter in the center arm, an addition funnel and glass stopper in the side arm, and a stir bar in the bottom, was evacuated and filled with nitrogen. 25ml (0.1892 mol) of n-hexyl amine and 80ml of methanol were added to the round bottom flask and were subsequently chilled in an ice bath for 10 minutes. 0.2636g (1.0586×10^{-5} mol polymer, 0.001884 mol ester groups) of PEO-PEI generation 0.5 polymer were dissolved with 20ml of methanol in a 50ml erlenmeyer flask. This polymer/methanol solution was transferred to the addition funnel and was added dropwise over 10 minutes. The 50ml erlenmeyer flask and the addition funnel were rinsed with an additional 5ml of methanol, which was then added to the reaction flask, for a

total methanol volume of 105ml. The reaction flask was covered with aluminum foil to prevent the polymer from yellowing, and the solution was allowed to warm to room temperature. After five days of stirring at room temperature, the majority of the methanol and excess n-hexyl amine were removed by vacuum distillation, and the polymer was left to dry under vacuum for a day. The polymer was redissolved in methanol and was purified by ultrafiltration in methanol through a BIOMAX polyethersulfone 5000 NMWL membrane to remove traces of n-hexyl amine. The pure polymer/methanol ultrafiltration solution was concentrated by vacuum distillation, and the polymer was again dried under vacuum overnight. The polymer was a light yellow, viscous liquid. Yield = 0.1122g. 66% substitution. ^1H NMR in MeOH-*d*: 3.69 (unreacted $-\text{CH}_2-\text{CH}_2-\text{CO}-\text{OCH}_3$), 3.66 ($-\text{O}-\text{CH}_2-\text{CH}_2-$), 3.19 ($-\text{CO}-\text{NH}-\text{CH}_2-\text{CH}_2-(\text{CH}_2)_3-\text{CH}_3$), 2.81 ($-\text{CH}_2-\text{CH}_2-\text{CO}-\text{NH}-$), 2.61 ($-\text{N}-\text{CH}_2-\text{CH}_2-$), 2.51 (unreacted $-\text{CH}_2-\text{CH}_2-\text{CO}-\text{OCH}_3$), 2.37 ($-\text{CH}_2-\text{CH}_2-\text{CO}-\text{NH}-$), 1.51 ($-\text{CO}-\text{NH}-\text{CH}_2-\text{CH}_2-(\text{CH}_2)_3-\text{CH}_3$), 1.35 ($-\text{CO}-\text{NH}-\text{CH}_2-\text{CH}_2-(\text{CH}_2)_3-\text{CH}_3$), 0.93 ($-\text{CO}-\text{NH}-\text{CH}_2-\text{CH}_2-(\text{CH}_2)_3-\text{CH}_3$). FTIR, ν cm^{-1} : 3281, 3072, 2955, 2924, 2857, 2820, 1738, 1646, 1554, 1461, 1363, 1259, 1197, 1117, 1037, 730.

Poly(ethylene oxide)-poly(ethylene imine) dendritic diblock generation 1.0-octyl terminated

All glassware were oven dried prior to use. A two-necked, 250ml round bottom flask equipped with a condenser and vacuum adapter in the center arm, an addition funnel and glass stopper in the side arm, and a stir bar in the bottom, was evacuated and filled with nitrogen. 29ml (0.1768 mol) of n-octyl amine and 90ml of methanol were added to the round bottom flask and were subsequently chilled in an ice bath for 10 minutes. 0.2430g (9.7590×10^{-6} mol polymer, 0.001737 mol ester groups) of PEO-PEI generation 0.5 polymer were dissolved with 20ml of methanol in a 50ml erlenmeyer flask. This polymer/methanol solution was transferred to the addition funnel and was added dropwise over 10 minutes. The 50ml erlenmeyer flask and the addition funnel were rinsed with an additional 6ml of methanol, which was then added to the reaction flask, for a total methanol volume of 116ml. The reaction flask was covered with aluminum foil to prevent the polymer from yellowing, and the solution was allowed to warm to room temperature. After five days of stirring at room temperature, the majority of the methanol and excess n-octyl amine were removed by vacuum distillation, and the polymer was left to dry under vacuum for a day. The polymer was redissolved in methanol and was purified by ultrafiltration in methanol through a BIOMAX polyethersulfone 5000 NMWL membrane to remove traces of n-octyl amine. The pure polymer/methanol ultrafiltration solution was concentrated by vacuum distillation, and the polymer was again dried under vacuum overnight. The polymer was a light yellow, viscous liquid. Yield = 0.0816g. 72% substitution. ^1H NMR in MeOH-*d*: 3.69 (unreacted $-\text{CH}_2-\text{CH}_2-\text{CO}-\text{OCH}_3$), 3.65 ($-\text{O}-\text{CH}_2-\text{CH}_2-$), 3.19 ($-\text{CO}-\text{NH}-\text{CH}_2-\text{CH}_2-(\text{CH}_2)_5-\text{CH}_3$), 2.82 ($-\text{CH}_2-\text{CH}_2-\text{CO}-\text{NH}-$), 2.61 ($-\text{N}-\text{CH}_2-\text{CH}_2-$), 2.50 (unreacted $-\text{CH}_2-\text{CH}_2-\text{CO}-\text{OCH}_3$), 2.38 ($-\text{CH}_2-\text{CH}_2-\text{CO}-\text{NH}-$), 1.51 ($-\text{CO}-\text{NH}-\text{CH}_2-\text{CH}_2-(\text{CH}_2)_5-\text{CH}_3$), 1.33 ($-\text{CO}-\text{NH}-\text{CH}_2-\text{CH}_2-(\text{CH}_2)_5-\text{CH}_3$), 0.93 ($-\text{CO}-\text{NH}-\text{CH}_2-\text{CH}_2-(\text{CH}_2)_5-\text{CH}_3$). FTIR, ν cm^{-1} : 3281, 3072, 2950, 2924, 2857, 2820, 1738, 1640, 1554, 1461, 1363, 1252, 1117, 724.

Poly(ethylene oxide)-poly(ethylene imine) dendritic diblock generation 1.0-decyl terminated

All glassware were oven dried prior to use. A two-necked, 100ml round bottom flask equipped with a condenser and vacuum adapter in the center arm, an addition funnel and glass stopper in the side arm, and a stir bar in the bottom, was evacuated and filled with nitrogen. 18ml (0.0900 mol) of n-decyl amine and 18ml of methanol were added to the round bottom flask and were

subsequently chilled in an ice bath for one hour. 0.2506g (1.0064×10^{-5} mol polymer, 0.001790 mol ester groups) of PEO-PEI generation 0.5 polymer were dissolved with 15 ml of methanol in a 50ml erlenmeyer flask. This polymer/methanol solution was transferred to the addition funnel and was added dropwise over 5 minutes. The 50ml erlenmeyer flask and the addition funnel were rinsed with an additional 12ml of methanol, which was added to the reaction flask, for a total methanol volume of 45ml. The reaction flask was covered with aluminum foil to prevent the polymer from yellowing, and the solution was allowed to warm to room temperature. After five days of stirring at room temperature, the majority of the methanol and excess n-decyl amine were removed by vacuum distillation, and the polymer was left to dry under vacuum for a day. The polymer was redissolved in methanol and was purified by ultrafiltration in methanol through a BIOMAX polyethersulfone 5000 NMWL membrane to remove traces of n-decyl amine. The pure polymer/methanol ultrafiltration solution was concentrated by vacuum distillation, and the polymer was again dried under vacuum overnight. The polymer was a light yellow, viscous liquid. Yield = 0.1081g. 58% substitution. ^1H NMR in MeOH-*d*: 3.70 (unreacted $-\text{CH}_2-\text{CH}_2-\text{CO}-\text{OCH}_3$), 3.65 ($-\text{O}-\text{CH}_2-\text{CH}_2-$), 3.19 ($-\text{CO}-\text{NH}-\text{CH}_2-\text{CH}_2-(\text{CH}_2)_7-\text{CH}_3$), 2.83 ($-\text{CH}_2-\text{CH}_2-\text{CO}-\text{NH}-$), 2.61 ($-\text{N}-\text{CH}_2-\text{CH}_2-$), 2.52 (unreacted $-\text{CH}_2-\text{CH}_2-\text{CO}-\text{OCH}_3$), 2.38 ($-\text{CH}_2-\text{CH}_2-\text{CO}-\text{NH}-$), 1.53 ($-\text{CO}-\text{NH}-\text{CH}_2-\text{CH}_2-(\text{CH}_2)_7-\text{CH}_3$), 1.32 ($-\text{CO}-\text{NH}-\text{CH}_2-\text{CH}_2-(\text{CH}_2)_7-\text{CH}_3$), 0.93 ($-\text{CO}-\text{NH}-\text{CH}_2-\text{CH}_2-(\text{CH}_2)_7-\text{CH}_3$). FTIR, ν cm^{-1} : 3278, 3066, 2963, 2925, 2854, 2816, 1741, 1644, 1551, 1464, 1367, 1253, 1117, 726.

Poly(ethylene oxide)-poly(ethylene imine) dendritic diblock generation 1.0-dodecyl terminated

All glassware were oven dried prior to use. A two-necked, 100ml round bottom flask equipped with a condenser and vacuum adapter in the center arm, an addition funnel and glass stopper in the side arm, and a stir bar in the bottom, was evacuated and filled with nitrogen. 16.7397g (0.09031 mol) of n-dodecyl amine were dissolved with 15ml of methanol in a 125ml erlenmeyer flask and were subsequently added to the round bottom flask. The solution was cooled in an ice bath for 15minutes. 0.2513g (1.0092×10^{-5} mol polymer, 0.001796 mol ester groups) of PEO-PEI generation 0.5 polymer were dissolved with 15ml of methanol in a 50ml erlenmeyer flask. This polymer/methanol solution was transferred to the addition funnel and was added dropwise over 5 minutes. The erlenmeyer flask and the addition funnel were rinsed with an additional 20ml of methanol, which was added to the reaction flask, for a total methanol volume of 50ml. The reaction flask was covered with aluminum foil to prevent the polymer from yellowing, and the solution was allowed to warm to room temperature. After five days of stirring at room temperature, the majority of the methanol and excess n-dodecyl amine were removed by vacuum distillation, and the polymer was left to dry under vacuum for a day. The polymer was redissolved in methanol and was purified by ultrafiltration in methanol through a BIOMAX polyethersulfone 5000 NMWL membrane to remove traces of n-dodecyl amine. The pure polymer/methanol solution was concentrated by vacuum distillation, and the polymer was again dried under vacuum for another day. The polymer was a light yellow, soft solid. Yield = 0.0398g. 89% substitution. ^1H NMR in MeOH-*d* and CDCl_3 : 3.69 (unreacted $-\text{CH}_2-\text{CH}_2-\text{CO}-\text{OCH}_3$), 3.66 ($-\text{O}-\text{CH}_2-\text{CH}_2-$), 3.19 ($-\text{CO}-\text{NH}-\text{CH}_2-\text{CH}_2-(\text{CH}_2)_9-\text{CH}_3$), 2.81 ($-\text{CH}_2-\text{CH}_2-\text{CO}-\text{NH}-$), 2.61 ($-\text{N}-\text{CH}_2-\text{CH}_2-$), 2.38 ($-\text{CH}_2-\text{CH}_2-\text{CO}-\text{NH}-$), 1.53 ($-\text{CO}-\text{NH}-\text{CH}_2-\text{CH}_2-(\text{CH}_2)_9-\text{CH}_3$), 1.31 ($-\text{CO}-\text{NH}-\text{CH}_2-\text{CH}_2-(\text{CH}_2)_9-\text{CH}_3$), 0.92 ($-\text{CO}-\text{NH}-\text{CH}_2-\text{CH}_2-(\text{CH}_2)_9-\text{CH}_3$). FTIR, ν cm^{-1} :

Poly(ethylene oxide)-poly(ethylene imine) dendritic diblock generation 1.0-octadecyl terminated

All glassware were oven dried prior to use. A three-necked, 50ml round bottom flask equipped with a condenser and vacuum adapter in the center arm, an addition funnel and glass stopper in one of the side arms, a glass stopper in the other side arm, and a stir bar in the bottom, was evacuated and filled with nitrogen. 1.5160g (0.005636 mol) n-octadecyl amine and 7ml of methanol were placed in a 50ml Erlenmeyer flask. The n-octadecyl amine did not dissolve with stirring, so the flask was heated, which induced dissolution. The flask was allowed to cool to room temperature and a small amount of octadecyl amine fell back out of solution, as indicated by the formation of a white precipitate on the bottom of the flask; however, the majority of the n-octadecyl amine remained in solution. This n-octadecyl amine/methanol solution was transferred to the reaction flask, and the 50ml Erlenmeyer flask was rinsed with an additional 3ml of methanol which were also added to the reaction flask. 0.2464g (9.8956×10^{-6} mol polymer, 0.001761 mol ester groups) of PEO-PEI generation 0.5 polymer were dissolved with 10ml of methanol in a 25ml erlenmeyer flask. This polymer/methanol solution was transferred to the addition funnel and was added dropwise over 5 minutes at room temperature. The addition funnel was rinsed with an additional 5ml of methanol for a total methanol volume of 25ml. The reaction flask was covered with aluminum foil to prevent the polymer from yellowing, and the solution was allowed to react at room temperature. After 18 hours, an oil bath was placed beneath the reaction flask and the solution was heated at 60°C. After four days of heating, the methanol was removed by removed by vacuum distillation and the polymer was left to dry under vacuum for a day. The polymer was redissolved in methanol and with time and exposure to air, the octadecyl amine fell out of solution as a white precipitate. The precipitate was removed by repeated vacuum filtration until no more precipitate appeared. The polymer/methanol solution was then purified by ultrafiltration in methanol through a PLBC regenerated cellulose 3000 NMWL membrane to remove traces of n-octadecyl amine. The pure polymer/methanol solution was concentrated by vacuum distillation, and the polymer was again dried under vacuum for another two days. The polymer was an off-white solid. Yield = 0.0669. 73% substitution. ^1H NMR in CDCl_3 : 3.67 (unreacted $-\text{CH}_2-\text{CH}_2-\text{CO}-\text{OCH}_3$), 3.65 ($-\text{O}-\text{CH}_2-\text{CH}_2-$), 3.21 ($-\text{CO}-\text{NH}-\text{CH}_2-\text{CH}_2-(\text{CH}_2)_{15}-\text{CH}_3$), 2.77 ($-\text{CH}_2-\text{CH}_2-\text{CO}-\text{NH}-$), 2.68 ($-\text{N}-\text{CH}_2-\text{CH}_2-$), 2.33 ($-\text{CH}_2-\text{CH}_2-\text{CO}-\text{NH}-$), 1.50 ($-\text{CO}-\text{NH}-\text{CH}_2-\text{CH}_2-(\text{CH}_2)_{15}-\text{CH}_3$), 1.28 ($-\text{CO}-\text{NH}-\text{CH}_2-\text{CH}_2-(\text{CH}_2)_{15}-\text{CH}_3$), 0.90 ($-\text{CO}-\text{NH}-\text{CH}_2-\text{CH}_2-(\text{CH}_2)_{15}-\text{CH}_3$). FTIR, $\nu \text{ cm}^{-1}$: 3298, 3060, 2951, 2918, 2854, 2822, 1734, 1644, 1566, 1470, 1360, 1116, 762, 665.

2.A.3 References

- (1) Dust, J. M.; Fang, Z. H.; Harris, J. M. "Proton NMR characterization of poly(ethylene glycols) and derivatives," *Macromolecules* 1990, 23, 3742-3746.
- (2) Overberger, C. G.; Peng, L. "Synthesis of poly(ethylene glycol methyl ether)-b-poly(ethylenimine) and its derivatives containing thymine and amino-acids as pendants," *Journal of Polymer Science Part A-Polymer Chemistry* 1986, 24, 2797-2813.

Appendix 5.A DSC Data

5.A.1 Generational Polymers

| Polymer | Physical Description | T _m (°C) | T _g (°C) |
|------------------------|------------------------------------|--|---------------------|
| PEO-PEI | light yellow, hard solid | 30.6 - PEO 38.6 - PEO 52.5 - PEI (dehydrated) 67.6 - PEI (partly hydrated) 76.0 - PEI (hydrated) | |
| PEO-PEI Generation 0.5 | light yellow, waxy solid | 39.0 - PEO | |
| PEO-PEI Generation 1.0 | light yellow solid | 40.7 - PEO | -13.2 – dendrimer |
| PEO-PEI Generation 1.5 | yellow, viscous liquid | 38.4 - PEO | |
| PEO-PEI Generation 2.0 | yellow solid | 37.6 - PEO | -1.9 – dendrimer |
| PEO-PEI Generation 2.5 | golden yellow, very viscous liquid | 39.6 - PEO (very weak) | |
| PEO-PEI Generation 3.0 | orange solid | 39.9 - PEO (very weak) | -0.4 – dendrimer |
| PEO-PEI Generation 3.5 | orange, very viscous liquid | 46.3 - PEO (very weak) | -20.2 – dendrimer |
| PEO-PEI Generation 4.0 | brown solid | 38.7 - PEO (very weak) | 5.3 – dendrimer |
| PEO-PEI Generation 4.5 | brown, sticky solid | 40.9 - PEO (very weak) | -3.3 - dendrimer |

5.A.2 Alkyl Terminated Polymers

5.A.2.1 Generation 1.0

| Polymer | Physical Description | T _m (°C) | T _g (°C) |
|----------------------------------|------------------------------|-----------------------------------|---------------------|
| PEO-PEI Generation 1.0-butyl | light yellow, viscous liquid | 22.7 - alkyl chains 39.3 - PEO | -13.4 - dendrimer |
| PEO-PEI Generation 1.0-hexyl | light yellow, viscous liquid | 21.3 - alkyl chains 38.4 - PEO | -23.4 - dendrimer |
| PEO-PEI Generation 1.0-octyl | light yellow, viscous liquid | 22.8 - alkyl chains 37.6 - PEO | -23.6 - dendrimer |
| PEO-PEI Generation 1.0-decyl | light yellow, viscous liquid | 22.4 - alkyl chains 37.1 - PEO | -25.3 - dendrimer |
| PEO-PEI Generation 1.0-dodecyl | light yellow, soft solid | 17.8 - alkyl chains 39.4 - PEO | -16.2 - dendrimer |
| PEO-PEI Generation 1.0-octadecyl | white, hard solid | 41.6 - PEO 50.0 - alkyl chains | |

5.A.2.2 Generation 2.0

| Polymer | Physical Description | T _m (°C) | T _g (°C) |
|----------------------------------|------------------------|---|---------------------|
| PEO-PEI Generation 2.0-butyl | yellow, viscous liquid | 22.3 - alkyl chains 30.9 - PEO 33.6 - PEO | -16.0 - dendrimer |
| PEO-PEI Generation 2.0-hexyl | yellow, viscous liquid | 21.9 - alkyl chains 28.0 - PEO | -10.6 - dendrimer |
| PEO-PEI Generation 2.0-octyl | yellow, viscous liquid | 20.7 - alkyl chains | -17.4 - dendrimer |
| PEO-PEI Generation 2.0-decyl | yellow, soft solid | 17.8 - alkyl chains 29.2 - PEO | -19.1 - dendrimer |
| PEO-PEI Generation 2.0-dodecyl | yellow, soft solid | 21.0 - alkyl chains 36.6 - PEO 43.8 - PEO | -20.5 - dendrimer |
| PEO-PEI Generation 2.0-octadecyl | light yellow solid | 37.7 - PEO 51.8 - alkyl chains 57.9 - alkyl | -1.3 - dendrimer |

5.A.2.3 Generation 3.0

| Polymer | Physical Description | T _m (°C) | T _g (°C) |
|----------------------------------|------------------------------------|---|---------------------|
| PEO-PEI Generation 3.0-butyl | golden yellow, very viscous liquid | 21.2 - alkyl chains 38.9 - PEO (very weak) | 5.0 - dendrimer |
| PEO-PEI Generation 3.0-hexyl | golden yellow, very viscous liquid | 21.0 - alkyl chains 34.1 - PEO (very weak) | 0.07 - dendrimer |
| PEO-PEI Generation 3.0-octyl | golden yellow, very viscous liquid | 21.0 - alkyl chains 34.4 - PEO (very weak) | -3.7 - dendrimer |
| PEO-PEI Generation 3.0-decyl | golden yellow, very viscous liquid | 22.2 - alkyl chains 34.1 - PEO (very weak) | -2.5 - dendrimer |
| PEO-PEI Generation 3.0-dodecyl | yellow, soft solid | 21.7 - alkyl chains 34.4 - PEO | -4.4 - dendrimer |
| PEO-PEI Generation 3.0-octadecyl | opaque, yellow solid | 51.0 - alkyl chains | 6.7 - dendrimer |

5.A.2.4 Generation 4.0

| Polymer | Physical Description | T _m (°C) | T _g (°C) |
|----------------------------------|----------------------------|--|---------------------|
| PEO-PEI Generation 4.0-butyl | golden yellow sticky solid | 21.6 - alkyl chains (very weak) | 10.8 - dendrimer |
| PEO-PEI Generation 4.0-hexyl | golden yellow sticky solid | 23.2 - alkyl chains (very weak) | 4.8 - dendrimer |
| PEO-PEI Generation 4.0-octyl | golden yellow sticky solid | 22.1 - alkyl chains (very weak) | 0.8 - dendrimer |
| PEO-PEI Generation 4.0-decyl | golden yellow sticky solid | 22.1 - alkyl chains (very weak) | 3.1 - dendrimer |
| PEO-PEI Generation 4.0-dodecyl | clear, yellow solid | 22.1 - alkyl chains (very weak) | 2.2 - dendrimer |
| PEO-PEI Generation 4.0-octadecyl | opaque, yellow solid | 49.4 - alkyl chains 59.1 - alkyl chains | -4.7 - dendrimer |

5.A.2.5 Generation 5.0

| Polymer | Physical Description | T _m (°C) | T _g (°C) |
|----------------------------------|----------------------|---------------------|---------------------|
| PEO-PEI Generation 5.0-dodecyl | clear, yellow solid | 18.0 - alkyl chains | -0.5 - dendrimer |
| PEO-PEI Generation 5.0-octadecyl | opaque, yellow solid | 49.1 – alkyl chains | -7.4 - dendrimer |

